UNIVERSITAT DE BARCELONA

Development of Iron-Catalyzed Hydrogen Atom Transfer Driven Cross-Coupling and Cyclization Reactions: Use of Isocyanides, Heterocycles and Tosylhydrazones as Radical Acceptors

Jordi Puig Bosch

UNIVERSITAT DE BARCELONA

FACULTAT DE FARMÀCIA I CIÈNCIES DE L'ALIMENTACIÓ

DEPARTAMENT DE FARMACOLOGIA, TOXICOLOGIA I QUÍMICA TERAPÈUTICA

DEVELOPMENT OF IRON-CATALYZED HYDROGEN ATOM TRANSFER DRIVEN CROSS-COUPLING AND CYCLIZATION REACTIONS: USE OF ISOCYANIDES, HETEROCYCLES AND TOSYLHYDRAZONES AS RADICAL ACCEPTORS

JORDI PUIG BOSCH

2024

UNIVERSITAT DE BARCELONA

FACULTAT DE FARMÀCIA I CIÈNCIES DE L'ALIMENTACIÓ

DEPARTAMENT DE FARMACOLOGIA, TOXICOLOGIA I QUÍMICA TERAPÈUTICA

PROGRAMA DE DOCTORAT DE QUÍMICA ORGÀNICA

DEVELOPMENT OF IRON-CATALYZED HYDROGEN ATOM TRANSFER DRIVEN CROSS-COUPLING AND CYCLIZATION REACTIONS: USE OF ISOCYANIDES, HETEROCYCLES AND TOSYLHYDRAZONES AS RADICAL ACCEPTORS

Memòria presentada per: Jordi Puig Bosch, per optar al títol de doctor per la Universitat de Barcelona

Dirigida per:

Dr. Ben Bradshaw

Prof. Josep Bonjoch

Jordi Puig Bosch

Barcelona, 2024

Financial support for this research was provided by PID2019-104188GB-I00 and PID2022-139257NB-I00 funded by MCIN/AEI/10.13039/501100011033 from the ministry of Economy and Competitiveness of Spain (MINECO).

La font constant arriba sempre al mar
i el riu que riu ho explica amb mots d'Homer:
és l'odissea obscura el foc del far
que revesteix la barca humil d'acer!

El cosmos es col·lapsa en un sospir,
etern i efímer com un meteor:
és l'esperança l'únic elixir
que l'alquimista mescla fins que mor.

Sols cal mirar la vida com un rar
llampec que ens crea i torna al cos d'atzur,
i entendre al cor que és sols un joc d'atzar
allò que, necis, suposem futur.

A tres de quatre,
Jordi Cussà Balaguer

Acknowledgements

En primer lloc vull agrair als meus directors, Ben i Josep, l'oportunitat d'haver pogut dur a terme la meva tesi amb ells, així com tot el suport i dedicació que m'han ofert, pel bon clima de treball i per transmetre'm els seus coneixements.

En segon lloc, voldria agrair als meus companys de laboratori. En especial al Sergi J. per acompanyar-me en els meus primers passos al laboratori, i a la Mar S. per introduir-me al món de les HAT, per ajudar-me sempre, però també per tots els viatges i estones que hem compartit i totes les hores invertides a les rondes de Barcelona. De la mateixa manera, vull donar el meu agraïment a la Clàudia M. i a la Laura R. per les estones compartides, i pel bon ambient al laboratori i al grup. També als companys Albert R., Vale P., Sergi O. i Arnau C. per fer més lleugers els esmorzars i dinars i poder-hi compartir inquietuds.

Als meus amics de la Garriga, la colla, pels anys compartits, per acompanyar-me tot aquest temps, suportar-me, i estimar-me. Al Pol, amb qui ens hem fet farmacèutics junts i mútuament, per fer de la terra la seva ciència.

Als meus pares, per haver-me ajudat incondicionalment, per guiar-me i ajudar-me a arribar fins aquí, per haver-me recolzat sempre en els moments bons i en els dolents. Als meus avis i àvies, per tota l'estima que n'he rebut des de ben xic, i per tot el coneixement que m'han transmès. A l'avi Joan, que, sense saber massa de ciència, era un gran científic i que em va inculcar la passió per aprendre i la feina ben feta. A l'àvia Mercè, per cuidar-me i ensenyar-me a ser pacient, pels valors transmesos.

I finalment a la Laura, per cuidar-me, animar-me i estimar-me, per fer-me feliç, per ser-hi sempre.

TABLE OF CONTENTS

Abstract

Radical reactions have been proven valuable tools in C-C bond generation because the initial radical can evolve to form additional C-C bonds until the new radical species is trapped. With the careful design of the substrates and the control of the reaction conditions, tandem radical reactions can be developed that allow the construction of complex structures starting from simple starting materials.

Metal-catalyzed hydrogen atom transfer (MHAT) reactions are radical-based reactions that allow mild and non-toxic conditions, with high chemo- and site-selectivity and a wide functional group tolerance (*Scheme 1*).

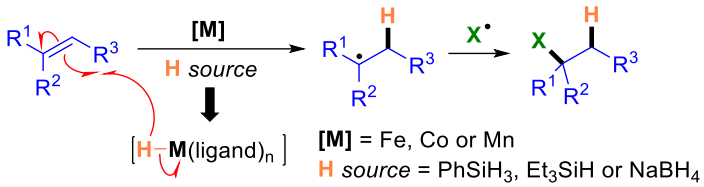

Scheme 1. Metal-catalyzed Hydrogen Atom Transfer (MHAT).

Our group has developed several MHAT C-C bond-forming reactions of non-activated alkenes with a wide variety of acceptor groups such as aldehydes, ketones, Cbz hydrazones, and tosylhydrazones. Despite the many advantages presented by MHAT-based radical reactions and their potential for developing new tandem reactions, few examples have yet been reported in the literature. In the present thesis, the aim was to expand the scope of radical acceptors that can be used in MHAT reactions as well as develop novel tandem reaction processes.

First, isocyanides have been studied as radical acceptors to carry out a tandem reaction to obtain functionalized nitrogen heterocycles, highly valued compounds in medicinal chemistry (*Scheme 2*). The reaction uses MHAT conditions to generate a radical from an alkene that carries out a first radical addition step on the isocyanide, followed by subsequent intramolecular cyclization to give rise to the functionalized heterocycle. A wide range of different nitrogen-containing heterocycles can be synthesized using this methodology. In cases where the alkene substitution made it more challenging, combining HAT-Minisci conditions made the coupling possible. The

reductive cyclization of these isocyanides has also been shown to be effective, in the absence of alkene, to give rise to the corresponding unfunctionalized heterocycles.

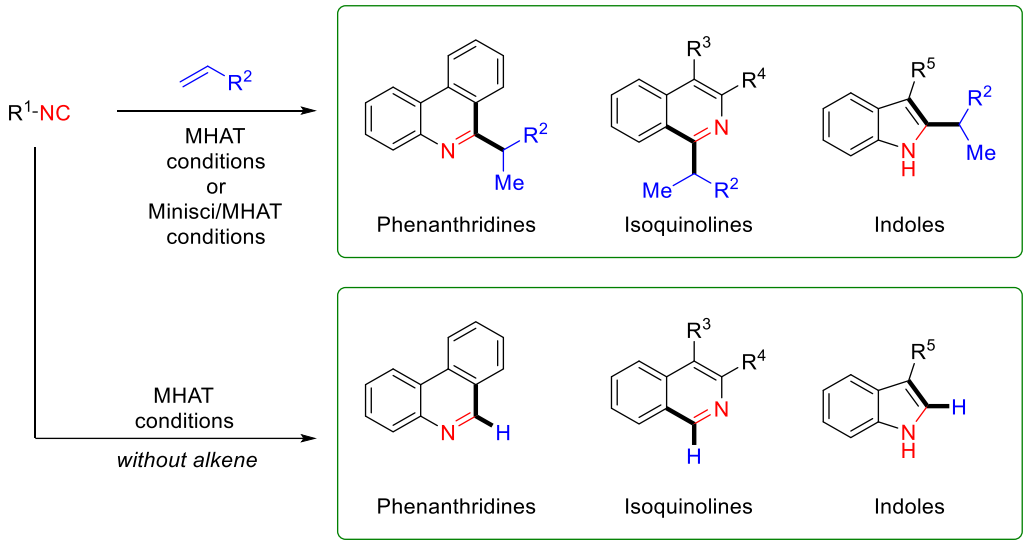

Scheme 2. Isocyanides as radical acceptors

Secondly, a cross-dehydrogenative coupling reaction has been developed from the initial serendipitously observed side reaction. Using conditions derived from MHAT and Minisci, it has been possible to generate radicals through C-H activation on the α-position of ethers, amides, and alkanes to carry out the radical coupling on activated heterorenes (*Scheme 3*). This reaction has the potential to be applied in medicinal chemistry for late-stage functionalization under mild conditions.

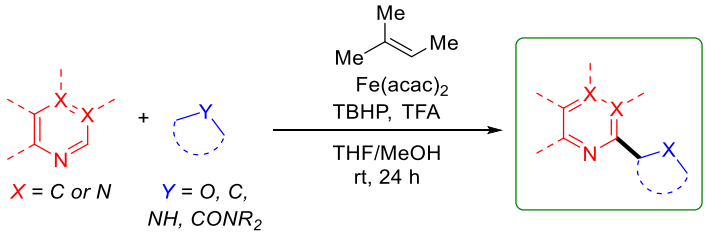

Scheme 3. C-H functionalization of heteroarenes.

Thirdly, the use of tosylhydrazones as acceptor groups in MHAT reactions has been studied to carry out a tandem reaction that begins with intramolecular cyclization followed by in situ fragmentation of the tosylhydrazine and subsequent intermolecular trapping of the generated tertiary radical with a Michael acceptor in a Giese-type addition (*Scheme 4*). This reaction allows the generation of two adjacent quaternary centers in a single reaction via the formation of two geminal C-C bonds. This methodology has been used to prepare functionalized adamantane-like derivatives,

which are very interesting scaffolds from the point of view of medicinal chemistry and other fields. Further transformations also allowed the preparation of adamantane-substituted heterocycles.

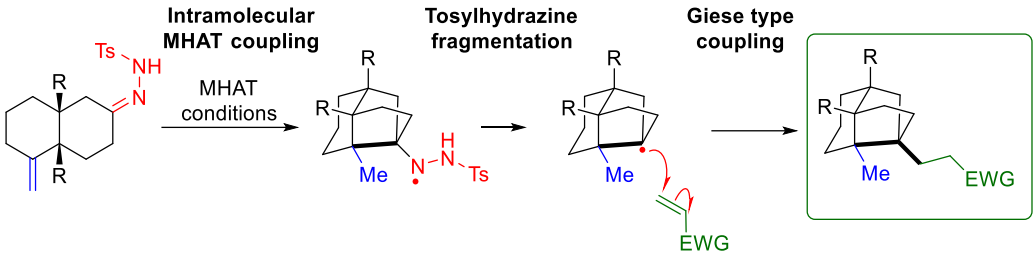

Scheme 4. Use of tosylhydrazones as radical acceptors.

List of Abbreviations and Acronyms

In this manuscript, the abbreviations and acronyms most commonly used in organic chemistry have been used following the recommendations from "Guidelines for Authors" of *J. Org. Chem.* **2020***.*

1,4-CHD	1,4-cyclohexadiene
4-CzIPN	1,2,3,5-tetrakis(carbazol-9-yl)-4,6-dicyanobenzene
p-ABSA	4-acetamidobenzenesulfonyl azide
Ac	acetyl
acac	acetylacetonate
ADME	absorption, distribution, metabolism and excretion
AIBN	azobisisobutyronitrile
aq	aqueous
Ar	aromatic substituent
ATA	α-*tert*-amines
ax	axial
Bn	benzyl
Boc	*tert*-butoxycarbonyl
BPO	benzoyl peroxide
bpy	2,2'-bipyridine
br	broad
t-Bu	*tert*-butyl
Bz	benzoyl
calcd	calculated
Cbz	benzyloxycarbonyl
CCDC	Cambridge crystallographic data centre
ChCl	choline chloride
Cp	cyclopentadienyl
m-CPBA	3-chloroperbenzoic acid
d	doublet
δ	chemical shift
DABCO	1,4-diazabicyclo[2.2.2]octane

DBU	1,5-diazabicyclo[5.4.0]undec-5-ene
DCP	dicumyl peroxide
DHB	2,5-dihydroxybenzoic acid
DCE	dichloroethane
DCM	dichloromethane
dd	doublet of doublets
ddd	doublet of doublets of doublets
dddd	doublet of doublets of doublets of doublets
DEAD	diethyl azodicarboxylate
DEG	diethylene glycol
dibm	diisobutyrylmethane
DIPEA	*N*,*N*-diisopropylethylamine
DMA	dimethylacetamide
DMAP	dimethylaminopyridine
DME	1,2-dimethoxyethane
DMF	*N*,*N*-dimethylformamide
DMPU	1,3-dimethyl-3,4,5,6-tetrahydro-2(1*H*)-pyrimidinone
DMSO	dimethylsulfoxide
DPEphos	bis[(2-diphenylphosphino)phenyl] ether
dpm	dipivaloylmethanato
dq	doublet of quatriplets
dr	diastereomeric ratio
dt	doublet of triplets
DTBP	di-*tert*-butyl peroxide
e.g.	*exempli gratia* (for example)
EI	electron ionization
eq	equatorial
equiv or eq.	equivalent
ESI	electrospray ionization
et al.	*et alii* (and others)
EWG	electro withdrawing group

FDA	Food and Drug Administration
GC-MS	gas chromatography-mass spectrometry
HAT	hydrogen atom transfer
HMPA	hexamethylphosphoramide
HRMS	high resolution mass spectrum
i.e.	*id est* (that is)
*i*Pr	isopropyl
J	coupling constant
KHMDS	potassium bis(trimethylsilyl)amide
LDA	lithium diisopropylamide
LEDs	light-emitting diodes
m	multiplet
M^+	molecular ion
m/z	mass to charge ratio
Mes	mesityl (1,3,5-trimethylbenzene)
$MesAcr^+BF_4^-$	9-mesityl-10-methylacridinium tetrafluoroborate
MHAT	metal catalysed hydrogen atom transfer
Ms	mesyl (methanesulfonyl)
MS	mass spectrometry
MTBE	methyl *tert*-butyl ether
NHC	*N*-heterocyclic carbene
NHPI	*N*-hydroxyphthalimide
NMDA	*N*-methyl-D-aspartate
NMO	4-methylmorpholine *N*-oxide
NMP	*N*-methyl-2-pyrrolidone
NMR	nuclear magnetic resonance
Oct	octyl
PCC	pyridinium chlorochromate
PCET	proton-coupled electron transfer
PIFA	(bis(trifluoroacetoxy)iodo)benzene
pin	pinacol

PMHS	polymethylhydrosiloxane
ppm	parts per million
ppy	2-phenylpyridine
PT	5,7,12,14-pentacenetetrone
Py	pyridine
qt	quadruplet of triplets
quint	quintuplet
R	generalized alkyl group or substituent
R_f	retention factor
rt	room temperature
s	singlet
SET	single electron transfer
t	triplet
TBAB	Tetrabutylammonium bromide
TBADT	Tetra-*n*-butylammonium decatungstate
TBDPS	*tert*-butyldiphenylsilyl
TBHP	*tert*-butyl hydroperoxide
TBPB	*tert*-butyl peroxybenzoate
TBS	*tert*-butyldimethylsilyl
TCB	trichlorobenzene
td	triplet of doublets
TEMPO	2,2,6,6-tetramethyl-1-piperidinyloxy
TES	triethylsilyl
Tf	triflate
TFA	trifluoroacetic acid
THF	tetrahydrofuran
TIPS	triisopropylsilyl
TLC	thin layer chromatography
TMS	tetramethylsilane
TRIP-SH	2,4,6-triisopropyl benzenethiol
Ts	tosyl (*p*-toluenesulfonyl)

TsOH	*p*-toluenesulfonic acid
W	watts
WMK	Wieland-Miescher ketone
XanthPhos	(9,9-dimethyl-9H-xanthene-4,5-diyl)bis(diphenylphosphane)

1. INTRODUCTION AND OBJECTIVES

1.1. INTRODUCTION

1.1.1. Radical Reactions in Organic Synthesis

In 1900, Moses Gomberg, a professor at the University of Michigan, tried to synthesize hexaphenylethane by reacting triphenylmethyl halides with sodium in benzene when he obtained a mysterious and unstable white crystalline powder. This highly reactive compound oxidized with the oxygen in the air and rapidly reacted with halogens, properties that did not agree with those expected for hexaphenylethane. After trying to study the compound more thoroughly, he concluded that the compound he had isolated had to be a free radical, the triphenylmethyl radical.[1] Gomberg's conclusions were taken with skepticism since the majority of the scientific community was still convinced that carbon must be tetravalent and that a deeper explanation of the existence of free radicals would not come until years later from scientists such as G. N. Lewis, W. Kossel, or I. Langmuir.[2]

Initially, these compounds garnered limited attention as they were perceived as highly reactive intermediates prone to rapid and uncontrolled reactions. However, in the 1980s radical chemistry began to emerge as a highly efficient strategy in organic synthesis[3] becoming a powerful tool for constructing C-C bonds through the addition of carbon-centered radicals to unsaturated bonds.[4]

In contrast to their ionic counterparts, radical reactions operate under mild conditions, exhibit high chemoselectivity, possess wide functional group tolerance, and facilitate the generation of complex structures via tandem reactions.[5] In more recent times, the advent of innovative methodologies for radical generation under environmentally benign conditions, including photochemical[6] and electrochemical techniques,[7] coupled with the fusion of radical chemistry with other areas such as organometallic coupling reactions[8] and organocatalysis,[9] has unlocked a plethora of previously inaccessible transformations. As a result, radical chemistry now occupies a central role at the forefront of synthetic methodology development, driving forward new avenues of exploration in the field and establishing radicals as indispensable elements in contemporary organic synthesis.

1.1.2. Metal-Hydrogen Atom Transfer (MHAT)

A landmark in the field of radical chemistry was the metal-catalyzed generation of radicals from alkenes through hydrogen atom transfer to initiate coupling reactions.[10] In this process, a non-toxic, earth-abundant metal such as cobalt, iron, or manganese,[11] is combined with a suitable hydride source, usually $PhSiH_3$, Et_3SiH, or $NaBH_4$, to generate a putative metal hydride species (*Scheme 1.1*). This metal hydride species undergoes hydrogen atom transfer to the less substituted position of an alkene, generating a carbon-centered radical that is subsequently trapped by an extensive range of electrophiles ($X^{\bullet}$) to give the corresponding addition product with Markovnikov selectivity.[12]

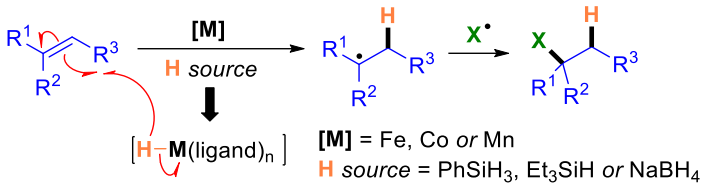

Scheme 1.1. Metal-catalyzed Hydrogen Atom Transfer (MHAT).

These types of reactions have focused the attention of many synthetic chemists in recent years, and this is due, in large part, to the numerous advantages that these procedures present. First, alkenes are very stable pro-radicals, making it possible to carry them through many steps of a synthetic sequence until the desired radical reaction occurs. As a result, MHAT reactions have been employed as the key step in the synthesis of complex natural products.[13] In addition, alkenes are inexpensive common feedstock chemicals, making them ideal starting materials for organic synthesis. Further advantages of MHAT reactions include their high chemoselectivity exhibited for alkenes, making these reactions exhibit a wide functional group tolerance. Furthermore, these reactions often exhibit high site selectivity,[14] making it possible to selectively react with one alkene over another if they have different substitution patterns. Finally, the mild reaction conditions employed make performing these reactions relatively straightforward. The reactions often occur at room temperature, at standard pressure, and without the need to exclude moisture. While the reactions are usually carried out under an inert atmosphere, a number of MHAT reactions perform

better open to the air. The fact that the metal catalysts can often be employed in low quantities and are non-toxic provides a further advantage over many classical radical reactions.

1.1.3. Historical background of MHAT reactions

The first application of an MHAT reaction on a double bond was studied in the 1960s by Kwiatek and Seyler, who managed to hydrogenate different alkenes using a cobalt catalyst.[15] Drago subsequently reported the first selective catalytic oxidation of terminal olefins using cobalt complexes in 1982.[16] However, it was not until 1989, when Mukayama described the catalytic hydration of alkenes using molecular oxygen, phenylsilane, and $Co(acac)_2$,[17] that organic chemists started to take an interest in this type of reaction. Notably, this reaction has been used extensively in many natural product syntheses.[18]

Since then, hydrofunctionalizations of alkenes to form C-O (hydroperoxydation[19] and hydroalkylation[20]), C-N (hydroamination,[21] hydrohydrazination, and hydroazidation,[22] nitrosation[23]), C-S (hydrothiolation[24]), C-X (hydrofluorination,[25] hydrochlorination,[26] hydrobromination, and hydroiodination[27]), C-H (hydrogenation[28]) and C-Se (hydroselenation[29]) bond formation have been developed using MHAT conditions (*Scheme 1.2*).[30]

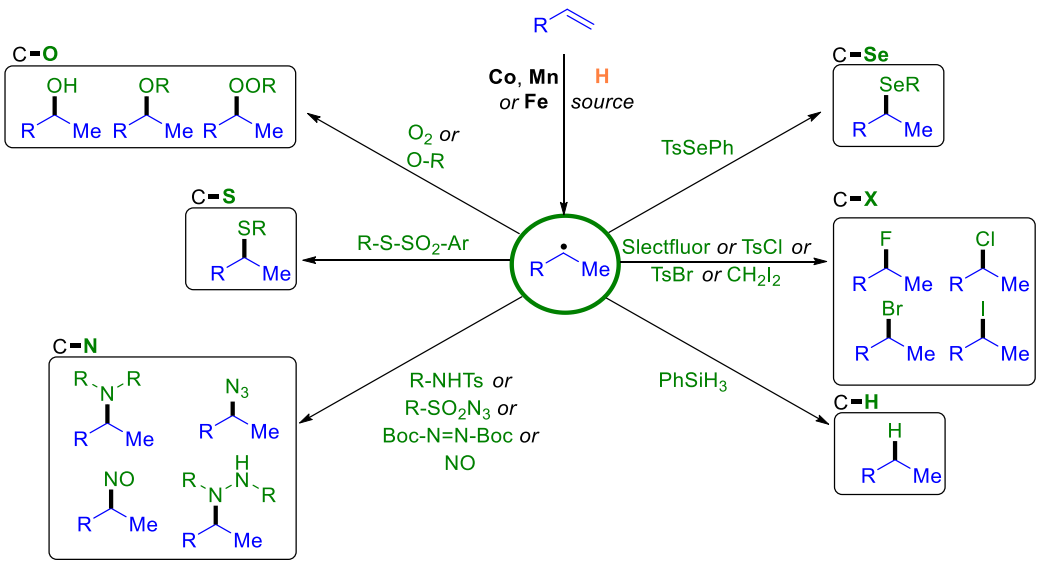

Scheme 1.2. Radical-based alkene hydrofunctionalization enabled by hydrogen atom transfer.

1.1.4. Carbon-Carbon Bond Formation by MHAT Reactions

However, it was not until relatively recently that general C–C bond formation reactions were developed using MHAT conditions. As a result, MHAT reactions have now become a powerful tool in organic synthesis.

As this thesis focuses on developing new MHAT C-C reactions, we will briefly outline all the C-C reactions developed to date, which we have grouped according to the type of radical acceptor used.

Electron-deficient alkenes as acceptors

In 2014, Baran and co-workers reported the first general method for C-C coupling,[31] where the intra- and intermolecular coupling between non-activated alkenes and electron-deficient olefins was described. $Fe(acac)_3$ was used as a metal catalyst, and $PhSiH_3$ was employed as a hydride source to generate structures such as bicyclic systems, cyclopropanes, and vicinal quaternary centers (*Scheme 1.3*).

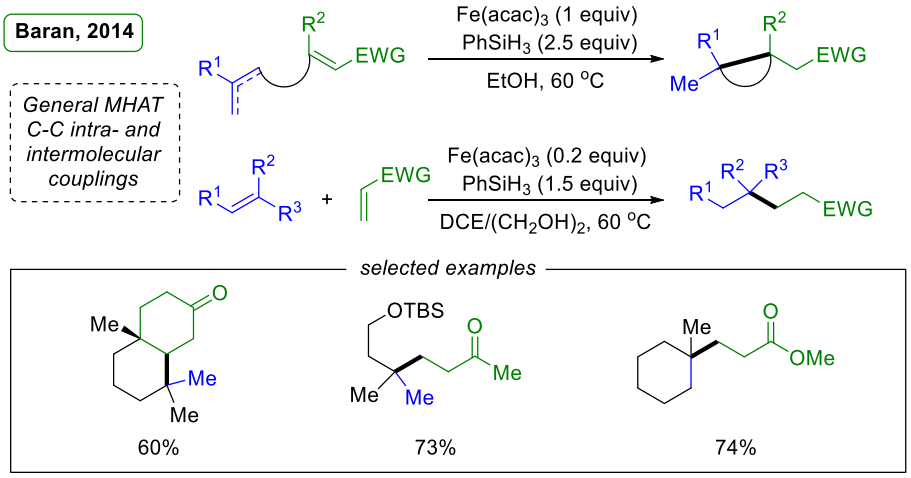

Scheme 1.3. Baran's reductive olefin coupling.

Shortly after, the scope of the reaction was expanded to include alkenes that presented a heteroatom adjacent to the carbon on which the radical is formed (*Scheme 1.4*).[32] This reaction performed better with $Fe(dipm)_3$ as the catalyst instead of $Fe(acac)_3$ and with Na_2HPO_4 as an additive.

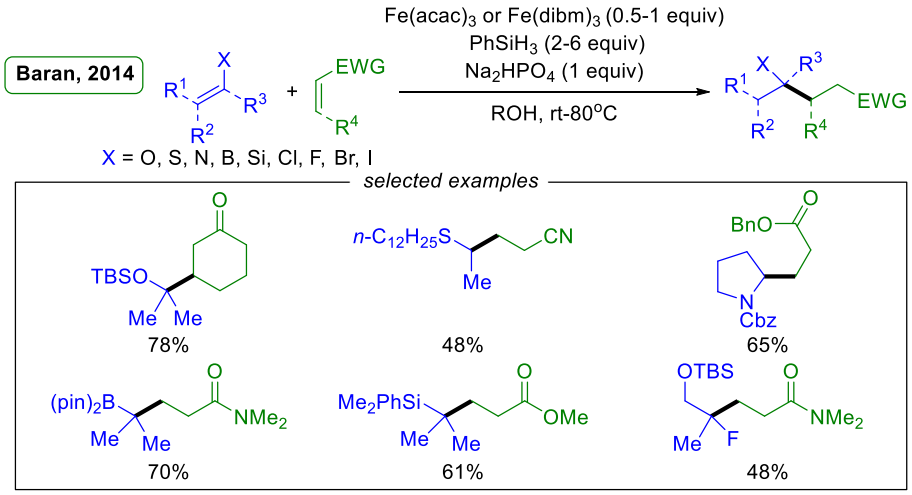

Scheme 1.4. Baran's functionalized olefin cross-coupling.

In 2017, Baran and Holland elucidated the mechanism with experimental evidence.[33] As shown in *Scheme 1.5*, it is a very complex cycle in which both the catalyst and the hydride source evolve into several species to form the metal hydride responsible for the radical attack to the alkene that will give rise to the C-C coupling. It was discovered that a Fe^{II} species formed in a secondary catalytic cycle involving $PhSiH_3$ independent of the substrate. These studies also showed that phenylsilane was converted to a much more reactive substituted ethoxy version in this secondary cycle. It should be noted that by excluding air from the reaction, the conversion of Fe^{II} to Fe^{III} does not occur.

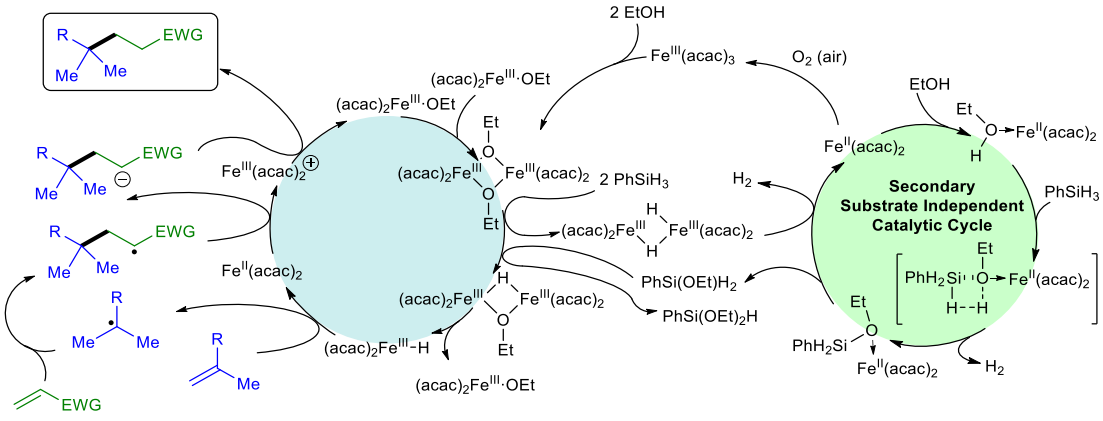

Scheme 1.5. Baran and Holland's mechanistic proposal for the alkene cross-coupling.

Furthermore, Poli and Holland reported an analysis of this MHAT C-C coupling using DFT calculations.[34] They concluded that Fe species decrease the amount of free radicals in solution by forming Fe-C and Fe-O bonds. These results are strongly related to the persistent radical effect (PRE),[35] which prolongs the life of active radical species through the reversible formation of a Fe-C bond; this stabilizes the radicals, decreasing

their concentration in the reaction medium and prolonging their life. Therefore, this PRE effect would help reduce unwanted bimolecular terminations and increase cross-coupling selectivity. The mechanisms for most of the subsequently outlined MHAT reactions are based on this mechanistic proposal; however, a simpler version that omits the secondary catalytic cycle and displays the iron species in its monomeric forms is usually presented. We will not outline the mechanism for all the subsequently described reactions due to space constraints; instead, we refer the reader to the corresponding publication for details.

In 2015, Cui used β-nitroalkenes as the acceptor group.[36] The alkene adds to the β-nitroalkene, generating a benzyl radical. Subsequently, the nitro group is eliminated, regenerating the double bond. This allows access to secondary- and tertiary-alkylated styrene derivatives, although this reaction is limited to aromatic β-nitroalkenes (*Scheme 1.6*).

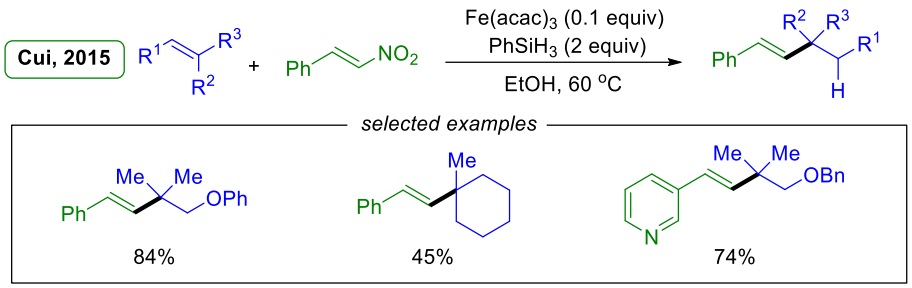

Scheme 1.6. Cui's reductive coupling of unactivated alkenes with β-nitroalkenes.

In 2016, Cui also reported a 1,6-addition of alkenes with *p*-quinone methides,[37] using the formation of the aromatic phenol ring as the driving force (*Scheme 1.7*).

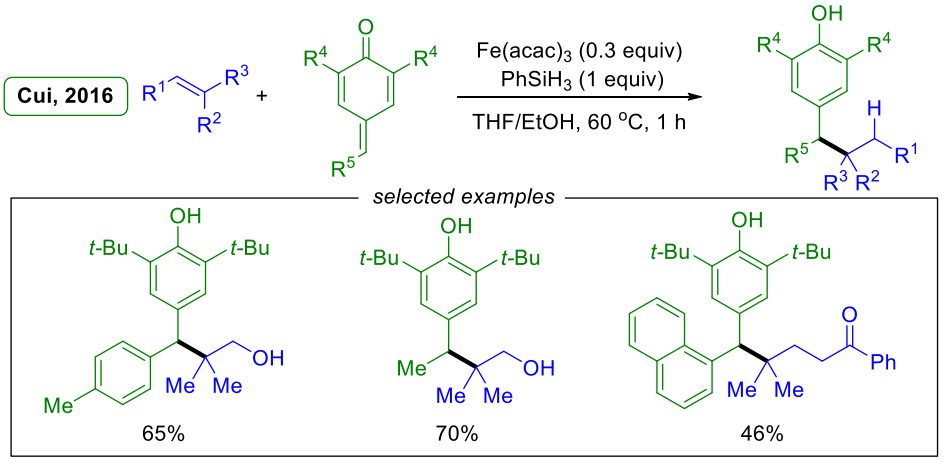

Scheme 1.7. Cui's hydroalkylation of olefins with p-quinone methides.

A few years later, in 2018, Cui continued to expand the range of MHAT reactions to make C-C bonds when he reported an alternative to the Baran reaction, incorporating a leaving group in the α-position of the Michael acceptor.[38] After alkene addition to the Morita-Baylis-Hillman adducts used as substrates in this reaction, the acetate group was eliminated to regenerate the double bond. Various mono-, di-, and trisubstituted alkenes were successfully transformed into cinnamate derivatives (*Scheme 1.8*).

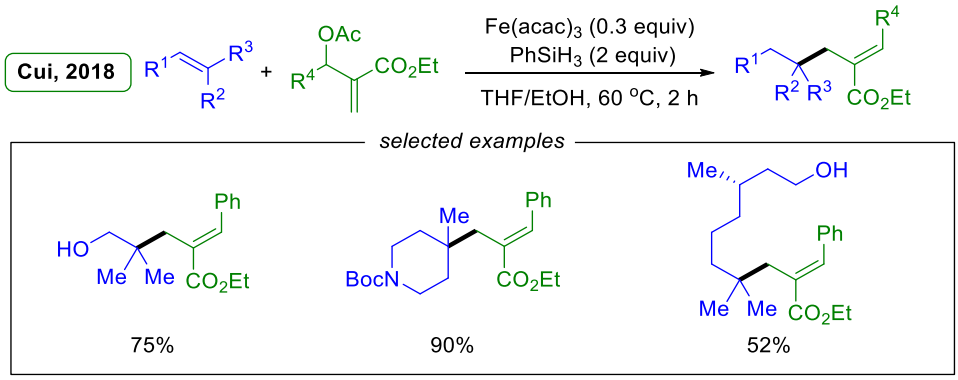

Scheme 1.8. Cui's hydroallylation of unactivated alkenes with Morita-Baylis-Hillman adducts.

The same year, Wang developed an analogous reaction to Cui's β-nitroalkene coupling, replacing the nitro group for two fluorine atoms.[39] In this case, the reaction proceeds like Cui's coupling, eliminating a fluorine atom and regenerating the double bond to give the corresponding substituted fluoroalkenes with excellent *Z*-selectivity under air- and water-tolerant conditions (*Scheme 1.9*). The reaction can also be carried out using mono-fluoroalkenes to provide the corresponding alkyl-substituted alkene.

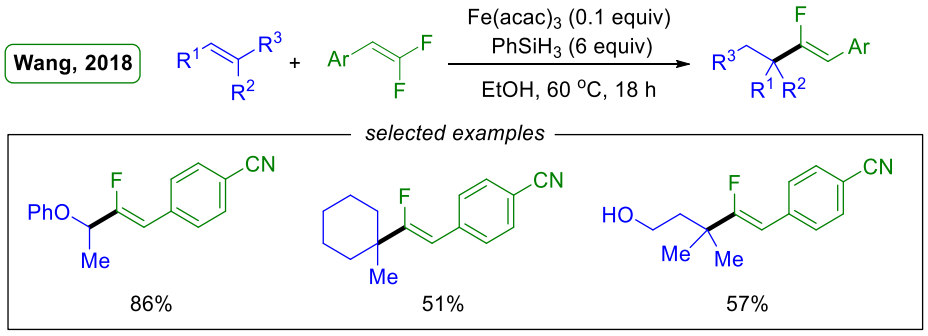

Scheme 1.9. Wang's defluorinative cross-coupling of donor alkenes with gem-difluoroalkenes.

In 2019, Compain and co-workers applied the conditions of the Baran reaction to furans and pyrans to functionalize sugars in their anomeric position via the intermediacy of tertiary pseudoanomeric radicals.[40] In this way, they achieved complete stereocontrol to quaternize the adjacent ether position (*Scheme 1.10*).

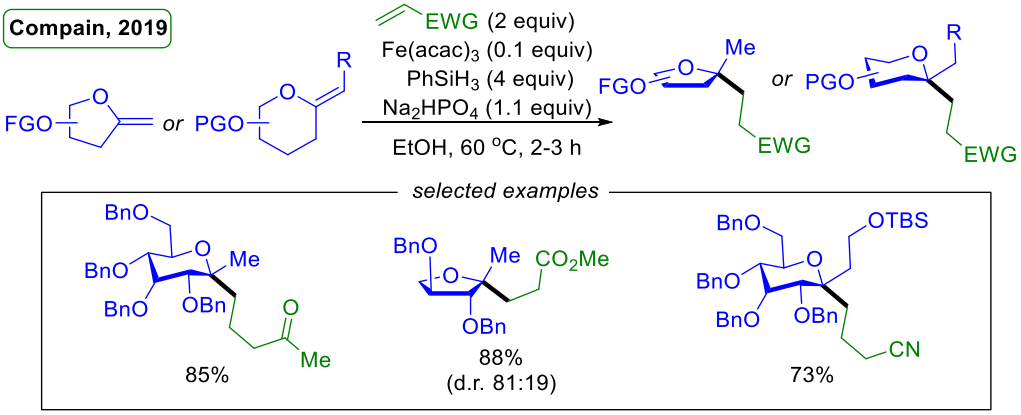

Scheme 1.10. Synthesis of C, C*-glycosides from exo-glycals.*

In parallel, Li developed a reaction analogous to that of Cui with β-nitroalkenes, but in this case, he used nitrodienes (*Scheme 1.11*).[41] It is worth noting the use of $Na_2HPO_4{\cdot}7H_2O$ as an additive, which they determined helped to accelerate the formation of the $PhSi(OEt)H_2$ species responsible for transferring the hydride to the metal catalyst.

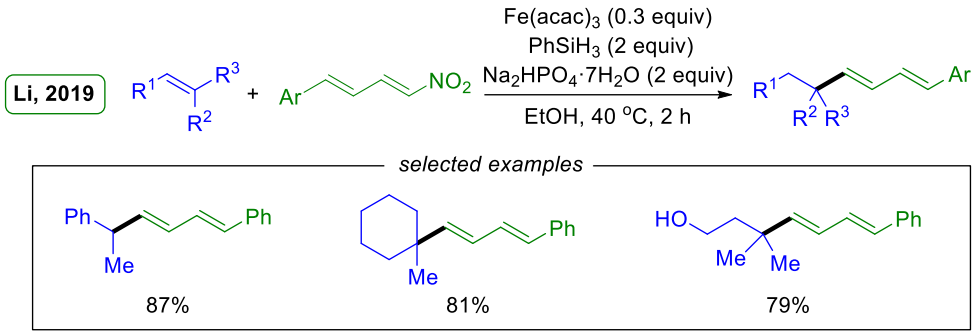

Scheme 1.11. Reductive coupling of nitrodienes with unactivated alkenes.

In the same year, Xu's group reported another variant of the Baran reaction in which unsaturated imines were used as radical acceptors to react with alkenes to give structurally diversified benzofurans, benzothiophene, and benzofuran-fused heterocycles (*Scheme 1.12*).[42]

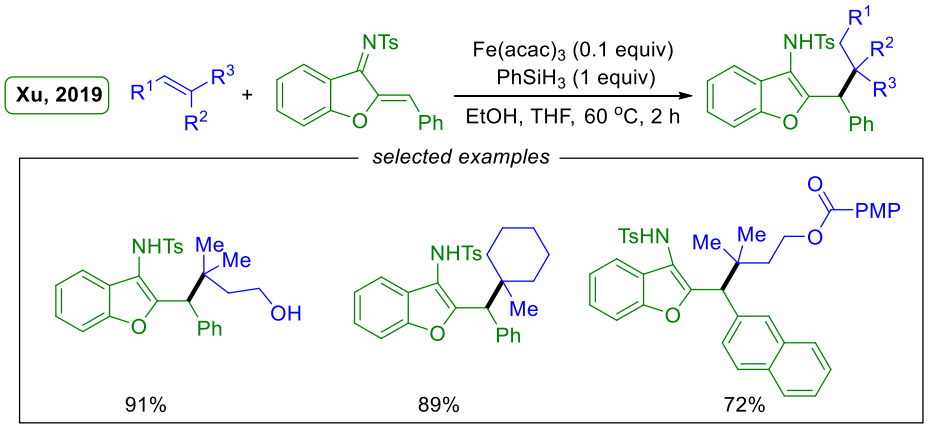

Scheme 1.12. Reductive coupling of alkenes with unsaturated imines.

In 2022, Zhao and co-workers described another variant of the Baran reaction,[43] in which the conjugate addition was carried out between an unactivated alkene with a Michael acceptor with two nitriles as electron-withdrawing groups. This allowed obtaining a wide range of substituted malononitriles (*Scheme 1.13*).

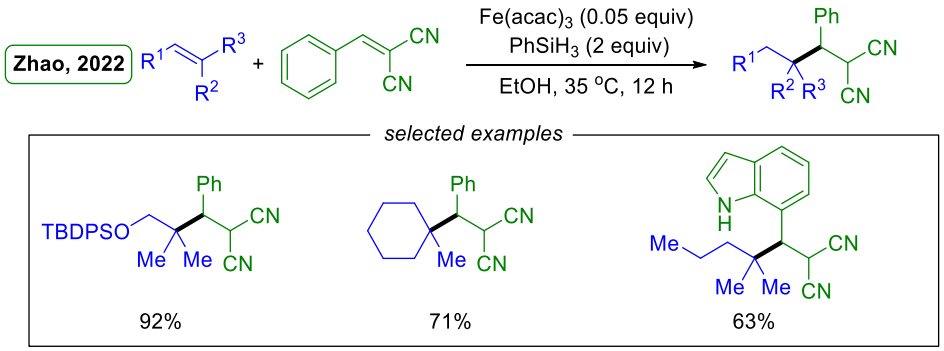

Scheme 1.13. Synthesis of functionalized malonitriles via MHAT.

At the same time, Luo's group used photocatalysis to carry out the Baran reaction using a cobalt catalyst.[44] Notably, during the reaction, the double bond is reformed as the α-hydrogen of the substrate is transferred to the cobalt species at the end of the reaction. This results in the regeneration of the hydride species; therefore, only a catalytic amount of $PhSiH_3$ is needed to start the reaction. It should be noted, however, that the substrates are limited to those that contain an oxygen atom adjacent to where the radical is generated or to 4-membered rings (*Scheme 1.14*).

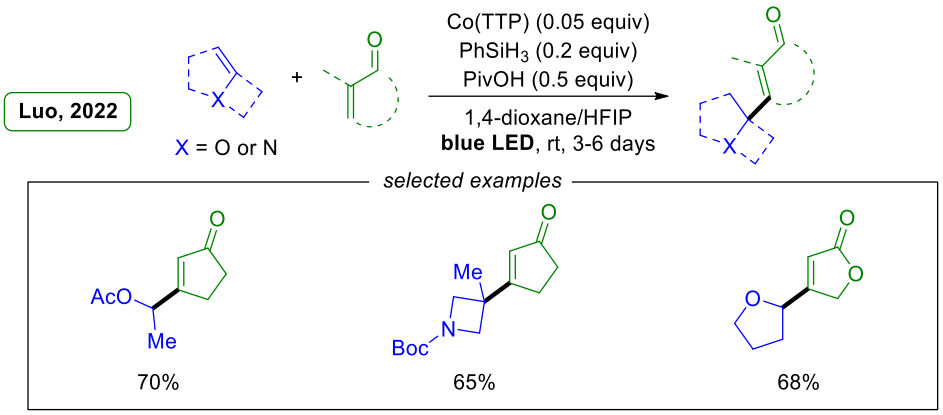

Scheme 1.14. Visible-light promoted olefin couple.

Finally, Studer published another alternative to the Baran reaction, expanding the scope by reacting allylboronic esters with Michael acceptors.[45] Upon addition of the metal hydride to the alkene, a 1,2-boron shift occurs to give the more stable radical intermediate, which the Michael acceptor traps to provide the corresponding borylated compounds (*Scheme 1.15*).

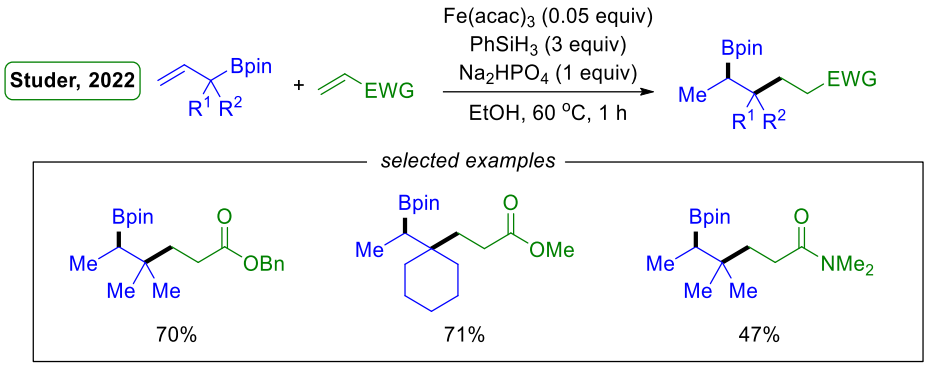

Scheme 1.15. 1,3-Hydroalkylation of allylboronic esters with Michael acceptors.

Electron-neutral alkenes as acceptors

In 2014, parallel to Baran's work using electron-deficient alkenes, Shenvi's group presented one of the first MHAT C-C couplings demonstrating that non-activated alkene radicals would intermolecularly couple with adjacent neutral alkenes.[46] It should be noted that this work was part of a mechanistic study on the formation of radical intermediates to carry out hydrogenations using MHAT and was not developed into a general C-C coupling methodology (*Scheme 1.16*).

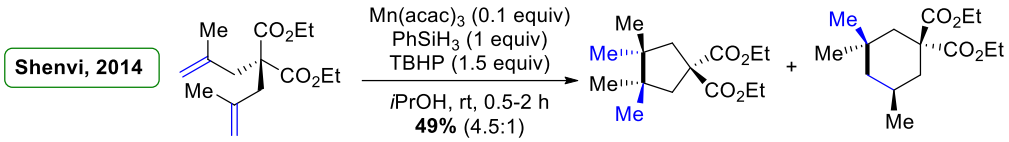

Scheme 1.16. Reductive cyclization of neutral alkenes.

In the same year, Shenvi[47] discovered that if a Cobalt catalyst was used in low amounts, the addition of the radical was found to be reversible, leading to the formation of more substituted alkenes; if the same reaction was carried out in the presence of another tethered alkene, then intramolecular cyclization will occur (*Scheme 1.17*).

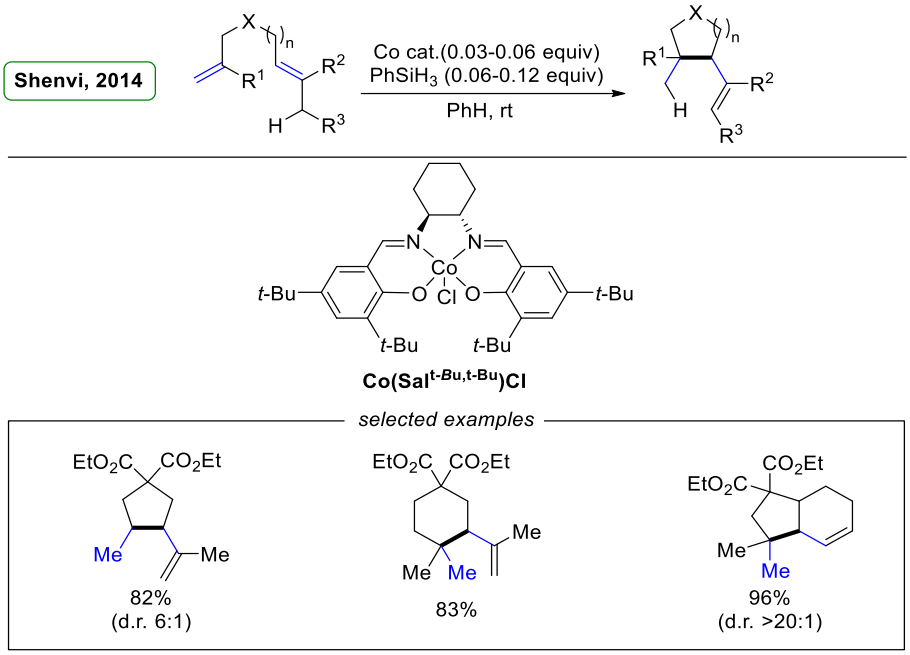

Scheme 1.17. Diene cycloisomerization.

Norton and co-workers reported a variation of this reaction to form furans.[48] Instead of the usual Fe, Co, or Mn catalysts, Norton used $HV(CO)_4$dppe to carry out these 5-*exo* cyclizations and used styrene as the acceptor group (*Scheme 1.18*).

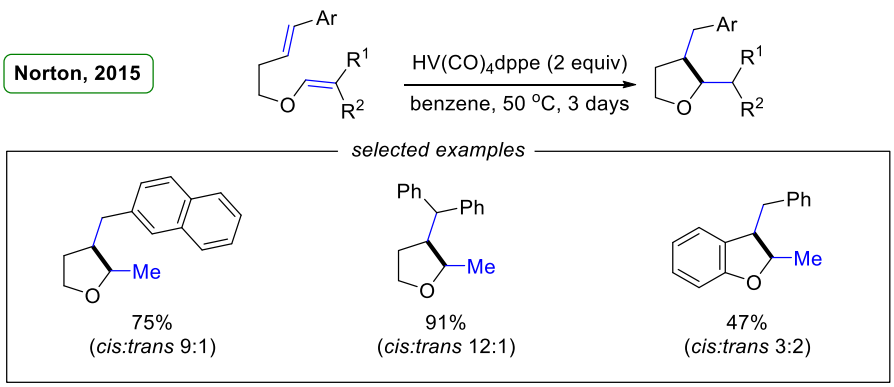

Scheme 1.18. Enol ether cyclization.

Recently, the Baran group used the Shenvi reaction described above in *Scheme 1.17* to demonstrate the potential of electrochemistry in MHAT reactions.[49] The changes compared to Shenvi's reaction are notable since, for example, instead of adding a $PhSiH_3$ as a hydride donor, they use electrochemical means to generate hydride from protons in the medium (*Scheme 1.19*).

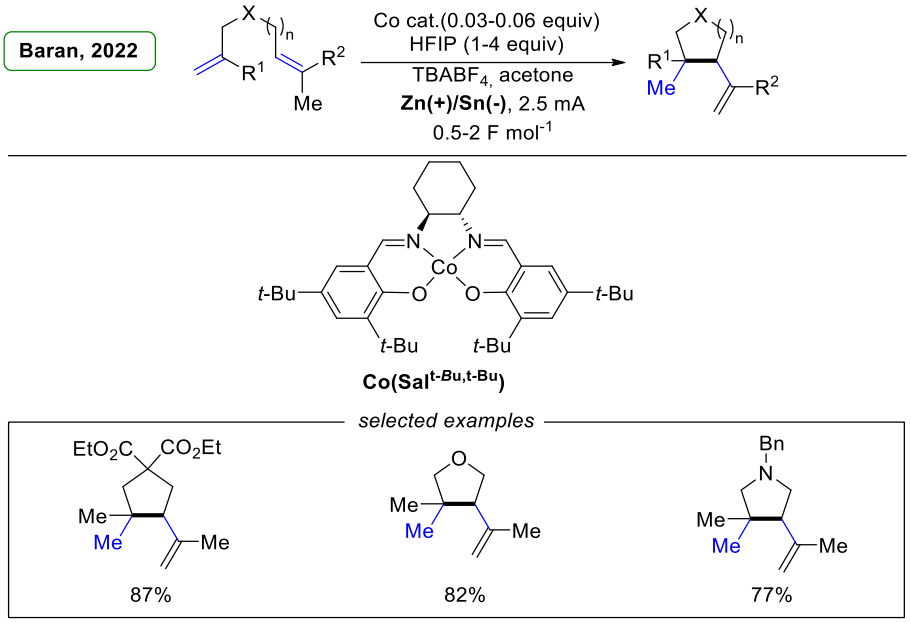

Scheme 1.19. Cobalt-electrocatalytic HAT for functionalization of unsaturated C-C bonds.

Alkynes as acceptors

In 2017, the Cui group developed a Fe^{III}-promoted hydroalkynylation of unactivated alkenes toward Csp−Csp^3 bond formation (*Scheme 1.20*). They showed that mono-, di-, and trisubstituted alkenes could be coupled with various substituted aromatic and heterocyclic alkynyl bromides. [50]

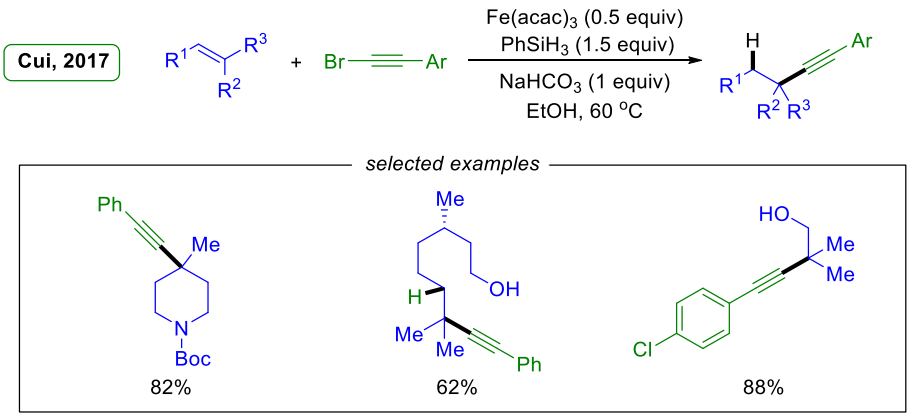

Scheme 1.20. Hydroalkynylation of unactivated alkenes.

Interestingly, in the work above, the triple bond remains inert in the HAT reaction medium once the desired product is formed. In contrast, in 2019, Wang and co-workers showed that 1,6-enynes could be reacted via an intramolecular cyclization to form heterocycles,[51] such as 3-acylbenzofurans and thiophenes (*Scheme 1.21*). The radical generated from hydrogen transfer to the alkene with the metal hydride species added intramolecularly to the triple bond, forming the 5-membered ring with the formation of an alkenyl radical. This, in turn, was oxidized by the oxygen present in the medium to give the product.

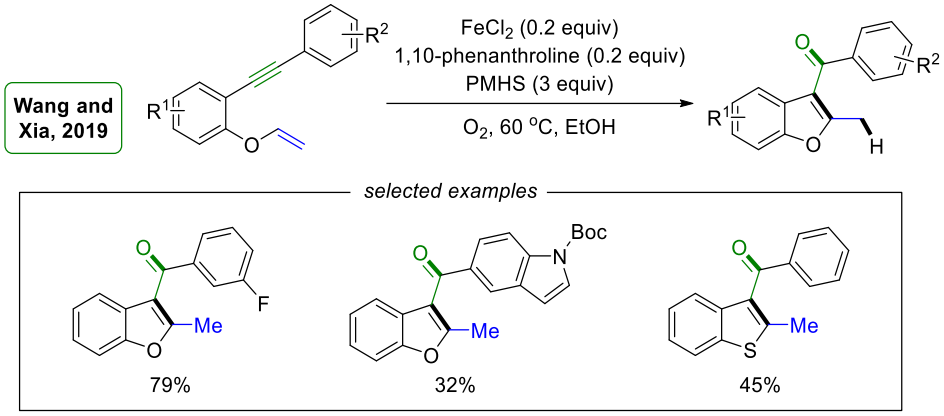

Scheme 1.21. Reductive cyclization of 1,6-enynes for the synthesis of 3-acylbenzofurans and thiophenes.

Two years later, the same group increased the scope of this reaction when they captured the formed vinyl radical after cyclization with NO instead of oxygen. Once the radical was trapped, it tautomerized to give access to ketoximes (*Scheme 1.22*).[52] Notably, this strategy could also be applied to synthesizing pyrrolo[3,2-*d*]isoxazoles with a quaternary stereocenter in a two-step transformation.

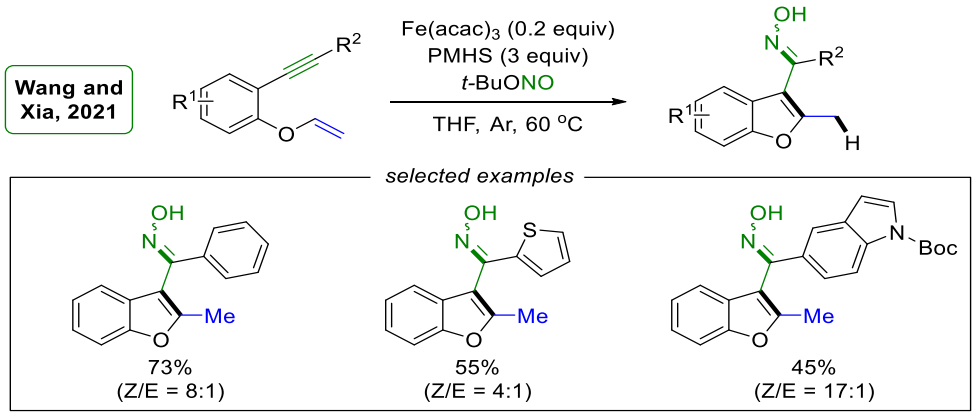

Scheme 1.22. Cyclization of 1,6-enynes for the synthesis of ketoximes.

Finally, in 2022, Shi's group reported the coupling of alkynes with alkenes analogously to that described by Cui. However, they used acetylenic sulfones instead of starting from alkynyl halides (*Scheme 1.23*).[53]

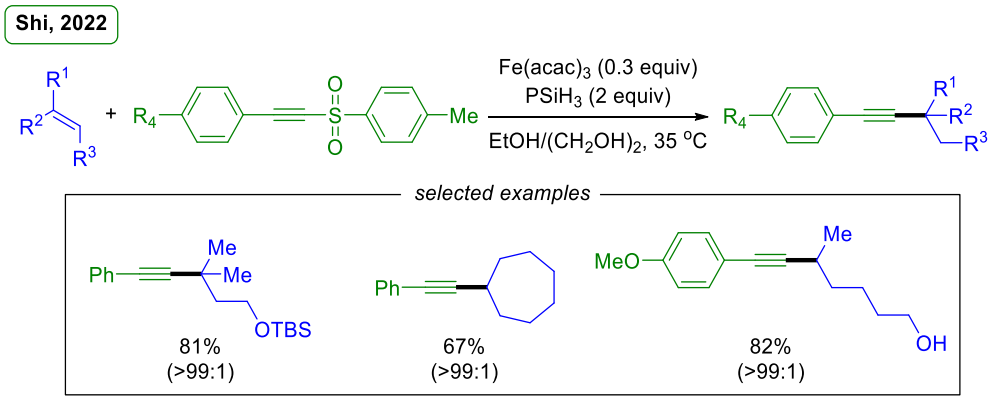

Scheme 1.23. Alkynylation of alkenes using sulfones.

Carbonyls as acceptors

In 2018, our group reported the first use of carbonyls as acceptors in MHAT reactions.[54] The use of catalytic amounts of $Fe(acac)_3$ with $PhSiH_3$ as a hydride source and using ethanol as a solvent at 60 °C allowed the intramolecular cyclization of different keto-alkenes for the synthesis of bi- and tricyclic compounds (*Scheme 1.24*). Notably, this reaction is generally unfavorable due to the instability of the alkoxy radical, which favors the reverse reaction. However, under the reaction conditions, excellent yields of the alcohol were achieved in many cases. Later, our group applied this methodology to synthesize natural products containing the skeleton of trans-fused hydrindanols structurally related to botrydial compounds.[55]

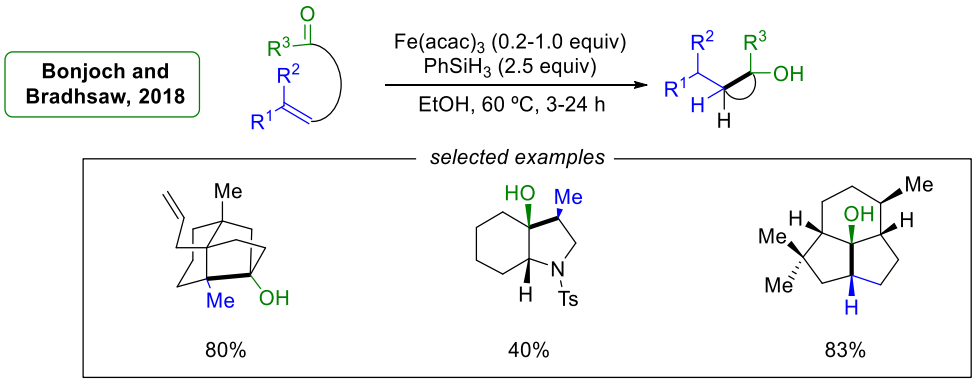

Scheme 1.24. HAT-triggered cyclization of alkenes onto ketones.

Subsequently, the Shenvi group tried to develop the intermolecular version of our reaction using aldehydes as acceptor groups.[56] However, they found that the unfavorable nature of the reaction only allowed the coupling to occur in low yields. They overcame this setback by transmetalation of the cobalt alkyl derivative to the chromium compound with $CrCl_3$. This allowed them to conduct a Nozaki–Hiyama–Kishi reaction type coupling to form the corresponding alcohol. In this way, they avoided the formation of unstable alkoxy radicals (*Scheme 1.25*).

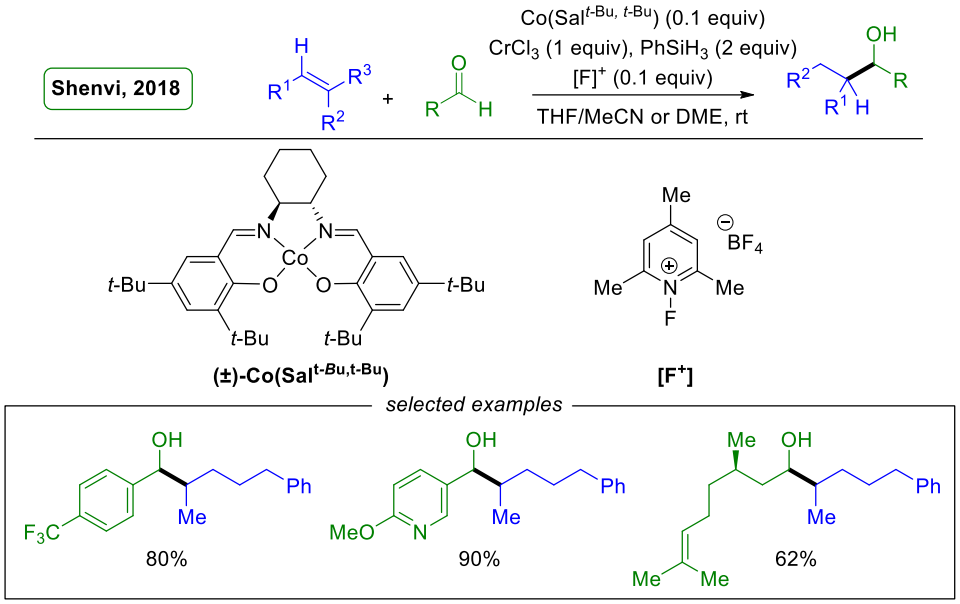

Scheme 1.25. Addition of unactivated olefins into aldehydes.

At the same time Shenvi group was developing the intermolecular version of our reported intramolecular alkene-carbonyl coupling, our group was also trying to develop the intermolecular version.[57] As the Shenvi group had found, we also obtained low yields of the coupled product. It was known from analyzing the reaction mechanism that the unstable alkoxy radical was reduced to an alkoxide by a Fe^{II} species (formed after initial atom transfer) to regenerate Fe^{III} and complete the catalytic cycle. We, therefore, proposed that adding extra Fe^{II} may facilitate the reaction by trapping the unstable alkoxy radical. Indeed, by using a combination of Fe^{III}/Fe^{II}, good yields of the coupled products could be formed (*Scheme 1.26*).

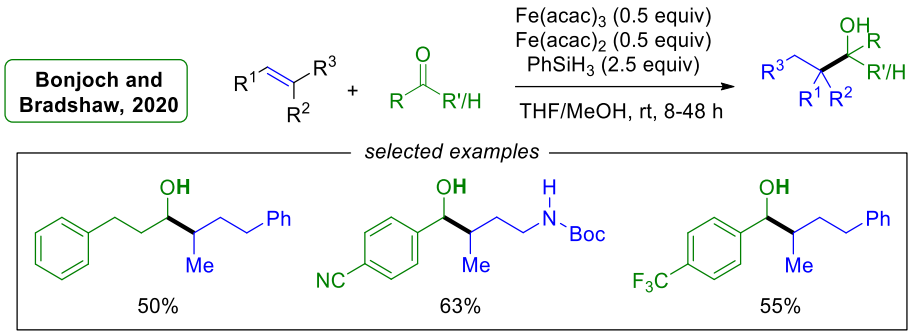

Scheme 1.26. Intermolecular addition of alkenes to aldehydes.

Furthermore, applying these new conditions to previously developed intramolecular alkene coupling to ketones resulted in significantly improved yields (*Scheme 1.27*).

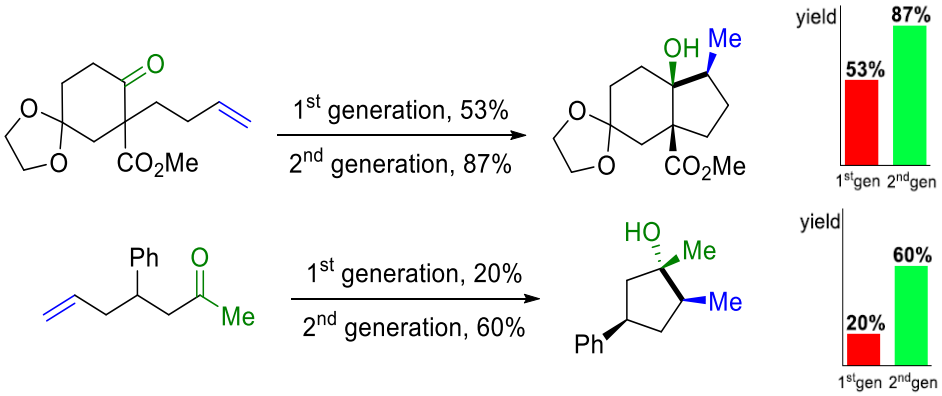

Scheme 1.27. Improved conditions for the intramolecular coupling.

Zhu's group also reported using carbonyls as acceptors; in this case, they overcame the unfavorable formation of the alkoxy radical by using acylsilanes to obtain a silyl enol ether.[58] The formed alkoxy radical immediately underwent a [1,2]-radical Brook rearrangement (RBR), trapping the radical and regenerating the double bond with the help of iodine as an oxidant. (*Scheme 1.28*).

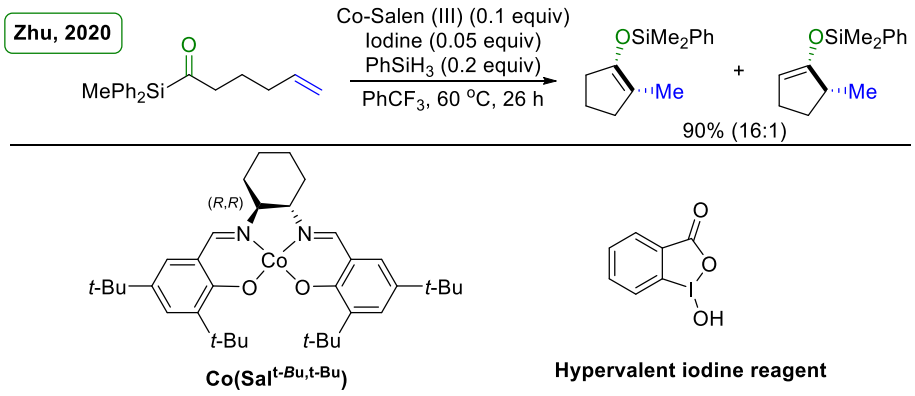

Scheme 1.28. Cyclization of unsaturated silanes.

The reaction was also tested in the presence of a Michael acceptor, and the α-siloxy radical could be trapped to form the corresponding substituted acylsilanes (*Scheme 1.29*).

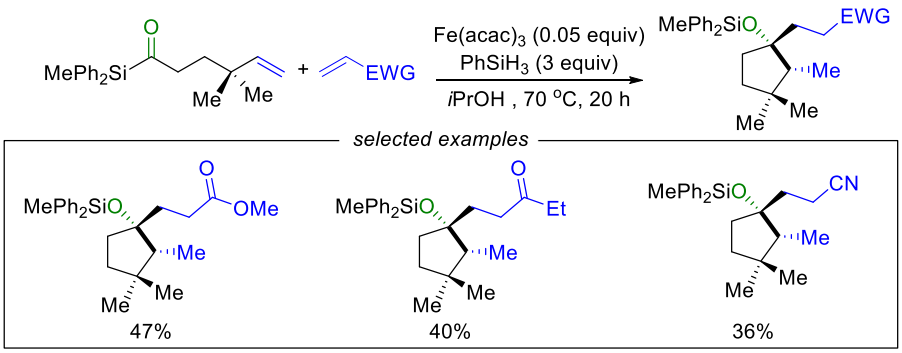

Scheme 1.29. Cyclization of unsaturated silanes followed by trapping.

Li's group has reported using acylphosphonates as acceptors[59] in MHAT reactions. Once the alkoxy radical was formed, a β-cleavage reaction removed the phosphoryl group to obtain the corresponding acylation product (*Scheme 1.30*).

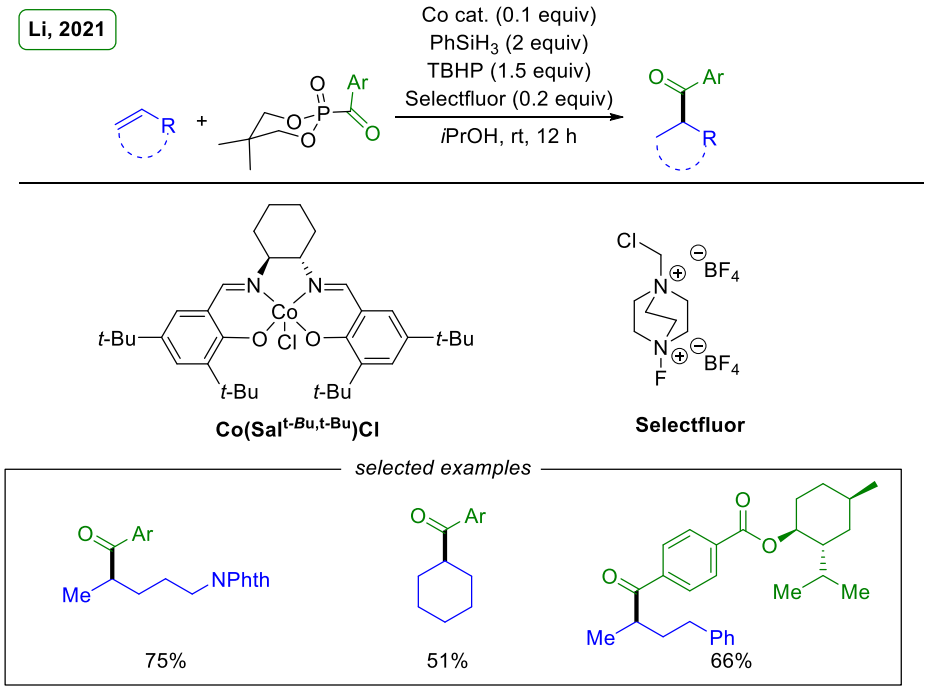

Scheme 1.30. Hydroacylation of unactivated alkenes.

Although our group developed the intermolecular coupling of unactivated alkenes with aldehydes under MHAT conditions, the analogous reaction with ketones remained unresolved. Recently, the Teskey group[60] showed that dienes could be coupled with diarylcarbonyls under photochemical conditions. The ketone forms a persistent ketyl-radical, which undergoes a radical-radical coupling with the radical generated from the diene under the MHAT conditions. This avoids the formation of the alkoxy radical, allowing the desired intermolecular coupling to take place in good yields (*Scheme 1.31*).

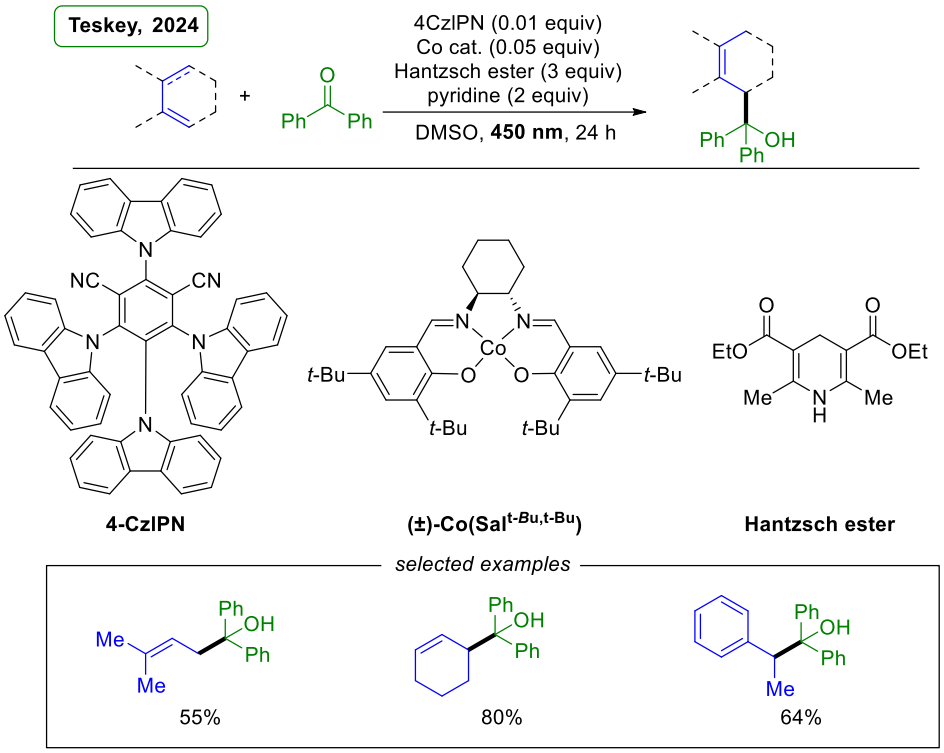

Scheme 1.31. Reductive MHAT coupling of dienes and ketones.

This same year, Shi and co-workers[61] also developed an intermolecular coupling of aldehydes with allenes and conjugated dienes. The use of a titanium catalyst is key to stabilizing the unstable alkoxy radical intermediate, allowing the allylation and radical crotylation of aldehydes by photoredox and titanium dual catalysis (*Scheme 1.32*). Notably, they do not use a conventional hydride source but instead, form the metal hydride Co-H from the protonation of Co^{I} formed during the catalytic cycle.

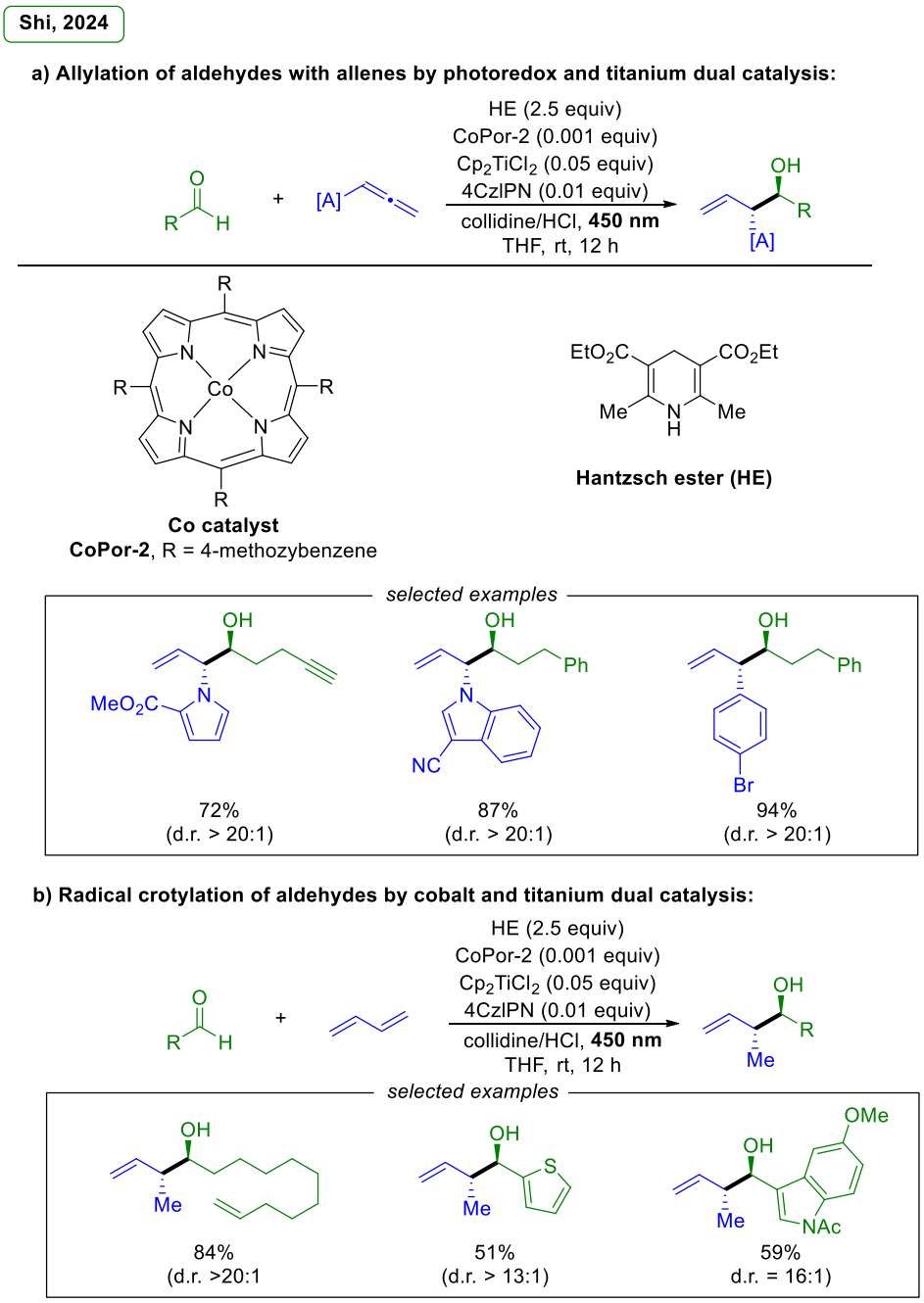

Scheme 1.32. Radical allylation and crotylation of aldehydes by cobalt and titanium dual catalysis.

Heterocycles as acceptors

In 2016, the Herzon group[62] showed that MHAT conditions could be applied to the Minisci reaction using pyridine salts as radical acceptors to carry out a hydropyridylation reaction of unactivated alkenes with high site-selectivity for the construction of tertiary and quaternary centers (*Scheme 1.33*).

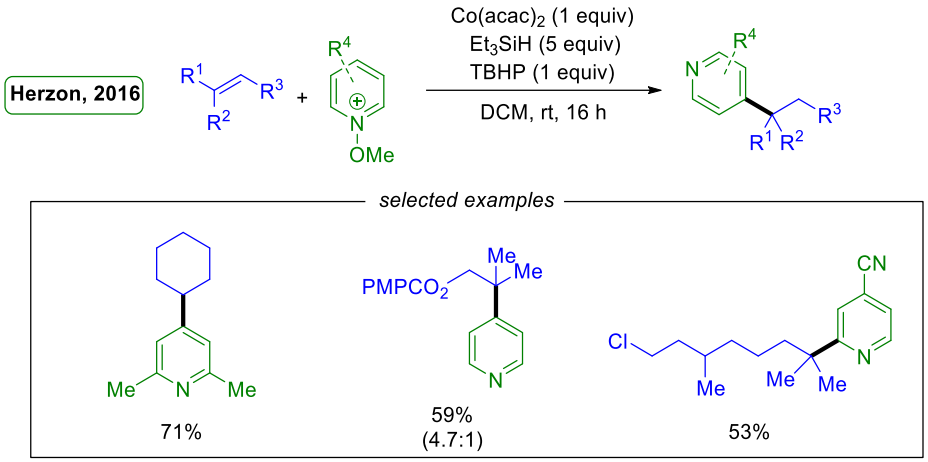

Scheme 1.33. Intermolecular hydropyridylation of unactivated alkenes.

Later, Starr[63] developed an intramolecular version of this reaction and showed that starting from pre-formed pyridine salts was unnecessary. Instead, *in situ* protonation was used to activate the heterocycle. This methodology allowed the construction of dihydropyrano-pyridine and 1,2,3,4-tetrahydronaphthyridine type scaffolds (*Scheme 1.34*).

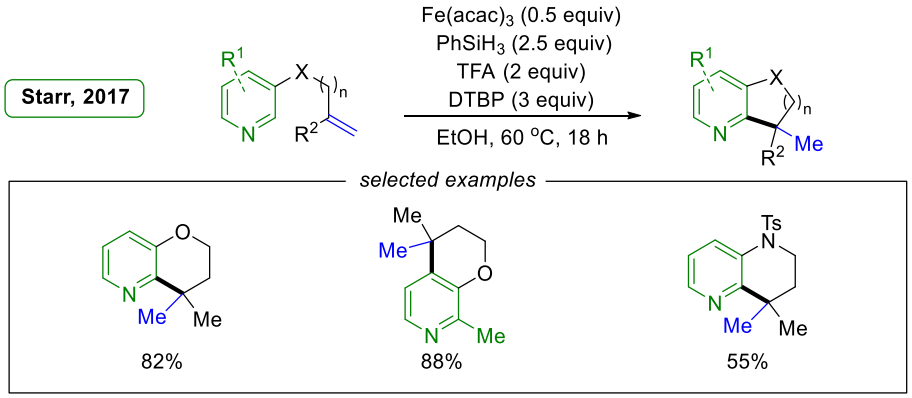

Scheme 1.34. Intramolecular hydropyridylation of olefins.

In 2017, Baran and co-workers developed another version of the intermolecular Minisci reaction,[64] using conditions similar to those developed by Starr but changing the acid from TFA to $BF_3{\cdot}OEt_2$. No co-oxidant was used, requiring stoichiometric quantities of the iron catalyst to be employed. In this same work, they described the use of *N*-oxides to carry out a selective alkylation on C-2 of the corresponding heterocycle, thus solving the site-selectivity problems that these Minisci-type reactions can present (*Scheme 1.35*).

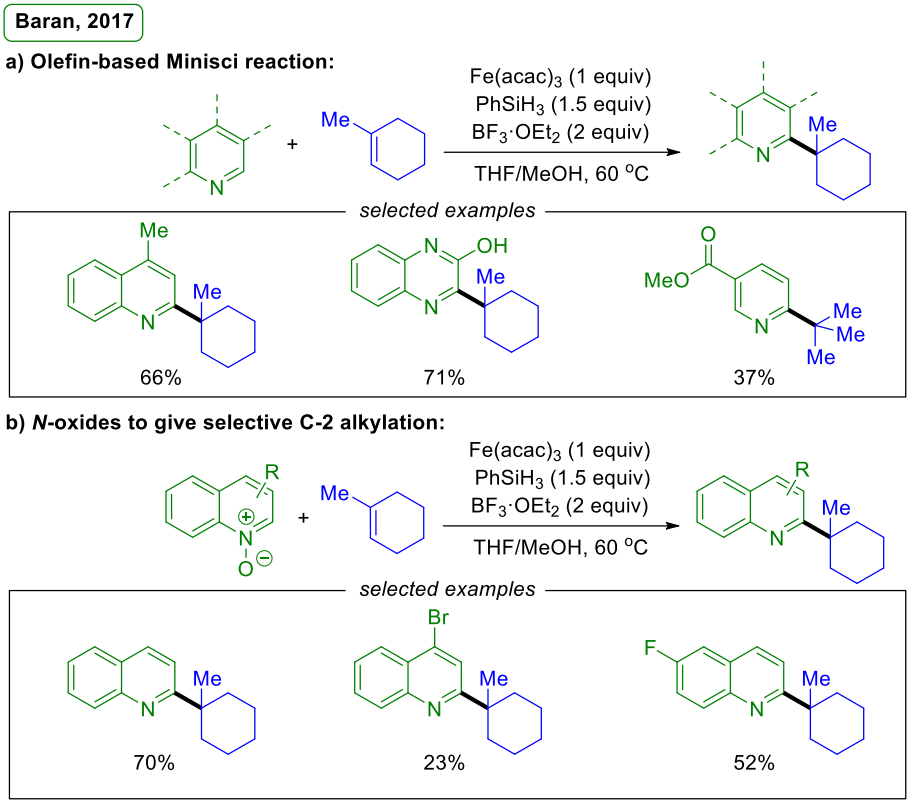

Scheme 1.35. Olefin-based Minisci reaction functionalizes heterocycles and their N-oxides.

In 2023, Teskey used the same principles developed for his photocatalyzed intermolecular ketone coupling (see *Scheme 1.31*), showing that phosphopyridines could also act as persistent radicals.[65] Dienes and pyridyl phosphonium salts were coupled in the presence of a cobalt catalyst via a radical-radical coupling. The reaction presented selectivity for the C-4 position of the pyridine substrates (*Scheme 1.36*).

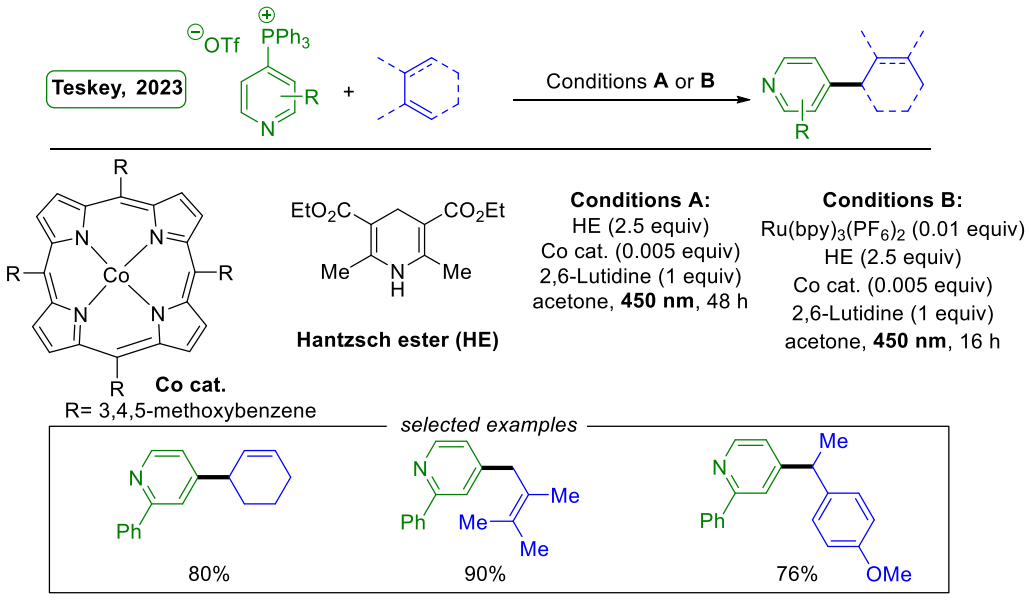

Scheme 1.36. Reductive coupling of pyridines and dienes.

Shortly after, Shi's group published[61] the same reaction as Teskey to couple phosphopyridine salts with conjugated dienes (*Scheme 1.37*) but using a titanium co-catalyst based on their work previously discussed in the carbonyls section (*Scheme 1.32*).

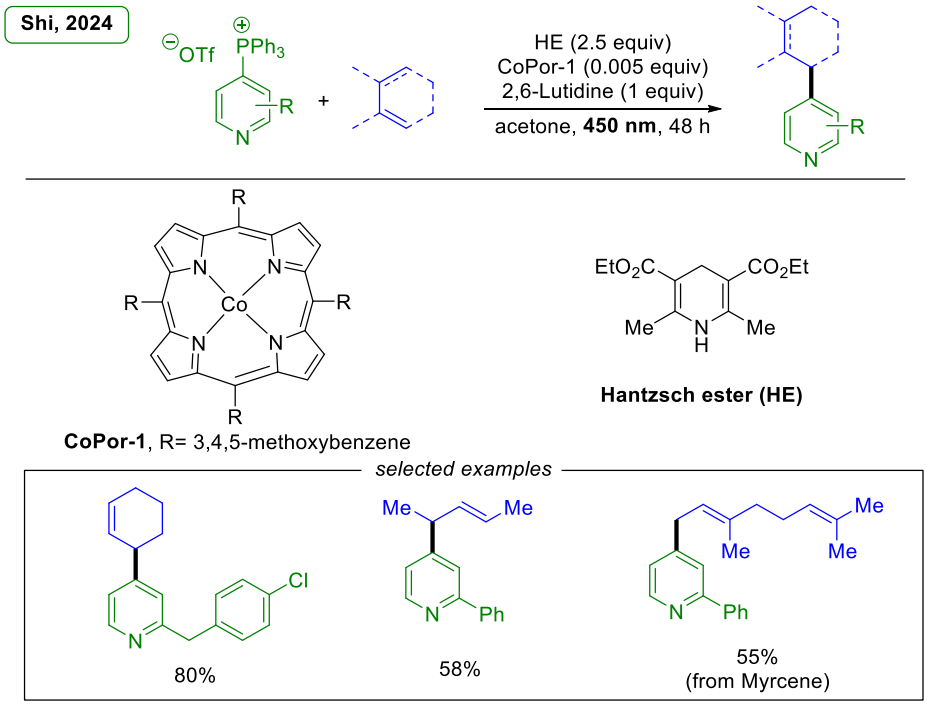

Scheme 1.37. Photoinduced cobalt catalyzed reductive coupling of pyridines and dienes.

Finally, Narang's group has recently reported using alkenyl indoles and pyrroles to carry out an intramolecular cyclization that allows the generation of the corresponding fused derivatives (*Scheme 1.38*). Notably, these protocols could be applied for the formal synthesis of bruceolline J and the total synthesis of bruceolline E and H.[66]

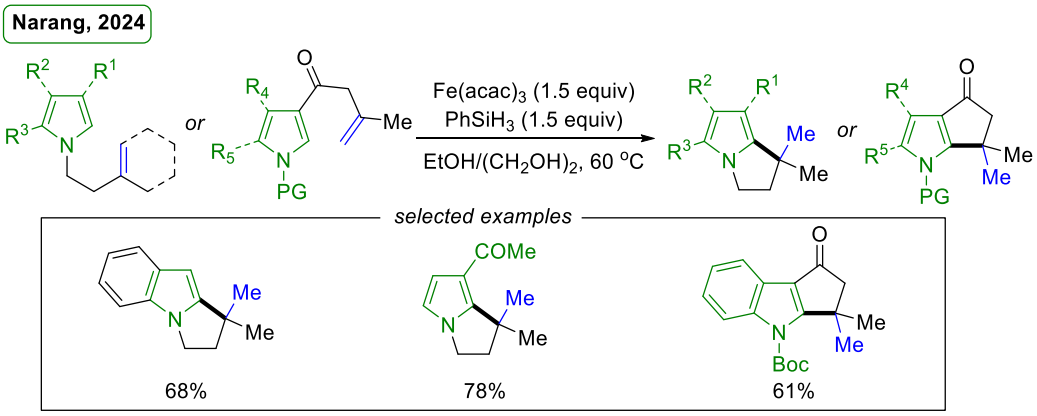

Scheme 1.38. Radical cyclization of alkenyl indoles and pyrroles to give their fused derivatives.

Aromatic rings as acceptors

Shenvi's group reported the first olefin hydroarylation using MHAT to couple alkenes with iodoarenes by joining the MHAT catalytic cycle with the Ni catalytic cycle (*Scheme 1.39*).[67] The nickel forms an aryl nickel complex that the Co-alkene species intercepts to carry out the desired coupling.

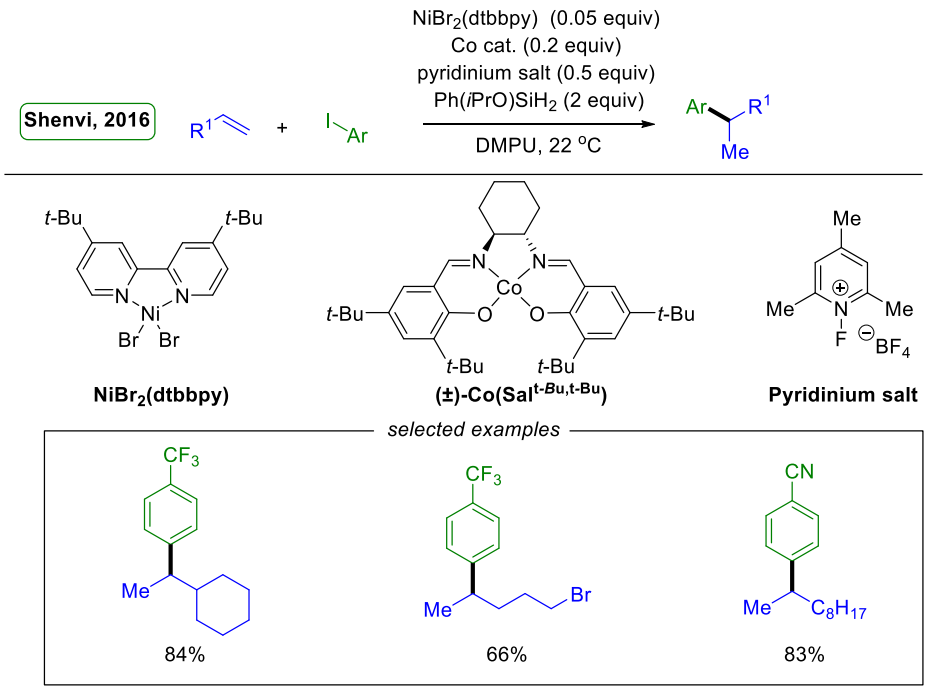

Scheme 1.39. Iodoarene-olefin cross-coupling.

The same year, Shenvi reported a method to generate 8-arylmenthol-type scaffolds from arylsulfonated isopulegol derivatives.[68] The radical derived from the alkene via MHAT couples to the aromatic ring; the substrate then undergoes a Smiles-Truce radical rearrangement, and SO_2 is released to form the alcohol (*Scheme 1.40*).

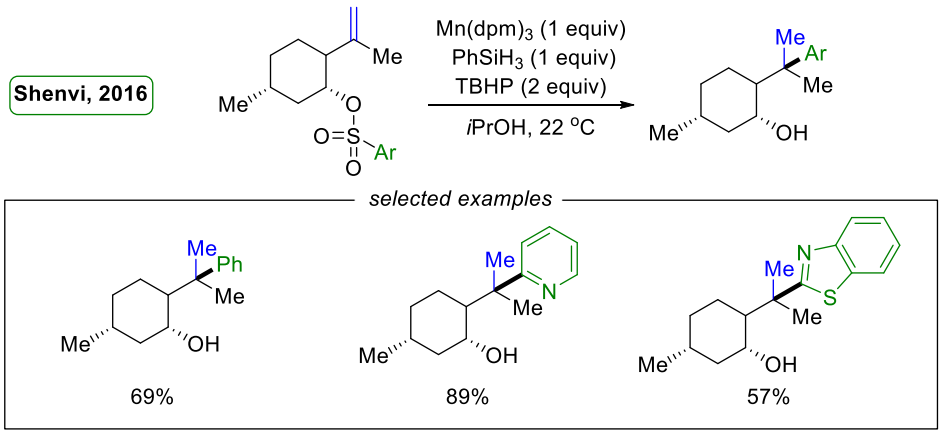

Scheme 1.40. Radical arylation of isopulegol.

At the same time, Hiroya published the intramolecular hydroarylation of unactivated olefins using a cobalt catalyst, disiloxane reagent as a hydride source, and an *N*-fluoro pyridinium salt that helped to form the active catalyst species.[69] With these conditions, it was possible to synthesize six-membered benzocyclic compounds from mono-, 1,1-, *trans*-1,2-di-, and trisubstituted olefins (*Scheme 1.41*).

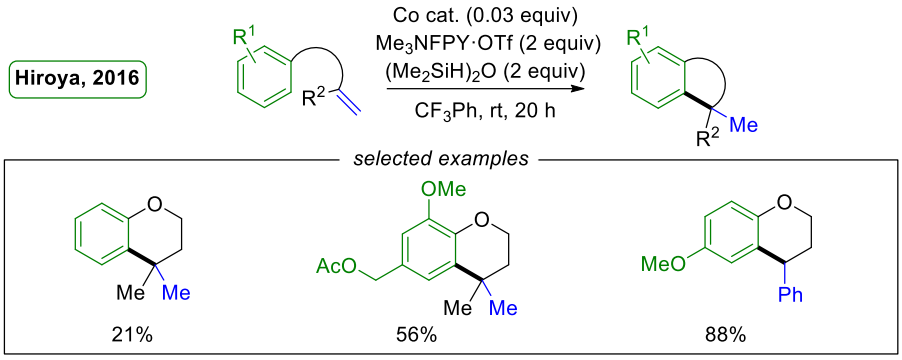

Scheme 1.41. Hydroarylation of unactivated olefins.

Later, Gao and co-workers applied a MHAT hydroarylation reaction using a cobalt catalyst and phenylsilane to synthesize natural products.[70] Specifically, they used this reaction to carry out the C-ring formation of the natural products viridin and viridiol (*Scheme 1.42*).

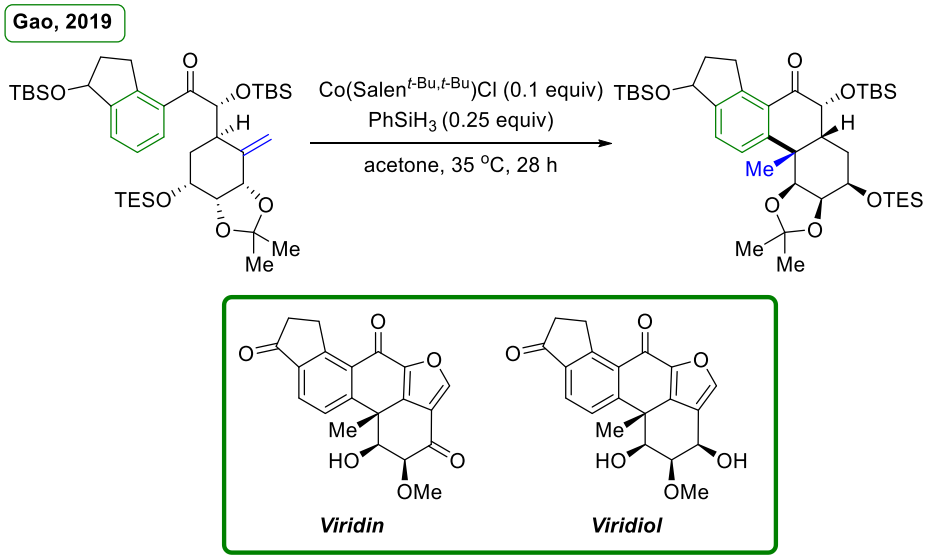

Scheme 1.42. Gao's total synthesis of Viridin and Viridiol.

Cyanides as acceptors

In 2007, the Carreira group introduced cyanides as a new group in the MHAT toolbox.[71] In this work, he documented the hydrocyanation of non-activated alkenes to give

access to secondary and tertiary nitriles, using TsCN as a cyanating agent, a cobalt catalyst, phenylsilane as a hydride source, and TBHP as an oxidant (*Scheme 1.43*).

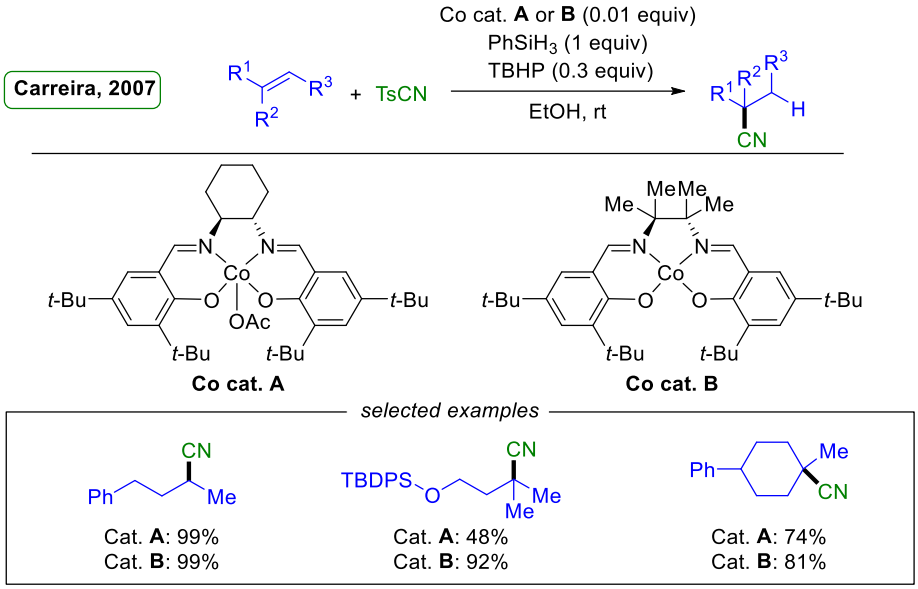

Scheme 1.43. Carreira's hydrocyanation of olefins with tosyl cyanide.

A few years later, in 2018, Ma and co-workers used an MHAT reaction to carry out an intramolecular reductive cyclization reaction between an alkene and a nitrile as a key step to synthesize the natural product navirine C (*Scheme 1.44*). [72] While this was the first reported use of a cyano group in a reductive MHAT coupling reaction, the authors did not develop this work into a general methodological procedure.

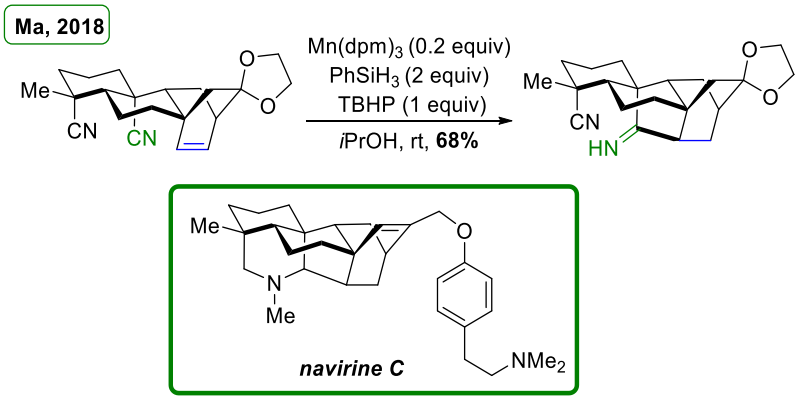

Scheme 1.44. Key cyclization reaction in the total synthesis of navirine C.

However, in the same year, Murphy described the intramolecular cyclization between alkenes and nitriles[73] using $Fe(acac)_3$ and $PhSiH_3$ and carried out a complete methodological study of the reaction (*Scheme 1.45*). Upon completion of the coupling, treatment of the imine intermediate with acid allowed access to the corresponding

ketone. The scope of the reaction is noteworthy, as they manage to form sterically hindered ketones, fused cyclic systems, and spirocycles.

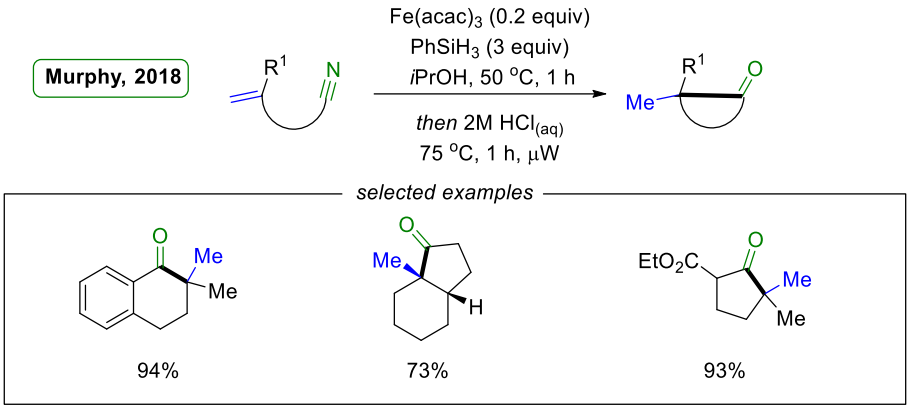

Scheme 1.45. Murphy's cyclization of nitriles.

Two years later, the same group would again use cyanides, in this case, to carry out an intramolecular cyclization of *N*-cyanamide alkenes (*Scheme 1.46*). In this domino-type cyclization, oxygen in the medium is key to carrying out an oxidation step and converting to the desired quinazolinone over the mono-cyclized intermediate.[74]

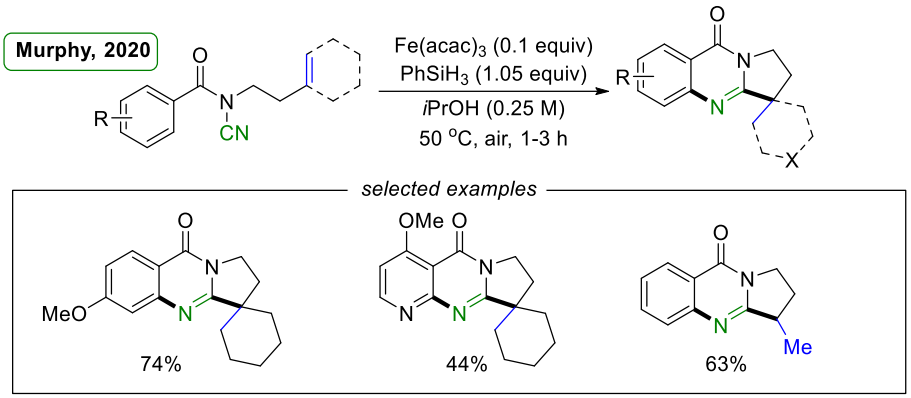

Scheme 1.46. MHAT cyclization to access (spiro)quinazolinones.

Lin's group later described the enantioselective version of Carreira's work combining a cobalt-mediated HAT with copper-promoted radical cyanation using a chiral ligand under electrochemical reaction conditions.[75] These conditions allowed them to obtain the hydrocyanation of alkenes with good yields and excellent enantiomeric excess (*Scheme 1.47*).

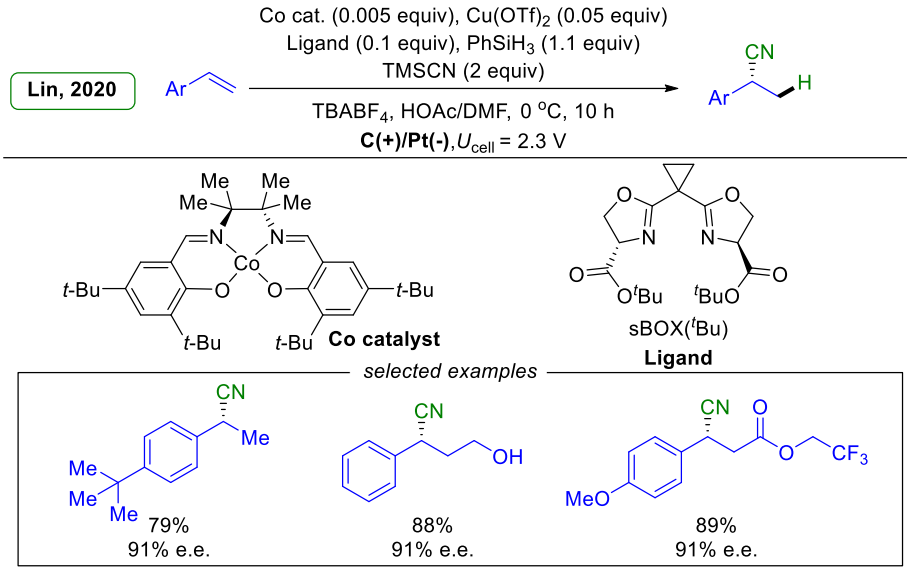

Scheme 1.47. Enantioselective hydrocyanation of conjugated alkenes.

Imines as acceptors

In 2009, Carreira reported the first example of using imines as a radical acceptor group in MHAT reactions[76], using phenyl sulfonyl oximes to introduce *o*-benzyloximes or oxymonitriles with a cobalt catalyst and $PhSiH_3$. In an additional step, the prepared compounds could be transformed into the corresponding aldehydes and amidoximes (*Scheme 1.48*).

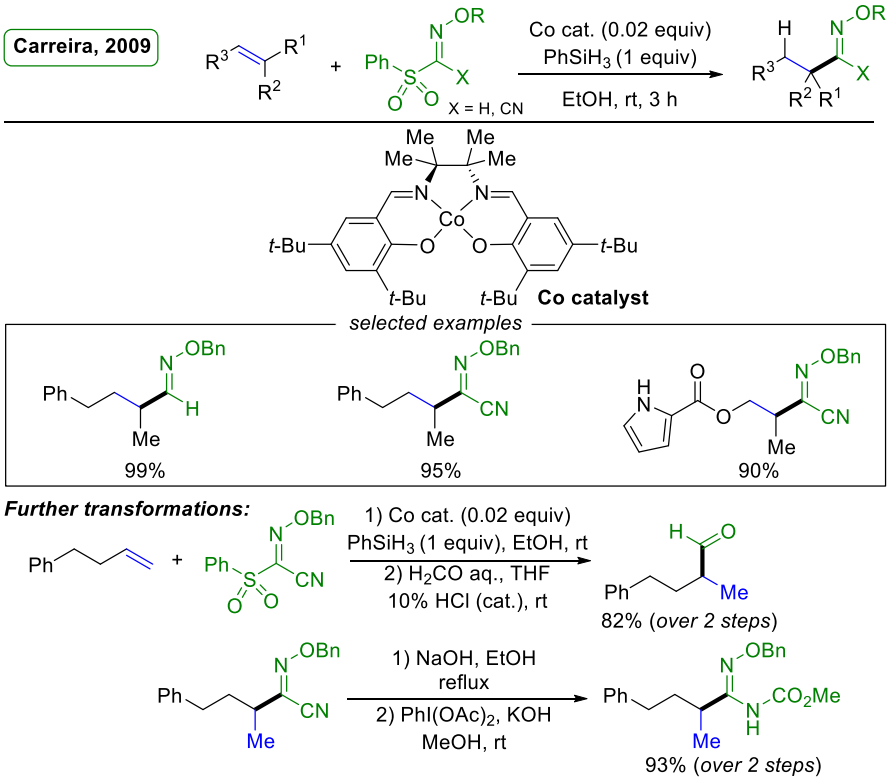

Scheme 1.48. Carreira's functionalization of olefins.

In 2015, Baran's group reported a hydromethylation consisting of adding the tosylhydrazone formed *in situ* between a hydrazine and formaldehyde. The subsequent cleavage of the tosylhydrazone resulted in the formal reductive methylation of alkene.[77] This method made it possible to obtain the methylation of mono-, di-, and trisubstituted alkenes and exhibits potential as a method for the late-stage functionalization of natural products and pharmaceuticals (*Scheme 1.49*).

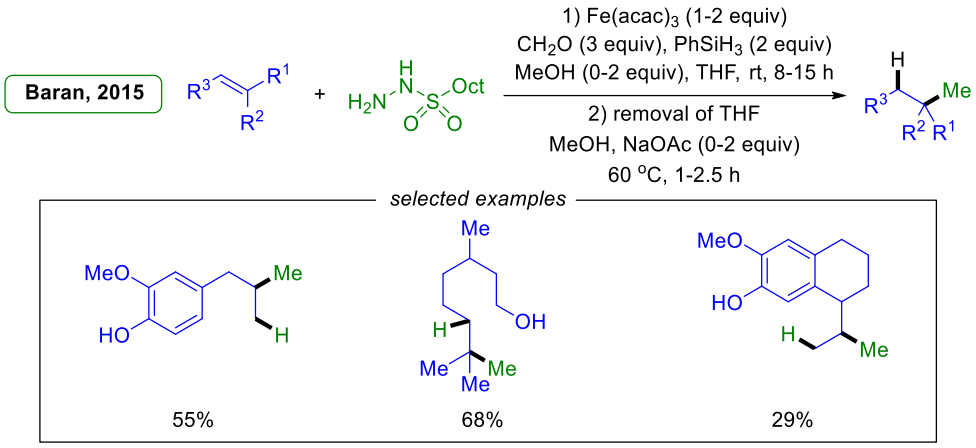

Scheme 1.49. Baran's hydromethylation of unactivated olefins.

Subsequently, in 2018, our group developed the inter- and intramolecular coupling of Cbz-hydrazones with alkenes.[78] Unlike Baran's reaction, in this case, the nitrogenated adduct did not fragment and could be hydrogenated to give the corresponding tertiary amine compounds, a structural motif found in many pharmaceuticals and alkaloids (*Scheme 1.50*).

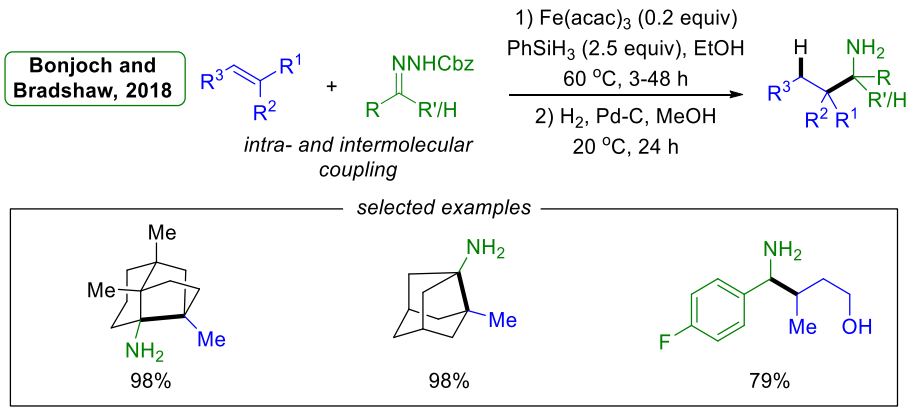

Scheme 1.50. Intra- and intermolecular coupling of alkenes with hydrazones.

In the same year, the Shenvi group reported the same reaction but using glyoxylimines as the acceptor group. This allowed the corresponding sulfinimines to be obtained,

with potential applications in synthesizing sterically hindered unnatural amino acids with good diastereoselectivities (*Scheme 1.51*).[79]

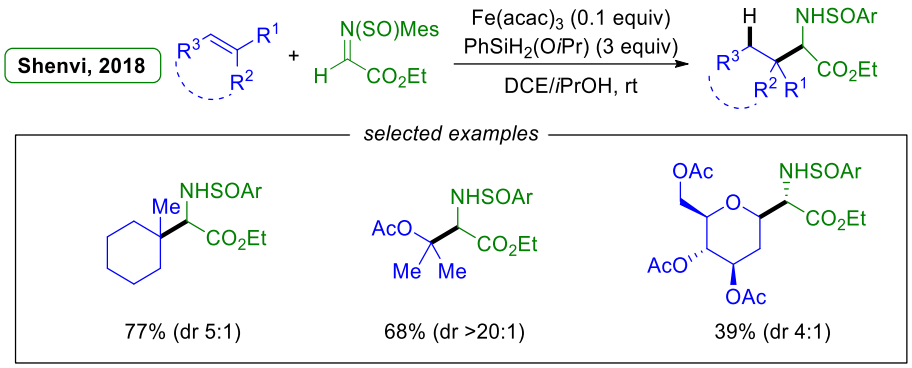

Scheme 1.51. Addition of unactivated olefins into imines.

Later on, Bode's group demonstrated that imines could be used in intramolecular MHAT cyclization reactions, allowing for the formation of bridged, spiro-, and fused rings.[80] Since imines are unstable, the imine was formed *in situ* from the corresponding amine (*Scheme 1.52*).

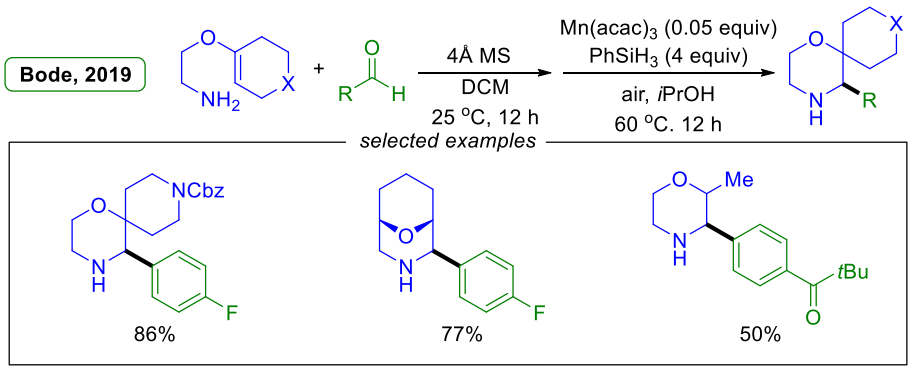

Scheme 1.52. Synthesis of bridged bicyclic and spirocyclic saturated N-heterocycles.

During studies to find the ideal acceptor group for the reaction detailed above by our group (see *Scheme 1.50*), we observed that tosylhydrazones underwent spontaneous fragmentation under the reaction conditions. However, due to the volatility of the compounds formed, isolation of the product proved difficult. To counter this, an intermolecular reaction was developed with substrates of higher molecular weight (*Scheme 1.53*).[81] It should be noted that although this reaction is analogous to Baran's methylation, that reaction was limited to using formaldehyde. In contrast, we demonstrated that a range of aldehyde compounds could form the corresponding tosylhydrazones. After coupling, the tosylhydrazine was eliminated using Et_3N,

resulting in a formal alkylation reaction. Notably, unlike the Baran reaction, simple tosyl hydrazones could be used instead of the bespoke octyl sulfonyl hydrazines.

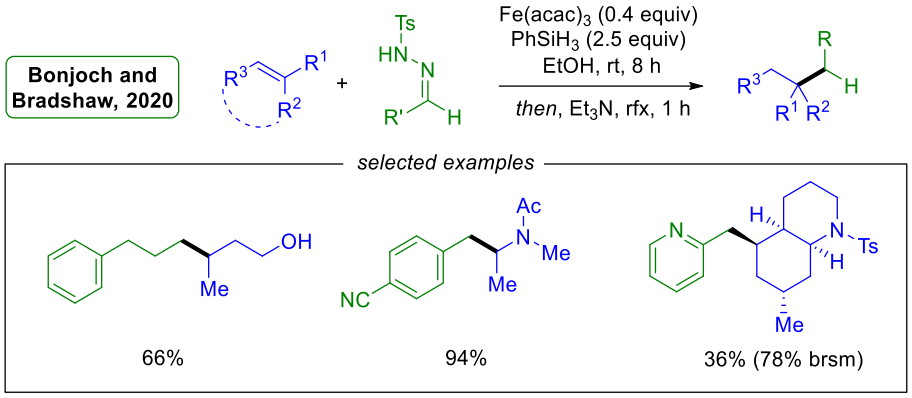

Scheme 1.53. Reductive alkylation of unactivated alkenes using tosylhydrazones.

Haloalkanes as acceptors

In 2019, Shenvi and co-workers reported the first use of alkyl halides as radical acceptors[82] to form hydroalkylated compounds containing a tertiary or quaternary carbon. Using a Mn/Ni dual catalytic system, an Mn MHAT-generated tertiary radical could be intercepted by a Ni species derived from an alkyl halide species (*Scheme 1.54*).

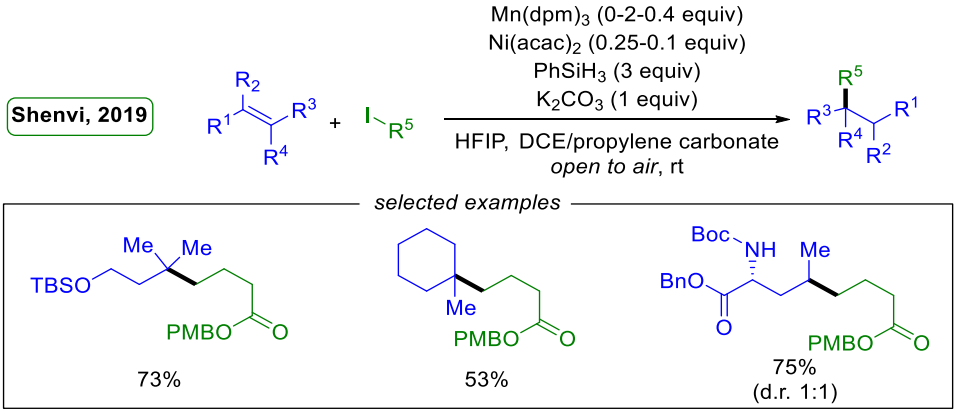

Scheme 1.54. Hydroalkylation of olefins to form quaternary carbons.

In 2023, the group of Liu applied a similar methodology, with a cobalt catalyst for the β-selective synthesis of 2-deoxy-C-glycosides from glycals (*Scheme 1.55*).[83] In this case, unlike the Mn/Ni dual-catalysis used by Shenvi, the activation of alkyl halide took place in the cobalt catalytic cycle to reoxidize the metal.

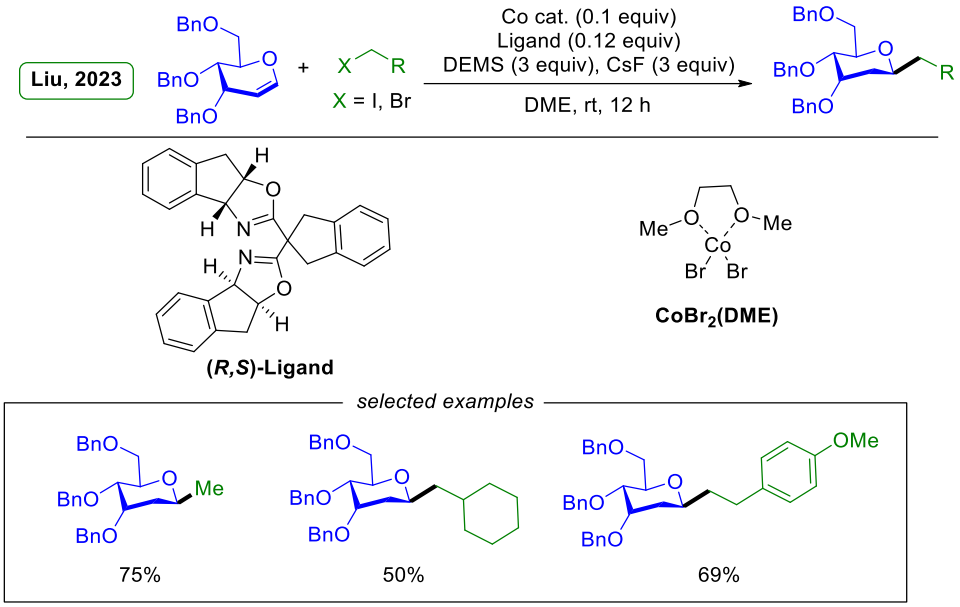

Scheme 1.55. Synthesis of 2-deoxy-C-glycosides from glycals.

In the same year, the group of Liu also re-applied this methodology with haloalkanes for C-alkyl glycosylation to access 2-deoxy-β-C-glycosides diastereoselectively with the help of a chiral ligand (*Scheme 1.56*).[84] In addition, they were able to carry out mechanistic studies where they determined that the hydrometallation of glycal with the Co-H ligated species would be the turnover-limiting step and the determining step of the stereoselectivity in this hydroalkylation.

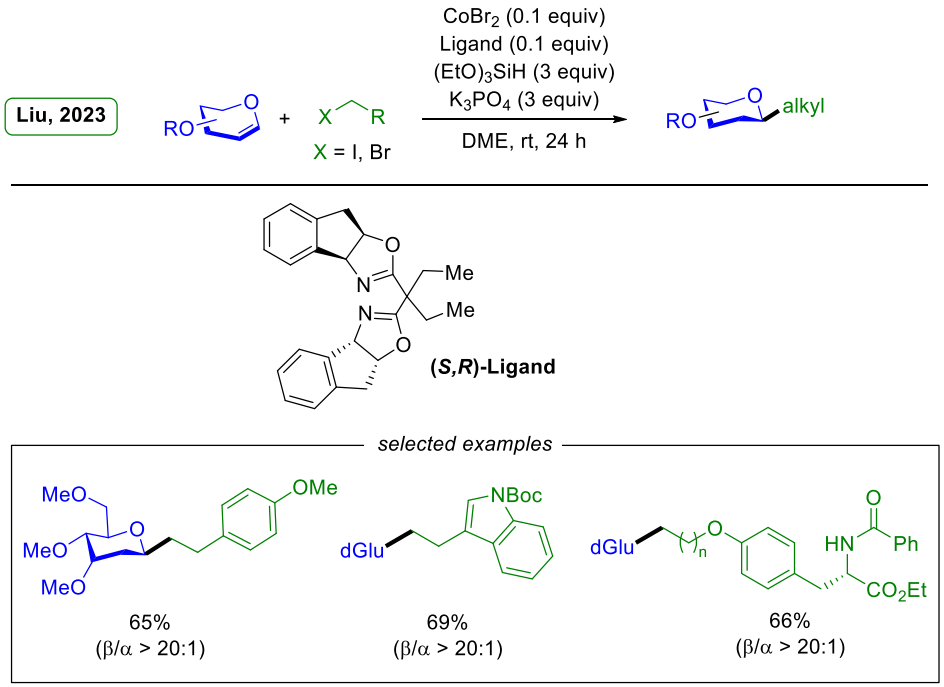

Scheme 1.56. Stereoselective synthesis of 2-deoxy-β-C-glycosides.

1.2. OBJECTIVES

The aim of this thesis is to expand the pool of radical acceptors in MHAT reactions for C-C bond formation and develop MHAT-based tandem reactions. When our research group began working in the field of MHAT reactions, only a few reported C-C bond-forming reactions were described in the literature. Since then, there has been a massive growth in the number of reported reactions, and now most of the common functional groups have been employed as acceptors in MHAT reactions. One of the groups that had not been used is the isocyanide group. The first objective of this thesis was to explore if they could be used as viable acceptor groups in MHAT reactions to construct heterocycles. The details of this study will be discussed in Chapter 2 of this thesis. During the course of this work, the serendipitous discovery that ethers could be coupled to heterocycles under MHAT-type conditions led us to explore this new C-H based cross dehydrogenative coupling (*Objective 2*). The results of this work will be discussed in Chapter 3. Finally, we wanted to explore the development of a novel MHAT-based tandem reaction based on the work of our group using tosylhydrazones as acceptor groups to obtain functionalized derivatives of the adamantane nucleus (*Objective 3*). The results of this work will be discussed in Chapter 4.

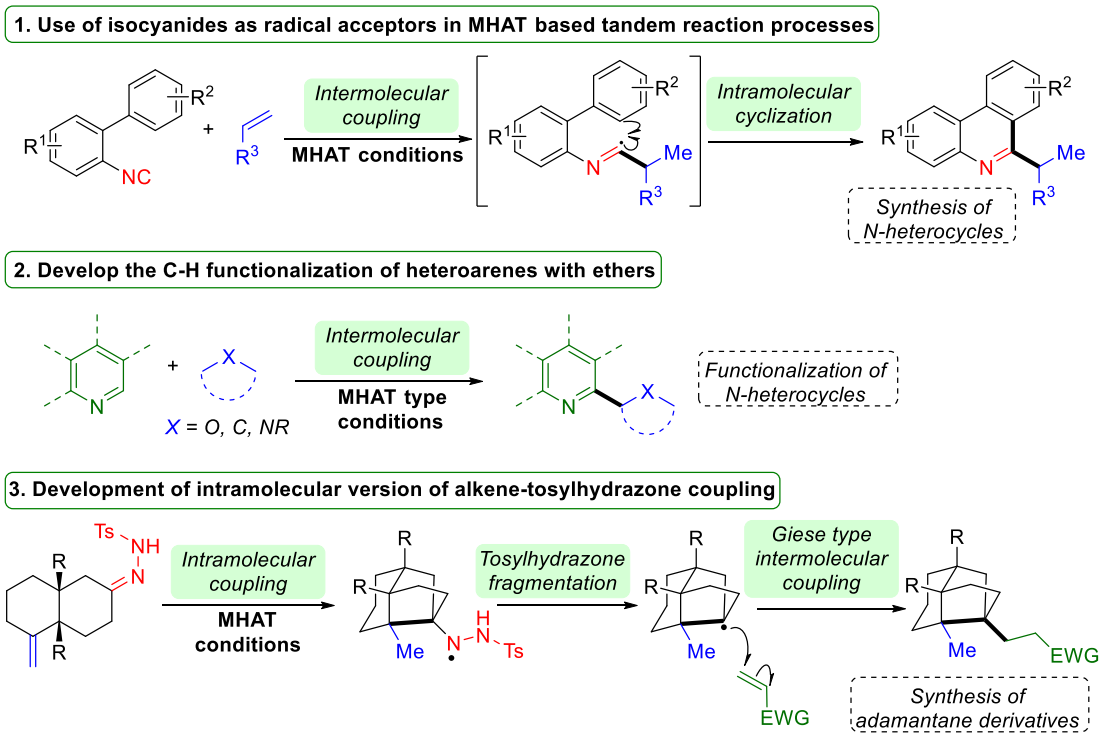

Scheme 1.57. Main objectives of this thesis.

2. ISOCYANIDES AS ACCEPTOR GROUPS IN MHAT REACTIONS WITH UNACTIVATED ALKENES

2.1. INTRODUCTION

In this chapter, we describe the use of isocyanides as acceptors groups in MHAT coupling reactions with alkenes leading to the formation of various types of biologically relevant heterocycles, such as phenanthridines, isoquinolines, and indoles.[85]

2.1.1. Heterocycles as synthetic targets

Nitrogen-containing heterocycles are one of the most important structural classes of compounds, observed in many natural, biologically active, and pharmaceutical products.[86] The FDA list of approved drugs reveals that 59% of small-molecule drugs contain at least one nitrogen heterocycle[87] with the most prominent structures, such as indole and pyridine. Additionally, these heterocyclic structures feature prominently in countless natural products of biological importance, such as alkaloids. Examples of these nitrogen heterocycle nuclei include Trisphaeridine,[88] a phenanthridine with neuroprotective properties, Papaverine,[89] an isoquinoline with antispasmodic properties or Melatonin,[90] an indole hormone that regulates circadian rhythms (*Figure 2.1*).

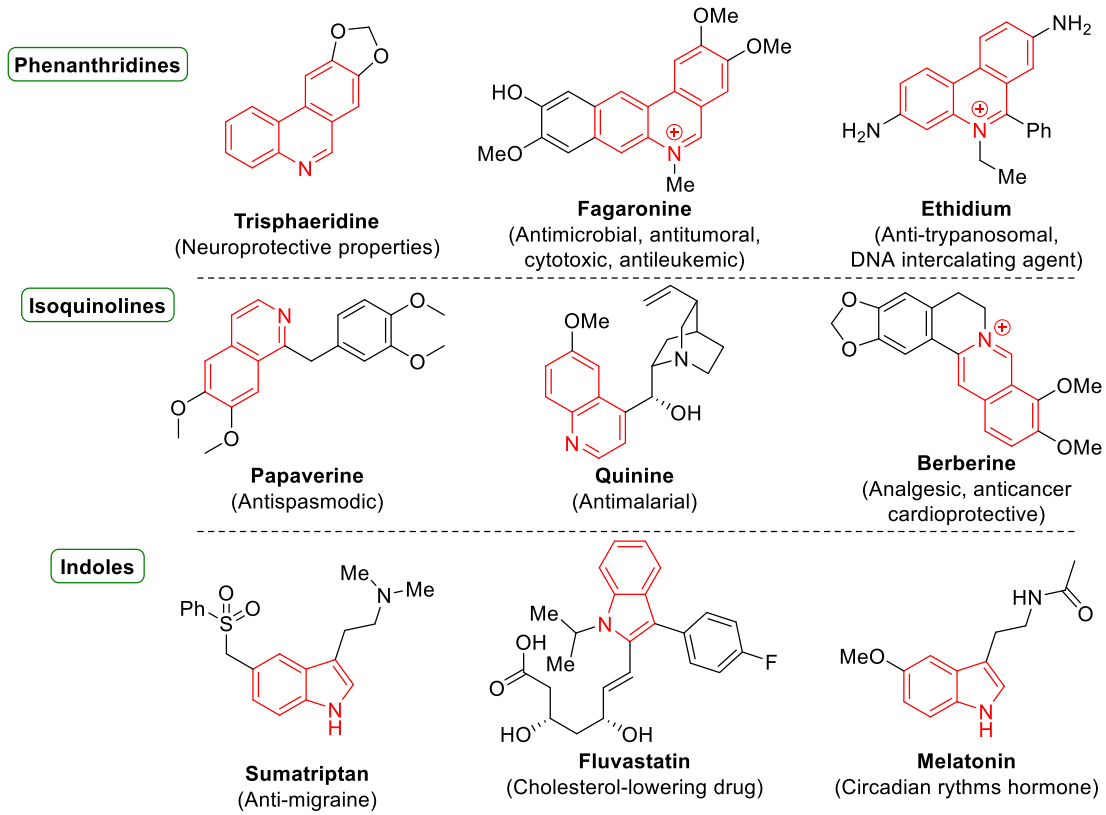

Figure 2.1. Pharmacologically active alkaloids, including heterocyclic core.

Due to the importance of nitrogen-containing heterocyclic structures, in particular phenanthridines, indoles, or isoquinolines, which have gained prominence in organic, medicinal, and materials chemistry, the last decades have seen many innovative efforts devoted to developing new approaches to synthesize them. Among the methods developed, the insertion of isocyanides has stood out as a powerful strategy for their preparation, with transition metal-mediated insertion reactions being widely explored.[91] In contrast, radical isocyanide insertion, the focus of this chapter, has remained less investigated.[92]

2.1.2. Background on the chemistry and structure of isocyanides

Because isocyanides are not one of the most commonly encountered functional groups and because they have a somewhat unique chemistry, we will here provide a brief summary of isocyanide structure, synthesis, and reactivity.

Despite their very penetrating, unpleasant odor, isocyanides are a unique class of organic compounds because they are the only stable derivatives (apart from carbon monoxide) that contain a divalent carbon.[93] Their discovery dates back more than 130 years to work by Lieke, Gautier, and Hofman. However, studies on its chemical reactivity did not appear until the 1960s,[94] when efficient syntheses of isocyanides were developed (*Scheme 2.1*).

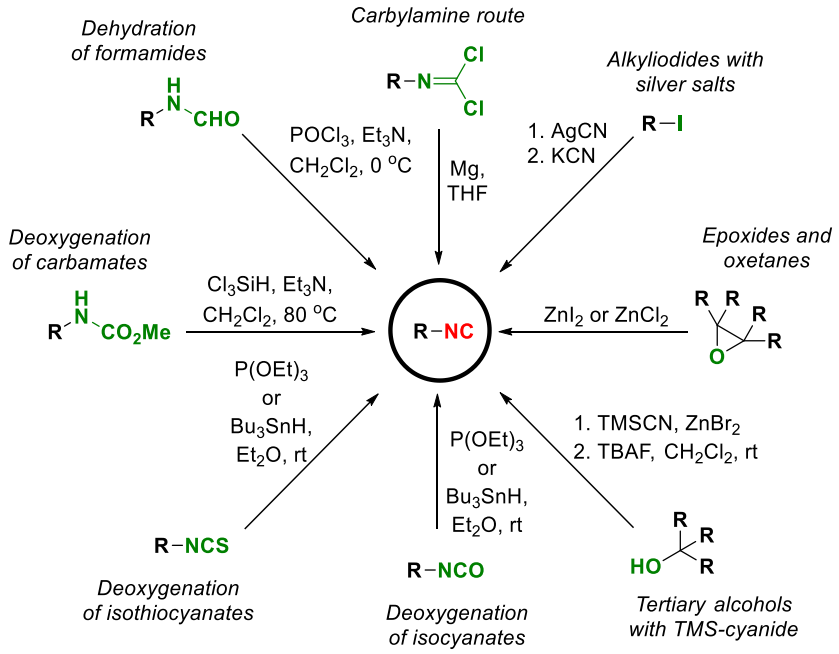

Scheme 2.1. Methods for the synthesis of isocyanides.

Since their discovery, there have been two classical routes for the synthesis of isocyanides.

(i) The carbylamine reaction, which consists of the reaction of chloroform and a strong base with a primary amine, that leads to the addition of the dichlorocarbene to the amino group, followed by the elimination of the hydrogen chloride.[95]

(ii) The alkylation route, where the treatment of metal cyanides with alkylating agents such as halogenated compounds or dialkyl sulfides leads to the formation of a mixture of the corresponding cyanides and isocyanides derivatives.[96]

Both methods have been discarded due to the small amounts of pure isocyanide they produce, their limited substrate scope, and the use of toxic metal cyanides and chloroform. Nowadays, the primary method to produce isocyanide derivatives is known as the "dehydration method". This synthetic strategy was first reported by Hagedorn and co-workers in 1956.[97] It consisted of transforming primary amines into formamides using formic acid or derivates, followed by dehydration using phosgene or phosphorous oxychloride with a base like triethylamine or diisopropylamine. Several other methods have been reported, such as Mukayama's reduction of isocyanates[98] or isothiocyanates,[99] epoxide opening with silyl cyanides,[100] deoxygenation of carbamates,[101] and the use of silyl cyanides on tertiary alcohols.[102]

With efficient methods for their preparation, isocyanide chemistry has not stopped growing due to their great versatility. Examples of important reactions developed using isocyanides consist of the attack of an electrophilic species onto the nucleophilic carbon of the isocyanide, such as Ritter-type processes[103] or the Ugi and Passerini reaction.[104]

The isocyanide structure can be seen as a divalent carbon atom, but in valence bond terms, the two resonance structures, **a** and **b**, are required (*Scheme 2.2*). This partial carbenoid character confers particular and rich reactivity properties to isocyanides.[105] Although the physical properties indicate that the dipolar form **a** is the one that contributes most to generating its nucleophilic character, in terms of radical chemistry, the divalent form **b** is the most interesting because it shows that isocyanide acts like a

geminal acceptor/donor synthon, so the acceptor carbon itself will become the donor through the imidoyl intermediate.

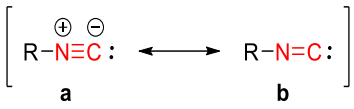

Scheme 2.2. Resonance in isocyanide structure.

So, despite being like alkynes in terms of molecular orbitals and electron density, they show different reactivity, possibly because isocyanides present some stereoelectronic differences. For example, the C-end of the isocyanide shows a σ-hole, which is important in modulating its stability and reactivity. Also, the π*-orbital is significantly more polarized than in the alkynes due to the electronegativity difference between the nitrogen and carbon.

These differences are represented in the reactivity of isocyanides with radicals since the addition of alkynes proceeds in a 1,2-manner, where the new bonds are formed in the two different carbons; in the isocyanides a 1,1-manner occurs, forming both bonds at the same end-carbon, showing its carbene nature (*see Scheme 2.3*). This 1,1-bond formation pattern has gained the attention of synthetic chemists, enabling participation in many interesting radical cascades.[93]

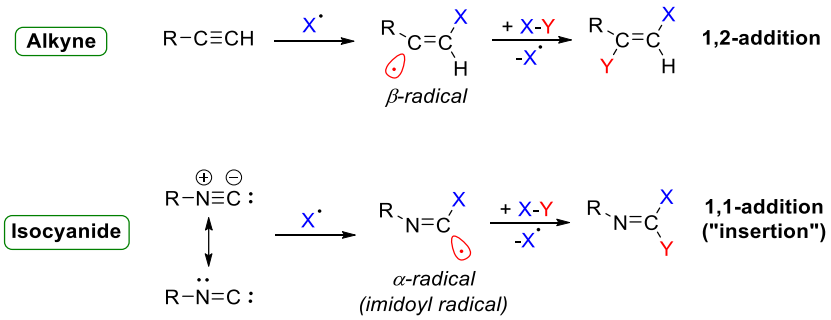

Scheme 2.3. Addition Pattern differences between Alkynes and Isocyanides.

The first reported example of a radical addition to isocyanides was described by Shaw and co-workers,[106] where DTBP was used in catalytic amounts with heat to produce the isomerization of an isocyanide to the corresponding cyanide, involving the addition of methyl radicals to the isocyanide followed by the β-scission of the resulting radical adduct (imidoyl radical). This fragmentation led to the rise of an alkyl radical responsible for converting the starting isocyanide to the cyanide. Then Saegusa studied

the feasibility of a radical attack on the isocyanide carbon using tributyltin hydride and alkyl isocyanides, using AIBN as initiator, enabling the addition of tin radicals to the isocyanide (*Scheme 2.4*).[107]

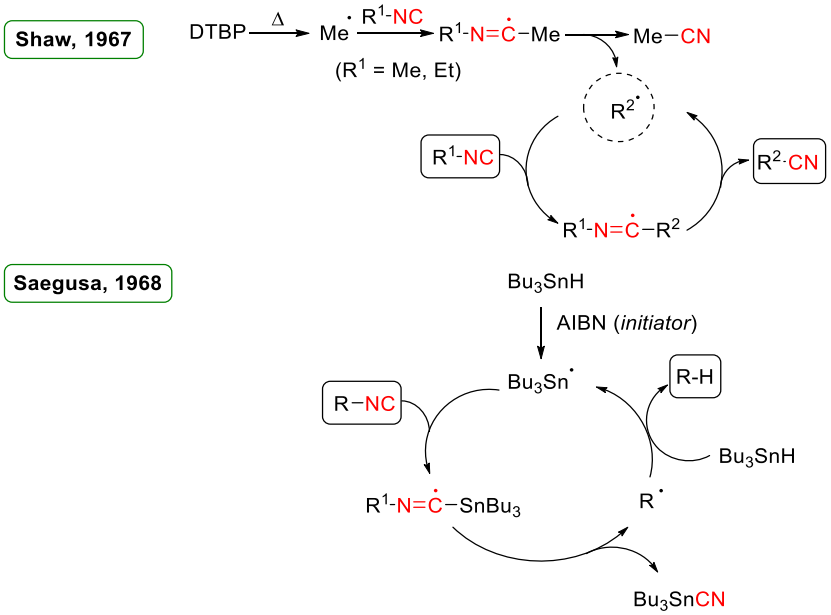

Scheme 2.4. First examples of radical addition to isocyanides proposed by Shaw and Saegusa.

Between 1970 and 1980, several papers reported the addition of carbon, oxygen, sulfur, silicon, phosphorous, and tin radicals to isocyanides.[108] Interestingly, in those studies, it was demonstrated that the nature of the attacking radical and the alkyl group of the isocyanide define the fragmentation that will take place on the imidoyl intermediate (*see Scheme 2.5*). While oxygen- and sulfur-centered radicals will lead to α-fragmentation to give isocyanates or isothiocyanates, carbon, tin, and silicon radicals will undergo β-fragmentation, leading to the corresponding cyanide. However, this behavior may differ from this general rule since the stability of the radical can determine the fragmentation pathway.

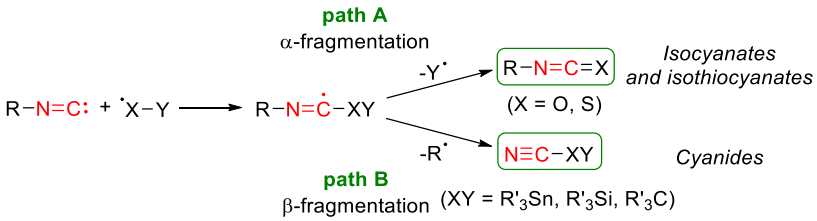

Scheme 2.5. Fragmentation pathways of imidoyl radicals.

Imidoyl radicals have been very useful intermediates for synthesizing *N*-heterocycles, but historically, they have always been generated from imines or imidoyl derivatives as

precursors.[109] This changed in 1991 when Curran and co-workers developed a pioneering work using isocyanides as radical acceptors to develop a radical cascade for constructing *N*-heterocycles.[110] Different radical species can be inserted to form the corresponding imidoyl intermediate, which will carry out the subsequent cyclization to obtain the corresponding nitrogenous heterocycle. This work opened the doors to further studies, where, for example, they used the [4+1] radical annulation strategy to synthesize pharmacologically interesting molecular structures such as Camptothecin, an antitumor agent (*Scheme 2.6*).

These reactions allowed the obtention of cyclopentane-fused quinolines through the addition of the alkyne to the isocyanide, through a 5-*exo*-*dig*-cyclization of the imidoyl intermediate onto the triple bond of the alkyne with a subsequent ring closure of the vinyl radical.[111] This cascade radical reaction supposed an incredible breakthrough for synthesizing Camptothecin and derivatives such as Topotecan and Irinotecan, where authors demonstrated a regioselective, asymmetric, and widely applicable protocol with a broad scope and functional-group tolerance.[112]

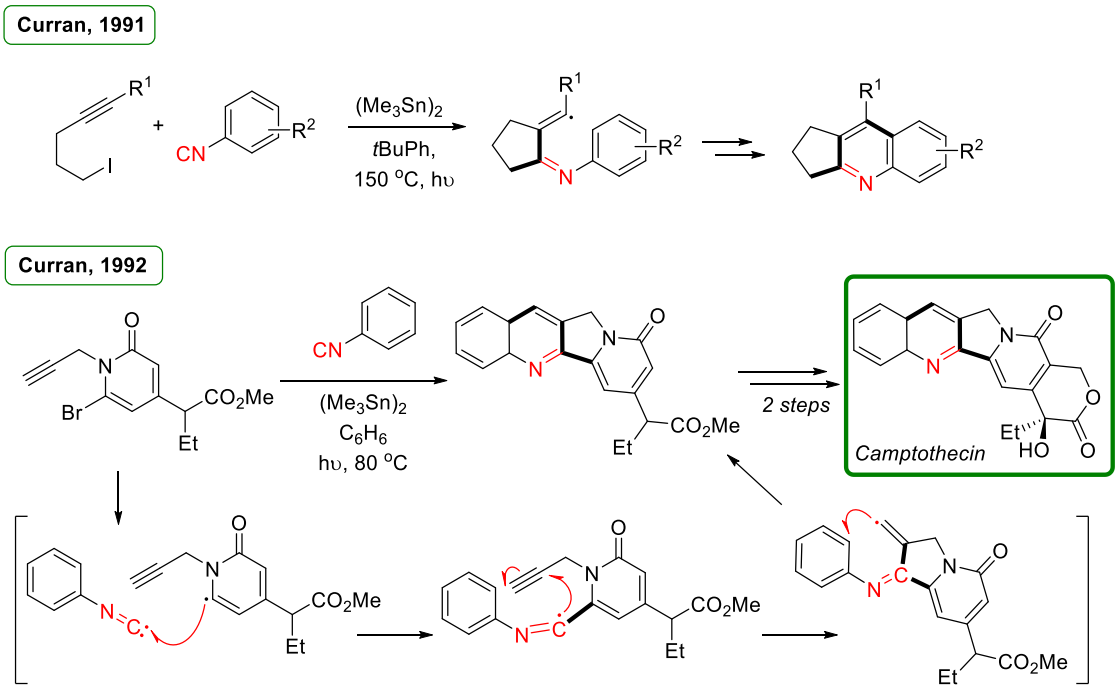

Scheme 2.6. Curran annulation for cyclopentane-fused quinolines and Camptothecin derivatives.

Analogous reactions were carried out in the same years by Tundo and co-workers[113] using aromatic isocyanides and alkyl and sulfanyl radicals with a cyano-substituted

sidechain. In 1998, Nanni also showed the applications of alkyl and sulfanyl radicals for synthesizing cyclopentaquinoxalines.[114] In 2000, Lenoir demonstrated the use of γ-iodoalkynes or iodonitriles for a [4+1] radical annulation to afford cyclopentane-fused pyridines and pyrazines (*Scheme 2.7*).[115]

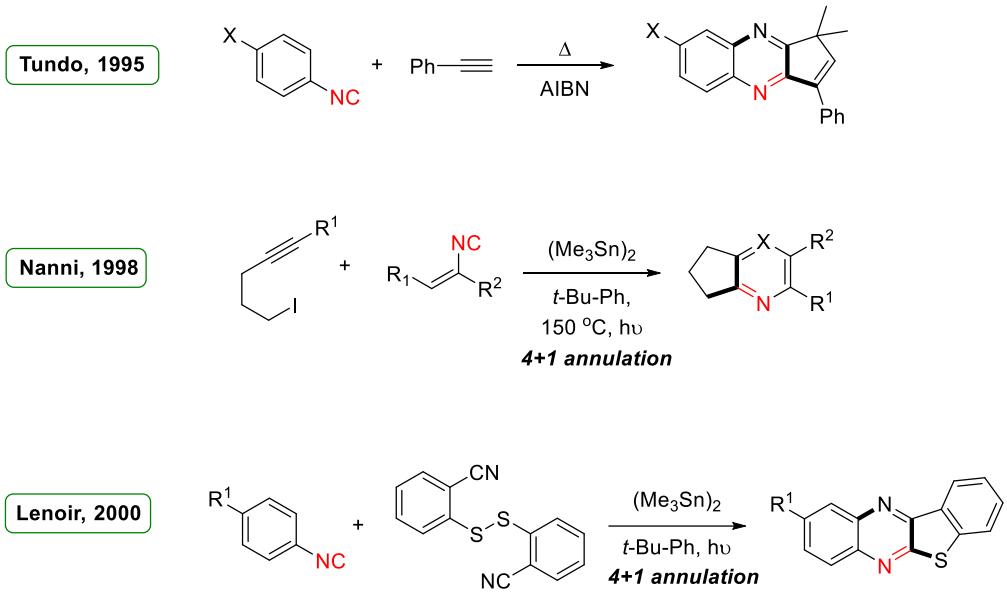

Scheme 2.7. Tundo, Nanni and Lenoir synthesis of pyridines and pyrazines.

Fukuyama successfully employed *ortho*-alkenyl-substituted aryl isocyanides in the synthesis of indole derivatives.[116] Tin radicals were used for the cyclization, and *ortho*-alkenyl-substituted thioanilides were also demonstrated to carry thus cyclization.[117] This synthesis represented an interesting innovation for synthesizing 2,3-substituted indoles and has been utilized as an approach to the key intermediates of indole-containing alkaloids, such as Discorhabdin A or Vincadifformine (*Scheme 2.8*).[118]

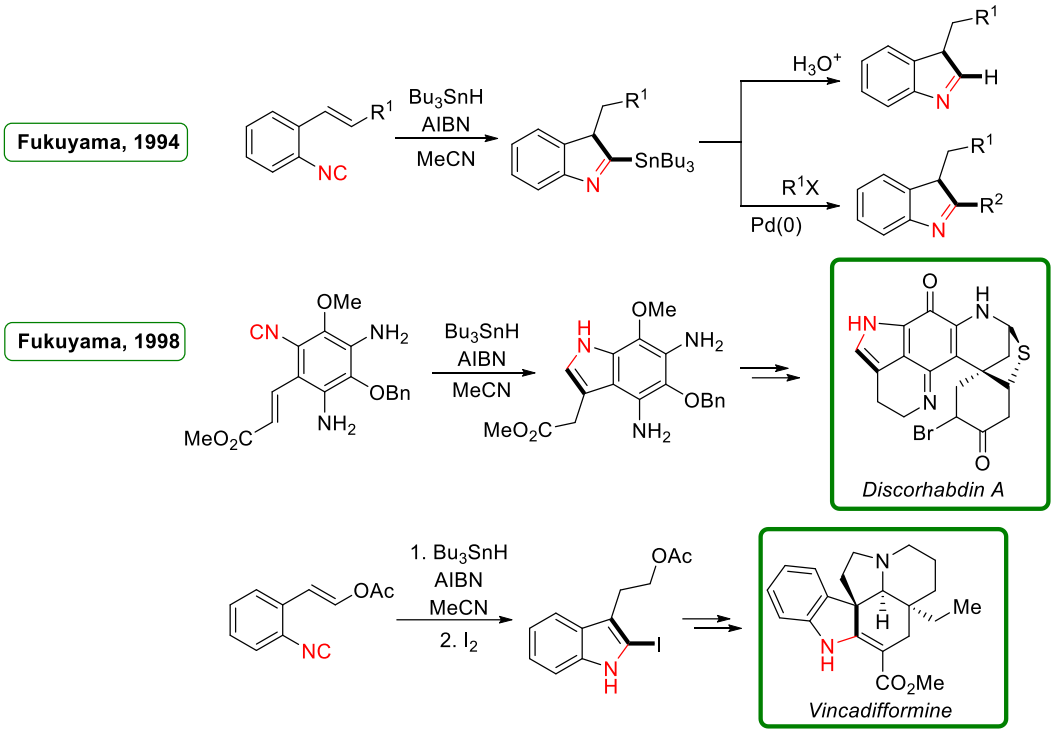

Scheme 2.8. Fukuyama's indole synthesis and application in alkaloid synthesis.

In this approach, the tri-*n*-butyltin radical attacks the isocyanide to form the α-stannoimidoyl radical, which leads, through a radical cyclization and further tautomerization, to the formation of the 2-stannylindole (*Scheme 2.9*).

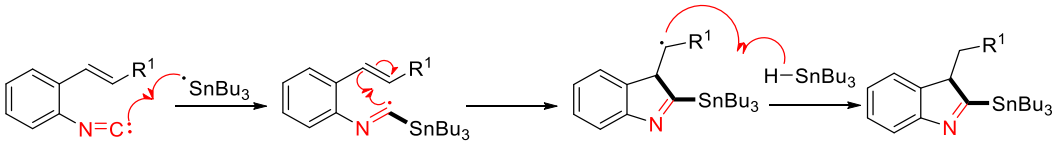

Scheme 2.9. Fukuyama's indole synthesis mechanism.

In a similar approach, Rainier and co-workers demonstrated that *ortho*-alkynyl-substituted aryl isocyanides with a TMS group linked can also be employed in this kind of tin-radical-mediated cyclization (*Scheme 2.10*).[119]

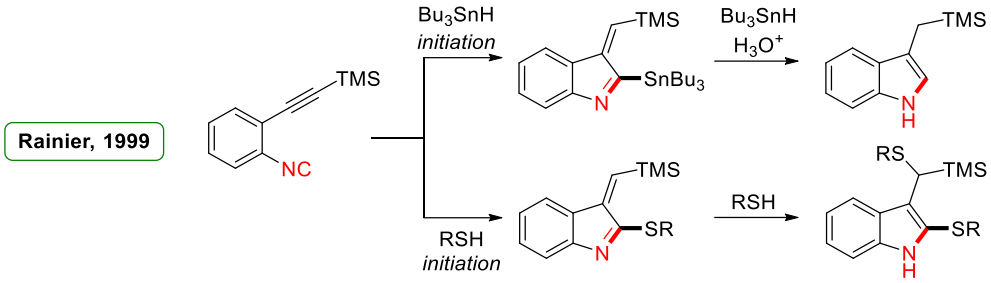

Scheme 2.10. Rainier synthesis of indole derivatives.

In 1970, Saegusa described the radical addition of thiols to isocyanides.[107] However, it was not until the 1990s that Bachi and co-workers developed synthetic methods based on Segusa's work to synthesize 5-membered nitrogen heterocycles.

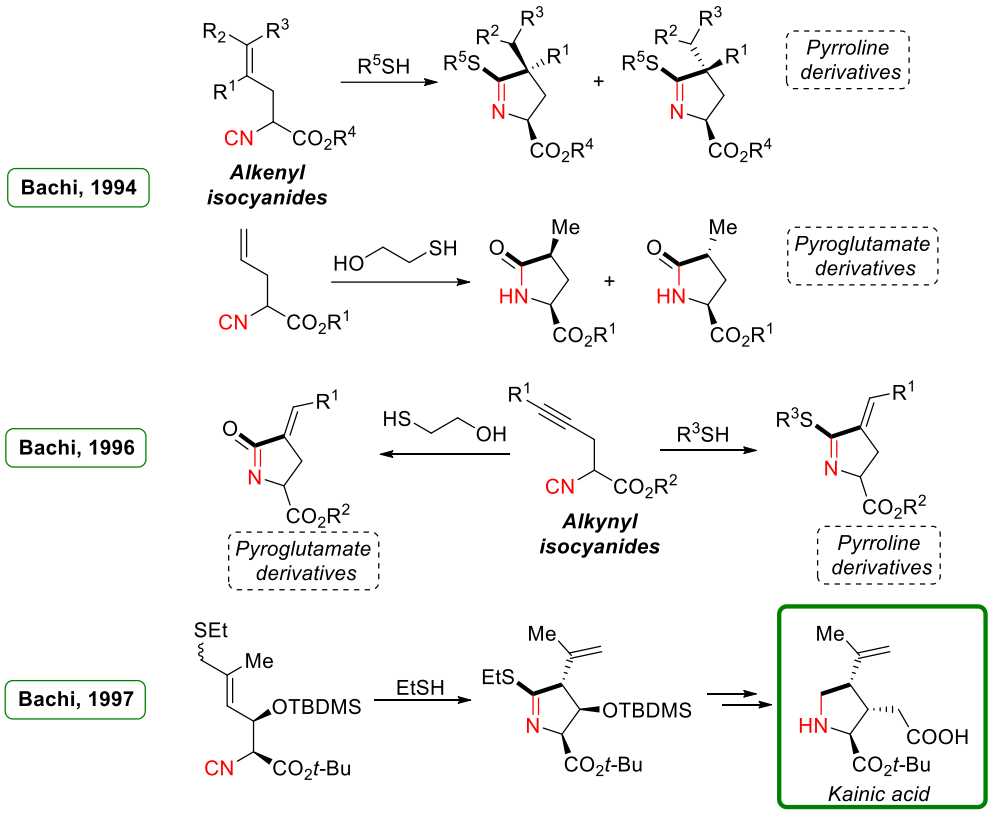

Scheme 2.11. Bachi's synthesis of pyrrolines and pyroglutamates with alkenyl and alkynyl isocyanides and its application in the synthesis of Kainic acid.

They demonstrated the synthesis of pyrrolines and pyroglutamates from alkenyl-substituted isocyanides, silylated alkynyl isocyanides, and allyl sulfides.[120] The methodology developed by Bachi was also used as a key step in the synthesis of (±)- and (-)-α-kainic acid in a stereo- and enantioselective way (*Scheme 2.11*).[121]

2.1.3. Literature precedents for the radical-based synthesis of heterocycles

Phenanthridines

During the 20th century, phenanthridine derivatives were neglected in pharmaceutical chemistry due to some studies highlighting their carcinogenic properties.[122] Later studies served to discover analogs of phenanthridine alkaloids, as well as phenanthridine derivatives with anti-parasitic properties, which served to increase the interest in this type of core again. Consequently, during the beginning of the 21st century, many scientific publications have focused on the functionalization of phenanthridines. Most notably, several synthetic routes have been developed, starting from the corresponding isocyanide to provide 6-substituted phenanthridine nuclei (*see Schemes 2.12 and 2.13*).

One of the most common pathways is using C-H activation to introduce different kinds of groups, such as alkanes,[123] ethers,[124] amides,[125] or acyls,[126] mainly via the use of oxidants. This led to C-H activation generating the carbon-tethered radical of the aforementioned functional groups, which attack the carbon of the isocyanide, leading to cyclization and formation of the heterocycle. On the other hand, another common method has also been using photochemistry to generate the radical species.

Another commonly explored route to introduce these substituents and produce the subsequent cyclization has been the use of carboxylic acids. In this case, using different metals promotes decarboxylation, generating a carbon-centered radical that attacks the isocyanide carbon, generating the imidoyl intermediate and posterior cyclization.[127] Notably, metal-free protocols also exist in which using a base like potassium carbonate in combination with heat leads to decarboxylation.[128] Similarly, *N*-(acyloxy)phthalimides have been used via photoredox-induced decarboxylation to generate an alkyl radical addition to isocyanides.[129]

It's also noteworthy that alkyl and acyl halides are used as proradicals to initiate this class of isocyanide insertion. In this field, alkyl bromides,[130] α-bromo esters,[131] perfluoroalkyl iodides,[132] alkyl iodides,[133] and iodonium ylides[134] have been employed, using metal catalysts or photochemistry to generate the radical cascade cyclization to access phenanthridine derivatives.

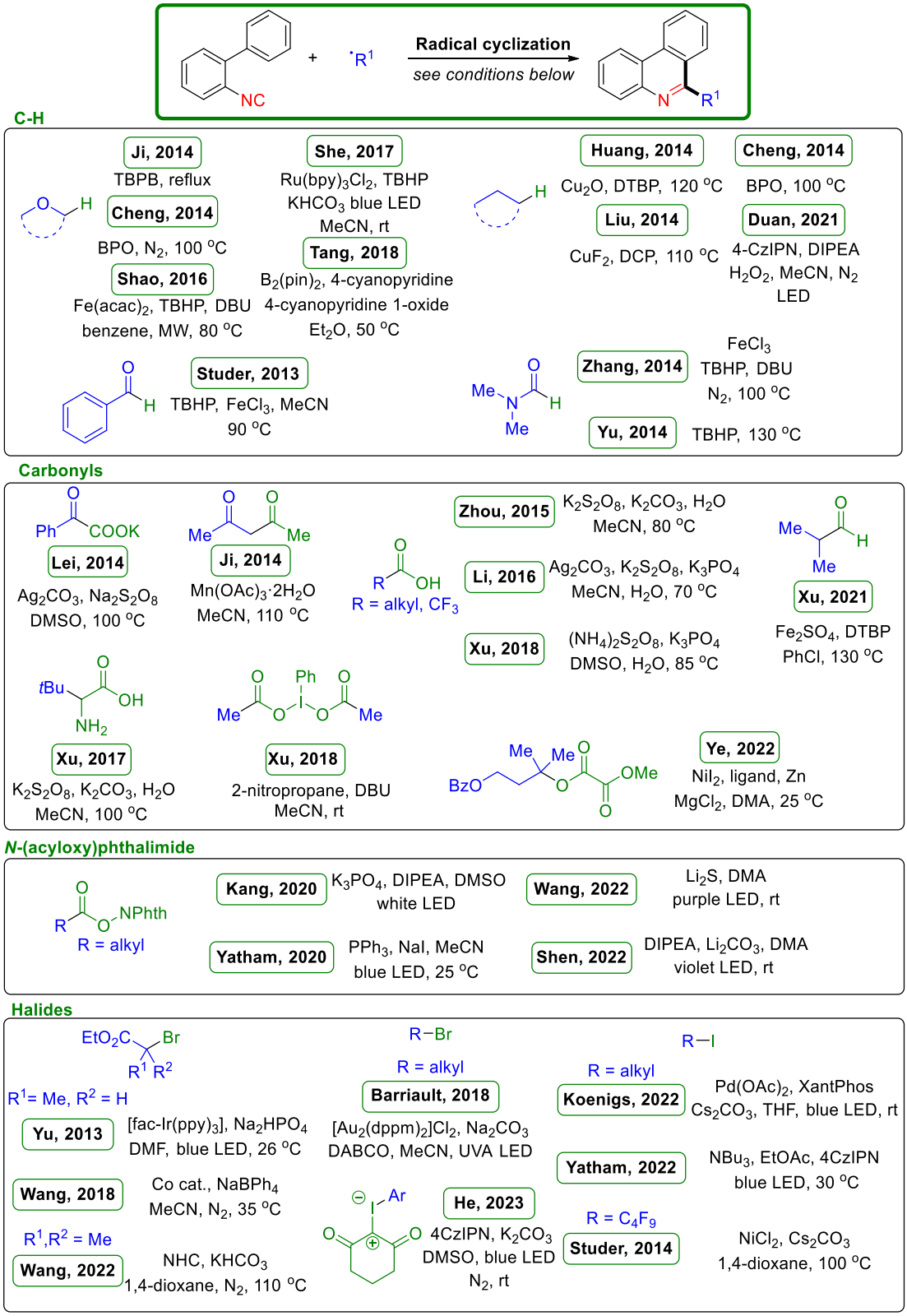

Scheme 2.12. Methods for phenanthridine synthesis using radicals.

Nitrogenated compounds such as amines,[135] hydrazines,[136] or diazo compounds[137] have also been used to generate radical species by photochemical methods, metal catalysts, or oxidants.

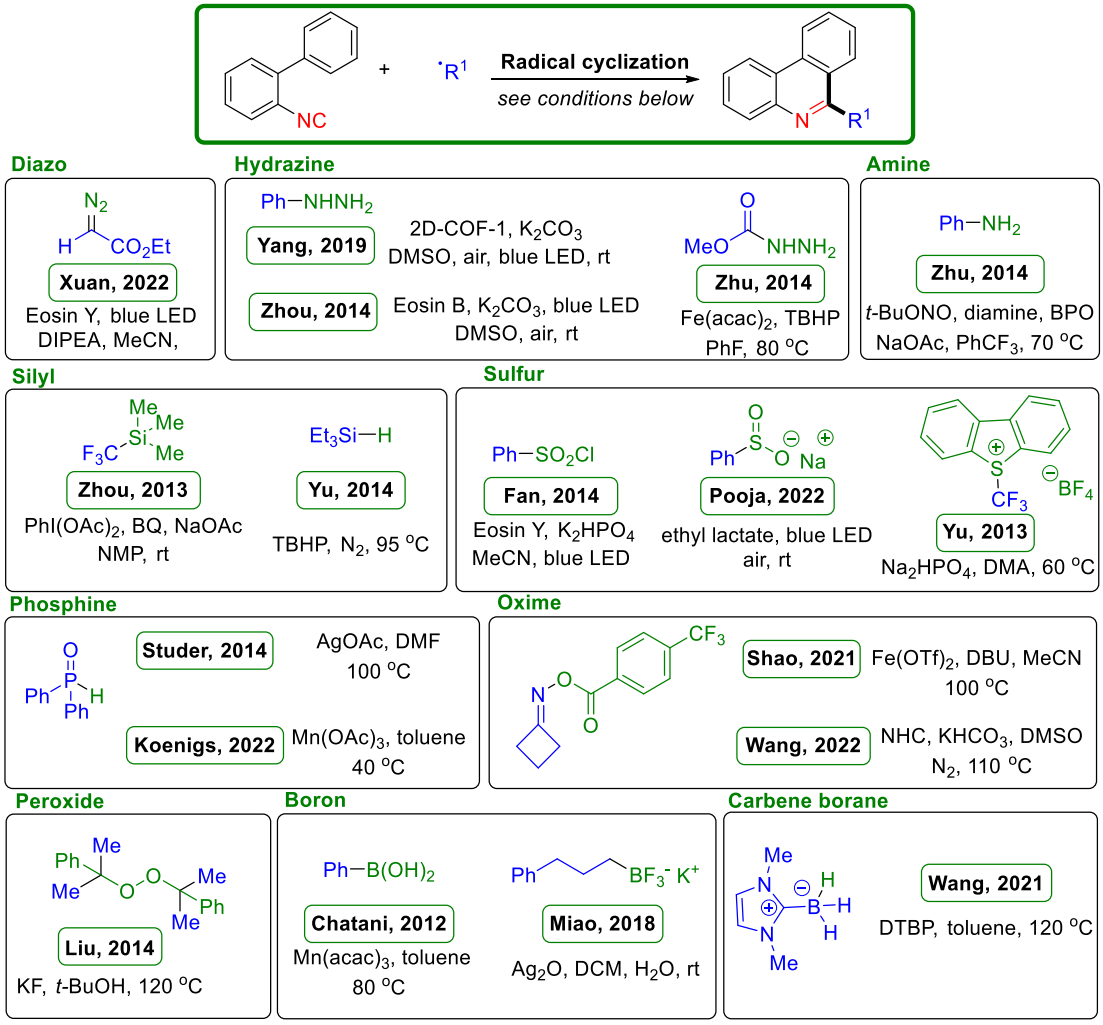

Scheme 2.13. Further methods for phenanthridine synthesis using radicals.

Although to a lesser extent, many other functional groups have been studied to achieve the introduction of different carbon skeletons through radical cascade cyclization. Among them, we can find the use of peroxides,[138] phosphines,[139] oximes,[140] sulfates,[141] and silyls, used both to introduce alkyls[142] and to introduce the silyl group itself,[143] borates,[144] or carbene borane,[145] used to introduce the borane itself into the phenanthridine nucleus.

Despite the extensive list of groups described in the literature, to our knowledge, alkenes have never previously been used to carry out this type of cyclization to functionalize phenanthridines.

Isoquinolines

Isoquinolines are another type of nitrogen heterocycle that has been attracting increasing interest over the years due to the discovery of derivatives with interesting pharmacological activities, such as inhibition of HIV-1, antibacterial, antituberculosis, antifungal, or antimalarial properties.[146]

This has led synthetic chemists to try to develop more efficient ways to obtain functionalized derivatives of this type of structure. As seen above, using C-H activation using metal catalysts or oxidants to generate carbon-centered radicals in alkanes,[147] ethers,[148] or alcohols[149] has been widely used. Radicals have also been generated from decarboxylation,[150] halides, [151]hydrazines,[152] isoxazolines,[153] borates,[154] or sulfur compounds (Umemoto's reagent)[155] (*Scheme 2.14*).

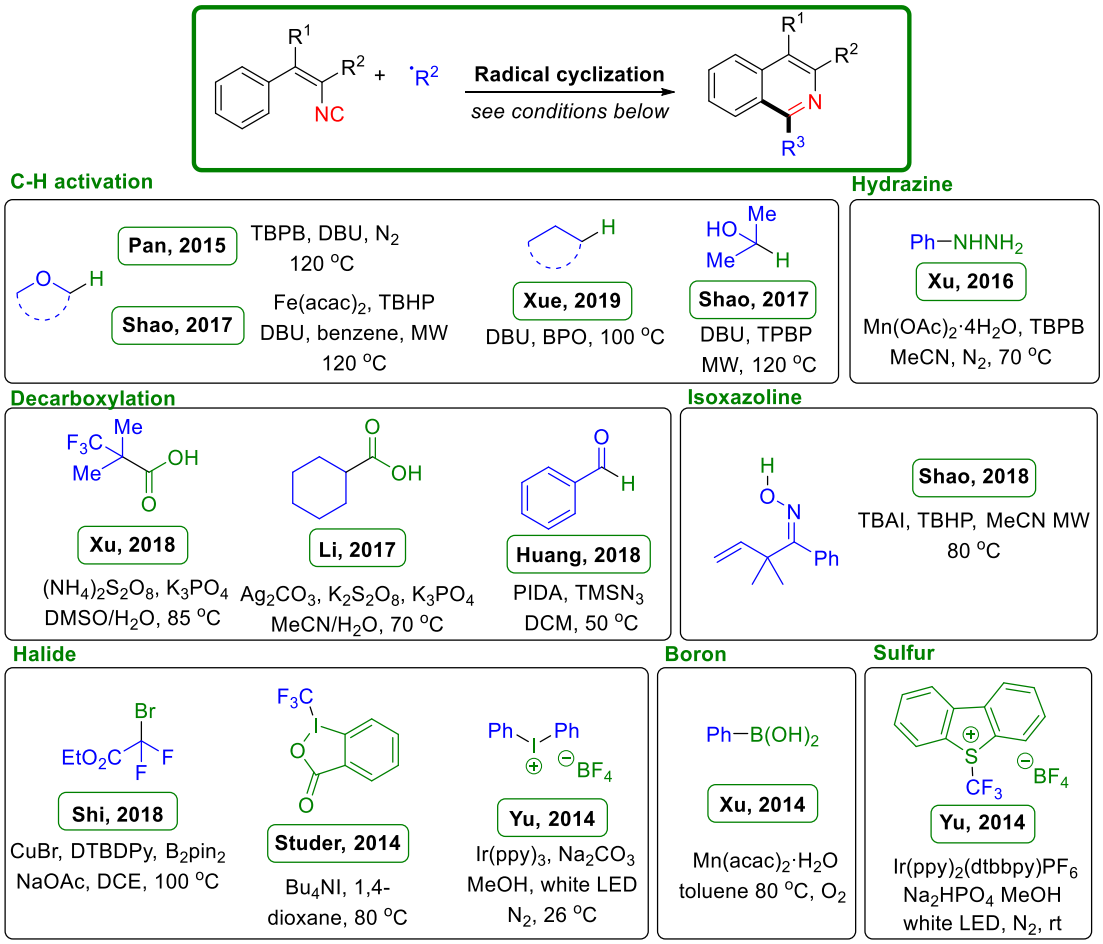

Scheme 2.14. Methods for isoquinoline synthesis using radicals.

Indoles

Many compounds that show biological activity contain the indole core, which, like the previously described ring systems, has led synthetic chemists to look for new ways to construct them. For example, a large class of natural indole diterpenoids has potent cytotoxic, antiviral, and antibacterial properties.[156]

Since Fukuyama's work using tributyltin hydride,[17] many groups have devoted their research to functionalizing this type of nucleus (*Scheme 2.15*) by inserting isocyanides through radical cyclization. Among them, the use of borates stands out, both to incorporate the borate group[157] and to introduce aryl groups.[158] Halogens,[159] carboxylic acids,[160] silyls,[161] diazo compounds,[162] thiols,[163] and other sulfonated groups have also been used,[164] as we have seen in the previous cases.

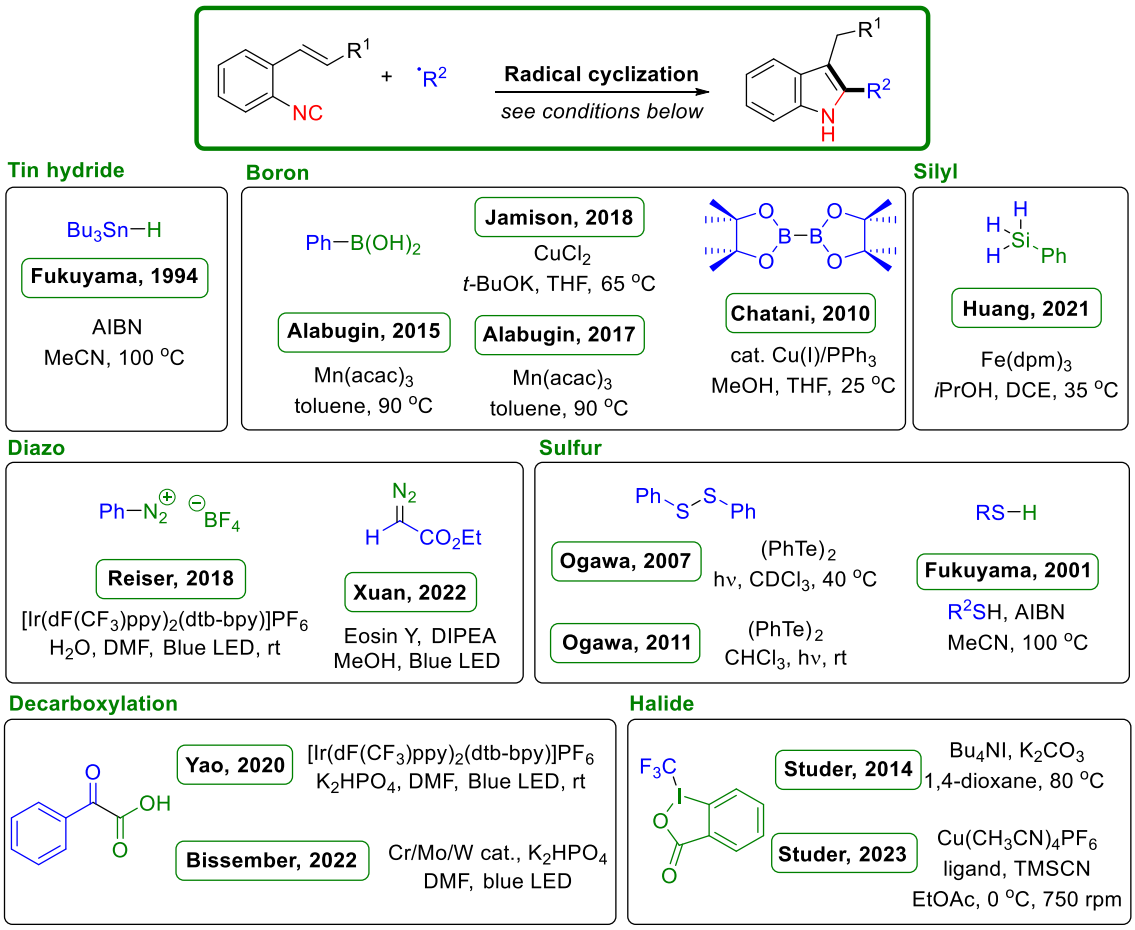

Scheme 2.15. Methods for indole synthesis using radicals.

Using AIBN and Bu_3SnH to obtain 2-stannyl-3-substituted indoles through a 5-*exo-trig* cyclization of the imidoyl radical intermediate, Fukuyama's approach opened the door to subsequent functionalization (*Scheme 2.16*). For example, in 1994, Fukuyama used this 2-stannyl indole in a Stille coupling, using aryl and vinyl halides, palladium catalyst, and triethylamine to obtain the 2-arylated indole.[17] Later, in 2011, he used the same method but this time using allylic systems to synthesize Tryprostatin A.[165] Similarly, in further studies of the same group, they also transformed the 2-stannyl indole through iodine to the corresponding 2-iodoindole, which would then serve as a substrate for palladium-mediated cross-coupling reactions to generate a large variety of 2,3-disubstituted indoles.[166] The work of Rainier,[119] where an alkyl thiol was used with AIBN to substitute the stannyl group, is also noteworthy.

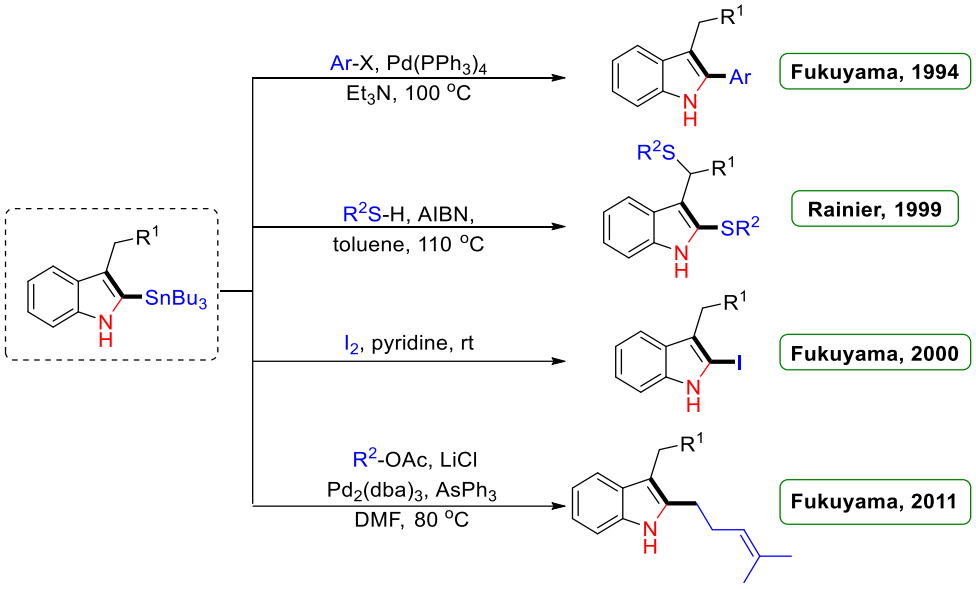

Scheme 2.16. Functionalization of 2-stannyl-3-susbtituted indoles.

2.2. OBJECTIVES

The main object of this chapter was to investigate using isocyanides as radical acceptors in MHAT reactions. The reaction would generate a carbon-centered radical from an unactivated alkene followed by an intermolecular coupling with an aryl isocyanide and subsequent intramolecular addition to a π-system. This would allow us to access different heterocyclic structures, such as phenanthridines, isoquinolines, and indoles, and to emulate Curran's Camptothecin synthesis (*Scheme 2.17*).

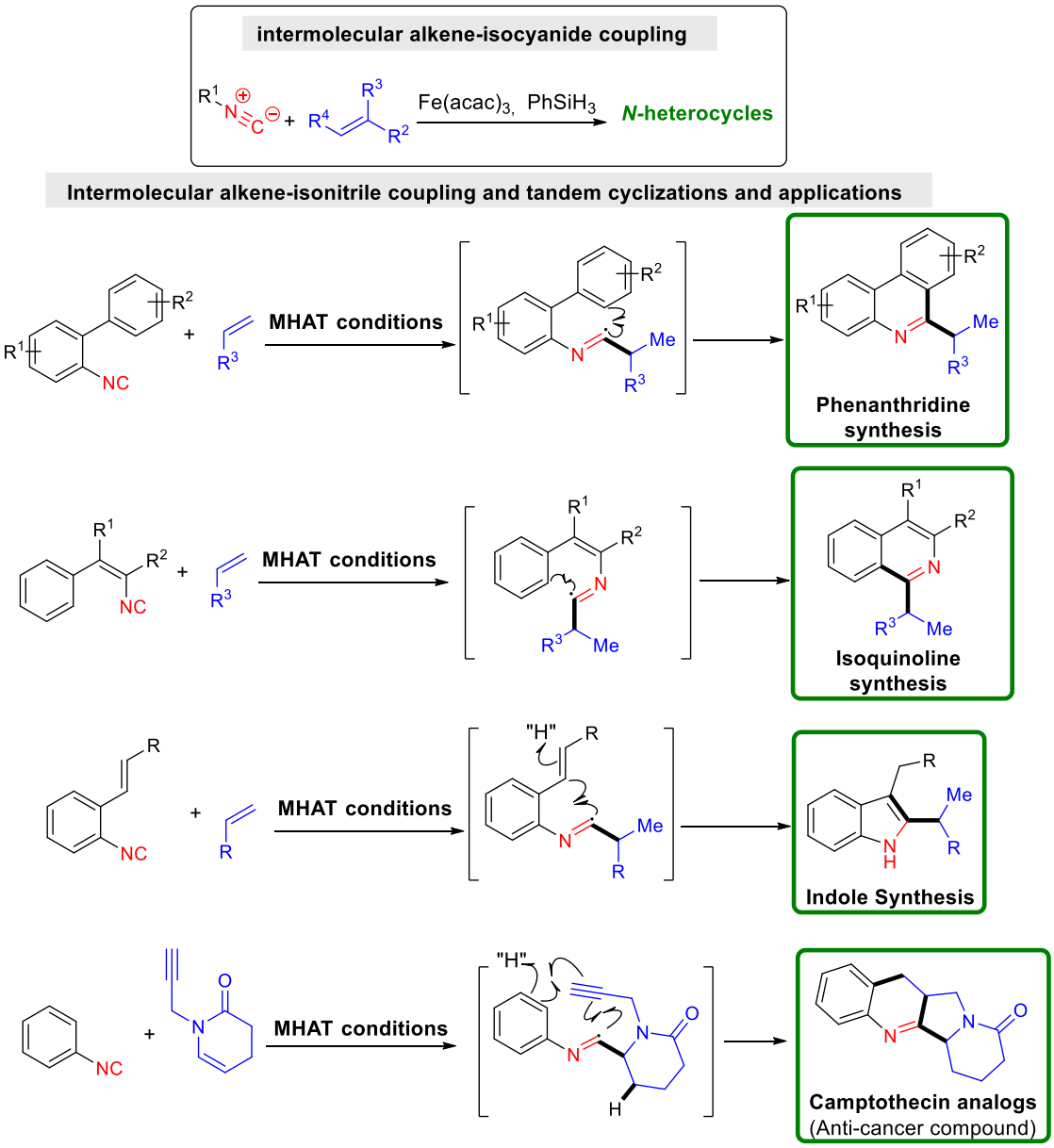

Scheme 2.17. Main objectives of this chapter.

2.3. RESULTS AND DISCUSSION

2.3.1. Synthesis of phenanthridines via MHAT coupling with isocyanides

Synthesis of the substrates

Functionalized biphenylamines **3a-3e** were prepared by a Suzuki coupling,[167] starting from the corresponding bromoanilines (**1a**-**1e**) and phenylboronic acids (**2a**-**2e**). $Pd(OAc)_2$ was employed in catalytic concentration, with K_2CO_3 as a base, in an EtOH/H_2O solution at 100 °C for 2 h. The corresponding biphenylamines were obtained with good to excellent yields without notable differences between electron-donating or electron-withdrawing groups (*see Scheme 2.18*).

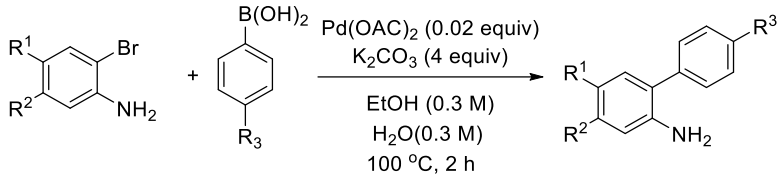

1a, R^1, R^2 = H **2a,** R^3 = H **3a**, R^1, R^2, R^3 = H, **99%**
1b, R^1, R^2 = H **2b**, R^3 = Me **3b**, R^1,R^2 = H, R^3 = Me, **99%**
1c, R^1, R^2 = H **2c,** R^3 = F **3c**, R^1, R^2 = H, R^3 = F, **77%**
1d, R^1 = H, R^2 = MeO **2d**, R^3 = H **3d**, R^1, R^3 = H, R^2 = MeO, **64%**
1e, R^1 = CF_3, R^2 = H **2e**, R^3 = H **3e**, R^1 = CF_3,R^2, R^3 = H, **88%**

Scheme 2.18. Suzuki coupling to achieve functionalized biphenylamines.

Subsequently, the corresponding isocyanides (**4a**-**4e**) were prepared from the functionalized biphenylamines by a two-step procedure (*see Scheme 2.19*).[168] First, the amines were *N*-formylated by refluxing them in toluene with formic acid for 5 h. The formylation was carried out in preliminary tests using acetic formic anhydride,[169] prepared by stirring formic acid and acetic anhydride at 55 °C for 2.5 h. However, the acetylated product was obtained in large quantities and was not reactive in the subsequent dehydration.

In initial attempts, we purified the formamides before the subsequent dehydration step, but we discovered that these compounds had limited stability, resulting in low recovered yields. We therefore proceeded directly to the dehydration of the formamide without further purification.

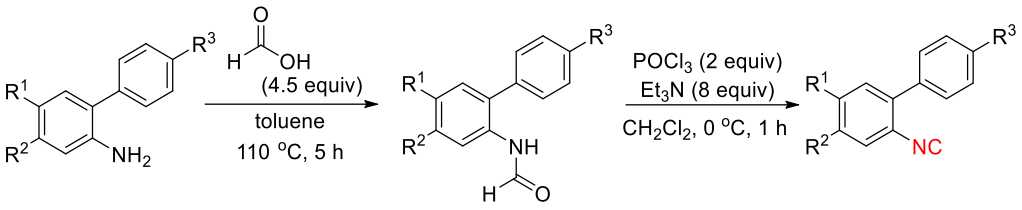

3a, R^1, R^2, R^3 = H
3b, R^1,R^2 = H, R^3 = Me
3c, R^1, R^2 = H, R^3 = F
3d, R^1, R^3 = H, R^2 = MeO
3e, R^1 = CF_3,R^2, R^3 = H

4a, R^1, R^2, R^3 = H, **91%** (*over two steps*)
4b, R^1,R^2 = H, R^3 = Me, **88%** (*over two steps*)
4c, R^1, R^2 = H, R^3 = F, **84%** (*over two steps*)
4d, R^1, R^3 = H, R^2 = MeO, **71%** (*over two steps*)
4e, R^1 = CF_3,R^2, R^3 = H **77%** (*over two steps*)

Scheme 2.19. Dehydration method for the preparation of biphenyl isocyanides.

Once the formamide was formed, the solvent was evaporated under reduced pressure, and the crude was cooled to 0 °C and stirred with Et_3N in dichloromethane. Then $POCl_3$ was added, and after 1 h, the corresponding isocyanides were obtained after purification by column chromatography with good to excellent yields.

Purifying these compounds was straightforward due to their low polarity and the fact that the crude reaction product is usually relatively clean after the work-up. Also, the pungent smell of these isocyanides makes it easy to detect when you have the product.

Reaction optimization

At the start of this work, it was thought that a key challenge in developing the alkene coupling would be the competition between the alkene and the isocyanide group as the metal hydride acceptor. On the first attempts of the alkene coupling, using MHAT conditions, it was seen that a lot of cyclized phenanthridine **5** and the corresponding biphenylamine **3a** was recovered. This led us to conclude that the hydride species formed under the MHAT conditions would directly compete with the alkene radical formed.

With this knowledge, it was decided to optimize the conditions of this reductive cyclization to understand the reaction better and help achieve a chemoselective control when the coupling with the alkene was attempted (*Table 2.1*).

Table 2.1. Optimization table of reductive cyclization to form phenanthridines.

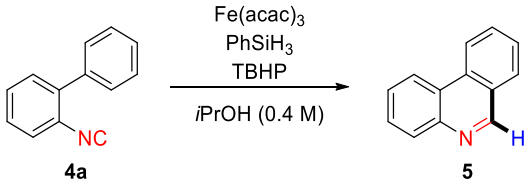

4a **5**

Entry	$Fe(acac)_3$	$PhSiH_3$	TBHP	T°	time	5
1	0.2	1	1.5 [a]	50 °C	2 h	43%
2	0.2	2.5	1.5 [b]	50 °C	2 h	40%
3	0.2 [c]	1	1.5 [b]	50 °C	2 h	55%
4[d]	0.2	1	1.5 [b]	rt	2 h	23%
5	0.2	1	1.5[a]	rt	24 h	51%
6	0.2	3	1.5[a]	rt	24 h	74%
7	0.2	3	1.5[a]	50 °C	24 h	62%
8	1	3	-	rt	2 h	-
9	0.2	3	1[a]	rt	2 h	50%
10	1	3	1[a]	rt	2 h	44%
11	0.2	3	3[a]	rt	2 h	40%

[a]TBHP 70% in water. [b]TBHP 5.5 M in decane. [c]$Fe(acac)_2$ instead of $Fe(acac)_3$. [d]*i*PrOH 0.04 M.

To develop the reductive cyclization, we began our studies by utilizing isocyanide **4a** in the presence of 0.2 equivalent of $Fe(acac)_3$, one equivalent of $PhSiH_3$ and 1.5 equivalent of TBHP in EtOH at 50 °C (*entry 1*), and we observed that phenanthridine **5** was obtained in a moderate yield of 43%. From this point, several factors were modified, such as $PhSiH_3$ equivalents (*entry 2*), catalyst (*entry 3*), oxidant (*entries 2, 3, and 4*), temperature (*entries 4 and 5*), or solvent concentration (*entry 4*). Despite not significantly increasing the yield of the process, these initial experiments indicated that the use of TBHP solution in water and carrying the reaction at room temperature presented some benefits. Also, it was thought that an excess of $PhSiH_3$ could favor the reductive cyclization, so these three conditions were applied together (*entry 6*), and a 74% yield was obtained.

From this point, other changes in conditions were evaluated (*entries 7 to 11*), such as the catalyst loading, reaction time, or combinations of different factors, but no further improvement was obtained.

MHAT coupling

Once we optimized the reductive cyclization conditions, we turned to the MHAT coupling reaction of alkenes, beginning with but-3-en-1-ol as the donor alkene (*Table 2.2*). Using the conditions of the previous work of our group[54] (*entry 1*), trace amounts of the desired compound **5a** were obtained. From this point, different solvents like tetrahydrofuran, *tert*-butanol, acetonitrile, or isopropanol and their concentrations were studied, showing isopropanol in a 0.4 molar concentration as the most appropriate. Various quantities of iron catalyst, phenylsilane, and temperature were studied (*entries 2 to 7*) but did not significantly improve the reaction yield. Only large amounts of reduced phenanthridine **5** were observed. However, we did not quantify how much was formed in these initial exploratory experiments, where we were focused only on obtaining reasonable amounts of the desired coupled product **5a**. It was seen that it could be beneficial to add an oxidant to reoxidize the iron catalyst so we could reduce it to catalytic quantities without compromising the reaction yield (*entry 9*). From this point, significant improvements were achieved in the reaction yield (*entries 9 to 18*), and small changes led us to the best conditions obtained (*entry 18*) with a good 75% yield. From here, other modifications were tried, such as modifying the quantity of isocyanide or alkene (*entries 21* and *22*), using different forms of iron-bearing larger ligands (*entries 17* and *19*), and using another hydride source (*entry 32*). However, no improvements to the reaction were observed. The addition of base (*entries 26 to 29*) was also evaluated to see if it had any benefit in the reoxidation and rearomatizing of the new-formed phenanthridine ring system or preventing undesired H transfer to the isocyanide,[124] but no improvement was found.

Finally, a mechanistic experiment (*entry 37*) demonstrated that the coupling and subsequent cyclization proceeded through radical addition to the isocyanide, not the phenanthridine. When we treated phenanthridine **5** to the optimized conditions from Table 1, no coupled product **5a** was observed, demonstrating that the reaction occurs via a MHAT coupling of the alkene to the isocyanide instead of forming the heterocycle first and then reacting with the alkene via a Minisci-type process.

Table 2.2. Optimization table of MHAT alkene coupling with isocyanides.

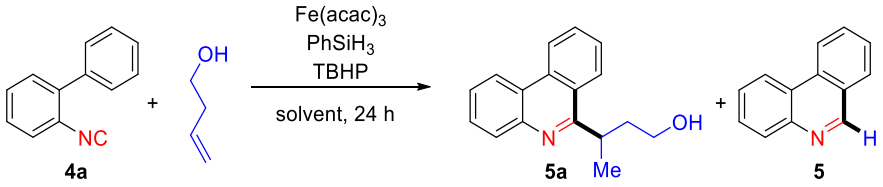

Entry	4a:alk	Fe	$PhSiH_3$	TBHP	solvent	T°	5a	5
1	1:1	1.0	2.5	-	EtOH 0.04 M	rt	9%	-
2	1:1	0.2	2.5	-	EtOH 0.04 M	rt	20%	-
3	1:1	0.2	2.5	-	THF 0.04 M[a]	rt	19%	
4	1:1	2.0	2.5	-	THF 0.04 M[a]	rt	20%	-
5	1:1	2.0	2.5	-	*t*-BuOH 0.04M	rt	6%	-
6	1:1	2.0	2.5	-	MeCN 0.04 M	rt	5%	-
7	1:1	0.4	2.5	-	MeCN 0.04 M	90 °C	29%	-
8	1:1	0.2	1	1.5	MeCN 0.4 M	60 °C	18%	-
9	1:1	0.4	2.5	1.5	*i*PrOH 0.4 M	rt	30%	30%
10	1:1	0.4	1	1.5	*i*PrOH 0.4 M	rt	40%	30%
11	1:1	0.2	1	1.5	*i*PrOH 0.4 M	rt	63%	25%
12	1:1[b]	0.2	1	1.5	*i*PrOH 0.4 M	rt	53%	3%
13	1:1	0.05	1	1.5	*i*PrOH 0.4 M	rt	41%	41%
14	1:1	0.2	0.5	1.5	*i*PrOH 0.4 M	rt	42%	22%
15	1:1	0.2	1[c]	1.5	*i*PrOH 0.4 M	rt	50%	17%
16[d]	1:1	0.2	1	1.5	*i*PrOH 0.4 M	rt	33%	11%
17	1:1	0.2[e]	1	1.5	*i*PrOH 0.4 M	rt	40%	50%
18	1:1	0.2	1	1.5	*i*PrOH 0.4 M	60 °C	75%	13%
19	1:1	0.2[f]	1	1.5	*i*PrOH 0.4 M	60 °C	23%	72%
20	1:1	0.2	1	1.5	*i*PrOH 0.4 M	100 °C	53%	40%
21	2:1	0.2	1	1.5	*i*PrOH 0.4 M	60 °C	40%	35%
22	1:2	0.2	1	1.5	*i*PrOH 0.4 M	60 °C	40%	46%
23	1:1	0.2	1	3	*i*PrOH 0.4 M	60 °C	17%	22%
24	1:1	0.2	1	0.5	*i*PrOH 0.4 M	60 °C	39%	50%
25	1:1	0.2	1	1.5[g]	*i*PrOH 0.4 M	60 °C	42%	10%
26[h]	1:1	0.2	1	1.5	*i*PrOH 0.4 M	60 °C	31%	29%
27[i]	1:1	0.2	1	1.5	*i*PrOH 0.4 M	60 °C	-	-
28[j]	1:1	0.2	1	1.5	*i*PrOH 0.4 M	60 °C	18%	32%
29[k]	1:1	0.2	1	1.5	*i*PrOH 0.4 M	60 °C	33%	45%
30	1:1	0.2	1	1.5	*t*-BuOH 0.4 M	60 °C	43%	29%
31	1:1	0.05	1	1.5	*t*-BuOH 0.4 M	60 °C	54%	36%
32	1:1	0.2	5.5[l]	1.5	*t*-BuOH 0.4 M	60 °C	26%	26%
33	1:1	0.4	1	-	*i*PrOH 0.4 M	rt	38%	20%
34	1:1	0.2	1	1.5	THF[a]	60 °C	23%	52%
35[m]	1:1	0.2	1	1.5	*i*PrOH 0.4 M	rt	32%	30%
36	1:1	0.4	1	1.5	*i*PrOH 0.2 M	rt	30%	40%
37	1[n]:1	0.2	1	1.5	*i*PrOH 0.4 M	60 °C	-	100%

[a]MeOH (10 equiv) was added. [b]Addition of isocyanide by syringe pump. [c]Addition of $PhSiH_3$ by syringe pump. [d]Without argon purge. [e]$Fe(dibm)_3$ instead of $Fe(acac)_3$ was used. [f]$Fe(acac)_2$ instead of $Fe(acac)_3$ was used. [g]DTBP was used as oxidant instead of TBHP. [h]Na_2HPO_4 (1 equiv) used as a base. [i]DBU (0.5 equiv) used as a base. [j]Na_2CO_3 (1.5 equiv) used as a base. [k]$NaHCO_3$ (1 equiv) used as a base. [l]PMHS (5.5 equiv) used instead of $PhSiH_3$. [m]4 h instead of 24 h. [n]**5** was used instead of **4a** as starting material.

Minisci coupling

When different alkenes were tried using the optimized conditions of the previous section, it was found that more substituted alkenes were less effective donors, and low yields of the corresponding products were obtained. It was thought that the increasing stability of the radical donor and increasing steric hindrance shifted the balance of reactivity, making the reductive cyclization more competitive compared to the desired coupling reaction. To overcome this problem, we proposed combining the MHAT reductive cyclization with a Minisci-type reaction (*Table 2.3*).[170] For a detailed explanation of the Minisci reaction see *Section 3.1.2*. For previously developed MHAT-Minisci reactions see *Section 1.1.4* (pages 37–40).

We started our optimization based on the work of Baran,[171] who used boron trifluoride diethyl etherate as a Lewis acid to activate the α-carbon of the nitrogen heterocycle and increase its electrophilicity. Under these conditions, we obtained a moderate 40% yield (*entry 1*) of the coupled compound **5l**. Interestingly, unlike typical Minisci reactions, no reoxidation of the ring was observed, and the only product obtained was the reduced compound. We then changed the acid to trifluoroacetic acid, and the reaction yield increased dramatically to 86%.

With this promising result, we decided to see if reducing the quantity of iron catalyst by adding an oxidant to the reaction was possible. (*entries 3 and 4*), but the yield dramatically decreased to 10-12%. Evaluation of different solvents (*entries 5-17*) in combination with an oxidant did not improve initial results and led us to return to using THF/MeOH mixtures. Interestingly, reexamination of the use of this solvent combination with an oxidant led to none of the product **5h** being formed. Further analysis determined that this was due to a furan-coupled subproduct that had formed in the reaction, presumably from the THF used as the solvent, leading us to abandon the use of an oxidant in the reaction (the structure of this compound will be discussed in the next section). Further optimization established that increasing the reaction time to 24 h, not purging the reaction, and leaving the flask open to air was beneficial for the reaction yield, allowing us to obtain the desired coupled heterocycle in an excellent 94% yield (*entry 29*).

Table 2.3. Optimization table for Minisci alkene coupling with phenanthridine.

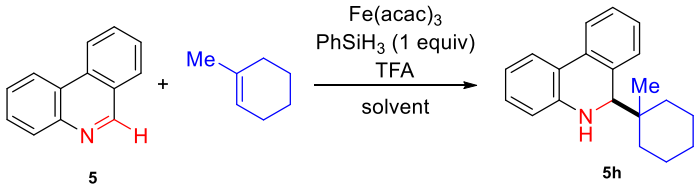

5 5h

Entry	5:alk	Fe(acac)$_3$	TBHP	Acid	solvent	T°	time	5h
1	1:3	1	-	2[a]	THF/MeOH 0.2 M	60 °C	2 h	40%
2	1:3	1	-	2	THF/MeOH 0.2 M	60 °C	2 h	86%
3	1:3	0.2	1.5	2[a]	THF/MeOH 0.2 M	60 °C	2 h	12%
4	1:3	0.2	1.5	2	THF/MeOH 0.2 M	rt	2 h	10%
5	1:3	0.4	1	2	*i*PrOH 0.2 M	rt	2 h	31%
6	1:3	0.4	1	2	CH_2Cl_2 0.2 M	40 °C	7 h	25%
7	1:3	0.4	1.5	2	Toluene/MeOH 0.2M	60 °C	24 h	42%
8	1:3	0.4	1.5	2	MeCN/MeOH 0.2 M	60 °C	24 h	26%
9	1:3	0.4	1.5	2	*t*-BuOH/MeOH 0.2M	60 °C	24 h	35%
10	1:3	0.4	1.5	2	DMF/MeOH 0.2 M	60 °C	24 h	17%
11	1:3	0.4	1.5	2	DCE/MeOH 0.2 M	60 °C	24 h	37%
12	1:3	1	1.5	2	DCE/MeOH 0.2 M	60 °C	24 h	29%
13[b]	1:3	0.4	1.5	2	DCE/MeOH 0.2 M	60 °C	24 h	38%
14	1:3	0.2	1.5	2	EtOH 0.2 M	60 °C	24 h	63%
15	1:3	0.2	1.5	2	DCE 0.2 M	60 °C	24 h	34%
16	1:3	0.2	1.5	2	DCE/MeOH 0.2 M	60 °C	24 h	35%
17	1:3	1	-	2	*i*PrOH 0.2 M	60 °C	3 h	30%
18	1:3	0.2[c]	1.5	2	THF/MeOH 0.2 M	rt	2 h	11%
19[d]	1:3	0.2[c]	1.5	2	THF/MeOH 0.2 M	rt	2 h	-
20[d]	1:3	0.2:0.2[c]	1.5	2	THF/MeOH 0.2 M	rt	4 h	-
21[d]	1:3	0.2[c]	1.5	2	THF/MeOH 0.2 M	rt	4 h	-
22[e]	1:3	1	-	2	THF/MeOH 0.2 M	60 °C	2 h	-
23	1:3	1	1.5[f]	2	THF/MeOH 0.2 M	60 °C	4 h	45%
24[g]	1:3	0.2	-	2	THF/MeOH 0.2 M	60 °C	24 h	31%
25[h]	1:3	1	-	2	THF/MeOH 0.2 M	60 °C	2 h	-
26	1:3	0.2	-	2	THF/MeOH 0.2 M	60 °C	2 h	25%
27	1:3	1	-	2	THF/MeOH 0.2 M	60 °C	24 h	44%
28	1:3	1	-	-	THF/MeOH 0.2 M	60 °C	24 h	5%
29[g]	1:3	1	-	2	THF/MeOH 0.2 M	60 °C	2 h	94%

[a]$BF_3{\cdot}Et_2O$ added instead [b]2.5 equiv of $PhSiH_3$ was added. [c] $Fe(acac)_2$ was used instead. [d]No $PhSiH_3$ was added. [e]After 2 h chloranil (2 equiv) was added. [f]TBHP was added after 2 h of reaction. [g]Without argon purge. [h]MnO_2 added after the reaction is completed.

MHAT-Minisci combined conditions

Once we proved the Minisci-type reaction as a viable alternative for the coupling of more substituted alkenes with the heterocycle, we envisioned the possibility of forming it from the corresponding isocyanide by one-pot synthesis by combining the reductive cyclization and by the Minisci coupling reaction together (*Table 2.4*).

*Table 2.4. Optimization table for MHAT cyclization-Minisci alkene coupling from isocyanide **4a**.*

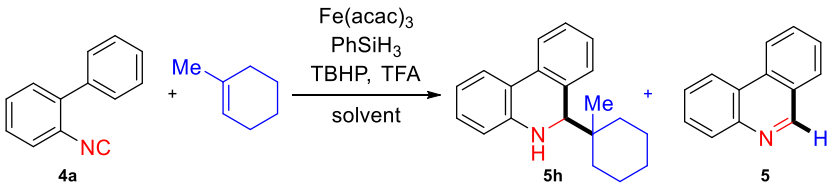

Entry	4a:alk	$Fe(acac)_3$	$PhSiH_3$	TBHP	TFA	solvent	T°	time	5h	5
1	1:3	1	1	-	2[a]	THF/MeOH 0.2 M	60 °C	2 h	-	-
2[b]	1:3	1	1	-	2[a]	THF/MeOH 0.2 M	60 °C	2 h	30%	-
3[c]	1:3	2	2.5	-	2	*i*PrOH 0.2 M	60 °C	2 h	20%	-
4	1:3	0.2	1	1.5	2	THF/MeOH 0.2 M	rt	2 h	20%	
5[d]	1:3	1	3	1	2	MTBE/MeOH 0.2 M	rt to 60 °C	2.5 h	56%	-

[a]$BF_3{\cdot}Et_2O$ added instead. [b]Acid was added 1 hour later. [c]Acid and alkene were added 10 min after the addition of $PhSiH_3$. [d]See *Supporting Information*: Method 3 - Sequential MHAT-Minisci Coupling from the corresponding isocyanide.

Studies began using the conditions we had tested as best for Minisci coupling, but the coupled product (*entry 1*) was not obtained. It was then decided to add the Lewis acid an hour later to let the reductive cyclization come to completion, and then, once the heterocycle was formed, activate the nitrogen to allow the Minisci reaction to proceed with the alkene coupling (*entry 2*). In this case, a small amount of product was observed. Using isopropanol as a solvent and increasing the equivalents of phenylsilane was tried next but was detrimental to the reaction yield (*entry 3*). Next, we tried to make the reaction catalytic by decreasing the iron equivalents and adding an oxidant. Unfortunately, this gave low yields as we obtained a significant amount of the product **5j** resulting from the coupling of tetrahydrofuran with the heterocycle (*Scheme 2.20*). This secondary reaction led us to study what was happening to understand the reaction better, and the results will be extensively discussed in *Chapter 3* of this thesis.

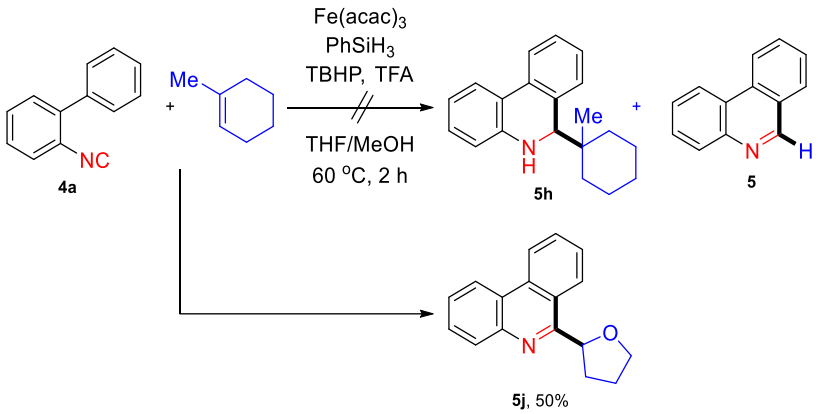

Scheme 2.20. Formation of unexpected ether coupling.

At this point, seeing that adding an oxidant could lead to the coupling of ethers with the heterocycle, it was decided to choose a solvent that would be unlikely to carry out this coupling, such as methyl *tert*-butyl ether (MTBE). We proposed that since the energy barrier to forming a primary radical would be higher and would likely not form.

A two-step protocol was then established to carry out a one-pot synthesis. This consists in first adding an equivalent of the isocyanide, accompanied by 0.2 equivalents of $Fe(acac)_3$, and dissolving it in a 0.4 molar solution in a 4:1 ratio of methyl *tert*-butyl ether and methanol. To this solution degassed with argon, one equivalent of *tert*-butyl hydroperoxide and three equivalents of phenylsilane are added and allowed to react for 15 minutes at room temperature. The reaction flask is then opened to air, MTBE is added to a concentration of 0.2 molar, 0.8 equivalents of $Fe(acac)_3$, two equivalents of trifluoroacetic acid, and three equivalents of alkene are added, and the reaction is left for three hours at 60 °C.

As can be seen, these conditions come from putting together the best conditions used to perform the reductive cyclization first, followed by the best conditions found to perform the Minisci reaction. This protocol allowed us to obtain the desired product **5h** in 56% yield in a one-pot reaction. Therefore, it allows us to increase the range of compounds we can obtain from isocyanides, achieving our goal of using the HAT methodology to couple alkenes to generate functionalized nitrogen heterocycles.

Substrate scope

With the optimized conditions, we investigated the reaction scope using different isocyanides and alkenes. All the alkenes used in the study were commercially available, except for but-3-en-1-yl benzoate and 2-(but-3-en-1-yl)isoindoline-1,3-dione, which were prepared according to standard procedures as indicated below (*Scheme 2.21*).

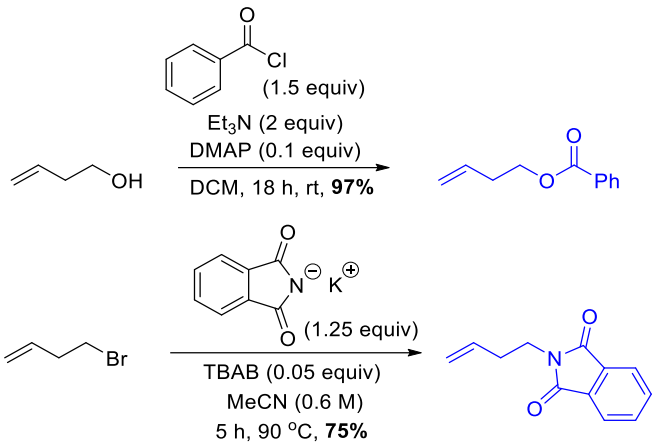

Scheme 2.21. Synthesis of non-commercially available alkenes.

Different alkenes were investigated, with other functional groups and chain lengths (*Scheme 2.22*). First, the MHAT coupling protocol (Method A) was applied for the less-hindered alkenes, obtaining moderate to good yields for all the alkenes studied. As expected, the yields dropped dramatically when this protocol was used with more substituted alkenes. For this reason, we used the Minisci method (Method B) from the corresponding heterocycle **5** to obtain the desired compounds. As discussed previously, compound **5h**, the product of coupling with a tertiary radical, produced only the reduced form. The same was observed for the formation of **5i**. Subsequent attempts to oxidize these compounds with MnO_2 were unsuccessful. Attempts to use 2,3-dihydrofuran as an alkene to evaluate the introduction of heteroatoms into the coupled products only gave traces of the corresponding product **5j** which stands in contrast to the easy manner it could be formed using the conditions of *Scheme 2.20*. With the scope of the coupling evaluated, we then showed it was feasible to prepare compounds **5f**-**5i** directly from the isocyanide **4a** via the one-pot combined HAT-Minisci conditions we had developed (Method C).

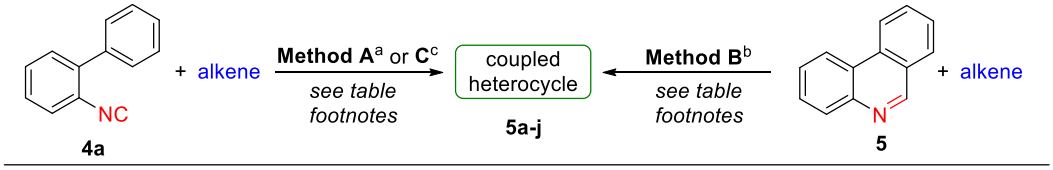

Alkene	Product	Alkene	Product
	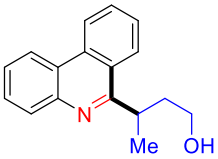 **5a**, Method **A**: 75% Method **B**: 21%		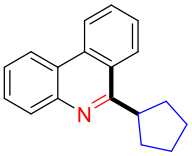 **5f**, Method **A**: 26% Method **B**: 70% Method **C**: 62%
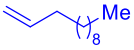	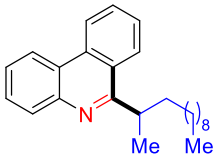 **5b**, Method **A**: 54% Method **B**: 63%		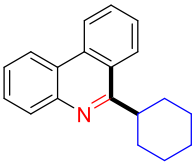 **5g**, Method **A**: 14% Method **B**: 63% Method **C**: 58%
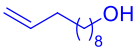	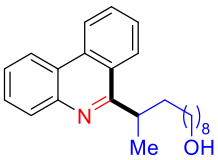 **5c**, Method **A**: 59% Method **B**: 71%	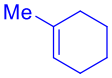	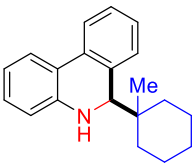 **5h**, Method **A**: 5% Method **B**: 94% Method **C**: 56%
	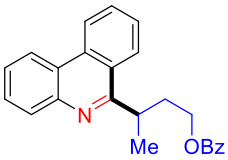 **5d**, Method **A**: 53% Method **B**: 76%	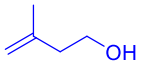	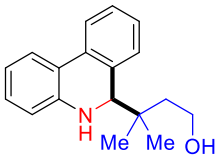 **5i**, Method **A**: nd Method **B**: 86% Method **C**: 52%
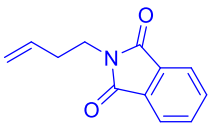	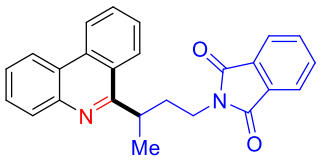 **5e**, Method **A**: 62% Method **B**: 76%		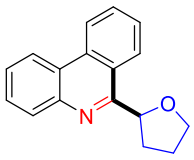 **5j**, Method **A**: traces Method **C**: traces

*Scheme 2.22. Substrate scope of HAT coupling between isocyanide **4a** and alkenes.* [a]Method **A:** Isocyanide/alkene (1:1), $Fe(acac)_3$ (0.2 equiv), $PhSiH_3$ (1 equiv), *i*PrOH [0.4 M], TBHP (1.5 equiv), 60 °C, 24 h. [b]Method **B:** Phenanthridine/alkene(1:3), $Fe(acac)_3$ (1 equiv), TFA (2 equiv), $PhSiH_3$ (1 equiv), THF/MeOH (0.2 M, 4:1), 3 h, 60 °C, open to air. [c]Method **C:** Isocyanide (1 equiv), $Fe(acac)_3$ (1 equiv), $PhSiH_3$ (3 equiv), TBHP (1 equiv), MTBE/MeOH (0.2 M), rt, 15 min, then TFA (2 equiv), alkene (3 equiv), 60 °C, 2.5 h, open to air.

Next, we evaluated the coupling of the differently substituted 2-isocyanobiphenyls **4b-4e** (*Scheme 2.23*). The corresponding phenanthridines **5k**-**5n** were prepared in good yields, and no significant effect of the substituent (either electron-donor or electron-withdrawing) was observed to influence the reaction outcome.

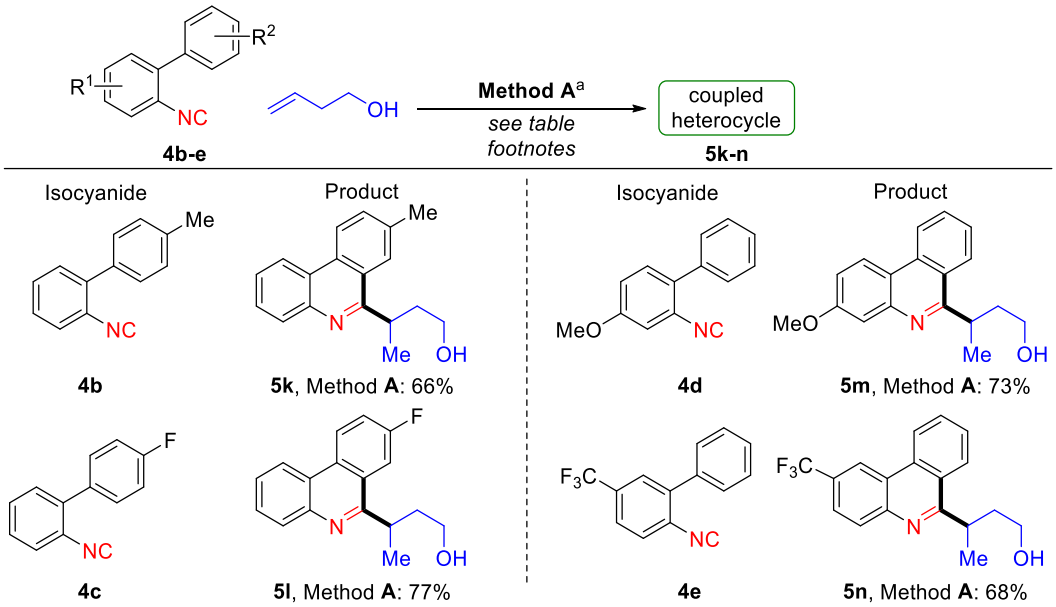

Scheme 2.23. Substrate scope of substituted isocyanides with but-3-en-1-ol. [a]Method **A**: Isocyanide/alkene (1:1), $Fe(acac)_3$ (0.2 equiv), $PhSiH_3$ (1 equiv), iPrOH [0.4 M], TBHP (1.5 equiv), 60 °C, 24 h.

Mechanistic discussion

The proposed mechanism for the reaction is outlined in *Scheme 2.24*. Phenylsilane acts as a hydride donor to form an iron hydride species, which adds to the alkene to generate a carbon-centered radical **A**, which adds to the isocyanide to form the corresponding imidoyl radical **B**. This imidoyl intermediate will go through the subsequent 6-*endo*-trig cyclization to generate the cyclohexadienyl radical **C**, which will be deprotonated by hydroxyl anion which is formed by the reaction of TBHP and Fe^{II} to give the anion **D**. This anion reduces TBHP by a single electron transfer to provide the desired coupled product **5a**. Alternatively, intermediate radical **C** can undergo a one-electron oxidation via Fe^{III} species or TBHP, resulting in rearomatization. Finally, the catalytic cycle is completed by the oxidation of Fe^{II} species by TBHP.

On the other hand, if HAT from the iron hydride species occurs to **4a** (i.e., in the absence of alkene), the non-coupled product **5** will be formed instead through the analogous process to that previously mentioned. The addition of TFA at this point activates the heterocycle to give the intermediate **E**, allowing the Minisci coupling reaction with more impeded alkenes. Initially, the formation of intermediate **F** and a subsequent reoxidation produced by a SET process from the Fe^{III} species would provide intermediate **G** that provides product **5g** (R^2 = H), which is then deprotonated upon work-up. In the case of trisubstituted alkenes (R^2 = Me), the additional steric impediment inhibits the process, resulting in a SET process directly to the nitrogen and obtaining the reduced heterocycle **5h.**

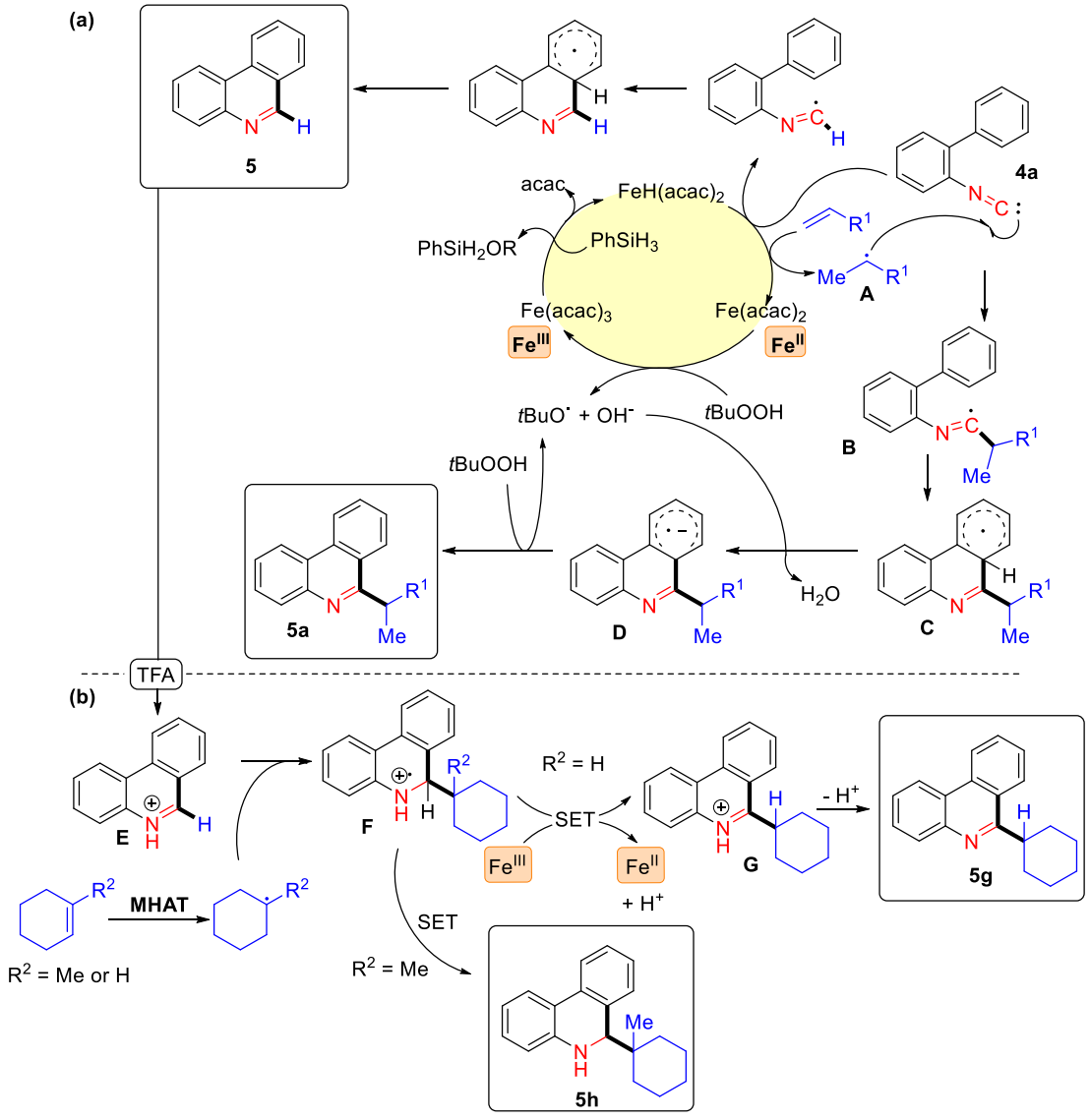

Scheme 2.24. Proposed mechanism for the MHAT couplings with isocyanides (a) direct coupling of the alkene (b) switching to MHAT-Minisci coupling mode via the addition of TFA.

Notably, without the addition of TFA, the Minisci reaction does not take place to any significant degree (*Table 2.3, entry 28*), discarding the possibility that the heterocycle is the coupling partner instead of isocyanide, for example, under the optimized conditions of *Table 2.2*. This possibility is also discarded, as commented above, in *Table 2.2* (*entry 37*), where it was proven that starting from phenanthridine **5** and applying optimized conditions for HAT coupling, no coupled product could be observed, and only non-reacted heterocycle could be recovered from the reaction.

2.3.2. Studies towards the Camptothecin nuclei

Seeing the potential of MHAT reactions to couple alkenes with isocyanide acceptors to generate nitrogen heterocycles, we next decided to attempt to emulate Curran's synthesis of Camptothecin (*see Section 2.1.2, Scheme 2.5*).

In our design, unlike Curran's work, where he started from an alkyl halide to generate the radical, it was thought that 3,4-dihydropyridinone **B** could act as a radical donor for a subsequent addition to phenyl isocyanide **A**. The resulting imidoyl radical would add to the alkyne to form a vinyl radical, which would then add to the aromatic ring. Rearomatization would then give the final product (*see Scheme 2.25*).

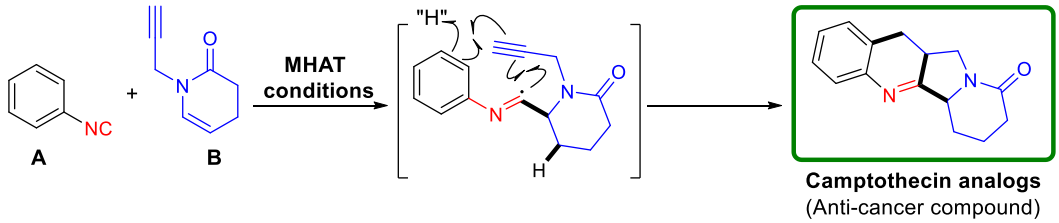

Scheme 2.25. MHAT conditions to generate Camptothecin analogs.

Synthesis of the substrates

The preparation of the used alkene (*Scheme 2.26*)[172] started with the *N*-alkylation of glutarimide **6** using 3-bromoprop-1-yne to introduce the propargyl group, using K_2CO_3 and TBAI suspended in acetone at room temperature for 20 h.

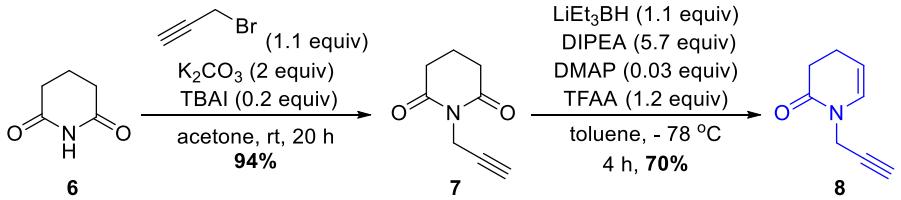

Scheme 2.26. Preparation of 1-(prop-2-yn-1-yl)-3,4-dihydropyridin-2(1H)-one.

The corresponding 1-(prop-2-yn-1-yl)piperidine-2,6-dione **7** was afforded in an excellent 94% yield. Subsequent reduction of the carbonyl with $LiEt_3BH$ (SuperHydride), with DIPEA, DMAP, and TFAA in toluene at -78 °C for 4 h, gave the reduced product **8** in a 70% yield.

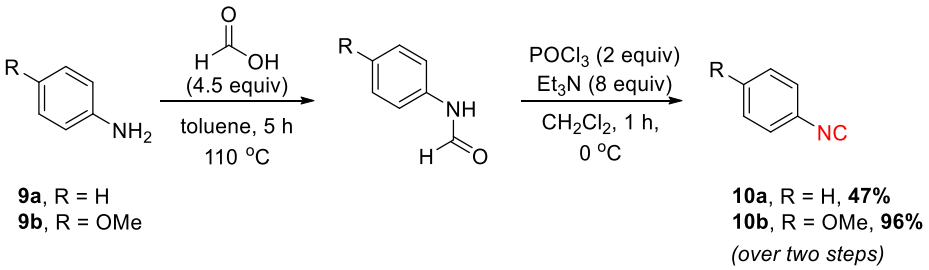

Scheme 2.27. Preparation of phenyl isocyanides.

The isocyanides **10a** and **10b** were prepared according to the above-mentioned dehydration method of the formamides prepared from the corresponding amines **9a** and **9b** (*Scheme 2.27*).

The volatility of compound **10a** proved problematic, making isolation challenging. Solvent removal had to be carried out by controlled distillation at atmospheric pressure instead of on a rotary evaporator. This resulted in a lower yield than for compound **10b**, which could be handled more straightforwardly. In both cases, the foul smell of the resulting isocyanides made the manipulation extremely unpleasant.

Reaction optimization

Once the starting materials were synthesized, the MHAT-triggered tandem radical cyclization was evaluated. Unfortunately, employing the conditions previously studied for phenanthridine cyclization was unsuccessful, and only complex mixtures were isolated. Attempts were made to purify the mixture to see if any of the desired products or related intermediates could be detected; however, no conclusive evidence could be found that the reaction was taking place (*Table 2.5*). We tried switching to the alternative Fe catalyst $Fe(dpm)_3$, which is known to work better for alkenes with an adjacent heteroatom (*entries 2 and 3*);[31] however, no product was detected. The use of isocyanide **10b** (*entry 4*) was also unsuccessful. Given our experience with the competitive reduction of the isocyanide moiety during our phenanthridine studies, it seemed likely that this unwanted reaction might play a significant part as the

isocyanides are less impeded than those studied previously (e.g., isocyanide **4a**). Therefore, with these unfruitful initial results and consideration of the potential difficulty of the reaction, it was decided to put these studies on one side and study the synthesis of other heterocycles, which showed more promising initial results.

Table 2.5. Reaction optimization table of MHAT cyclization.

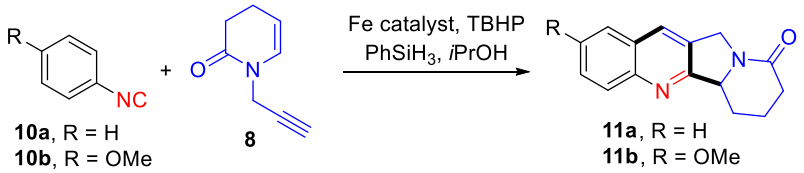

Entry	10a:8	Fe	$PhSiH_3$	TBHP	*i*PrOH	T°	Time	11
1	1:1	0.2[a]	1	1.5	0.4 M	50 °C	24 h	-
2	1:1	1[b]	1	-	0.04 M	rt	24 h	-
3	1:1	0.2[b]	1	1.5	0.04 M	100 °C	24 h	-
4	1[c]:1	0.2[a]	1	1.5	0.4 M	50 °C	24 h	-

[a]$Fe(acac)_3$ used as Fe catalyst. [b]$Fe(dibm)_3$ used as Fe catalyst. [c]**10b** was used as isocyanide.

2.3.3. Synthesis of isoquinolines via MHAT coupling with isocyanides

Synthesis of the substrates

The preparation of 2-isocyano-3,3-diphenylacrylate **14** (*Scheme 2.28*) started with the condensation of benzophenone **12** and methyl 2-isocyanoacetate using NaH as a base in THF at room temperature for 2 hours. After recrystallization from methanol, formamide **13** was obtained with a good 77% yield.[173] Subsequent dehydration of the formamide was carried out using the protocol mentioned above to provide the corresponding isocyanide **14** in an excellent 90% yield.

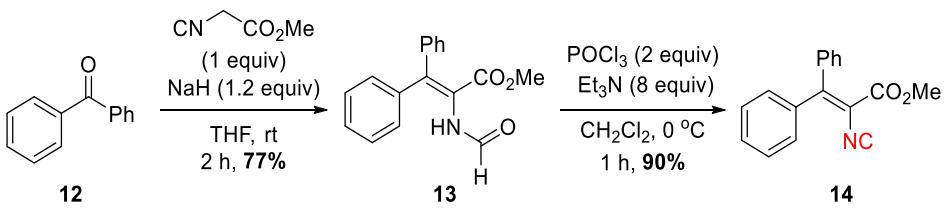

Scheme 2.28. Preparation of 2-isocyano-3,3-diphenylacrylate.

Reaction optimization

Reductive cyclization

While studies of phenanthridine were in progress, we had started investigating the synthesis of isoquinolines. This reaction was thought to share many similarities with the MHAT synthesis of phenanthridines, so similar reaction conditions were used as the initial starting point.

We started with the optimization of the core heterocycle by omitting the alkene using the same conditions as phenanthridine studies (*Table 2.6*). However, only a poor 9% yield of the desired product **15** was obtained. From this point, modifications such as solvent (*entry 2*), temperature (*entry 3*), iron source (*entry 4*), or TBHP (*entry 5*) were applied. These initial tests showed us that the reaction worked best at room temperature, and *tert*-butyl peroxide was better in a 70% water solution than in a 5.5 M anhydrous decane solution. Finally, by increasing the phenylsilane to three equivalents, we could achieve an excellent 86% yield (*entry 6*).

Table 2.6. Optimization table for reductive cyclization of isoquinoline.

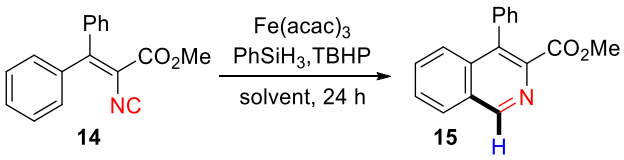

Entry	$Fe(acac)_3$	$PhSiH_3$	TBHP	solvent	T°	15
1	0.2	1	1.5[a]	*i*PrOH 0.4 M	50 °C	9%
2	0.2	1	1.5[a]	THF 0.4 M[b]	50 °C	9%
3	0.2	1	1.5[a]	*i*PrOH 0.4 M	rt	34%
4	0.2[c]	1	1.5[d]	*i*PrOH 0.4 M	rt	51%
5	0.2	1	1.5[d]	*i*PrOH 0.4 M	rt	83%
6	0.2	3	1.5[d]	*i*PrOH 0.4 M	rt	86%

[a]TBHP 5.5 M in decane. [b]MeOH (10 equiv) were added. [c]$Fe(acac)_2$ was used instead of $Fe(acac)_3$. [d]TBHP 70% in water.

MHAT coupling

Next, we optimized the MHAT coupling of alkenes with isoquinolines (*Table 2.7*). We started by applying the best conditions for phenanthridines (*see Table 2.2, entry 18*), but unfortunately, a poor yield of coupled product was obtained. Next, we tried varying the concentration of solvent (*entry 2*) and increasing the equivalents of phenylsilane (*entry 3*), but this did not result in a significant increase in reaction yield. When the reaction was carried out at room temperature instead of at 60 °C, a slight improvement in the yield was observed (*entry 4*). We then screened different concentrations of Fe, solvent concentration, and equivalents of phenylsilane (*entries 4 to 8*), until a good yield of 61% could be reached, using 0.2 equivalents of $Fe(acac)_3$, 3 equivalents of phenylsilane, room temperature and a 0.4 M concentration of isopropanol (entry 9).

In summary, the key differences with respect to the HAT coupling of phenanthridines with alkenes lie in the fact that three equivalents of phenylsilane are needed instead of one, and room temperature instead of heating to 60 °C. These conditions were denoted as Method A.

Table 2.7. Optimization table for the HAT coupling with alkene.

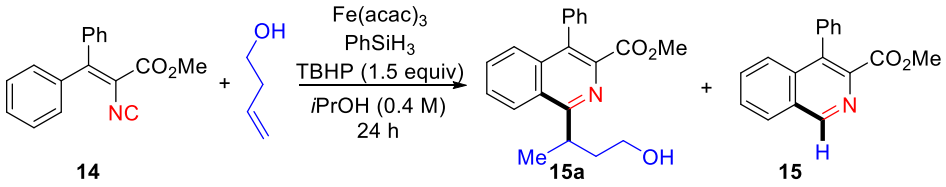

Entry	14:alk	$Fe(acac)_3$	$PhSiH_3$	T°	15a	15
1[a]	1:1	0.2	1	60 °C	23%	29%
2[a,b]	1:1	0.2	1	60 °C	17%	-
3[a]	1:1	0.2	3	60 °C	21%	40%
4[a,b]	1:1	0.2	3	rt	46%	38%
5[a]	1:1	0.2	1	rt	38%	40%
6[a]	1:1	0.4	3	rt	33%	57%
7[a]	1:1	0.1	3	rt	25%	54%
8[c]	1:1	0.2	3	rt	53%	22%
9[a]	1:1	0.2	3	rt	61%	27%

[a]TBHP 70% in water. [b]*i*PrOH (0.04 M). [c]TBHP 5.5 M in decane.

Minisci coupling

To carry out the Minisci reaction, the best conditions of the phenanthridines (*Table 2.3, entry 29*) were taken as the initial starting point and modified according to the previous observations for isoquinolines. Three equivalents of phenylsilane and room temperature were used to obtain good yields (see the scope in *Scheme 2.29*). As a result, no further optimization was carried out. Therefore, the conditions used consisted of one equivalent of heterocycle **15**, three equivalents of alkene, one equivalent of $Fe(acac)_3$, two equivalents of TFA, and three equivalents of phenylsilane in a 0.2 M mixture of tetrahydrofuran in methanol in a ratio of 4: 1, at room temperature for 3 hours. These conditions were denoted as Method B.

MHAT-Minisci combined conditions

Finally, the sequential MHAT-Minisci synthesis was attempted to couple more hindered alkenes to the isocyanide **14**. To do this, the optimized conditions of the phenanthridines were used (see *Table 2.4, entry 5*), and we obtained the desired products **15d** and **15e** with good yields (*see Scheme 2.29*). These conditions were denoted as Method C.

Substrate scope

The scope of the reaction is illustrated in *Scheme 2.29,* where we applied the three different methods we had developed to synthesize isoquinolines. Coupling the isocyanide **14** with the different alkenes gave the substituted isoquinolines **15a**-**15e** in moderate to good yields. Notably, the addition of trisubstituted alkenes only gave fully oxidized products unlike in the phenanthridine series.

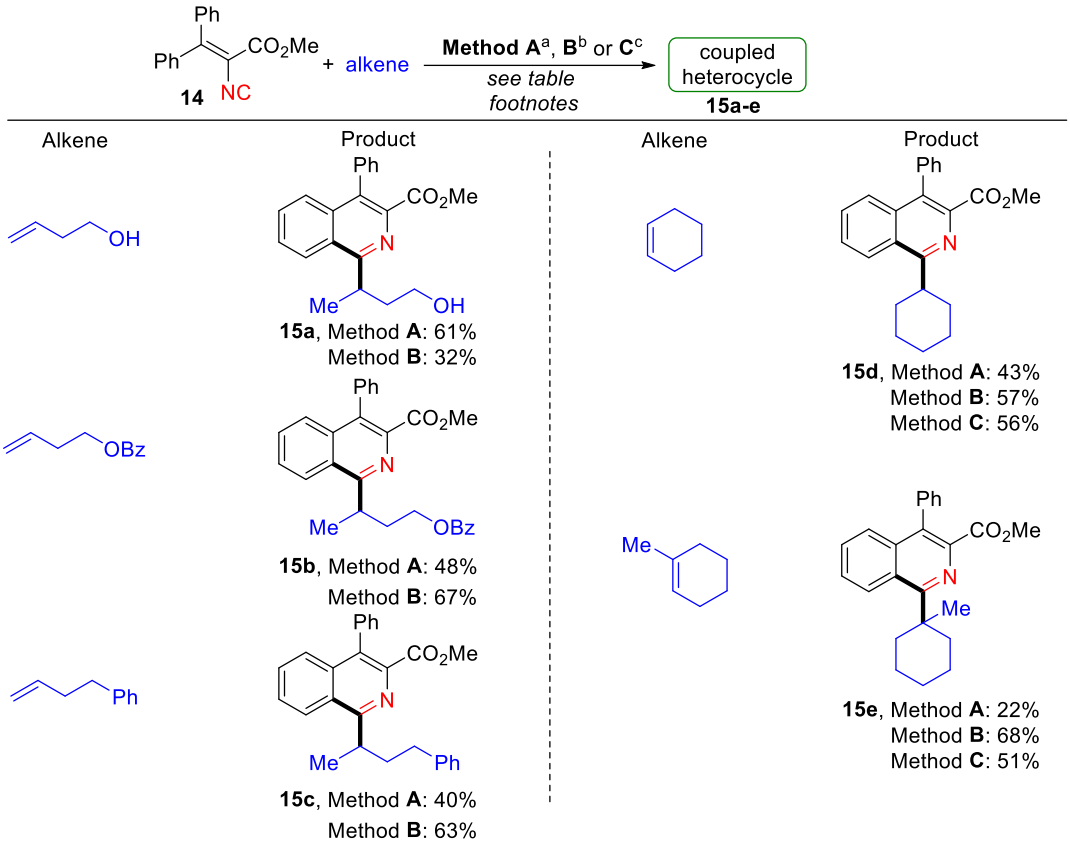

Scheme 2.29. Scope table of coupled isoquinolines. [a]Method **A**: Isocyanide/alkene (1:1), $Fe(acac)_3$ (0.2 equiv), $PhSiH_3$ (3 equiv), *i*PrOH [0.4 M], TBHP (1.5 equiv), rt, 24 h. [b]Method **B**: Isoquinoline/alkene(1:3), $Fe(acac)_3$ (1 equiv), TFA (2 equiv), $PhSiH_3$ (3 equiv), THF/MeOH (0.2 M, 4:1), 3 h, rt, open to air. [c]Method **C**: $Fe(acac)_3$ (1 equiv), $PhSiH_3$ (3 equiv), TBHP (1 equiv), MTBE/MeOH (0.2 M), rt, 15 min, then TFA (2 equiv), alkene (3 equiv), 60 °C, 2.5 h, open to air. [c]Isocyanide/alkene (1:1), $Fe(acac)_3$ (0.2 equiv), $PhSiH_3$ (1 equiv), *i*PrOH (0.04 M], rt, 24 h.

Mechanistic discussion

The proposed mechanism for this reaction occurs very similarly to that previously outlined for phenanthridines (*Scheme 2.30*). The reaction begins by forming the metal hydride species, which adds to the double bond, generating the radical **A** on the most substituted carbon. This will add on the isocyanide, generating the imidoyl intermediate **B**, which will carry out the subsequent 6-*endo*-trig cyclization, forming the cyclohexadienyl radical **C**. A hydroxyl anion then deprotonates **C** to generate the **D** anion, which is then oxidized by the TBHP, giving the coupled isoquinoline **15a**.

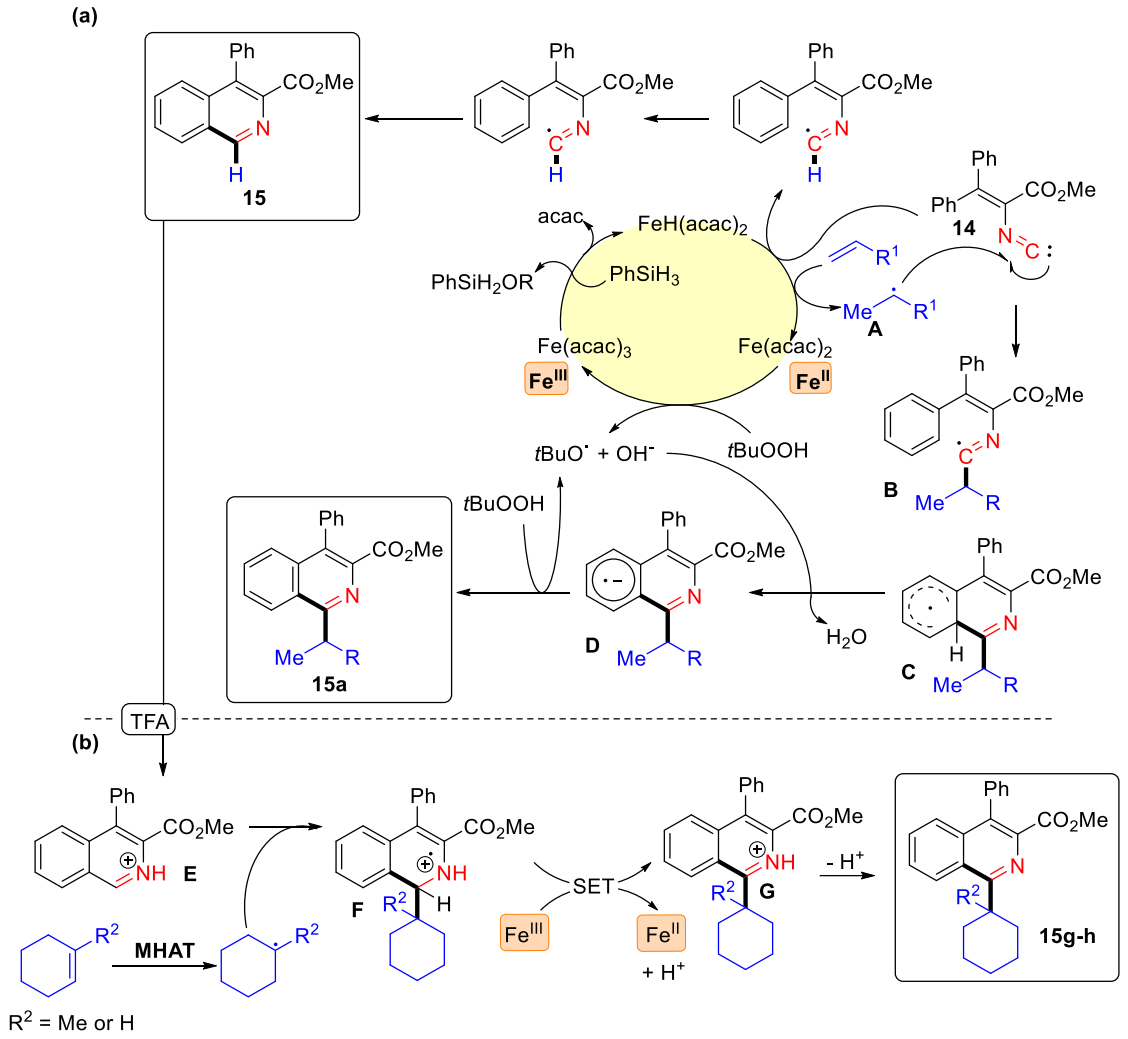

Scheme 2.30. Proposed mechanism for the MHAT couplings with isocyanides (a) direct coupling of the alkene (b) switching to MHAT-Minisci coupling mode via the addition of TFA.

Alternatively, if the hydrogen atom transfer from the metal hydride occurs to compound **14**, product **15** will be analogous to that described for **15a**. In this case, adding TFA will activate our heterocycle to give intermediate **E**, allowing the Minisci reaction to occur with more hindered alkenes. This activated heterocycle will be attacked by the radical formed on the alkene through a HAT process to form intermediate **F**, where the subsequent reoxidation produced by a SET process by Fe^{III} species will give intermediate **G**, which through deprotonation will allow us to obtain the desired products **15g** and **15h**.

2.3.4. Synthesis of indoles via MHAT coupling with isocyanides

Synthesis of the substrates

The preparation of isocyanide **19** (*Scheme 2.31*) started with condensing 2-nitrobenzaldehyde **16** and acetophenone, using NaOH as a base in methanol at room temperature to obtain the nitrophenyl compound **17**. Subsequently, the nitro group was reduced with iron powder and hydrochloric acid in ethanol to give the corresponding aniline **18**.[174]

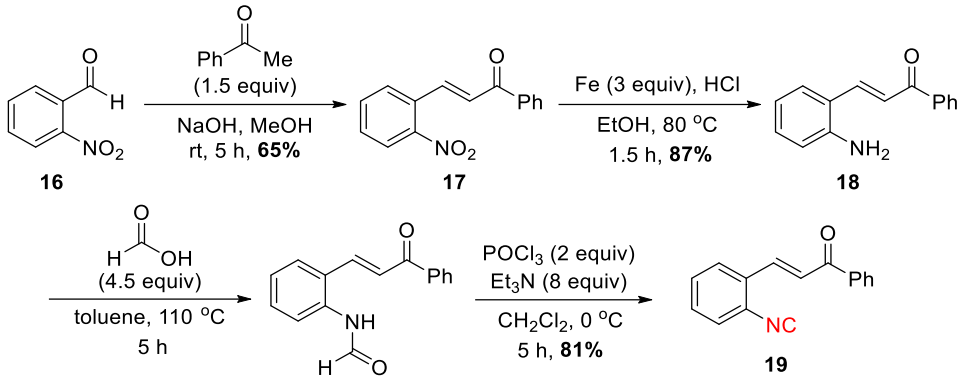

Scheme 2.31. Preparation of 3-(2-isocyanophenyl)-1-phenylprop-2-en-1-one.

The final conversion to the corresponding isocyanide **19** was carried out analogously to the previous synthesis of isocyanides, with the formylation and subsequent dehydration.

For the preparation of compound **24**, the synthesis started with the Horner–Wadsworth–Emmons reaction of compound **21** with 2-nitrobenzaldehyde **16**. For this reaction, compound **21** was previously prepared by an Arbuzov reaction of the ethyl 2-bromoacetate **20** with triethyl phosphite (*Scheme 2.32*).[175]

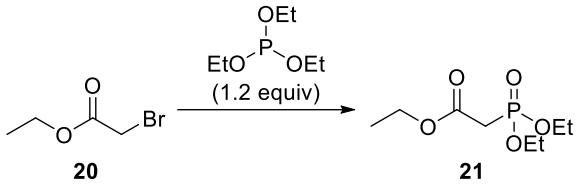

Scheme 2.32. Preparation of ethyl 2-(diethoxyphosphoryl)acetate.

Once the nitro compound **22** was prepared, the preparation proceeded with the reduction of the nitro group to the corresponding amine using the conditions above-mentioned for the synthesis of compound **19** to obtain compound **23** *(Scheme 2.33)*.

Once the amine was synthesized, the preparation of the corresponding isocyanide followed the same steps as the previous synthetic routes.[176]

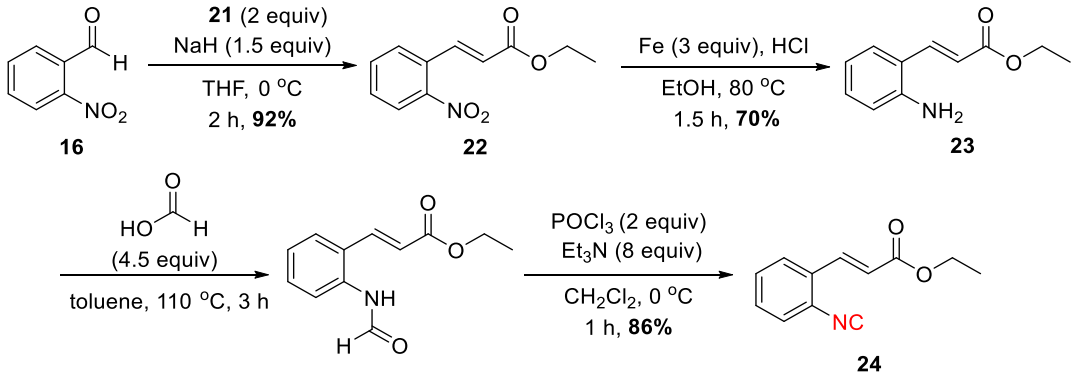

Scheme 2.33. Preparation of Ethyl 2-(2-isocyanophenyl)acrylate.

Preparation of compound **27** (*Scheme 2.34*) started with the reduction of compound **23** using diisobutylaluminium hydride and sodium hydride in tetrahydrofuran at 0 °C to achieve the corresponding alcohol **25** in an excellent 92% yield. Subsequent methylation of the alcohol was carried out using methyl iodide and sodium hydride in tetrahydrofuran at 0 °C, and the product was obtained in a good 65% yield.[177]

From this point, the obtention of the corresponding isocyanide followed the same synthetic path as the previously prepared compounds.

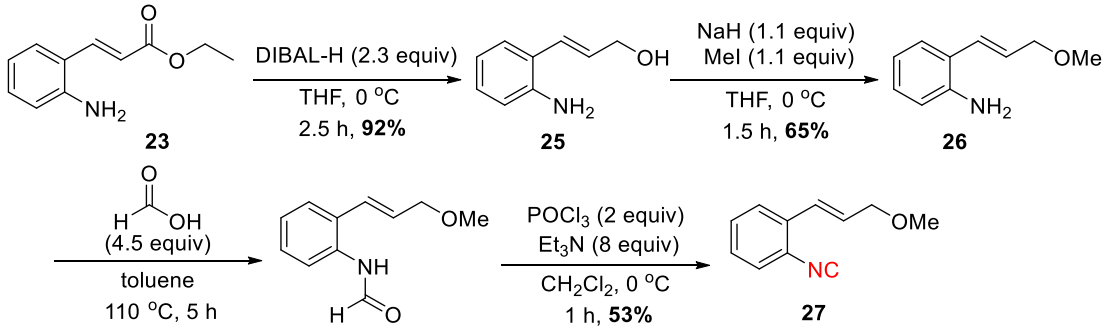

Scheme 2.34. Preparation of 1-isocyano-2-(3-methoxyprop-1-en-1-yl)benzene.

To obtain compound **31** (*Scheme 2.35*), the synthesis started with the obtention of isocyanide **30** from 2-bromoaniline **28**, using the same procedure mentioned above. Once the isocyanide was obtained, it was treated with methyl formate and *n*-butyl lithium in tetrahydrofuran at -78 °C to give the 2-aminobenzaldehyde **31**.[178]

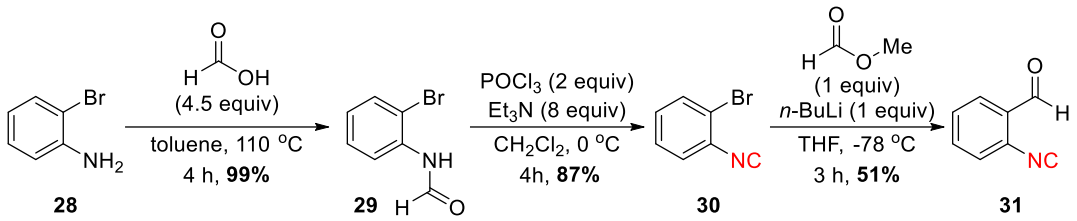

Scheme 2.35. Preparation of 2-isocyanobenzaldehyde.

Finally, to obtain compound **34** (*Scheme 2.36*), 1-(2-aminophenyl)ethan-1-one **32** was treated with the previously used conditions to convert the amine into the isocyanide in a good overall yield.

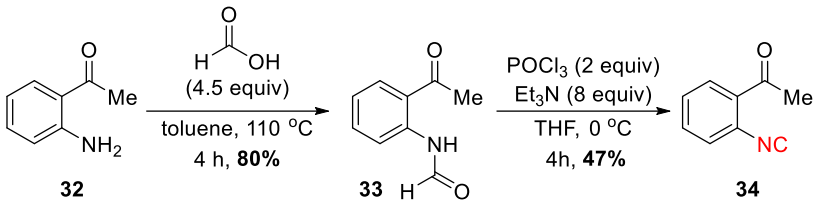

Scheme 2.36. Preparation of 1-(2-isocyanophenyl)ethan-1-one.

Reaction optimization

Reductive cyclization

In the same way, as with the previous heterocycles, we also started by optimizing the reductive cyclization (*Table 2.8*). To do this, we began by using the optimized conditions for phenanthridine at room temperature (*Table 2.8, entry 1*), applying them to isocyanide **19** containing an electron-poor alkene. Unfortunately, the cyclized product **35** was not obtained. We decided to lower the solvent concentration to 0.04 M (*entry 2*), and for the first time, it was possible to obtain the product with a yield of 47%.

Several modifications were tried here, such as replacing the solvent with ethanol. However, this proved detrimental to the reaction. Attempts to decrease the amount of $Fe(acac)_3$ or use a mixture of $Fe(acac)_3$ with $Fe(acac)_2$ proved similarly unsuccessful (*entries 3 and 4*). Finally, when the solvent was replaced by a mixture of 0.04 M tetrahydrofuran with methanol (10 equiv) and three equivalents of phenylsilane were added at 60 °C, the product could be obtained in good yield of 75% (*entry 5*).

In the case of indoles, no oxidant is used since the Fe^{III} species are regenerated during the reduction of the α-radical formed, similar to Baran's MHAT reaction of electron-deficient alkenes.[33]

Table 2.8. Indoles reductive cyclization.

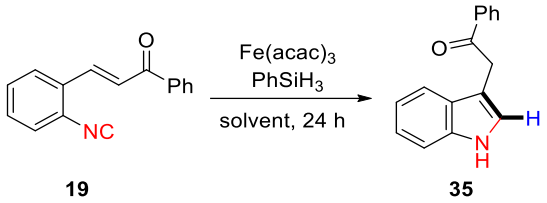

19 **35**

Entry	19	$Fe(acac)_3$	$PhSiH_3$	solvent	T°	35
1	1	0.2[a]	1	*i*PrOH 0.4 M	rt	-
2	1	0.2	1	*i*PrOH 0.04 M	rt	47%
3	1	0.05	1	EtOH 0.04 M	60 °C	11%
4	1	0.05/0.15[b]	1	*i*PrOH 0.04 M	rt	37%
5	1	0.2	3	THF 0.04 M[c]	60 °C	75%

[a]$Fe(acac)_2$ was used instead of $Fe(acac)_3$. [b]A combination of $Fe(acac)_3$ and $Fe(acac)_2$ was used. [c]MeOH (10 equiv) were added.

With the optimum conditions in hand, the range of previously synthesized isocyanides were shown to undergo the desired reductive cyclization (*Scheme 2.37*). Isocyanide **24**, bearing an electron-poor chain, was obtained in an excellent 91% yield. However, when the other isocyanides **27**, **31**, and **34** were subjected to the same conditions, only a complex mixture was obtained, and no detection of the corresponding cyclized products was possible. In the case of isocyanide **27**, we presumed this was due to the substrate having an electron-rich alkene chain. In the case of isocyanides **31** and **34** with carbonyls as radical acceptors, the cyclization reaction would imply the formation of an unstable alkoxy radical intermediate, which could revert and undergo decomposition. While we have previously demonstrated that aldehydes and ketones are viable acceptors in MHAT reactions,[54] none of the desired products **38** and **39** were detected in this case.

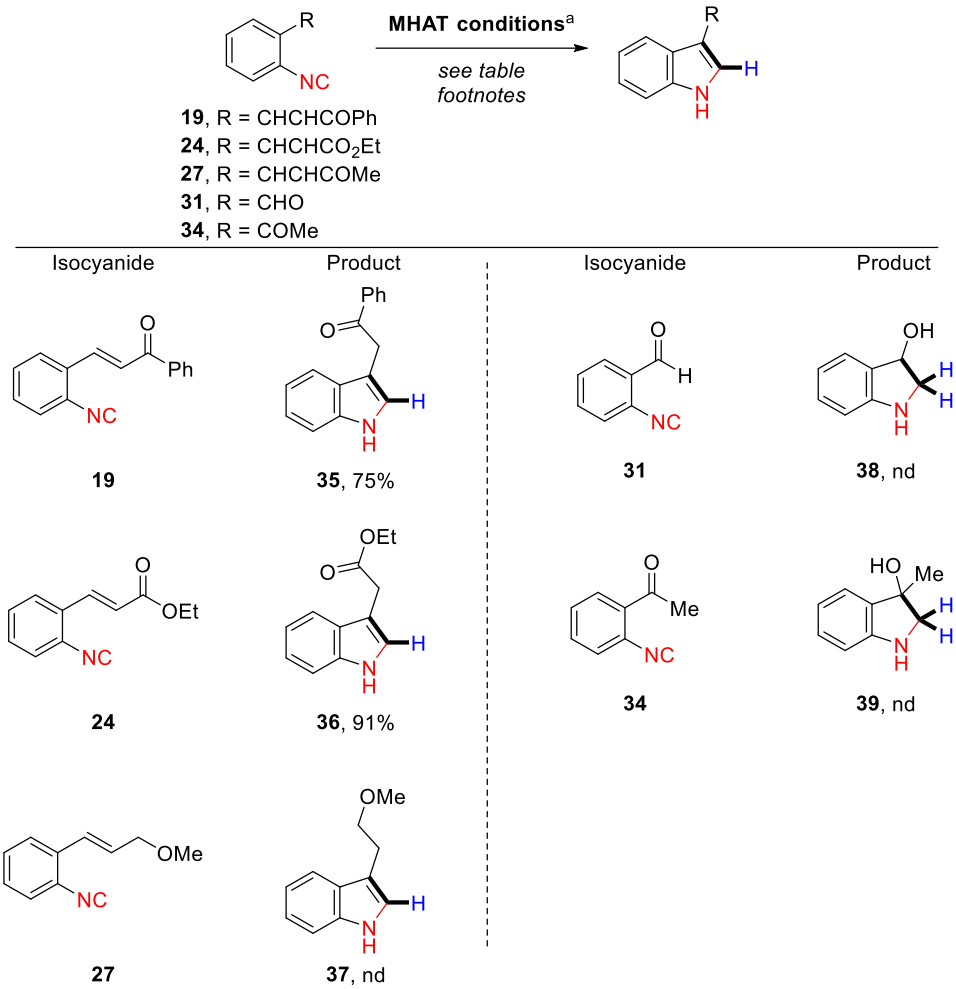

Scheme 2.37. Reductive cyclization scope on different substituted isocyanides. [a]$Fe(acac)_3$ (0.2 equiv), $PhSiH_3$ (3 equiv), THF (0.04 M), MeOH (10 equiv), 60 °C, 24 h.

MHAT coupling

Once the optimal conditions for the reductive cyclization were obtained, the coupling with alkenes was studied. This became significantly more challenging because isocyanides were more susceptible to reductive cyclization than the rest of the previous compounds studied so far.

The optimization started using the optimal conditions for the phenanthridines (*Table 2.9, entry 1)* but without an oxidant because, as previously discussed in the reductive cyclization section, it is not required. The conditions were then modified by diluting the concentration to 0.04 M (*entry 2*); the desired product **35a** could be obtained, albeit in a low yield of 14%. From here, different modifications were carried out, such as changing the solvent to dichloroethane (*entry 6*), dichloroethane/isopropanol mixture

(*entry 11*), acetonitrile/water mixture (*entry 25*), or tetrahydrofuran (*entries 3, 5, 7, 8 and 14-21*). During the course of our studies, Ramón and co-workers published a study of Baran's coupling of unactivated alkenes with electron-deficient alkenes, where they used deep eutectic solvents as a reaction medium.[179] These tend to be combinations of two or more components that form a eutectic liquid mixture via electrostatic and hydrogen bond interactions.

*Table 2.9. Optimization table for the formation of indole **35a.***

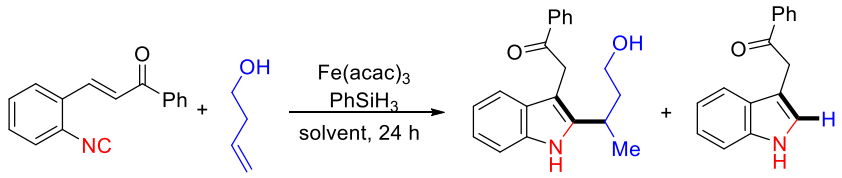

19 **35a** **35**

Entry	19:alk	$Fe(acac)_3$	$PhSiH_3$	solvent	T°	35a	35
1	1:1	0.2	1	*i*PrOH 0.4 M	rt	-	22%
2	1:1	0.4	1	*i*PrOH 0.04 M	rt	15%	29%
3	1:1	1	1	THF 0.04 M[a]	rt	23%	33%
4	1:1	0.05	5	*i*PrOH 0.04 M	rt	5%	40%
5	1:1	1	3	THF 0.04 M[a]	rt	9%	47%
6	1:1	1	3	DCE 0.04 M[a]	rt	19%	58%
7	1:1	0.2	3	THF 0.04 M[a]	60 °C	-	80%
8	1:1[b]	0.4[c]	1	THF 0.04 M[a]	rt	8%	37%
9	1:1	0.4	1	EtOH/EG (5:1) 0.2 M	rt	16%	28%
10	1:3	0.1	5.5[d]	ChCl/EG (1:2) 0.2 M	60 °C	8%	11%
11	1:3	0.4[e]	1	*i*PrOH/DCE (1:1) 0.2 M	60 °C	11%	73%
12	1:1	0.2	3	EtOH 0.04 M	rt	10%	55%
13	1:3	0.4	3	*i*PrOH 0.04 M	rt	15%	41%
14	1:1	0.1	1	THF 0.04 M[a]	rt	11%	43%
15	1:1	0.05[c]	1	THF 0.04 M[a]	rt	19%	59%
16	2:1[f]	1	1	THF 0.04 M[a]	rt	18%	57%
17	1:1	2	1	THF 0.04 M[a]	rt	14%	38%
18	1:1	1	1	THF 0.04 M[g]	rt	9%	58%
19	1:1	1	1	THF 0.004 M[a]	rt	31%	40%
20	1:1	1	1	THF 0.04 M[a]	0 °C	21%	38%
21	1:3	1	1	THF 0.02 M[h]	0 °C	9%	33%
22	1:1	1	1	*i*PrOH 0.02 M	rt	14%	35%
23	1:1	0.2[i]	1	*i*PrOH 0.04 M	rt	-	44%
24	1:1	0.2[j]	1	*i*PrOH 0.04 M	rt	-	-
25	1:1	0.2	1	MeCN/H_2O (1:1) (0.0125 M)	rt	-	21%
26	1:1	0.2	1	*i*PrOH 0.04 M	rt	47%	16%

[a]MeOH (10 equiv) were added. [b]4-phenylbutene used as alkene. [c]$Fe(acac)_2$ (0.4 equiv) were added. [d]PMHS was used instead of $PhSiH_3$. [e]$Fe(dpm)_3$ was used instead of $Fe(acac)_3$. [f]Second equivalent of isocyanide was added 2 h later. [g]*i*PrOH (10 equiv) were added. [h]*i*PrOH (50 equiv) were added. [i]Co(salen) was used instead of $Fe(acac)_3$. [j]$Mn(dpm)_3$ was used instead of $Fe(acac)_3$.

It was therefore decided to test its conditions, using mixtures of ethanol/ethylene glycol (*entry 9*) and choline chloride/ethylene glycol (*entry 10*), as well as poly(methylhydrosiloxane) (PMHS) as a hydride source, but very poor yields were obtained.

Changing the catalyst to one with more bulky ligands, such as $Fe(dpm)_3$ (*entry 11*), Co(salen) (*entry 23*), or $Mn(dpm)_3$ (*entry 24*), was unsuccessful. Carrying out the reaction at room temperature, at 60 ^oC (*entries 7, 10, and 11*) or at 0 ^oC (*entries 20 and 21*) to try to make the reductive cyclization less active and slower were also investigated, including different quantities of catalyst, as well as different amounts of phenylsilane. Various amounts of alkene were also tried (*entries 10, 11, 13, and 21*). In all previously mentioned cases, no substantial improvement in yield was achieved, and in most cases, large amounts of the reduced heterocycle **35** were formed, demonstrating, as we commented above, that the reductive cyclization outcompeted the desired coupling of the isocyanide with the alkene.

Finally, similar conditions to those tested initially, isopropanol, one equivalent of alkene, 0.2 equivalents of $Fe(acac)_3$, one equivalent of phenylsilane, and room temperature but with a dilution of 0.04 M (*entry 26*), gave us access to the desired coupled indole **35a** in a moderate yield of 47% which is a good result considering the difficulty of the reaction.

Substrate scope

Finally, after extensive screening, compounds **35a**, **35b**, **36a**, and **36b** could be obtained with moderate yields (*Scheme 2.38*). Compound **35c**, using isocyanide **19** and a tertiary alkene, could only be obtained in trace amounts. In this case, the one-pot conditions of Minisci-HAT could not be applied due to the electron-rich nature of the indoles.

Attempts to couple isocyanides **27**, **31**, and **34** to give the corresponding coupled indoles **37a**, **38a**, and **39a** were unsuccessful, as we had found in the reductive cyclization studies discussed previously.

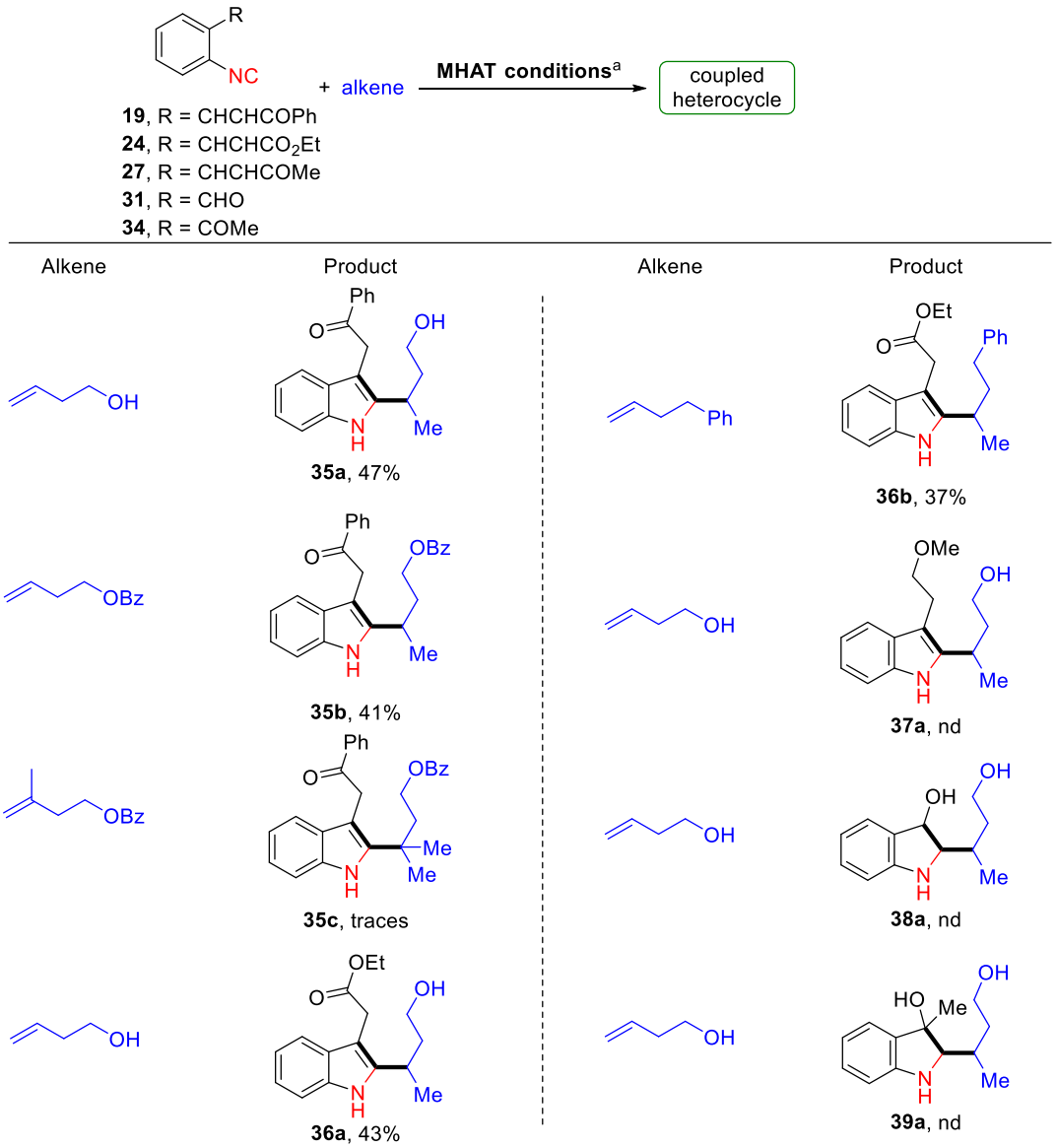

Scheme 2.38. Scope table for indole coupling using MHAT conditions. [a]Isocyanide/alkene (1:1), $Fe(acac)_3$ (0.2 equiv), $PhSiH_3$ (1 equiv), *i*PrOH [0.04 M], rt, 24 h.

During the course of our studies, Huang and co-workers reported a MHAT reductive cyclization to form indoles (*Scheme 2.39*).[180] This method was limited to investigating the reductive cyclization reaction and to just one substrate type.

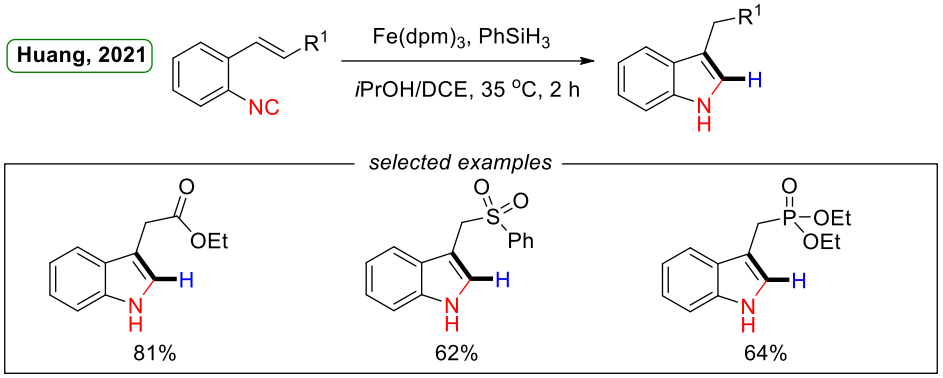

Scheme 2.39. Reductive indole synthesis using MHAT.

After the publication of our work, an alternative hydrogen atom transfer cyclization to phenanthridine was described by the same group (*Scheme 2.40*).[181] They showed that the hydride donor could be formed from triphenylphosphine and water using photocatalytic conditions. Despite the potential of this process, it was not applied to the coupling of alkenes with isocyanides to make substituted phenanthridines or any other heterocyclic ring system.

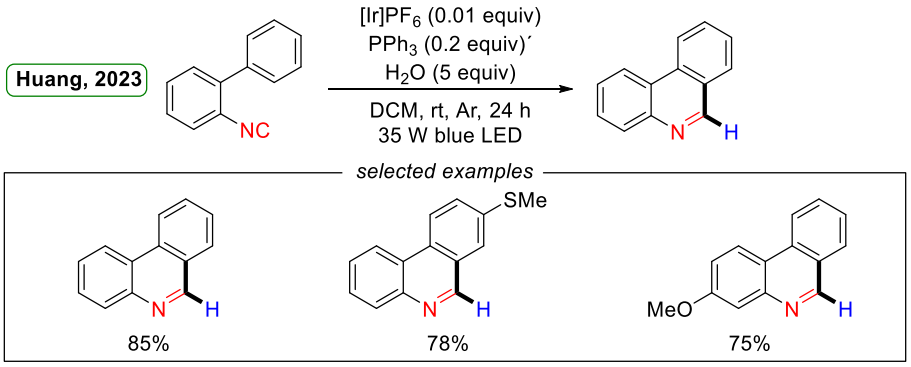

Scheme 2.40. Photoredox/PPh_3 dual catalysis for phenanthridine synthesis.

Mechanistic discussion

The mechanism is similar to that previously outlined for phenanthridines and isoquinolines but presents some key differences (*Scheme 2.41*).

The reaction begins with replacing a metal ligand with a hydride from the phenylsilane. This metal hydride is transferred to the alkene, generating a radical in the most substituted position, which then attacks the carbon of the isocyanide, forming the imidoyl intermediate **A**. This intermediate will subsequently carry out a 5-*exo-trig* cyclization on the nearest carbon of the vinyl chain, forming a 5-membered ring to give intermediate **B**. At this point, the mechanism diverges from the phenanthridine and isoquinoline series. The new carbon-centered radical is located next to a carbonyl, which, in accordance with mechanistic studies carried out by Baran for the coupling reaction of alkenes with Michael acceptors,[32] will be reduced by an electron from the Fe^{II} species to form an enolate anion **C**. Subsequent protonation and tautomerization of the ring will give the desired product **35a**. This final step makes the reaction catalytic; therefore, no oxidant is required to regenerate the Fe^{III} species.

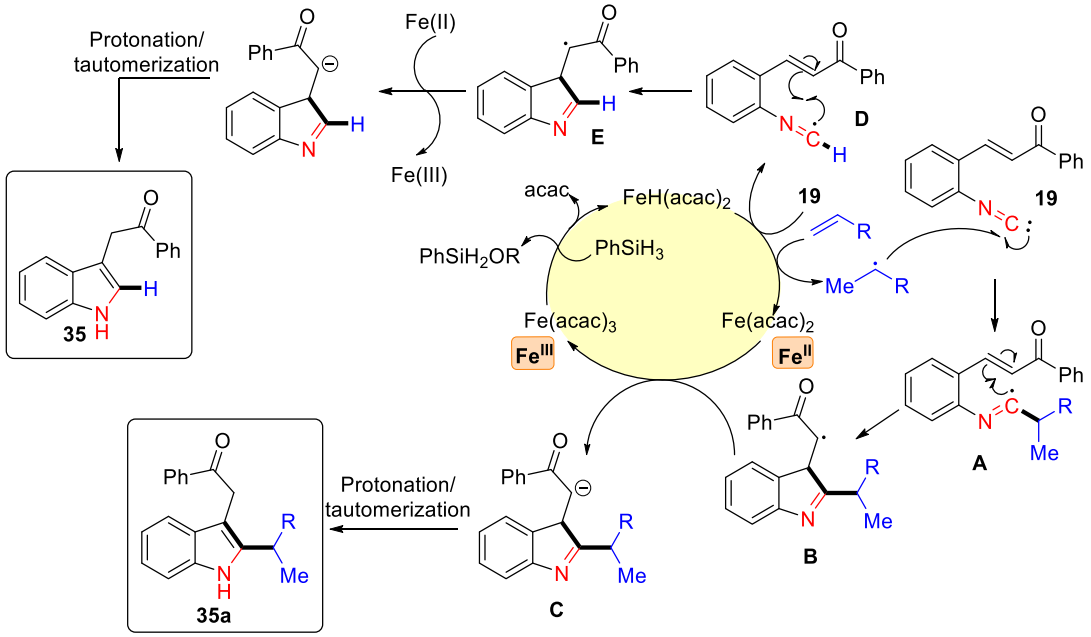

Scheme 2.41. Proposed mechanism for the alkene coupling and reductive cyclization of indoles.

On the other hand, if the metal hydride species directly attacks the isocyanide, it forms the imidoyl intermediate **D**, which undergoes a 5-*exo-trig* cyclization and form the intermediate **E**, which subsequently, following the same mechanism explained above, will reoxidize the Fe to generate the enolate. After subsequent protonation and tautomerization, product **35** is formed.

3. MHAT-MINISCI COUPLING OF HETEROCYCLES WITH ETHERS

3.1. INTRODUCTION

In this chapter, we discuss the development of a serendipitously discovered cross-dehydrogenative coupling reaction chapter that allows the coupling of electron-deficient heteroarenes with non-prefunctionalized ethers under mild conditions using catalytic amounts of iron, peroxide, and a trisubstituted alkene as an additive.

3.1.1. Discovery of Minisci-type coupling of furan to phenanthridine

In the previous chapter, during the development of the MHAT-Minisci conditions to couple more substituted alkenes with isocyanides, it was observed that when catalytic amounts of Fe were used together with TBHP as the reoxidant in the presence of TFA, a molecule of THF (used as the solvent) coupled instead of the alkene. Notably, when we tried to obtain the same coupled compound under MHAT conditions (from the isocyanide) or MHAT-Minisci conditions (from the phenanthridine) using 2,3-dihydrofuran we observed only traces of the coupled product (*Scheme 3.1*).

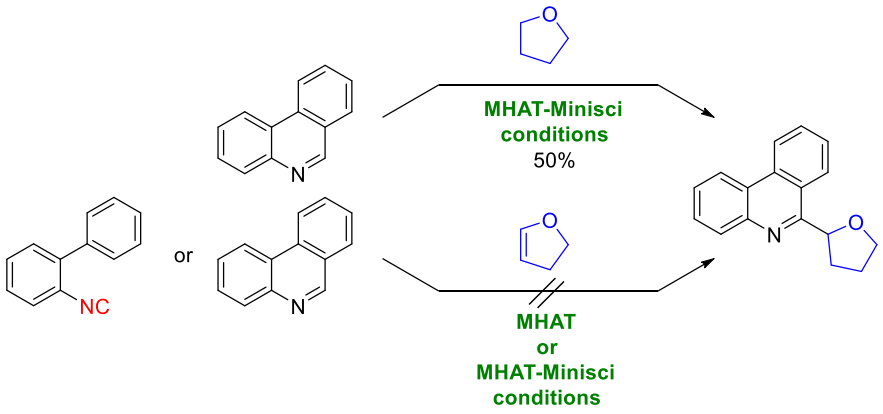

Scheme 3.1. Serendipitous discovery of Minisci-type coupling of tetrahydrofuran and failed coupling of 2,3 dihydrofuran under MHAT and MHAT-Minisci conditions.

This serendipitously discovered reaction was envisaged as the basis of a new general strategy to carry out Minisci-type cross-dehydrogenative coupling reactions between heterocycles and ethers. Notably, the mild reaction conditions and the fact the same type of compound could not be prepared from the corresponding alkene under standard MHAT conditions made the reaction warrant further study.

3.1.2. Overview of the Minisci reaction

The Minisci reaction consists of the substitution of protonated heterocycles by nucleophilic carbon-centered radicals. This reaction represented a significant breakthrough in the functionalization of C-H bonds of unsaturated systems and has attracted the attention of many synthetic chemists during the last decades.[182]

In 1964, Lynch and co-workers showed that mixtures of isomers obtained in the phenylation of pyridine could be directed to C-2 when the reaction was carried out in acetic acid. This is attributed to the formation of the more reactive pyridinium intermediate.[183] In 1968, Minisici's work demonstrated that strong acid conditions could direct the addition of alkyl radicals to the C-2 and C-4 positions of pyridine, with no C-3 product observed (*Scheme 3.2*).[184]

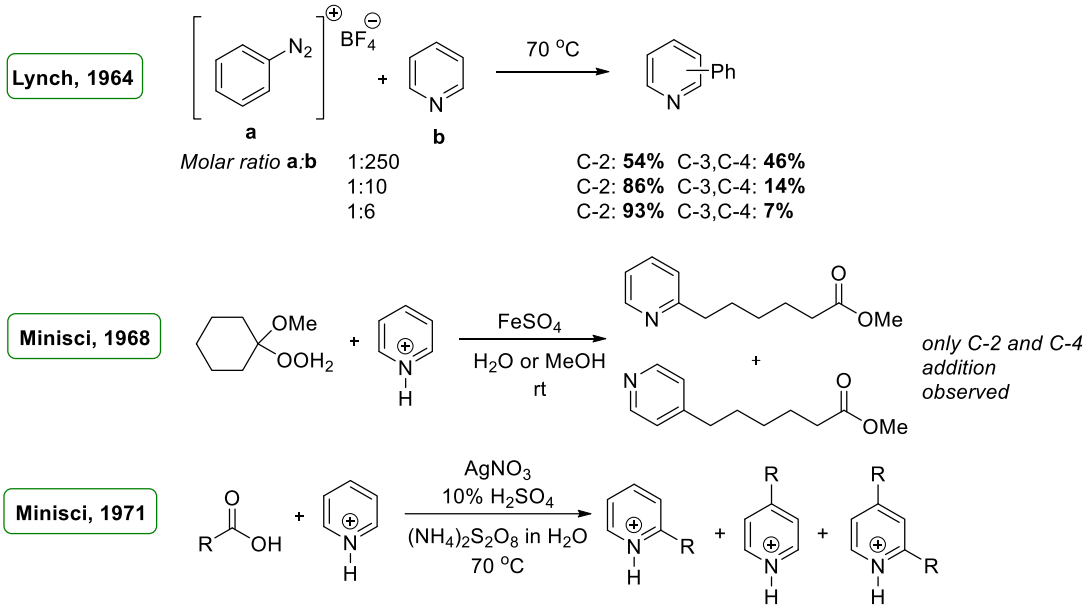

Scheme 3.2. Lynch and Minisci additions of radicals to electron-deficient heteroarenes.

In 1970, Minisci also published another study where he generated radicals from various peroxides.[185] In 1971, he published what would give rise to the name "Minisci reaction" in a study where he demonstrated that an aliphatic carboxylic acid undergoes oxidative decarboxylation using a silver and peroxydisulfate catalyst, coupling the generated radical with pyridines and quinolines.[186] This method was seen to be of great use in the pharmaceutical industry, where many molecules incorporate this type of functionalized heteroarene core.[187] As a key advantage, the specificity of the reaction for basic heteroarenes stands out in contrast to other methods, such as the Friedel-Crafts

aromatic substitution, which presents opposite reactivity and selectivity. However, classical protocols also had some limitations, such as obtaining mixtures of regioisomers, which are difficult to separate, and moderate yields. Still, the easy access to pharmaceutically desirable scaffolds often outweighs these limitations.[188] Modern studies have revealed that this lack of regioselectivity can be overcome, being determinant of the nature of the radical, solvent polarity, or the acid used for the activation.[189]

The mechanism of the Minisci reaction starts with an initial step where a carbon-centered nucleophilic radical is added to a basic heteroarene. Acid is used in stoichiometric quantities to protonate this heteroarene, lowering its LUMO energy to facilitate this radical addition. The LUMO energy of C-2 and C-4 are usually very similar, explaining the mixture of regioisomers typically obtained.[190] As Minisci's work showed,[191] the nature of this radical will determine whether the addition of the radical is reversible or not. Once the radical cation **A** is formed (*see Scheme 3.3*), two different pathways can eliminate the acidic α-proton. Pathway **1** involves the hydrogen atom transfer (HAT) from the radical intermediate to rearomatize the pyridine in one step. Pathway **2** consists of a deprotonation step to produce the neutral radical **B**. Final oxidation through a single-electron transfer (SET) would lead to the rearomatized pyridine. The specific pathway in each reaction would depend on several factors, such as the substrate in question or the reaction conditions.

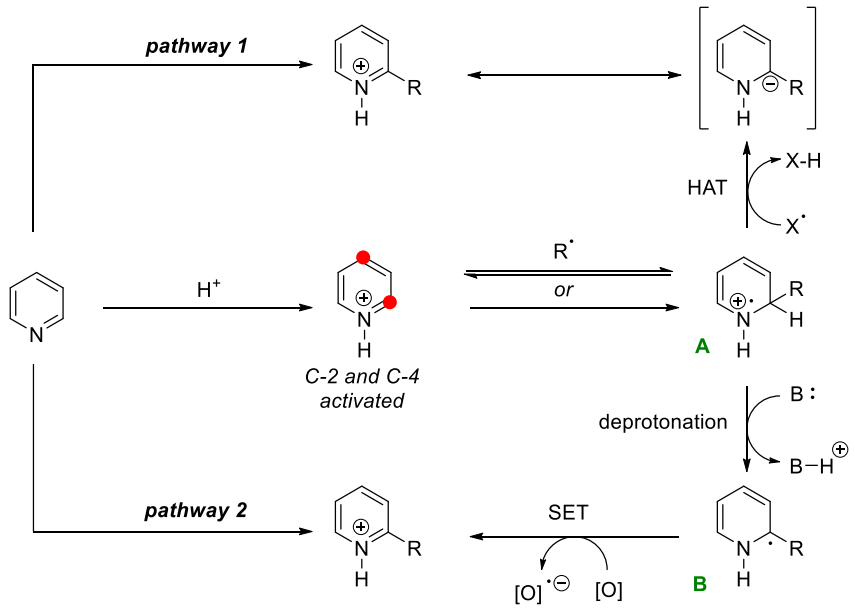

Scheme 3.3. Overview of mechanistic pathways in Minisci-type reactions.

A wide range of heterocycles have been used as radical acceptors in the Minisci reaction, such as 5-membered, 6-membered, 6,5-bicyclic, 6,6-bicyclic or polycyclic systems (*see Scheme 3.4*), highlighting the versatility of this transformation. It should also be noted that the reaction has been successfully used in non-basic systems such as furan and thiophene[192], using $Mn(OAc)_3$ as oxidant and arylboronic acids as radical donors, or pyrrole[193], using alkyl iodides, H_2O_2 and catalytic Fe in DMSO to generate electrophilic carbon-centered radicals. The preferred positions of the radical attack on the heterocycle are indicated, with most showing a preference for the α-position to the nitrogen. Notable exceptions are quinazoline, where the C-4 position is more active than the C -2, or the case of 1,2,3-triazine, in which the most active position is C-5.

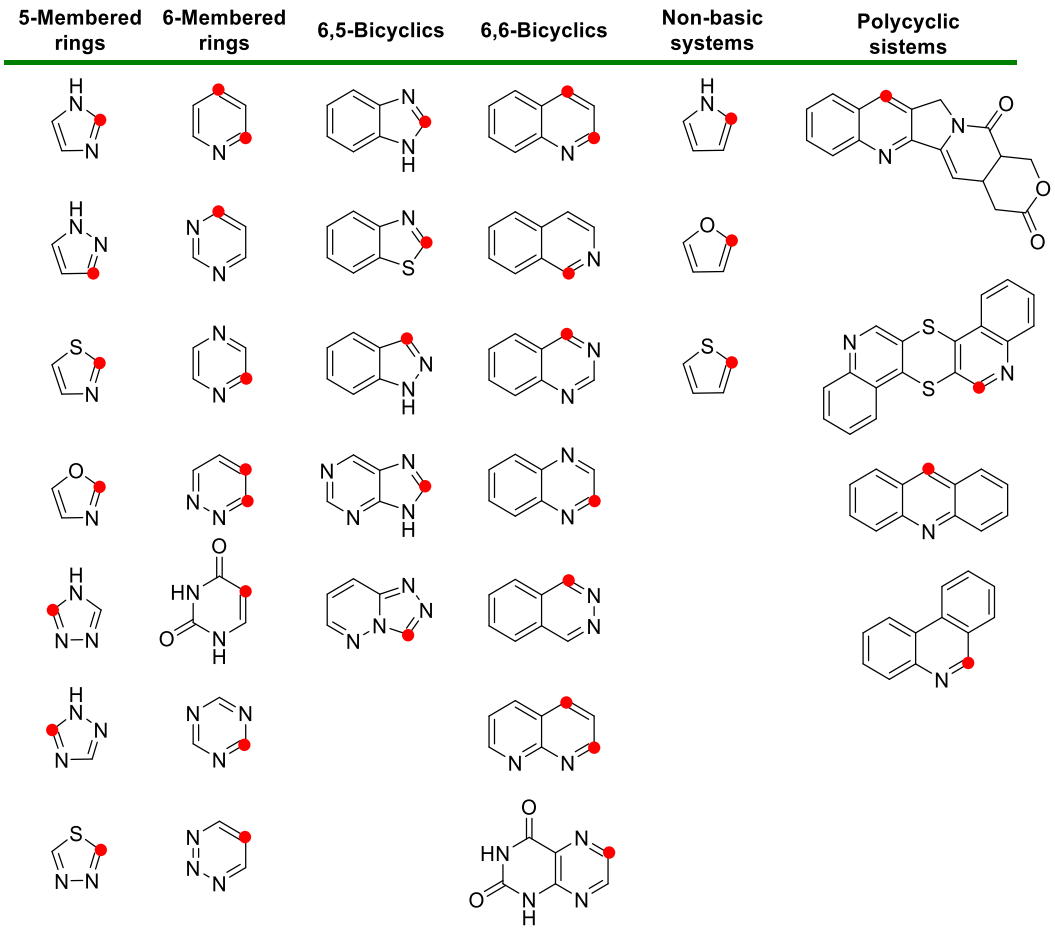

Scheme 3.4. Commonly used heterocyclic partners in Minisci reaction and its preferred positions of radical attack of the protonated form.

In *Scheme 3.5*, the different radical donors are summarized. Many different types of functional groups can be employed in the reaction, providing a broad spectrum of possibilities for heterocycle functionalization.

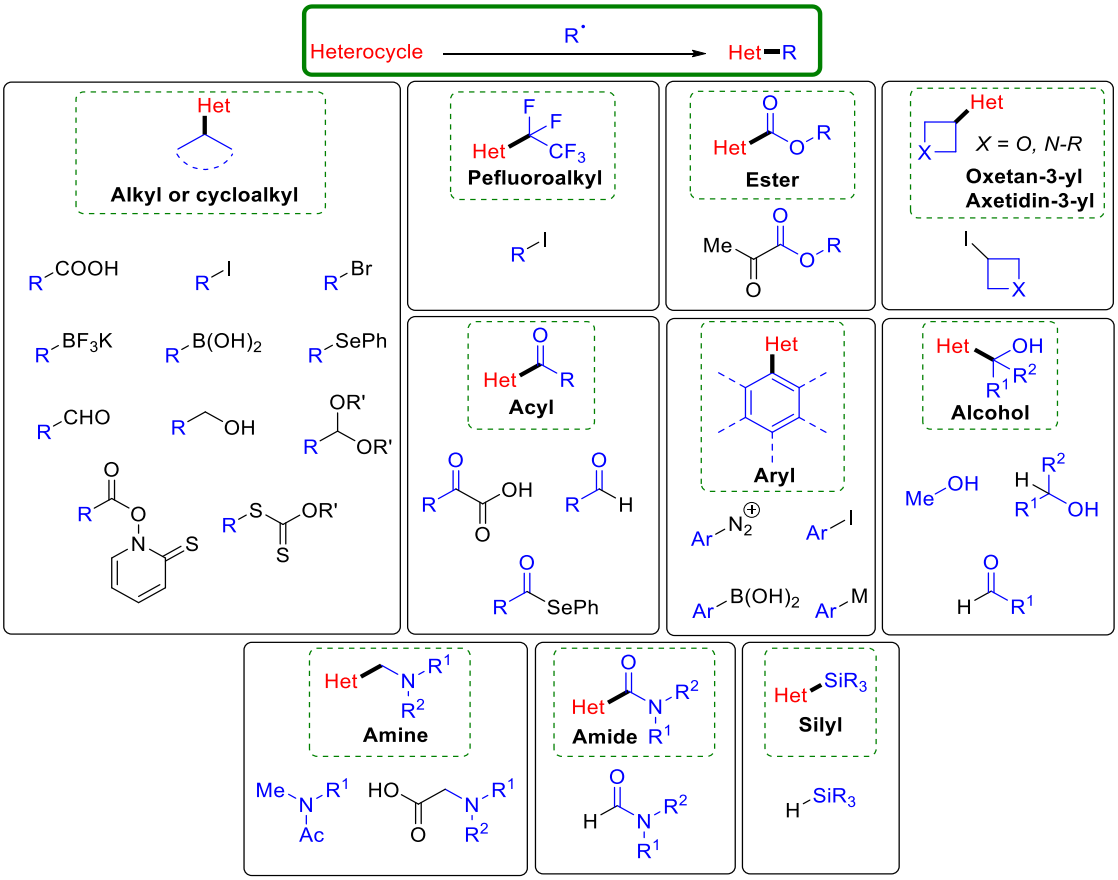

Scheme 3.5. Representative groups added to different heterocycles using Minisci reaction.

Despite the numerous advantages of the Minisci reaction, it has three main limitations. The first is the lack of regioselectivity; in most cases where two positions can act as acceptors, a mixture of the corresponding regioisomers is usually obtained. Secondly, yields have traditionally been moderate, mainly due to the recovery of unreacted starting material. Thirdly, and as a consequence of the previous two points, the purification of the products is often complex.

Even so, the benefits usually outweigh the limitations since the reaction allows us to perform C-H functionalization in a very selective way. Since radicals are the reactive intermediates, protection strategies are generally unnecessary, making synthetic sequences more direct.

3.1.3. Use of Minisci reaction in medicinal chemistry

It has been said that the best way to discover new drugs is to modify known ones. As many pharmaceuticals contain aromatic heterocycles, one key use of the Minisci reaction has been to create large libraries of new compounds for screening via modifications to existing pharmaceutical compounds (*Scheme 3.6*).

The pharmaceutical industry usually depends on a relatively small range of highly proven and dependable reactions, many of them directed toward the functionalization of heterocycles.[194]

In this context, the Minisci reaction has been used extensively in medicinal chemistry as a highly useful tool for preparing chemical libraries[188] and highlights the need to develop new variations of this reaction.

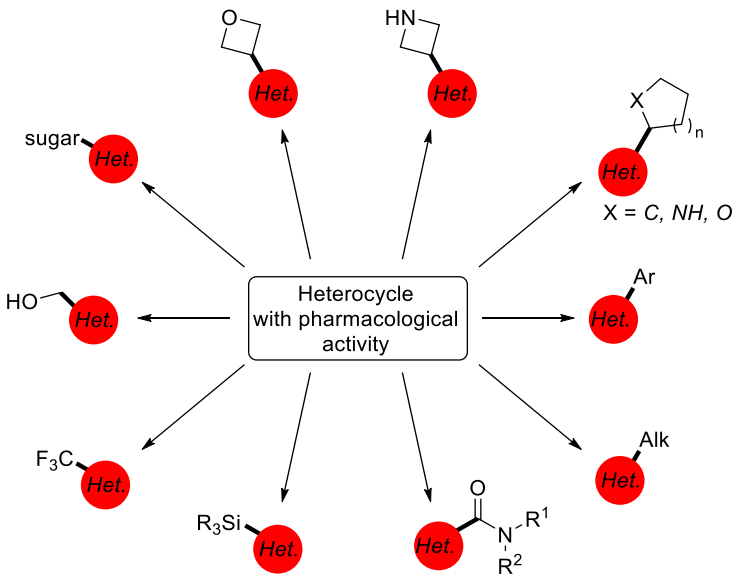

Scheme 3.6. Potential use of Minisci reaction to produce chemical libraries of functionalized heterocycles.[188]

3.1.4. Examples of biologically relevant Cα-heteroarylated compounds

Structures containing a Cα-heteroarylated ether functionality are interesting since many natural products and pharmaceuticals with important biological properties have functionalized acyclic and cyclic ethers as part of their structure (*Figure 3.1*). The most common examples are those containing 5- and 6-cyclic ethers.[195] Ethers can act as hydrogen bond acceptors and decrease lipophilicity, reducing metabolic labilities and increasing aqueous solubility.[196] Therefore, synthetic methods directly incorporating these motifs into complex heterocycles without prefunctionalization are powerful approaches to producing small-molecule drugs.

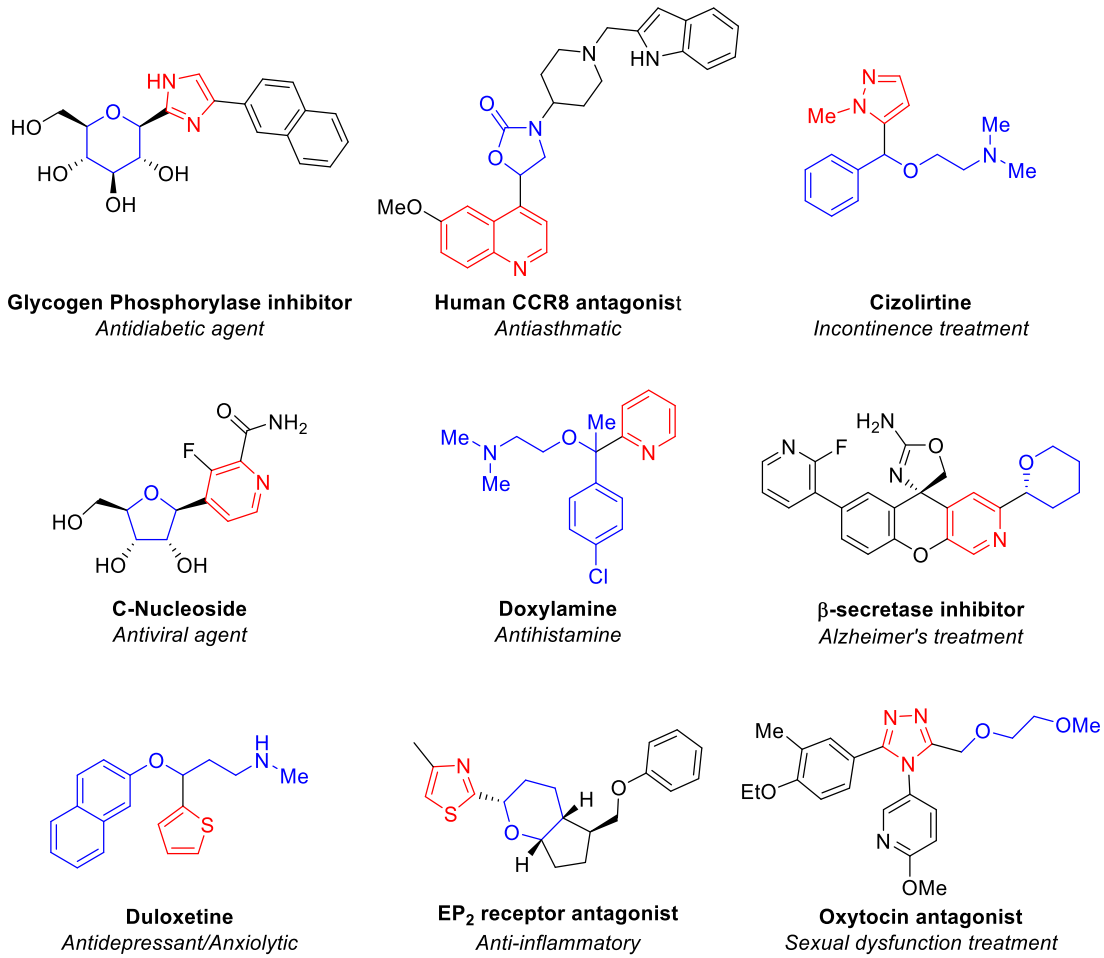

Figure 3.1. Selected bioactive compounds containing Cα-heteroarylated ether functionalities.

3.1.5. Literature precedents for the C(sp^3)-H bond activation of ethers

During the last decades, many methodologies have been developed to carry out C-H activation of ethers with nitrogen-containing heterocycles through radical chemistry. In this field, we can divide the methods developed into two large groups: the reactions that use oxidants and heat to generate the radical on the C_α of the ether and the reactions that use photochemistry to generate this same type of radical (*Scheme 3.7*). Within this first group of reactions, we can see how they all use Minisci's methodology to activate the heteroarene, either with the use of a Brönsted acid, as is the case of Togo[197] or Barriault[198] who use trifluoroacetic acid, Huang, who uses the Lewis acid $Sc(OTf)_3$[199] or using species generated in the medium itself, as is the case of Singh,[200] who use $K_2S_2O_8$ to generate the radical on the ether, but at the same time, one of the derivatives of this compound in the medium is HSO_4^- which serves to activate the heteroarene; or in the case of Antonchick,[201] which generates trifluoroacetic acid from secondary reactions of the PIFA used to generate the ether radical.

Those who do not use acids instead start from the *N*-oxide of the heterocycle, as in the case of Wu,[202] or an *N*-iminopyridinium ylide, as in the case of Wang.[203] Finally, the synthetic route used by Cheng[204] is also noteworthy, which, analogously to what was discussed in the previous chapter of this thesis, forms the radical with an oxidant such as BPO and heat and attacks an isocyanide instead of the heterocycle to carry out the corresponding cyclization. All of the outlined procedures, except for the case of Antonchick, require oxidizing species combined with vigorous heating to generate the radical species.

In the second group, we can see the methodologies that use photochemistry to generate the radical. Among them, we see the use of different photochemical methods, such as MacMillan's use of an iridium catalyst,[205] which uses it to carry out a SET on $S_2O_8^{2-}$ which subsequently performs a HAT on the ether to generate the radical. Li used a tungsten catalyst to generate the radical via SET,[206] and Gonzalez-Gomez used an acridine catalyst to generate the radical with light and transfer it via SET to ether.[207] Tong[208] uses this methodology with $FeCl_3$ to generate a radical on chlorine with light and transfer it to the ether using HAT. In the same way, through different compounds, Shah,[209] Li,[210] Zhang,[211] Jin,[212] or Li[213] end up carrying out the same HAT process. Li also

did this through a SET from species derived from $K_2S_2O_8$. Finally, Guin,[214] using O_2, and Terent'ev,[215] using NHPI, generate a radical intermediate that carries out a hydrogen abstraction on the ether to generate the corresponding radical.

Finally, it is also interesting to highlight the work of Wang[216] and Li,[217] who have successfully applied photochemistry to carry out the coupling with amines and amides.

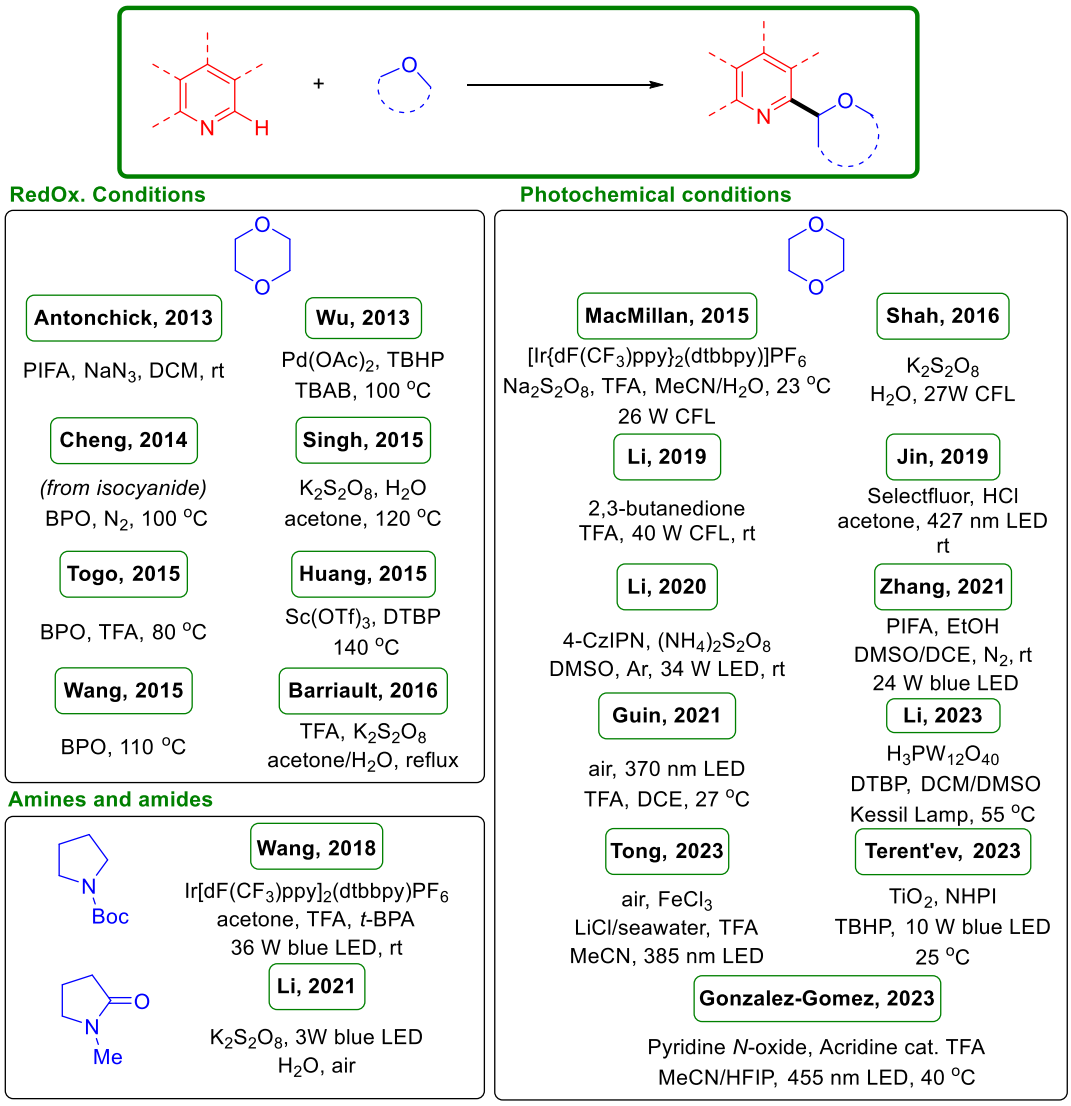

Scheme 3.7. Main coupling methods of ethers with heteroarenes using C-H activation.

3.2. OBJECTIVES

Based on these precedents from the literature combined with our serendipitous discovery of the coupling of THF to heterocycles under MHAT-type conditions, we believed it would be possible to develop a general cross-dehydrogenative coupling reaction under mild conditions. The first objective would be to determine the reagents needed to carry out the reaction and optimize the reaction to obtain more synthetically useful yields. The second objective would be to determine the scope of the reaction by using different ethers and other donor groups. The third objective would be determining the scope of the heterocycles that could be used in the reaction.

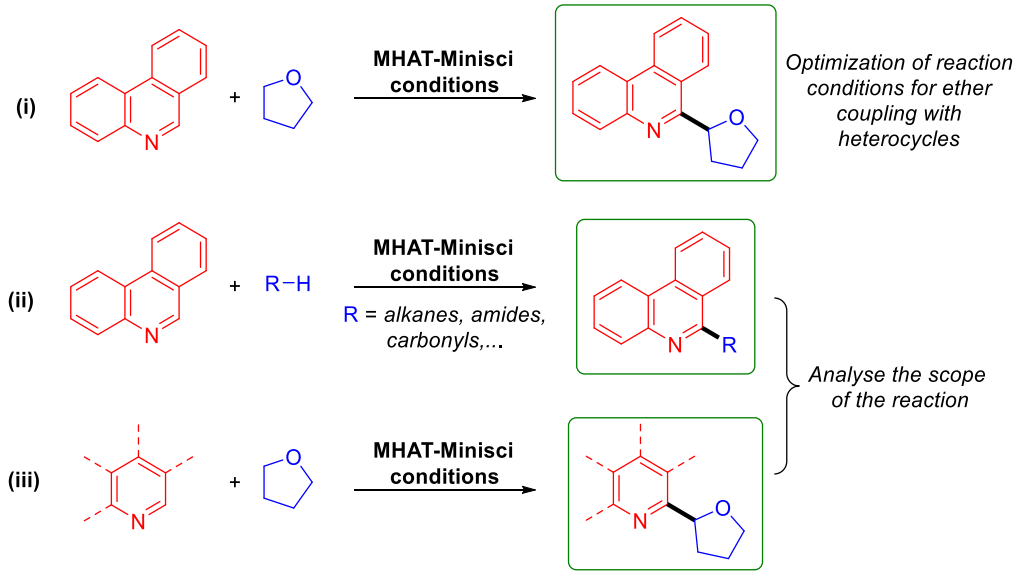

Scheme 3.8. Main objectives of Chapter 3.

3.3. RESULTS AND DISCUSSION

3.3.1. Reaction optimization

Determination of necessary reagents for the reaction

To begin our studies, we proceeded to analyze which components were necessary for the reaction to take place and which components had either no effect or had a negative impact on the reaction. Compared to the serendipitously discovered conditions (*Table 3.1, entry 1*), using Fe^{II} led to a slight improvement in yield (*entry 2*). Notably, removing the alkene resulted in a significant drop in yield (*entry 3*). This was particularly surprising given that the alkene would appear to be unnecessary for the reaction. The omission of the hydride donor $PhSiH_3$ (*entry 4*) gave a slightly better yield, likely because it is superfluous for the reaction mechanism, and its omission resulted in cleaner reactions. The omission of methanol led to the formation of impurities, resulting in a drop in yield and making the product harder to isolate in pure form (*entry 5*). To determine any synergistic effects that might be taking place, Fe^{II} was used without the addition of $PhSiH_3$ (*entry 6*) to give the highest yield so far (65%). However, the same conditions without the alkene did not perform well, providing only a 23% yield (*entry 7*), indicating the alkene must perform an essential role in the reaction.

Table 3.1. Determination of necessary reagents for coupling of phenanthridine with THF.

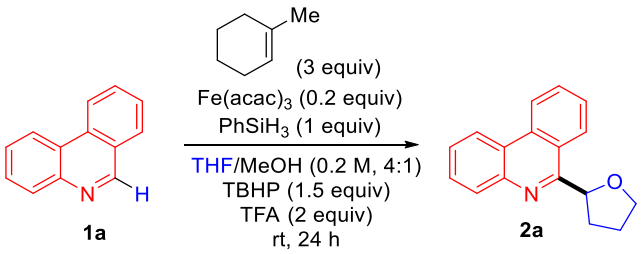

Entry	Variation from initial conditions	Yield
1	No variation	50%
2	$Fe(acac)_2$ instead of $Fe(acac)_3$	58%
3	No alkene	13%
4	No $PhSiH_3$	52%
5	No MeOH	60%
6	$Fe(acac)_2$ instead of $Fe(acac)_3$, no $PhSiH_3$	65%
7	$Fe(acac)_2$ instead of $Fe(acac)_3$, no alkene, no $PhSiH_3$	23%

Optimization of reaction conditions

Having identified which components are essential for the reaction, we optimized the reaction using the result from *entry 6* of *Table 3.1* as the new baseline conditions.

First, we wanted to test whether different alkenes could improve the performance of the reaction (*Table 3.2*). 2-methylbut-2-ene was evaluated instead of 1-methylcyclohex-1-ene, obtaining an improvement of up to 73% (*entry 2*). Styrene (*entry 3*) was also assessed, but yields similar to baseline conditions were obtained. β-pinene was tested (*entry 4*) due to its exocyclic double bond, which could provide greater reactivity, but only a moderate yield of 42% was obtained. Finally, increasing the amount of 2-methylbut-2-ene to 5 equivalents slightly decreased the yield (*entry 5*).

Table 3.2. Determination of the most appropriate alkene.

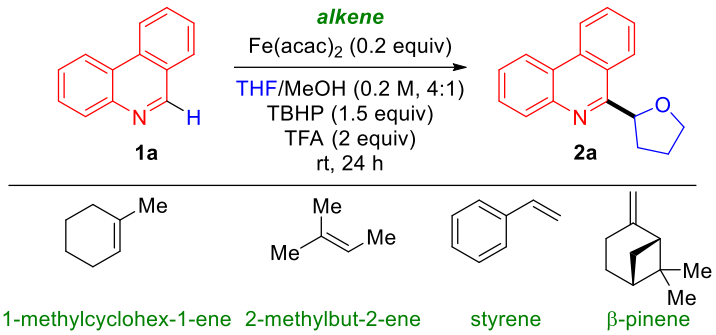

Entry	Variation from initial conditions	Yield
1	1-methylcyclohex-1-ene (3 equiv)	50%
2	2-methylbut-2-ene (3 equiv)	73%
3	Styrene (3 equiv)	65%
4	β-pinene (3 equiv)	42%
5	2-methylbut-2-ene (5 equiv)	66%

Once the most suitable alkene for the reaction had been determined, we investigated the effect of temperature on the reaction (*Table 3.3*). It was seen that increasing the temperature to 60 °C (*entry 2*) led to a dramatic drop in yield to 7%. On the other hand, lowering the temperature to 0 °C was also detrimental to the reaction, which dropped to 28% yield (*entry 3*).

Table 3.3. Determination of the most appropriate temperature.

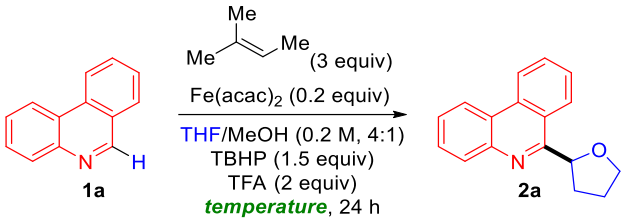

Entry	Variation from initial conditions	Yield
1	Room temperature	73%
2	60 °C	7%
3	0 °C	28%

The next step was determining the optimal reaction time (*Table 3.4*). It was seen that 3 hours was not enough (*entry 2*), and a yield below 50% was obtained. The reaction was also left for 48 (*entry 3*) and 72 hours (*entry 4*). Yields similar to the baseline conditions were obtained, indicating that the reaction did not progress further but that the product formed was not significantly degraded in the medium.

Table 3.4. Determination of the most appropriate reaction time.

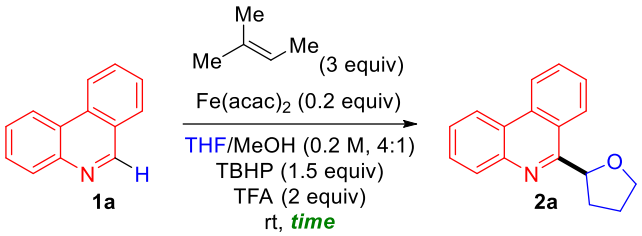

Entry	Variation from initial conditions	Yield
1	24 h	73%
2	3 h	47%
3	48 h	70%
4	72 h	68%

Next, we wanted to evaluate different oxidants and their optimum amount (*Table 3.5*). Different oxidants were tested, such as DTBP (*entry 2*), where no product formation was observed, DBPO (*entry 3*), and H_2O_2 (*entry 4*), both giving poor yields. Then, different quantities of TBHP were evaluated. Increasing to 3 equivalents of oxidant resulted in a drop in yield to 30% (*entry 5*), and adding the oxidant in two portions, starting with 1.5 equivalents and adding 1.5 more after 8 hours, also resulted in no improvement (*entry 6*).

Table 3.5. Determination of the most appropriate oxidant.

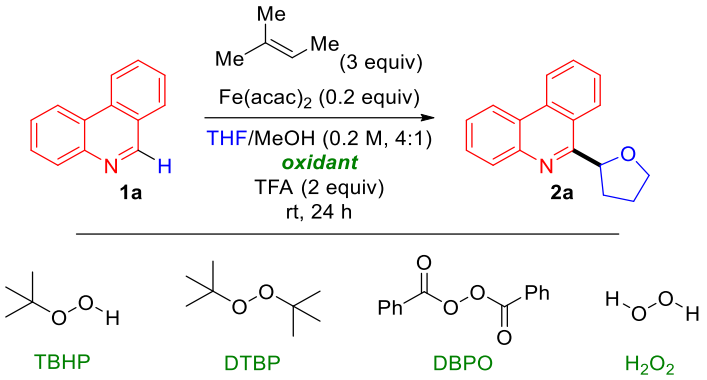

Entry	Variation from initial conditions	Yield
1	TBHP (1.5 equiv)	73%
2	DTBP (1.5 equiv)	nr
3	DBPO (1.5 equiv)	13%
4	H_2O_2 (1.5 equiv)	44%
5	TBHP (3 equiv)	30%
6	2nd addition of TBHP (1.5 equiv) after 8 h	48%

Next, the role of the acid in the reaction was also studied (*Table 3.6*). Different Brönsted acids, such as *p*-toluenesulfonic acid (*entry 2*) or sulfuric acid (*entry 3*), resulted in inferior reaction performance. The Lewis acid boron trifluoride diethyl etherate was also tested but also led to a reduced yield (*entry 4*). Finally, increasing the amount of TFA to 5 equivalents (*entry 5*) was found to be detrimental to the reaction.

Table 3.6. Determination of the most appropriate acid.

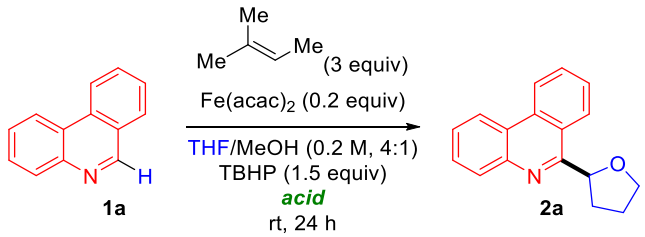

Entry	Variation from initial conditions	Yield
1	TFA (2 equiv)	73%
2	*p*-TsOH (1.5 equiv)	39%
3	H_2SO_4 (1.5 equiv)	6%
4	$BF_3{\cdot}OEt_2$ (1.5 equiv)	27%
5	TFA (5 equiv)	65%

The optimization process continued by evaluating the catalyst (*Table 3.7*). $Fe(acac)_3$ was reevaluated with the new optimum conditions (*entry 2*); however, only a 44% yield was obtained, certifying that the reduced form of iron was much better for the reaction. To explore other metal catalysts, cobalt(II) acetylacetonate was evaluated (*entry 3*), but only traces of the desired product were observed. The reaction was also carried out

without any catalyst (*entry 4*) to rule out that the reaction did not proceed under metal-free conditions (for example, via light-generated radicals). However, no reaction was observed, confirming the need for the metal catalyst to generate the radical species. Finally, different amounts of the optimum catalyst were evaluated, and it was observed that increasing the catalyst loading to 1 equivalent was detrimental to the reaction (*entry 5*), as was reducing it to 0.1 equivalents but to a lesser extent (*entry 6*).

Table 3.7. Determination of the most appropriate catalyst.

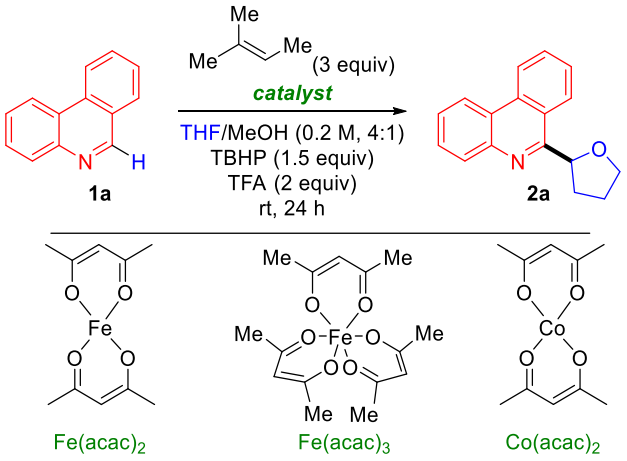

Entry	Variation from initial conditions	Yield
1	$Fe(acac)_2$ (0.2 equiv)	73%
2	$Fe(acac)_3$ (0.2 equiv)	44%
3	$Co(acac)_2$ (0.2 equiv)	traces
4	No catalyst	nr
5	$Fe(acac)_2$ (1 equiv)	45%
6	$Fe(acac)_2$ (0.1 equiv)	63%

Finally, we wanted to study the effect of using a cosolvent to reduce the amount of ether employed (*Table 3.8*). This would enable the use of solid ethers and expensive or non-commercially available ethers. First, it was evaluated whether using methanol as a cosolvent was necessary (*entry 2*). However, the omission of MeOH led to a reduced yield of 32%. We then evaluated different concentrations of THF/methanol, and it was seen that when the reaction was concentrated to 0.1 M (*entry 3*) and when it was diluted to 0.4 M (*entry 4*), the yield dropped. Ethanol (*entry 5*), water (*entry 6*), and *tert*-butanol (*entry 7*) were also studied as cosolvents instead of methanol but did not provide any benefit to the reaction, reducing the yields to 20-40%. Then, the reaction was tried in a mixture of tetrahydrofuran and dichloroethane without methanol (*entry 8*), but no reaction was observed. Keeping the final concentration at 0.2 M was tested to add a third component to the THF/MeOH mixture with dichloroethane (*entry 9*),

tert-butylmethyl ether (*entry 10*), acetonitrile (*entry 11*), and 1,1,1,3,3,3-hexafluoroisopropanol (*entry 14*). Although these tests did not improve upon the previously obtained 73% yield, the acetonitrile mixture allowed us to obtain the product in a respectable 58% yield. Finally, the THF/MeCN/MeOH mixture was studied to see if the equivalents of THF could be further reduced without this detrimentally affecting the reaction. Therefore, ratios of 1:3:1 (*entry 12*) and 0.5:3:1 (*entry 13*) were tested, and in both cases, the yield decreased slightly, but no significant difference between the two concentrations was found.

Table 3.8. Determination of the most appropriate cosolvent and concentration.

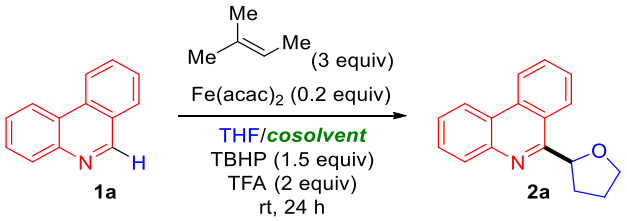

Entry	Variation from initial conditions	Yield
1	THF/MeOH (0.2 M, 4:1)	73%
2	THF (0.2 M)	32%
3	THF/MeOH (0.1 M, 4:1)	56%
4	THF/MeOH (0.4 M, 4:1)	45%
5	THF/EtOH (0.2 M, 4:1)	22%
6	THF/H_2O (0.2 M, 4:1)	43%
7	THF/*t*-BuOH (0.2 M, 4:1)	20%
8	THF/DCE (0.2 M, 4:1)	nr
9	THF/DCE/MeOH (0.2 M, 2:2:1)	48%
10	THF/*t*-BuOMe/MeOH (0.2 M, 2:2:1)	53%
11	THF/MeCN/MeOH (0.2 M, 2:2:1)	58%
12	THF/MeCN/MeOH (0.2 M, 1:3:1)	49%
13	THF/MeCN/MeOH (0.2 M, 0.5:3.5:1)	47%
14	THF/HFIP/MeOH (0.2 M, 2:2:1)	12%

While it can be observed that using the ether as the solvent is preferable, the conditions of entries 11-13 provide an alternative to allow us to test the reaction with ethers that are solids at room temperature or are too expensive to be employed as the solvent.

3.3.2. Substrate scope

Once we had optimized the reaction, we proceeded to analyze the scope, examining different mono- and polysubstituted heterocycles as the radical acceptor with different types of donors, including cyclic and acyclic ethers, amides, and nitriles.

Scope of donors

Cyclic ethers

The first group of ethers we examined were cyclic ethers (**2a**-**2i**). As observed in *Scheme 3.9*, increasing the ring size from 5 to 6 gave **2b** in an excellent 84% yield. Using 1,4-dioxane also allowed the desired compound **2c** to be obtained in a good yield of 86%. When benzo[*d*][1,3]dioxole was subjected to the reaction conditions, the product **2d** could also be isolated in an excellent yield of 95%, but in contrast, when its analog with an extra carbon was tried, the desired product **2e** was not obtained, recovering almost all the mass of the starting materials in the crude reaction mixture.

When 1,3-dioxolane was used, the reaction was achieved with 97% yield, obtaining constitutional isomers in a 19:1 ratio (**2f**-**2f'**) with preference for the position between the two oxygen atoms. When using 2-methyltetrahydrofuran as a donor, only the coupled product with the methyl at the 5' position **2g** was obtained in a diastereomeric mixture of 1.5:1, and none of the product with the methyl at the 2' position was observed.

Finally, it was thought that it might be interesting to study the coupling with crown ethers for their biological applications[218] and their importance in coordination chemistry.[219] Unfortunately, 1,3,5-trioxane and 18-crown-6 were tested**,** only complex mixtures were obtained that did not allow the isolation of the desired products.

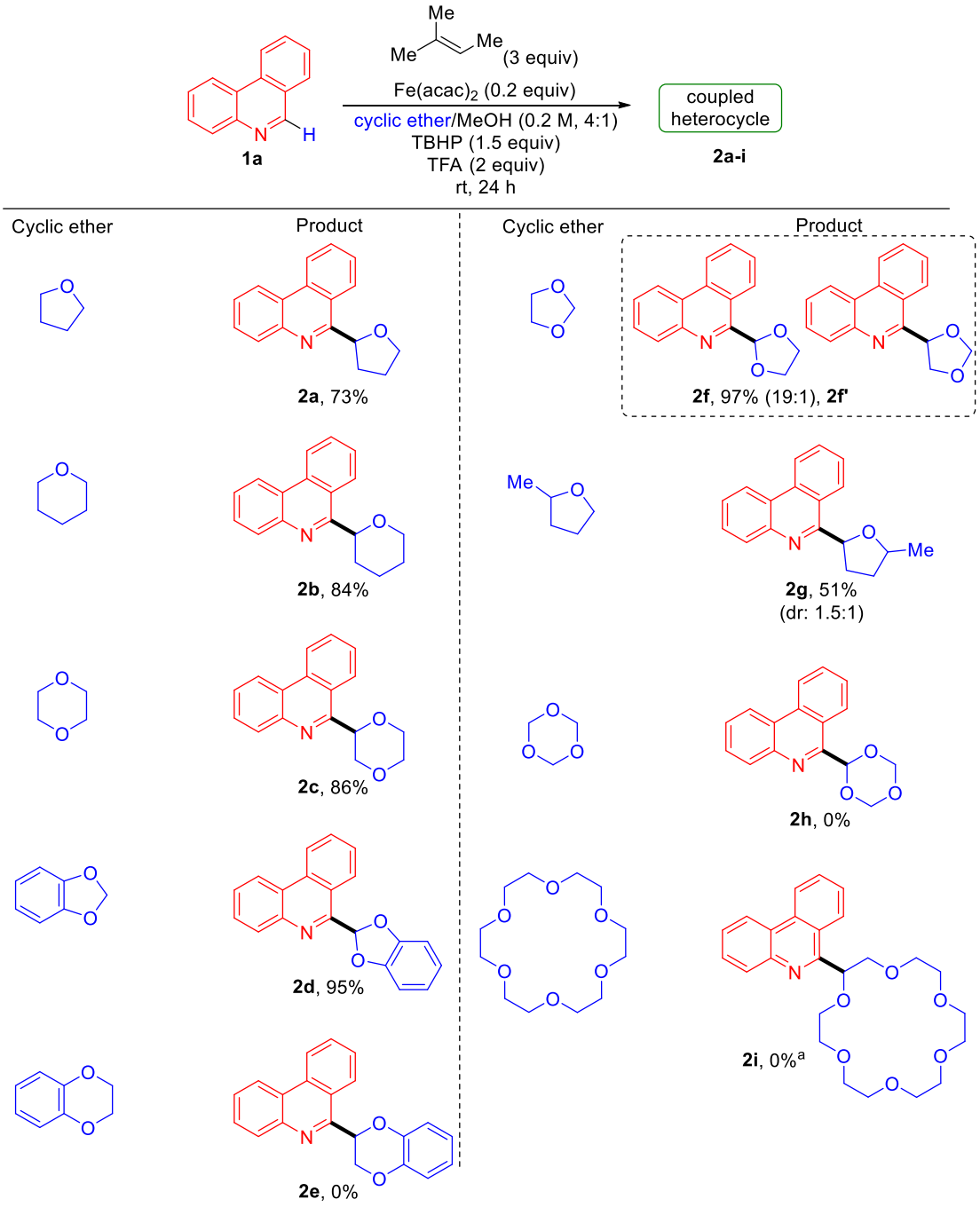

Scheme 3.9. Scope of cyclic ethers. [a]MeCN/MeOH (0.2 M, 4:1) was used as solvent and 18-crown-6 (5 equiv) as donor.

Acyclic ethers

Next, we proceeded to evaluate acyclic ethers as radical donors. We obtained excellent yields with diethyl ether, *n*-propyl ether and dimethoxyether to give compounds **2j-l** respectivley. Surprisingly, when the dibenzyl ether was used, 6-benzoylphenanthridine **2m** was obtained in a moderate yield of 32% instead of the expected product. A reasonable explanation would be that, in a similar way to the work described by

Gonzalez-Gomez[220] and Peng,[221] after hydrogen abstraction from Bn_2O, a β-fragmentation would give rise to a benzyl radical and an alkoxy radical, the latter could be oxidized by TBHP, and give an acyl radical which would attack the heterocycle to achieve the observed product. When *tert*-butyl methyl ether was used, none of the coupled product **2n** was observed. Additionally, when diisopropyl ether was used, no reaction to **2o** was observed either. These results show the preference of the reaction to only couple with secondary radical positions. Consequently, as they are unreactive, ethers such as methyl tert-butyl ether and diisopropyl ether can potentially be used as solvents in the reaction.

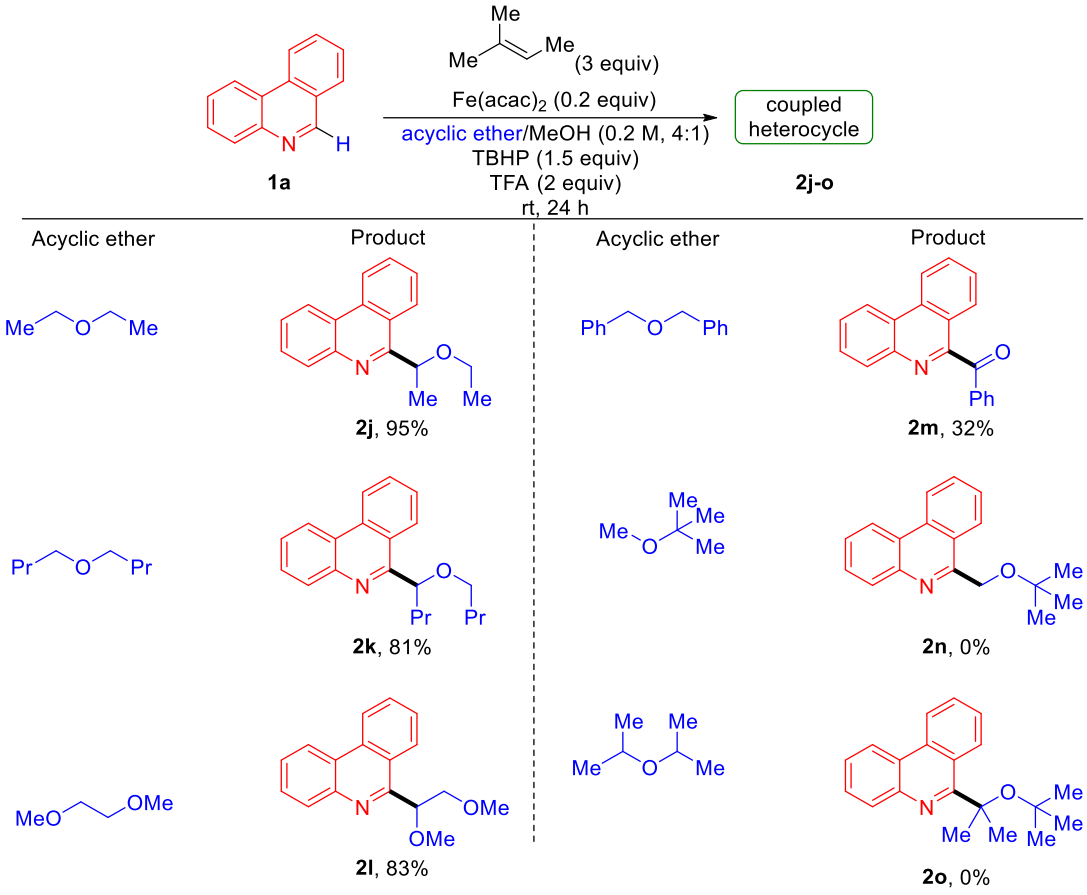

Scheme 3.10. Scope of acyclic ethers.

Notably, when diisopropyl ether was used, we observed the formation of an aldehyde next to the nitrogen atom, giving compound **3a** a 27% yield. The formation of this product appears because the methanol acts as a formylating agent, a reaction documented in the literature.[222] The mechanism starts with the homolytic cleavage of the radical initiator TBHP to give the hydroxyl radical, which abstracts a hydrogen atom from methanol to afford the hydroxymethyl radical **A** and a *tert*-butoxyl radical

(*Scheme 3.11.*). This radical intermediate **A** then undergoes a Minisci reaction with phenanthridine **B** to yield intermediate **C**, which oxidizes through *tert*-butoxyl radicals to achieve intermediate **D**. Finally, the aldehyde is obtained by the oxidation of the alcohol **D** enabled by the Fe catalyst.

While the formation of this byproduct was of concern, removing methanol from the reaction seems unnecessary as the side-reaction only predominates when the donor is unreactive, and there is no alternative pathway. When this is not the case (as stated in *Table 3.8*), methanol exerts an overall beneficial effect on the reaction.

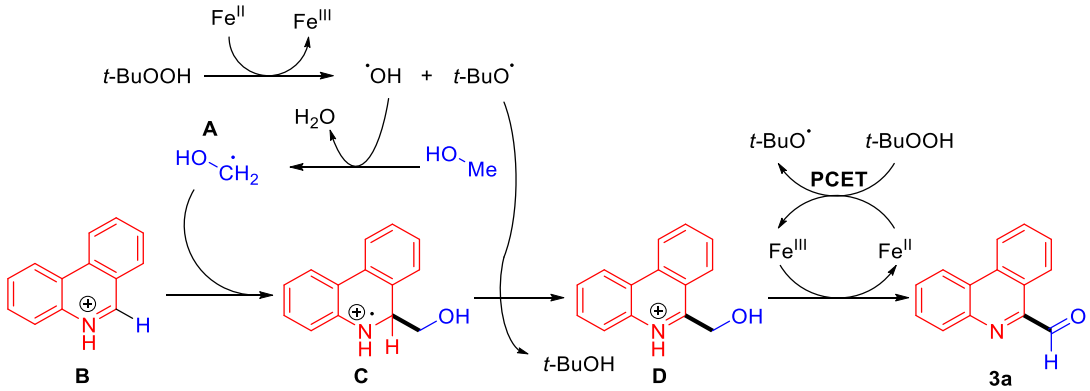

Scheme 3.11. Mechanism for the formation of the aldehyde product.

We thought it could be interesting to develop this reaction further, allowing the formation of formylated heterocycles under mild conditions.[223] Using our optimized reaction conditions but omitting THF and using only MeOH as a solvent, we were pleased to observe that the desired formylated phenanthridine **3a** was formed in a good 77% (*Table 3.9, entry 1*). Notably, the desired product was only formed in trace amounts when the same reaction was carried out without the alkene additive (*entry 2*).

*Table 3.9. Study of the best conditions to produce aldehyde **3a**.*

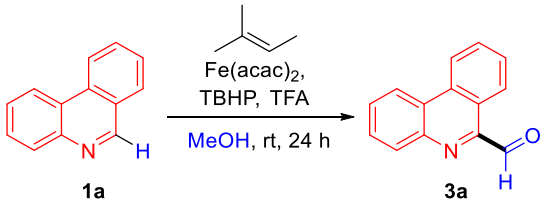

Entry	alkene	$Fe(acac)_2$	TBHP	TFA	T°	MeOH	time	Prod.
1	3	0.2	1.5[a]	2	rt	0.2 M	24 h	77%
2	-	0.2	1.5[a]	2	rt	0.2 M	24 h	3%

[a]TBHP 5.5 M in decane.

We briefly considered evaluating if these conditions could be extrapolated to other heterocycles, such as quinoline. Unfortunately, when we exposed lepidine **1b** to the reaction conditions, the reaction was more sluggish, giving only 4% of the aldehyde **3b** and 25% of the alcohol precursor **3b'** after 24 h (*Table 3.10, entry 1*). Attempts to use quinoxaline (*entry 2*) proved even less successful. Given the results for lepidine, we evaluated forcing the reaction by lengthening the reaction time to 96 h and adding double the quantity of oxidant. We were pleased that this gave a moderate 44% yield of the aldehyde and 50% of the alcohol product. However, we did not continue with this optimization due to time constraints.

*Table 3.10. Study of the best conditions to produce aldehyde **3b**.*

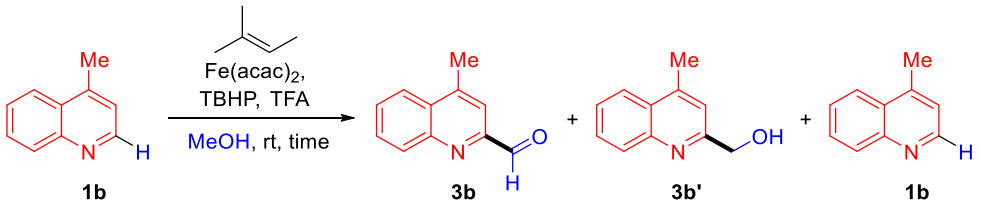

Entry	alkene	$Fe(acac)_2$	TBHP	TFA	T°	MeOH	time	3b	3b'	1b
1	3	0.2	1.5[a]	2	rt	0.2 M	24 h	4%	28%	68%
2[b]	3	0.2	1.5[a]	2	rt	0.2 M	24 h	2%	7%	42%
3	5	0.2	3[a]	2	rt	0.2 M	96 h	44%	40%	10%
4	3	0.5[c]	1.5[a]	2	rt	0.2 M	72 h	28%	60%	12%

[a]TBHP 5.5 M in decane. [b]Quinoxaline as heterocycle. [c]0.5 equiv of $Fe(acac)_3$ also added.

Amides and carbamates

Once we finished examining different ethers, we wanted to analyze the potential of amides and carbamates that have been demonstrated to behave similarly to ethers under radical coupling conditions. The reaction was successfully carried out with *N*-methyl-2-pyrrolidone, yielding a mixture of constitutional isomers **2p** and **2p´** in a 2:1 ratio, as seen in *Scheme 3.12*. Contrarily, no product **2q** was observed when we used pyrrolidine protected with Boc, possibly due to the bulkiness of the Boc group or electronic effects. Similarly, the use of oxopyrrolidine did not give the desired product **2r**. We then proceeded to examine non-cyclic amides and nitriles. When *N,N*-dimethylacetamide was used, the desired compound **2s** was achieved with a good 75% yield. Surprisingly, when *N*, *N*-Dimethylformamide was studied, the carbonyl side **2t** coupled product was obtained in good yield instead of reacting with the methyl group as in the previous compound.

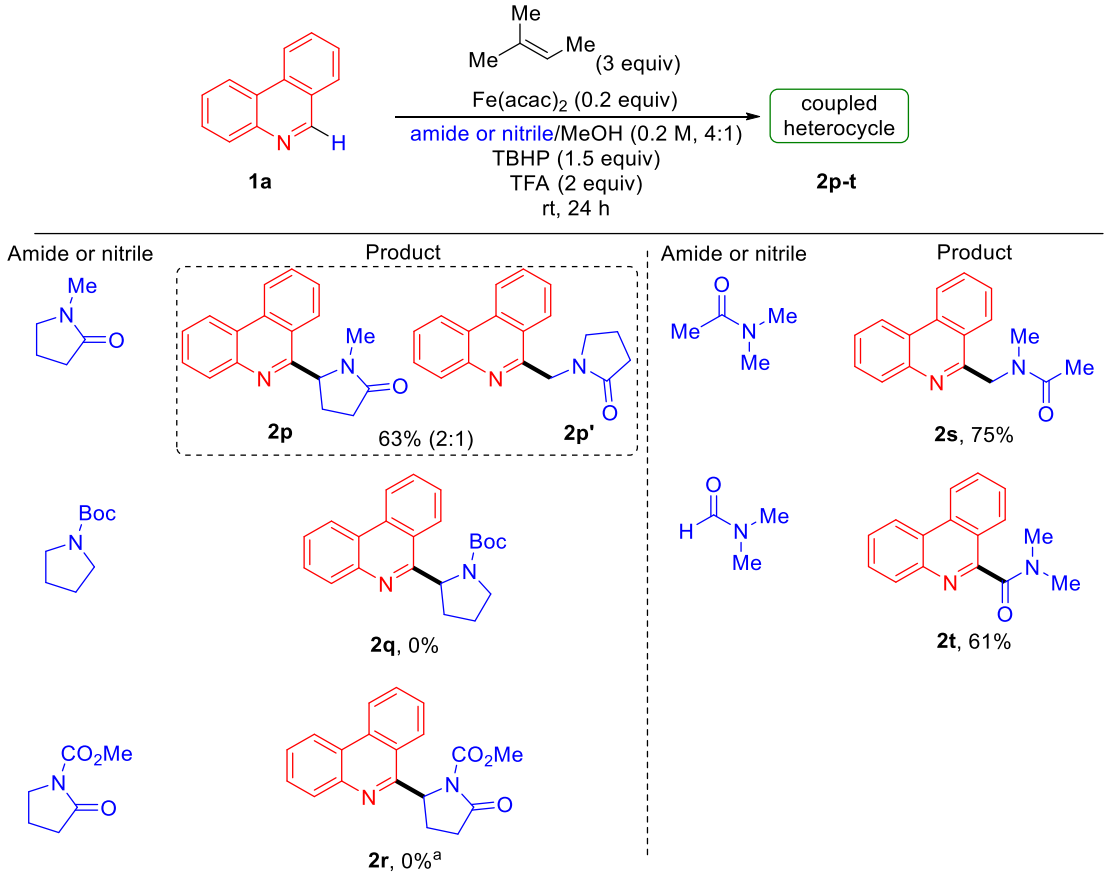

Scheme 3.12. Scope of amides and nitriles. [a]MeCN/MeOH (0.2 M, 4:1) was used as solvent and methyl 2-oxopyrrolidine-1-carboxylate (5 equiv) as donor.

Subsequent literature revision showed the preference for formyl hydrogen abstraction rather than *N*-methyl one in the case of DMF and the preference for *N*-methyl hydrogen abstraction instead of the acetyl group in the case of DMA due to stereo-electronic effects.[224]

Miscellaneous donors

Finally, we examined the potential of this methodology applied to aldehydes, ketones, and alkanes (*Scheme 3.13*). When 4-methoxybenzaldehyde was subjected to the reaction conditions, the formation of the desired product was not detected. In the same way, cyclohexanone gave no detected product. Notably, the use of cyclohexane did result in the formation of the desired product **2w**, albeit in a poor 11% yield. We postulate that the fundamental problem here is the effect of the polarity of the donor compound on the reaction when used as a solvent. In the initial examples, the polarity of the donors likely makes them too polar as solvents. In the case of cyclohexane, the effect is the opposite, and it is too apolar as a solvent. A deeper study of these groups had to be left due to lack of time. Still, the promising results of compound **2w** open the door to optimizing the reaction in the future.

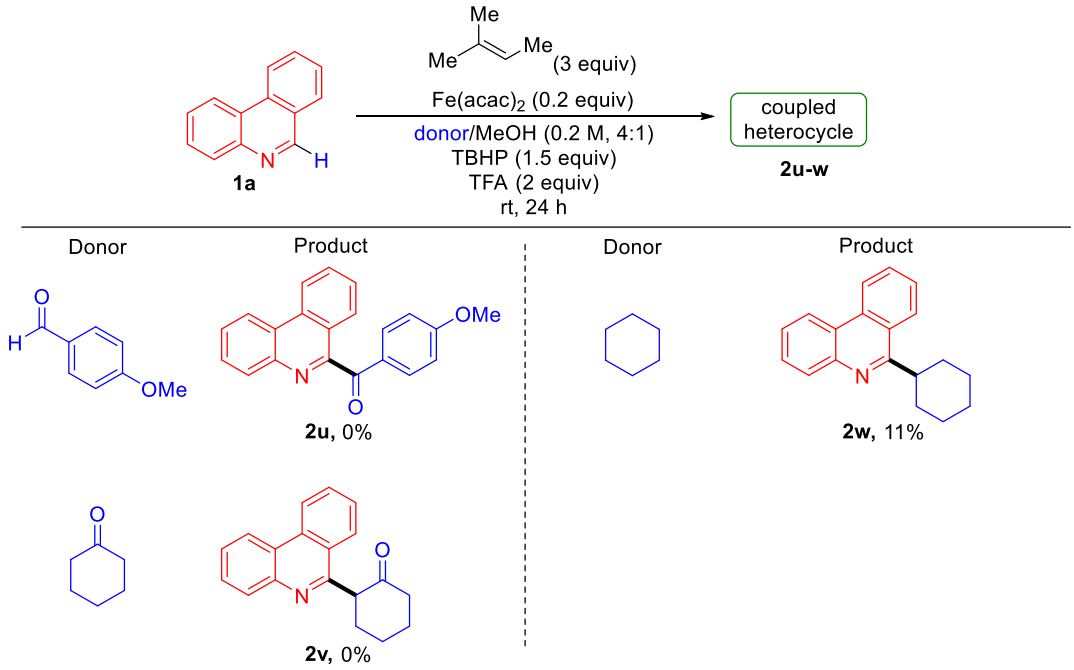

Scheme 3.13. Scope of miscellaneous donors.

Scope of acceptors

Mononitrogenated polycyclic heterocycles

After completing the scope of donors, we examined the scope of acceptors using different heterocycles. We began using mononitrogenated polycyclic heterocycles, keeping THF constant as the radical donor (*Scheme 3.14*).

Lepidine **1b** and isoquinoline **1c** gave the desired product in good yields, giving a single product since the C-4 position is blocked in both cases. However, when quinoline **1d** was used, both the C-2 and C-4 coupled products **4d** and **4d'** were obtained in 67% yield and a ratio of constitutional isomers of 1.6:1. Next, 2-methylquinoline **1e** was examined, and the product could be obtained with a good yield of 74%. Finally, benzo[*d*]thiazole **1f** was also tried to see how the presence of a sulfur atom affected the reaction. Unfortunately, none of the desired product **4f** was obtained.

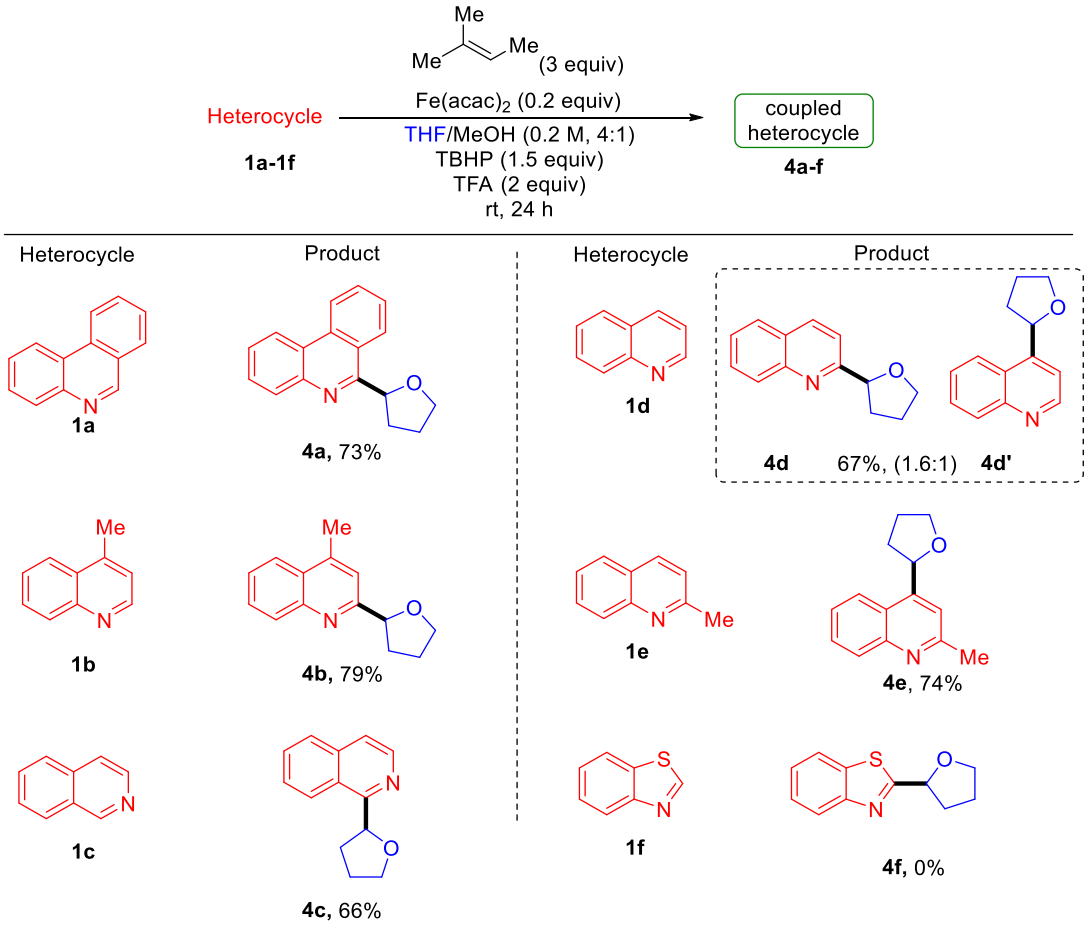

Scheme 3.14. Scope of mononitrogenated polycyclic heterocycles.

Substituted pyridines

Next, we explored substituted pyridines (*Scheme 3.15*). When 4-cyanopyridine **1g** and 4-cyanopyridine **1h** were treated, only traces of the desired products were obtained, which could be seen by NMR but could not be isolated on the corresponding chromatographic columns. When methyl isonicotinate **1i** was tested, no product was isolated either. In contrast, when methyl nicotinate **1j** was tested, the expected product **4j** could be obtained in a moderate yield of 44%, probably due to the increased electron deficiency of the heterocyclic ring resulting from the ester group, notably becoming more apparent at the C-3 position than at the C-4 position. Moreover, when 4-phenylpyridine **1k** was used, only 5% of impure product **4k** was obtained. Finally, 2,6-lutidine **1l** was used, but no reaction was observed, indicating the 4-position was not reactive, or the heterocycle itself was too electron-rich due to the two methyl groups.

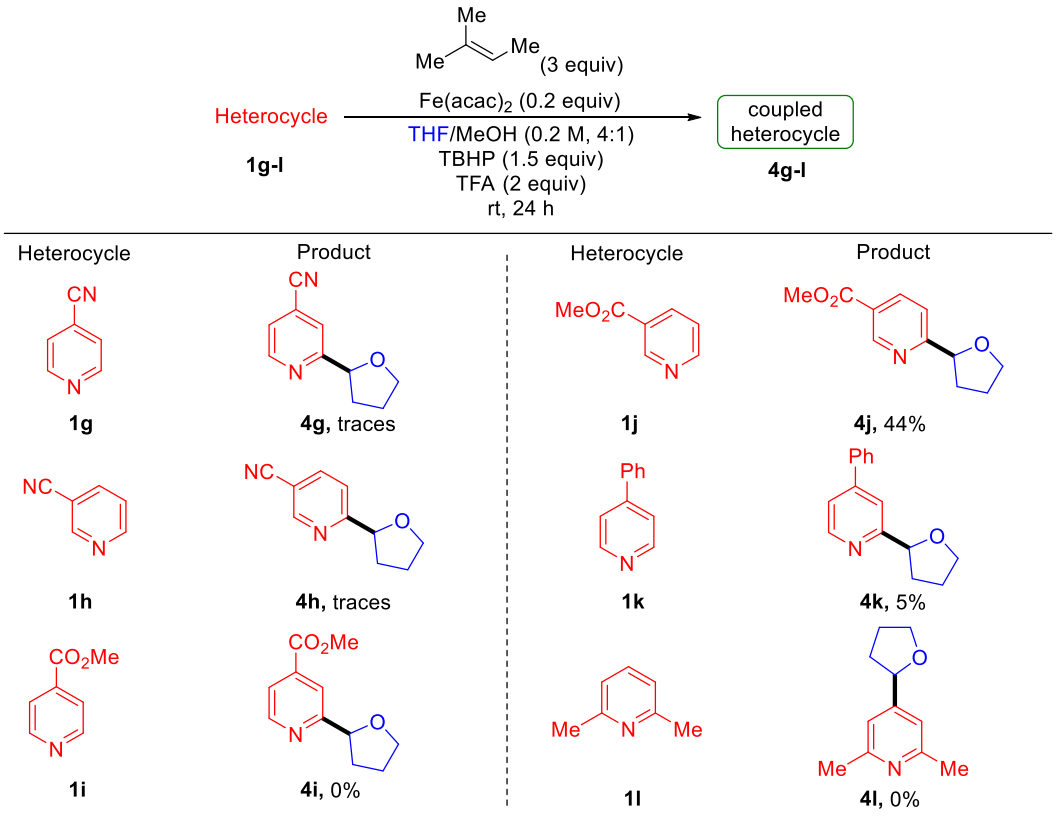

Scheme 3.15. Scope of substituted pyridines.

Polynitrogenated heterocycles

Finally, it was decided to study the behavior of different mono- or bicyclic polynitrogenated heterocycles (*Scheme 3.16*). The initial tests yielded very low amounts of the desired compounds with two equivalents of acid, probably due to double protonation, meaning there was no acid left over for the formation of the radical, so it was decided to put twice as many equivalents of TFA (4 equiv).

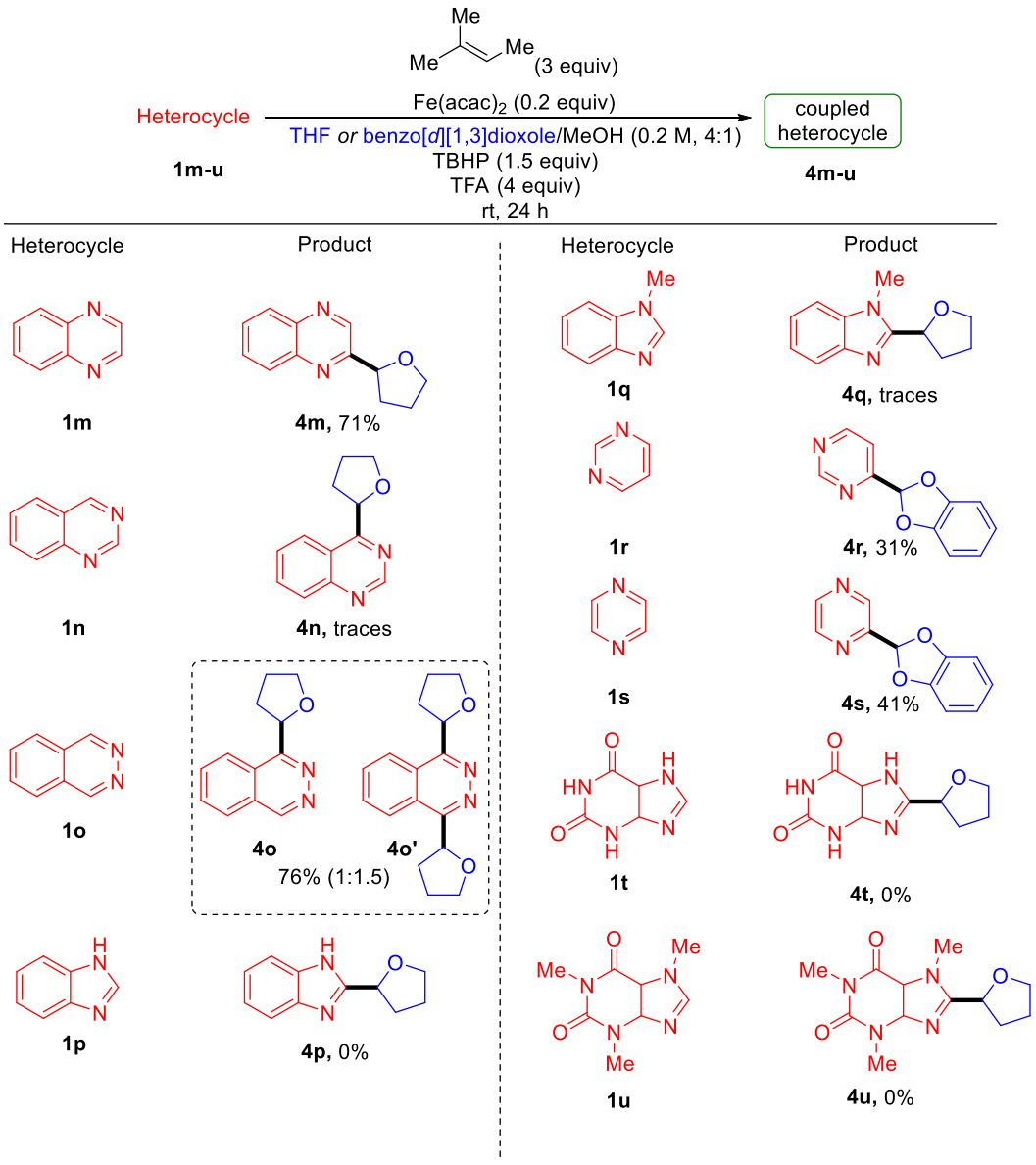

Scheme 3.16. Scope of polynitrogenated heterocycles.

Under these conditions, quinoxaline **1m** gave the expected product **4m** in 71%. In contrast, when its isomer, quinazoline **1n**, was tested, only traces of product **4n** could be identified. On the other hand, phthalazine **1o** coupled readily to give a 1:1.5 mixture

of the mono- and dicoupled compounds **4o** and **4o'** in a 76% yield. Next, 1H-benzo[*d*]imidazole **1p** and its methylated version, 1-methyl-1H-benzo[*d*]imidazole **1q**, were tested. Still, in the first case, no product formation was seen, and in the second, traces of the product **4q** could be identified by NMR, but it could not be isolated.

Two diazines, compounds **1r** and **1s**, were also evaluated; since both pyrazine and pyrimidine are volatile, we coupled these acceptors with 1,3-benzodioxole instead of THF to increase the coupled products' boiling points. In both cases, moderate yields of the coupled heterocycles **4r** and **4s** were obtained. However, **4r** could not be fully purified. Finally, two xanthine bases were studied, xanthine **1t** and caffeine **1u**, but in neither case could the formation of the expected products be observed.

Overview of the Reaction Scope

In summary, in schemes *3.17* and *3.18,* we can see the summarized scope separated by the analysis of donors and acceptors, previously discussed more specifically. Twenty-three radical donors were tested, and fourteen successfully gave the desired product. Twenty-one heterocycles were also tested, of which eleven reacted successfully.

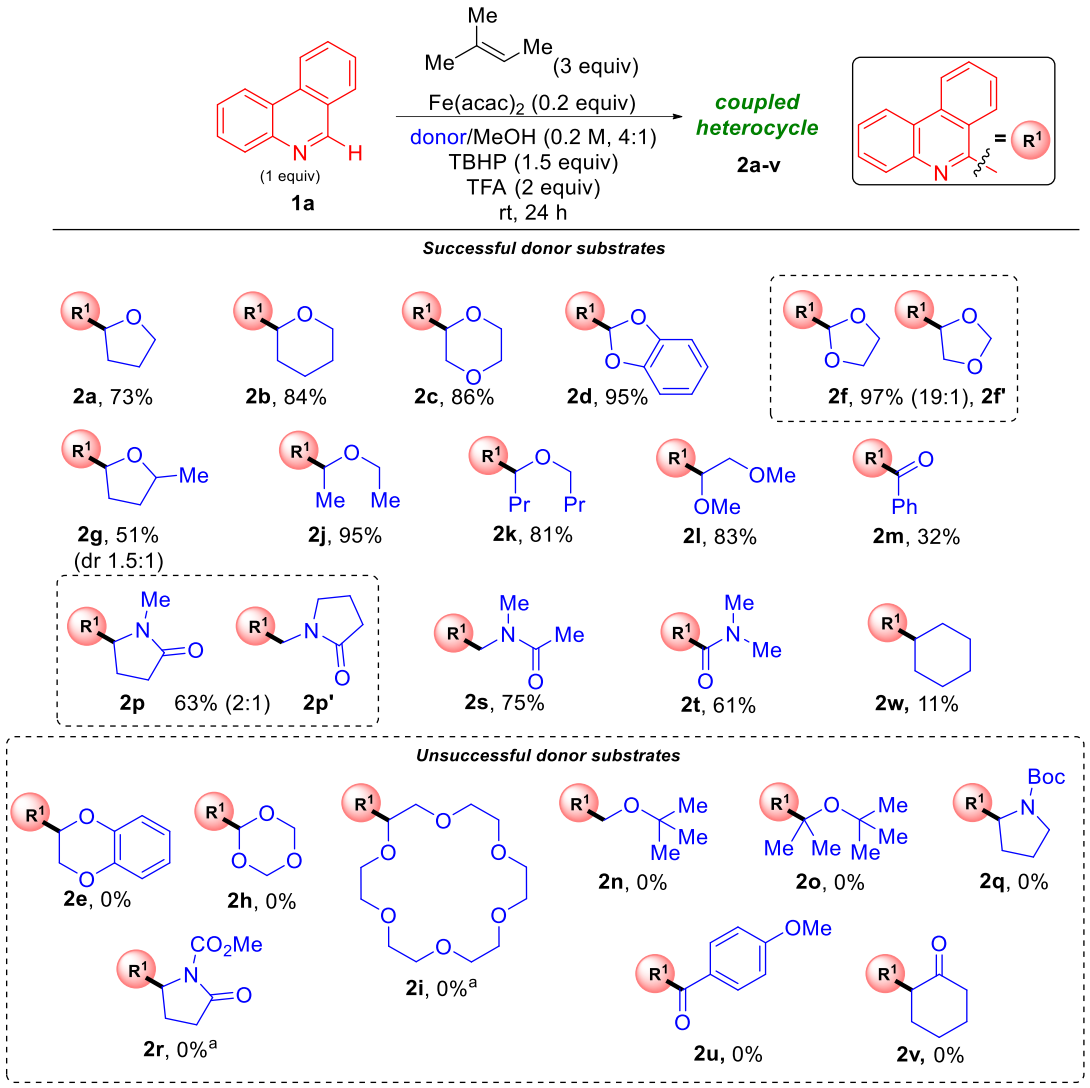

Scheme 3.17. Overview of the scope of different donor substrates. [a]MeCN/MeOH (0.2 M, 4:1) was used as solvent and donor (5 equiv).

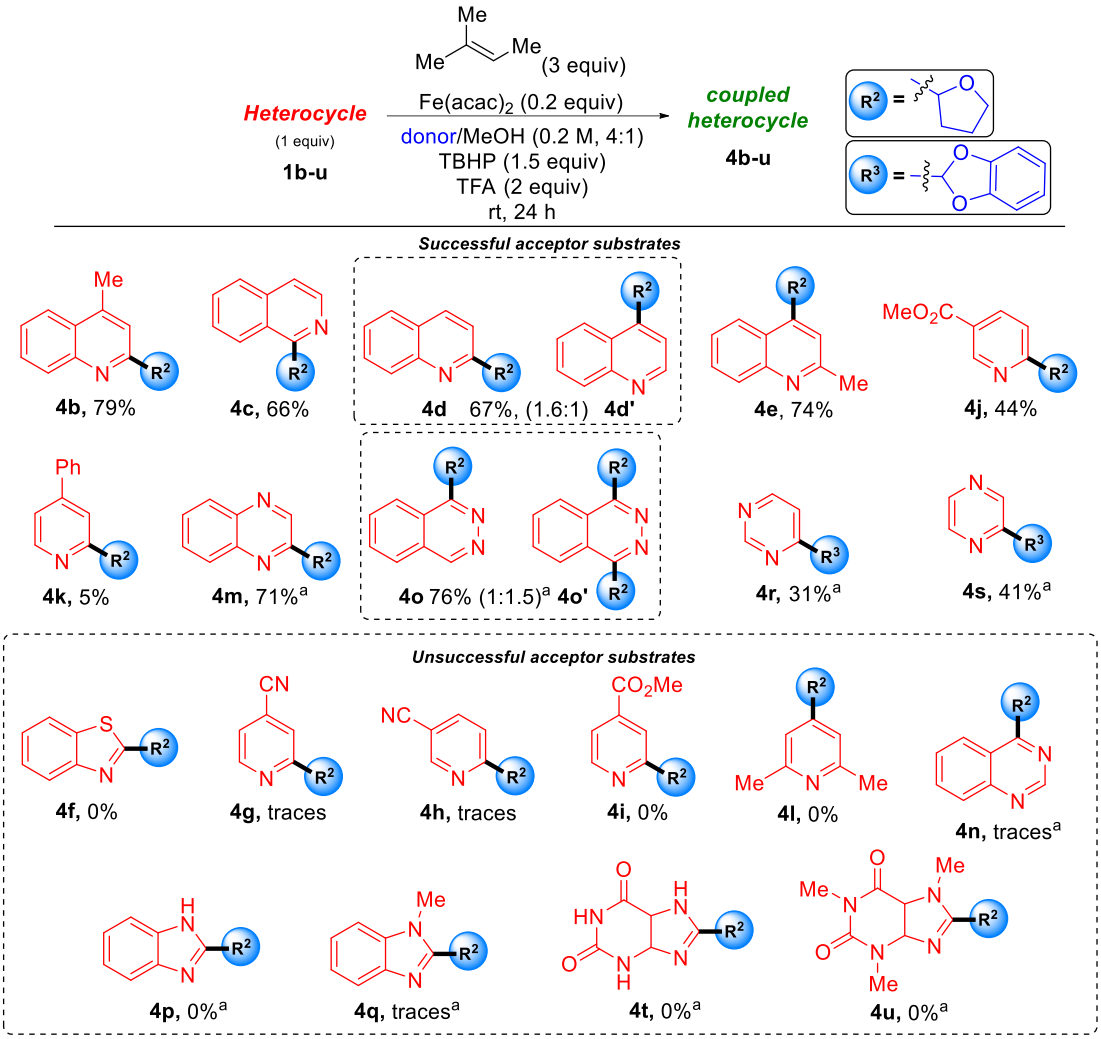

Scheme 3.18. Scope overview of acceptor substrates. [a]TFA (4 equiv) was used.

3.3.3. Mechanistic discussion

Finally, a plausible mechanism is outlined in *Scheme 3.19*. An initial PCET reaction enabled by Fe^{II} generates the *t*-BuO· radical which undergoes a HAT reaction to generate α-oxyalkyl radical. This α-radical will attack the heterocycle activated with TFA **A** to form the coupled radical cation product **B**. Next, a SET reaction between the coupled radical cation and the Fe^{III} formed will regenerate the Fe^{II}, thus completing the catalytic cycle. Alternatively, the generation of the oxidized intermediate **C** could also occur by a HAT reaction between the radical *t*-BuO· and the coupled radical cation **B**. Final deprotonation during the work-up of the reaction would give rise to the coupled heterocycle **2a**. In this process, the role of methanol is notable since it was observed that in its absence, the yield drops (*see Table 3.8*) and may serve to stabilize the radical species.

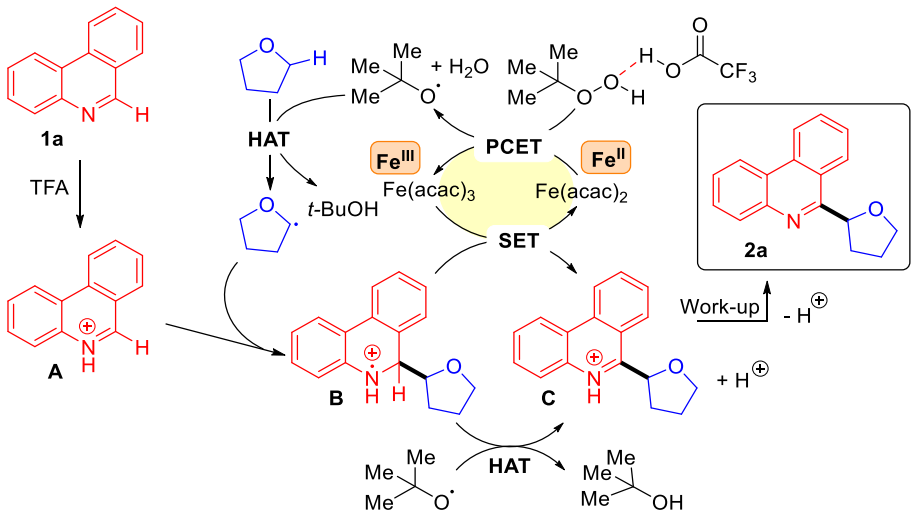

Scheme 3.19. Proposed mechanism for the Minisci C-H cross-coupling of heterocycles with ethers.

As we observed during the reaction optimization (see *Section 3.3.1*), the alkene was essential to obtain a good reaction yield, so we proposed to study its function in the reaction. Among the options contemplated, two seemed most likely: (i) It acts as a hydrogen acceptor from the reduced coupled heterocycle, allowing the reoxidation of the aromatic ring of the phenanthridine (see *Scheme 3.19*), or (ii) It acts as a scavenger in an analogous manner to the Pinnick reaction, which uses the same alkene. To be

able to analyze the alkene after the reaction, two different higher molecular weight alkenes, **6** and **8**, were synthesized (*Scheme 3.20*) that could be recovered at the end of the reaction, unlike the highly volatile 2-methylbut-2-ene.

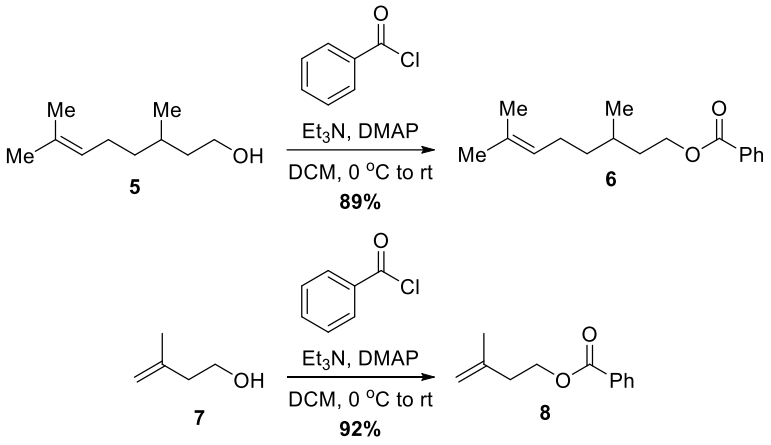

*Scheme 3.20. Preparation of alkenes **6** and **8**.*

Reaction under the optimized reaction conditions was carried out by substituting 2-methylbut-2-ene for either alkene **6** or **8**, giving the desired compound **2a** in good yield indicating the change of alkene was not too detrimental to the reaction performance (*Scheme 3.21*). We focused on the isolation of the alkene or by-products, and surprisingly, in both cases, almost all the unreacted alkene was recovered, thus giving us little information about its role in the reaction. To explain this, we considered the recovery of the intact alkenes to be due to hydride addition, followed by subsequent hydride transfer donors to regenerate the double bond.[47] However, this possibility was ruled out as alkene **8** was recovered with the methylene group intact and a hydrogen transfer mechanism was in operation; then, the more stable substituted double bond would be formed.

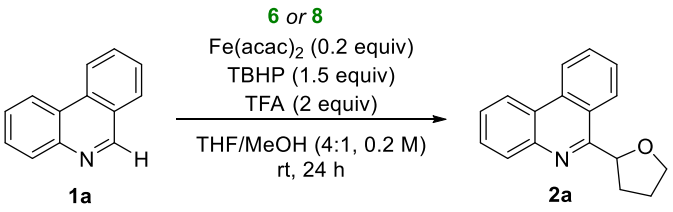

Alkene used	2a	
6 (3 equiv)	50%	*Unreacted alkene was almost fully recovered*
8 (1 equiv)	61%	

Scheme 3.21. Mechanism studies to understand alkene function.

We therefore propose that the role of the alkene is to act as a radical scavenger by inhibiting non-desirable pathways. It is known that 2-methylbut-2-ene is added to solvents such as chloroform and dichloromethane for this purpose. In our reaction, reactive oxygen species (ROS) may be formed as a result of using peroxides or via residual atmospheric oxygen, leading to the formation of various unwanted species such as hydroxy radical ($HO^{\bullet}$), hydroxide (HO^{-}), triplet oxygen ($^{3}O_2$), hydroperoxide (HOO^{-}), peroxide (O_2^{-}), and superoxide radical ($O_2^{-\bullet}$).[225] By neutralizing these species, the alkene may prevent undesirable reaction pathways leading to lower yields. Finally, it is notable that reactions involving peroxides usually require high temperatures (see *Scheme 3.7*) and it cannot be ruled out that the alkene acts as a radical transfer agent to facilitate the abstraction of the hydrogen atom of the ether.

3.3.4. Future work

As future work to investigate (*Scheme 3.22*), it would be interesting to try the use of Michael acceptors such as cyclohex-2-en-1-one[226] or naphthalene-1,4-dione[227] to see if this reaction can serve not only to couple nitrogenated heterocycles, but also other types of radical acceptors in a Giese type coupling. On the other hand, to continue expanding the scope of radical donors, it would be interesting to improve the coupling of heterocycles with alkanes, alcohols,[203] and aldehydes[228] which require further optimization to make the reactions synthetically useful.

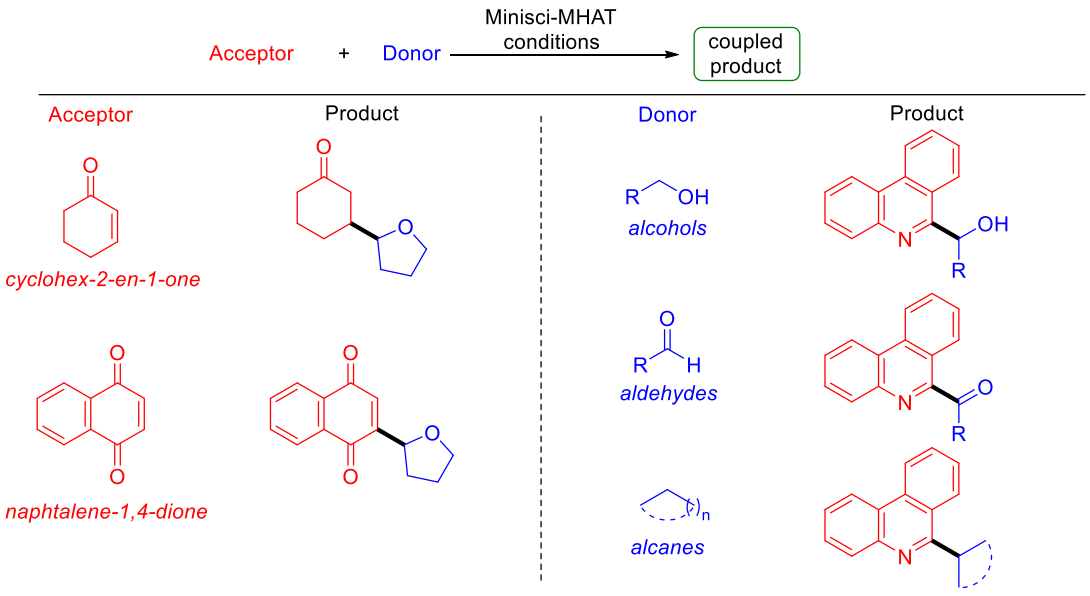

Scheme 3.22. Future studies to expand the scope.

4. ADAMANTANE BUILDING-BLOCK SYNTHESIS USING MHAT

4.1. INTRODUCTION

In this chapter, we will discuss the development of a MHAT tandem reaction for the synthesis of adamantane-like building blocks via an intramolecular MHAT of coupling tosylhydrazones, followed by fragmentation and a final Giese type coupling.

4.1.1. Adamantane and Amantadine: discovery and importance

Adamantane is a stable tricycloalkane first isolated from crude oil in 1933.[229] In 1941, Prelog and Seiwerth achieved the first synthesis of this simple diamondoid from Meerwein's ester in a five-step synthesis with a poor 1.5 % global yield.[230] Stetter reported improvements in this route a few years later, but the overall yield only increased to 6.5%.[231] However, it was not until 1957 that Schleyer demonstrated a more efficient synthesis through a Lewis-acid-induced rearrangement from dicyclopentadiene.[232]

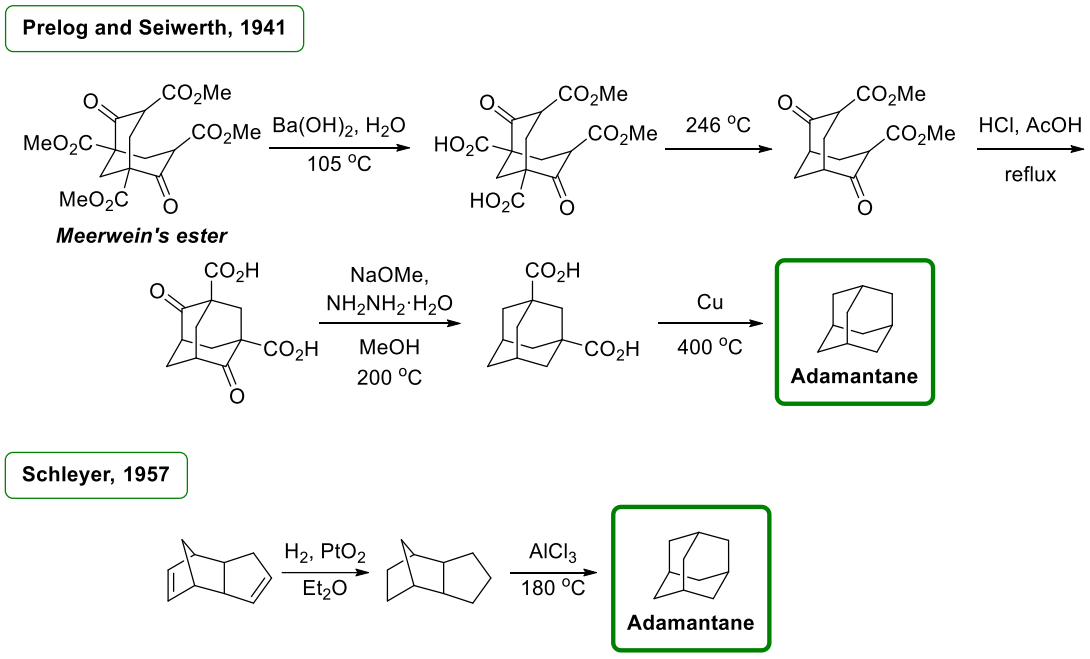

Scheme 4.1. The first reported syntheses of Adamantane by Prelog, Seiwerth, and Schleyer.

Later studies done by the groups of Olah[233] and McKervey[234] used superacid catalysis, which improved the procedures for obtaining adamantane, diamantane, and superior diamondoids.

In 1959, Stetter, Schwarz, and Hirschhorn reported the first halogenation of this nucleus to obtain 1-bromoadamantane (*Scheme 4.2*).[235] In the same year, Webber and

Harthoorn demonstrated insecticidal properties in chloroadamantanes, thus beginning the study of the biological properties of this type of nuclei.[236]

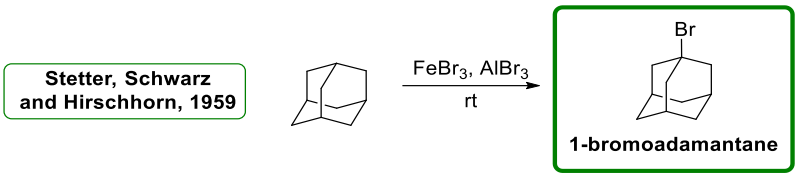

Scheme 4.2. First reported synthesis of 1-bromoadamantane.

Ever since adamantane attracted the interest of synthetic chemists, its functionalization became a subject of study. In 1959, Wulff used the previously mentioned bromination to conduct the first synthesis of 1-aminoadamantane, better known as amantadine (*Scheme 4.3*). Using a Ritter reaction, he prepared *N*-1-adamantylacetamide from 1-bromoadamantane and acetonitrile.[237] Subsequent hydrolysis using sodium hydroxide and diethylene glycol led to 1-aminoadamantane with a good overall yield.

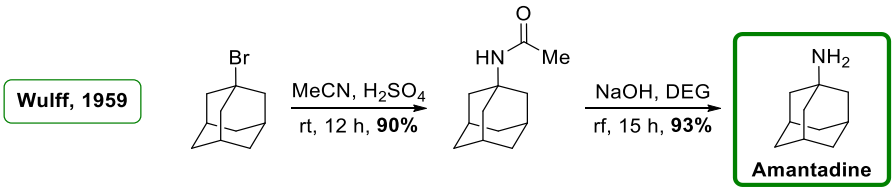

Scheme 4.3. First reported synthesis of Amantadine.

The interesting pharmacological properties of amantadine and other adamantane derivatives (see Section 4.1.2) attracted the interest of synthetic chemists in further functionalizing this type of scaffold.

4.1.2. Pharmaceuticals incorporating the Adamantane scaffold

A few years later, in 1964, amantadine was identified as an antiviral compound against *Influenza A*, inhibiting virus replication by interfering with the enzyme that transcribes DNA to RNA.[238] Further studies revealed the utility of amantadine in relieving symptoms in the early stages of Parkinson's disease and dyskinesia.[239] Similarly, rimantidine,[240] a chiral aminoadamantane, and tromantadine[241] were discovered and also presented antiviral properties for *Influenza A* and *Herpes Simplex* respectively. Shortly after, memantine, a bi-methylated amantadine, was synthesized by Eli Lilly and

Company as antidiabetic. It was later found to be a treatment for Alzheimer's disease due to its noncompetitive NMDA-receptor antagonist properties (*Figure 4.1*).[242]

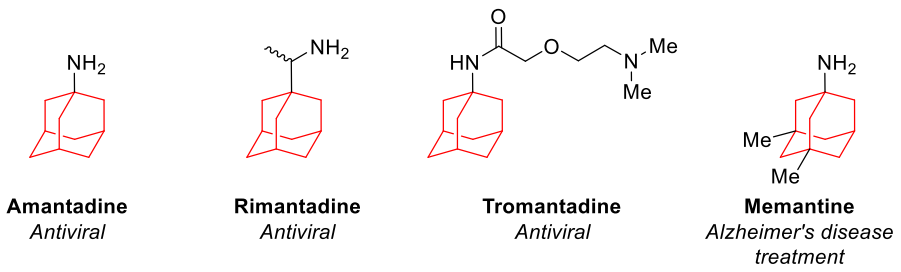

Figure 4.1. First adamantane derivatives with pharmacological properties.

Since these early discoveries, the adamantane scaffold has been incorporated into multiple pharmacological products with diverse biological activities. These include antiviral compounds, which have been used to treat *Influenza A*, *Herpes Simplex*, Hepatitis C, or HIV; antimalarials; antibiotics; anticancer agents; and acne treatments. It has also been incorporated into compounds for the treatment of neurological disorders such as Parkinson's, Alzheimer's, or central nervous system disorders; enzymatic inhibition, inhibiting DPP-IV for diabetes control or inhibiting epoxide hydrolases, protein phosphatases or hydroxysteroid dehydrogenases (*Figure 4.2*).[243]

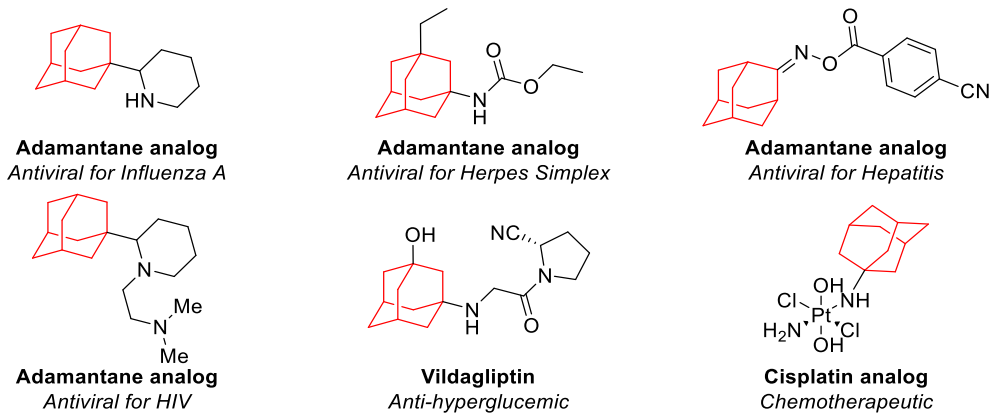

Figure 4.2. Selected examples of pharmacologically active compounds containing the adamantane scaffold.

The adamantane or heteroadamantane scaffold plays an important role in the three-dimensional adjustment of the pharmacophores into the respective binding site of the receptor, historically known as the "lock and key" principle, or more currently called

"induced-fit", referring to greater dynamism in the ligand-receptor interaction. Not only have adamantane derivatives proven to be pharmacologically active, but the adamantane scaffold has also been used to modify known pharmaceuticals, thus increasing its lipophilicity and stability and improving the pharmacokinetics, with a success rate second only to the methyl group. The role played by the three-dimensional structure with the ADME characteristics is noteworthy since it plays a crucial role in the organism's absorption, distribution, and metabolism. Therefore, in prodrug concepts, these drug carriers are used to guide the drug and direct it to the desired therapeutic target. For example, this methodology has been employed in the modification of hypoglycemic sulfonylureas,[244] nucleosides,[245] or anabolic steroids.[246]

4.1.3. Catalysts incorporating the adamantyl moiety

In the same way that the adamantane scaffold can be used to provide beneficial modifications to drugs, it can also be used as a building block to modify catalysts due to its rigid and symmetrical structure, inert hydrocarbon reactivity, and steric bulk. The rigidity of the adamantane structure provides a stable molecular platform that can be beneficial in maintaining the shape of the metal-ligand complex during catalytic reactions, thus increasing its efficiency and selectivity. The inherent prochirality of adamantanes can be exploited to design chiral ligands, which are useful in asymmetric reactions, as they can induce selectivity in the formation of stereoisomers.[247] In addition, adamantanes can offer several coordination points to the central metal in a coordination complex, increasing its stability and facilitating interaction with reagents.

The reactivity and stability of catalysts is dependent on their steric saturation and electronic richness.[248] One of the most effective ways that have been developed to study this is by the calculation of the Tolman cone angles, which can be defined as a measure of the angular spacing that a ligand would occupy around a metal in a coordination complex.[249] Adamantane ligands often have large Tolman angles, which can provide sufficient space for larger molecules or bulky reactants, favoring certain catalytic reactions. The low cost, relative ease of functionalization, ready availability, and stereoelectronic properties make adamantane a very attractive structure to incorporate into catalysts. Over the last decade, the number of catalysts containing the adamantyl moiety has increased steadily. Representative examples of adamantane

acting as a ligand can be found in many reactions (Figure *4.3*), among them in aryl palladium couplings, such as Suzuki, Heck, or Palladium-mediated cross-coupling reactions,[250] where di(adamantly)phosphines have played a significant role. In C-H activation reactions,[251] Arduengo's adamantyl-substituted carbene has been widely used. The Grubbs catalyst was modified by incorporating the adamantane skeleton, thus improving the selective synthesis of *Z*-olefins in metathesis reactions.[252] The incorporation of adamantyl moiety in Jacobsen's chiral chromium catalyst allowed and efficient, highly diastereo- and enantioselective hetero-Diels-Alder reaction.[253] In hydrogenations, chiral phosphine adamantane derivatives chelated to the rhodium center furnished the corresponding hydrogenated products in excellent *ee* of up to >99.9%.[254] Mukherjee has reported the use of thioureas that incorporate the adamantane skeleton as ligands for the asymmetric vinylogous Michael addition of butenolides to *N*-phenylmaleimides.[255]

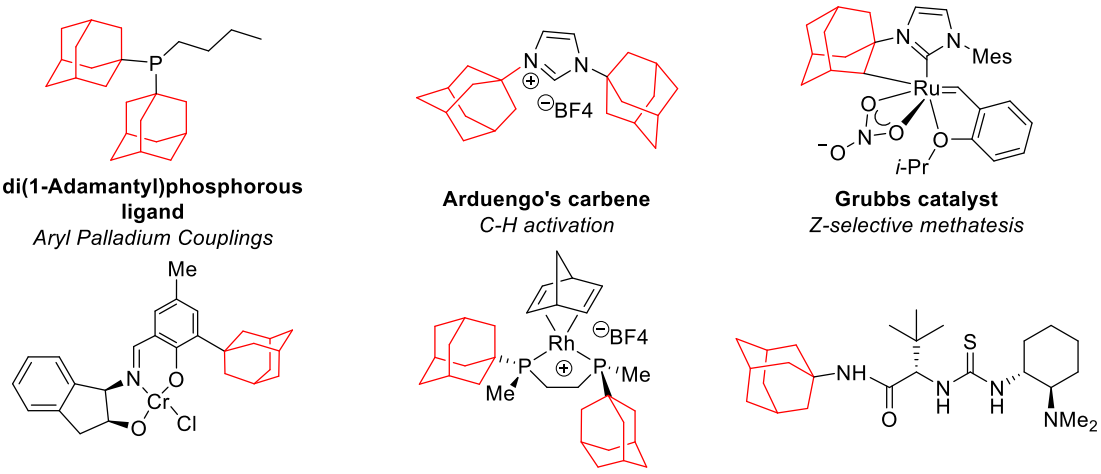

Figure 4.3. Selected examples of catalysts containing adamantane scaffold.

4.1.4. Adamantane in Natural Products

The Adamantane motif is also present in natural products (*Figure 4.4*). Examples include the Sampsoniones A-H,[256] found in *Hypericum sampsonii,* Plukenetione A,[257] isolated from *Clusia plukenetii,* and Hyperibone K,[258] isolated from *Hypericum scrabum.* These compounds have been found to have antiviral and anticancer properties.

Interestingly, analogs incorporating oxygen into their structure have also been isolated, as is the case of Tetrodotoxin, secreted by the puffer fish (*Tora fugu*), a selective blocker of voltage-gated Na^+ channels, where the rigid structure of dioxadamantane orients the groups to block the channel.[259] Also noteworthy is the case of Muamvatin,[260] which was the first natural product with a trioxadamantane core isolated from *Siphonaria normalis*, or Caloundrin B,[261] extracted from *Siphonaria zelandica* and with the same core. Some natural products containing this trioxadamantane nucleus have been revealed as sedatives and can play a role in SARS coronavirus replication inhibition.[262]

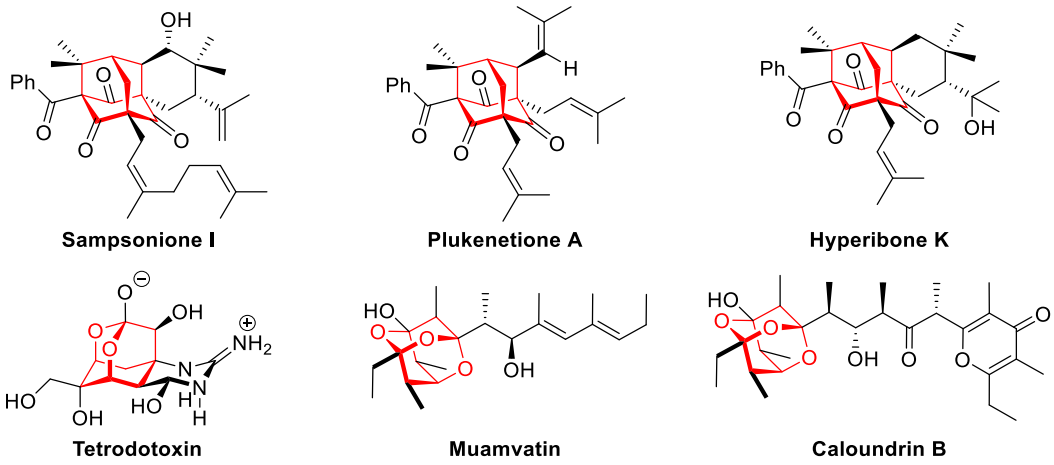

Figure 4.4. Natural products containing adamantane and heteroadamantane core.

4.1.5. Adamantane and diamondoids in nanoscience

Adamantane, and many members of the diamondoid family, have unique characteristics such as electron-donating ability, low dielectric constants, negative electron affinity, large steric bulk, rigid, hard, and saturated structure, and high thermal and chemical stability. These characteristics have made them highly desired in the field of nanoscience.[263]

Among its applications, we can find the use of these compounds in polymers to increase the hardness and thermal stability of the matrix, improve transparency and increase the refractive index, decrease its dielectric constant, and increase its porosity. They are also helpful in connecting unsaturated linkers and chromophores to optical materials and nanoscale frameworks.[264] These properties have made them suitable for developing electron emitters, such as electron-beam lithography and high-resolution electron microscopy.[265] We can also find them in ultrasensitive catalyst-based electrochemiluminescence or gas sensors.[266] They have also been used for host materials in blue organic light-emitting diodes (OLEDs) as efficient π-conjugation disruption.[267] Interestingly, they have also been applied to the construction of nanomachines, as is the case of their use as the wheels of a nanocar (*Figure 4.5*).[268]

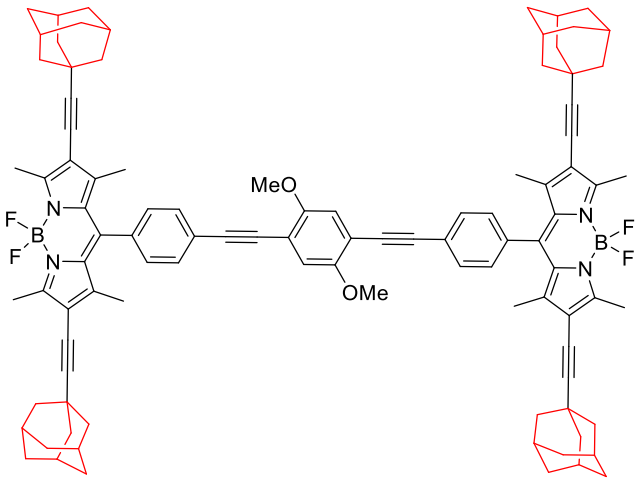

Figure 4.5. Adamantane-wheeled nanocar.

Considering the large number of applications this type of compound has in the field of nanoscience, it becomes clear that functionalizing these structures is necessary to increase their potential applications.

4.1.6. Chemistry of Adamantanes: Functionalization

The functionalization of adamantanes usually involves the substitution of halogenated intermediates, which can be converted to the desired functionalized product through the formation of the corresponding radical by traditional methods or carbocation intermediate via S_N1-type substitution with different carbon or heteroatom nucleophiles (*Scheme 4.4*). It should be noted that the radical intermediate **A** is destabilized due to the conformation. In contrast, the tertiary carbocation **B** is unusually stable because of the hyperconjugation with filled bonding orbitals within the rigid cage.[269]

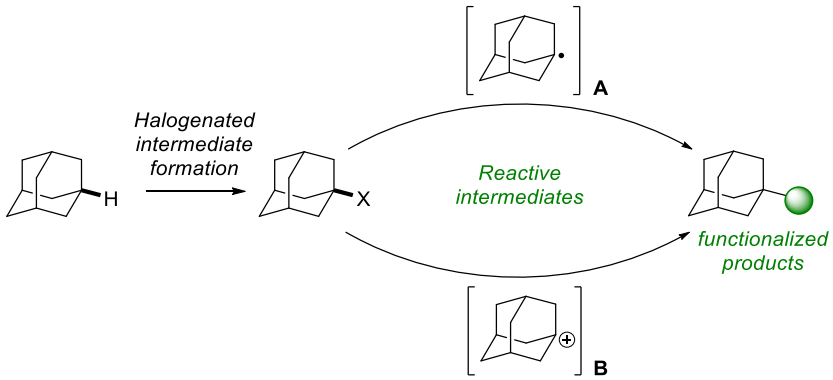

Scheme 4.4. Adamantane functionalization through radical or carbocation intermediates.

Different radical functionalization methods have been developed in recent decades to add several functional groups directly to the adamantane skeleton without passing through a halogenated intermediate. Since adamantane has two types of carbons, where the hydrogen abstraction takes place will be vital in determining the regioselectivity of the reaction. Among these multiple transformations achieved (*Scheme 4.5*), acylations, such as chlorocarbonylation,[270] acetylation,[271] formylation,[272] esterification,[273] and amidation,[274] stand out. It's also necessary to highlight the carbon monoxide carbonylations, which could be carried out using a wide range of reaction conditions.[275] Alkylation of adamantane has been achieved by adding alkenes using peroxides as catalysts[276] or through photochemistry.[277] Alkenes and alkynes have also been used in addition-fragmentation processes that have allowed decarboxylative alkenylation,[278] photochemical allylation,[279] and alkenylation,[280] and alkenylation catalyzed by metals[281] and alkynylation[282] to be carried out. Arylation processes have

also been carried out using photooxidation,[283] Minisci-type conditions,[284] metal catalysts,[285] or cascade reactions involving aromatic systems.[286] Finally, it has also been possible to introduce nitrogen-containing groups with cyanation[287] or aminoalkylation.[288]

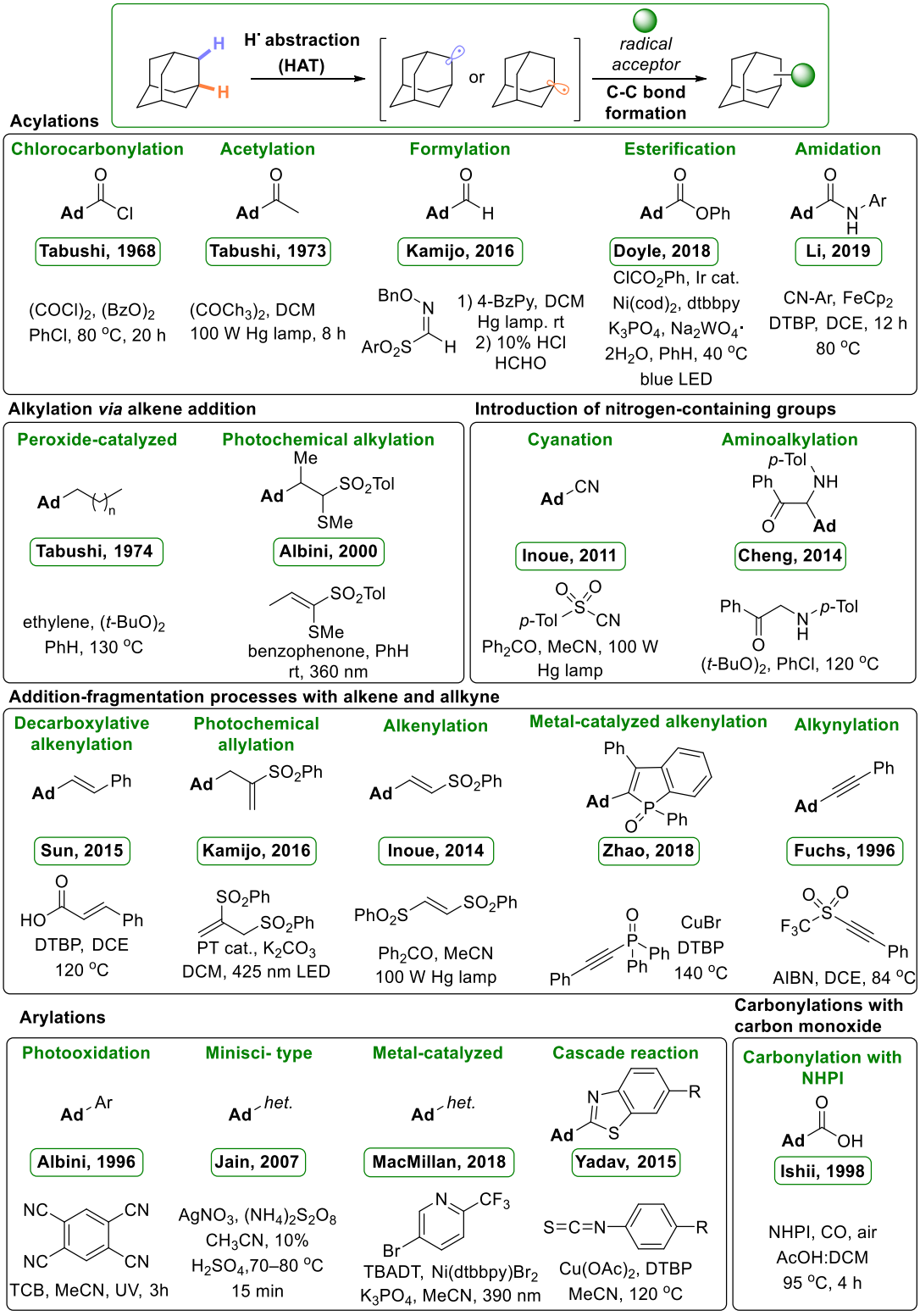

Scheme 4.5. Selected examples for adamantane functionalization using radicals.

4.1.7. Previous work in our research group

In 2018, our group reported the synthesis of α-tertiary amines via MHAT. Different types of hydrazones, as well as other C=N derivatives like oximes and imines, were evaluated and subjected to radical cyclization conditions using $Fe(acac)_3$ (0.2 equiv) and $PhSiH_3$ (2.5 equiv) in EtOH at 60 °C for 3 h. These studies revealed Cbz-hydrazones as the most suitable derivative for this reaction, allowing the one-pot formation of the hydrazone and subsequent cyclization with an excellent 93% yield. Subsequent cleavage of the hydrazine bond was successfully achieved by hydrogenation in an 85% yield (*Scheme 4.6*).

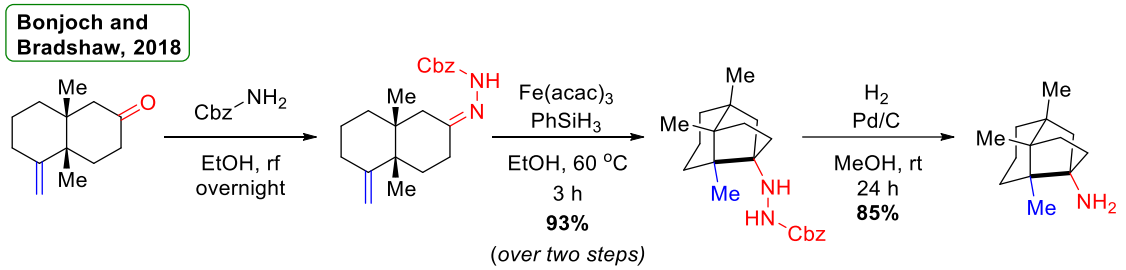

Scheme 4.6. MHAT route to access α-tertiary amines.

During these studies, when the best hydrazone group to carry out the radical cyclization was being sought, it was seen that tosylhydrazone **A**, in the presence of catalytic amounts of iron and heating, would undergo intramolecular coupling to give the intermediate tosylhydrazine **B**. Additionally, *in situ* fragmentation of the tosylhydrazone radical was believed to generate the corresponding tricyclic adamantane-like compound **C** (*Scheme 4.7*). Products **D** and **E** were thought to arise from the formation of a carbocation intermediate under the reaction conditions followed by an attack of the solvent or the metal ligand, respectively. When the reaction was repeated with two equivalents of $Fe(acac)_3$, the quantity of product **C** isolated was much higher, and similar yields were found for the byproducts **D** and **E**.

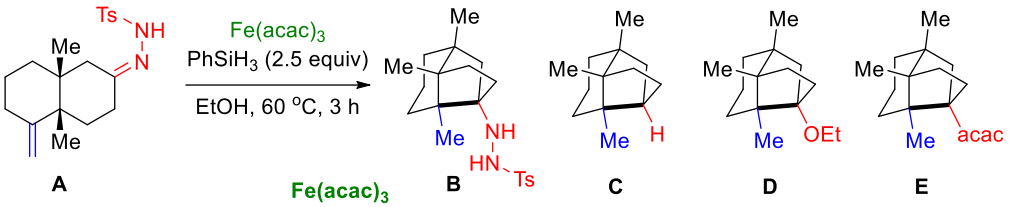

$Fe(acac)_3$	B	C	D	E
0.2 equiv	18%	15%	13%	11%
2.0 equiv	nd	51%	14%	20%

*Scheme 4.7. Radical cyclization and fragmentation of tosylhydrazone **A**.*

Attempts to repeat the reaction to characterize compound **C** fully were complicated by its high volatility and lack of chromophore. Our group therefore focused on the intermolecular version of the reaction (*Scheme 4.8*). Due to the nature of the substrates used, most of which contained a substituted aromatic ring, these compounds were no longer challenging to manipulate, and this led to the development of radical reductive alkylation of unactivated alkenes using tosylhydrazones.[81]

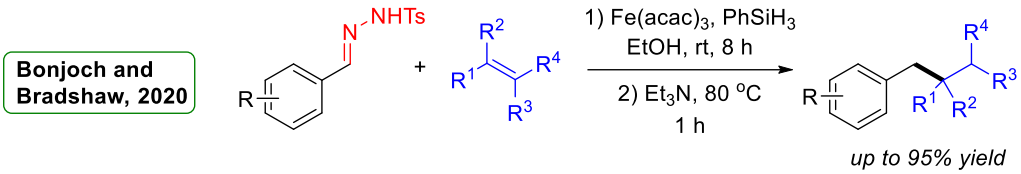

Scheme 4.8. Intramolecular alkylation of unactivated alkenes.

With additional experience, we decided to reevaluate the intramolecular version of the reaction. Kim and co-workers have described precedents for an analogous type of reaction by coupling an alkyl halide proradical with *N*-aziridinyl amines[289] with subsequent trapping with various Michael acceptors (*Scheme 4.9*). Kim's synthesis uses 1-amino-2-phenylaziridine, which must be synthesized carefully because it is potentially explosive, requiring strict control measures for its preparation and storage.[290] Additionally, all subsequent hydrazone derivatives of this compound are potentially explosive and must also be handled with care.

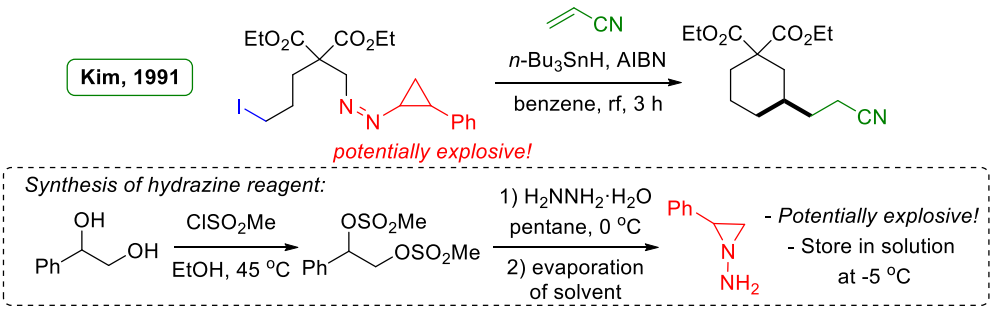

Scheme 4.9. Intramolecular cyclization of N-Aziridinyl Imines.

We, therefore, proposed carrying out an analogous process, trapping the tertiary radical intermediate with a Michael acceptor via a Giese-type reaction (*Scheme 4.10*). Initial attempts by our group led to the formation of the desired product in low yields but provided proof of concept of the reaction.

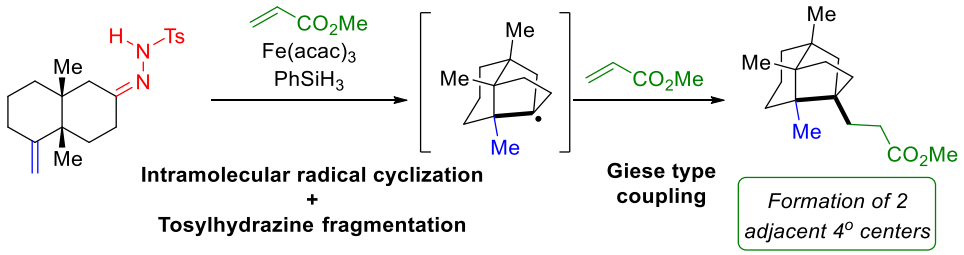

Scheme 4.10. Tandem coupling of tosylhydrazones and Michael acceptors.

4.2. OBJECTIVES

This work aimed to optimize the tandem reaction leading to adamantane-type structures (*Scheme 4.11*). The principal objective was to optimize the reaction process to obtain synthetically useful yields. Next, we would examine the scope of the Michael acceptors that could be used in the reaction. Finally, we would explore the scope of different tosylhydrazone precursors that could be used in the reaction. Notably, in contrast to the reported methods, this methodology would employ stable pro-radicals (alkenes) and stable nonexplosive hydrazines. It would also permit the formation of densely congested structures via the formation of two adjacent quaternary centers.

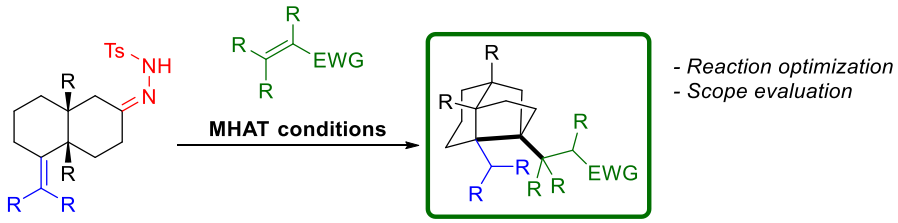

Scheme 4.11. Optimization of the tandem MHAT reaction to access adamantane-like structures.

The realization of this methodology would allow us to synthesize different adamantane-like compounds for a wide range of applications, as outlined in the introduction of this chapter, such as pharmaceuticals, catalysts, and materials, as well as application to natural product synthesis.

4.3. RESULTS AND DISCUSSION

4.3.1. Synthesis of the substrates

The synthesis of the ketone starting material for the tandem reaction began with preparing the corresponding Wieland-Miescher ketone (WMK) and its analogs **3a-c**.[291] The diketones **1a-c** were mixed with but-3-en-2-one and a catalytic amount of Et_3N to obtain the corresponding triketones **2a-c** in excellent yields via a solvent-free Michael conjugate addition. Then, the subsequent Robinson annulation with pyrrolidine in toluene at reflux provided the desired WMK analogs **3a-c** with good yields (*Scheme 4.12*).

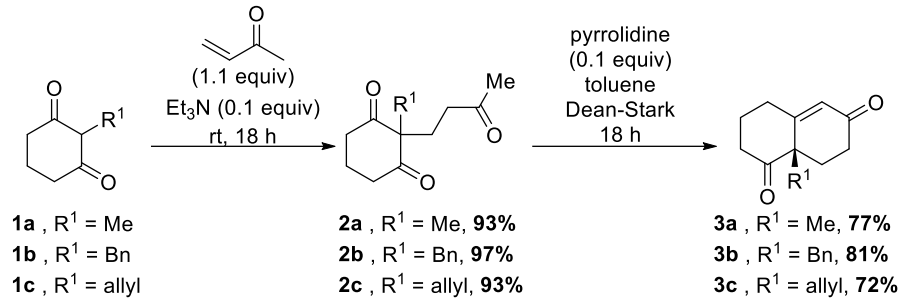

*Scheme 4.12. Preparation of Wieland-Miescher ketone analogs **3a-c**.*

Conjugate addition of the methyl cuprate formed by MeLi and CuI in diethyl ether to **3a** gave the methylated decalone, which was then converted to the acetal **4a** using 2-ethyl-2-methyl-1,3-dioxolane and *p*-toluenesulfonic acid. Wittig reaction using methyltriphenylphosphonium bromide and potassium *tert*-butoxide, followed by the deprotection of the acetal using a 10% aqueous HCl solution, allowed the obtention of the desired ketone **5a** (*Scheme 4.13*) in excellent overall yield.

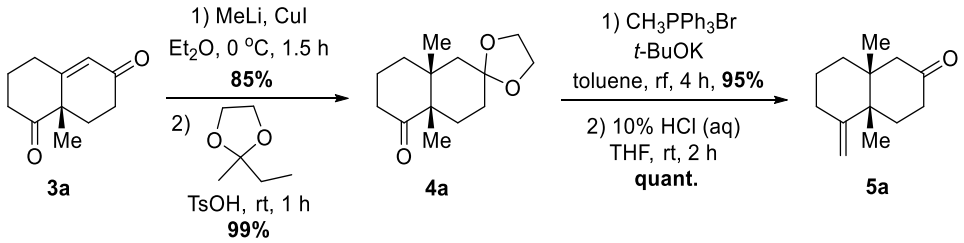

*Scheme 4.13. Preparation of C-8a methylated decalone **5a**.*

Although the formation of compound **5a** proceeds with good yield, it is difficult to scale up the process due to the excess MeLi that must be used to achieve good diastereoselectivity in the conjugate addition. As can be seen in *Figure 4.6*, the

formation of *cis*-decalin in a diastereoselective manner is due to the formation of π-complex intermediates that have been identified and fully characterized, showing that the β-face-π-intermediate is the most stable and populated species, leading to the exclusive formation of β-methyloctalone.[292] Effectively, at least two equivalents of the cuprate are needed to form this complex, which equates to 4 equivalents of MeLi. Typically, five equivalents are required to ensure a small excess of the reagent is available, meaning that the reaction becomes prohibitively expensive on a large scale. Combined with the fact that large volumes of anhydrous ether are required for the reaction means that quenching the reaction on a large scale was of concern.

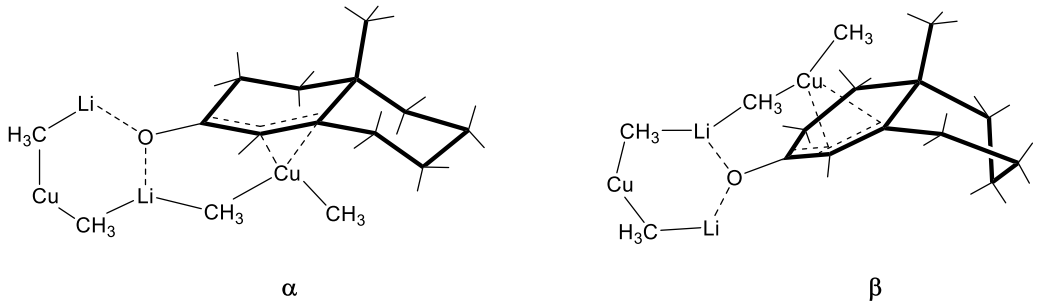

Figure 4.6. Conformation of π-complex intermediate of WMK-$(Me_2CuLi)_2$.

Therefore, we considered alternative strategies that avoided the conjugate addition step when making the analogs needed for this study. One alternative was hydrogenation to give the C-8a hydrogenated analogs **7a-c**.[293] Hydrogenation of **3a-c**, using palladium on carbon and a balloon filled with hydrogen, gave the reduced compounds, which were directly converted to their corresponding acetals using 2-ethyl-2-methyl-1,3-dioxolane and *p*-toluenesulfonic acid to provide the desired decalones **6a-c** with good to excellent yields. Subsequent Wittig reaction using methyltriphenylphosphonium bromide and potassium *tert*-butoxide, followed by the deprotection of the acetals using a 10% aqueous HCl solution, allowed the obtention of the desired ketones **7a-c** (*Scheme 4.14*).

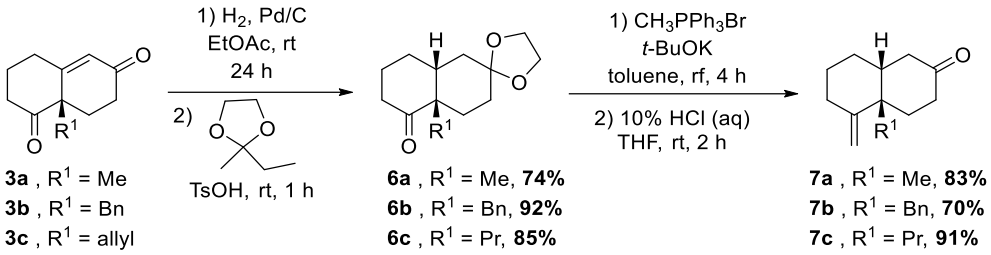

*Scheme 4.14. Preparation of decalones **7a-c**.*

Intermediate **6a** also allowed the obtention of ketone **7d** by the corresponding Wittig reaction using butyltriphenylphosphonium bromide, and subsequent deprotection of the acetal achieved the desired compound with a moderate 52% yield (*Scheme 4.15*).

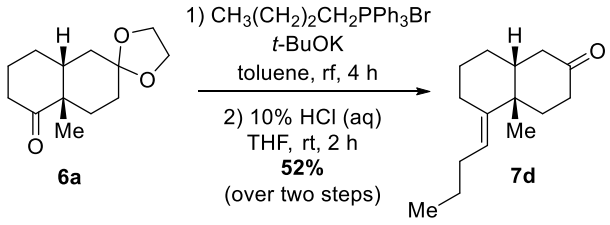

*Scheme 4.15. Preparation of ketone **7d**.*

Compound **5b**, with the alkene and ketone groups reversed in relation to compound **5a**, was prepared following the method previously developed by our group.[54] WMK **3a** was submitted to conjugate addition conditions to form the C-8a methylated diketone. Subsequently, a Wittig reaction was performed, at the less impeded ketone to obtain the methylene in the reversed position (*Scheme 4.16*).

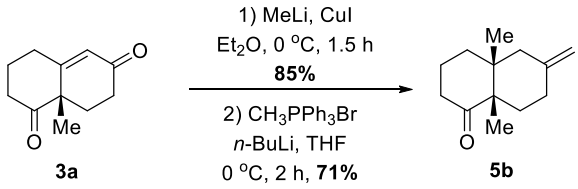

*Scheme 4.16. Synthesis of decalone **5b**.*

Once these decalones were successfully prepared, other substrates were synthesized to test that the reaction could work in different scaffolds containing the ketone and the alkene necessary for the reaction. Compound **8** was synthesized from 1,3-Adamantanediol through a Grob-type fragmentation using *p*-toluenesulfonyl chloride, benzene, and pyridine in an excellent yield. However, the compound's volatility made its manipulation very difficult (*Scheme 4.17*).[294]

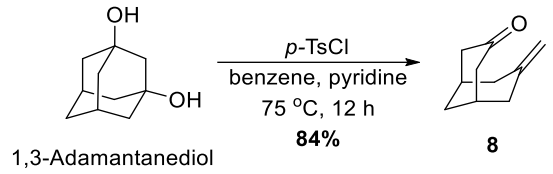

*Scheme 4.17. Synthesis of 7-methylenebicyclo[3.3.1]nonan-3-one **8**.*

Ketone **9** was prepared from the alkylation of ethyl 2-oxocyclohexane-1-carboxylate using 4-bromobut-1-ene and potassium *tert*-butoxide as a base with good yield (*Scheme 4.18*).[295]

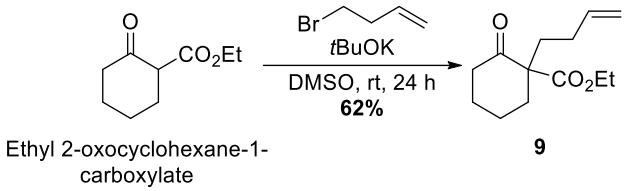

*Scheme 4.18. Synthesis of substrate **9**.*

Finally, Ito and co-workers' synthetic route of presilphiperfolan-8-ol core[296] was used to synthesize ketone **10** from (+)-pulegone through a 1,4-addition of allyltrimethylsilane and subsequent isomerization using potassium hydroxide and methanol with good yield (*Scheme 4.19*).

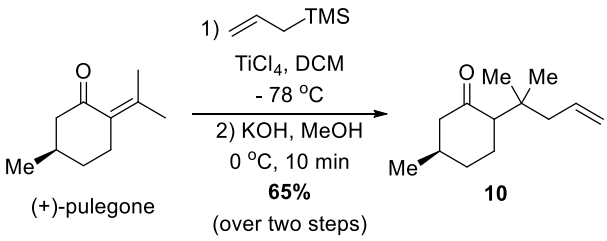

*Scheme 4.19. Preparation of ketone **10**.*

To prepare the starting material for the reaction optimization, ketone **5a** was mixed with *p*-toluenesulfonyl hydrazine in ethanol for 3 hours at room temperature to form the tosylhydrazone **11a** in an excellent 98% yield (*Scheme 4.20*).

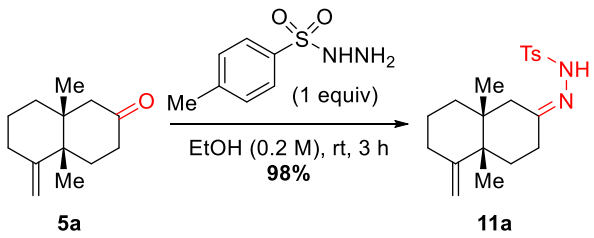

*Scheme 4.20. Preparation of tosylhydrazone **11a**.*

4.3.2. Reaction optimization

The conditions for the reaction optimization are outlined in Table 4.1. In each case, methyl acrylate was used as the acceptor group. In the initial tests, it was seen that heating the reaction to 60 °C was positive for the reaction (*entry 2*), but the use of a bulkier catalyst such as $Fe(dpm)_3$ was detrimental to the performance (*entry 3*). Using ten equivalents of Michael acceptor was beneficial (*entry 4*), as was using two equivalents of Fe (*entry 5*). Since ethanol, a polar protic solvent may favor the formation of the carbocation byproduct (see *Scheme 4.7*). Substitution with THF (*entry 6*) didn't result in an improvement, potentially due to the radical destabilizing effect of THF since it is an aprotic solvent. However, adding ten equivalents of *t*-BuOH increased the yield to 62% (*entry 7*).

Table 4.1. Reaction screening and optimization.

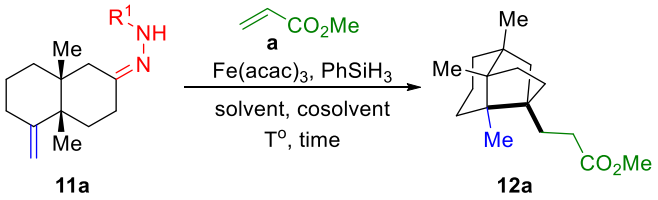

11a **12a**

Entry	a	R^1	Fe	$PhSiH_3$	solvent[a]	Cosolvent[b]	t	T°	10a
1	1.5	Ts	1.0	2.5	EtOH	-	5 h	rt	15%
2	1.5	Ts	1.0	2.5	EtOH	-	5 h	60 °C	44%
3	1.5	Ts	1.0[c]	2.5	EtOH	-	5 h	60 °C	24%
4	10	Ts	1.0	2.5	EtOH	-	5 h	60 °C	49%
5	10	Ts	2.0	2.5	EtOH	-	5 h	60 °C	55%
6	10	Ts	2.0	2.5	THF	-	5 h	60 °C	36%
7	10	Ts	2.0	2.5	THF	*t*BuOH	5 h	60 °C	62%
8	1.5	Ts	2.0	2.5	THF	*t*BuOH	5 h	60 °C	33%
9	10	Ts	1.0	2.5	THF	*t*BuOH	5 h	60 °C	39%
10	10	Ts	2.0[d]	2.5	THF	*t*BuOH	5 h	60 °C	19%
11[e]	10	Ts	0.4	2.5	THF	*t*BuOH	5 h	60 °C	nd
12	10	Ts	2.0	5.0	THF	*t*BuOH	5 h	60 °C	44%
13	10	Ts	2.0	2.5	DCE	*t*BuOH	5 h	60 °C	13%
14	10	Mes	2.0	2.5	THF	*t*BuOH	5 h	60 °C	21%
15	10	Ts	2.0	2.5	THF	*t*BuOH	24 h	60 °C	94%
16	10	Ts	2.0	2.5	THF	MeOH	24 h	60 °C	84%
17	10	Ts	2.0	1.0	THF	*t*BuOH	24 h	60 °C	53%
18	10	Ts	2.0	2.5	THF	*t*BuOH	24 h	100 °C	nd
19[f]	10	Ts	2.0	2.5	THF	*t*BuOH	24 h	60 °C	72%
20[f]	10	Ts	2.0	2.5	THF	MeOH	24 h	60 °C	82%

[a]0.08 M concentration. [b]10 equivalents were added. [c]$Fe(dpm)_3$ used instead of $Fe(acac)_3$. [d]$Fe(dibm)_3$ used instead of $Fe(acac)_3$. [e]TBHP (1.5 equiv) were added. [f]1 mmol scale.

From that point, different conditions were selectively modified, such as the methyl acrylate equivalents (*entry 8*), the catalyst loadings (*entry 9*), $Fe(dibm)_3$ instead of $Fe(acac)_3$ (*entry 10*), all without improvement. Catalytic amounts of $Fe(acac)_3$ in combination with TBHP as the reoxidant were tried (*entry 11*), but no product formed, showing that the presence of oxidant is detrimental to the reaction. Additionally, other modifications included increasing the equivalents of $PhSiH_3$ (*entry 12*), DCE instead of THF (*entry 13*), or the use of a different hydrazine such as mesityl hydrazine (*entry 14*), but all trials led to no improvement in yield.

A significant breakthrough was observed when the mixture was allowed to react for 24 hours (*entry 15*), increasing the yield to an excellent 94%, showing that the reaction was not completed in 5 hours. Modifying the cosolvent to methanol (*entry 16*) led to a slight decrease in the yield. Phenylsilane loading was also decreased to 1 equivalent (*entry 17*) but also led to lower yield, and increasing heating to 100 ^{o}C (*entry 18*) did not improve the reaction performance. Finally, the two best conditions of the optimization table were conducted in a 1 mmol scale (*entries 19 and 20*), and it was confirmed that *t*-BuOH was a better cosolvent than MeOH and proved that the reaction worked well when scaled up.

It should be noted that although it was initially thought that trapping the radical with a Michael acceptor would make the resulting compound less volatile and easier to visualize by TLC, we found that the compound remained significantly volatile and was hard to visualize. For this reason, during the optimization, and in the following scope tables, we developed a specific isolation protocol for the coupled products. After chromatographic separation, the fractions were allowed to evaporate at room temperature overnight. The next day, the TLC analysis was easier due to the more concentrated nature of the fractions. The desired fractions were combined and left again to evaporate overnight at room temperature. Trace amounts of solvent could then be removed on a rotatory evaporator with as little vacuum as possible and for the shortest time.

4.3.3. Substrate Scope

Scope of acceptors

At the start of the scope evaluation, it was seen that tosylhydrazones were not very stable and that they decomposed in the chromatographic column or under prolonged storage. Therefore, it was decided to synthesize the tosylhydrazone *in situ*.

With the optimum conditions in hand, we investigated the scope of the suitable Michael acceptors (*Scheme 4.21*). Ketone **5a** was chosen as the alkene donor, and different Michael acceptors were submitted to MHAT conditions to evaluate the viability. Different kinds of primary alkenes bearing an electron-withdrawing group were used, showing a wide tolerance of functional groups. Esters like methyl acrylate gave us the desired product **12a** in an excellent 94%, and hexyl acrylate gave us the expected compound **12b** in a good 63% yield. Acrylonitrile allowed the obtention of **12c** in an excellent yield, and *N*, *N*-dimethylacrylamide also provided **12d** in good yield. More substituted acrylates, such as methyl methacrylate, were used, and the corresponding product **12e** was obtained in a good 68% yield as a mixture of epimers. Then, methyl (*E*)-but-2-enoate was tested and the product **12f** was obtained with a good 77% yield, also as a mixture of epimers.

Next, we wanted to test cyclic acceptors. Naphthalene-1,4-dione gave the desired product **12g** in good yield. Since it is a high molecular weight compound, it was not necessary to take strict measures when evaporating the solvent from the compound. However, the observation that the acceptor and the product had very similar *Rf* values caused us to lower the acceptor equivalents to 2.5 to enable the purification of the product. Cyclohex-2-en-1-one was also tested, and compound **12h** was obtained in an excellent 82% yield. It wasn't easy to see by ^{1}H NMR that we had the compound, as the spectrum does not present very characteristic signals. However, we were able to confirm the structure from the ^{13}C spectra, which confirmed the presence of the carbonyl group and by mass spectrometry, which gave the correct molecular ion. Subsequently, more hindered alkenes were evaluated. First, (*E*)-1,4-diphenylbut-2-ene-1,4-dione was tested, and product **12i** could be isolated in an excellent 92% yield as a mixture of diastereomers. This compound also did not present volatility issues, so the

acceptor was reduced to 2.5 equivalents to avoid purification problems. In contrast, the desired diester product **12j** could not be obtained when diethyl fumarate was tested. Nor was the expected product obtained when diethyl 2-benzylidenemalonate was used.

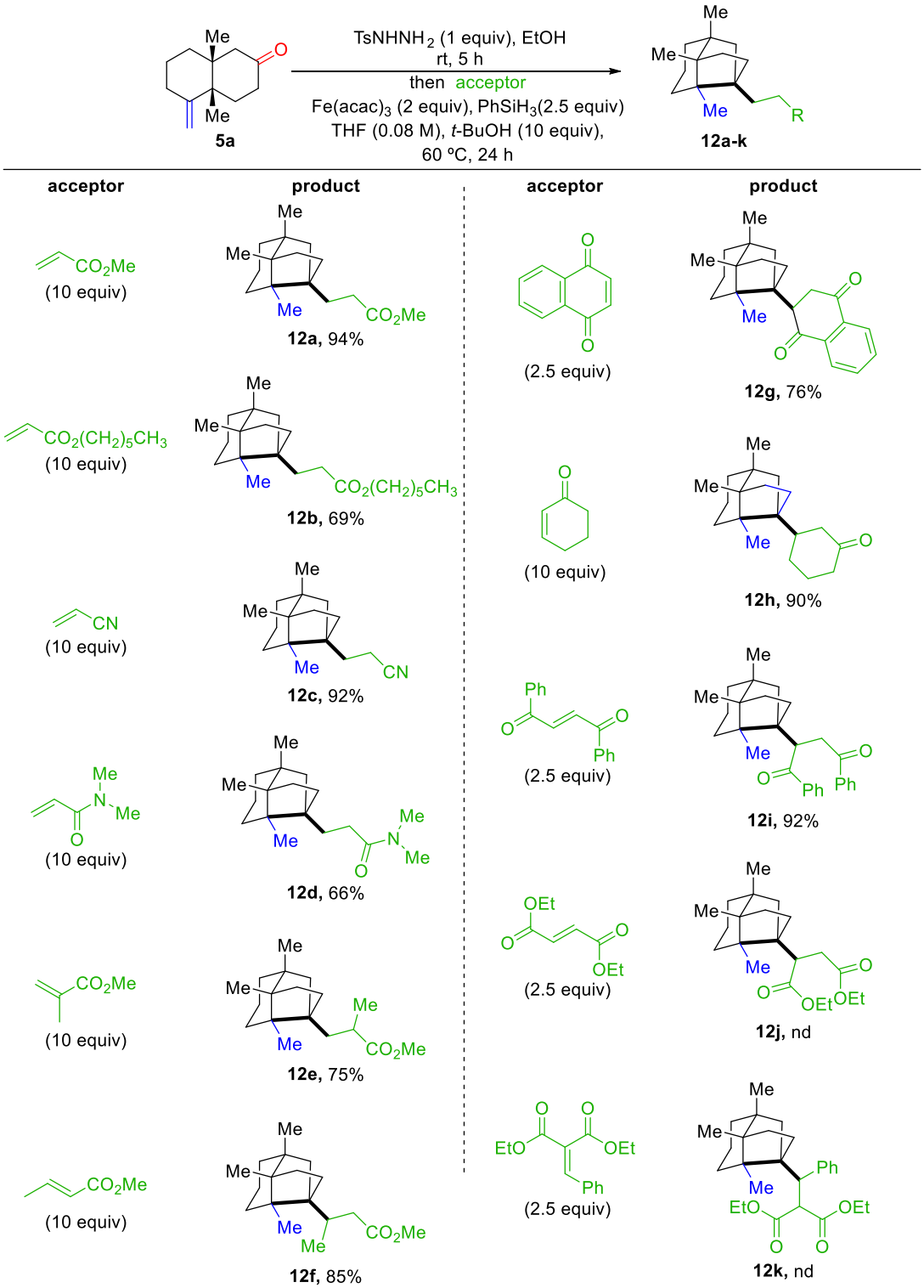

Scheme 4.21. Scope of acceptors.

Scope of alkene donors

Next to be evaluated was the scope of tosylhydrazone acceptors (*Scheme 4.22*). For this study, methyl acrylate was selected as the Michael acceptor. While this continued to give us problems with the volatility of the obtained compounds, it showed good yields and did not present the product as a mixture of diastereomers.

Different decalones were evaluated, giving good to excellent results, except for compounds **7d** and **5b**, from which the desired product could not be isolated. Other ketones containing an alkene tether were also evaluated, but the formation of the desired products could not be observed.

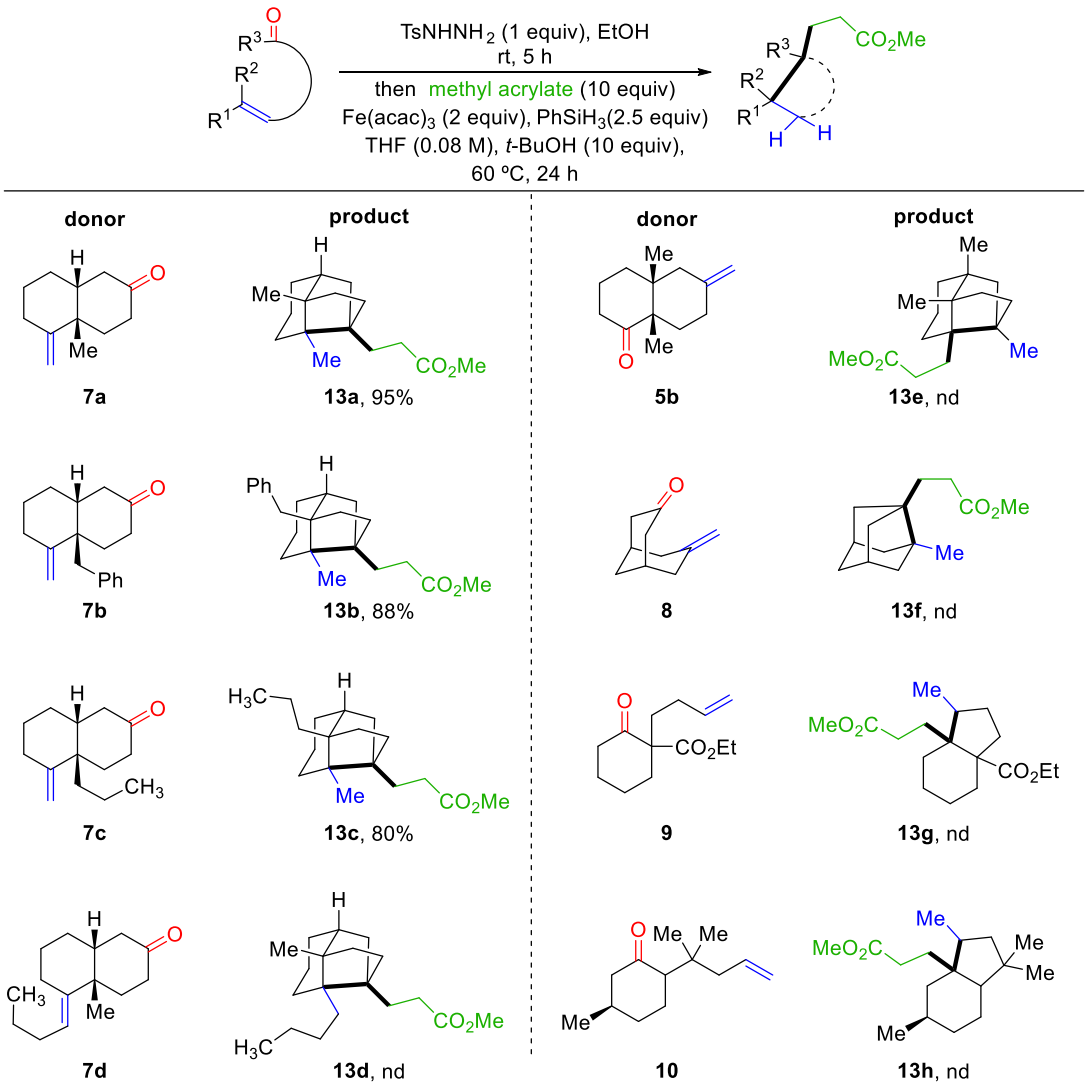

Scheme 4.22. Scope of alkene donors.

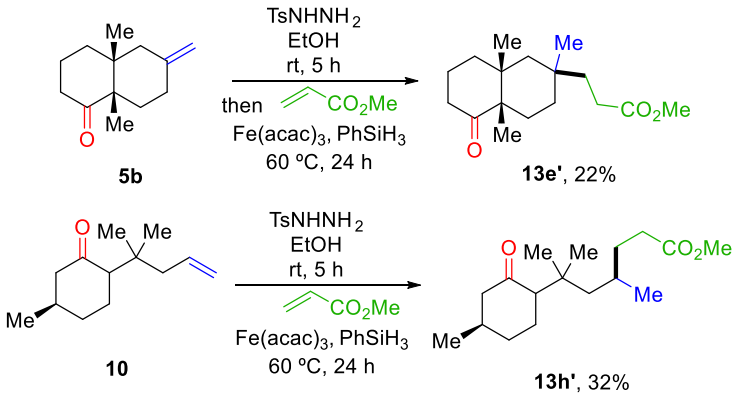

*Scheme 4.23. Formation of unexpected by-products with ketones **5b** and **10**.*

Notably, in further studies on the unsuccessful substrates, the crude of the reactions of **5b** and **10** allowed the isolation of two apparent compounds similar to the desired products by NMR but presenting noticeable differences. After studying it more thoroughly and with the help of mass spectrometry, it was possible to determine that the products obtained in these two cases came from the coupling of the two alkenes (*Scheme 4.23*). A plausible explanation for both cases is depicted in *Scheme 4.24*, using compound **10** as an example.

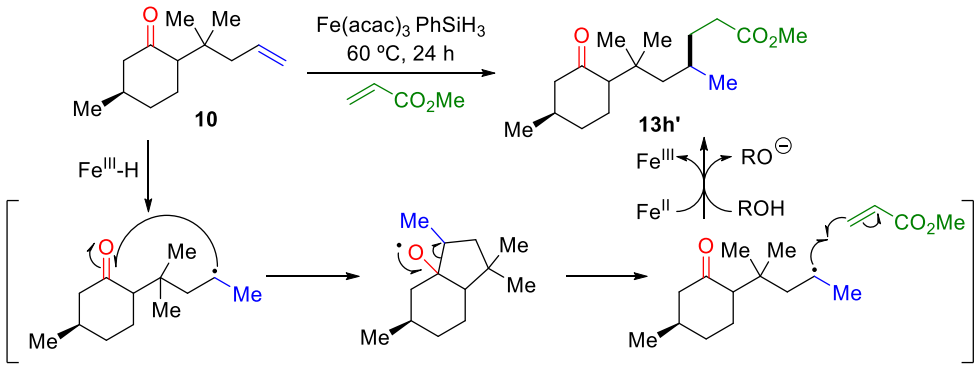

*Scheme 4.24. Mechanism of formation of byproducts **13e'** and **13h'**.*

Because the ketone is very close to a quaternary center, it is possible that the expected tosylhydrazone may not have been formed. This would mean that the ketone had reacted instead. This would mean that the radical would attack the carbon of the carbonyl, similar to what was reported by our group in previous studies.[54] This would form an unstable alkoxy radical that would perform a β-fragmentation, recovering the initial radical that would later couple with the Michael acceptor. Future studies should

focus on first ensuring the formation of the tosylhydrazone before proceeding to the MHAT cyclization.

4.3.4. Heterocycles incorporating adamantane building block

From compound **12i**, Paal-Knorr synthesis of pyrroles could be carried out using ammonium acetate to obtain pyrrole **14** in very good yield. Similarly, when compound **10i** was reacted with *p*-toluenesulfonic acid under reflux, the furane derivative **15** could also be obtained with excellent yield (*Scheme 4.25*).

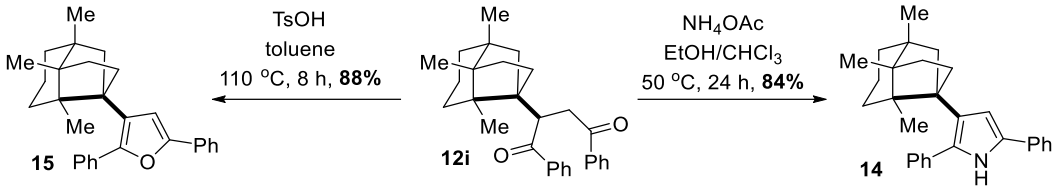

*Scheme 4.25. Synthesis of heterocycles **14** and **15**.*

Given the importance of heterocycles in the pharmaceutical industry and seeing in this present chapter the great utility of adamantane derivatives in the pharmacological modulation of drugs, it was thought that the synthesis of compound **12i** or analogs could be used to obtain functionalized heterocycles of interest. For example, further modifications could be achieved by changing the nitrogen substitution and functionalizing the heterocyclic ring to give compounds similar to Atorvastatin, one of the most successful developed drugs (*Scheme 4.26*).

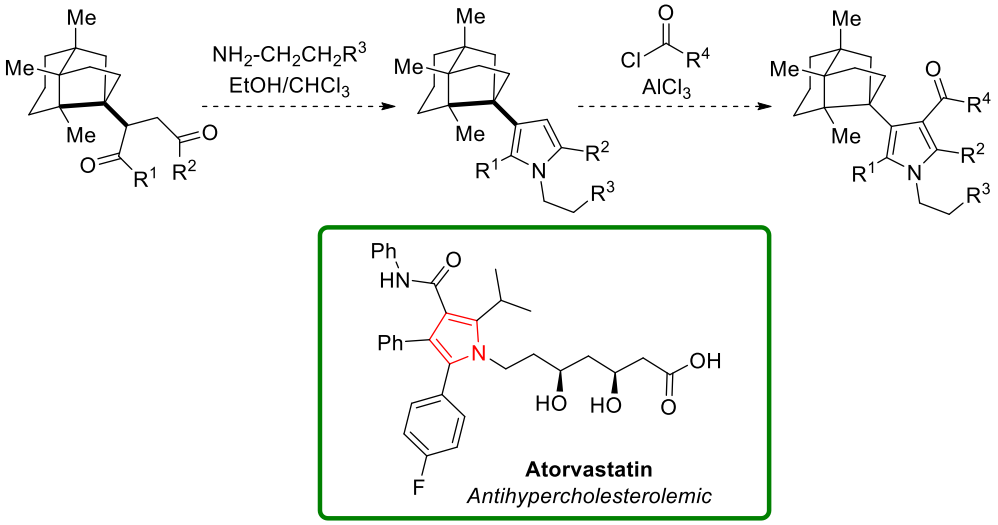

*Scheme 4.26. Proposed construction of pharmaceutical compounds based on the synthesis of compound **14**.*

4.3.5. Mechanistic discussion

Based on previous knowledge of the reaction, we suggest a plausible mechanism for forming the desired product **G** and the observed byproducts **H**, **I**, **K**, and **L**. The formation of the metal hydride species would proceed with a catalytic cycle analogously to that described by Baran.[33] Once the tosylhydrazone **A** is formed, the attack of the metal hydride species on the alkene would generate the tertiary radical **B,** which would attack the tosylhydrazone, forming the cyclized species **C.** At this point, a SET process favored by heating (discussed in more detail in *Scheme 4.34*) would lead to fragmentation of the tosylhydrazone radical, giving the tertiary radical **D**, which can be trapped by a Michael acceptor to generate the desired product **G** through Fe radical reduction to the corresponding anion followed by proton transfer (*Scheme 4.27*).

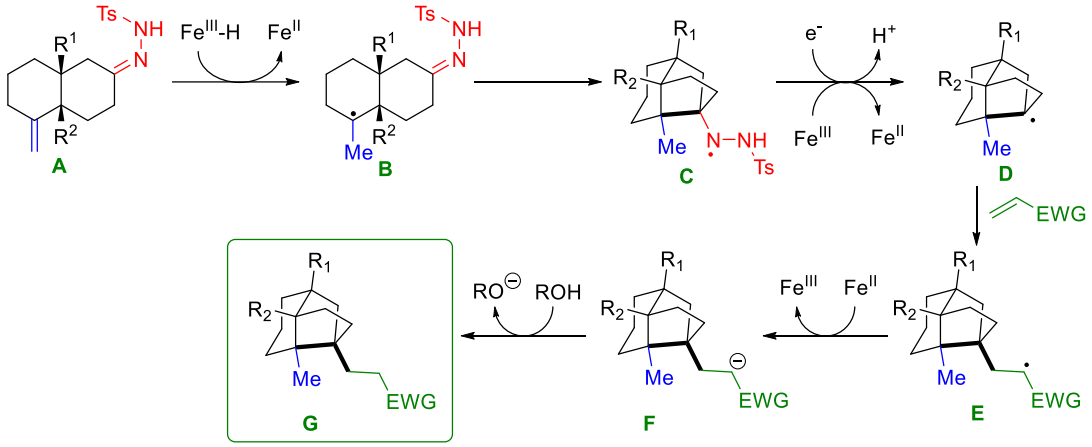

Scheme 4.27. Proposed reaction mechanism.

The formation of intermediate **D** from **C** can involve two different radical pathways (*Scheme 4.28*). Path **A** may involve a SET between the Fe and the nitrogen, leading to hydrogen abstraction that gives a diradical or leads directly to the double bond formation. This process is analogous to that observed in the final oxidation step of the heterocycle in the Minisci reaction. Fragmentation then gives nitrogen gas and a tosyl radical. This would explain why our reaction is not catalytic. Path **B** involves direct fragmentation, expulsing a tosyl radical, which abstracts the hydrogen. Loss of nitrogen then gives intermediate **D**.

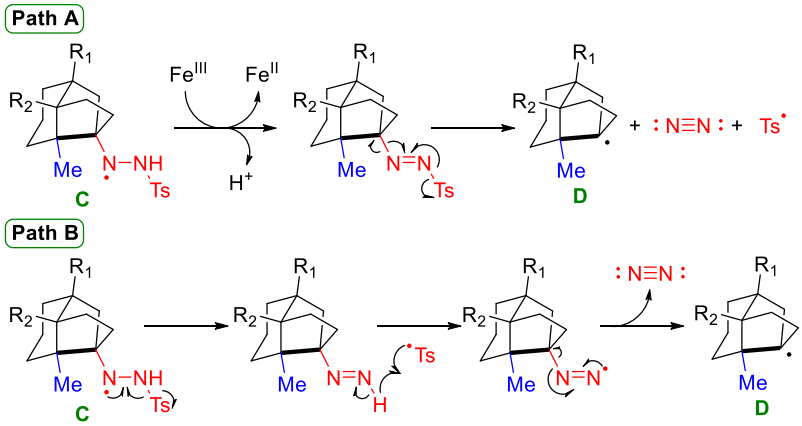

Scheme 4.28. Tosylhydrazone fragmentation possible pathways.

For the formation of the by-products (*Scheme 4.29*), hydrogen transfer to the nitrogen radical of the Ts hydrazine **C** can lead to the formation of **H**. If this hydrogen transfer process occurs on the tertiary radical of species **D**, it will give rise to the reduced adamantane analog **I**. If a SET with the metal species takes place on this same species **D**, it will give rise to the carbocation **J**. This reaction is especially favored when a polar protic solvent is used, and as seen in *Section 4.3.2*, This carbocation then reacts with the EtOH to give the compound **K**, or it may react with the catalyst ligand to provide **L**.

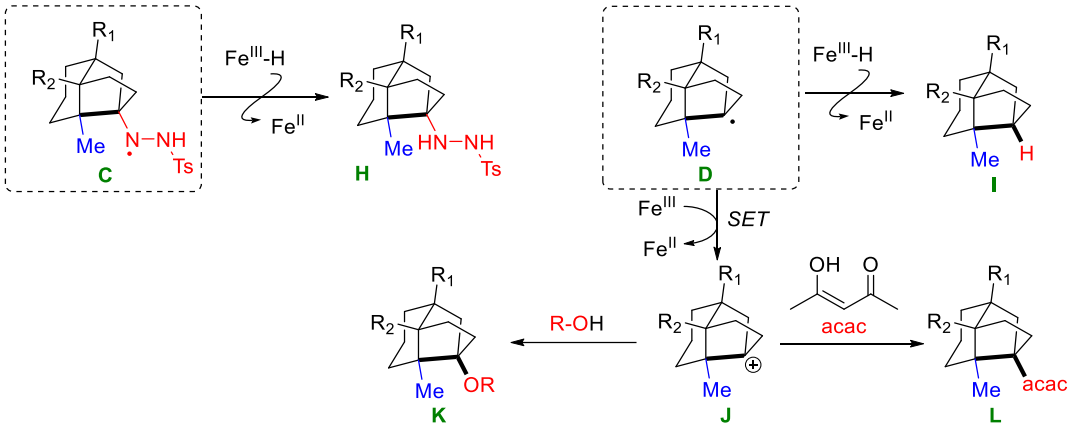

Scheme 4.29. Formation of isolated byproducts.

5. CONCLUSIONS

Throughout the presented work, five new radical carbon-carbon bond-forming reactions have been developed based on metal-catalyzed hydrogen atom transfer (MHAT) conditions. From the obtained results, we can conclude the following:

1. - The synthetic methods developed present new disconnection possibilities to form C-C bonds. Additionally, these reactions employ ubiquitous and stable functional groups such as alkenes, ethers, amides, and aromatic heterocycles. Moreover, the methodologies presented use cheap and non-toxic reagents such as the iron catalysts used in all the reactions developed. The methods presented have the potential to be used in a wide variety of applications, particularly for the synthesis of natural products and pharmaceuticals.

2. - Isocyanides could be reductively coupled using an iron-mediated HAT reaction to form different heterocyclic structures, including phenanthridines, isoquinolines, and indoles (*Scheme 5.1*).

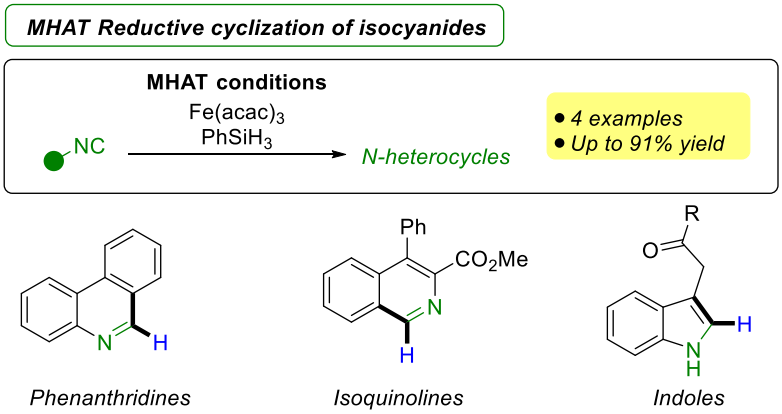

Scheme 5.1. Reductive cyclization of isocyanides.

3. - Unactivated alkenes can be coupled with isocyanides using an iron-mediated HAT reaction (*Scheme 5.2*). The tandem reaction process consists of an intermolecular coupling between the alkene and the isocyanide followed by an intramolecular radical cyclization via an imidoyl radical species. This reaction allowed the formation of several different functionalized heterocycles, such as phenanthridines, isoquinolines, and indoles. Notably, despite the extensive use of various types of isocyanides in radical

coupling-cyclization reactions to form heterocycles, this is the first example of a radical coupling using alkenes as the radical precursor.

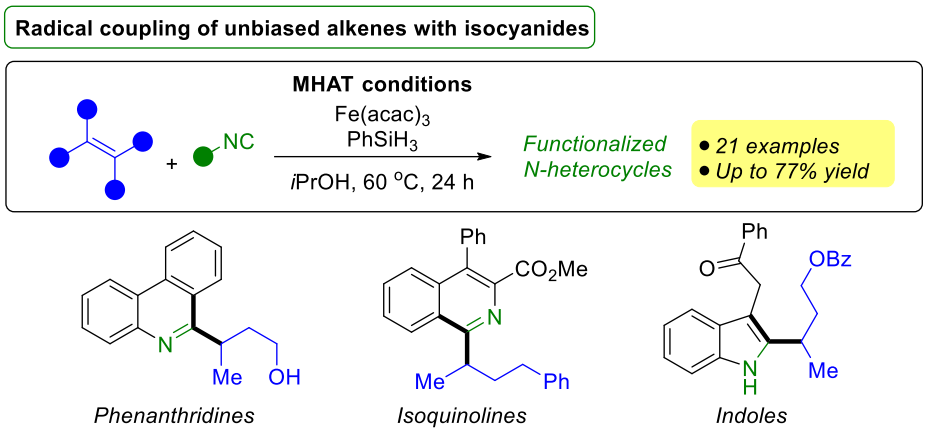

Scheme 5.2. Coupling of unbiased alkenes with isocyanides.

4. The coupling of more substituted alkenes with aryl isocyanides proved challenging, leading to the development of new conditions (*Scheme 5.3*). To form these more impeded compounds, a two-step process was devised. First, a reductive MHAT cyclization of the isocyanide formed the non-substituted heterocycle. Second, an MHAT Minisci-type coupling with the alkene gave the substituted heterocycle. These reactions could be carried out separately or combined in a one-pot process.

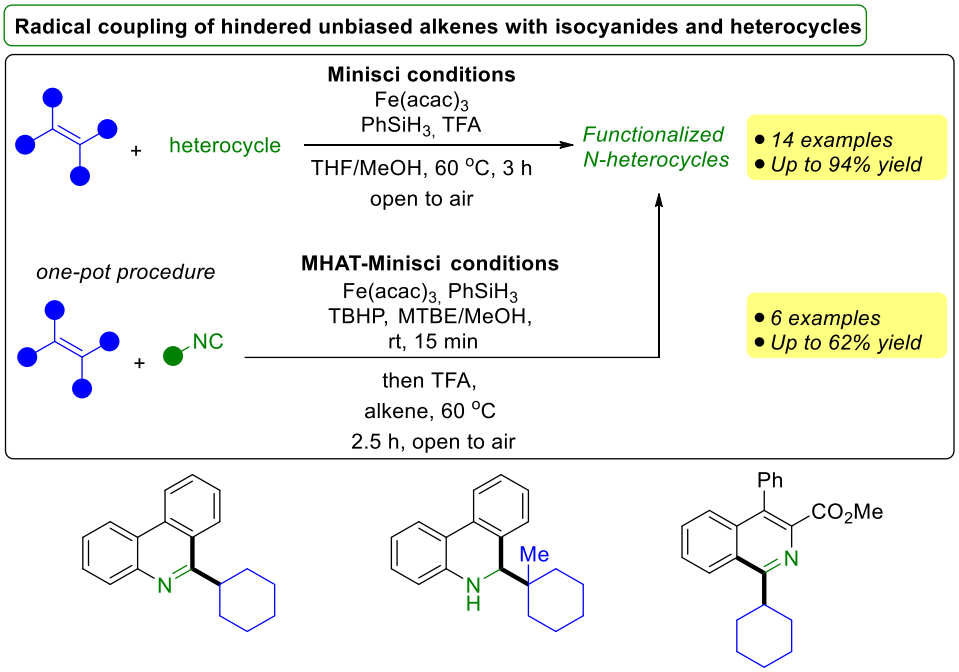

Scheme 5.3. Coupling of hindered unbiased alkenes with isocyanides and heterocycles.

5. - A cross-dehydrogenative coupling reaction of ethers with heterocycles has been developed from an initial serendipitously observed side reaction when employing MHAT conditions for the Minsici reaction when THF was used as the solvent in the presence of an oxidant. The coupling proceeds under very mild conditions (room temperature) compared to similar processes requiring heating. Optimization of the reaction revealed that the alkene, instead of functioning as a radical precursor, is likely acting as an essential additive in the reaction to prevent autooxidation or act as a radical scavenger. A wide range of different nitrogen-containing heterocycles and ethers can be coupled.

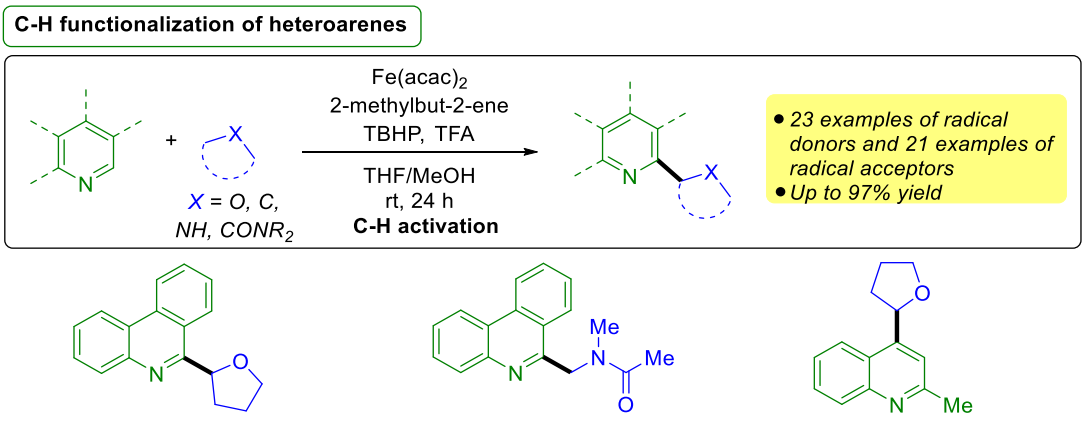

Scheme 5.4. C-H functionalization of heteroarenes.

6. - A tandem reaction using MHAT conditions was developed to form adamantane-like compounds (*Scheme 5.5*). An intramolecular cyclization between an alkene and a tosylhydrazone generated a tosylhydrazine radical, which underwent fragmentation under the conditions of the reaction to form a tertiary carbon-centered radical, which was trapped with a range of Michael acceptors. The reaction generates two adjacent quaternary centers in a single reaction via the formation of two geminal C-C bonds. Further transformations also allowed the preparation of adamantane-substituted heterocycles.

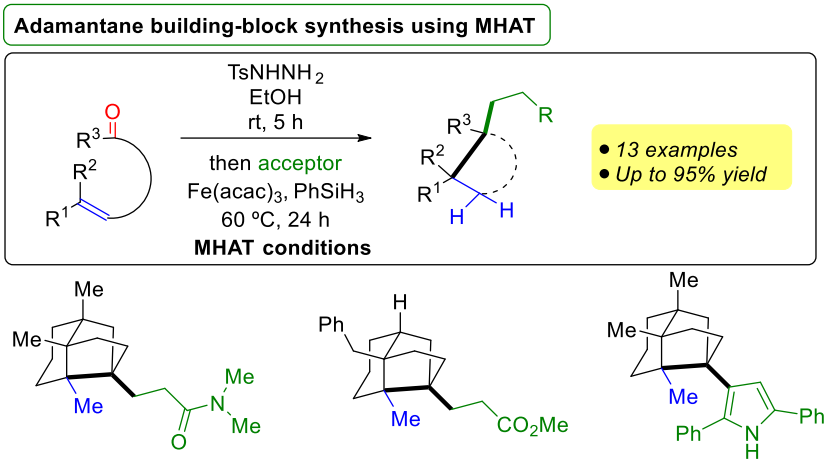

Scheme 5.5. Adamantane building block synthesis.

7. – In the work reported in this thesis, Iron-mediated HAT reactions have been shown to initiate tandem radical processes to form multiple C-C bonds in a single reaction. This represents the first reported examples of MHAT processes being used in cascade processes.

8. – It should also be mentioned at the start of this thesis that the development of an MHAT intermolecular coupling of unactivated alkenes with aldehydes was worked on in conjunction with another research group member (Dr. Mar Saladrigas). The results of that work were published in their doctoral thesis[297] and a published article[57] and, therefore, have not been commented on here.

Summary and outlook

In conclusion, the objectives outlined at the beginning of this thesis have been achieved, and new MHAT methodologies have been developed for the formation of C-C bonds, two of which involve tandem reaction processes. It has also been possible to develop a C-H activation cross-dehydrogenative coupling reaction. This method holds promise for the late-stage derivatization of pharmaceuticals containing aromatic rings to modify their properties. We believe these methodologies should find potential applications for forming and functionalizing heterocycles and developing new biologically active products. The method developed to form adamantane-like structures holds promise as a way to construct pharmaceuticals or provide building blocks for the modification of pharmaceuticals and catalysts.

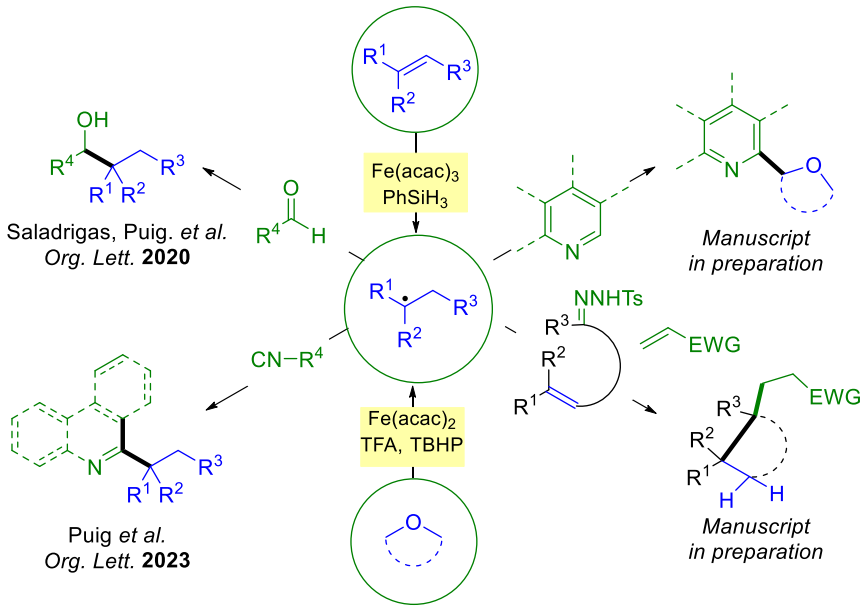

Scheme 5.6. Summary.

6. EXPERIMENTAL PART

General Information

All reactions were carried out under an argon atmosphere with dry, freshly distilled solvents under anhydrous conditions. All product mixtures were analyzed by thin-layer chromatography using TLC silica gel plates (Merck silica gel 60 F_{254}), and the spots were located by short-wave UV light as the visualizing agent and with 1% aqueous $KMnO_4$ or 2% ethanolic anisaldehyde and heat as developing agents. Chromatography refers to flash chromatography was carried out on SiO_2 (silica gel 60 Å, 35-75 µm, 230-240 mesh) or aluminum oxide (neutral) pH 6.5-7.5 (63-200 µm). Drying of organic extracts during workup of reactions was performed over anhydrous Na_2SO_4. Solvent evaporation was accomplished with a rotatory evaporator. NMR spectra were recorded in $CDCl_3$, except were stated otherwise, on a Bruker 400 MHz or Bruker 500 MHz. Chemical shifts of ^1H, ^{13}C and ^{19}F NMR spectra are reported in ppm downfield (δ) from Me_4Si or from $CDCl_3$. All NMR data assignments are supported by gCOSY and gHSQC experiments.

2. ISOCYANIDES AS ACCEPTOR GROUPS IN MHAT REACTIONS WITH UNACTIVATED ALKENES

Alkenes used are commercially available, except for but-3-en-1-yl benzoate,[298] and 2-(but-3-en-1-yl)isoindoline-1,3-dione,[299] which were prepared according to the literature. Compounds **8**,[300] **10a**, **10b**,[301] **31**[302] and **34**[303] were prepared according to reported procedures.

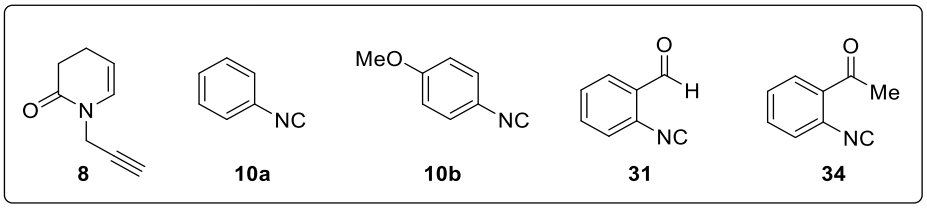

8 **10a** **10b** **31** **34**

Preparation of starting materials

Preparation of biphenylamines 3a-3e

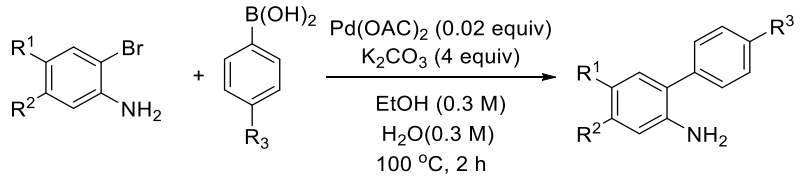

1a, R^1, R^2 = H
1b, R^1, R^2 = H
1c, R^1, R^2 = H
1d, R^1 = H, R^2 = MeO
1e, R^1 = CF_3, R^2 = H

2a, R^3 = H
2b, R^3 = Me
2c, R^3 = F
2d, R^3 = H
2e, R^3 = H

3a, R^1, R^2, R^3 = H, **99%**
3b, R^1,R^2 = H, R^3 = Me, **99%**
3c, R^1, R^2 = H, R^3 = F, **77%**
3d, R^1, R^3 = H, R^2 = MeO, **64%**
3e, R^1 = CF_3,R^2, R^3 = H, **88%**

General Procedure for the preparation of biphenylamines: The corresponding bromoaniline **1a**-**1e** (1 equiv), boronic acid **2a**-**2e** (1.5 equiv), $Pd(OAc)_2$ (0.02 equiv), and K_2CO_3 (4 equiv) were mixed in a flask. Then, H_2O (0.3 M) and EtOH (0.3 M) were added, and the reaction was refluxed at 100 °C for 2 h. When the reaction was completed, the mixture was taken to room temperature and extracted with EtOAc. The combined organic extracts were dried and concentrated. Purification by column chromatography gave the corresponding biphenylamines **3a**-**3e**. Spectral data were identical to those previously reported.[304]

2-Isocyano-1,1'-biphenyl (4a)

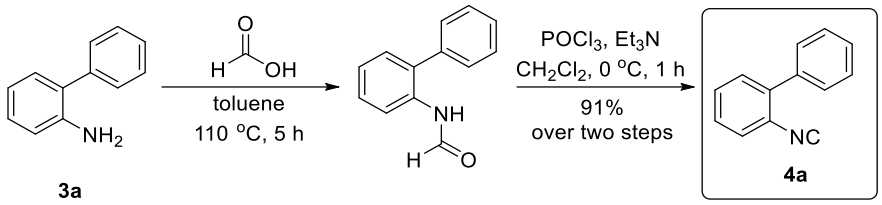

General procedure for the preparation of isocyanides: A solution of **3a** (3 g, 17.7 mmol) and formic acid (98%, 3.1 mL, 79.8 mmol) in toluene (1 M, 18 mL) was refluxed using a Dean-Stark apparatus for 5 h. The reaction was quenched with a saturated aq. Na_2CO_3 solution (10 mL) and extracted with CH_2Cl_2 (3 × 10 mL). The combined organic extracts were washed with brine, dried and concentrated. The formamide was shown to be an unstable compound, so the two steps were conducted consecutively. Using material from a separate experiment a small sample was purified by chromatography (hexane → hexane/EtOAc 50:50) to give a mixture of rotamers; ^{1}H NMR (400 MHz, $CDCl_3$) δ 8.46–8.43 (m, 0.5H), 8.27 (dd, *J* = 8.2 Hz, 1H), 8.12–8.10 (m, 0.5H), 7.53 (br s, 1H), 7.41 (t, *J* = 7.2 Hz, 2H), 7.36–7.27 (m, 4H), 7.24–7.19 (m, 1H), 7.15 (t, *J* = 7.2 Hz, 1H). To a solution of the crude formamide (3.5 g, 17.7 mmol) and Et_3N (20 mL, 0.14 mol) in anhydrous dichloromethane (36 mL) at 0 °C, was added $POCl_3$ (3.3 mL, 35.5 mmol) dropwise and the mixture was stirred for 1 h at 0 °C. The reaction was quenched by slowly adding a saturated aq. Na_2CO_3 solution (10 mL) and the mixture was allowed to stir for a further 1 h. The mixture was extracted with CH_2Cl_2 (3 × 15 mL) and combined organic extracts were washed with water and brine, dried and concentrated. Purification by chromatography (hexane → hexane/EtOAc 95:5) gave **4a** (2.90 g, 91% over two steps) as a green oil; ^{1}H NMR (400 MHz, $CDCl_3$) δ 7.54–7.43 (m, 8H, Ph), 7.40–7.36 (m, 1H, Ph); ^{13}C NMR (101 MHz, $CDCl_3$) δ 166.5 (NC), 138.8 (C_{ipso}), 136.9 (C_{ipso}), 130.5 (Ph), 129.5 (Ph), 128.9 (Ph), 128.5 (Ph), 128.3 (Ph), 128.1 (Ph), 127.8 (Ph). Spectral data were identical to those previously reported.[305]

2-isocyano-4'-methyl-1,1'-biphenyl (4b)

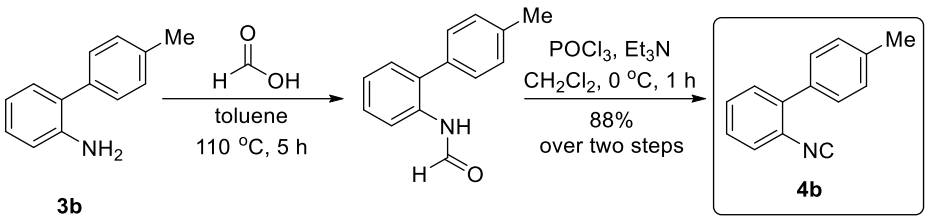

According to the general procedure for the preparation of isocyanides, **3b** (500 mg, 2.73 mmol) and formic acid (98%, 0.46 mL, 12.3 mmol) in toluene (1 M, 3 mL) gave formamide as a white solid; ^{1}H NMR (400 MHz, $CDCl_3$) δ 8.69 (d, *J* = 11.2 Hz, 0.5 H), 8.38 (d, *J* = 6.8 Hz, 0.5 H), 8.29 (d, *J* = 2 Hz, 0.5 H), 7.39–7.14 (m, 8H), 2.49 (s, 1.5 H), 2.41 (s, 1.5 H). The crude formamide (576 mg, 2.73 mmol), Et_3N (3 mL, 21.8 mmol), anhydrous dichloromethane (5.5 mL) and $POCl_3$ (0.51 mL, 5.46 mmol) gave after purification by chromatography (hexane → hexane/EtOAc 97.5:2.5) **4b** (465 mg, 88% over two steps) as a green oil; ^{1}H NMR (400 MHz, $CDCl_3$) δ 7.50–7.44 (m, 5H, Ph), 7.38–7.32 (m, 3H, Ph), 2.46 (s, 3H, Me); ^{13}C NMR (101 MHz, $CDCl_3$) δ 166.5 (NC), 138.8 (C_{ipso}), 138.2 (C_{ipso}), 134.1 (C_{ipso}), 130.5 (Ph), 129.5 (Ph), 129.3 (Ph), 128.8 (Ph), 127.9 (Ph), 127.8 (Ph), 21.2 (Me). Spectral data were identical to those previously reported.[306]

4'-fluoro-2-isocyano-1,1'-biphenyl (4c)

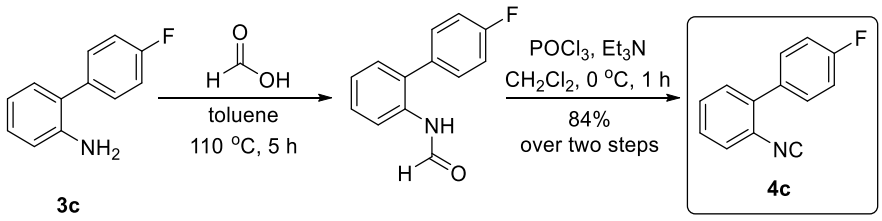

According to the general procedure for the preparation of isocyanides, **3c** (800 mg, 4.27 mmol) and formic acid (98%, 0.72 mL, 19.2 mmol) in toluene (1 M, 4.30 mL) gave formamide as a brownish solid; ^{1}H NMR (400 MHz, $CDCl_3$) δ 8.67 (d, *J* = 11.2 Hz, 0.5 H), 8.34 (d, *J* = 9.2 Hz, 0.5 H), 8.30 (d, *J* = 1.6 Hz, 0.5 H), 7.41–7.28 (m, 4H), 7.24–7.14 (m, 4H). The crude formamide (920 mg, 4.27 mmol), Et_3N (4.76 mL, 34.2 mmol), anhydrous dichloromethane (8.5 mL) and $POCl_3$ (0.80 mL, 8.55 mmol) gave after purification by chromatography (hexane → hexane/EtOAc 97.5:2.5) **4c** (710 mg, 84% over two steps) as a green oil; ^{1}H NMR (400 MHz, $CDCl_3$) δ 7.51–7.44 (m, 4H, Ph), 7.41–7.36 (m, 2H,

Ph), 7.17 (t, *J* = 8.8 Hz, 2H); ^{13}C NMR (101 MHz, $CDCl_3$) δ 166.9 (NC), 162.9 (d, *J* = 249.1 Hz, C-F), 137.9 (C_{ipso}), 133.1 (d, *J* = 3.6 Hz, C_{ipso}), 130.9 (d, *J* = 8.3 Hz, Ph), 130.6 (Ph), 129.7 (Ph), 128.4 (Ph), 127.9 (Ph), 115.7 (d, *J* = 21.5 Hz, Ph); ^{19}F NMR (376 MHz, $CDCl_3$) δ −113.38 (dd, *J* = 13.9, 8.6, 5.6 Hz). Spectral data were identical to those previously reported.[306]

2-isocyano-4-methoxy-1,1'-biphenyl (4d)

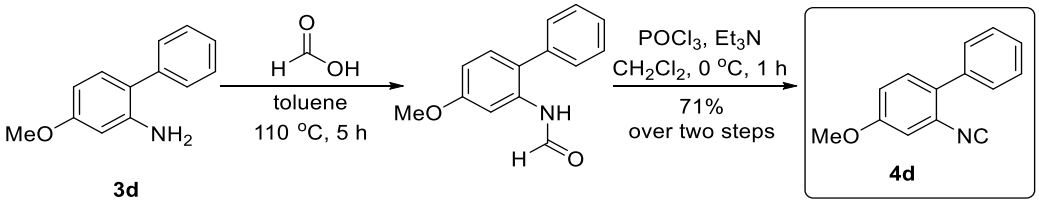

According to the general procedure for the preparation of isocyanides, **3d** (600 mg, 3.01 mmol) and formic acid (98%, 0.51 mL, 13.5 mmol) in toluene (1 M, 3 mL) gave formamide as a yellowish oil; ^{1}H NMR (400 MHz, $CDCl_3$) δ 8.67 (d, *J* = 11.6 Hz, 0.5 H), 8.28 (d, *J* = 2 Hz, 0.5 H), 8.08 (d, *J* = 2.8 Hz, 0.5 H), 7.49–7.22 (m, 5H), 7.14 (d, *J* = 8.4 Hz, 1 H), 6.83–6.74 (m, 2H), 3.86 (s, 3H). To a solution of the crude formamide (684 mg, 3.01 mmol), Et_3N (3.35 mL, 24.1 mmol), anhydrous dichloromethane (6 mL) and $POCl_3$ (0.56 mL, 6.02 mmol) gave after purification by chromatography (hexane → hexane/EtOAc 95:5) **4d** (630 mg, 71% over two steps) as a pale green solid; ^{1}H NMR (400 MHz, $CDCl_3$) δ 7.52–7.46 (m, 4H, Ph), 7.43–7.39 (m, 1H, Ph), 7.36–7.33 (m, 1H, Ph), 7.04–7.01 (m, 2H, Ph), 3.86 (s, 3H, Me); ^{13}C NMR (101 MHz, $CDCl_3$) δ 166.4 (NC), 159.1 (C_{ipso}), 136.9 (C_{ipso}), 131.5 (Ph), 131.4 (C_{ipso}), 129.0 (Ph), 128.6 (Ph), 127.9 (Ph), 116.2 (Ph), 112.8 (Ph), 55.8 (Me). Spectral data were identical to those previously reported.[306]

2-isocyano-5-(trifluoromethyl)-1,1'-biphenyl (4e)

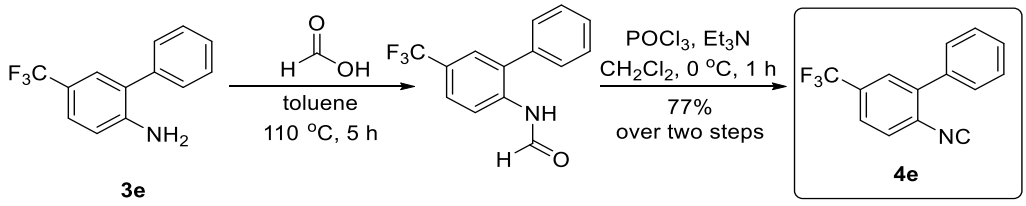

According to the general procedure for the preparation of isocyanides **3e** (850 mg, 3.58 mmol) and formic acid (98%, 0.61 mL, 16.1 mmol) in toluene (1 M, 3.60 mL) gave

formamide as a white solid; ^{1}H NMR (400 MHz, $CDCl_3$) δ 8.81 (d, *J* = 11.2 Hz, 0.5 H), 8.60 (d, *J* = 8.8 Hz, 0.5 H), 8.34 (d, *J* = 2 Hz, 0.5 H), 7.63 (d, *J* = 8.4 Hz, 1H), 7.57–7.47 (m, 3H), 7.43–7.33 (m, 2H), 7.28–7.24 (m, 1H), 7.19–7.14 (m, 1H). To a solution of the crude formamide (950 mg, 3.58 mmol), Et_3N (4 mL, 28.7 mmol), anhydrous toluene (7.2 mL) and $POCl_3$ (0.67 mL, 7.17 mmol) gave after purification by chromatography (hexane → hexane/EtOAc 97.5:2.5) **4e** (684 mg, 77% over two steps) as a brownish oil; ^{1}H NMR (400 MHz, $CDCl_3$) δ 7.72 (s, 1H, Ph), 7.67–7.61 (m, 2H, Ph), 7.54–7.48 (m, 5H, Ph); ^{13}C NMR (101 MHz, $CDCl_3$) δ 169.6 (NC), 139.8 (C_{ipso}), 135.7 (C_{ipso}), 131.6 (q, *J* = 33.2 Hz, C-F_3), 129.2 (Ph), 129.0 (Ph), 128.9 (Ph), 128.5 (Ph), 127.9 (q, *J* = 4 Hz, Ph), 125.2 (q, *J* = 3.6 Hz, Ph), 124.7 (Ph), 122.0 (Ph); ^{19}F NMR (376 MHz, $CDCl_3$) δ −62.91 (s) ppm. Spectral data were identical to those previously reported.[306]

Methyl 2-isocyano-3,3-diphenylacrylate (14)

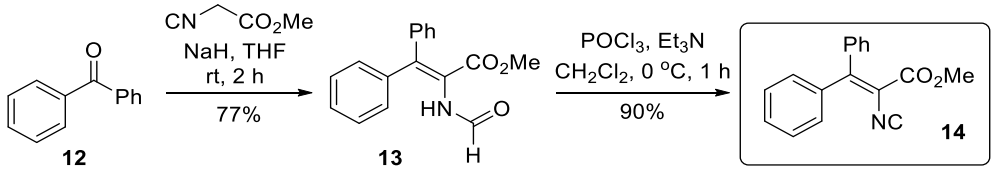

To a solution of NaH (90%, 88 mg, 3.29 mmol) in THF (2.7 mL) a mixture of benzophenone **12** (500 mg, 2.74 mmol) and methyl isocyanoacetate (272 mg, 2.74 mmol) in THF (2.7 mL) at room temperature was added and stirred for 2 h. The reaction was quenched by adding a 10% AcOH aq. solution at 0 °C until there is no hydrogen release. The solvent was removed under reduced pressure and extracted with CH_2Cl_2 (3 × 10 mL). The organic layer was washed with water and brine, dried, concentrated and recrystallized with MeOH to give **13** (594 mg, 77%) as a white solid. ^{1}H NMR (400 MHz, $CDCl_3$) δ 7.45–7.35 (m, 8H, Ph), 7.17–7.15 (m, 2H, Ph), 3.68 (s, 3H, Me); ^{13}C NMR (101 MHz, $CDCl_3$) δ 169.9 (C-1), 162.3 (NC), 154.5 (C-3), 137.8 (C_{ipso}), 137.4 (C_{ipso}), 130.3 (Ph), 129.9 (Ph), 129.6 (C-2), 129.1 (Ph), 128.5 (Ph), 128.3 (Ph), 52.9 (Me). The formamide **13** (300 mg, 1.07 mmol) was dissolved in anhydrous dichloromethane (2.2 mL) with Et_3N (1.2 mL, 8.53 mmol) and cooled to 0 °C. Then, $POCl_3$ (200 μL, 2.13 mmol) was added dropwise and the mixture was stirred for 1 h at 0 °C. The mixture was quenched by slowly adding a saturated aq. Na_2CO_3 solution (3 mL) and the mixture was stirred for 1 h. The mixture was extracted with CH_2Cl_2 and washed with water and brine, dried and

concentrated. Purification by chromatography (hexane → hexane/EtOAc 90:10) gave **14** (254 g, 90%) as a brownish solid; ^{1}H NMR (400 MHz, $CDCl_3$) δ 7.45–7.35 (m, 8H, Ph), 7.17–7.15 (m, 2H, Ph), 3.68 (s, 3H, Me); ^{13}C NMR (101 MHz, $CDCl_3$) δ 169.9 (C-1), 162.3 (NC), 154.5 (C-3), 137.8 (C_{ipso}), 137.4 (C_{ipso}), 130.3 (Ph), 129.9 (Ph), 129.6 (C-2), 129.1 (Ph), 128.5 (Ph), 128.3 (Ph), 52.9 (Me). Spectral data were identical to those previously reported.[307]

3-(2-Isocyanophenyl)-1-phenylprop-2-en-1-one (19)

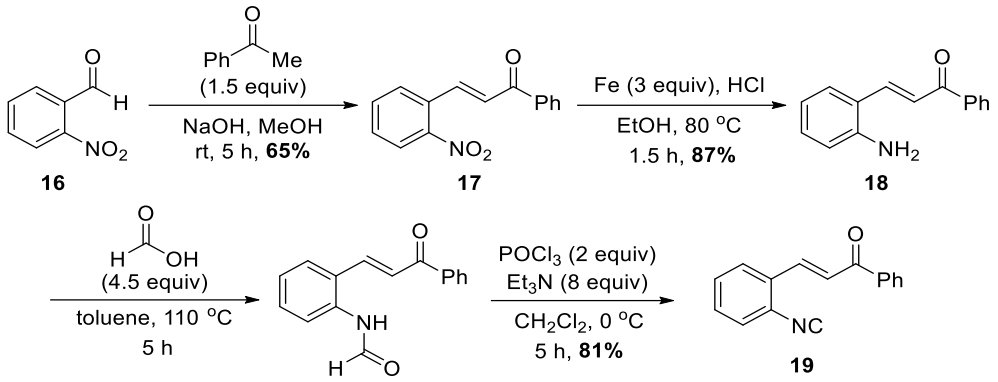

To a solution of 2-nitrobenzaldehyde **16** (4.00 g, 26.5 mmol) and acetophenone (4.77 g, 39.7 mmol), was added a solution of NaOH (10% in MeOH, 5.3 mL) and the mixture stirred for 5 h at room temperature. The reaction mixture was purified by trituration with MeOH to give **17** (4.30 g, 65%) as a brownish solid; ^{1}H NMR (400 MHz, $CDCl_3$) δ 8.13 (d, *J* = 15.6 Hz, 1H), 8.08 (d, *J* = 8 Hz, 1H), 8.02 (d, *J* = 7.2 Hz, 2H), 7.76–7.67 (m, 2H), 7.63–7.58 (m, 2H), 7.56–7.51 (m, 2H), 7.31 (d, *J* = 15.6 Hz, 1H). To a solution of **17** (1.5 g, 5.92 mmol) in EtOH (19 mL) was added Fe powder (992 mg, 17.8 mmol) followed by HCl (0.1 N, 5.95 mL) and the mixture was stirred at 80 °C for 1.5 h. The reaction was cooled to room temperature, diluted with EtOAc and filtered through Celite. The filtrate was washed with saturated aq. Na_2CO_3 solution, dried and concentrated. Purification by chromatography (hexane → hexane/EtOAc 75:25) gave **18** (1.32 g, 87%) as orange solid; ^{1}H NMR(400 MHz, $CDCl_3$) δ 8.04–7.98 (m, 3H), 7.61–7.47 (m, 5H), 7.21 (ddd, *J* = 8, 7.2, 1.6 Hz, 1H), 6.80 (t, *J* = 7.6 Hz, 1H), 6.73 (d, *J* = 8 Hz, 1H), 4.07 (s, 1H). To a solution of amine **18** (1.15 g, 5.15 mmol) in toluene (0.5 M, 10.3 mL) was added acetic formic acid (1.4 mL, 10.3 mmol) and the mixture was stirred at reflux for 5 h. The resulting mixture was concentrated and purified by chromatography (hexane → hexane/EtOAc 50:50) to give the formamide (1.29 g, 90%) as yellow solid as

a mixture of rotamers; ^{1}H NMR (400 MHz, $CDCl_3$) δ 8.54–8.48 (m, 1H), 8.09–7.98 (m, 3H), 7.72 (dd, *J* = 18.4, 7.6 Hz, 1H), 7.57–7.42 (m, 5H), 7.34–7.21 (m, 1H), 5.29 (s, 1H). The formamide was shown to be an unstable compound, so the two steps were conducted consecutively. To a solution of formamide (1.16 g, 4.64 mmol) and Et_3N (2.6 mL, 18.6 mmol) in anhydrous THF (9.3 mL) at 0 °C, $POCl_3$ (651 μL, 6.96 mmol) was added dropwise and the mixture was stirred for 5 h at 0 °C. The reaction was quenched by slowly adding a saturated aq. Na_2CO_3 solution (3 mL) and the reaction was allowed to stir for a further 1 h. The mixture was extracted with Et_2O (10 mL) and washed with water and brine, dried and concentrated. Purification by chromatography (hexane → hexane/EtOAc 75:25) gave **19** (873 mg, 81%) as a brownish solid; ^{1}H NMR (400 MHz, $CDCl_3$) δ 8.05–8.02 (m, 2H, Ph), 8.03 (d, *J* = 16 Hz, 1H, H-3), 7.79–7.76 (m, 1H, Ph), 7.63–7.59 (m, 1H, Ph), 7.62 (d, *J* = 16 Hz, 1H, H-2), 7.54 (s, 1H, Ph), 7.52 (s, 1H, Ph), 7.47 (t, *J* = 2.4 Hz, 1H, Ph), 7.45 (m, 2H, Ph); ^{13}C NMR (101 MHz, $CDCl_3$) δ 189.9 (C-1), 169.1 (NC), 137.9 (C-3), 137.6 (C_{ipso}), 133.1 (Ph), 131.3 (C_{ipso}), 130.7 (Ph), 129.6 (Ph), 128.7 (Ph), 128.6 (Ph), 127.9 (Ph), 127.5 (Ph), 126.1 (C-2). Spectral data were identical to those previously reported.[308]

Ethyl 3-(2-isocyanophenyl)acrylate (24)

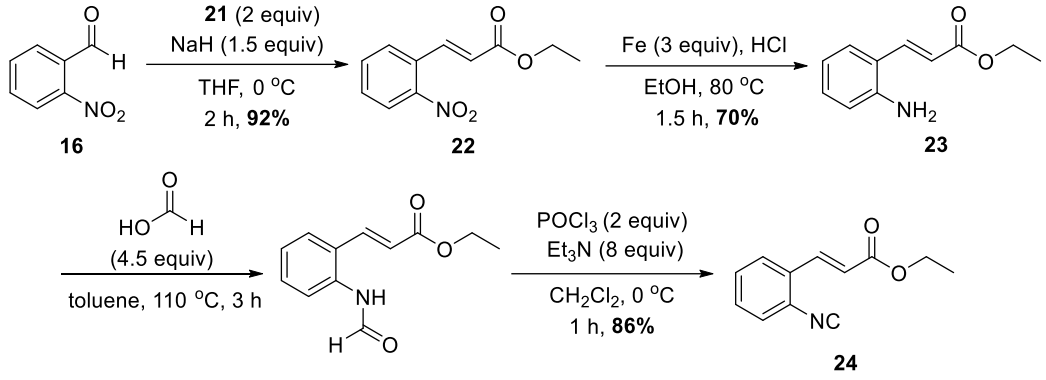

Ethyl 2-(diethoxyphosphoryl)acetate **21** (1.48 g, 6.62 mmol) was added at 0 °C to a suspension of NaH (90%, 132 mg, 4.69 mmol) in dry THF (5 mL) and stirred for 30 min under argon atmosphere. A solution of 2-nitrobenzaldehyde **16** (500 mg, 3.31 mmol) in dry THF (2 mL) was then added and the reaction mixture was stirred for 2 h at 0 °C. The reaction was quenched with a saturated aq. NH_4Cl solution (5 mL) and extracted with EtOAc (3 × 15 mL). The organic layer was then washed with brine, dried and concentrated. Purification by chromatography (hexane → hexane/EtOAc 75:25) gave

22 (663 mg, 92%) as green solid; ^{1}H NMR (400 MHz, $CDCl_3$) δ 8.11 (d, *J* = 15.6 Hz, 1H), 8.04 (d, *J* = 8 Hz, 1H), 7.67–7.63 (m, 2H), 7.57–7.52 (m, 1H), 6.37 (d, *J* = 16.4 Hz, 1H), 4.29 (q, *J* = 7.2 Hz, 2H), 1.35 (t, *J* = 6.8 Hz, 3H). To a solution of **22** (663 mg, 2.99 mmol) in CH_2Cl_2:EtOH (1:1, 9 mL) was added Fe powder (1.17 g, 20.9 mmol) followed by AcOH (3 mL) and H_2O (3 mL) and the mixture was stirred at room temperature for 16 h. The reaction was quenched with saturated aq. $NaHCO_3$ solution (10 mL) and filtered. The mixture was extracted with CH_2Cl_2 (3 × 10 mL), washed with water and brine, dried and concentrated without further purification to give **23** (402 mg, 70%) as orange solid; ^{1}H NMR (400 MHz, $CDCl_3$) δ 7.87 (d, *J* = 16 Hz, 1H), 7.41 (d, *J* = 8 Hz, 1H), 7.21 (t, *J* = 7.6 Hz, 1H), 6.82 (q, *J* = 7.2 Hz, 2H), 6.37 (d, *J* = 16 Hz, 1H), 4.25 (q, *J* = 14, 6.8 Hz, 2H), 1.33 (t, *J* = 7.2 Hz, 3H). A solution of amine **23** (3.1 g, 16.2 mmol) and formic acid (98%, 2.8 mL, 72.9 mmol) in toluene (1 M, 16 mL) was refluxed using a Dean-Stark apparatus for 3 h. The reaction was quenched with a saturated aq. Na_2CO_3 solution (10 mL), extracted with CH_2Cl_2 (3 × 10 mL) and washed with brine, dried and concentrated. The formamide was shown to be an unstable compound, so the two steps were conducted consecutively. Further purification (hexane → hexane/EtOAc 75:25) revealed a mixture of rotamers; ^{1}H NMR (400 MHz, $CDCl_3$) δ 8.94 (d, *J* = 10.4 Hz, 0.5H), 8.48–8.43 (m, 1H), 7.93–7.87 (m, 1H), 7.55 (dd, *J* = 25.2, 8 Hz, 1H), 7.39–7.31 (m, 1H), 7.24 (t, *J* = 7.6 Hz, 0.5 Hz), 7.19–7.12 (m, 1H), 6.37 (dd, *J* = 16, 10.8 Hz, 1H), 4.19 (q, *J* = 7.2 Hz, 2H), 1.26 (q, *J* = 14.8, 7.2 Hz, 3H). To a solution of the crude formamide (3.55 g, 16.2 mmol) and Et_3N (18 mL, 0.13 mol) in anhydrous CH_2Cl_2 (33 mL) at 0 °C, was added $POCl_3$ (3.03 mL, 32.4 mmol) dropwise and the mixture was stirred for 1 h at 0 °C. The reaction was quenched by slowly adding a saturated aq. Na_2CO_3 solution (10 mL), and the mixture was stirred for 1 h. The mixture was extracted with CH_2Cl_2 and washed with water and brine, dried and concentrated. Purification by chromatography (hexane → hexane/EtOAc 95:5) gave **24** (2.79 g, 86% over two steps) as a brownish solid; ^{1}H NMR (400 MHz, $CDCl_3$) δ 7.96 (d, *J* = 16.4 Hz, 1H, H-3), 7.67–7.65 (m, 1H, Ph), 7.45–7.40 (m, 3H, Ph), 6.53 (d, *J* = 16 Hz, 1H, H-2), 4.29 (q, *J* = 7.2 Hz, 2H, $OC\underline{H}_2CH_3$), 1.35 (t, *J* = 7.2 Hz, 3H, $OCH_2C\underline{H}_3$); ^{13}C NMR (101 MHz, $CDCl_3$) δ 168.8 (C-1), 165.9 (NC), 137.6 (C-3), 130.8 (C_{ipso}), 130.6 (Ph), 129.6 (Ph), 127.7 (Ph), 126.9 (Ph), 122.5 (C-2), 60.9 ($O\underline{C}H_2CH_3$), 14.2 ($OCH_2\underline{C}H_3$). Spectral data were identical to those previously reported.[309]

1-Isocyano-2-(3-methoxyprop-1-en-1-yl)benzene (27)

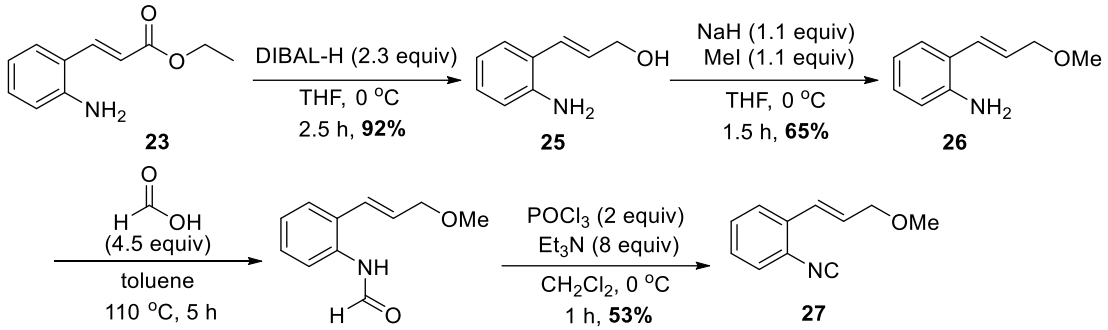

To a solution of amine **23** (3.36 g, 15.1 mmol) in dry THF (19 mL) at 0 °C was added DIBAL-H (1M in hexane, 45 mL, 45.2 mmol). The reaction was allowed to stir for 2.5 h at room temperature. The reaction was quenched by adding MeOH (10 mL) and Rochelle salt solution (10 mL) and the mixture was stirred for another 1 h. The resulting mixture was filtered, and the resulting phases separated. The aqueous phase was extracted with EtOAc (3 × 10 mL). The organic layers were mixed and washed with water and brine, dried and concentrated. Purification by chromatography (hexane → hexane/EtOAc 50:50) gave **25** (2.07 g, 92%) as a brownish solid; ^{1}H NMR (400 MHz, $CDCl_3$) δ 7.19 (d, *J* = 8 Hz, 1H), 7.03 (t, *J* = 7.6 Hz, 1H), 6.72 (t, *J* = 7.6 Hz, 1H), 6.61 (t, *J* = 8 Hz, 2H), 6.15 (dt, *J* = 15.6, 5.6 Hz, 1H), 4.22 (d, *J* = 5.6 Hz, 1H), 3.56 (br s, 3H). To a solution of NaH (90%, 268 mg, 10.1 mmol) in dry THF (90 mL) at 0 °C was added **25** (1.00 g, 6.70 mmol) in THF (5 mL) and the solution was stirred for 30 min. Then, MeI (670 μL, 10.1 mmol) was added and the mixture was stirred for 1.5 h at 0 °C. The reaction was quenched with H_2O (20 mL). The aqueous phase was extracted with EtOAc (3 × 15 mL). The organic phases were collected and washed with water and brine, dried and concentrated. Purification by chromatography (hexane → hexane/EtOAc 90:10) gave **26** (708 mg, 65%) as a brownish oil; ^{1}H NMR (400 MHz, $CDCl_3$) δ 7.26 (d, *J* = 8.8 Hz, 1H), 7.06 (t, *J* = 7.6 Hz, 1H), 6.75 (t, *J* = 7.6 Hz, 1H), 6.66 (d, *J* = 8 Hz, 1H), 6.64 (d, *J* = 5.6 Hz, 1H), 6.17 (dt, *J* = 16, 6 Hz, 1H), 4.09 (dd, *J* = 6, 1.6 Hz, 2H), 3.63 (br s, 2H), 3.39 (s, 3H). A solution of amine **26** (107 mg, 0.66 mmol) and formic acid (98%, 136 mg, 2.95 mmol) in toluene (1 M, 0.7 mL) was refluxed using a Dean-Stark apparatus for 5 h. The reaction was quenched with saturated aq. Na_2CO_3 solution (2 mL) and extracted with CH_2Cl_2 (3 × 3 mL), washed with brine, dried and concentrated. The crude was used for the next step without further purification. To a

solution of the crude formamide (125 mg, 0.65 mmol) and Et_3N (730 μL, 5.23 mmol) in anhydrous CH_2Cl_2 (1.3 mL) at 0 °C, was added $POCl_3$ (122 μL, 1.31 mmol) dropwise and the mixture was stirred for 1 h at 0 °C. The reaction was quenched by slowly adding a saturated aq. Na_2CO_3 solution (1 mL), and the mixture was stirred for 1 h. The mixture was extracted with CH_2Cl_2 (3 × 3 mL) and washed with water and brine, dried and concentrated. Purification by chromatography (hexane → hexane/EtOAc 90:10) gave **27** (60 mg, 53% over two steps from **26**) as a brownish oil; ^{1}H NMR (400 MHz, $CDCl_3$) δ 7.60–7.58 (m, 1H, Ph), 7.36 (t, *J* = 6.8 Hz, 2H, Ph), 7.28–7.24 (m, 1H, Ph), 6.93 (d, *J* = 16 Hz, 1H, H-1), 6.40 (dt, *J* = 16, 6 Hz, 1H, H-2), 4.15 (dd, *J* = 6, 1.6 Hz, 2H, H-3), 3.42 (s, 3H, Me); ^{13}C NMR (101 MHz, $CDCl_3$) δ 166.8 (NC), 160.6 (C_{ipso}), 133.1 (C_{ipso}), 130.7 (C-2), 129.4 (Ph), 128.2 (Ph), 127.1 (Ph), 126.0 (Ph), 125.9 (C-1), 72.7 (C-3), 58.3 (Me). Spectral data were identical to those previously reported.[310]

Synthesis of core heterocycles via MHAT

Phenanthridine (5)

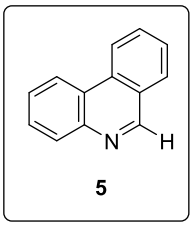

5

To a solution of isocyanide **4a** (315 mg, 1.76 mmol, 1 equiv) and $Fe(acac)_3$ (124 mg, 0.35 mmol, 0.2 equiv) in *i*PrOH (0.4 M, 4.4 mL) was added TBHP (70%, 377 μL, 2.64 mmol, 1.5 equiv) and the mixture was degassed and bubbled with argon for 5 min. $PhSiH_3$ (570 mg, 5.27 mmol, 3 equiv) was added (Caution: continuous argon purge with outlet was maintained to avoid over pressurization of the reaction flask.). The reaction mixture was stirred at room temperature for 24 h. The mixture was concentrated and purified by chromatography (hexane → hexane/EtOAc 90:10) to give **5** (233 mg, 74%) as brownish solid; ^{1}H NMR (400 MHz, $CDCl_3$) δ 9.30 (s, 1H, H-6), 8.63 (d, *J* = 7.6 Hz, 1H, H-1), 8.59 (dd, *J* = 8.4, 1.6 Hz, 1H, H-10), 8.20 (dd, *J* = 8, 2 Hz, 1H, H-4), 8.06 (d, *J* = 8 Hz, 1H, H-7), 7.88 (ddd, *J* = 8.4, 7.2, 1.6 Hz, 1H, H-9), 7.78–7.68 (m, 3H, H-2, H-3 and H-8); ^{13}C NMR (101 MHz, $CDCl_3$) δ 153.5 (C-6), 144.3 (C-4a), 132.5 (C-10a), 131.0 (C-9), 130.0 (C-4), 128.8 (C-7), 128.7 (C-3), 127.5 (C-8), 127.1 (C-2), 126.3 (C-6a), 124.1 (C-10b), 122.2 (C-1), 121.8 (C-10). HRMS (ESI) *m/z*: $[M+H]^+$ calcd for $[C_{13}H_{10}N]^+$ 180.0813, found 180.0819. Spectral data were identical to those previously reported.[311]

3-Methoxycarbonyl-4-phenylisoquinoline (15)

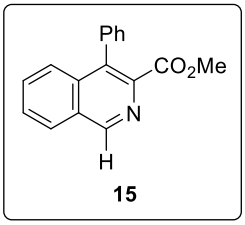

15

To a solution of isocyanide **14** (100 mg, 0.38 mmol, 1 equiv) and $Fe(acac)_3$ (27 mg, 0.076 mmol, 0.2 equiv) in *i*PrOH (0.4 M, 1 mL), was added TBHP (70%, 81 μL, 0.57 mmol, 1.5 equiv) and the mixture was degassed and bubbled with argon for 5 min. $PhSiH_3$ (153 mg, 1.14 mmol, 3 equiv) was added and the reaction mixture was stirred at room temperature for 24 h. The reaction mixture was concentrated and purified by chromatography (hexane → hexane/EtOAc 75:25) to give **15** (86 mg, 86%) as a brownish oil; ^{1}H NMR (400 MHz, $CDCl_3$) δ 9.32 (s, 1H, H-1), 8.07 (d, *J* = 8 Hz, 1H, H-8), 7.72–7.61 (m, 3H, H-5, H-6, H-7), 7.53–7.47 (m, 3H, Ph), 7.35–7.32 (m, 2H, Ph), 3.75 (Me); ^{13}C NMR (101 MHz, $CDCl_3$) δ 167.0 (C=O), 151.7 (C-1), 140.9 (C-3), 135.9 (C_{ipso}), 135.7 (C-4), 134.9 (C-4a), 131.1 (C-6), 129.5 (Ph), 129.0 (C-8a), 128.8 (C-7), 128.2 (Ph), 127.9 (Ph), 127.6 (C-8), 126.5 (C-5), 52.4 (Me). HRMS (ESI) *m/z*: $[M+H]^+$ calcd for $[C_{17}H_{14}NO_2]^+$ 264.1024, found 264.1025. Spectral data were identical to those previously reported.[312]

3-(2-Oxo-2-phenylethyl)indole (35)

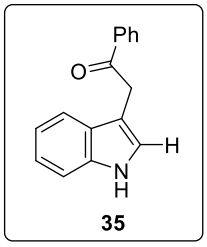

35

Isocyanide **19** (100 mg, 0.43 mmol, 1 equiv) and $Fe(acac)_3$ (30 mg, 0.086 mmol, 0.2 equiv) were dissolved in THF (0.04 M, 11 mL) and MeOH (174 μL, 4.29 mmol, 10 equiv) degassed and bubbled with argon for 5 min. $PhSiH_3$ (139 mg, 1.29 mmol, 3 equiv) was added and the reaction mixture was stirred at 60 °C for 24 h. The reaction mixture was concentrated and purified by chromatography (hexane → hexane/EtOAc 75:25) to give **35** (76 mg, 75%) as brownish oil ; ^{1}H NMR (400 MHz, $CDCl_3$) δ 8.11 (br s, 1H, NH), 8.05 (d, *J* = 7.2 Hz, 2H, Ph), 7.61 (d, *J* = 8 Hz, 1H, H-4), 7.54 (t, *J* = 7.2 Hz, 1H, Ph), 7.44 (t, *J* = 8 Hz, 2H, Ph), 7.33 (d, *J* = 8 Hz, 1H, H-7), 7.19 (t, *J* = 7.2 Hz, 1H, H-6), 7.13 (t, *J* = 8 Hz, 1H, H-5), 7.10 (s, 1H, H-2), 4.41 (s, 2H, CH_2); ^{13}C NMR (101 MHz, $CDCl_3$) δ 197.9 (C=O), 136.7 (C-7a), 136.1 (C_{ipso}), 132.9 (Ph), 128.6 (Ph), 128.5 (Ph), 127.3 (C-3a), 123.2 (C-2), 122.1 (C-6), 119.6 (C-5), 118.7 (C-4), 111.2 (C-7), 108.8 (C-3), 35.5 (CH_2). HRMS (ESI) *m/z*: $[M+H]^+$ calcd for $[C_{16}H_{14}NO]^+$ 236.1075, found 236.1076. Spectral data were identical to those previously reported.[313]

Ethyl 3-indoleacetate (36)

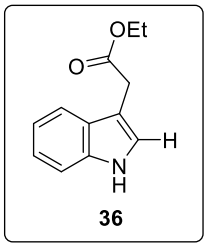

36

Isocyanide **24** (100 mg, 0.50 mmol, 1 equiv), $Fe(acac)_3$ (35 mg, 0.10 mmol, 0.2 equiv) were dissolved in THF (0.04 M, 12.4 mL) and MeOH (201 μL, 4.97 mmol, 10 equiv), degassed and bubbled with argon for 5 min. $PhSiH_3$ (161 mg, 1.49 mmol, 3 equiv) was added and the reaction mixture was stirred at 60 °C for 24 h. The reaction mixture was concentrated and purified by chromatography (hexane → hexane/EtOAc 75:25) to give **36** (92 mg, 91%) as a brownish oil; ^{1}H NMR (400 MHz, $CDCl_3$) δ 8.17 (br s, 1H, NH), 7.64 (d, *J* = 8.4 Hz, 1H, H-4), 7.32 (dt, *J* = 8, 1.2 Hz, 1H, H-7), 7.21 (ddd, *J* = 8.4, 7.2, 1.2 Hz, 1H, H-6), 7.15 (ddd, *J* = 8, 7.2, 1.6 Hz, 1H, H-5), 7.10 (d, *J* = 2.4 Hz, 1H, H-2), 4.19 (q, *J* = 7.2 Hz, 2H, $C\underline{H}_2CH_3$), 3.79 (s, 2H, CH_2), 1.28 (t, *J* = 6.8 Hz, 3H, $CH_2C\underline{H}_3$); ^{13}C NMR (101 MHz, $CDCl_3$) δ 172.3 (C=O), 136.2 (C-7a), 127.3 (C-3a), 123.2 (C-2), 122.2 (C-6), 119.7 (C-5), 118.9 (C-4), 111.3 (C-7), 108.5 (C-3), 60.9 ($\underline{C}H_2CH_3$), 31.5 (CH_2), 14.3 ($CH_2\underline{C}H_3$). HRMS (ESI) *m/z*: $[M+H]^+$ calcd for $[C_{12}H_{14}NO_2]^+$ 204.1024, found 204.1022. Spectral data were identical to those previously reported.[314]

Synthesis of coupled products via MHAT

General Methods

Method 1a – MHAT Coupling from the corresponding isocyanide.

To a solution of isocyanide (1 equiv), alkene (1 equiv) and $Fe(acac)_3$ (0.2 equiv) in *i*PrOH (0.4 M) was added TBHP (70% in water, 1.5 equiv) and the mixture was degassed and bubbled with argon for 5 minutes. The mixture was adjusted to the indicated temperature and $PhSiH_3$ (1 equiv) was then added via syringe. After 24 h at this temperature, the reaction mixture was concentrated and purified by column chromatography.

Method 1b – MHAT Coupling from the corresponding isocyanide.

A solution of isocyanide (1 equiv), alkene (1 equiv) and $Fe(acac)_3$ (0.2 equiv) in *i*PrOH (0.04 M) was degassed and bubbled with argon for 5 minutes. The mixture was adjusted to the indicated temperature and $PhSiH_3$ (1 equiv) was then added via syringe. After 24 h at this temperature, the reaction mixture was concentrated and purified by column chromatography.

Method 2 – MHAT-Minisci Coupling from the corresponding heterocycle.

To a solution of the heterocycle (1 equiv), alkene (3 equiv), and $Fe(acac)_3$ (1 equiv) in 4:1 THF/MeOH (0.2 M) was added TFA (2 equiv). The mixture was adjusted to the indicated temperature and $PhSiH_3$ (1 equiv) was added via syringe and stirred for 2 h open to the air. The reaction was quenched by the addition of saturated aq. $NaHCO_3$ solution, extracted with EtOAc, washed with brine, dried, concentrated and purified by column chromatography.

Method 3 – Sequential MHAT-Minisci Coupling from the corresponding isocyanide.

To a solution of isocyanide (1 equiv) and $Fe(acac)_3$ (0.2 equiv) in 4:1 MTBE/MeOH (0.4 M) was added TBHP (70% in water, 1 equiv) and the mixture was degassed and bubbled with argon for 5 minutes. $PhSiH_3$ (3 equiv) was added via syringe and the reaction mixture was stirred at room temperature for 15 min. Then, the reaction was opened to air, and MTBE (to a 0.2 M solution) was added, followed by $Fe(acac)_3$ (0.8 equiv), TFA (2 equiv) and alkene (3 equiv) and the reaction was heated to 60 °C and stirred for 3 h. The reaction was quenched by the addition of saturated aq. $NaHCO_3$ solution, extracted with EtOAc, washed with brine, dried, concentrated, and purified by column chromatography.

6-(4-hydroxybutan-2-yl)phenanthridine (5a)

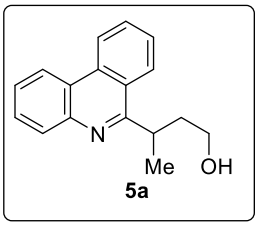

5a

Method 1a: Isocyanide **4a** (100 mg, 0.56 mmol), but-3-en-1-ol (40 mg, 0.56 mmol), $Fe(acac)_3$ (40 mg, 0.11 mmol), TBHP (70%, 120 μL, 0.84 mmol) and $PhSiH_3$ (60 mg, 0.56 mmol) in *i*PrOH (0.4 M, 1.4 mL) at 60 °C. Purification by chromatography (hexane → hexane/EtOAc 50:50) gave **6a** (105 mg, 75%) as a yellow oil.

Method 2: Phenanthridine **5** (50 mg, 0.28 mmol), but-3-en-1-ol (60 mg, 0.84 mmol), $Fe(acac)_3$ (98 mg, 0.28 mmol), TFA (43 μL, 0.56 mmol) and $PhSiH_3$ (30 mg, 0.28 mmol) in 4:1 THF/MeOH (0.2 M, 1.4 mL) at 60 °C. Purification by chromatography (hexane → hexane/EtOAc 50:50) gave **5a** (15 mg, 21%) as a yellow oil.

^{1}H NMR (400 MHz, $CDCl_3$) δ 8.66 (d, *J* = 8.4 Hz, 1H, H-1), 8.54 (d, *J* = 8 Hz, 1H, H-10), 8.36 (d, *J* = 8.4 Hz, 1H, H-7), 8.10 (d, *J* = 8.4 Hz, 1H, H-4), 7.85 (t, *J* = 8.4 Hz, 1H, H-2),

7.71 (t, *J* = 7.6 Hz, 2H, H-3 and H-8), 7.63 (t, *J* = 7.2 Hz, 1H, H-9), 4.97 (br s, 1H, OH), 4.28–4.20 (m, 1H, H-2'), 3.94–3.88 (m, 1H, H-4'), 3.84–3.79 (m, 1H, H-4'), 2.40–2.32 (m, 1H, H-3'), 2.28–2.20 (m, 1H, H-3'), 1.51 (d, *J* = 6.8 Hz, 3H, Me); ^{13}C NMR (101 MHz, $CDCl_3$) δ 165.2 (C-6), 142.7 (C-4a), 133.2 (C-10a), 130.5 (C-2), 129.0 (C-4), 128.7 (C-3), 127.4 (C-8), 126.6 (C-9), 125.9 (C-7), 124.8 (C-6a), 123.5 (C-10b), 122.7 (C-1), 121.9 (C-10), 59.7 (C-4'), 36.5 (C-3'), 35.2 (C-2'), 19.9 (Me); HRMS (ESI) *m/z*: $[M+H]^+$ calcd for $[C_{17}H_{18}NO]^+$ 252.1388, found 252.1387.

6-(dodecan-2-yl)phenanthridine (**5b**)

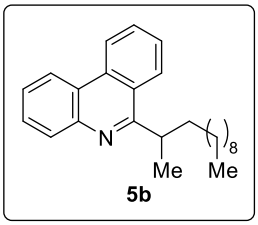

5b

Method 1a: Isocyanide **4a** (50 mg, 0.28 mmol), 1-dodecene (47 mg, 0.28 mmol), $Fe(acac)_3$ (20 mg, 0.056 mmol), TBHP (70%, 60 μL, 0.42 mmol) and $PhSiH_3$ (30 mg, 0.28 mmol) in *i*PrOH (0.4 M, 0.7 mL) at 60 °C. Purification by chromatography (hexane → hexane/EtOAc 99:1) gave **5b** (53 mg, 54%) as a yellow oil. **Method 2:** Phenanthridine **5** (50 mg, 0.28 mmol), 1-dodecene (140 mg, 0.84 mmol), $Fe(acac)_3$ (98 mg, 0.28 mmol), TFA (43 μL, 0.56 mmol) and $PhSiH_3$ (30 mg, 0.28 mmol) in 4:1 THF/MeOH (0.2 M, 1.4 mL) at 60 °C. Purification by chromatography (hexane → hexane/EtOAc 99:1) gave **5b** (61 mg, 63%) as a yellow oil.

^{1}H NMR (400 MHz, $CDCl_3$) δ 8.66 (d, *J* = 8 Hz, 1H, H-1), 8.55 (dd, *J* = 8, 1.2 Hz, 1H, H-10), 8.32 (d, *J* = 8.4 Hz, 1H, H-7), 8.14 (d, *J* = 8 Hz, 1H, H-4), 7.82 (ddd, *J* = 8, 6.8, 1.2 Hz, 1H, H-2), 7.70 (dddd, *J* = 9.6, 7.2, 6, 1.6 Hz, 2H, H-3 and H-8), 7.61 (ddd, *J* = 8.4, 7.2, 1.6 Hz, 1H, H-9), 3.83 (sext, *J* = 6.8 Hz, 1H, H-2'), 2.18–2.09 (m, 1H, H-3'), 1.81–1.72 (m, 1H, H-3'), 1.48 (d, *J* = 6.8 Hz, 3H, Me), 1.23 (br s, 16H, H-4'–H-11'), 0.87 (t, *J* = 6.8 Hz, 3H, Me); ^{13}C NMR (101 MHz, $CDCl_3$) δ 165.8 (C-6), 144.0 (C-4a), 133.2 (C-10a), 130.1 (C-4), 130.0 (C-2), 128.5 (C-3), 127.2 (C-8), 126.2 (C-9), 125.7 (C-7), 125.3 (C-6a), 123.4 (C-10b), 122.7 (C-1), 121.9 (C-10), 36.8 (C-2'), 36.4 (C-3'), 32.1 (CH_2), 30.0 (CH_2), 29.8 (CH_2), 29.8 (CH_2), 29.7 (CH_2), 29.5 (CH_2), 28.1 (CH_2), 22.8 (CH_2), 20.3 (Me), 14.3 (Me); HRMS (ESI) *m/z*: $[M+H]^+$ calcd for $[C_{25}H_{32}N]^+$ 346.2535, found 346.2540.

6-(11-hydroxyundecan-2-yl)phenanthridine (5c)

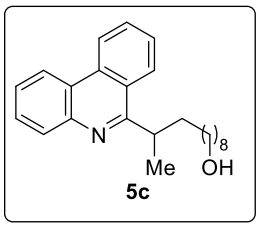

5c

Method 1a: Isocyanide **4a** (100 mg, 0.56 mmol), 10-undecen-1-ol (95 mg, 0.56 mmol), $Fe(acac)_3$ (40 mg, 0.11 mmol), TBHP (70%, 120 μL, 0.84 mmol) and $PhSiH_3$ (60 mg, 0.56 mmol) in *i*PrOH (0.4 M, 1.4 mL) at 60 °C. Purification by chromatography (hexane → hexane/EtOAc 90:10) gave **5c** (111 mg, 59%) as a yellow oil.
Method 2: Phenanthridine **5** (100 mg, 0.56 mmol), 10-undecen-1-ol (285 mg, 1.67 mmol), $Fe(acac)_3$ (197 mg, 0.56 mmol), TFA (85 μL, 1.12 mmol) and $PhSiH_3$ (60 mg, 0.56 mmol) in 4:1 THF/MeOH (0.2 M, 2.9 mL) at 60 °C. Purification by chromatography (hexane → hexane/EtOAc 90:10) gave **5c** (133 mg, 71%) as a yellow oil.

^{1}H NMR (400 MHz, $CDCl_3$) δ 8.65 (d, *J* = 8.4 Hz, 1H, H-1), 8.54 (d, *J* = 8.4 Hz, 1H, H-10), 8.32 (d, *J* = 8.4 Hz, 1H, H-7), 8.15 (d, *J* = 8 Hz, 1H, H-4), 7.82 (ddd, *J* = 8.4, 7.2, 1.6 Hz, 1H, H-2), 7.73–7.67 (m, 2H, H-3 and H8), 7.61 (ddd, *J* = 8.4, 6.8, 1.6 Hz, 1H, H-9), 3.83 (sext, *J* = 6.8 Hz, 1H, H-2'), 3.61 (t, *J* = 6.8 Hz, 2H, H-11'), 2.19–2.10 (m, 1H, CH_2), 1.81–1.72 (m, 1H, CH_2), 1.56–1.51 (m, 2H, CH_2), 1.49 (d, *J* = 6.8 Hz, 3H, Me), 1.36–1.26 (m, 12H, CH_2); ^{13}C NMR (101 MHz, $CDCl_3$) δ 165.8 (C-6), 143.9 (C-4a), 133.1 (C-10a), 130.1 (C-2), 129.9 (C-4), 128.5 (C-3), 127.2 (C-8), 126.3 (C-9), 125.7 (C-7), 125.3 (C-6a), 123.4 (C-10b), 122.7 (C-1), 121.9 (C-10), 63.1 (C-11'), 36.7 (C-2'), 36.4 (CH_2), 32.9 (CH_2), 29.9 (CH_2), 29.6 (CH_2), 29.5 (CH_2), 29.4 (CH_2), 28.0 (CH_2), 25.8 (CH_2), 20.3 (Me); HRMS (ESI) *m/z*: $[M+H]^+$ calcd for $[C_{24}H_{30}NO]^+$ 348.2327, found 348.2330.

6-(4-(benzoyloxy)butan-2-yl)phenanthridine (5d)

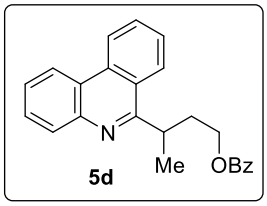

5d

Method 1a: Isocyanide **4a** (100 mg, 0.56 mmol), but-3-en-1-yl benzoate (98 mg, 0.56 mmol), $Fe(acac)_3$ (40 mg, 0.11 mmol), TBHP (70%, 120 μL, 0.84 mmol) and $PhSiH_3$ (60 mg, 0.56 mmol) in *i*PrOH (0.4 M, 1.4 mL) at 60 °C. Purification by chromatography (hexane → hexane/EtOAc 97.5:2.5) gave **5d** (105 mg, 53%) as a pale-yellow oil.
Method 2: Phenanthridine **5** (100 mg, 0.56 mmol), but-3-en-1-yl benzoate (295 mg, 1.67 mmol), $Fe(acac)_3$ (197 mg, 0.56 mmol), TFA (85 μL, 1.12 mmol) and $PhSiH_3$ (60 mg,

0.56 mmol) in 4:1 THF/MeOH (0.2 M, 2.8 mL) at 60 °C. Purification by chromatography (hexane → hexane/EtOAc 97.5:2.5) gave **5d** (150 mg, 76%) as a pale-yellow oil.

^{1}H NMR (400 MHz, $CDCl_3$) δ 8.65 (d, *J* = 8.4 Hz, 1H, H-10), 8.54 (d, *J* = 8 Hz, 1H, H-1), 8.33 (d, *J* = 8.4 Hz, 1H, H-7), 8.15 (dd, *J* = 8, 1.2 Hz, 1H, H-3), 7.95–7.93 (m, 2H, Ph), 7.81 (ddd, *J* = 8.8, 6.8, 1.2 Hz, 1H, H-9), 7.72 (ddd, *J* = 8.4, 7.2, 1.6 Hz, 1H, H-2), 7.65 (ddd, *J* = 8.4, 6.8, 1.2 Hz, 1H, H-8), 7.62 (ddd, *J* = 8.4, 7.2, 1.6 Hz, 1H, H-4), 7.53 (tt, *J* = 6.8, 1.2 Hz, 1H, Ph), 7.38 (t, *J* = 8.4 Hz, 2H, Ph), 4.55–4.49 (m, 1H, H-4'), 4.41–4.35 (m, 1H, H-4'), 4.12 (sext, *J* = 14.4, 6.8 Hz, 1H, H-2'), 2.78 (dq, *J* = 14, 6.8 Hz, 1H, H-3'), 2.28 (dq, *J* = 12, 6.8 Hz, 1H, H-3'), 1.55 (d, *J* = 6.8 Hz, 3H, Me); ^{13}C NMR (101 MHz, $CDCl_3$) δ 166.7 (C=O), 164.1 (C-6), 143.9 (C-4a), 133.2 (C-10a), 132.9 (Ph), 130.5 (C_{ipso}), 130.2 (C-3), 130.1 (C-9), 129.6 (Ph), 128.6 (C-2), 128.4 (Ph), 127.3 (C-8), 126.5 (C-4), 125.4 (C-7), 125.1 (C-6a), 123.5 (C-10b), 122.8 (C-10), 121.9 (C-1), 63.9 (C-4'), 34.7 (C-3'), 33.6 (C-2'), 20.9 (Me); HRMS (ESI) *m/z*: $[M+H]^+$ calcd for $[C_{24}H_{22}NO_2]^+$ 356.1650, found 356.1647.

6-(4-(1,3-dioxoisoindolin-2-yl)butan-2-yl)phenanthridine (5e)

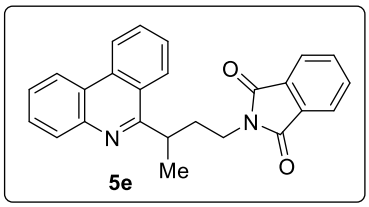

Method 1a: Isocyanide **4a** (100 mg, 0.56 mmol), 2-(but-3-en-1-yl)isoindoline-1,3-dione (112 mg, 0.56 mmol), $Fe(acac)_3$ (40 mg, 0.11 mmol), TBHP (70%, 120 μL, 0.84 mmol) and $PhSiH_3$ (60 mg, 0.56 mmol) in *i*PrOH (0.4 M, 1.4 mL) at 60 °C. Purification by chromatography (hexane → hexane/EtOAc 75:25) gave **5e** (132 mg, 62%) as a pale-yellow solid.

Method 2: Phenanthridine **5** (100 mg, 0.56 mmol), 2-(but-3-en-1-yl)isoindoline-1,3-dione (336 mg, 1.67 mmol), $Fe(acac)_3$ (197 mg, 0.56 mmol), TFA (85 μL, 1.12 mmol) and $PhSiH_3$ (60 mg, 0.56 mmol) in 4:1 THF/MeOH (0.2 M, 2.8 mL) at 60 °C. Purification by chromatography (hexane → hexane/EtOAc 75:25) gave **5e** (161 mg, 76%) as a pale-yellow solid.

^{1}H NMR (400 MHz, $CDCl_3$) δ 8.57 (d, *J* = 9.6 Hz, 1H, H-10), 8.43 (d, *J* = 8.4 Hz, 1H, H-1), 8.24 (d, *J* = 8 Hz, 1H, H-7), 8.08 (d, *J* = 8.4 Hz, 1H, H-4), 7.79 (ddd, *J* = 8.4, 7.2, 1.2 Hz, 1H, H-9), 7.69–7.63 (m, 2H, H-3 and H-8), 7.61–7.53 (m, 5H, H-2 and Ar), 3.98–3.86 (m, 2H, H-2' and H-4'), 3.83–3.76 (m, 1H, H-4'), 2.88 (dq, *J* = 15.6, 7.6 Hz, 1H, H-3'), 2.12 (dq, *J* = 13.2, 5.6 Hz, 1H, H-3'), 1.48 (d, *J* = 7.2 Hz, 3H, Me); ^{13}C NMR (101 MHz, $CDCl_3$) δ

168.4 (C=O), 163.9 (C-6), 143.7 (C-4a), 133.7 (Ar), 133.2 (C-10a), 132.1 (C_{ipso}), 130.1 (C-4 and C-9), 128.5 (C-3), 127.3 (C-8), 126.3 (C-2), 125.6 (C-7), 124.9 (C-6a), 123.4 (C-10b), 122.9 (Ar), 122.6 (C-10), 121.8 (C-1), 37.1 (C-4'), 35.1 (C-2'), 33.6 (C-3'), 21.5 (Me). HRMS (ESI) *m/z*: $[M+H]^+$ calcd for $[C_{25}H_{21}N_2O_2]^+$ 381.1603, found 381.1605.

6-cyclopentylphenanthridine (5f)

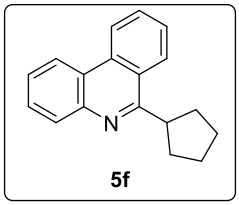

5f

Method 1a: Isocyanide **4a** (100 mg, 0.56 mmol), cyclopentene (38 mg, 0.56 mmol), $Fe(acac)_3$ (40 mg, 0.11 mmol), TBHP (70%, 120 μL, 0.84 mmol) and $PhSiH_3$ (60 mg, 0.56 mmol) in *i*PrOH (0.4 M, 1.4 mL) at 60 °C. Purification by chromatography (hexane → hexane/EtOAc 97.5:2.5) gave **5f** (36 mg, 26%) as a yellowish oil.

Method 2: Phenanthridine **5** (100 mg, 0.56 mmol), cyclopentene (114 mg, 1.67 mmol), $Fe(acac)_3$ (197 mg, 0.56 mmol), TFA (85 μL, 1.12 mmol) and $PhSiH_3$ (60 mg, 0.56 mmol) in 4:1 THF/MeOH (0.2 M, 2.9 mL) at 60 °C. Purification by chromatography (hexane → hexane/EtOAc 97.5:2.5) gave **5f** (97 mg, 70%) as a yellowish oil.

Method 3: Isocyanide **4a** (100 mg, 0.56 mmol), $Fe(acac)_3$ (40 mg, 0.11 mmol), TBHP (70%, 80 μL, 0.56 mmol) and $PhSiH_3$ (181 mg, 1.67 mmol) in 4:1 MTBE/MeOH (0.4 M, 1.4 mL) at room temperature. After 15 min, was added MTBE (to a 0.2 M solution, 1.4 mL), $Fe(acac)_3$ (157 mg, 0.45 mmol), TFA (85 μL, 1.12 mmol) and cyclopentene (153 μL, 1.67 mmol) at 60 °C, open to air. Purification by chromatography (hexane → hexane/EtOAc 97.5:2.5) gave **5f** (82 mg, 62%) as a yellowish oil.

^{1}H NMR (400 MHz, $CDCl_3$) δ 8.62 (d, *J* = 9.6 Hz, 1H, H-1), 8.53 (d, *J* = 8 Hz, 1H, H-10), 8.34 (d, *J* = 8,4 Hz, 1H, H-7), 8.18 (d, *J* = 8 Hz, 1H, H-4), 7.80 (ddd, *J* = 8.4, 7.2, 1.2 Hz, 1H, H-2), 7.73 (ddd, *J* = 8.4, 7.2, 1.6 Hz, 1H, H-3), 7.68 (ddd, *J* = 8.4, 7.2, 1.2 Hz, 1H, H-8), 7.61 (ddd, *J* = 8.4, 7.2, 1.6 Hz, H-9), 4.09 (q, *J* = 8 Hz, 1H, H-1'), 2.36–2.18 (m, 4H, CH_2), 2.04–1.94 (m, 2H, CH_2), 1.89–1.80 (m, 2H, CH_2); ^{13}C NMR (101 MHz, $CDCl_3$) δ 164.2 (C-6), 143.8 (C-4a), 132.9 (C-10a), 130.0 (C-2), 129.9 (C-4), 128.4 (C-3), 127.1 (C-8), 126.2 (C-9), 126.1 (C-7), 125.7 (C-6a), 123.5 (C-10b), 122.4 (C-1), 121.9 (C-10), 43.6 (C-1'), 32.2 (CH_2), 26.1 (CH_2); HRMS (ESI) *m/z*: $[M+H]^+$ calcd for $[C_{18}H_{18}N]^+$ 248.1439, found 248.1442. Spectral data were identical to those previously reported.[315]

6-cyclohexylphenanthridine (5g)

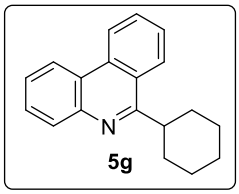

Method 1a: Isocyanide **4a** (50 mg, 0.28 mmol), cyclohexene (23 mg, 028 mmol), $Fe(acac)_3$ (20 mg, 0.056 mmol), TBHP (70%, 60 μL, 0.42 mmol) and $PhSiH_3$ (30 mg, 0.28 mmol) in *i*PrOH (0.4 M, 700 μL) at 60 °C. Purification by chromatography (hexane → hexane/EtOAc 95:5) gave **5g** (10 mg, 14%) as a yellow oil.

Method 2: Phenanthridine **5** (100 mg, 0.56 mmol), cyclohexene (137 mg, 1.67 mmol), $Fe(acac)_3$ (197 mg, 0.56 mmol), TFA (85 μL, 1.12 mmol) and $PhSiH_3$ (60 mg, 0.56 mmol) in 4:1 THF/MeOH (0.2 M, 2.9 mL) at 60 °C. Purification by chromatography (hexane → hexane/EtOAc 95:5) gave **5g** (92 mg, 63%) as a yellow oil.

Method 3: Isocyanide **4a** (100 mg, 0.56 mmol), $Fe(acac)_3$ (40 mg, 0.11 mmol), TBHP (70%, 80 μL, 0.56 mmol) and $PhSiH_3$ (181 mg, 1.67 mmol) in 4:1 MTBE/MeOH (0.4 M, 1.4 mL) at room temperature. After 15 min, was added MTBE (to a 0.2 M solution, 1.4 mL), $Fe(acac)_3$ (157 mg, 0.45 mmol), TFA (85 μL, 1.12 mmol) and 1-methyl-1-cyclohexene (170 μL, 1.67 mmol) at 60 °C, open to air. Purification by chromatography (hexane → hexane/EtOAc 95:5) gave **5g** (84 mg, 58%) as a yellow oil.

^{1}H NMR (400 MHz, $CDCl_3$) δ 8.65 (d, *J* = 9.6 Hz, 1H, H-1), 8.54 (dd, *J* = 8, 1.2 Hz, 1H, H-10), 8.32 (d, *J* = 8.4 Hz, 1H, H-7), 8.13 (dd, *J* = 8, 1.6 Hz, 1H, H-4), 7.81 (ddd, *J* = 8.4, 6.8, 1.2 Hz, 1H, H-2), 7.72–7.67 (m, 2H, H-3 and H-8), 7.60 (ddd, *J* = 8.4, 7.2, 1.6 Hz, 1H, H-9), 3.62 (tt, *J* = 11.2, 3.2 Hz, 1H, H-1'), 2.09–2.07 (m, 2H, CH_2), 1.99–1.93 (m, 4H, CH_2), 1.88–1.82 (m, 1H, CH_2), 1.63–1.55 (m, 2H, CH_2), 1.45 (tt, *J* = 12.8, 3.6 Hz, 1H, CH_2); ^{13}C NMR (101 MHz, $CDCl_3$) δ 165.4 (C-6), 144.0 (C-4a), 133.2 (C-10a), 130.1 (C-4), 130.0 (C-2), 128.5 (C-3), 127.2 (C-8), 126.3 (C-9), 125.7 (C-7), 124.9 (C-6a), 123.5 (C-10b), 122.7 (C-1), 121.9 (C-10), 42.1 (C-1'), 32.4 (CH_2), 27.0 (CH_2), 26.5 (CH_2); HRMS (ESI) *m/z*: $[M+H]^+$ calcd for $[C_{19}H_{20}N]^+$ 262.1595, found 262.1596. Spectral data were identical to those previously reported.[313]

6-(1-methylcyclohexyl)-5,6-dihydrophenanthridine (5h)

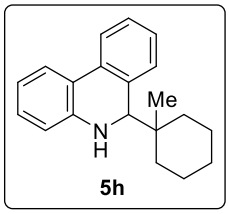

5h

Method 1a: Isocyanide **4a** (100 mg, 0.56 mmol), 1-methyl-1-cyclohexene (54 mg, 0.56 mmol), $Fe(acac)_3$ (40 mg, 0.11 mmol), TBHP (70%, 120 μL, 0.84 mmol) and $PhSiH_3$ (60 mg, 0.56 mmol) in *i*PrOH (0.4 M, 1.4 mL) at 60 °C. Purification by chromatography (hexane → hexane/EtOAc 97:2.5) gave **5h** (8 mg, 5%) as a colorless oil.

Method 2: Phenanthridine **5** (100 mg, 0.56 mmol), 1-methyl-1-cyclohexene (161 mg, 1.67 mmol), $Fe(acac)_3$ (197 mg, 0.56 mmol), TFA (85 μL, 1.12 mmol) and $PhSiH_3$ (60 mg, 0.56 mmol) in 4:1 THF/MeOH (0.2 M, 2.9 mL) at 60 °C. Purification by chromatography (hexane → hexane/EtOAc 97.5:2.5) gave **5h** (145 mg, 94%) as a colorless oil.

Method 3: Isocyanide **4a** (100 mg, 0.56 mmol), $Fe(acac)_3$ (40 mg, 0.11 mmol), TBHP (70% in water, 80 μL, 0.56 mmol) and $PhSiH_3$ (181 mg, 1.67 mmol) in 4:1 MTBE/MeOH (0.4 M, 1.4 mL) at room temperature. After 15 min, was added MTBE (to a 0.2 M solution, 1.4 mL), $Fe(acac)_3$ (157 mg, 0.45 mmol), TFA (85 μL, 1.12 mmol) and 1-methyl-1-cyclohexene (199 μL, 1.67 mmol) at 60 °C, open to air. Purification by chromatography (hexane → hexane/EtOAc 97.5:2.5) gave **5h** (86 mg, 56%) as a colorless oil.

^{1}H NMR (400 MHz, CD_3OD) δ 7.72 (d, *J* = 8 Hz, 1H, H-10), 7.60 (d, *J* = 7.6 Hz, 1H, H-1), 7.29 (tt, *J* = 7.2, 1.6 Hz, 1H, H-9), 7.17 (tt, *J* = 7.6, 2 Hz, 1H, H-8), 7.08 (d, *J* = 7.6 Hz, 1H, H-7), 7.00 (ddd, *J* = 8.4, 6.8, 1.2 Hz, 1H, H-3), 6.67 (d, *J* = 7.6 Hz, 1H, H-4), 6.62 (ddd, *J* = 7.2, 1.2 Hz, 1H, H-2), 4.03 (d, *J* = 2.4 Hz, 1H, H-6), 1.53–1.10 (m, 10H, CH_2) 0.67 (s, 3H, Me); ^{13}C NMR (101 MHz, CD_3OD) δ 146.9 (C-4a), 134.5 (C-10a), 132.9 (C-6a), 130.4 (C-7), 129.9 (C-3), 128.3 (C-9), 126.7 (C-8), 123.6 (C-1), 122.9 (C-10), 122.7 (C-10b), 118.0 (C-4), 114.8 (C-2), 65.2 (C-6), 43.0 (CH_2), 35.0 (CH_2), 34.9 (CH_2), 27.4 (CH_2), 22.9 (CH_2), 22.7 (Me), 19.4 (C-2'); HRMS (ESI) *m/z*: $[M+H]^+$ calcd for $[C_{20}H_{24}N]^+$ 278.1908, found 278.1903.

6-(4-hydroxy-2-methylbutan-2-yl)-5,6-dihydrophenanthridine (5i)

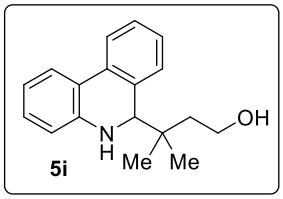

5i

Method 2: Phenanthridine **5** (200 mg, 1.12 mmol), 3-methylbut-3-en-1-ol (288 mg, 3.35 mmol), $Fe(acac)_3$ (394 mg,

1.12 mmol), TFA (171 μL, 2.232 mmol) and $PhSiH_3$ (121 mg, 1.12 mmol) in 4:1 THF/MeOH (0.2 M, 5.6 mL) at 60 °C. Purification by chromatography (hexane → hexane/EtOAc 90:10) gave **5i** (257 mg, 86%) as a white solid.

Method 3: Isocyanide **4a** (200 mg, 1.116 mmol), $Fe(acac)_3$ (79 mg, 0.223 mmol), TBHP (70% in water, 160 μL, 1.116 mmol) and $PhSiH_3$ (362 mg, 3.35 mmol) in 4:1 MTBE/MeOH (0.4 M, 2.8 mL) at room temperature. After 15 min, was added MTBE (to a 0.2 M solution, 2.8 mL), $Fe(acac)_3$ (315 mg, 0.89 mmol), TFA (171 μL, 2.23 mmol) and 3-methylbut-3-en-1-ol (338 μL, 3.35 mmol) at 60 °C, open to air. Purification by chromatography (hexane → hexane/EtOAc 90:10) gave **6i** (155 mg, 52%) as a white solid.

^{1}H NMR (400 MHz, CD_3CN) δ 7.70 (dd, *J* = 8, 1.6 Hz, 1H, H-10), 7.65 (dd, *J* = 7.6, 1.6 Hz, 1H, H-1), 7.35 (d, *J* = 7.6 Hz, 1H, H-7), 7.29 (t, *J* = 7.2 Hz, 1H, H-9), 7.21 (ddd, *J* = 8.8 7.6, 1.2 Hz, 1H, H-8), 7.12 (ddd, *J* = 8.8, 7.2, 1.6 Hz, 1H, H-3), 6.65 (ddd, *J* = 8.8, 7.6, 1.2 Hz, 1H, H-2), 6.51 (d, *J* = 8.4 Hz, 1H, H-4), 4.44 (s, 1H, H-6), 3.64 (t, *J* = 6.8 Hz, 2H, H-4'), 1.80 (t, *J* = 3.6 Hz, 2H, H-3'), 1.40 (s, 3H, Me), 0.93 (s, 3H, Me); ^{13}C NMR (101 MHz, CD_3CN) δ 146.9 (C-4a), 134.2 (C-10a), 133.3 (C-6a), 130.4 (C-3), 128.4 (C-9), 127.8 (C-8), 126.5 (C-7), 123.7 (C-1), 123.1 (C-10), 120.9 (C-10b), 117.4 (C-2), 112.5 (C-4), 68.4 (C-6), 68.3 (C-4'), 42.6 (C-2'), 39.9 (C-3'), 26.9 (Me), 21.7 (Me); HRMS (ESI) *m/z*: $[M+H]^+$ calcd for $[C_{18}H_{22}NO]^+$ 268.1701, found 268.1698.

6-(4-hydroxybutan-2-yl)-8-methylphenanthridine (5k)

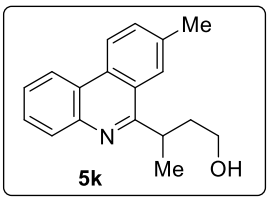

5k

Method 1a: Isocyanide **4b** (100 mg, 0.52 mmol), but-3-en-1-ol (37 mg, 0.52 mmol), $Fe(acac)_3$ (36 mg, 0.10 mmol), TBHP (70%, 111 μL, 0.78 mmol) and $PhSiH_3$ (56 mg, 0.52 mmol) in *i*PrOH (0.4 M, 1.3 mL) at 60 °C. Purification by chromatography (hexane → hexane/EtOAc 50:50) gave **5k** (91 mg, 66%) as a yellow oil. ^{1}H NMR (400 MHz, $CDCl_3$) δ 8.56 (d, *J* = 8.4 Hz, 1H, H-1), 8.51 (dd, *J* = 8, 1.6 Hz, 1H, H-2), 8.13 (br s, 1H, H-7), 8.08 (dd, *J* = 8, 1.6 Hz, 1H, H-9), 7.68 (ddd, *J* = 8.4, 7.2, 1.6 Hz, 2H, H-3 and H-4), 7.61 (ddd, *J* = 8.4, 7.2, 1.6 Hz, 1H, H-10), 4.28–4.20 (m, 1H, H-2'), 3.96–3.90 (m, 1H, H-4'), 3.84–3.79 (m, 1H, H-4'), 2.63 (s, 3H, Me), 2.39–2.31 (m, 1H, H-3'), 2.29–2.21 (m, 1H, H-3'), 1.51 (d, *J* = 7.2 Hz, 3H, Me); ^{13}C NMR (101 MHz, $CDCl_3$) δ 165.1 (C-6), 142.4 (C-4a), 137.5 (C-8

and C-10a), 132.5 (C-3), 129.1 (C-9), 128.4 (C-4), 126.8 (C-10), 125.6 (C-7), 125.1 (C-6a), 123.8 (C-10b), 122.8 (C-1), 121.9 (C-2), 59.9 (C-4'), 36.5 (C-3'), 35.4 (C-2'), 21.1 (Me), 20.1 (Me). HRMS (ESI) *m/z*: $[M+H]^+$ calcd for $[C_{18}H_{20}NO]^+$ 266.1545, found 266.1547.

6-(4-hydroxybutan-2-yl)-8-fluorophenanthridine (5l)

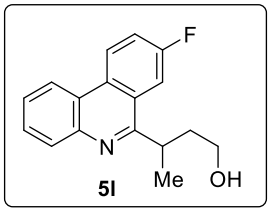

5l

Method 1a: Isocyanide **4c** (100 mg, 0.51 mmol), but-3-en-1-ol (36 mg, 0.51 mmol), $Fe(acac)_3$ (36 mg, 0.10 mmol), TBHP (70%, 110 μL, 0.76 mmol) and $PhSiH_3$ (55 mg, 0.51 mmol) in *i*PrOH (0.4 M, 1.3 mL) at 60 °C. Purification by chromatography (hexane → hexane/EtOAc 50:50) gave **5l** (105 mg, 77%) as a white solid. ^{1}H NMR (400 MHz, $CDCl_3$) δ 8.66 (dd, *J* = 9.2, 5.6 Hz, 1H, H-10), 8.49 (dd, *J* = 8, 1.2 Hz, 1H, H-1), 8.10 (dd, *J* = 8.8, 1.6 Hz, 1H, H-4), 7.98 (dd, *J* = 10.4, 2.8 Hz, 1H, H-7), 7.71 (ddd, *J* = 8.4, 6.8, 1.2 Hz, 1H, H-3), 7.64 (ddd, *J* = 8.4, 7,2, 1.6 Hz, 1H, H-2), 7.60 (ddd, *J* = 10.8, 8, 2.8 Hz, 1H, H-9), 4.13–4.04 (m, 1H, H-2'), 3.92–3.86 (m, 1H, H-4'), 3.84–3.78 (m, 1H, H-4'), 2.41–2.34 (m, 1H, H-3'), 2.25–2.17 (m, 1H, H-3'), 1.50 (d, *J* = 6.8 Hz, 3H, Me); ^{13}C NMR (101 MHz, $CDCl_3$) δ 164.5 (C-6), 161.7 (d, *J* = 248.7 Hz, C-8), 142.6 (C-4a), 130.0 (C-10a), 129.5 (C-4), 128.7 (C-3), 127.2 (C-2), 126.3 (d, *J* = 7.2 Hz, C-6a), 125.4 (d, *J* = 8.4 Hz, C-10), 123.2 (C-10b), 121.8 (C-1), 119.8 (d, *J* = 23.6 Hz, C-9), 110.8 (d, *J* = 21.9 Hz, C-7), 60.1 (C-4'), 36.8 (C-3'), 35.3 (C-2'), 20.0 (Me); ^{19}F NMR (376 MHz, $CDCl_3$) δ −111.87 (s). HRMS (ESI) *m/z*: $[M+H]^+$ calcd for $[C_{17}H_{17}FNO]^+$ 270.1294, found 270.1291.

6-(4-hydroxybutan-2-yl)-3-methoxyphenanthridine (5m)

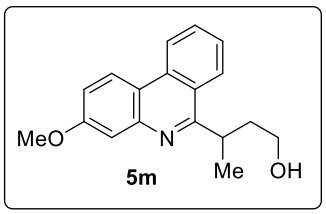

5m

Method 1a: Isocyanide **4d** (100 mg, 0.48 mmol), but-3-en-1-ol (34 mg, 0.48 mmol), $Fe(acac)_3$ (34 mg, 0.10 mmol), TBHP (70%, 103 μL, 0.72 mmol) and $PhSiH_3$ (52 mg, 0.48 mmol) in *i*PrOH (0.4 M, 1.2 mL) at 60 °C. Purification by chromatography (hexane → hexane/EtOAc 50:50) gave **5m** (98 mg, 73%) as a orange solid. ^{1}H NMR (400 MHz, $CDCl_3$) δ 8.55 (d, *J* = 8.4 Hz, 1H, H-10), 8.42 (d, *J* = 9.2 Hz, 1H, H-1), 8.32 (d, *J* = 8.4 Hz, 1H, H-7), 7.81 (ddd, *J* = 8.4, 6.8, 1.2 Hz, 1H, H-9), 7.63 (ddd, *J* = 8, 6.8, 1.2 Hz, 1H, H-8), 7.47 (d, *J* = 2.8 Hz, 1H, H-4), 7.26 (dd, *J* = 9.2, 2.8 Hz, 1H, H-2), 4.29–4.21 (m, 1H, H-2'), 3.98 (s, 3H, OMe), 3.95–3.89 (m, 1H, H-4'), 3.84–3.79 (m, 1H, H-4'), 2.38–2.31 (m, 1H, H-3'), 2.28–2.20 (m, 1H, H-3'), 1.51 (d, *J* = 6.8 Hz, 3H, Me); ^{13}C

NMR (101 MHz, $CDCl_3$) δ 165.9 (C-6), 160.4 (C-3), 144.5 (C-4a), 133.6 (C-10a), 130.8 (C-9), 126.5 (C-8), 126.1 (C-7), 124.0 (C-6a), 123.3 (C-1), 122.4 (C-10), 118.0 (C-2), 117.7 (C-10b), 108.8 (C-4), 59.9 (C-4'), 55.8 (OMe), 36.6 (C-3'), 35.4 (C-2'), 20.1 (Me); HRMS (ESI) *m/z*: $[M+H]^+$ calcd for $[C_{18}H_{20}NO_2]^+$ 282.1494, found 282.1496.

6-(4-hydroxybutan-2-yl)-2-(trifluoromethyl)phenanthridine (5n)

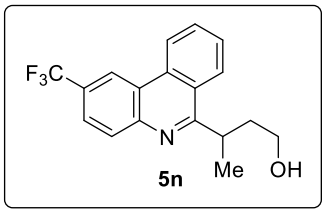

5n

Method 1a: Isocyanide **4f** (100 mg, 0.40 mmol), but-3-en-1-ol (29 mg, 0.40 mmol), $Fe(acac)_3$ (29 mg, 0.08 mmol), TBHP (70%, 87 μL, 0.61 mmol) and $PhSiH_3$ (44 mg, 0.40 mmol) in *i*PrOH (0.4 M, 1.0 mL) at 60 °C. Purification by chromatography (hexane → hexane/EtOAc 75:25) gave **5n** (77 mg, 68%) as a pale yellow solid. ^1H NMR (400 MHz, $CDCl_3$) δ 8.83 (s, 1H, H-1), 8.69 (d, *J* = 8 Hz, 1H, H-10), 8.42 (d, *J* = 8 Hz, 1H, H-7), 8.20 (d, *J* = 8.8 Hz, 1H, H-4), 7.94–7.89 (m, 2H, H-3 and H-9), 7.79 (ddd, *J* = 8.4 Hz, 7.2, 1.2 Hz, H-8), 4.18 (m, 1H, H-2'), 3.89–3.78 (m, 2H, H-4'), 2.45–2.37 (m, 1H, H-3'), 2.23–2.15 (m, 1H, H-3'), 1.52 (d, *J* = 6.8 Hz, 3H, Me); ^{13}C NMR (101 MHz, $CDCl_3$) δ 167.9 (C-6), 144.6 (C-4a), 132.9 (C-10a), 131.3 (C-9), 130.3 (C-4), 128.5 (C-8), 127.2 (q, *J* = 272.3 Hz, CF_3), 126.3 (C-7), 125.3 (C-6a), 124.8 (q, *J* = 3.3 Hz, C-3), 123.2 (C-10b), 122.9 (C-10), 119.9 (q, *J* = 4.2 Hz, C-1), 60.3 (C-4'), 37.1 (C-3'), 34.9 (C-2'), 20.3 (Me); ^{19}F NMR (376 MHz, $CDCl_3$) δ −61.75 (s). HRMS (ESI) *m/z*: $[M+H]^+$ calcd for $[C_{18}H_{17}F_3NO]^+$ 320.1262, found 320.1262.

1-(4-Hydroxybutan-2-yl)-3-methoxycarbonyl-4-phenylisoquinoline (15a)

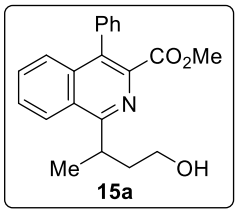

15a

Method 1a: Isocyanide **14** (100 mg, 0.38 mmol), but-3-en-1-ol (27 mg, 0.38 mmol), $Fe(acac)_3$ (27 mg, 0.076 mmol), TBHP (70%, 103 μL, 0.57 mmol) and $PhSiH_3$ (123 mg, 1.14 mmol) in *i*PrOH (0.4 M, 1 mL) at room temperature. Purification by chromatography (hexane → hexane/EtOAc 75:25) gave **15a** (78 mg, 61%) as a yellow oil.

Method 2: Isoquinoline **15** (100 mg, 0.38 mmol), but-3-en-1-ol (82 mg, 1.14 mmol), $Fe(acac)_3$ (134 mg, 0.38 mmol), TFA (58 μL, 0.76 mmol) and $PhSiH_3$ (123 mg, 1.14 mmol) in 4:1 THF/MeOH (0.2 M, 1.9 mL) at room temperature. Purification by chromatography (hexane → hexane/EtOAc 75:25) gave **15a** (41 mg, 32%) as a yellow oil.

^{1}H NMR (400 MHz, $CDCl_3$) δ 8.35 (d, *J* = 8.4 Hz, 1H, H-8), 7.71–7.67 (m, 1H, H-7), 7.64 (br s, 1H, H-6), 7.63 (br s, 1H, H-5), 7.52–7.46 (m, 3H, Ph), 7.35–7.29 (m, 2H, Ph), 4.25–4.19 (m, 1H, H-2'), 3.92–3.86 (m, 1H, H-4'), 3.80–3.74 (m, 1H, H-4'), 3.71 (s, 3H, Me), 2.38–2.30 (m, 1H, H-3'), 2.25–2.17 (m, 1H, H-3'), 1.50 (d, *J* = 6.8 Hz, 3H, Me); ^{13}C NMR (101 MHz, $CDCl_3$) δ 164.8 (C=O), 158.8 (C-1), 136.3 (C-3), 163.2 (Ph), 130.5 (C-6), 129.7 (Ph), 129.6 (Ph), 129.0 (C-4), 128.9 (C-8a), 128.6 (C-7), 128.3 (Ph), 128.2 (Ph), 128.1 (Ph), 127.9 (C-4a), 127.6 (C-5), 124.9 (C-8), 59.9 (C-4'), 52.3 (Me), 36.7 (C-3'), 34.9 (C-2'), 20.4 (Me); HRMS (ESI) *m/z*: $[M+H]^+$ calcd for $[C_{21}H_{22}NO_3]^+$ 336.1599, found 336.1597.

Methyl 1-(4-(Benzoyloxy)butan-2-yl)-4-phenylisoquinoline-3-carboxylate (15b)

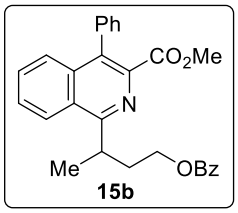

15b

Method 1a: Isocyanide **14** (50 mg, 0.19 mmol), but-3-en-1-yl benzoate (34 mg, 0.19 mmol), $Fe(acac)_3$ (14 mg, 0.038 mmol), TBHP (70%, 41 μL, 0.29 mmol) and $PhSiH_3$ (123 mg, 0.57 mmol) in *i*PrOH (0.4 M, 0.5 mL) at room temperature. Purification by chromatography (hexane → hexane/EtOAc 95:5) gave **15b** (40 mg, 48%) as a white solid.

Method 2: Isoquinoline **15** (100 mg, 0.38 mmol), but-3-en-1-yl benzoate (200 mg, 1.14 mmol), $Fe(acac)_3$ (134 mg, 0.38 mmol), TFA (58 μL, 0.76 mmol) and $PhSiH_3$ (41 mg, 0.38 mmol) in 4:1 THF/MeOH (0.2 M, 1.9 mL) at room temperature. Purification by chromatography (hexane → hexane/EtOAc 75:25) gave **15b** (112 mg, 67%) as a white solid.

^{1}H NMR (400 MHz, $CDCl_3$) δ 8.33–8.29 (m, 1H, H-8), 8.13–8.11 (m, 2H, Ph), 7.99–7.96 (m, 2H, Ph), 7.66–7.59 (m, 4H, H-5, H-6, H-7 and Ph), 7.55 (ddd, *J* = 8.8, 6.8, 1.6 Hz, 1H, Ph), 7.50–7.45 (m, 2H, Ph), 7.42 (t, *J* = 8 Hz, 1H, Ph), 7.35–7.28 (m, 1H, Ph), 4.52–4.46 (m, 1H, H-4'), 4.36–4.30 (m, 1H, H-4'), 4.11 (sext., *J* = 13.2, 6.8, 1H, H-2'), 3.65 (s, 3H, Me), 2.70 (dq, *J* = 14.4, 7.6 Hz, 1H, H-3'), 2.28 (dq, *J* = 13.2, 6 Hz, 1H, H-3'), 1.54 (d, *J* = 6.8 Hz, 3H, Me); ^{13}C NMR (101 MHz, $CDCl_3$) δ 170.9 (C=O), 168.4 (C=O), 164.0 (C-1), 141.6 (C-3), 136.4 (C-4), 136.1 (C_{ipso}), 133.9 (Ph), 132.9 (Ph), 131.6 (C-4a), 130.5 (C_{ipso}), 130.3 (Ph), 130.1 (C-6), 130.0 (Ph), 129.6 (Ph), 129.3 (C-8a), 128.6 (Ph), 128.5 (Ph), 128.3 (Ph), 128.2 (Ph), 127.9 (C-7), 127.4 (C-5), 127.1 (Ph), 124,5 (C-8), 63.9 (C-4'), 52.3

(Me), 34.9 (C-3'), 33.5 (C-2'), 21.1 (Me); HRMS (ESI) *m/z*: $[M+H]^+$ calcd for $[C_{28}H_{26}NO_4]^+$ 440.1862, found 440.1866.

Methyl 4-Phenyl-1-(4-phenylbutan-2-yl)isoquinoline-3-carboxylate (15c)

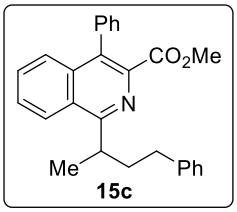

Method 1a: Isocyanide **14** (70 mg, 0.27 mmol), 4-phenyl-1-butene (35 mg, 0.27 mmol), $Fe(acac)_3$ (19 mg, 0.053 mmol), TBHP (70%, 57 μL, 0.40 mmol) and $PhSiH_3$ (87 mg, 0.81 mmol) in *i*PrOH (0.4 M, 0.7 mL) at room temperature. Purification by chromatography (hexane → hexane/EtOAc 95:5) gave **15c** (42 mg, 40%) as a pale-yellow solid.

Method 2: Isoquinoline **15** (70 mg, 0.27 mmol), 4-phenyl-1-butene (105 mg, 0.798 mmol), $Fe(acac)_3$ (94 mg, 0.27 mmol), TFA (41 μL, 0.53 mmol) and $PhSiH_3$ (29 mg, 0.27 mmol) in 4:1 THF/MeOH (0.2 M, 1.4 mL) at room temperature. Purification by chromatography (hexane → hexane/EtOAc 95:5) gave **15c** (66 mg, 63%) as a pale-yellow solid.

^{1}H NMR (400 MHz, $CDCl_3$) δ 8.16–8.11 (m, 1H, H-8), 7.67–7.63 (m, 1H, H-5), 7.63–7.59 (m, 2H, H-6 and H-7), 7.52–7.45 (m, 3H, Ph), 7.38–7.35 (m, 2H, Ph), 7.29–7.25 (m, 2H, Ph), 7.20–7.16 (m, 3H, Ph), 3.84 (sext., *J* = 13.6, 6.8 Hz, 1H, H-2'), 3.68 (s, 3H, Me), 2.70 (t, *J* = 8 Hz, 2H, H-4'), 2.55–2.46 (m, 1H, H-3'), 2.16–2.05 (m, 1H, H-3'), 1.51 (d, *J* = 6.8 Hz, 3H, Me); ^{13}C NMR (101 MHz, $CDCl_3$) δ 168.5 (C=O), 164.9 (C-1), 142.7 (C-3), 141.6 (C_{ipso}), 136.5 (C-4), 135.9 (C_{ipso}), 131.3 (C-4a), 130.1 (C-6), 130.0 (Ph), 128.4 (Ph), 128.3 (Ph), 128.0 (Ph), 127.9 (C-7), 127.1 (C-5), 127.1 (C-8a), 125.8 (Ph), 124.7 (C-8), 52.3 (Me), 37.9 (C-3'), 35.9 (C-2'), 34.2 (C-4'), 20.7 (Me); HRMS (ESI) *m/z*: $[M+H]^+$ calcd for $[C_{27}H_{26}NO_2]^+$ 396.1963, found 396.1963.

1-Cyclohexyl-3-methoxycarbonyl-4-phenylisoquinoline (15d)

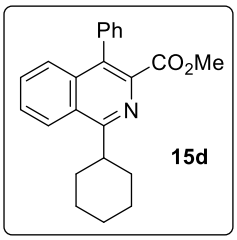

Method 1a: Isocyanide **14** (30 mg, 0.11 mmol), cyclohexene (9 mg, 0.11 mmol), $Fe(acac)_3$ (8 mg, 0.023 mmol), TBHP (70%, 24 μL, 0.17 mmol) and $PhSiH_3$ (37 mg, 0.34 mmol) in *i*PrOH (0.4 M, 285 μL) at room temperature. Purification by chromatography (hexane → hexane/EtOAc 97.5:2.5) gave **15d** (17 mg, 43%) as a yellow oil.

Method 2: Isoquinoline **15** (100 mg, 0.38 mmol), cyclohexene (94 mg, 1.14 mmol), $Fe(acac)_3$ (134 mg, 0.38 mmol), TFA (58 μL, 0.76 mmol) and $PhSiH_3$ (123 mg, 1.14 mmol) in 4:1 THF/MeOH (0.2 M, 1.9 mL) at room temperature. Purification by chromatography (hexane → hexane/EtOAc 97.5:2.5) gave **15d** (75 mg, 57%) as a yellow oil.

Method 3: Isocyanide **14** (86 mg, 0.33 mmol), $Fe(acac)_3$ (23 mg, 0.065 mmol), TBHP (70% in water, 47 μL, 0.33 mmol) and $PhSiH_3$ (106 mg, 0.98 mmol) in 4:1 MTBE/MeOH (0.4 M, 820 μL) at room temperature. After 15 min, was added MTBE (to a 0.2 M solution, 820 μL), $Fe(acac)_3$ (92 mg, 0.26 mmol), TFA (47 μL, 0.65 mmol) and cyclohexene (99 μL, 0.98 mmol) at 60 °C, open to air. Purification by chromatography (hexane → hexane/EtOAc 97.5:2.5) gave **15d** (63 mg, 56%) as a yellow oil.

^{1}H NMR (500 MHz, CD_3OD) δ 8.40 (d, *J* = 8.5 Hz, 1H, H-8), 7.73–7.70 (m, 1H, H-7), 7.68–7.65 (m, 1H, H-6), 7.62–7.60 (m, 1H, H-5), 7.51–7.45 (m, 3H, Ph), 7.31–7.29 (m, 2H, Ph), 3.74–3.67 (m, 1H, H-1'), 3.59 (s, 3H, CH_3), 1.99–1.83 (m, 6H, CH_2), 1.65–1.58 (m, 2H, CH_2), 1.45–1.38 (m, 1H, CH_2), 1.32–1.25 (m, 1H, CH_2); ^{13}C NMR (126 MHz, CD_3OD) δ 170.2 (C=O), 166.6 (C-1), 143.0 (C-3), 137.4 (C_{ipso}), 136.9 (C-4), 131.9 (C-4a), 131.6 (C-6), 131.1 (Ph), 129.4 (Ph), 129.3 (Ph), 129.1 (C-5), 127.8 (C-7), 127.7 (C-8a), 125.9 (C-8), 52.6 (CH_3), 42.7 (C-1'), 33.4 (CH_2), 27.7 (CH_2), 27.3 (CH_2); HRMS (ESI) *m/z*: $[M+H]^+$ calcd for $[C_{23}H_{24}NO_2]^+$ 346.1807, found 346.1810. Spectral data were identical to those previously reported.[316]

1-(1-Methylcyclohexyl)-3-methoxycarbonyl-4-phenylisoquinoline (15e)

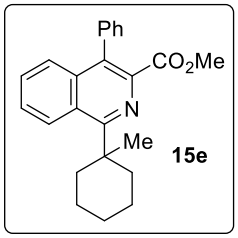

Method 1a: Isocyanide **14** (100 mg, 0.38 mmol), 1-methyl-1-cyclohexene (36 mg, 0.38 mmol), $Fe(acac)_3$ (27 mg, 0.076 mmol), TBHP (70%, 82 μL, 0.57 mmol) and $PhSiH_3$ (123 mg, 1.14 mmol) in *i*PrOH (0.4 M, 0.95 mL) at room temperature. Purification by chromatography (hexane → hexane/EtOAc 99:1) gave **15e** (30 mg, 22%) as a yellow oil.

Method 2: Isoquinoline **15** (100 mg, 0.38 mmol), 1-methyl-1-cyclohexene (109 mg, 1.14 mmol), $Fe(acac)_3$ (134 mg, 0.38 mmol), TFA (58 μL, 0.76 mmol) and $PhSiH_3$ (123

mg, 1.14 mmol) in 4:1 THF/MeOH (0.2 M, 1.9 mL) at room temperature. Purification by chromatography (hexane → hexane/EtOAc 99:1) gave **15e** (93 mg, 68%) as a yellow oil.

Method 3: Isocyanide **14** (86 mg, 0.33 mmol), $Fe(acac)_3$ (23 mg, 0.065 mmol), TBHP (70% in water, 47 μL, 0.33 mmol) and $PhSiH_3$ (106 mg, 0.98 mmol) in 4:1 MTBE/MeOH (0.4 M, 820 μL) at room temperature. After 15 min, was added MTBE (to a 0.2 M solution, 820 μL), $Fe(acac)_3$ (92 mg, 0.26 mmol), TFA (47 μL, 0.65 mmol) and 1-methyl-1-cyclohexene (116 μL, 0.98 mmol) at 60 °C, open to air. Purification by chromatography (hexane → hexane/EtOAc 99:1) gave **15e** (60 mg, 51%) as a yellow oil.

^{1}H NMR (400 MHz, CD_2Cl_2) δ 8.68–8.65 (m, 1H, H-8), 7.68–7.65 (m, 1H, H-7), 7.63–7.55 (m, 2H, H-5 and H-6), 7.52–7.46 (m, 3H, Ph), 7.35–7.33 (m, 2H, Ph), 3.63 (s, 3H, Me), 2.54–2.47 (m, 2H, CH_2), 1.96–1.89 (m, 2H, CH_2), 1.69 (s, 3H, Me), 1.67–1.62 (m, 4H, CH_2), 1.58–1.43 (m, 2H, CH_2); ^{13}C NMR (101 MHz, CD_2Cl_2) δ 168.6 (C=O), 166.8 (C-1), 140.6 (C-3), 137.4 (C-4), 136.9 (C_{ipso}), 131.6 (C-4a), 130.4 (Ph), 129.6 (C-6), 128.5 (Ph), 128.1 (C-7), 127.4 (C-8), 127.1 (C-8a), 126.9 (C-5), 52.2 (Me), 43.8 (CH_2), 39.3 (CH_2), 27.3 (C-1'), 26.9 (Me), 23.3 (CH_2). HRMS (ESI) *m/z*: $[M+H]^+$ calcd for $[C_{24}H_{26}NO_2]^+$ 360.1963, found 360.1959.

2-(4-Hydroxybutan-2-yl)-3-(2-oxo-2-phenylethyl)indole (35a)

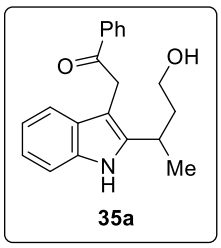

35a

Method 1b: Isocyanide **19** (100 mg, 0.43 mmol), but-3-en-1-ol (31 mg, 0.43 mmol) and $Fe(acac)_3$ (30 mg, 0.086 mmol) and $PhSiH_3$ (46 mg, 0.43 mmol) in *i*PrOH (0.04 M, 10.7 mL) at room temperature. Purification by chromatography (hexane → hexane/EtOAc 75:25) gave **35a** (62 mg, 47%) as a brownish oil. ^{1}H NMR (400 MHz, $CDCl_3$) δ 8.10 (d, *J* = 8.4 Hz, 2H, Ph), 8.03 (s, 1H, NH), 7.59 (t, *J* = 7.6 Hz, 1H, Ph), 7.49 (d, *J* = 8 Hz, 2H, Ph), 7.38 (d, *J* = 7.6 Hz, 1H, H-4), 7.30 (d, *J* = 8 Hz, 1H, H-7), 7.12 (t, *J* = 7.2 Hz, 1H, H-6), 7.05 (t, *J* = 7.6 Hz, 1H, H-5), 4.59 and 4.22 (2d, *J* = 16.8 Hz, 1H each, CH_2), 3.64–3.58 (m, 1H) and 3.56–3.49 (m, 1H, H-4'), 3.38–3.29 (m, 1H, H-2'), 2.56 (br s, 1H, OH), 2.01–1.93 (m, 1H) and 1.87–1.79 (m, 1H, H-3'), 1.32 (d, *J* = 6.8 Hz, 3H, Me); ^{13}C NMR (101 MHz, $CDCl_3$) δ 199.1 (C=O), 140.7 (C-2), 136.9 (C-7a), 135.4 (C_{ipso}), 133.2 (Ph), 128.6 (Ph), 128.5 (Ph), 128.3 (C-3a), 121.4 (C-6), 119.5 (C-5), 117.9 (C-4), 110.6 (C-7),

104.3 (C-3), 60.4 (C-4'), 39.5 (C-3'), 34.1 (CH_2), 27.9 (C-2'), 21.4 (Me). HRMS (ESI) *m/z*: $[M+H]^+$ calcd for $[C_{20}H_{22}NO_2]^+$ 308.1650, found 308.1652.

2-(4-(Benzoyloxy)butan-2-yl)-3-(2-oxo-2-phenylethyl)-1H-indole (35b)

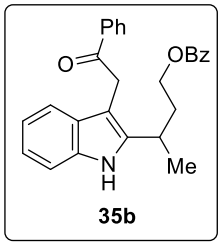

35b

Method 1b: Isocyanide **19** (100 mg, 0.43 mmol), but-3-en-1-yl benzoate (76 mg, 0.43 mmol) and $Fe(acac)_3$ (30 mg, 0.086 mmol) and $PhSiH_3$ (46 mg, 0.43 mmol) in *i*PrOH (0.04 M, 10.7 mL) at room temperature. Purification by chromatography (hexane → hexane/EtOAc 95:5) gave **35b** (72 mg, 41%) as a yellow solid. ^{1}H NMR (400 MHz, $CDCl_3$) δ 7.99–7.97 (m, 2H, Ph), 7.91–7.88 (m, 2H, Ph), 7.53–7.48 (m, 2H, Ph), 7.44 (d, *J* = 7.6 Hz, 1H, H-4), 7.38 (t, *J* = 7.6 Hz, 2H, Ph), 7.33–7.29 (m, 3H, H-7 and Ph), 7.13 (ddd, *J* = 8, 6.8, 1.2 Hz, 1H, H-6), 7.08 (ddd, *J* = 8, 7.2, 1.2 Hz, 1H, H-5), 4.36 (s, 2H, CH_2), 4.34–4.28 (m, 1H, H-4'), 4.21–4.15 (m, 1H, H-4'), 3.39–3.30 (m, 1H, H-2'), 2.17–2.02 (m, 2H, H-3'), 1.37 (d, *J* = 7.2 Hz, 3H, Me); ^{13}C NMR (101 MHz, $CDCl_3$) δ 197.7 (C=O), 166.7 (C=O), 139.7 (C-2), 136.9 (C-7a), 135.7 (C_{ipso}), 133.0 (Ph), 130.2 (C_{ipso}), 129.6 (Ph), 128.7 (Ph), 128.6 (C-3a), 128.5 (Ph), 121.7 (C-6), 119.8 (C-5), 118.4 (C-4), 110.8 (C-7), 104.8 (C-3), 63.3 (C-4'), 35.9 (C-3'), 34.8 (CH_2), 28.4 (C-2'), 21.0 (Me); HRMS (ESI) *m/z*: $[M+H]^+$ calcd for $[C_{27}H_{26}NO_3]^+$ 412.1912, found 412.1909.

Ethyl 2-(4-Hydroxybutan-2-yl)-3-indoleacetate (36a)

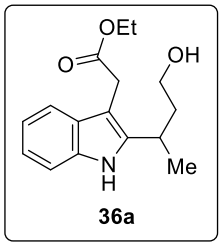

36a

Method 1b: Isocyanide **24** (100 mg, 0.50 mmol), but-3-en-1-ol (36 mg, 0.50 mmol), $Fe(acac)_3$ (35 mg, 0.099 mmol) and $PhSiH_3$ (54 mg, 0.50 mmol) in *i*PrOH (0.04 M, 12.4 mL) at room temperature. Purification by chromatography (hexane → hexane/EtOAc 50:50) gave **36a** (59 mg, 43%) as a yellow oil. ^{1}H NMR (400 MHz, $CDCl_3$) δ 8.15 (s, 1H, NH), 7.56 (d, *J* = 7.2 Hz, 1H, H-4), 7.28 (d, *J* = 8 Hz, 1H, H-7), 7.12 (m, 2H, H-5, H-6), 4.14 (q, *J* = 7.2 Hz, 2H, $OC\underline{H}_2CH_3$), 3.77 (d, *J* = 14.8 Hz, 1H, H-1'), 3.68 (d, *J* = 15.2 Hz, 1H, H-1'), 3.60–3.55 (m, 1H, H-4''), 3.45–3.37 (m, 2H, H-2'', H-4''), 2.03–1.96 (m, 1H, H-3''), 1.82–1.74 (m, 1H, H-3''), 1.33 (d, *J* = 7.2 Hz, 3H, H-1''), 1.26 (t, *J* = 7.2 Hz, 3H, $OCH_2C\underline{H}_3$); ^{13}C NMR (101 MHz, $CDCl_3$) δ 173.3 (C=O), 140.2 (C-2), 135.4 (C-7a), 128.1 (C-3a), 121.5 (C-6), 119.5 (C-5), 118.3 (C-4), 110.5 (C-7), 104.3 (C-3), 61.2 ($O\underline{C}H_2CH_3$), 59.8

(C-4''), 39.6 (C-3''), 30.4 (C-1''), 27.2 (C-2''), 21.5 (C-1''), 14.2 ($OCH_2\underline{C}H_3$). HRMS (ESI) *m/z*: $[M+H]^+$ calcd for $[C_{16}H_{22}NO_3]^+$ 276.1599, found 276.1599.

3-(Ethoxycarbonylmethyl)-2-(4-phenylbutan-2-yl)-1H-indole (36b)

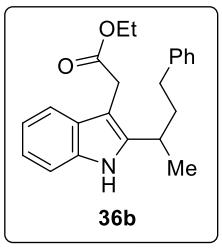

36b

Method 1b: Isocyanide **24** (100 mg, 0.50 mmol), 4-phenyl-1-butene (66 mg, 0.50 mmol) and $Fe(acac)_3$ (35 mg, 0.099 mmol) and $PhSiH_3$ (54 mg, 0.50 mmol) in *i*PrOH (0.04 M, 12.4 mL) at room temperature. Purification by chromatography (hexane → hexane/EtOAc 90:10) gave **36b** (62 mg, 37%) as a yellow oil. ^{1}H NMR (400 MHz, $CDCl_3$) δ 7.85 (br s, 1H, NH), 7.59 (d, *J* = 8.4 Hz, 1H, H-4), 7.31 (d, *J*= 6.8 Hz, 1H, H-7), 7.28–7.24 (m, 3H, Ph), 7.19–7.15 (m, 1H, Ph), 7.14–7.09 (m, 3H, H-5, H-6 and Ph), 4.09 (q, *J* = 7.2 Hz, 2H, $C\underline{H}_2CH_3$), 3.69 and 3.61 (2d, *J* = 15.2 Hz, 1H each, CH_2), 3.15 (sext., *J* = 14, 6.8 Hz, 1H, H-2'), 2.62–2.50 (m, 2H, H-4'), 2.06–1.95 (m, 2H, H-3'), 1.35 (s, *J* = 7.2 Hz, 3H, Me), 1.20 (t, *J* = 7.2 Hz, 3H, $CH_2C\underline{H}_3$); ^{13}C NMR (101 MHz, $CDCl_3$) δ 172.1 (C=O), 142.0 (C_{ipso}), 140.6 (C-2), 135.4 (C-7a), 128.6 (C-3a), 128.5 (Ph), 128.4 (Ph), 126.0 (Ph), 121.6 (C-6), 119.7 (C-5), 118.7 (C-4), 110.6 (C-7), 104.5 (C-3), 60.8 ($\underline{C}H_2CH_3$), 38.8 (C-3'), 33.9 (C-4'), 30.8 (C-2'), 30.7 (CH_2), 21.3 (Me), 14.4 ($CH_2\underline{C}H_3$); HRMS (ESI) *m/z*: $[M+H]^+$ calcd for $[C_{22}H_{26}NO_2]^+$ 336.1963, found 336.1962.

Copies of ^{1}H and ^{13}C NMR Spectra

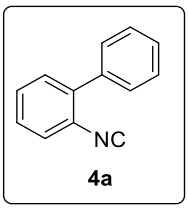

4a

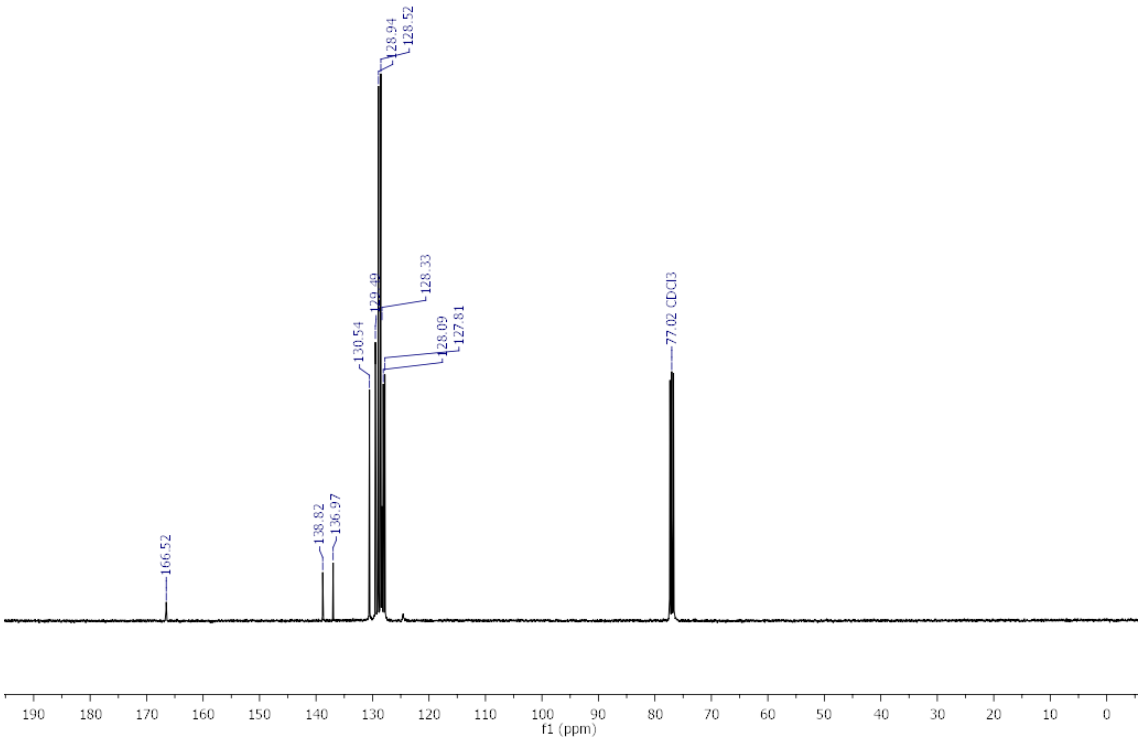

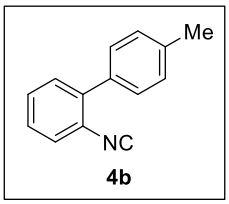
Me
NC

4b

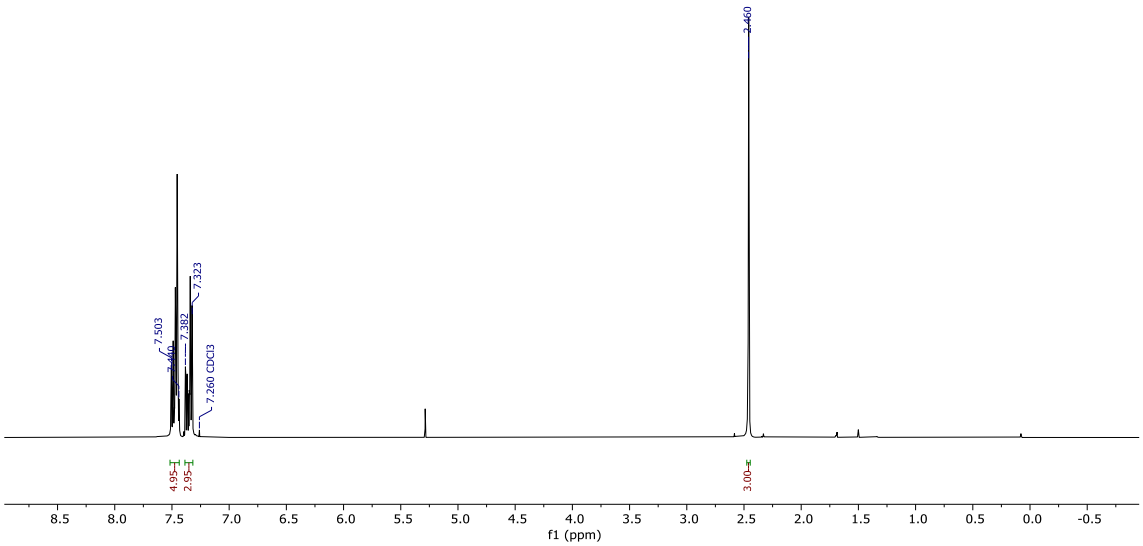
2.460
7.503
7.382
7.323
7.260 CDCl3
4.95
2.95
3.00
8.5 8.0 7.5 7.0 6.5 6.0 5.5 5.0 4.5 4.0 3.5 3.0 2.5 2.0 1.5 1.0 0.5 0.0 -0.5
f1 (ppm)

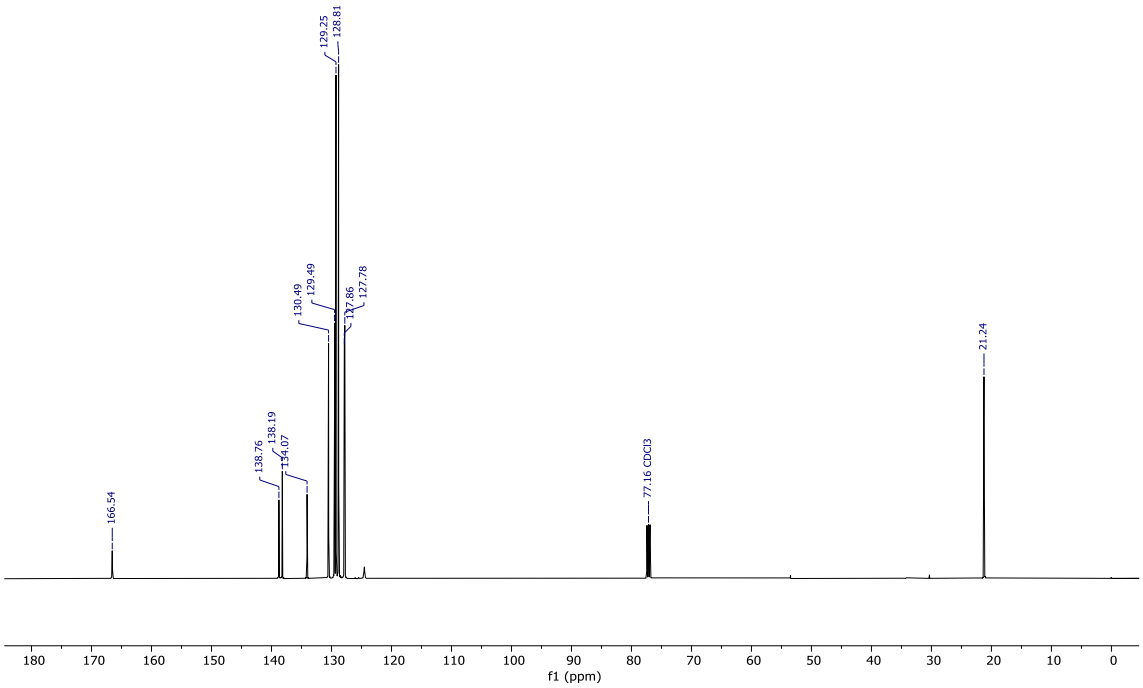
166.54
138.76
138.19
134.07
130.49
129.49
129.25
128.81
127.86
127.78
77.16 CDCl3
21.24
180 170 160 150 140 130 120 110 100 90 80 70 60 50 40 30 20 10 0
f1 (ppm)

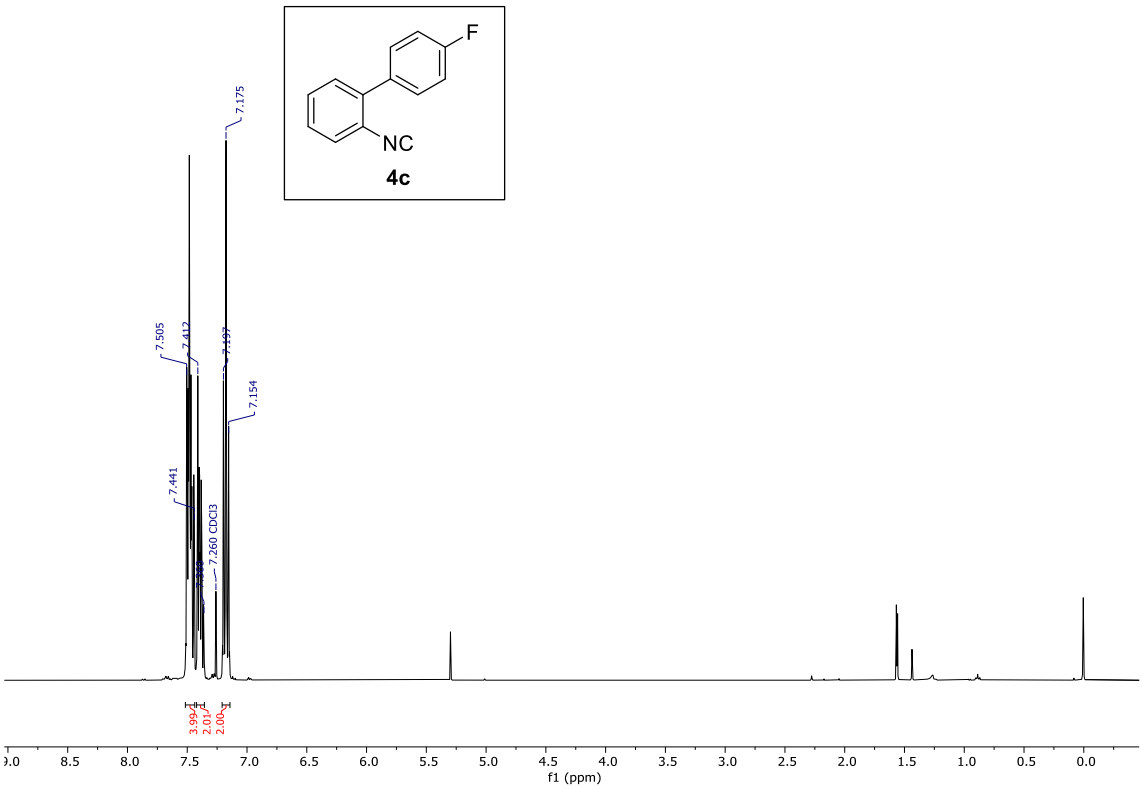
F
NC
4c
7.505
7.412
7.397
7.175
7.154
7.441
7.260 CDCl3
3.99
2.01
2.00
f1 (ppm)

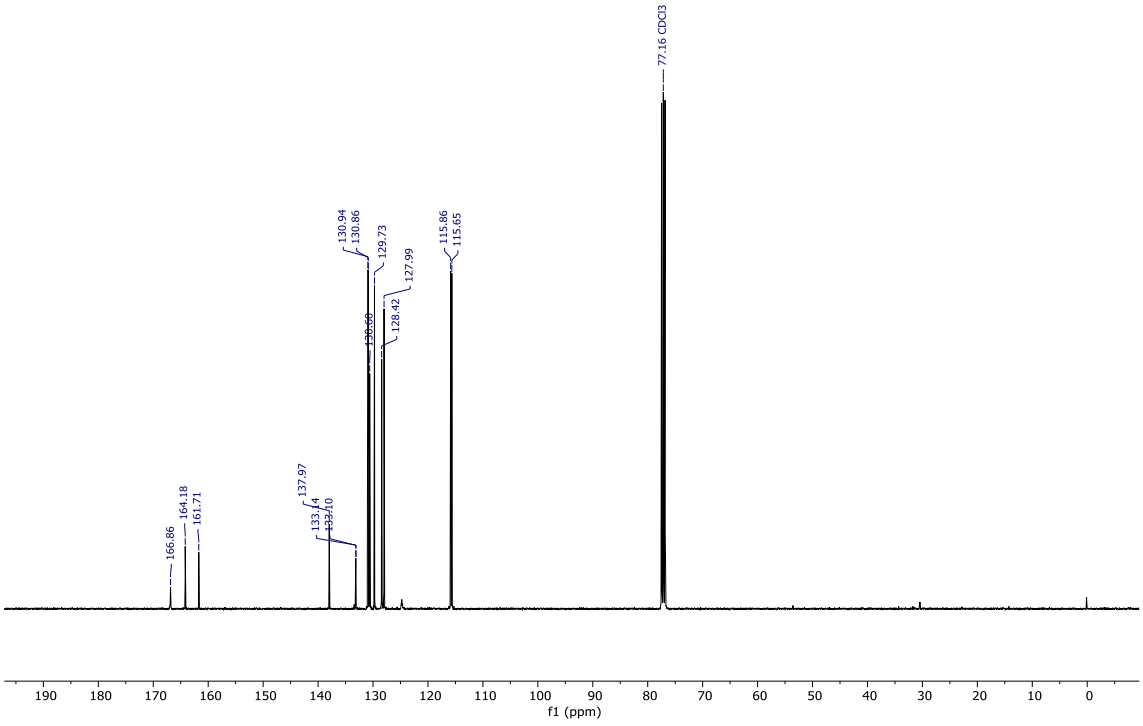
77.16 CDCl3
130.94
130.86
129.73
127.99
128.42
115.86
115.65
137.97
133.14
133.10
166.86
164.18
161.71
f1 (ppm)

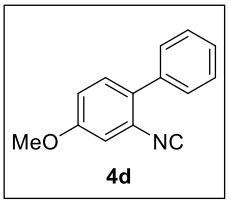
MeO
NC

4d

3.856
7.013
7.517
7.455
7.429
7.386
7.361
7.328
7.260 CDCl3
7.039
3.90
0.90
0.95
1.94
3.00
8.5 8.0 7.5 7.0 6.5 6.0 5.5 5.0 4.5 4.0 3.5 3.0 2.5 2.0 1.5 1.0 0.5 0.0
f1 (ppm)

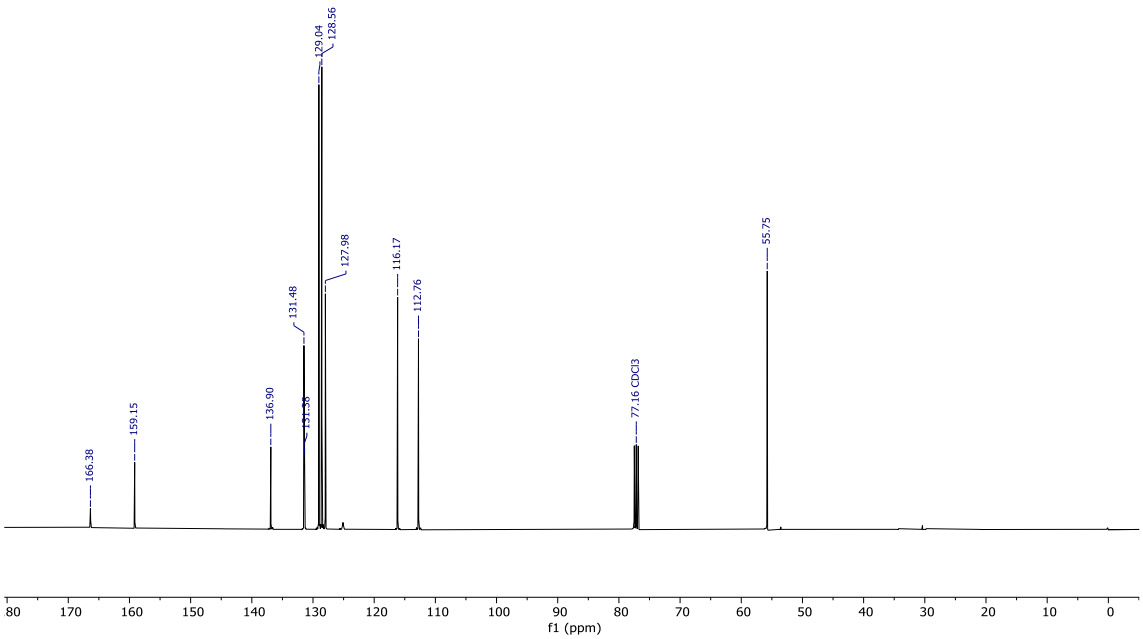
129.04
128.56
127.98
116.17
112.76
131.48
131.38
136.90
159.15
166.38
77.16 CDCl3
55.75
80 170 160 150 140 130 120 110 100 90 80 70 60 50 40 30 20 10 0
f1 (ppm)

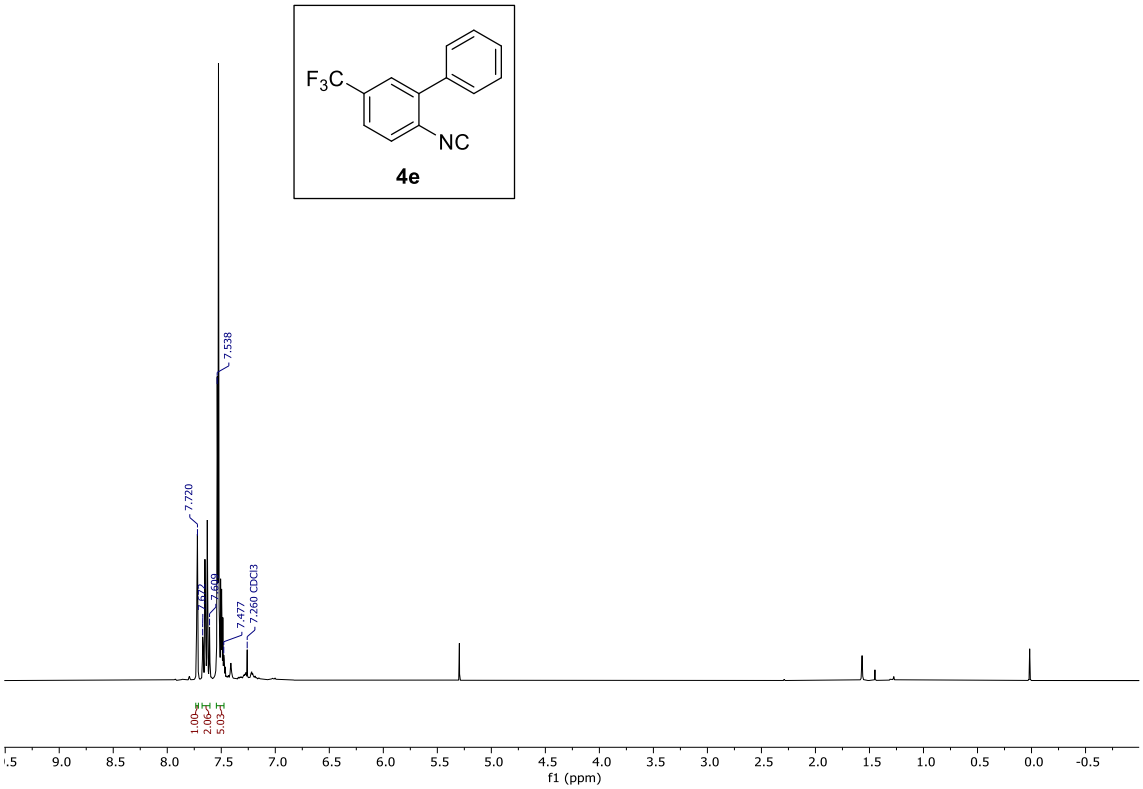
F3C
NC
4e
7.720
7.677
7.660
7.538
7.477
7.260 CDCl3
1.00
2.06
5.03
f1 (ppm)

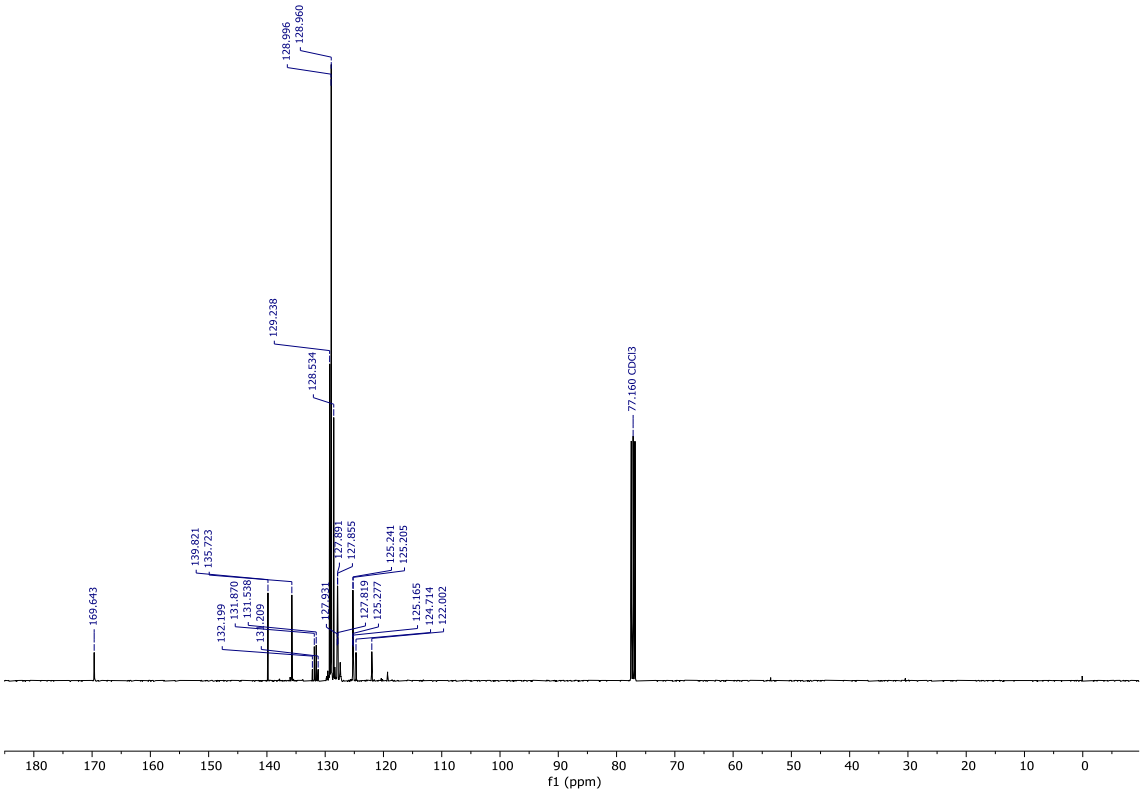
169.643
139.821
135.723
132.199
131.870
131.538
131.209
129.238
128.996
128.960
128.534
127.931
127.891
127.855
127.819
125.277
125.241
125.205
125.165
124.714
122.002
77.160 CDCl3
f1 (ppm)

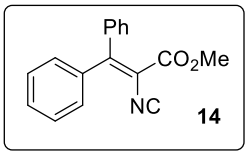
Ph
CO2Me
NC
14

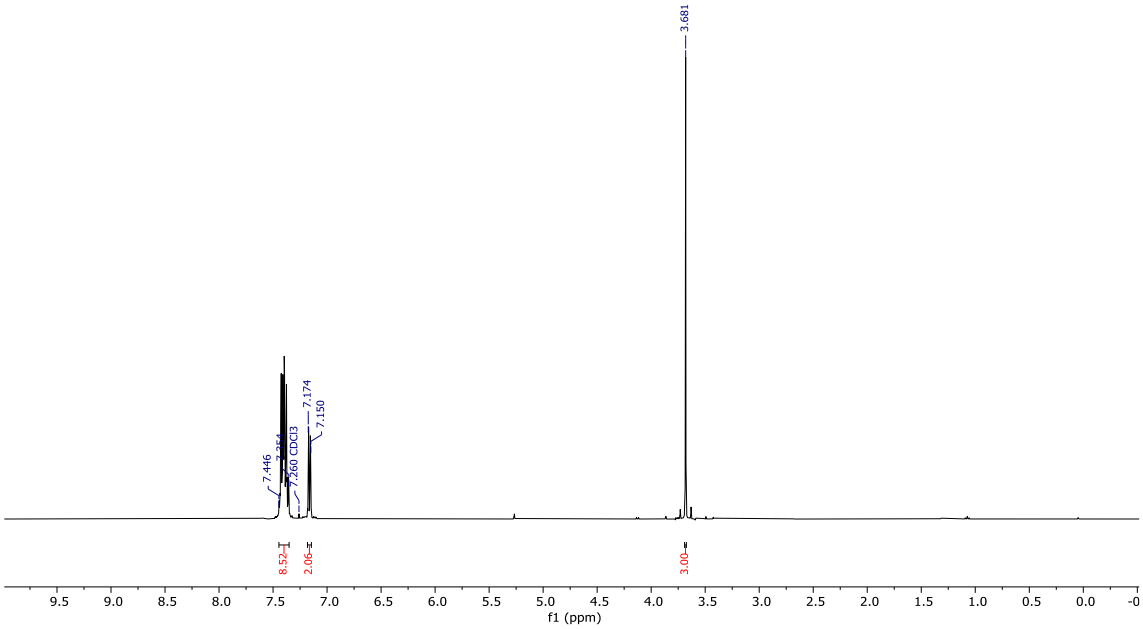
3.681
7.446
7.260 CDCl3
7.174
7.150
8.52
2.06
3.00
f1 (ppm)

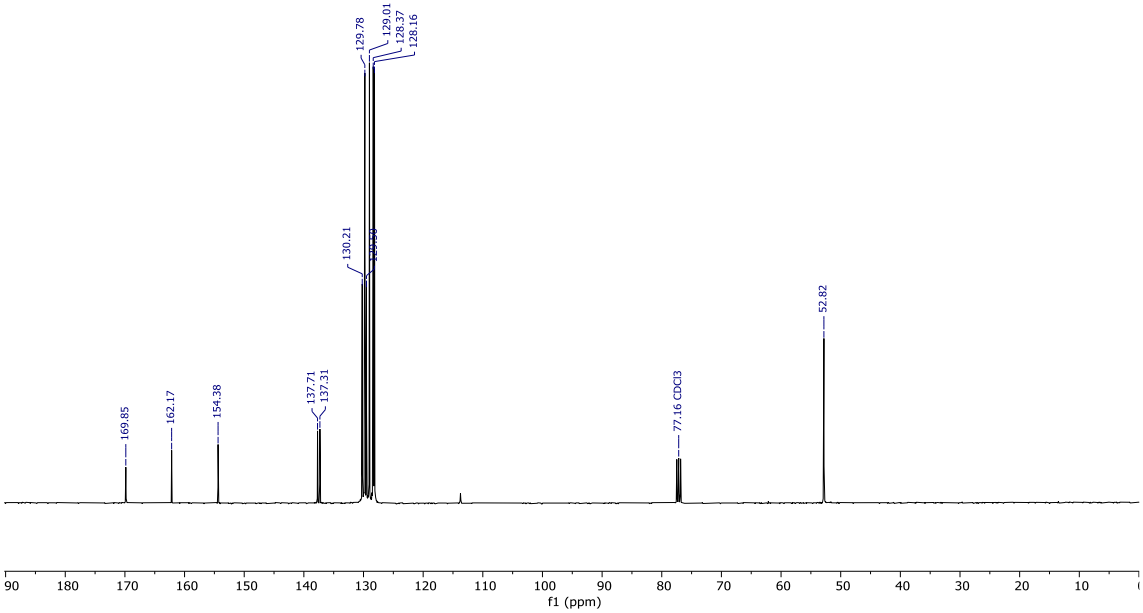
129.78
129.01
128.37
128.16
130.21
52.82
169.85
162.17
154.38
137.71
137.31
77.16 CDCl3
f1 (ppm)

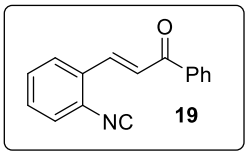
O
Ph
NC
19

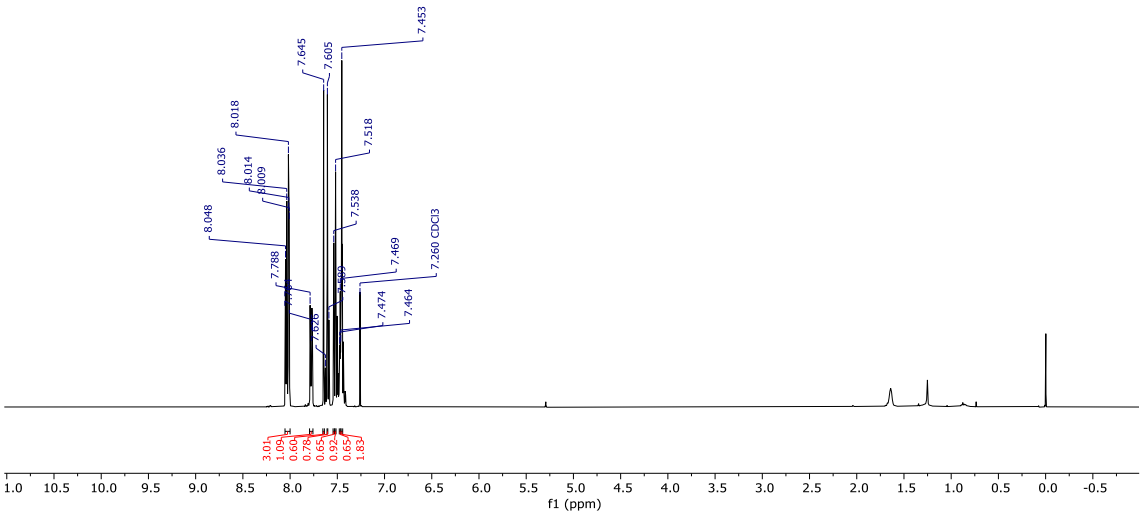
7.453
7.645
7.605
8.018
7.518
8.036
8.014
8.009
7.538
8.048
7.469
7.260 CDCl3
7.788
7.474
7.464
7.626
3.01
1.09
0.60
0.78
0.65
0.92
0.65
1.83
f1 (ppm)

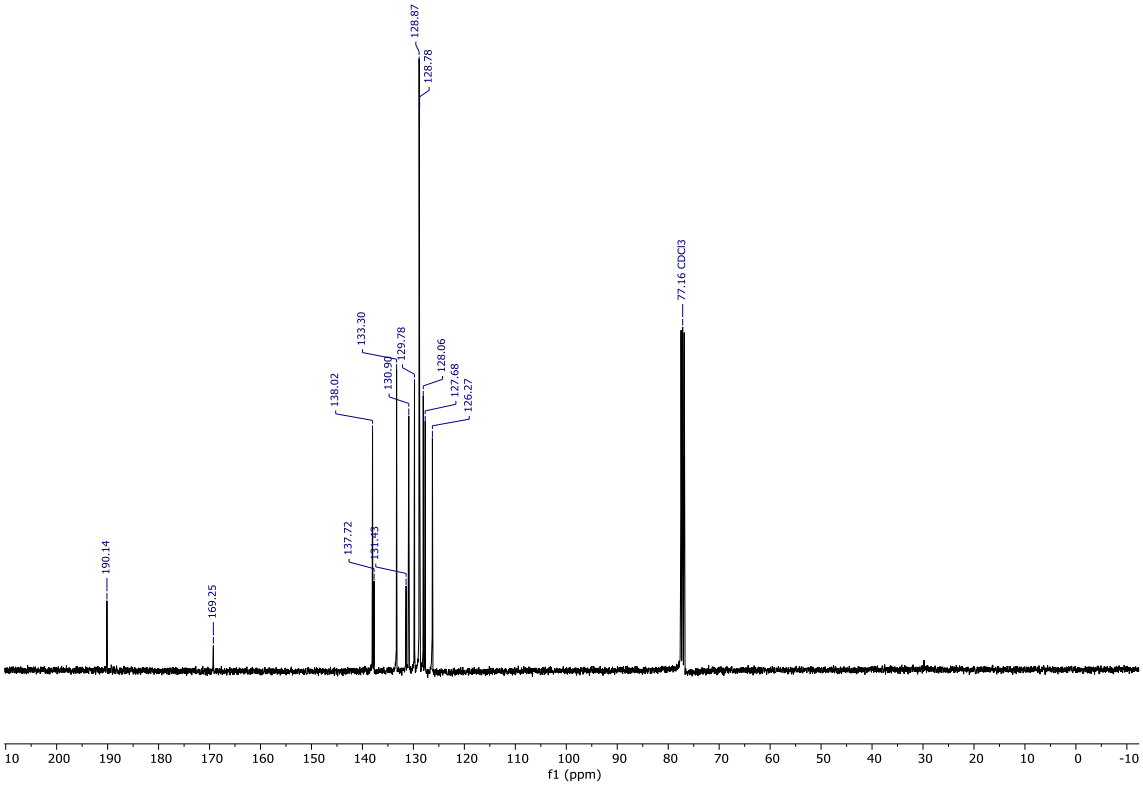
128.87
128.78
77.16 CDCl3
133.30
129.78
130.90
128.06
127.68
126.27
138.02
137.72
131.43
190.14
169.25
f1 (ppm)

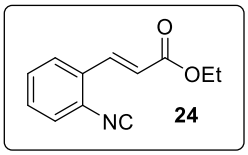
O
OEt
NC

24

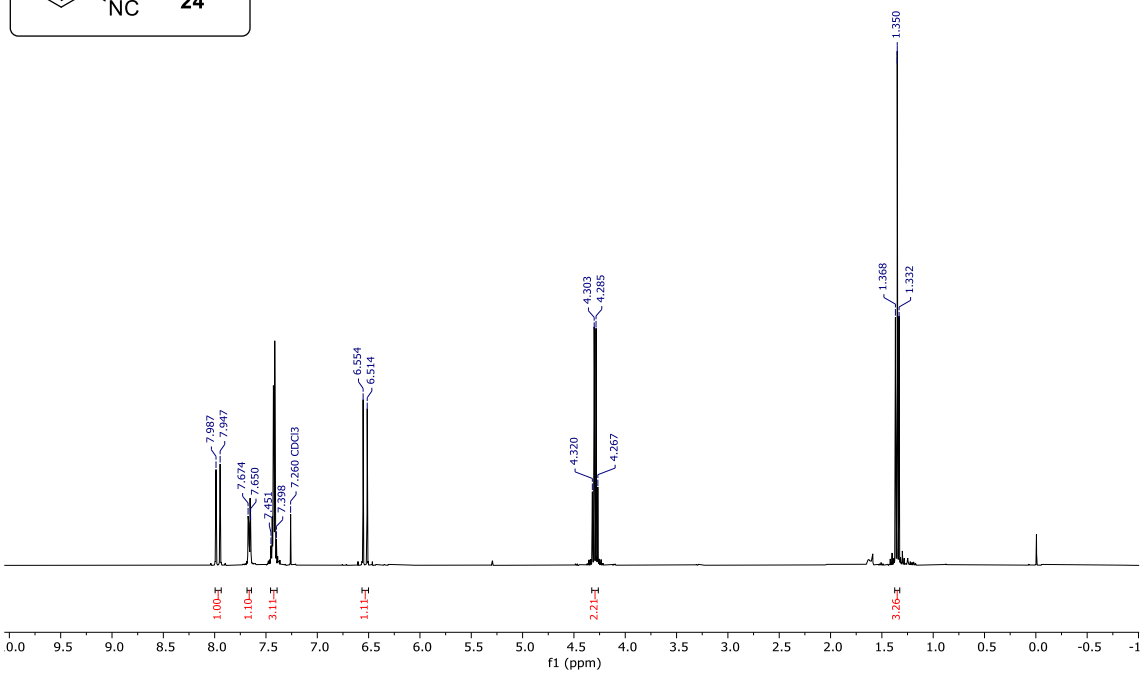
7.987
7.947
7.674
7.650
7.456
7.398
7.260 CDCl3
6.554
6.514
4.303
4.285
4.320
4.267
1.368
1.350
1.332
1.00
1.10
3.11
1.11
2.21
3.26
f1 (ppm)

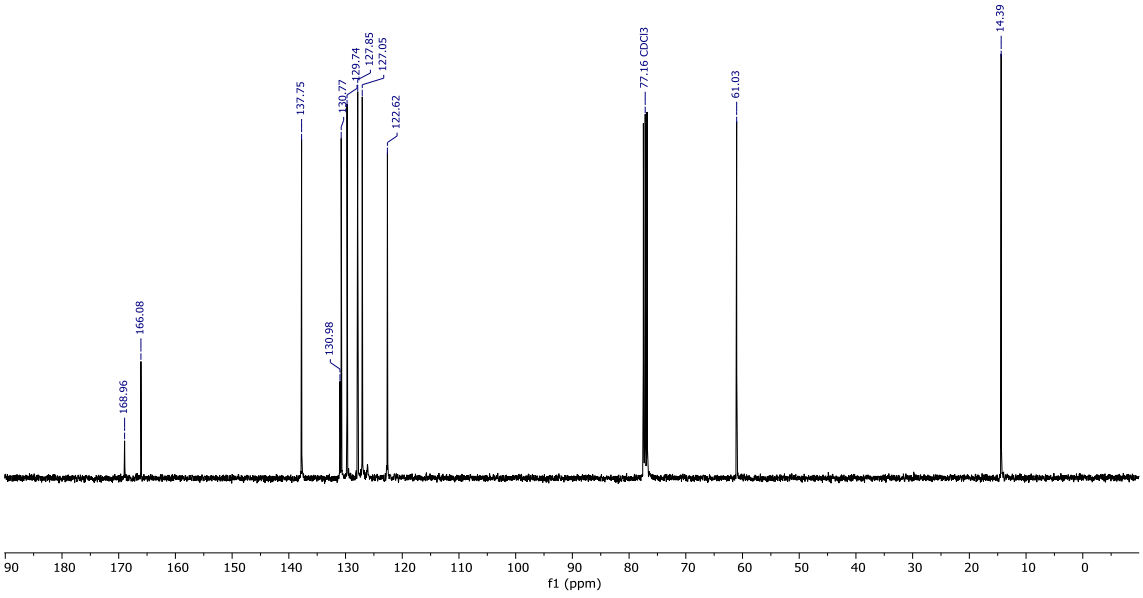
168.96
166.08
137.75
130.98
130.77
129.74
127.85
127.05
122.62
77.16 CDCl3
61.03
14.39
f1 (ppm)

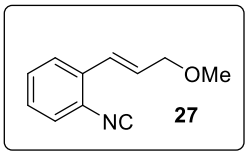
OMe
NC

27

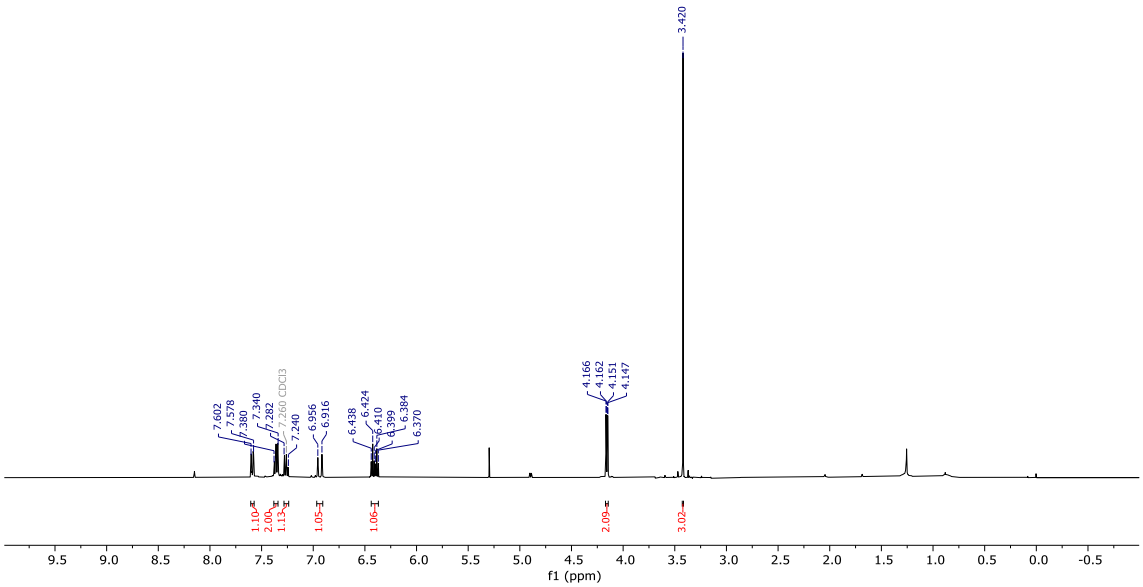
7.602
7.578
7.380
7.340
7.282
7.260 CDCl3
7.240
6.956
6.916
6.438
6.424
6.410
6.399
6.384
6.370
4.166
4.162
4.151
4.147
3.420
1.10
2.00
1.13
1.05
1.06
2.09
3.02
f1 (ppm)

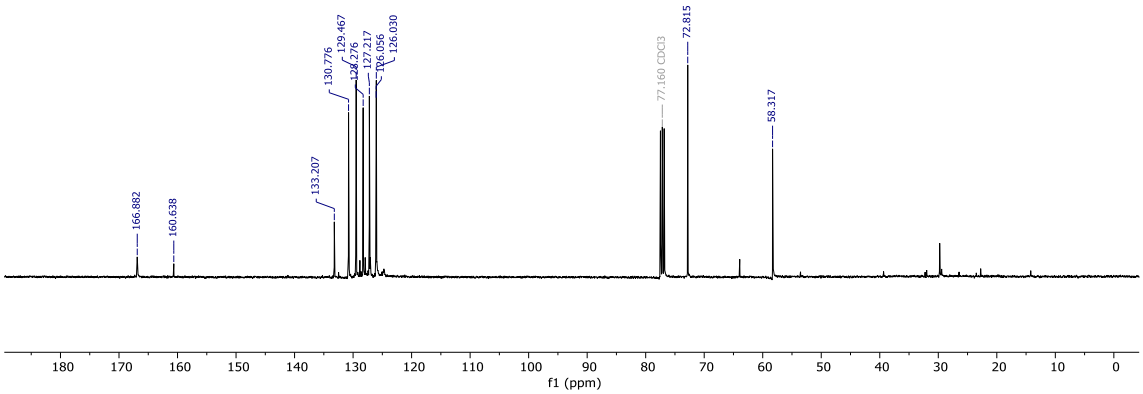
166.882
160.638
133.207
130.776
129.467
128.276
127.217
126.056
126.030
77.160 CDCl3
72.815
58.317
f1 (ppm)

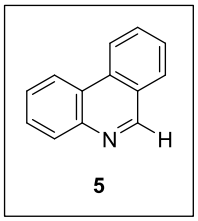
N
H

5

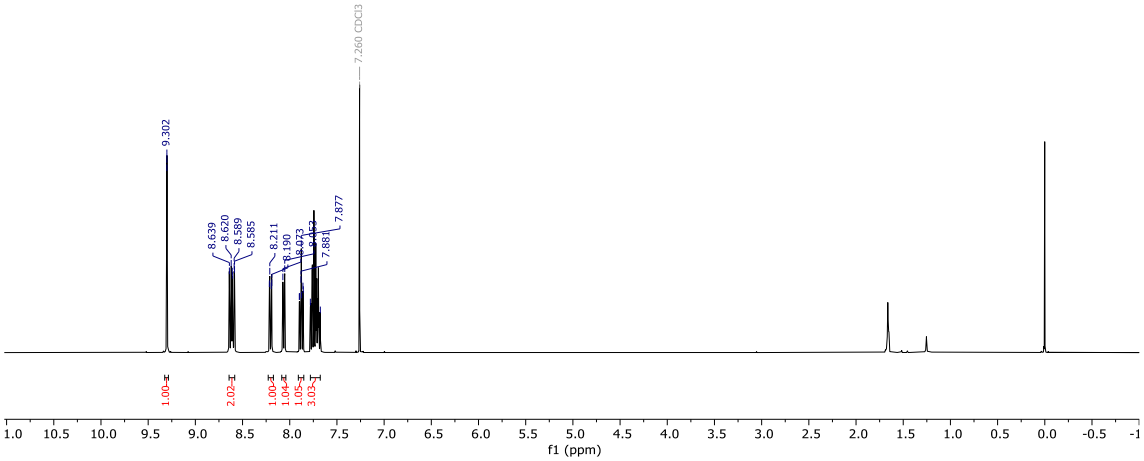
9.302
8.639
8.620
8.599
8.585
8.211
8.190
8.073
8.052
7.886
7.877
7.260 CDCl3
1.00
2.02
1.00
1.04
1.05
3.03
f1 (ppm)

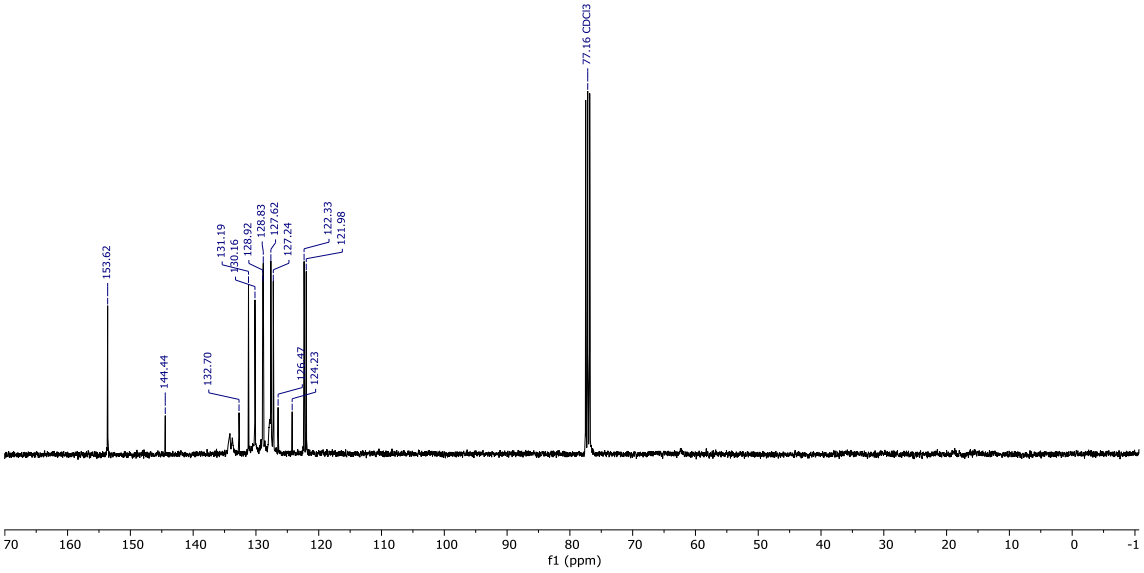
153.62
144.44
132.70
131.19
130.16
128.92
128.83
127.62
127.24
126.47
124.23
122.33
121.98
77.16 CDCl3
f1 (ppm)

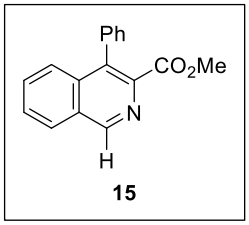
Ph
CO2Me
N
H

15

9.318
8.079
8.059
7.720
7.605
7.596
7.472
7.343
7.319
7.260 CDCl3
3.744
1.06
1.00
3.26
3.11
2.21
3.03
f1 (ppm)

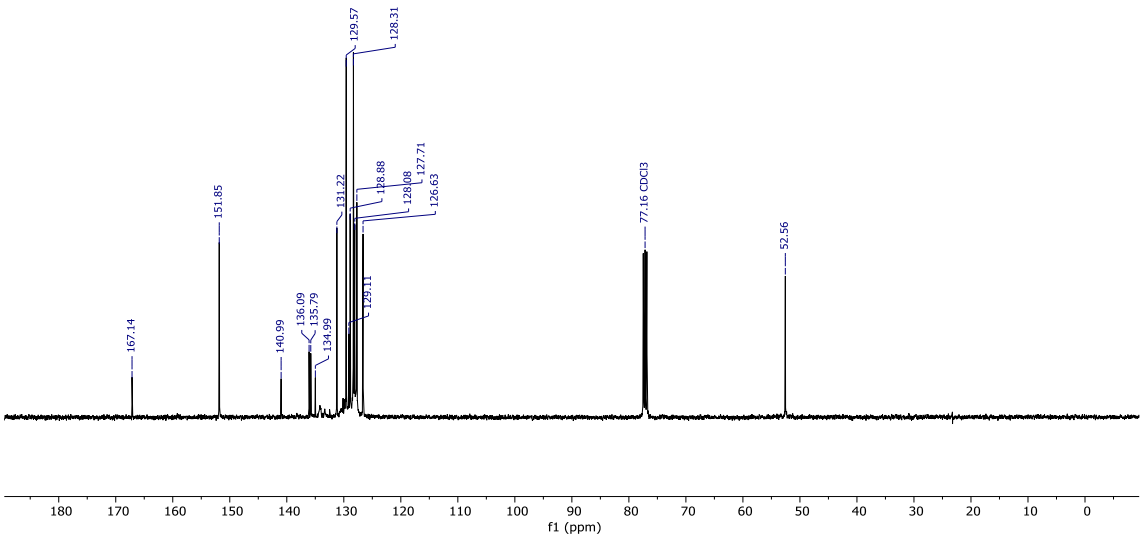
167.14
151.85
140.99
136.09
135.79
134.99
131.22
129.57
129.11
128.88
128.31
128.08
127.71
126.63
77.16 CDCl3
52.56
f1 (ppm)

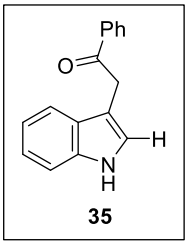
Ph
O
H
N
H

35

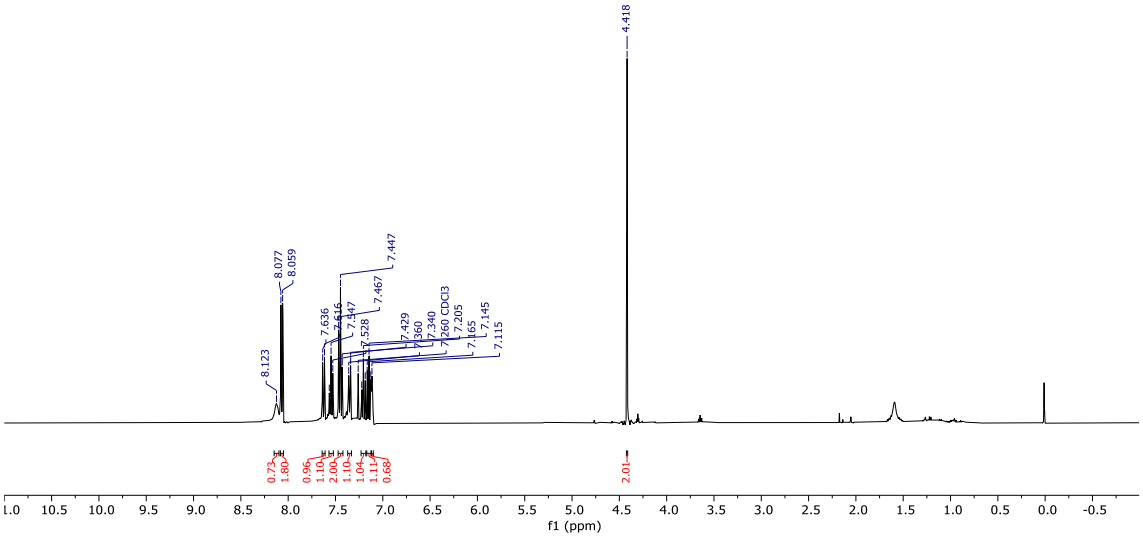
4.418
8.077
8.059
7.447
7.636
7.467
7.429
7.360
7.340
7.260 CDCl3
7.205
7.165
7.145
7.115
8.123
7.528
0.73
1.80
0.96
1.10
2.00
1.10
1.04
1.11
0.69
2.01
f1 (ppm)

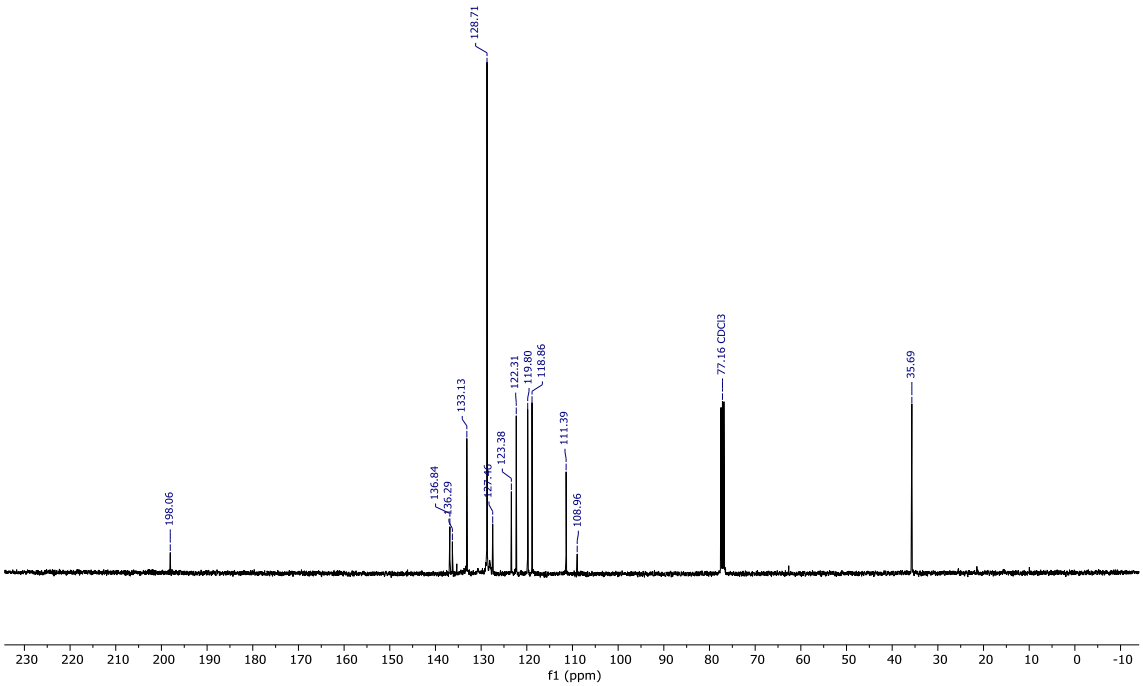
128.71
77.16 CDCl3
35.69
133.13
122.31
119.80
118.86
111.39
123.38
136.84
136.29
127.46
108.96
198.06
f1 (ppm)

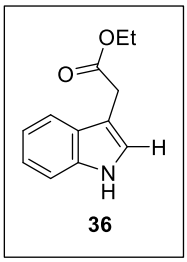
OEt
O
H
N
H

36

8.170
7.656
7.635
7.315
7.333
7.211
7.208
7.172
7.152
7.109
7.103
4.219
4.201
4.183
4.166
3.790
1.300
1.283
1.265
0.77
0.95
0.99
1.00
1.01
0.95
2.01
1.95
3.01
f1 (ppm)

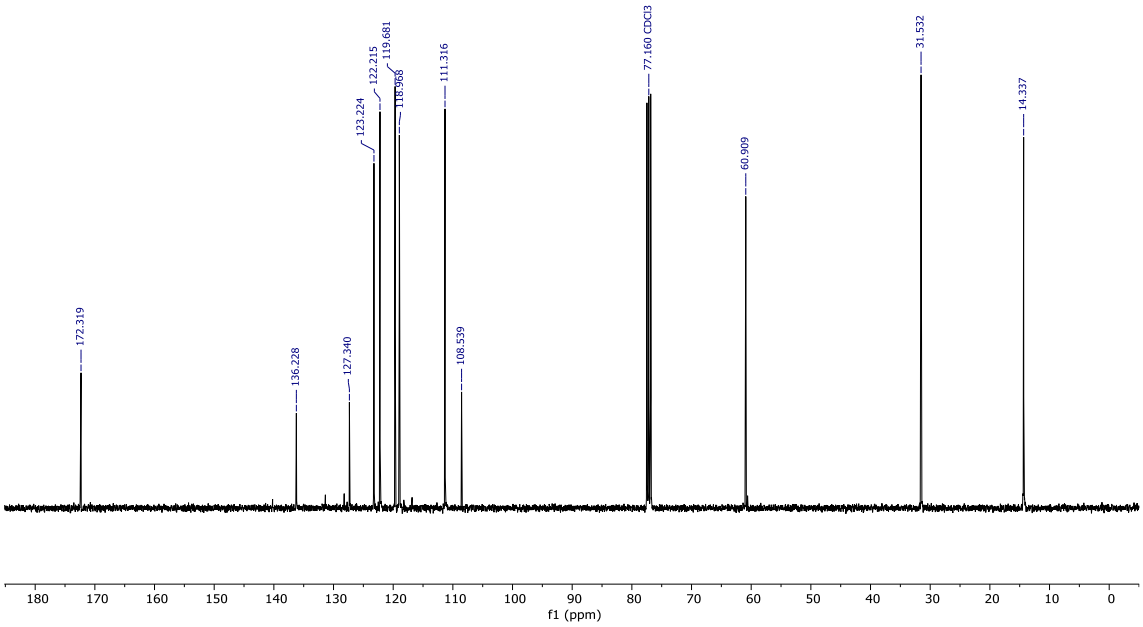
172.319
136.228
127.340
123.224
122.215
119.681
118.968
111.316
108.539
77.160 CDCl3
60.909
31.532
14.337
f1 (ppm)

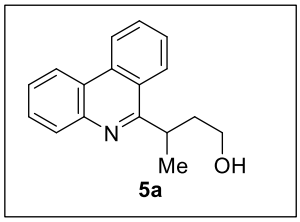
N
Me
OH

5a

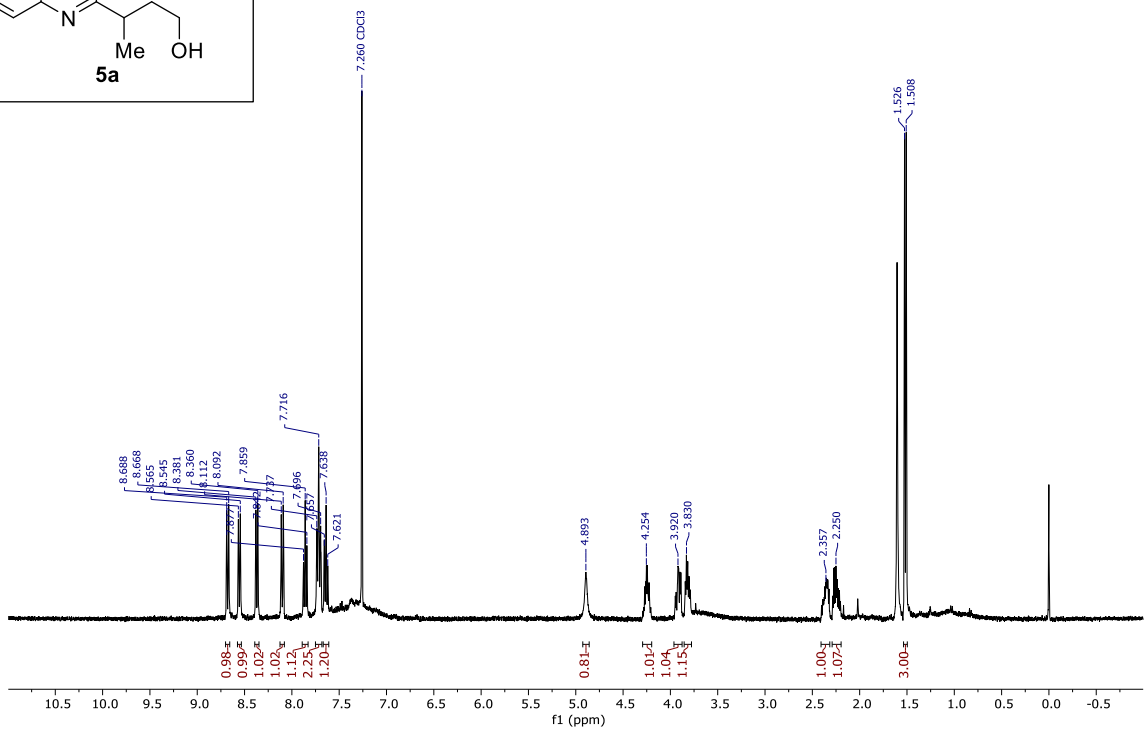
7.260 CDCl3
1.526
1.508
8.688
8.668
8.565
8.545
8.381
8.360
8.112
8.092
7.859
7.716
7.737
7.696
7.638
7.621
4.893
4.254
3.920
3.830
2.357
2.250
0.98
0.99
1.02
1.02
1.12
2.25
1.20
0.81
1.01
1.04
1.15
1.00
1.07
3.00
f1 (ppm)

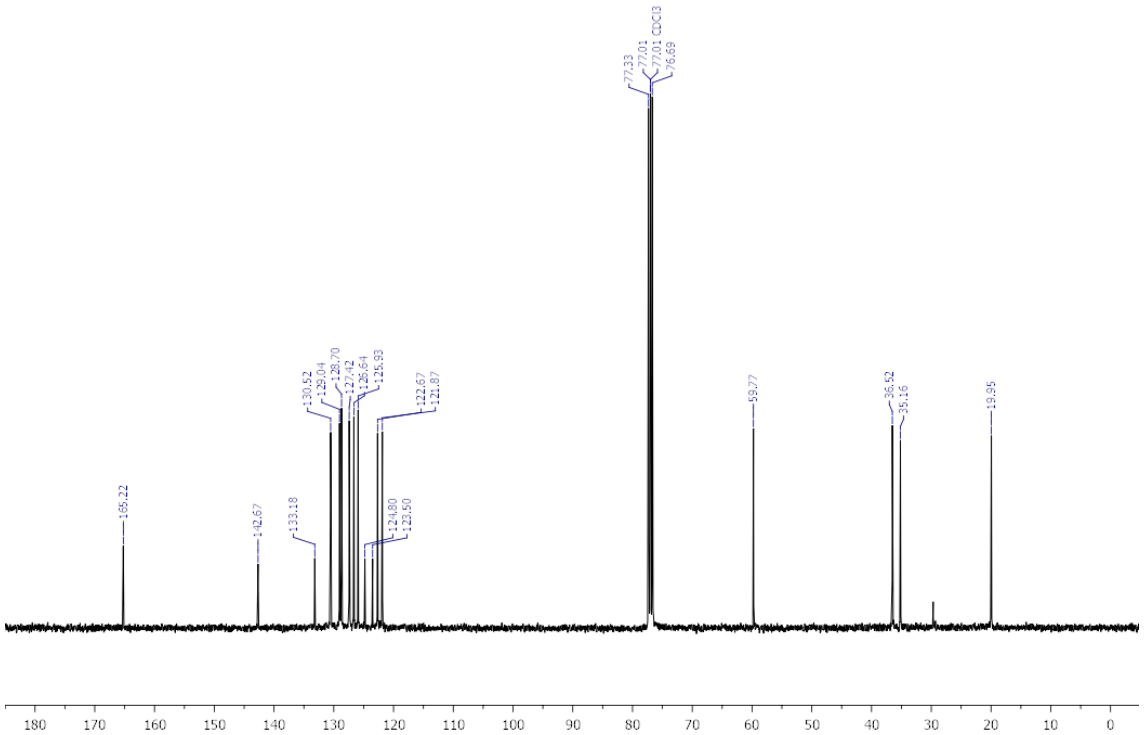
77.33
77.01
77.01 CDCl3
76.69
130.52
129.04
128.70
127.42
126.64
125.93
122.67
121.87
166.22
142.67
133.18
124.80
123.50
59.77
36.52
35.16
19.95

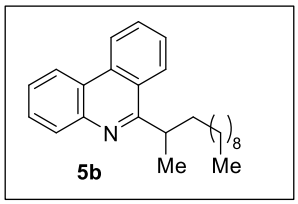
N
Me
Me
8
5b

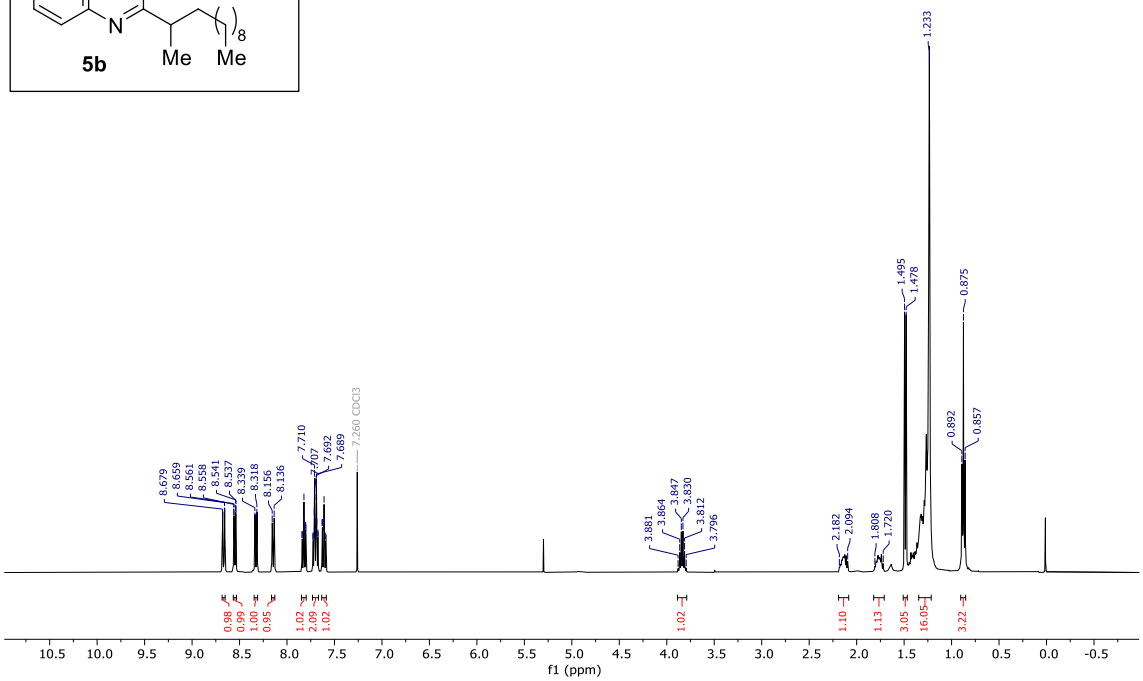
8.679
8.659
8.561
8.558
8.541
8.537
8.339
8.318
8.156
8.136
7.710
7.707
7.692
7.689
7.260 CDCl3
3.881
3.864
3.847
3.830
3.812
3.796
2.182
2.094
1.808
1.720
1.495
1.478
1.233
0.892
0.875
0.857
0.98
0.99
1.00
0.95
1.02
2.09
1.02
1.02
1.10
1.13
3.05
16.05
3.22
f1 (ppm)

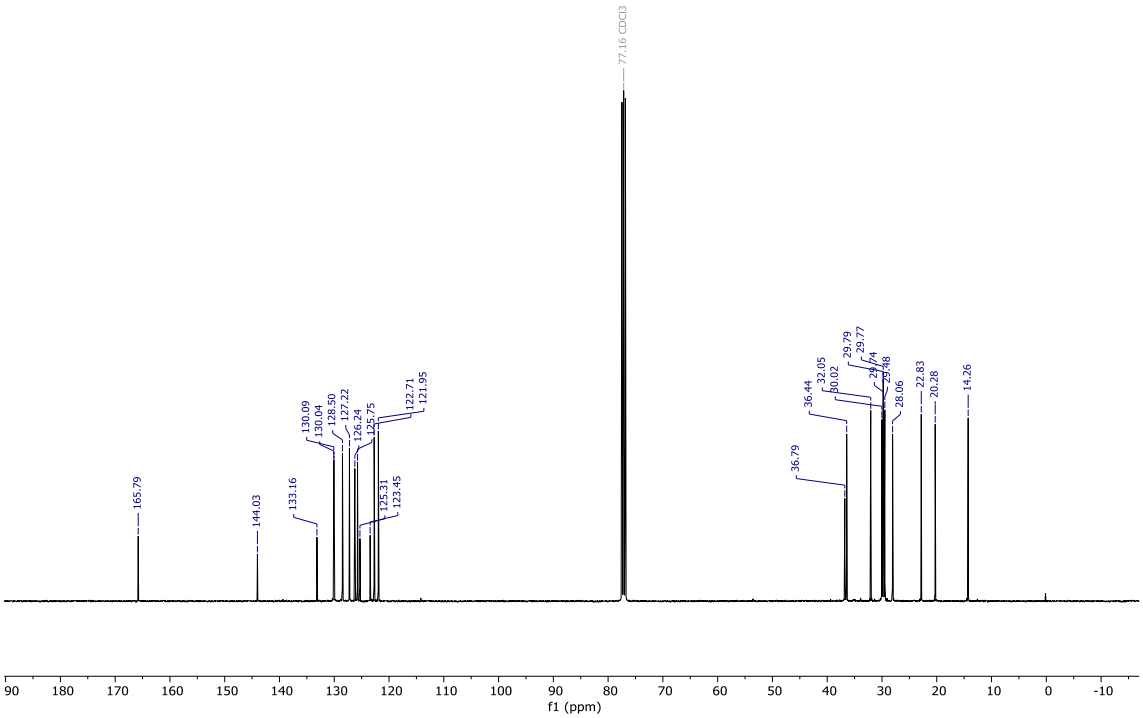
77.16 CDCl3
165.79
144.03
133.16
130.09
130.04
128.50
127.22
126.24
125.75
125.31
123.45
122.71
121.95
36.79
36.44
32.05
30.02
29.79
29.77
29.74
29.48
28.06
22.83
20.28
14.26
f1 (ppm)

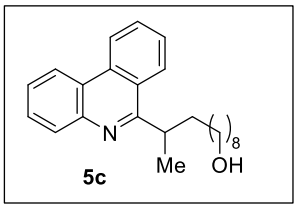
N
Me
OH
8
5c

8.668
8.667
8.556
8.535
8.333
8.312
8.169
8.149
7.820
7.607
7.604
7.260 CDCl3
3.881
3.864
3.847
3.829
3.812
3.609
3.626
3.592
2.185
2.098
1.812
1.724
1.564
1.541
1.498
1.481
1.255
1.356
1.02
1.00
0.98
0.93
1.01
1.13
2.03
0.99
1.04
2.00
1.06
1.18
2.29
2.99
12.07
f1 (ppm)

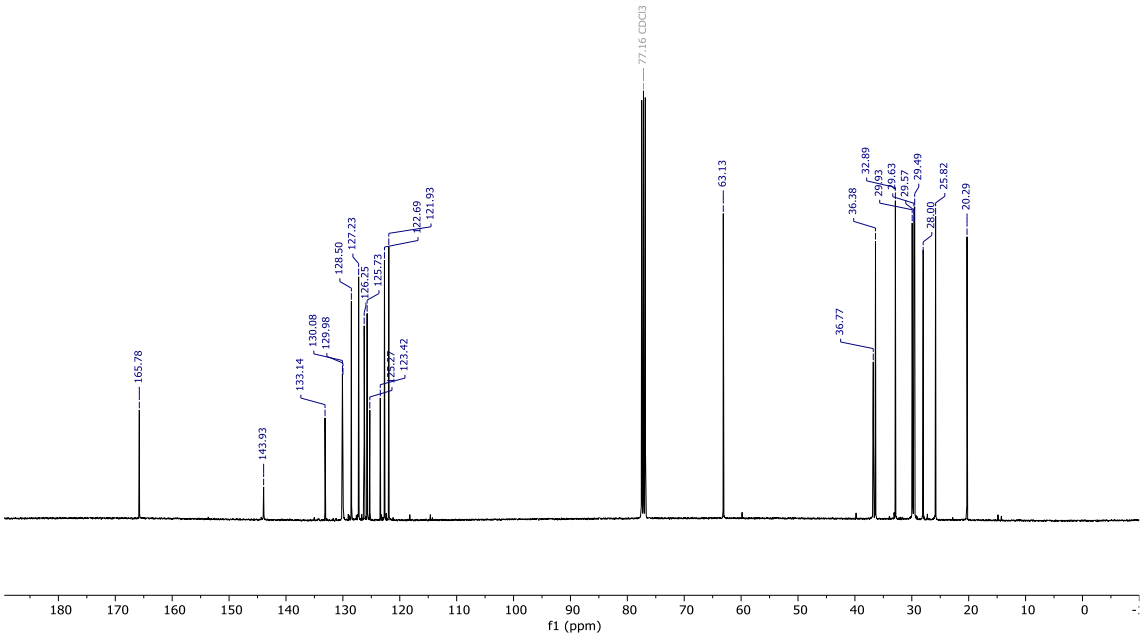
165.78
143.93
133.14
130.08
129.98
128.50
127.23
126.25
125.73
125.27
123.42
122.69
121.93
77.16 CDCl3
63.13
36.77
36.38
32.89
29.93
29.63
29.57
29.49
28.00
25.82
20.29
f1 (ppm)

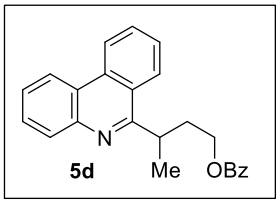
N
5d
Me
OBz

f1 (ppm)

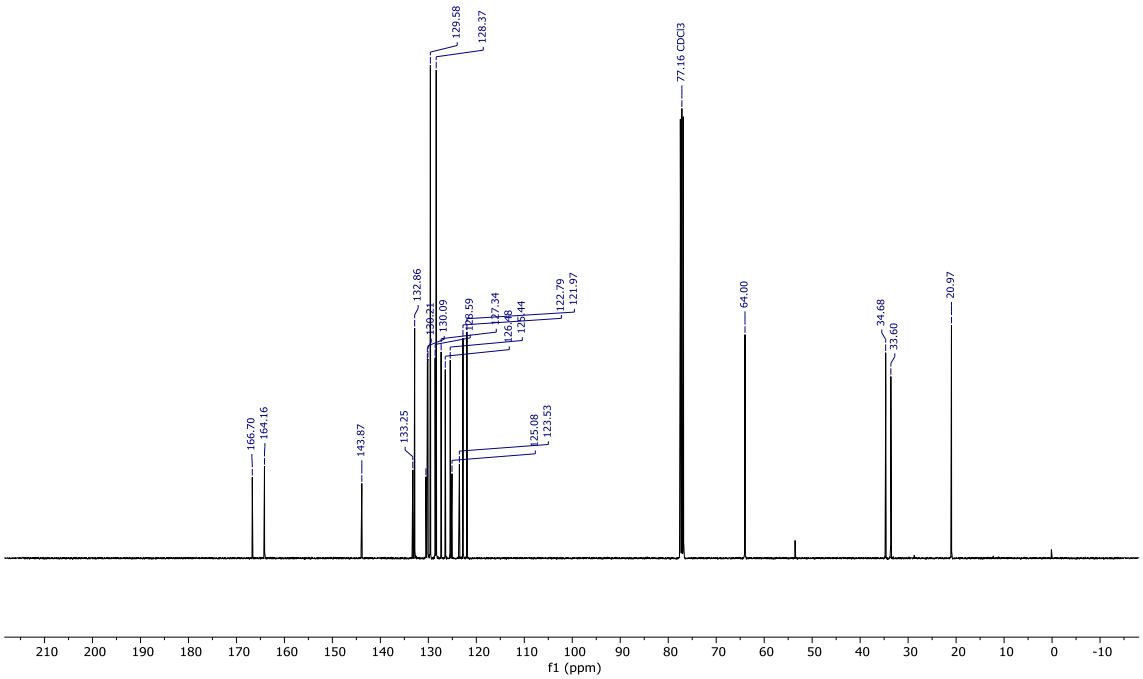
77.16 CDCl3
f1 (ppm)

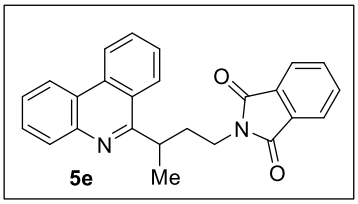
O
N
N
O
5e
Me

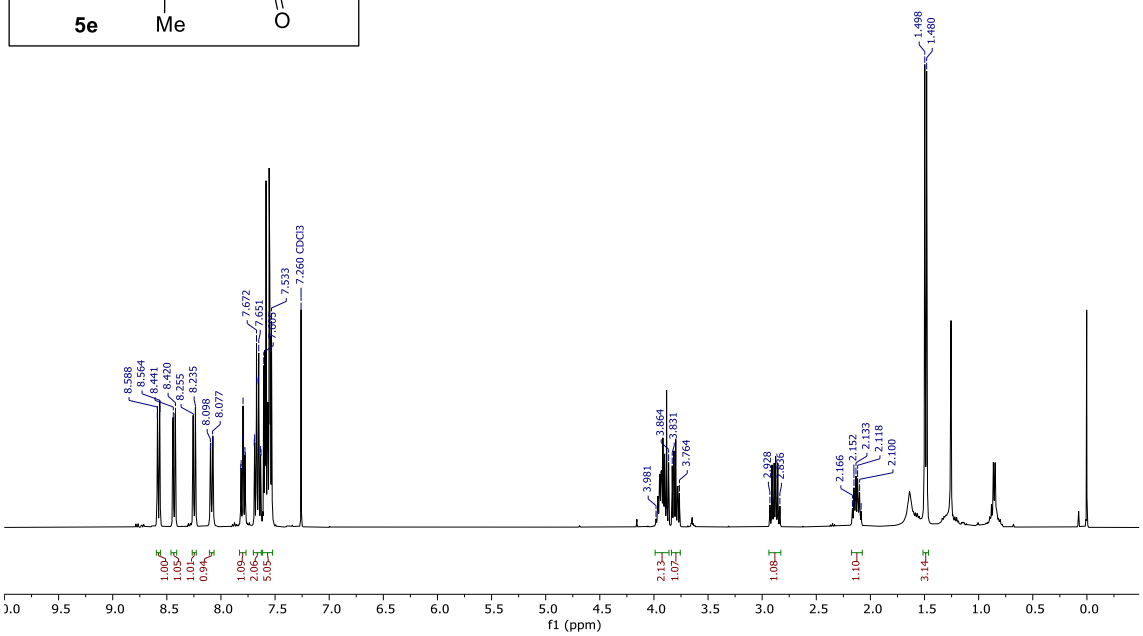
8.598
8.564
8.441
8.420
8.255
8.235
8.098
8.077
7.672
7.651
7.533
7.260 CDCl3
3.981
3.864
3.831
3.764
2.928
2.166
2.152
2.133
2.118
2.100
1.498
1.480
1.00
1.05
1.01
0.94
1.09
2.06
5.05
2.13
1.07
1.08
1.10
3.14
f1 (ppm)

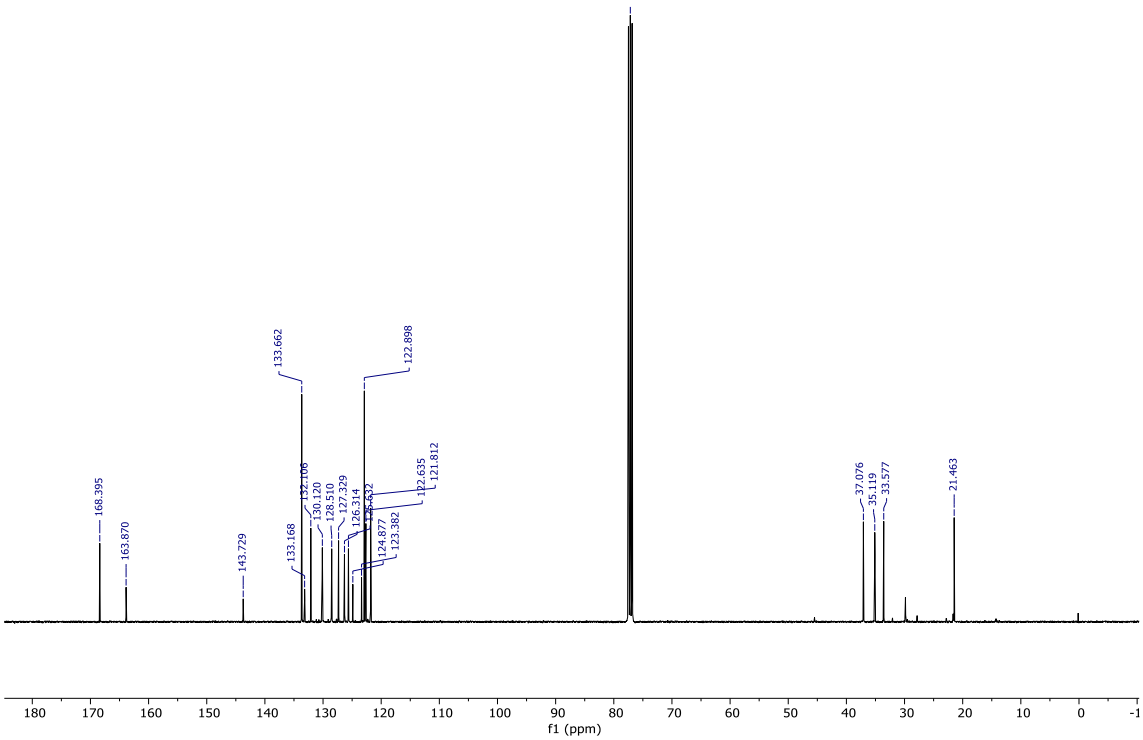
168.395
163.870
143.729
133.662
133.168
132.106
130.120
128.510
127.329
126.314
125.852
124.877
123.382
122.898
122.635
121.812
37.076
35.119
33.577
21.463
f1 (ppm)

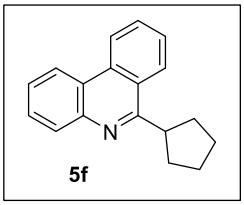
N

5f

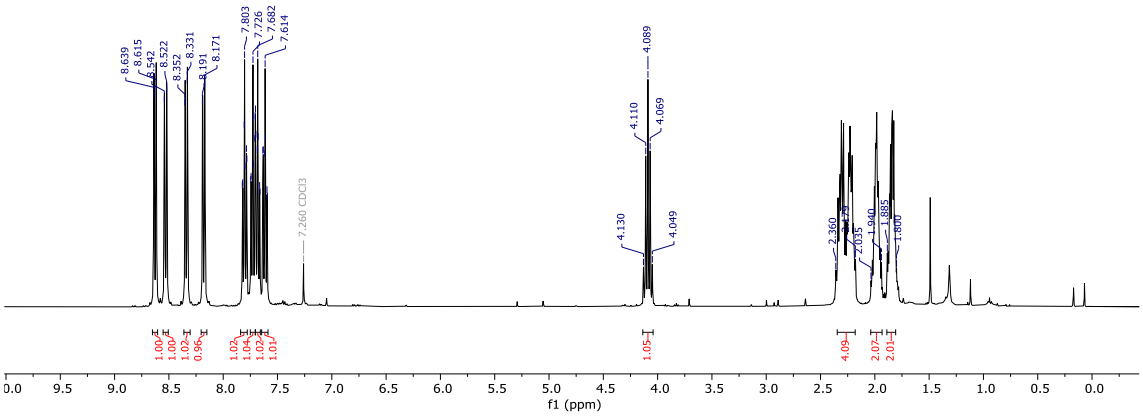
8.639
8.615
8.542
8.522
8.352
8.331
8.191
8.171
7.803
7.726
7.682
7.614
7.260 CDCl3
4.130
4.110
4.089
4.069
4.049
2.360
2.035
1.940
1.885
1.800
1.00
1.00
1.00
1.02
0.96
1.02
1.04
1.02
1.01
1.05
4.09
2.07
2.01
f1 (ppm)

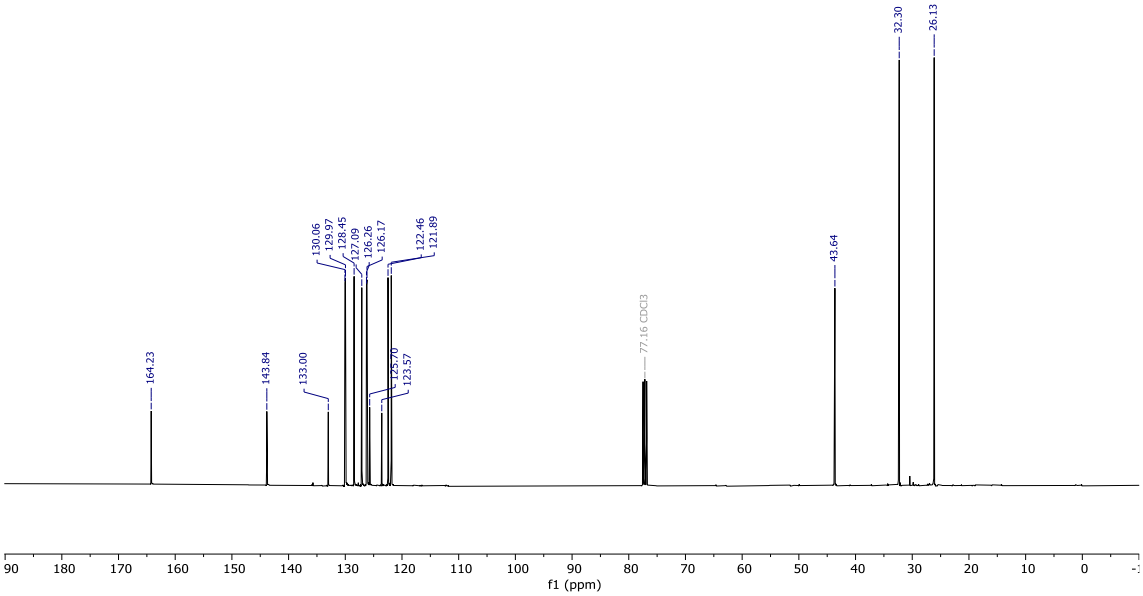
164.23
143.84
133.00
130.06
129.97
128.45
127.09
126.26
126.17
125.70
123.57
122.46
121.89
77.16 CDCl3
43.64
32.30
26.13
f1 (ppm)

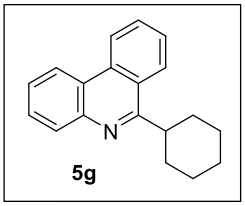
N

5g

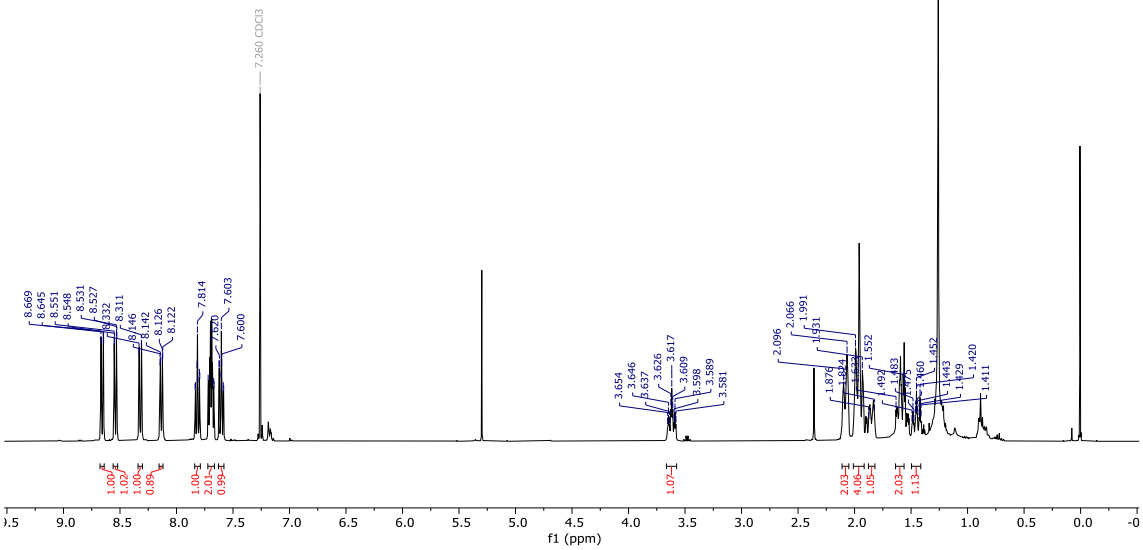
7.260 CDCl3
8.669
8.645
8.551
8.548
8.531
8.527
8.332
8.311
8.146
8.142
8.126
8.122
7.814
7.620
7.603
7.600
3.654
3.646
3.637
3.626
3.617
3.609
3.598
3.589
3.581
2.096
2.066
1.991
1.931
1.878
1.552
1.483
1.452
1.443
1.429
1.420
1.411
1.00
1.02
1.00
0.89
1.00
2.01
0.99
1.07
2.03
4.06
1.05
2.03
1.13
f1 (ppm)

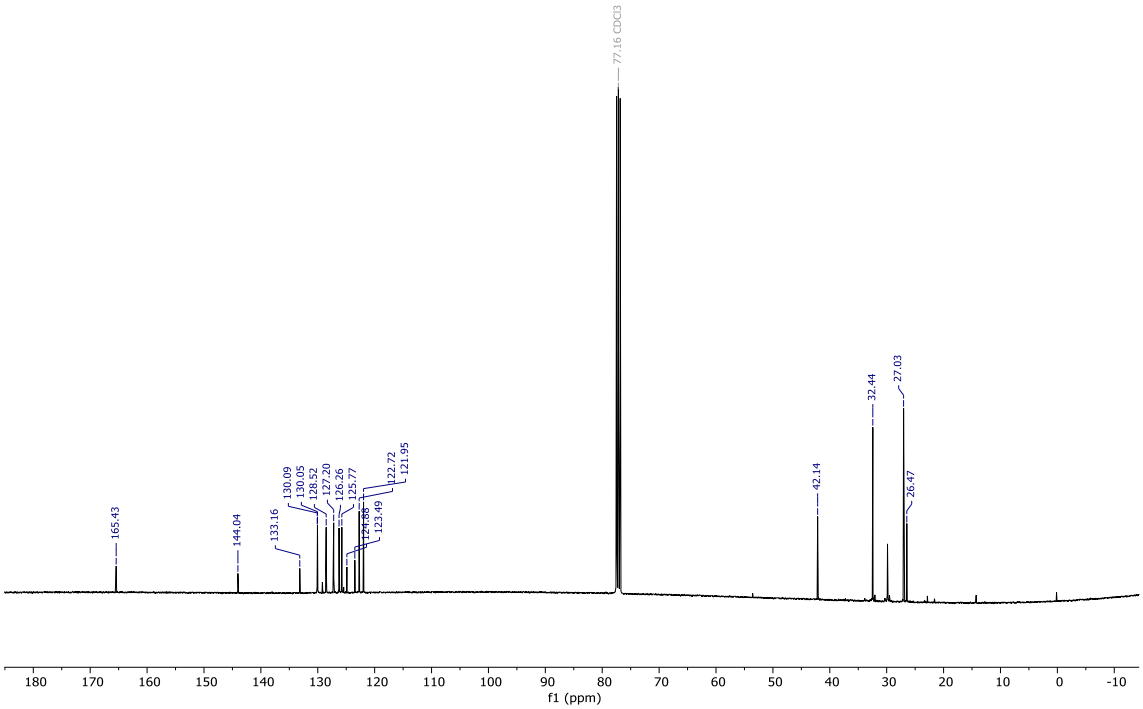
77.16 CDCl3
165.43
144.04
133.16
130.09
130.05
128.52
127.20
126.26
125.77
123.49
122.72
121.95
42.14
32.44
27.03
26.47
f1 (ppm)

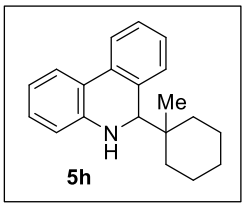
Me
N
H

5h

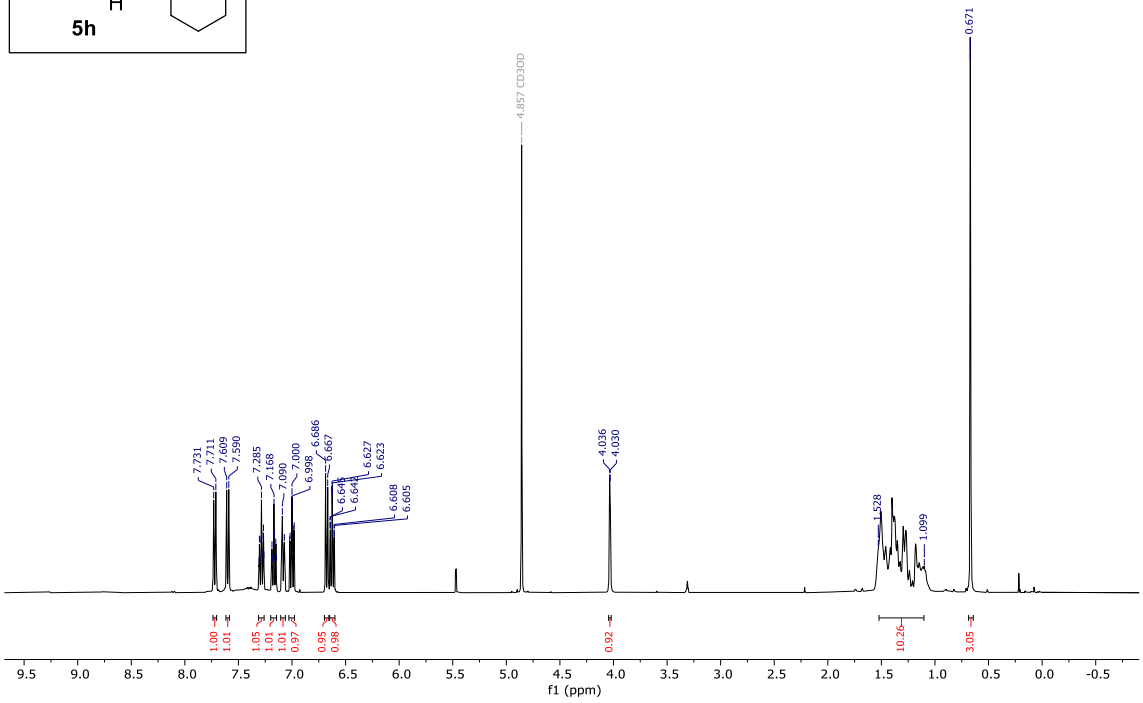
4.857 CD3OD
0.671
7.731
7.711
7.609
7.590
7.285
7.168
7.090
7.000
6.998
6.686
6.667
6.627
6.623
6.608
6.605
4.036
4.030
1.528
1.099
1.00
1.01
1.05
1.01
1.01
0.97
0.95
0.98
0.92
10.26
3.05
f1 (ppm)

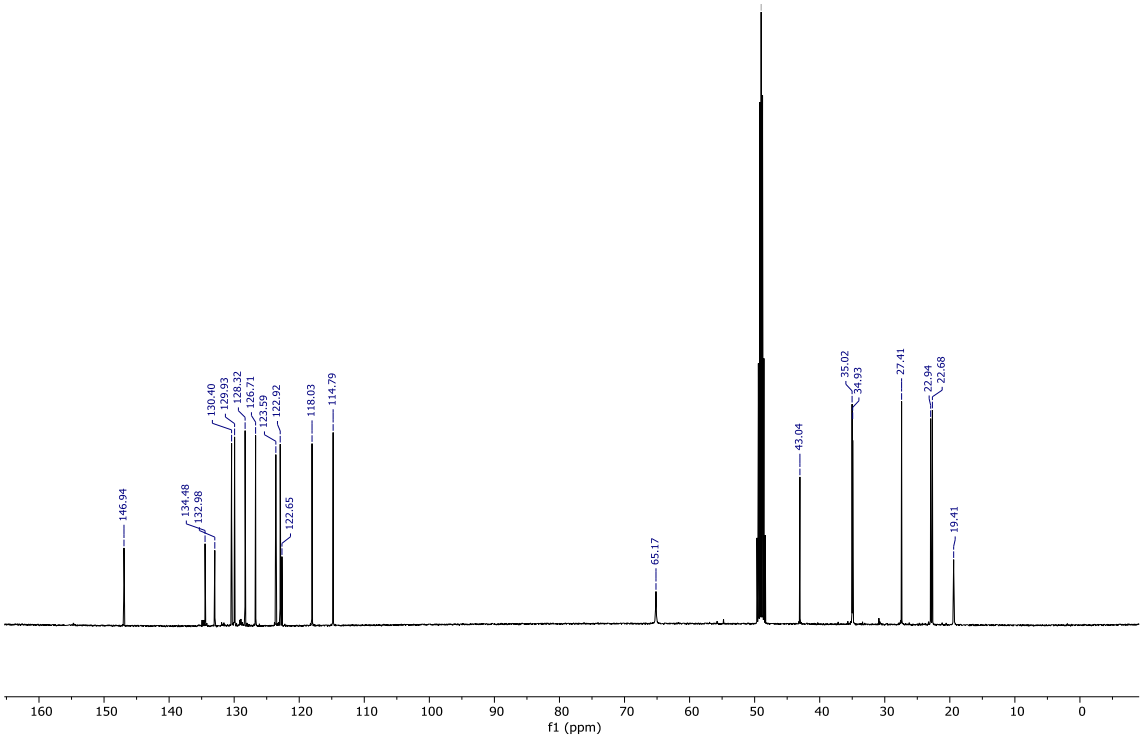
146.94
134.48
132.96
130.40
129.93
128.32
126.71
123.59
122.92
122.65
118.03
114.79
65.17
43.04
35.02
34.93
27.41
22.94
22.68
19.41
f1 (ppm)

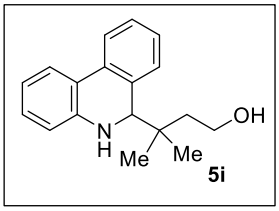
OH
N
H
Me
Me

5i

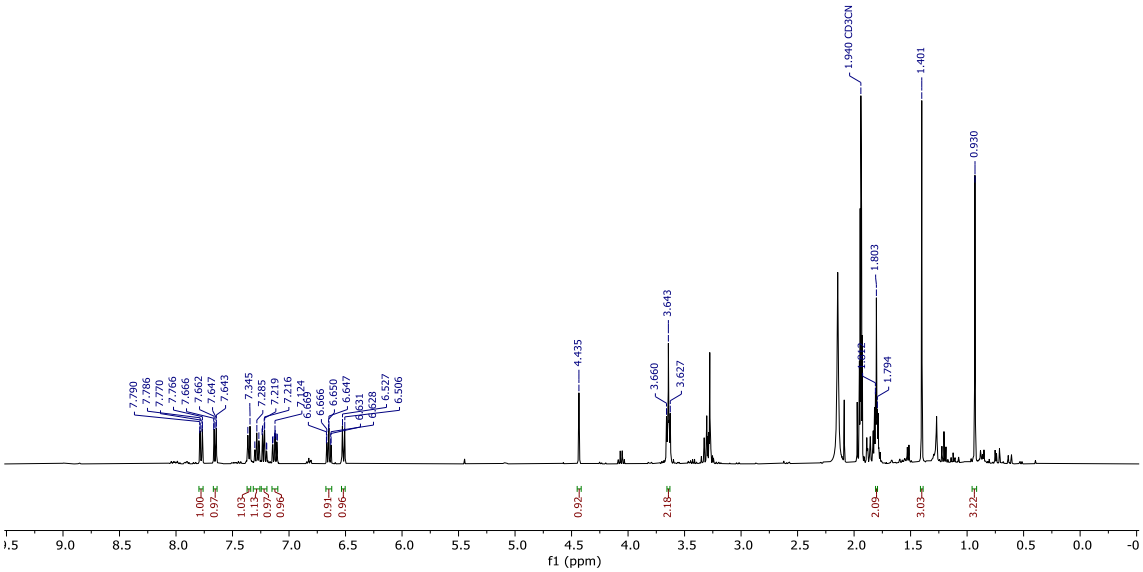
1.940 CD3CN
1.401
0.930
1.803
1.794
3.643
3.660
3.627
4.435
7.790
7.786
7.770
7.766
7.666
7.662
7.647
7.643
7.345
7.285
7.219
7.216
6.666
6.650
6.647
6.631
6.628
6.527
6.506
1.00
0.97
1.03
1.13
0.92
0.96
0.91
0.96
0.92
2.18
2.09
3.03
3.22
f1 (ppm)

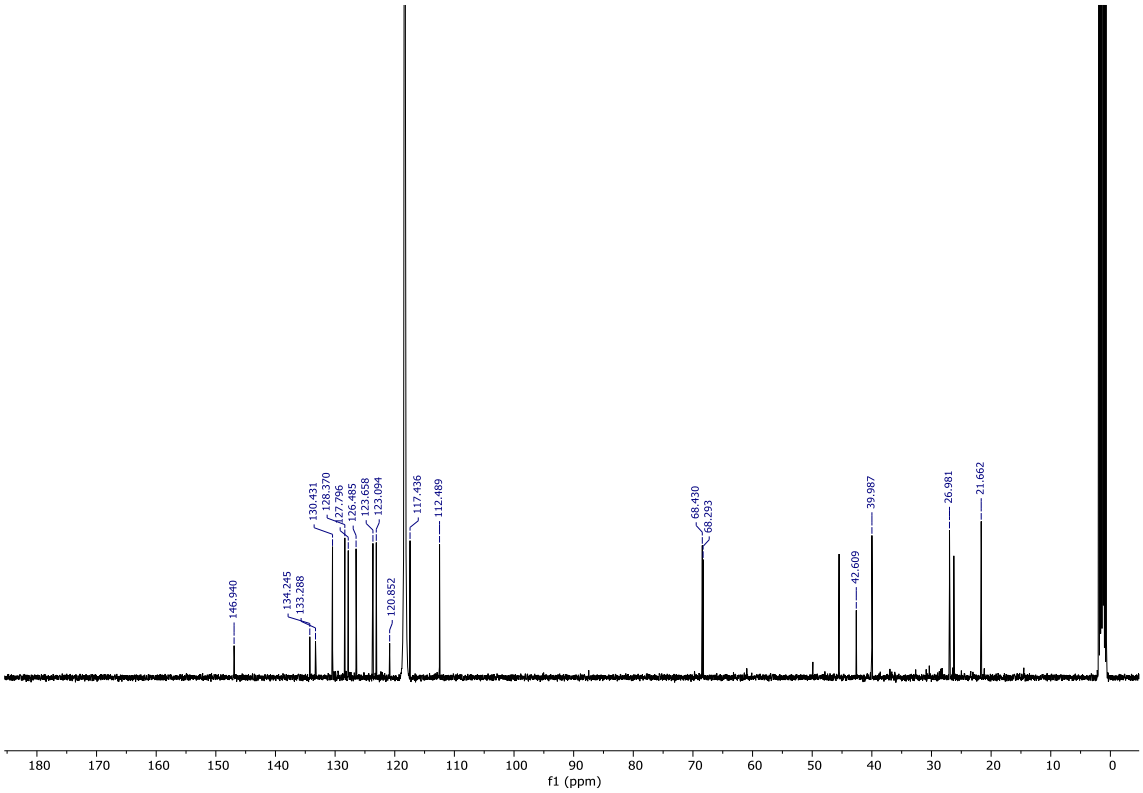
146.940
134.245
133.288
130.431
128.370
127.796
126.485
123.658
123.094
120.852
117.436
112.489
68.430
68.293
42.609
39.987
26.981
21.662
f1 (ppm)

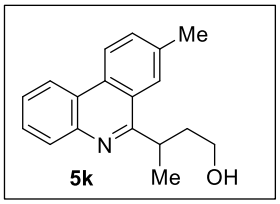
Me
N
Me
OH

5k

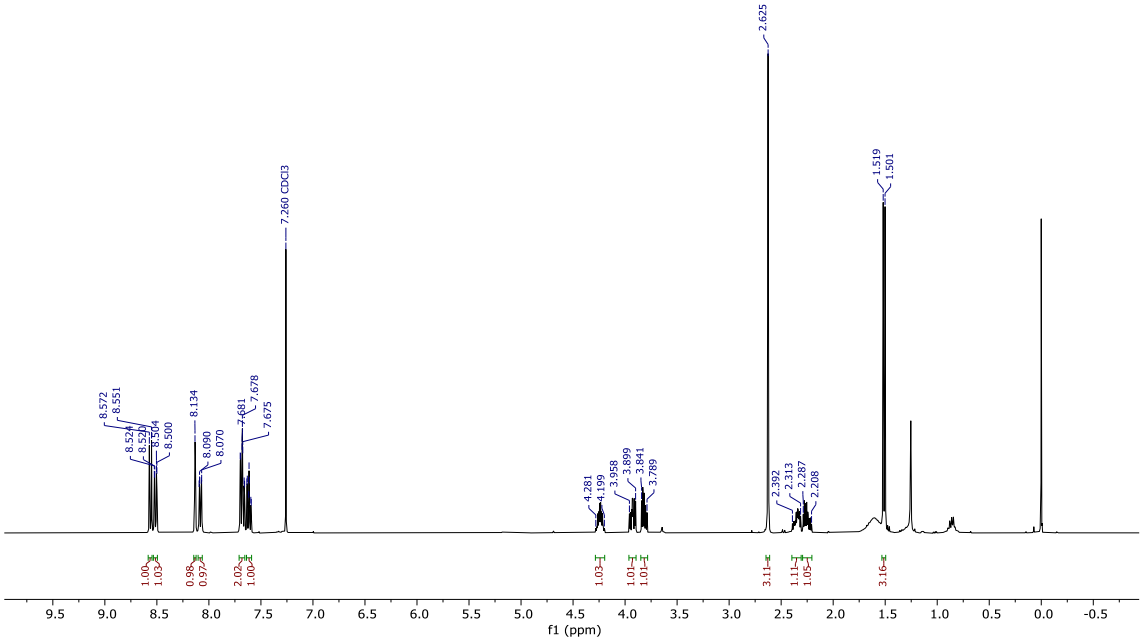
2.625
1.519
1.501
7.260 CDCl3
8.572
8.551
8.134
7.681
7.678
7.675
8.090
8.070
4.281
4.199
3.958
3.899
3.841
3.789
2.392
2.313
2.287
2.208
f1 (ppm)

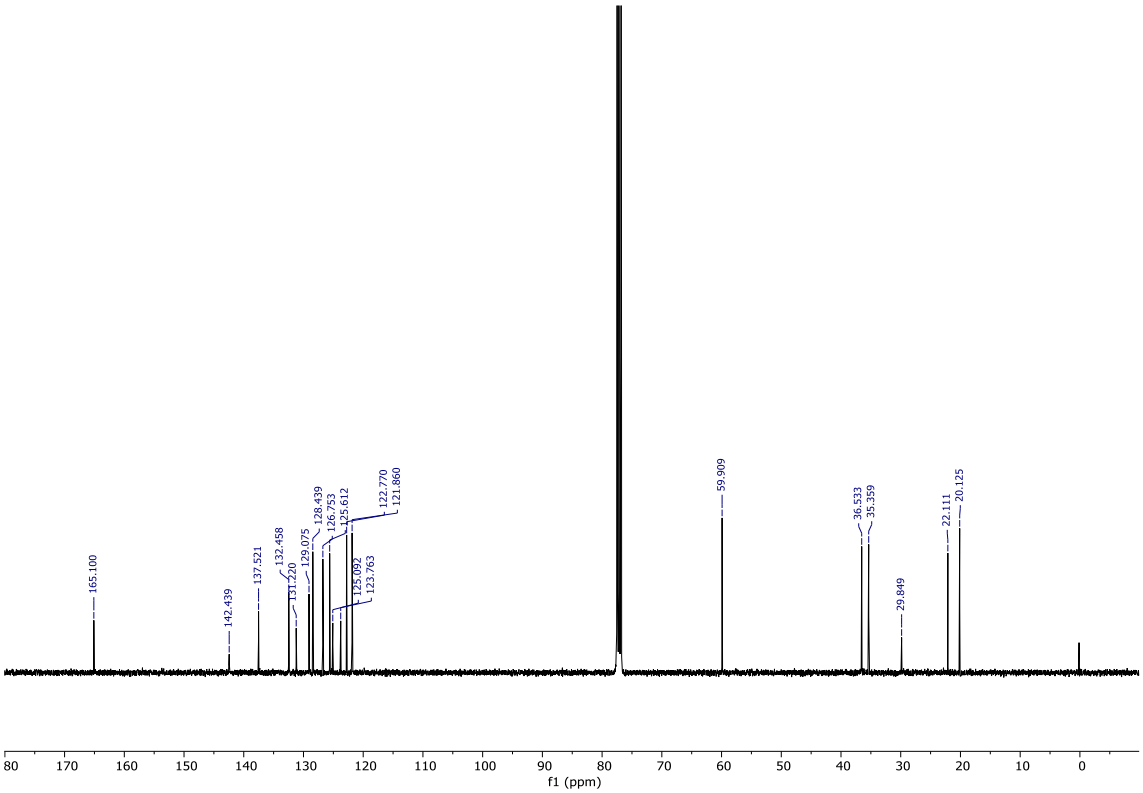
165.100
142.439
137.521
132.458
131.220
129.075
128.439
126.753
125.612
125.092
123.763
122.770
121.860
59.909
36.533
35.359
29.849
22.111
20.125
f1 (ppm)

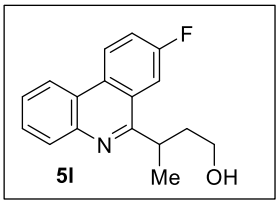
F
N
Me
OH

5l

1.513
1.496
7.260 CDCl3
8.682
8.668
8.659
8.645
8.500
8.497
8.480
8.476
8.114
8.096
8.094
7.707
7.691
7.642
7.621
4.127
4.044
3.917
3.858
3.836
3.782
2.414
2.335
2.248
2.168
1.03
1.05
1.00
0.92
0.97
1.02
0.95
0.96
0.94
0.94
0.98
0.98
3.05
f1 (ppm)

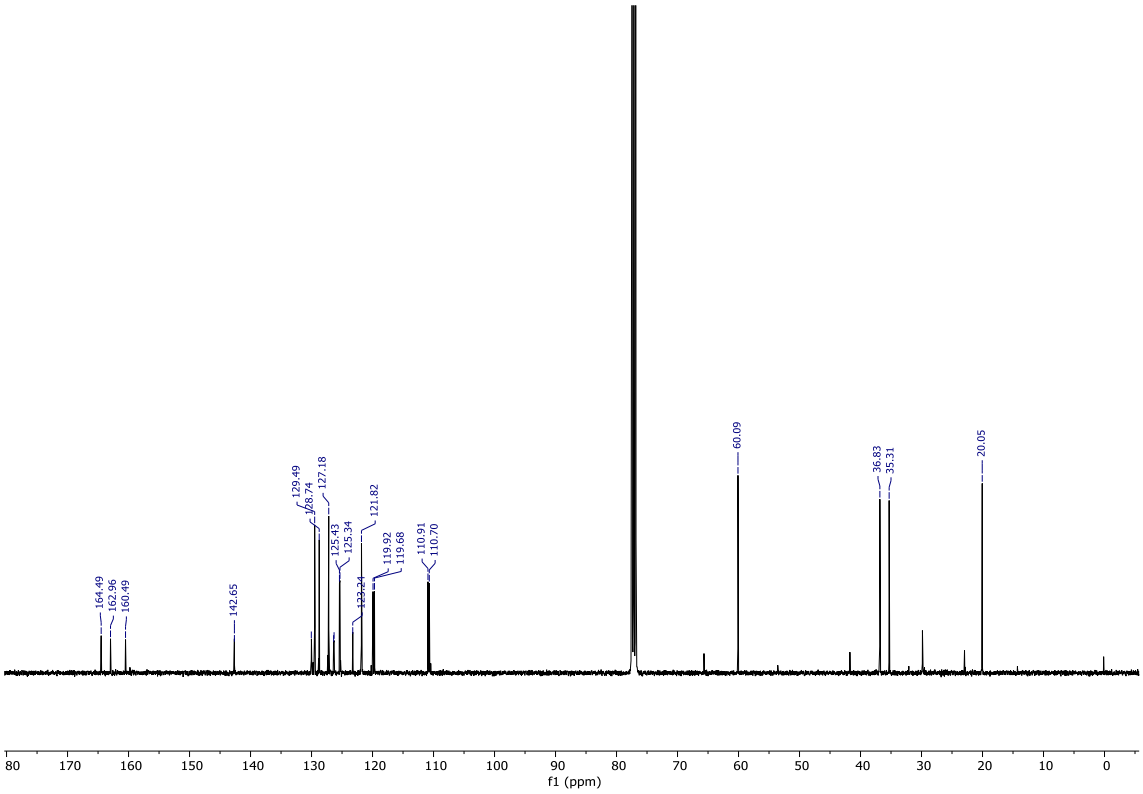
164.49
162.96
160.49
142.65
129.49
128.74
127.18
125.43
125.34
123.24
121.82
119.92
119.68
110.91
110.70
60.09
36.83
35.31
20.05
f1 (ppm)

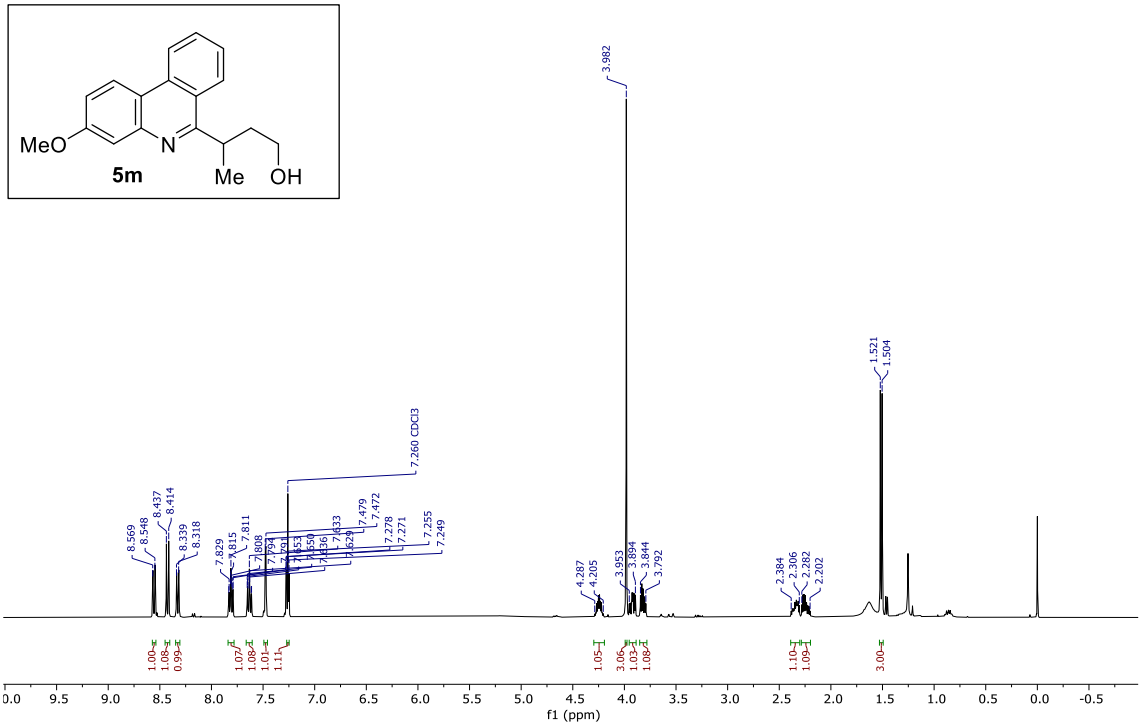
MeO
N
5m
Me
OH
3.982
7.260 CDCl3
1.521
1.504
8.569
8.548
8.437
8.414
8.339
8.318
7.829
7.815
7.811
7.808
7.794
7.791
7.479
7.472
7.278
7.271
7.255
7.249
4.287
4.205
3.953
3.894
3.844
3.792
2.384
2.306
2.282
2.202
1.00
1.08
0.99
1.07
1.04
1.01
1.11
1.05
3.06
1.03
1.08
1.10
1.09
3.00
f1 (ppm)

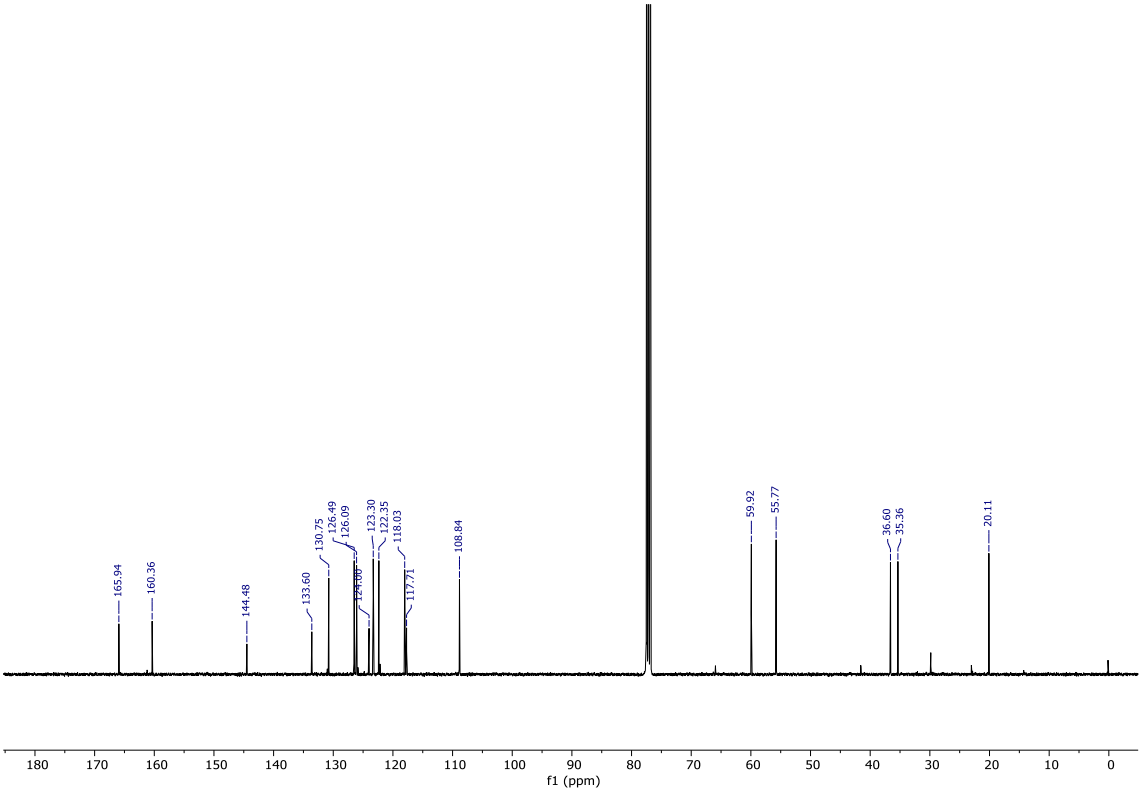
165.94
160.36
144.48
133.60
130.75
126.49
126.09
123.30
122.35
118.03
117.71
108.84
59.92
55.77
36.60
35.36
20.11
f1 (ppm)

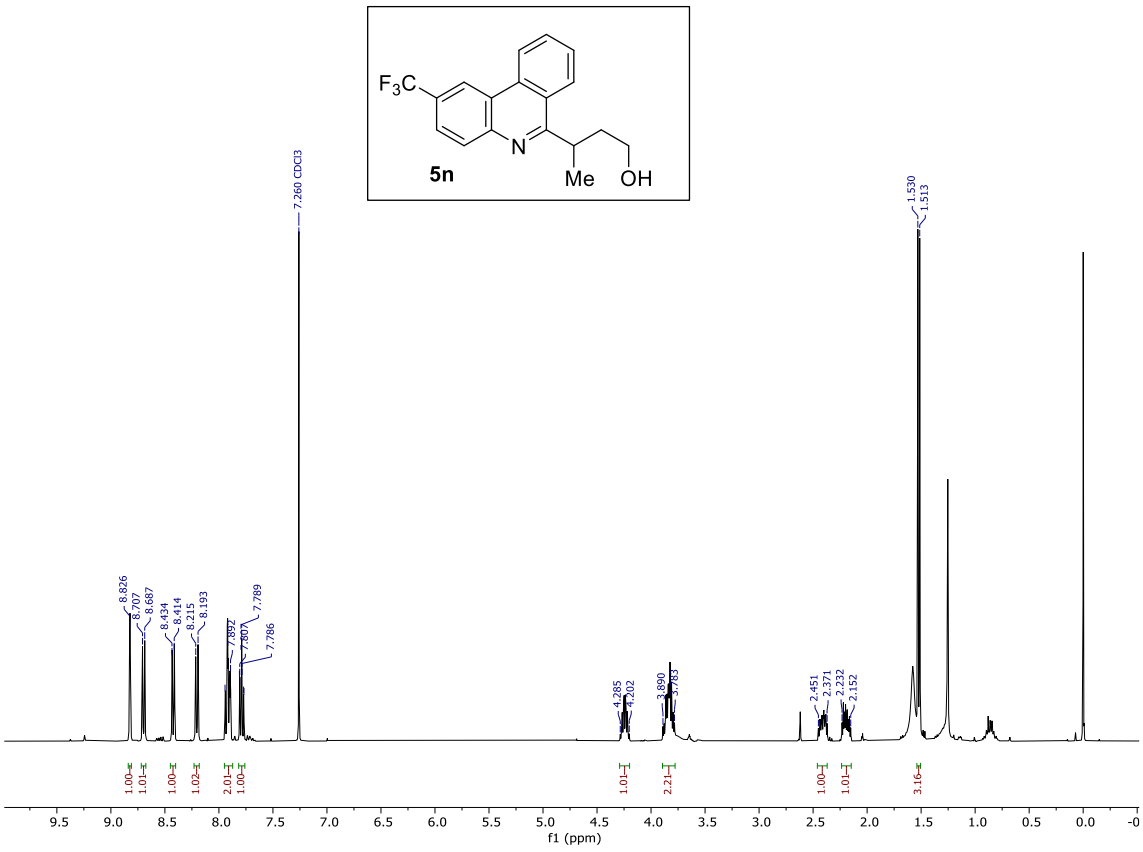
F3C
N
Me
OH
5n
7.260 CDCl3
1.530
1.513
8.826
8.707
8.687
8.434
8.414
8.215
8.193
7.892
7.807
7.789
7.786
4.285
4.202
3.890
3.785
2.451
2.371
2.232
2.152
1.00
1.01
1.00
1.02
2.01
1.00
1.01
2.21
1.00
1.01
3.16
f1 (ppm)

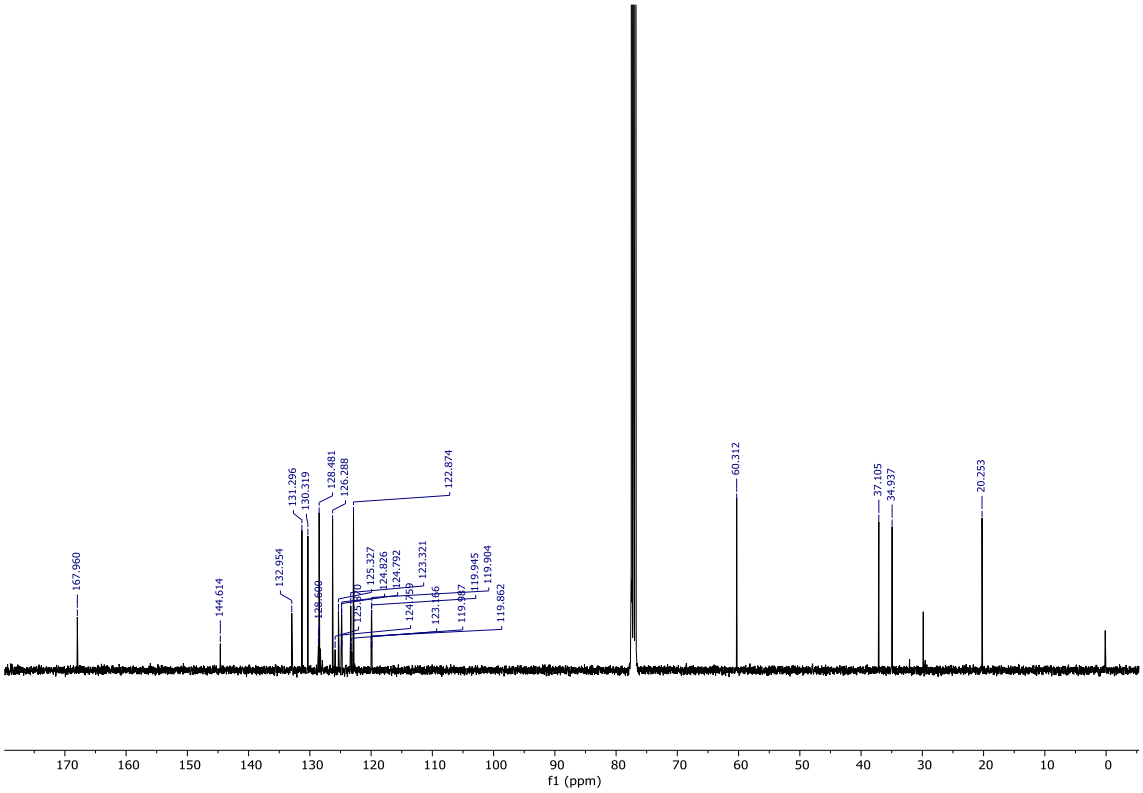
167.960
144.614
132.954
131.296
130.319
128.481
126.288
122.874
125.327
124.826
124.792
123.321
119.945
119.904
119.862
60.312
37.105
34.937
20.253
f1 (ppm)

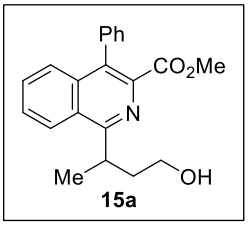
Ph
CO2Me
N
Me
OH

15a

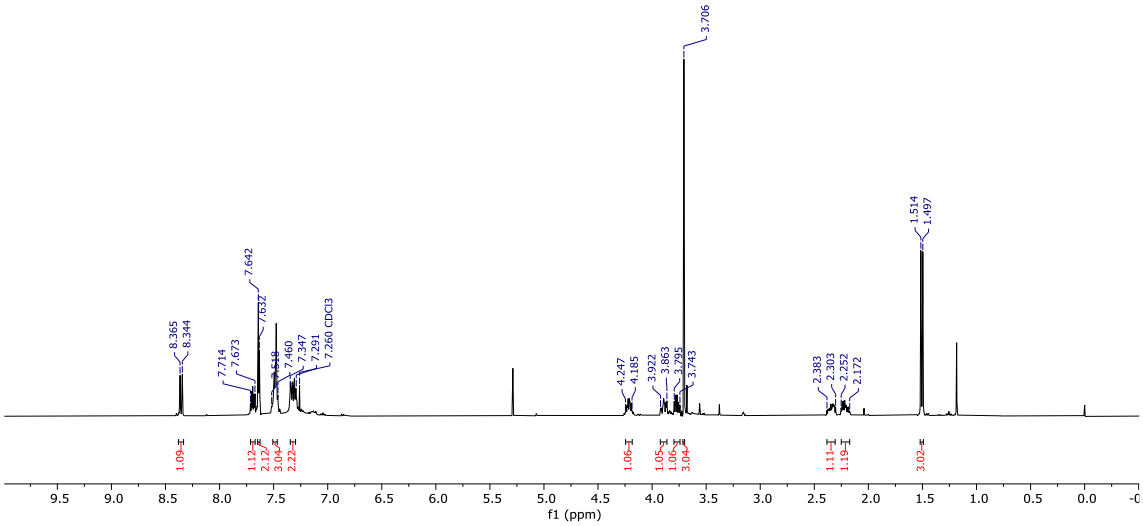
8.365
8.344
7.714
7.673
7.642
7.632
7.518
7.460
7.347
7.291
7.260 CDCl3
4.247
4.185
3.922
3.863
3.795
3.743
3.706
2.383
2.303
2.252
2.172
1.514
1.497
1.09
1.12
2.12
3.04
2.22
1.06
1.05
1.06
3.04
1.11
1.19
3.02
f1 (ppm)

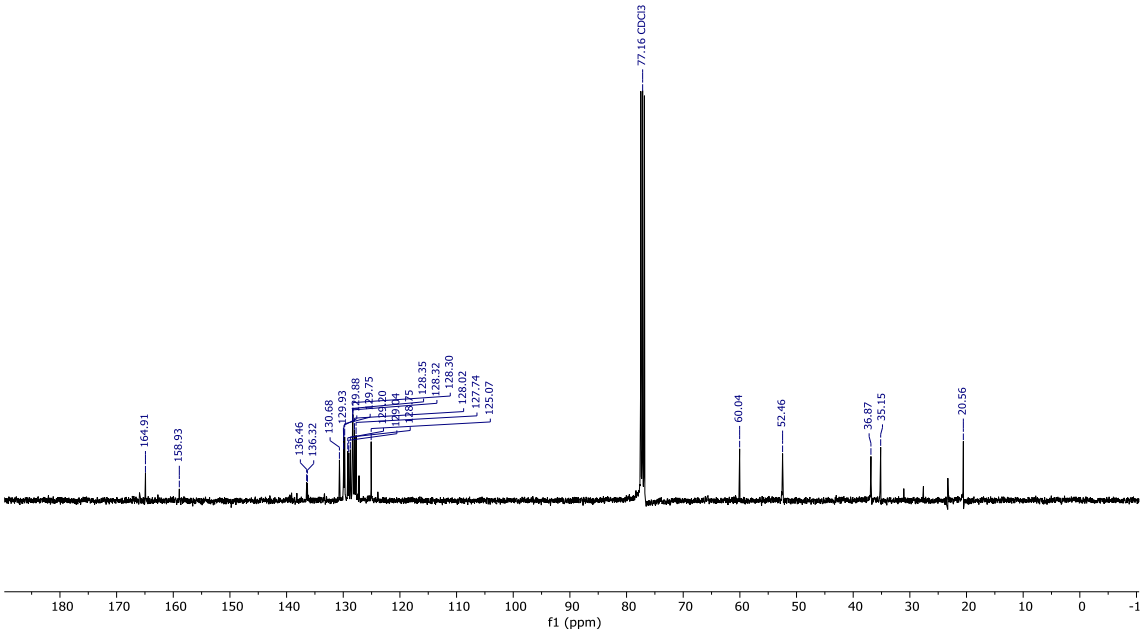
164.91
158.93
136.46
136.32
130.68
129.93
129.88
129.75
129.10
128.44
128.35
128.32
128.30
128.02
127.74
125.07
77.16 CDCl3
60.04
52.46
36.87
35.15
20.56
f1 (ppm)

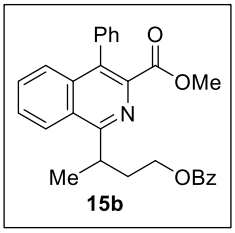
Ph
O
OMe
N
Me
OBz

15b

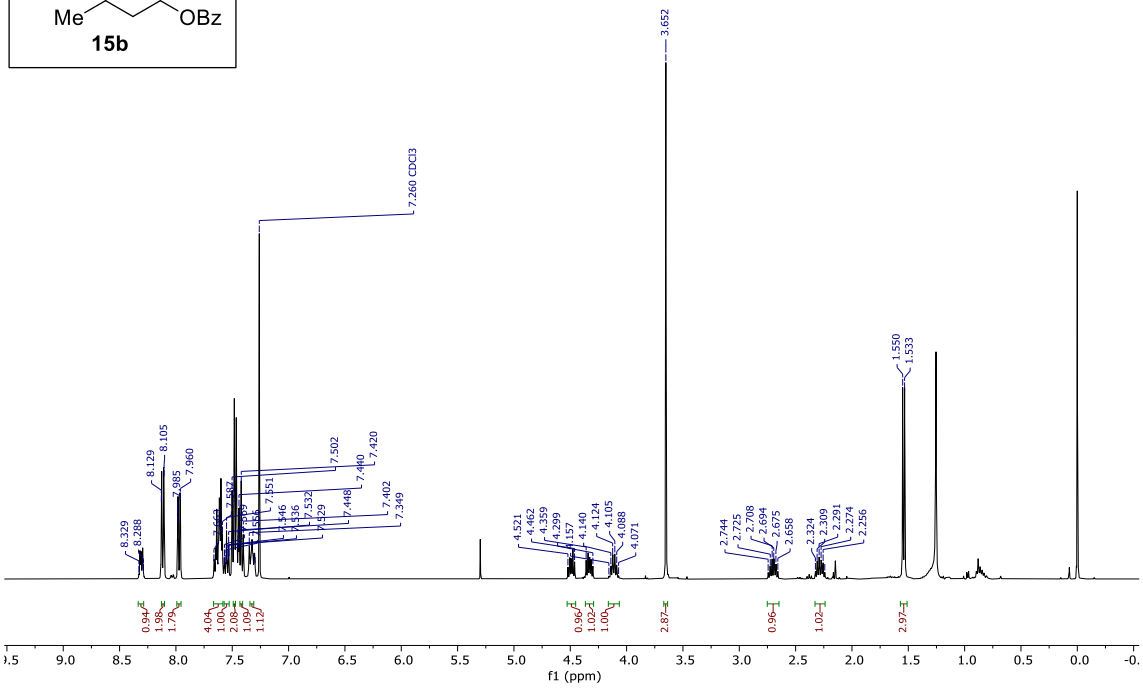
7.260 CDCl3
3.652
1.550
1.533
8.329
8.288
8.129
8.105
7.960
2.985
7.502
7.440
7.420
7.402
7.349
7.448
7.151
4.521
4.462
4.359
4.299
4.157
4.140
4.124
4.105
4.088
4.071
2.744
2.725
2.708
2.694
2.675
2.658
2.324
2.309
2.291
2.274
2.256
f1 (ppm)

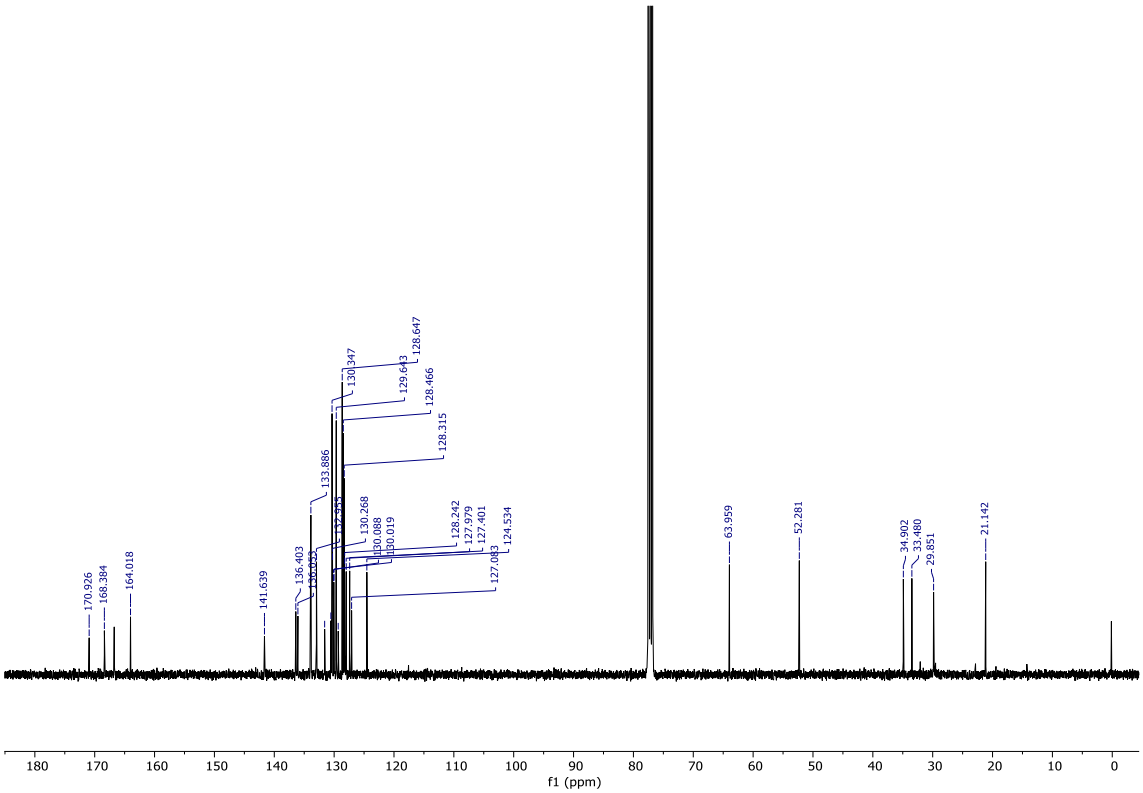
170.926
168.384
164.018
141.639
136.403
133.886
130.347
129.643
128.647
128.466
128.315
130.268
128.242
127.979
127.401
124.534
127.083
63.959
52.281
34.902
33.480
29.851
21.142
f1 (ppm)

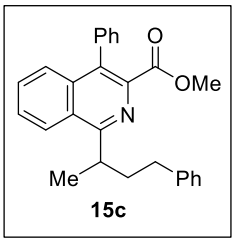
Ph
O
OMe
N
Me
Ph

15c

3.675
7.260 CDCl3
7.197
7.249
7.159
1.517
1.500
2.698
2.679
2.718
2.550
2.460
2.159
2.052
f1 (ppm)

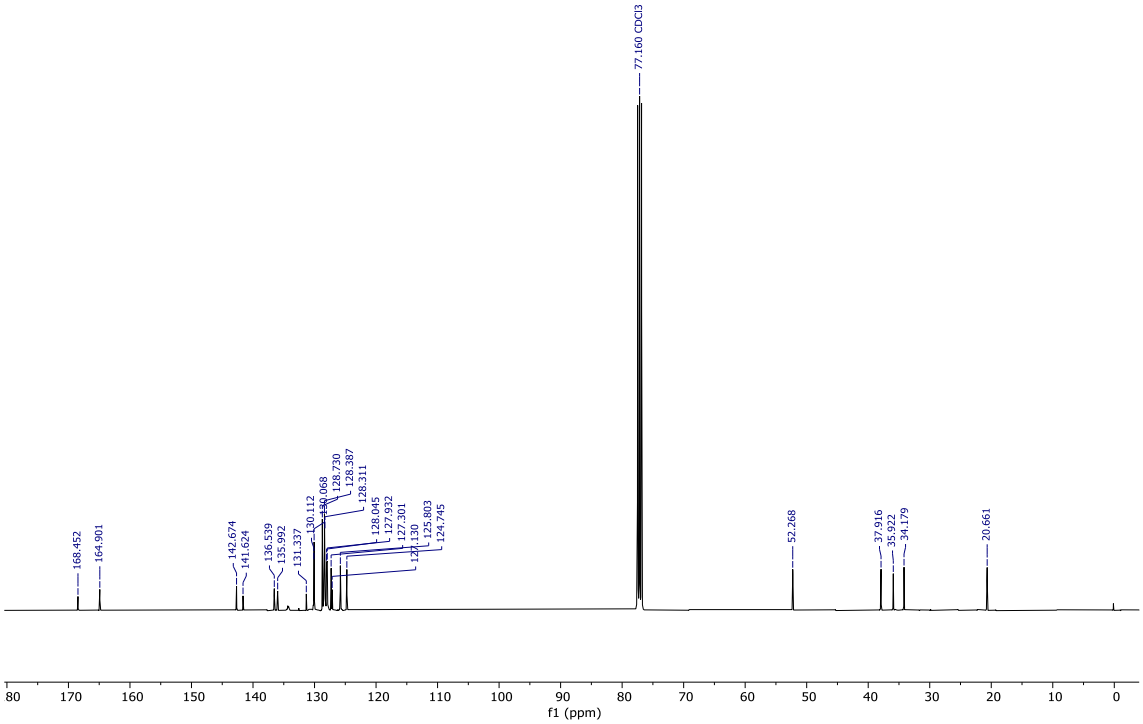
77.160 CDCl3
168.452
164.901
142.674
141.624
136.539
135.992
131.337
130.112
129.068
128.730
128.387
128.311
128.045
127.932
127.301
125.803
124.745
52.268
37.916
35.922
34.179
20.661
f1 (ppm)

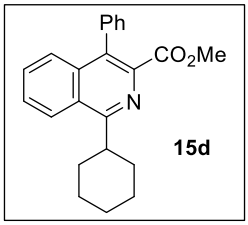
Ph
CO2Me
N

15d

4.870 CD3OD
3.592
8.412
8.395
7.733
7.700
7.683
7.617
7.601
7.311
7.288
3.739
3.665
1.991
1.828
1.652
1.575
1.453
1.379
1.321
1.252
f1 (ppm)

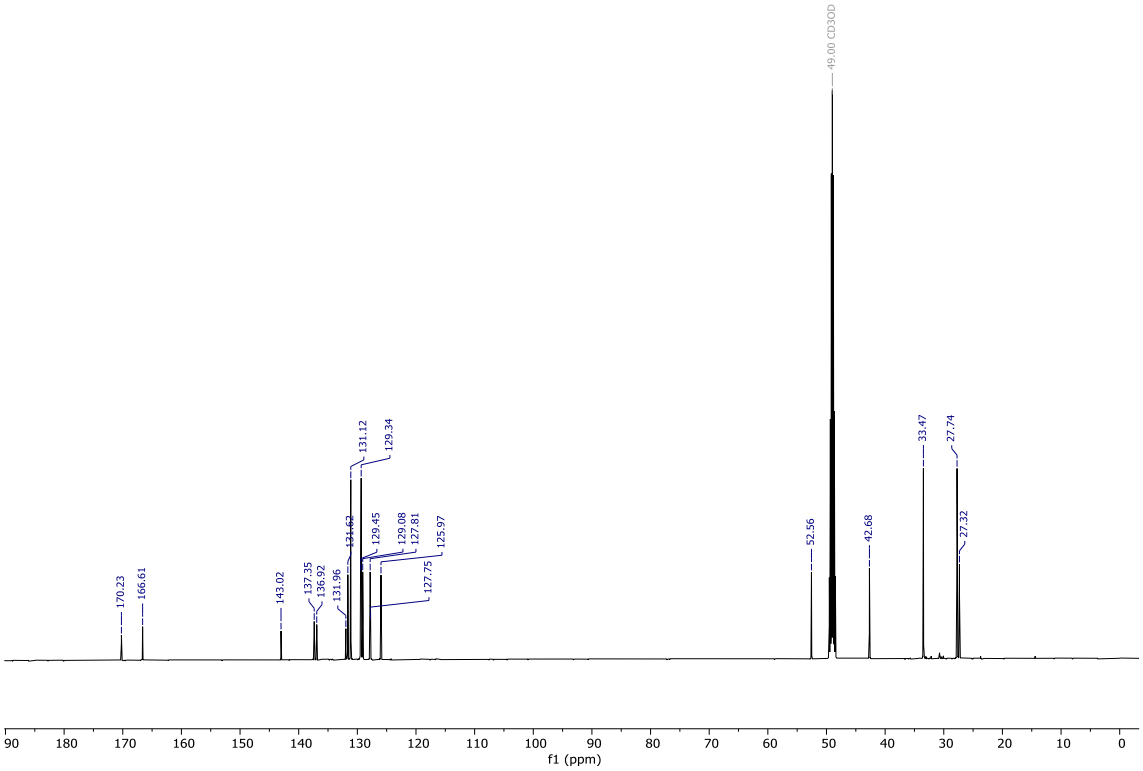
49.00 CD3OD
131.12
129.34
129.45
129.08
127.81
125.97
127.75
170.23
166.61
143.02
137.35
136.92
131.96
52.56
42.68
33.47
27.74
27.32
f1 (ppm)

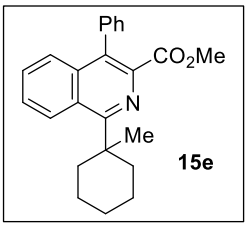
Ph
CO2Me
N
Me
15e

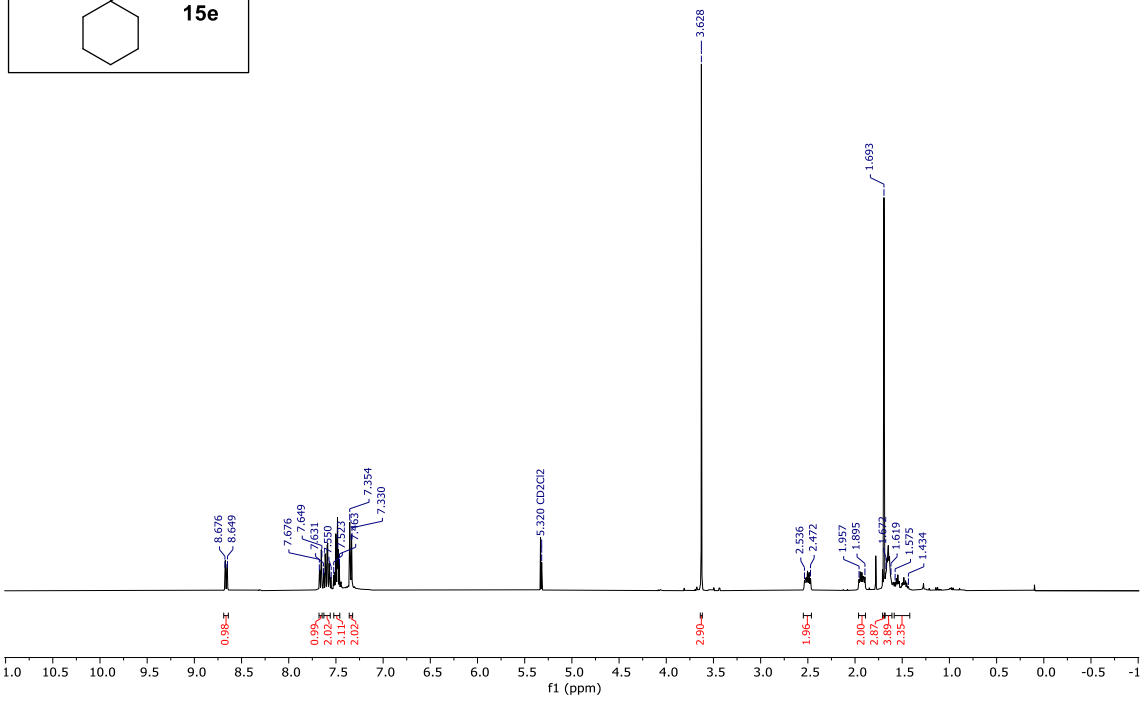
3.628
1.693
8.676
8.649
7.676
7.649
7.631
7.550
7.523
7.463
7.354
7.330
5.320 CD2Cl2
2.536
2.472
1.957
1.895
1.672
1.619
1.575
1.434
0.98
0.99
2.03
3.11
2.02
2.90
1.96
2.00
2.87
3.89
2.35
f1 (ppm)

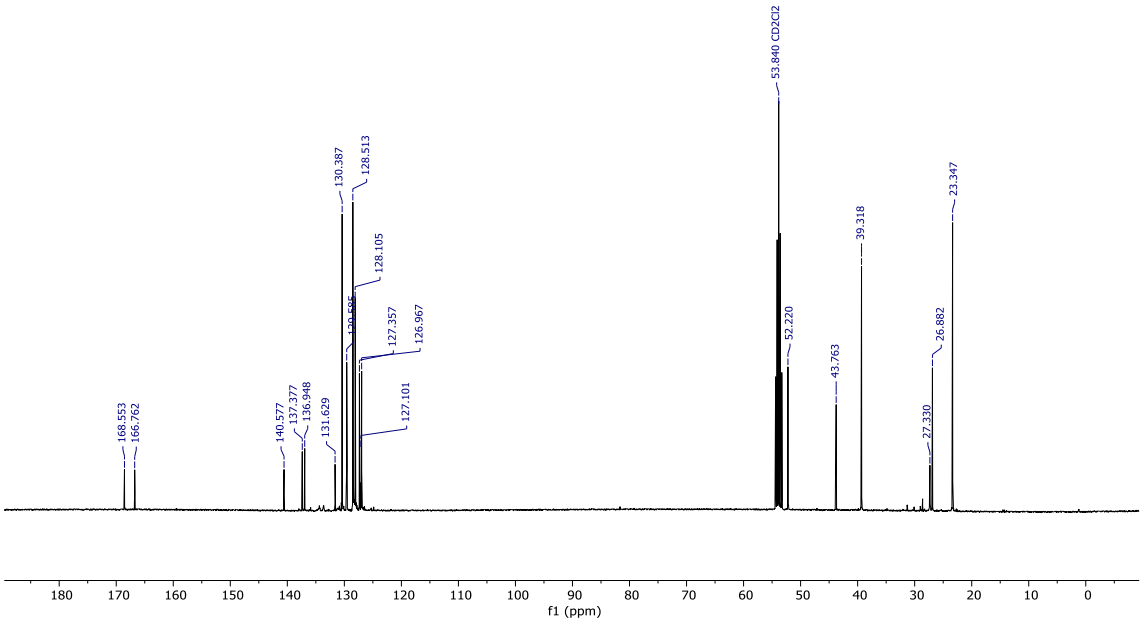
53.840 CD2Cl2
130.387
128.513
128.105
127.357
126.967
127.101
168.553
166.762
140.577
137.377
136.948
131.629
52.220
43.763
39.318
26.882
27.330
23.347
f1 (ppm)

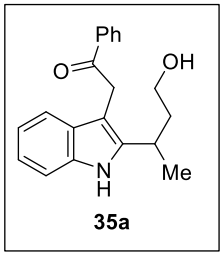
Ph
O
OH
N
H
Me

35a

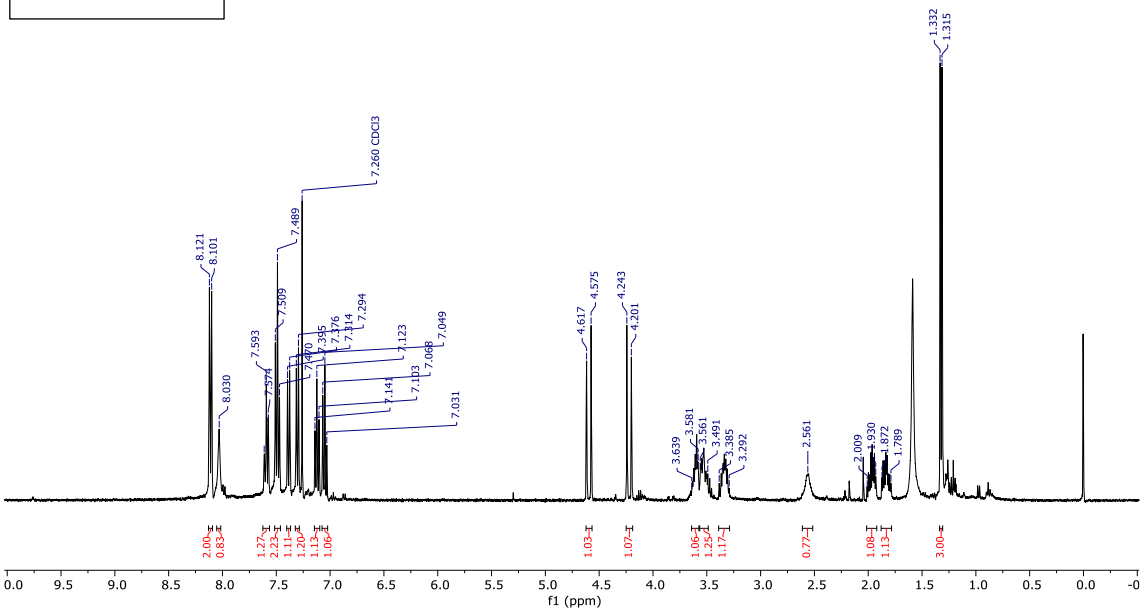
8.121
8.101
8.030
7.593
7.574
7.509
7.489
7.260 CDCl3
7.395
7.376
7.314
7.294
7.123
7.068
7.049
7.141
7.103
7.031
4.617
4.575
4.243
4.201
3.639
3.581
3.561
3.491
3.383
3.292
2.561
2.009
1.930
1.872
1.789
1.332
1.315
f1 (ppm)

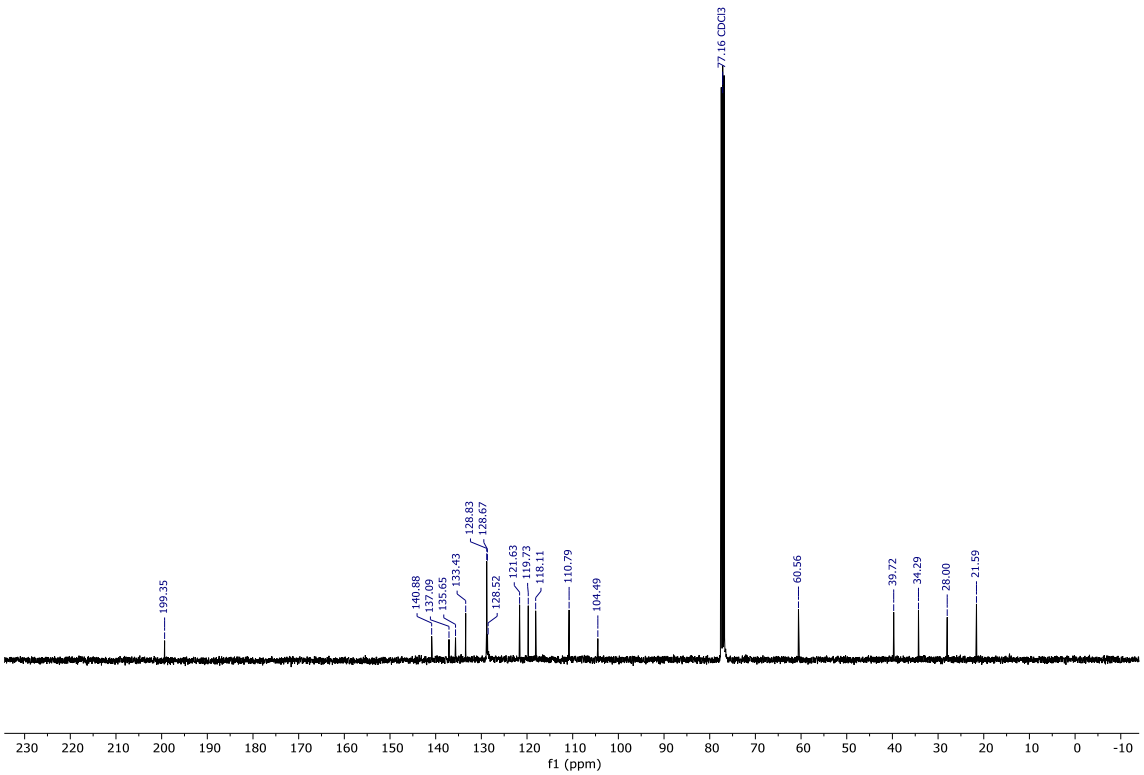
199.35
140.88
137.09
135.65
133.43
128.83
128.67
128.52
121.63
119.73
118.11
110.79
104.49
77.16 CDCl3
60.56
39.72
34.29
28.00
21.59
f1 (ppm)

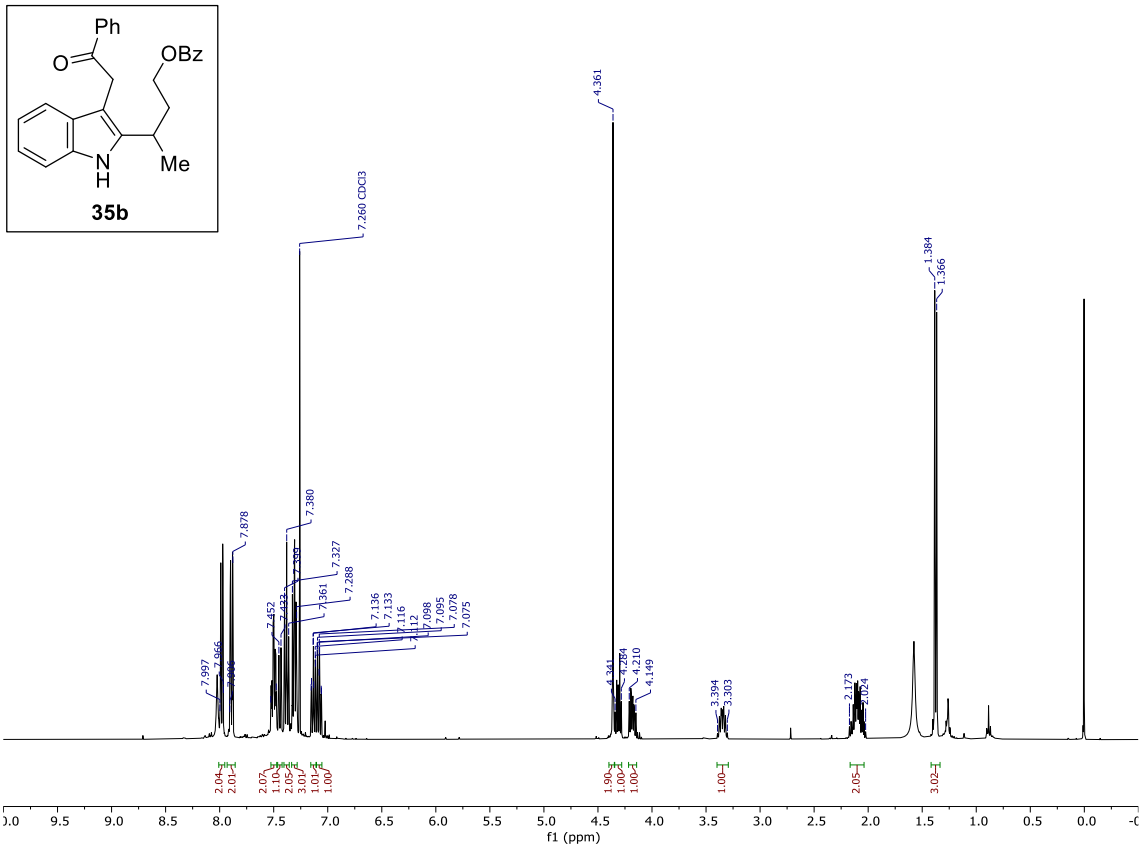
Ph
O
OBz
N
H
Me
35b
7.260 CDCl3
4.361
1.384
1.366
7.878
7.380
7.327
7.388
7.361
7.136
7.133
7.116
7.098
7.095
7.078
7.075
7.997
7.966
7.452
4.341
4.284
4.210
4.149
3.394
3.303
2.173
2.124
f1 (ppm)

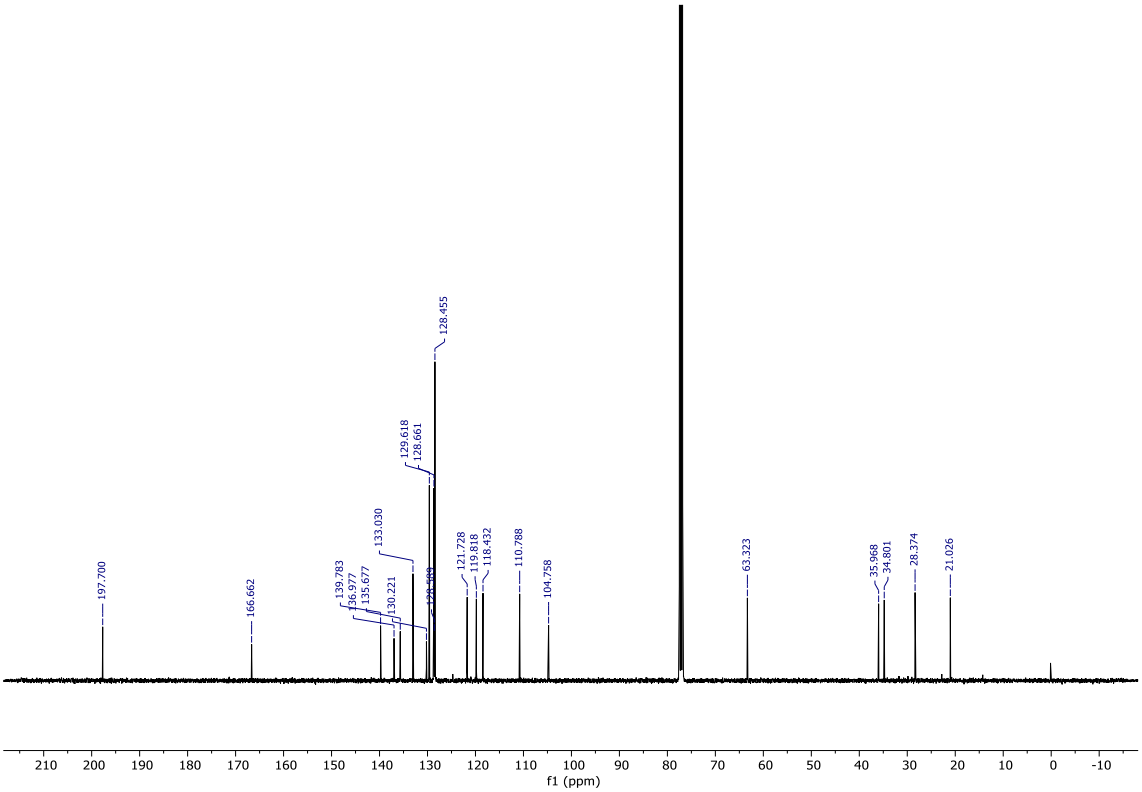
128.455
129.618
128.661
133.030
121.728
119.818
118.432
110.788
104.758
197.700
166.662
139.783
136.977
135.677
130.221
63.323
35.968
34.801
28.374
21.026
f1 (ppm)

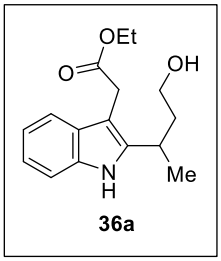
OEt
O
OH
N
H
Me

36a

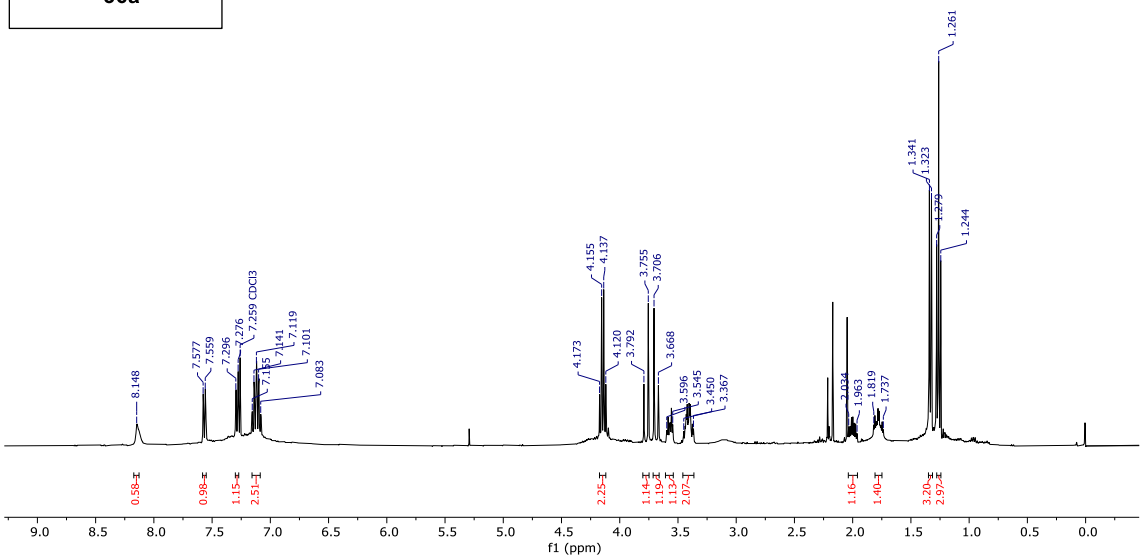
8.148
7.577
7.559
7.296
7.276
7.259 CDCl3
7.141
7.119
7.101
7.083
4.173
4.155
4.137
4.120
3.792
3.755
3.706
3.668
3.596
3.545
3.450
3.367
2.034
1.963
1.819
1.737
1.341
1.323
1.279
1.261
1.244
0.58
0.98
1.15
2.51
2.25
1.14
1.13
2.07
1.16
1.40
3.20
2.97
f1 (ppm)

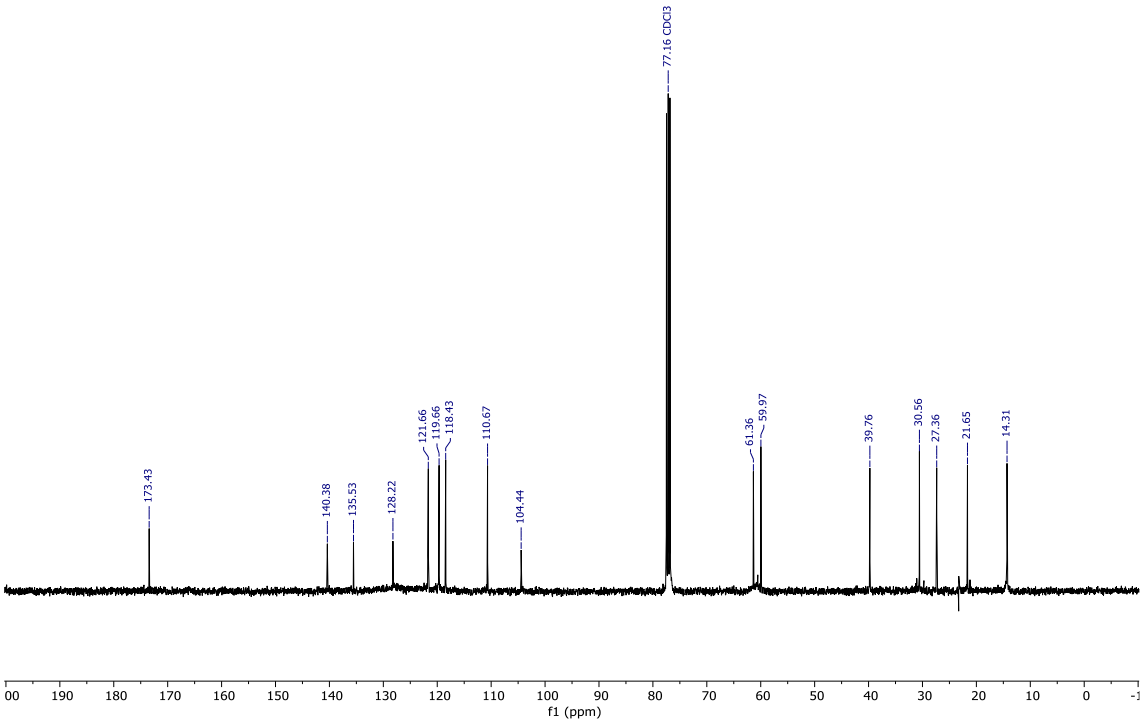
173.43
140.38
135.53
128.22
121.66
119.66
118.43
110.67
104.44
77.16 CDCl3
61.36
59.97
39.76
30.56
27.36
21.65
14.31
f1 (ppm)

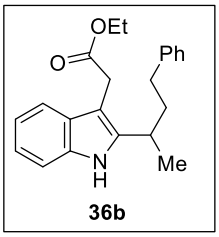
OEt
O
Ph
N
H
Me

36b

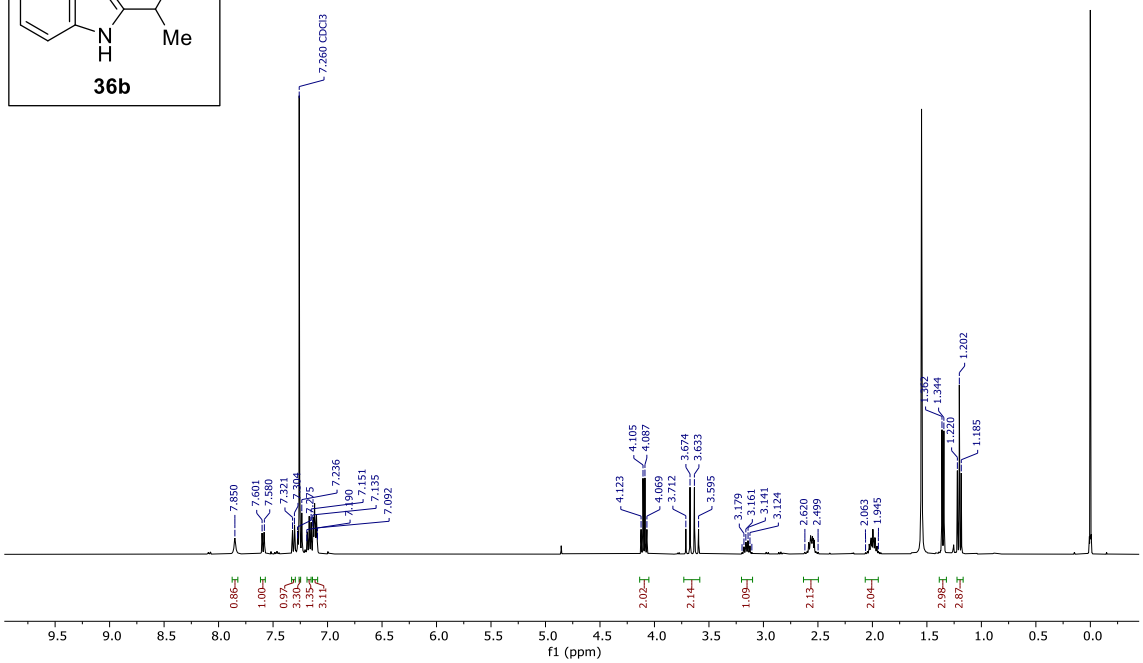
7.260 CDCl3
7.850
7.601
7.580
7.321
7.304
7.275
7.236
7.190
7.151
7.135
7.092
4.123
4.105
4.087
4.069
3.712
3.674
3.633
3.595
3.179
3.161
3.141
3.124
2.620
2.499
2.063
1.945
1.362
1.344
1.220
1.202
1.185
0.86
1.00
0.97
3.30
1.35
3.11
2.02
2.14
1.09
2.13
2.04
2.98
2.87
f1 (ppm)

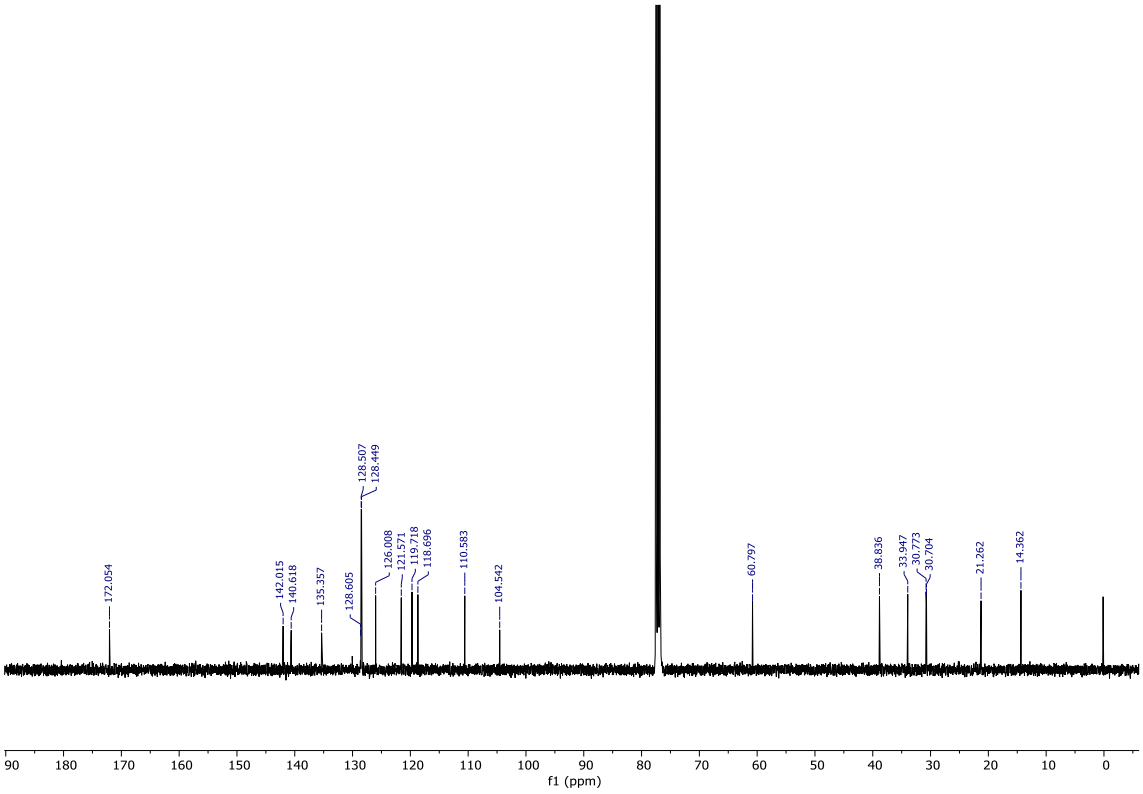
172.054
142.015
140.618
135.357
128.605
128.507
128.449
126.008
121.571
119.718
118.696
110.583
104.542
60.797
38.836
33.947
30.773
30.704
21.262
14.362
f1 (ppm)

Copies of ^{19}F NMR spectra

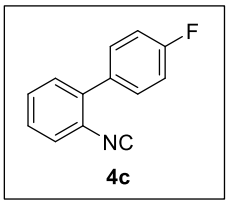

4c

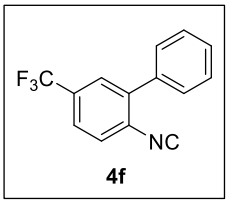

4f

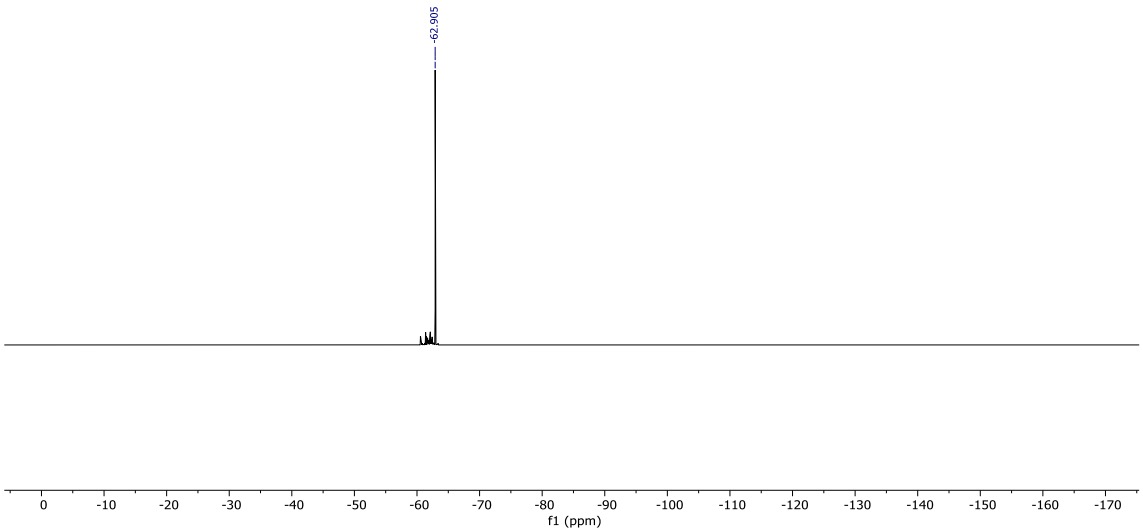

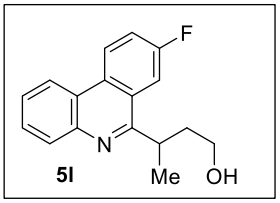
F
N
Me
OH

5l

-111.874
0
-10
-20
-30
-40
-50
-60
-70
-80
-90
-100
-110
-120
-130
-140
-150
-160
-170
f1 (ppm)

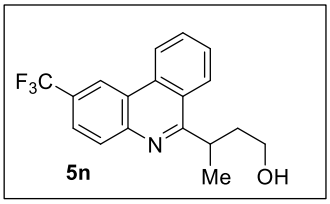
F3C
N
Me
OH

5n

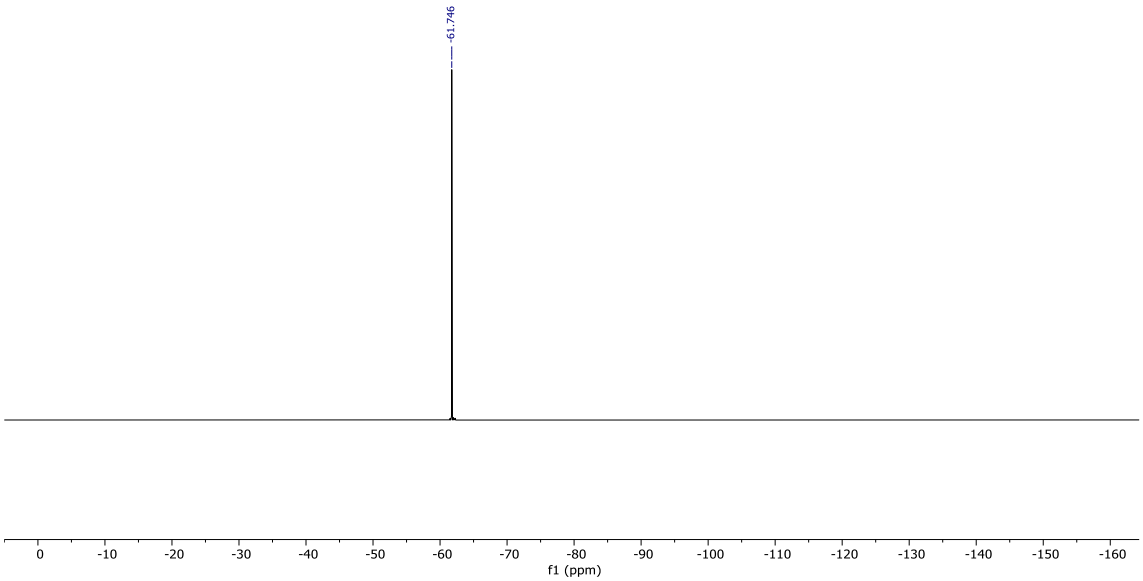
-61.746
0
-10
-20
-30
-40
-50
-60
-70
-80
-90
-100
-110
-120
-130
-140
-150
-160
f1 (ppm)

3. MHAT-MINISCI COUPLING OF HETEROCYCLES WITH ETHERS

Preparation of starting materials

All the substrates used are commercially available except for compounds *tert*-Butyl pyrrolidine-1-carboxylate,[317] Methyl 2-oxopyrrolidine-1-carboxylate,[318] **6**,[298] **8**[298] which were prepared according to the reported procedure.

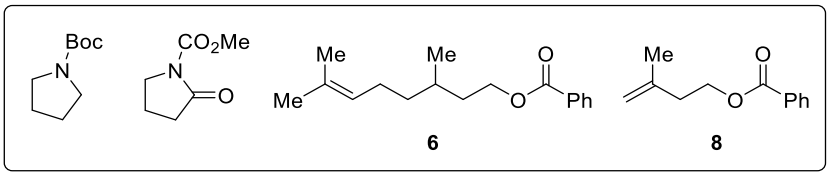

Scope of the Minisci C-H cross-coupling reaction

General method

To a solution of heterocycle (1 equiv), alkene (3 equiv) and $Fe(acac)_2$ (0.2 equiv) in a 4:1 mixture of the donor compound/MeOH (0.2 M) was added TFA (2 equiv) and the mixture was degassed and bubbled with argon for 5 minutes. Then, TBHP (5.5 M in decanes, 1.5 equiv) was added to the mixture and the solution was stirred overnight at room temperature under argon. After 24 h, the reaction was quenched by the addition of saturated aqueous $NaHCO_3$ solution, extracted three times with EtOAc, the combined organic extracts were washed with brine, dried with anhydrous Na_2SO_4, concentrated, and purified by column chromatography.

6-(Tetrahydrofuran-2-yl)phenanthridine (2a)

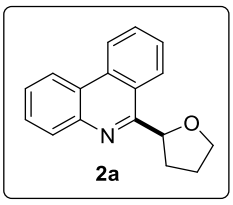

According to the general method for Minisci C-H cross-coupling, phenanthridine (100 mg, 0.558 mmol), 2-methylbut-2-ene (178 µL, 1.67 mmol), $Fe(acac)_2$ (29 mg, 0.112 mmol), TBHP (5.5 M in decanes, 152 µL, 0.837 mmol), TFA (85 µL, 1.12 mmol), in 4:1 THF/MeOH (0.2 M, 2.86 mL) at room temperature gave after purification by chromatography (hexane → hexane/AcOEt 75:25) **2a** (102 mg, 73%) as a pale yellow powder. ^{1}H NMR (400 MHz, $CDCl_3$) δ 8.65 (d, *J* = 8.4 Hz, 1H, H-1), 8.55 (d, *J* = 8 Hz, 1H, H-10), 8.45 (d, *J* = 8 Hz, 1H, H-4), 8.19 (d, *J* = 8.4 Hz, H-7), 7.83 (ddd, *J* = 8.4, 7.2, 1.2 Hz, 1H, H-9), 7.71 (dq, *J* = 8.4, 1.6 Hz, 2H, H-3 and H-8), 7.65 (ddd, *J* = 8, 6.8, 1.2 Hz, 1H, H-2), 5.78 (t, *J* = 6.8 Hz, 1H, H-2'), 4.21 (q, *J* = 14, 8 Hz, 1H, H-5'), 4.07 (q, *J* = 14.4, 8 Hz,

1H, H-5'), 2.75 (ddt, *J* = 15.2, 8.4, 6.8 Hz, 1H, H-3'), 2.47–2.39 (m, 1H, H-3'), 2.27–2.08 (m, 2H, H-4'); ^{13}C NMR (101 MHz, CDCl3) δ 159.4 (C-6), 143.4 (C-4a), 133.4 (C-10a), 130.6 (C-9), 130.4 (C-7), 128.6 (C-3), 127.3 (C-8), 127.0 (C-1), 126.6 (C-2), 124.9 (C-6a), 124.2 (C-10b), 122.5 (C-10), 121.9 (C-4), 79.8 (C-2'), 69.2 (C-5'), 30.1 (C-3'), 26.1 (C-4').

6-(Tetrahydro-2H-pyran-2-yl)phenanthridine (2b)

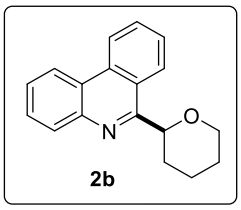

According to the general method for Minisci C-H cross-coupling, phenanthridine (100 mg, 0.558 mmol), 2-methylbut-2-ene (178 µL, 1.67 mmol), $Fe(acac)_2$ (29 mg, 0.112 mmol), TBHP (5.5 M in decanes, 152 µL, 0.837 mmol), TFA (85 µL, 1.12 mmol), in 4:1 tetrahydro-2H-pyran/MeOH (0.2 M, 2.86 mL) at room temperature gave after purification by chromatography (hexane → hexane/AcOEt 75:25) **2b** (123 mg, 84%) as a pale yellow powder. ^{1}H NMR (400 MHz, $CDCl_3$) δ 8.61 (d, *J* = 8.3 Hz, 1H, H-1), 8.54 (d, *J* = 5.0 Hz, 1H, H-10), 8.52 (dd, *J* = 7.2, 1.2 Hz, 1H, H-4), 8.24 (dd, *J* = 8.2, 1.0 Hz, 1H, H-7), 7.79 (ddd, *J* = 8.4, 7.0, 1.3 Hz, 1H, H-9), 7.73–7.60 (m, 3H, H-2, H-3 and H-8), 5.21 (dd, *J* = 11.2, 2.2 Hz, 1H, H-2'), 4.30 (dt, *J* = 11.5, 2.0 Hz, 1H, H-6'), 3.81 (td, *J* = 11.6, 2.3 Hz, 1H, H-6'), 2.34–2.24 (m, 1H, H-3'), 2.12–2.05 (m, 2H, H-3' and H-5'), 1.97–1.77 (m, 2H, H-5' and H-4'), 1.69 (d, *J* = 12.4 Hz, 1H, H-4'). ^{13}C NMR (101 MHz, $CDCl_3$) δ 159.6 (C-6), 143.4 (C-4a), 133.4 (C-10a), 130.4 (C-7), 130.3 (C-9), 128.5 (C-3), 127.1 (C-8), 127.0 (C-2), 126.7 (C-10), 124.4 (C-6a), 124.1 (C-10b), 122.4 (C-1), 121.9 (C-4), 80.6 (C-2'), 69.5 (C-6'), 30.6 (C-3'), 26.1 (C-4'), 23.9 (C-5').

6-(1,4-Dioxan-2-yl)phenanthridine (2c)

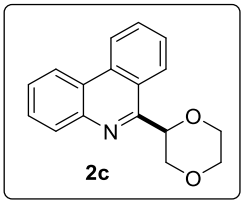

According to the general method for Minisci C-H cross-coupling, phenanthridine (100 mg, 0.558 mmol), 2-methylbut-2-ene (178 µL, 1.67 mmol), $Fe(acac)_2$ (29 mg, 0.112 mmol), TBHP (5.5 M in decanes, 152 µL, 0.837 mmol), TFA (85 µL, 1.12 mmol), in 4:1 1,4-dioxane/MeOH (0.2 M, 2.86 mL) at room temperature gave after purification by chromatography (hexane → hexane/AcOEt 75:25) **2c** (128 mg, 86%) as a brown powder. ^{1}H NMR (400 MHz, $CDCl_3$) δ 8.66 (d, *J* = 8.8 Hz, 1H, H-1), 8.56 (dd, *J* = 8, 1.6 Hz, 1H, H-10), 8.44 (d, *J* = 8 Hz, 1H, H-4), 8.21 (dd, *J* = 8.8, 0.8 Hz, 1H, H-7), 7.85 (ddd, *J* = 8.4, 7.2, 1.2 Hz, 1H, H-9), 7.75–7.70 (m, 2H, H-3 and H-2), 7.67 (ddd, *J* = 8, 6.8, 1.6 Hz,

1H, H-8), 5.49 (dd, *J* = 7.6, 5.2 Hz, 1H, H-2'), 4.35–4.29 (m, 2H, H-3'), 4.18–4.07 (m, 2H, H-6'), 4.97–3.89 (m, 2H, H-5'). ^{13}C NMR (101 MHz, $CDCl_3$) δ 156.1 (C-6), 143.2 (C-4a), 133.3 (C-10a), 130.5 (C-7 and C-9), 128.7 (C-3), 127.4 (C-2), 127.3 (C-8), 126.1 (C-4), 124.5 (C-6a), 124.1 (C-10b), 122.5 (C-1), 121.9 (C-10), 76.2 (C-2'), 70.1 (C-3'), 67.8 (C-6'), 66.6 (C-5').

6-(Benzo[d][1,3]dioxol-2-yl)phenanthridine (2d)

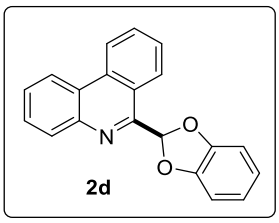

According to the general method for Minisci C-H cross-coupling, phenanthridine (100 mg, 0.558 mmol), 2-methylbut-2-ene (178 µL, 1.67 mmol), $Fe(acac)_2$ (29 mg, 0.112 mmol), TBHP (5.5 M in decanes, 152 µL, 0.837 mmol), TFA (85 µL, 1.12 mmol), in 4:1 1,3-benzodioxole/MeOH (0.2 M, 2.86 mL) at room temperature gave after purification by chromatography (hexane → hexane/AcOEt 75:25) **2d** (159 mg, 95%) as a pale brown powder. ^{1}H NMR (400 MHz, $CDCl_3$) δ 8.68 (d, *J* = 8.5 Hz, 1H, H-1), 8.60 (dd, *J* = 8.2, 1.6 Hz, 1H, H-10), 8.30–8.25 (m, 2H, H-7, H-4), 7.86 (ddd, *J* = 8.4, 7.1, 1.3 Hz, 1H, H-9), 7.76 (dddd, *J* = 9.7, 8.0, 6.1, 1.6 Hz, 2H, H-3 and H-8), 7.63 (dd, *J* = 8.4, 1.2 Hz, 1H, H-2), 7.45 (s, 1H, H-2'), 7.03–6.96 (m, 4H, H-4', H-5', H-6' and H-7'). ^{13}C NMR (101 MHz, $CDCl_3$) δ 152.5 (C-6), 147.5 (C-3a' and C-7a'), 142.9 (C-4a), 133.9 (C-10a), 131.0 (C-7), 130.9 (C-9), 129.0 (C-3), 128.4 (C-8), 127.8 (C-2), 126.0 (C-4), 125.0 (C-6a), 123.8 (C-10b), 122.7 (C-1), 122.4 (C-5' and C-6'), 122.2 (C-10), 112.2 (C-2'), 109.4 (C-4' and C-7').

6-(1,3-Dioxolan-2-yl)phenanthridine (2f) and 6-(1,3-Dioxolan-4-yl)phenanthridine(2f')

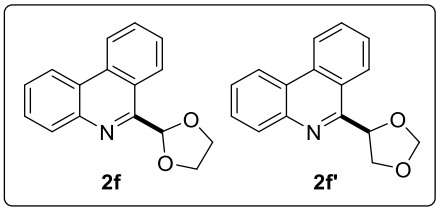

According to the general method for Minisci C-H cross-coupling, phenanthridine (100 mg, 0.558 mmol), 2-methylbut-2-ene (178 µL, 1.67 mmol), $Fe(acac)_2$ (29 mg, 0.112 mmol), TBHP (5.5 M in decanes, 152 µL, 0.837 mmol), TFA (85 µL, 1.12 mmol), in 4:1 1,3-dioxolane/MeOH (0.2 M, 2.86 mL) at room temperature gave after purification by chromatography (hexane → hexane/AcOEt 50:50) **2f** (136 mg, 97%) as a dark yellow oil. **2f'** could be seen in the crude NMR but was not isolated. ^{1}H NMR (400 MHz, $CDCl_3$) δ 8.61 (d, *J* = 8.4 Hz, 1H, H-1), 8.53 (dd, *J* = 8.1, 1.6 Hz, 1H, H-10), 8.49 (d, *J* = 8.4, 1H, H-4), 8.26 (dd, *J* = 8.3, 1.3 Hz, 1H, H-7), 7.81 (ddd, *J* = 8.4, 7.1, 1.4 Hz, 1H, H-9), 7.73 (ddd, *J* = 8.2, 7.1, 1.5 Hz, 1H, H-3),

7.66 (ddd, *J* = 7.1, 6.8, 2.0 Hz, 2H, H-2 and H-8), 6.50 (s, 1H, H-2'), 4.41–4.32 (m, 2H, H-4' and H-5'), 4.25–4.16 (m, 2H, H-4' and H-5'). ^{13}C NMR (101 MHz, $CDCl_3$) δ 154.8 (C-6), 143.0 (C-4a), 133.6 (C-10a), 130.8 (C-7), 130.6 (C-9), 128.7 (C-3), 127.7 (C-8), 127.3 (C-2), 126.6 (C-4), 124.6 (C-6a), 124.1 (C-10b), 122.3 (C-1), 122.0 (C-10), 104.2 (C-2'), 65.5 (C-4' and C-5').

6-(5-Methyltetrahydrofuran-2-yl)phenanthridine (2g)

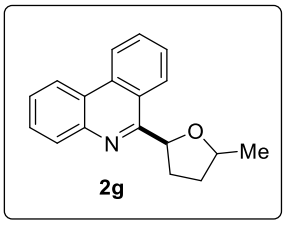

2g

According to the general method for Minisci C-H cross-coupling, phenanthridine (100 mg, 0.558 mmol), 2-methylbut-2-ene (178 µL, 1.67 mmol), $Fe(acac)_2$ (29 mg, 0.112 mmol), TBHP (5.5 M in decanes, 152 µL, 0.837 mmol), TFA (85 µL, 1.12 mmol), in 4:1 2-methyltetrahydrofuran/MeOH (0.2 M, 2.86 mL) at room temperature gave after purification by chromatography (hexane → hexane/AcOEt 75:25) **2g** as a mixture of diastereomers (1.5:1) (75 mg, 51%) as a pale yellow powder. ^{1}H NMR (400 MHz, $CDCl_3$) δ 8.64 (d, *J* = 8.4 Hz, 1H, H-1), 8.55 (d, *J* = 8.2 Hz, 1H, H-10), 8.47 (d, *J* = 8.2 Hz, 1H, H-4), 8.18 (ddd, *J* = 8.3, 3.9, 1.2 Hz, 1H, H-7), 7.83 (tt, *J* = 7.0, 1.5 Hz, 1H, H-9), 7.73–7.62 (m, 3H, H-3, H-8 and H-2), 5.92 (t, *J* = 6.9 Hz, 1H, H-2', M), 5.70 (t, *J* = 7.1 Hz, 1H, H-2', m), 4.52–4.44 (m, 1H, H-5', M), 4.37–4.29 (m, 1H, H-5', m), 2.91–2.76 (m, 1H, H-3'), 2.51–2.37 (m, 1H, H-3'), 2.36–2.19 (m, 1H, H-4'), 1.85–1.72 (m, 1H, H-4'), 1.40 (d, *J* = 6.1 Hz, 3H, Me, m), 1.39 (d, *J* = 6.1 Hz, 3H, Me, M). ^{13}C NMR (101 MHz, $CDCl_3$) δ 159.9 (C-6, M) 159.2 (C-6, m) 143.5 (C-4a, m), 143.4 (C-4a, M), 133.5 (C-10a, m), 133.4 (C-10a, M), 130.6 (C-7, M), 130.5 (C-7, m), 130.4 (C-9, M), 130.3 (C-9, m), 128.6 (C-3, M), 128.5, (C-3, m), 127.3 (C-8, M), 127.2 (C-8, m), 127.0 (C-2, m) 126.9 (C-2, M) 126.7 (C-4), 125.12 (C-6a, m), 124.9 (C-6a, M), 124.3 (C-10b, m), 124.2 (C-10b, M), 122.5 (C-1, M), 122.4 (C-1, m), 122.0 (C-10), 80.7 (C-2', m), 79.2 (C-2' M), 77.4 (C-5', m) 76.1 (C-5', M), 33.9 (C-4', M), 33.2 (C-4', m), 30.6 (C-3', M), 30.0 (C-3', m), 21.6 (Me, M), 21.4 (Me, m).

6-(1-Ethoxyethyl)phenanthridine (2j)

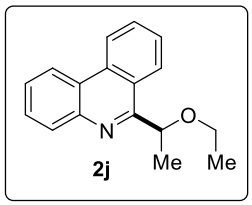

2j

According to the general method for Minisci C-H cross-coupling, phenanthridine (100 mg, 0.558 mmol), 2-methylbut-2-ene (178 µL, 1.67 mmol), $Fe(acac)_2$ (29 mg, 0.112 mmol), TBHP (5.5 M in

decanes, 152 µL, 0.837 mmol), TFA (85 µL, 1.12 mmol), in 4:1 diethyl ether/MeOH (0.2 M, 2.86 mL) at room temperature gave after purification by chromatography (hexane → hexane/AcOEt 75:25) **2j** (133 mg, 95%) as a yellow oil. ^{1}H NMR (400 MHz, $CDCl_3$) δ 8.88 (d, *J* = 8.4 Hz, 1H, H-1), 8.61 (d, *J* = 8.3 Hz, 1H, H-10), 8.51 (d, *J* = 7.3 Hz, 1H, H-4), 8.19 (dd, *J* = 8.4, 1.0 Hz, 1H, H-7), 7.79 (td, *J* = 7.1, 1.4 Hz, 1H, H-9), 7.71 (td, *J* = 6.9, 1.3 Hz, 1H, H-3), 7.67–7.59 (m, 2H, H-2 and H-8), 5.23 (q, *J* = 6.8 Hz, 1H, H-2'), 3.62–3.55 (m, 1H, H-4'), 3.50–3.43 (m, 1H, H-4'), 1.79 (d, *J* = 6.9 Hz, 3H, H-1'), 1.21 (t, *J* = 7.0 Hz, 3H, H-5'). ^{13}C NMR (101 MHz, $CDCl_3$) δ 161.9 (C-6), 143.3 (C-4a), 133.5 (C-10a), 130.4 (C-9), 130.0 (C-7), 128.6 (C-3), 127.0 (C-8), 126.9 (C-1), 126.8 (C-2), 124.1 (C-6a), 124.0 (C-10b), 122.4 (C-10), 121.9 (C-4), 81.4 (C-2'), 64.7 (C-4'), 21.5 (C-1'), 15.6 (C-5').

6-(1-Butoxybutyl)phenanthridine (2k)

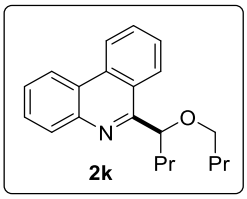

2k

According to the general method for Minisci C-H cross-coupling, phenanthridine (100 mg, 0.558 mmol), 2-methylbut-2-ene (178 µL, 1.67 mmol), $Fe(acac)_2$ (29 mg, 0.112 mmol), TBHP (5.5 M in decanes, 152 µL, 0.837 mmol), TFA (85 µL, 1.12 mmol), in 4:1 dibutyl ether/MeOH (0.2 M, 2.86 mL) at room temperature gave after purification by chromatography (hexane → hexane/AcOEt 90:10) **2k** (139 mg, 81%) as a pale yellow powder. ^{1}H NMR (400 MHz, $CDCl_3$) δ 8.92 (d, *J* = 8.2 Hz, 1H, H-1), 8.66 (d, *J* = 8.4 Hz, 1H, H-10), 8.57 (dd, *J* = 8.1, 1.6 Hz, 1H, H-4), 8.18 (d, *J* = 8.0 Hz, 1H, H-7), 7.84 (ddd, *J* = 8.4, 7.0, 1.3 Hz, 1H, H-9), 7.73 (ddd, *J* = 8.3, 7.0, 1.5 Hz, 1H, H-3), 7.70–7.63 (m, 2H, H-2 and H-8), 4.98 (dd, *J* = 8.8, 5.4 Hz, 1H, H-1'), 3.48–3.43 (m, 1H, H-6'), 3.42–3.36 (m, 1H, H-6'), 2.25–2.15 (m, 1H, H-2'), 1.99–1.90 (m, 1H, H-2'), 1.72–1.63 (m, 1H, H-3'), 1.59–1.52 (m, 2H, H-7'), 1.36–1.30 (m, 2H, H-8'), 0.95 (t, *J* = 7.4 Hz, 3H, H-4'), 0.83 (t, *J* = 7.4 Hz, 3H, H-9'). ^{13}C NMR (101 MHz, $CDCl_3$) δ 162.0 (C-6), 143.4 (C-4a), 133.6 (C-10a), 130.6 (C-9), 130.1 (C-7), 128.7 (C-3), 127.3 (C-1), 127.1 (C-8), 127.0 (C-2), 124.5 (C-6a), 124.2 (C-10b), 122.4 (C-10), 122.1 (C-4), 86.4 (C-1'), 69.5 (C-6'), 38.4 (C-2'), 32.2 (C-7'), 20.0 (C-3'), 19.5 (C-8'), 14.1 (C-4'), 14.0 (C-9').

6-(1,2-Dimethoxyethyl)phenanthridine (2l)

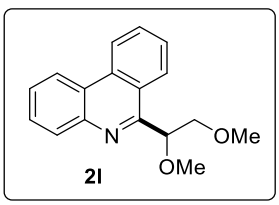

2l

According to the general method for Minisci C-H cross-coupling, phenanthridine (100 mg, 0.558 mmol), 2-methylbut-

2-ene (178 µL, 1.67 mmol), $Fe(acac)_2$ (29 mg, 0.112 mmol), TBHP (5.5 M in decanes, 152 µL, 0.837 mmol), TFA (85 µL, 1.12 mmol), in 4:1 dimethoxy ethane/MeOH (0.2 M, 2.86 mL) at room temperature gave after purification by chromatography (hexane → hexane/AcOEt 75:25) to give **2l** (123 mg, 83%) as a yellow oil. ^{1}H NMR (400 MHz, $CDCl_3$) δ 8.73 (d, *J* = 8.3 Hz, 1H, H-1), 8.67 (d, *J* = 8.3 Hz, 1H, H-10), 8.57 (dd, *J* = 8.2, 1.5 Hz, 1H, H-4), 8.22 (dd, *J* = 8.2, 1.1 Hz, 1H, H-7), 7.85 (dd, *J* = 7.1, 1.2 Hz, 1H, H-9), 7.78–7.61 (m, 3H, H-2, H-3 and H-8), 5.32 (dd, *J* = 8.1, 3.6 Hz, 1H, CH), 4.14 (dd, *J* = 11.0, 8.4 Hz, 1H, CH_2), 3.83 (dd, *J* = 10.8, 3.7 Hz, 1H, CH_2), 3.45 (s, 3H, OMe), 3.44 (s, 3H, OMe). ^{13}C NMR (101 MHz, $CDCl_3$) δ 158.0 (C-6), 143.5 (C-4a), 133.4 (C-10a), 130.7 (C-9), 130.4 (C-7), 128.8 (C-3), 127.5 (C-8), 127.3 (C-2), 126.5 (C-1), 124.9 (C-6a), 124.1 (C-10b), 122.5 (C-10), 122.0 (C-4), 84.9 (CH), 75.3 (CH_2), 59.4 (OMe), 57.5 (OMe).

6-Benzoylphenanthridine (2m)

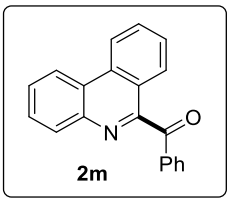

According to the general method for Minisci C-H cross-coupling, phenanthridine (100 mg, 0.558 mmol), 2-methylbut-2-ene (178 µL, 1.67 mmol), $Fe(acac)_2$ (29 mg, 0.112 mmol), TBHP (5.5 M in decanes, 152 µL, 0.837 mmol), TFA (85 µL, 1.12 mmol), in 4:1 dibenzyl ether/MeOH (0.2 M, 2.86 mL) at room temperature gave after purification by chromatography (hexane → hexane/AcOEt 95:5) to give **2m** (51 mg, 32%) as a colorless solid. ^{1}H NMR (400 MHz, $CDCl_3$) δ 8.73 (d, *J* = 8.4 Hz, 1H, H-1), 8.68–8.66 (m, 1H, H-10), 8.24–8.21 (m, 1H, H-8), 8.14 (d, *J* = 8 Hz, 1H, H-4), 8.04 (dd, *J* = 8.8, 1.6, 2H, Ph), 7.91 (ddd, *J* = 8.4, 7.2, 1.6 Hz, 1H, H-2), 7.80–7.77 (m, 2H, H-7 and H-9), 7.68 (ddd, *J* = 8, 6.8, 1.2 Hz, 1H, H-3), 7.63 (ddd, *J* = 8.8, 6.8, 1.2 Hz, 1H, Ph), 7.51–7.46 (m, 2H, Ph); ^{13}C NMR (101 MHz, $CDCl_3$) δ 194.9 (C=O), 157.6 (C-6), 142.7 (C-4a), 136.2 (C_{ipso}), 134.2 (Ph), 133.4 (C-10a), 131.5 (C-2), 130.9 (Ph), 130.7 (C-8), 128.7 (C-7 and C-9), 128.4 (Ph), 127.9 (C-3), 127.5 (C-4), 124.6 (C-6a), 123.9 (C-10b), 122.5 (C-1), 122.3 (C-10).

6-(1-Methyl-5-oxopyrrolidin-2-yl)phenanthridine (2p) and 6-((2-Oxopyrrolidin-1-yl)methyl)phenanthridine (2p')

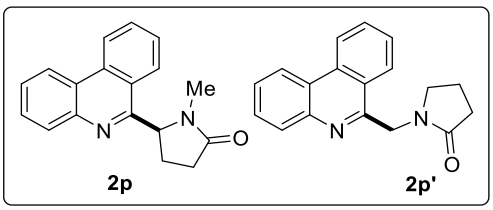

According to the general method for Minisci C-H cross-coupling, phenanthridine (100 mg, 0.558 mmol), 2-methylbut-2-ene (178 µL, 1.67 mmol), $Fe(acac)_2$ (29 mg, 0.112 mmol), TBHP

(5.5 M in decanes, 152 µL, 0.837 mmol), TFA (85 µL, 1.12 mmol), in 4:1 NMP/MeOH (0.2 M, 2.86 mL) at room temperature gave after purification by chromatography (CH_2Cl_2 → DCM/MeOH 95:5) **2p** and **2p'** as a mixture of constitutional isomers (2:1) (97 mg, 63%) as a pale yellow powder. ^{1}H NMR (400 MHz, $CDCl_3$) **2p** δ 8.71 (d, *J* = 8.7 Hz, 1H, H-1), 8.57 (d, *J* = 8.1 Hz, 1H, H-10), 8.18 (d, *J* = 8.7 Hz, 1H, H-4), 8.16–8.13 (dd, *J* = 8.0, 1.6 Hz,1H, H-7), 7.92–7.84 (m, 1H, H-9), 7.79–7.62 (m, 3H, H-2, H-3 and H-8), 5.56 (dd, *J* = 8.5, 3.7 Hz, 1H, H-2'), 2.92 (s, 3H, H-1'), 2.76–2.59 (m, 2H, H-4' and H-3'), 2.57–2.50 (m, 1H, H-4'), 2.22–2.13 (m, 1H, H-3'). ^{1}H NMR (400 MHz, $CDCl_3$) **2p'** δ 8.66 (d, *J* = 8.3 Hz, 1H, H-1), 8.57 (d, *J* = 8.1 Hz, 1H, H-10), 8.45 (d, *J* = 8.3 Hz, 1H, H-4), 7.92–7.84 (m, 1H, H-7), 7.79–7.62 (m, 4H, H-9, H-2, H-3 and H-8), 5.16 (s, 2H, H-1'), 3.36 (t, *J* = 7.1 Hz, 2H, H-5'), 2.47 (t, *J* = 8.1 Hz, 2H, H-3'), 1.95 (p, *J* = 7.4 Hz, 2H, H-4'). ^{13}C NMR (101 MHz, $CDCl_3$) **2p** δ 176.2 (C-5'), 157.8 (C-6), 143.4 (C-4a), 133.7 (C-10a), 130.8 (C-9), 130.7 (C-7), 129.0 (C-3), 127.7 (C-8), 127.4 (C-2), 124.5 (C-4), 124.0 (C-6a), 123.9 (C-10b), 123.2 (C-1), 122.0 (C-10), 63.0 (C-2'), 30.0 (C-4'), 29.4 (C-1'), 25.9 (C-3'). ^{13}C NMR (101 MHz, $CDCl_3$) **2p'** δ 174.9 (C-2'), 156.2 (C-6), 141.5 (C-4a), 133.2 (C-10a), 131.1 (C-7), 130.1 (C-3), 128.9 (C-9), 128.6 (C-8), 128.1 (C-2), 126.5 (C-4), 124.7 (C-6a), 124.4 (C-10b), 122.5 (C-1), 122.2 (C-10), 47.9 (C-1'), 47.2 (C-5'), 31.1 (C-3'), 18.0 (C-4').

6-((*N*-Methylacetamido)methyl)phenanthridine (2s)

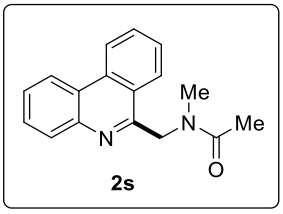

2s

According to the general method for Minisci C-H cross-coupling, phenanthridine (100 mg, 0.558 mmol), 2-methylbut-2-ene (178 µL, 1.67 mmol), $Fe(acac)_2$ (29 mg, 0.112 mmol), TBHP (5.5 M in decanes, 152 µL, 0.837 mmol), TFA (85 µL, 1.12 mmol), in 4:1 *N,N*-Dimethylacetamide/MeOH (0.2 M, 2.86 mL) at room temperature gave after purification by chromatography (AcOEt) **2s** as a mixture (1:0.2) of *anti* and *syn* isomers[319] (110 mg, 75%) as a pale yellow oil. ^{1}H NMR (400 MHz, $CDCl_3$) δ 8.63 (d, *J* = 8.4 Hz, 1H, H-1), 8.56 (dd, *J* = 8, 1.6 Hz, 1H, H-10), 8.43 (d, *J* = 8.4 Hz, 1H, H-8), 8.16 (dd, *J* = 8.4, 1.6 Hz, 1H, H-4), 7.85 (ddd, *J* = 8.4, 7.2, 1.2 Hz, 1H, H-2), 7.75–7.65 (m, 3H, H-3, H-7, and H-9), 5.32 (s, 2H, CH_2), 3.01 (s, 3H, N-Me), 2.19 (s, 3H, COMe); ^{13}C NMR (101 MHz, $CDCl_3$) δ 170.8 (C=O), 156.9 (C-6), 143.7 (C-4a), 133.2 (C-10a), 130.9 (C-2), 130.1 (C-4), 128.8 (C-9), 127.9 (C-7), 127.7 (C-6a), 127.3 (C-3), 126.6 (C-8), 124.2 (C-10b), 122.4 (C-1), 122.1 (c-10), 51.2 (CH_2), 35.6 (N-Me), 22.1 (COMe).

6-(Dimethylcarbamoyl)phenanthridine (2t)

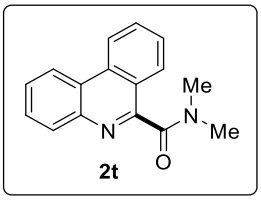

According to the general method for Minisci C-H cross-coupling, phenanthridine (100 mg, 0.558 mmol), 2-methylbut-2-ene (178 µL, 1.67 mmol), $Fe(acac)_2$ (29 mg, 0.112 mmol), TBHP (5.5 M in decanes, 152 µL, 0.837 mmol), TFA (85 µL, 1.12 mmol), in 4:1 N,N-dimethylformamide/MeOH (0.2 M, 2.86 mL) at room temperature gave after purification by chromatography (hexane → hexane/AcOEt 50:50) to give **2t** (117 mg, 61%) as a colorless oil. ^{1}H NMR (400 MHz, $CDCl_3$) δ 8.66 (dd, *J* = 8, 1.2 Hz, 1H, H-1), 8.59 (dd, *J* = 8, 2 Hz, 1H, H-10), 8.19 (dd, *J* = 8, 1.2 Hz, 1H, H-4), 8.07 (dd, *J* = 8.4, 2 Hz, 1H, H-7), 7.89 (ddd, *J* = 8.4, 7.2, 1.6 Hz, 1H, H-2), 7.79–7.68 (m, 3H, H-3, H-8, and H-9), 3.31 (s, 3H, Me), 2.93 (s, 3H, Me); ^{13}C NMR (101 MHz, $CDCl_3$) δ 168.3 (C=O), 156.4 (C-6), 143.2 (C-4a), 133.3 (C-10a), 131.5 (C-2), 130.4 (C-4), 129.2 (C-3), 128.0 (C-9), 127.9 (C-8), 127.2 (C-7), 124.2 (C-6a), 123.3 (C-10b), 122.4 (C-1), 122.2 (C-10), 38.5 (Me), 34.9 (Me).

6-Cyclohexylphenanthridine (2w)

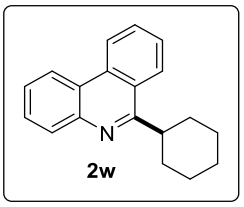

According to the general method for Minisci C-H cross-coupling, phenanthridine (100 mg, 0.558 mmol), 2-methylbut-2-ene (178 µL, 1.674 mmol), $Fe(acac)_2$ (29 mg, 0.112 mmol), TBHP (5.5 M in decanes, 152 µL, 0.837 mmol), TFA (85 µL, 1.116 mmol), in 4:1 cyclohexane/MeOH (0.2 M, 2.86 mL) at room temperature gave after purification by chromatography (hexane → hexane/AcOEt 90:10) **2w** (16 mg, 11%) as a transparent oil. ^{1}H NMR (400 MHz, $CDCl_3$) δ 8.65 (d, *J* = 9.6 Hz, 1H, H-1), 8.54 (dd, *J* = 8, 1.2 Hz, 1H, H-10), 8.32 (d, *J* = 8.4 Hz, 1H, H-7), 8.13 (dd, *J* = 8, 1.6 Hz, 1H, H-4), 7.81 (ddd, *J* = 8.4, 6.8, 1.2 Hz, 1H, H-2), 7.72–7.67 (m, 2H, H-3 and H-8), 7.60 (ddd, *J* = 8.4, 7.2, 1.6 Hz, 1H, H-9), 3.62 (tt, *J* = 11.2, 3.2 Hz, 1H, H-1'), 2.09–2.07 (m, 2H, CH_2), 1.99–1.93 (m, 4H, CH_2), 1.88–1.82 (m, 1H, CH_2), 1.63–1.55 (m, 2H, CH_2), 1.45 (tt, *J* = 12.8, 3.6 Hz, 1H, CH_2); ^{13}C NMR (101 MHz, $CDCl_3$) δ 165.4 (C-6), 144.0 (C-4a), 133.2 (C-10a), 130.1 (C-4), 130.0 (C-2), 128.5 (C-3), 127.2 (C-8), 126.3 (C-9), 125.7 (C-7), 124.9 (C-6a), 123.5 (C-10b), 122.7 (C-1), 121.9 (C-10), 42.1 (C-1'), 32.4 (CH_2), 27.0 (CH_2), 26.5 (CH_2); HRMS (ESI) *m/z*: $[M+H]^+$ calcd for $[C_{19}H_{20}N]^+$ 262.1595, found 262.1596.

Phenanthridine-6-carbaldehyde (3a)

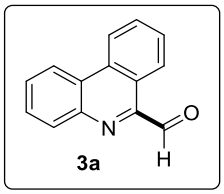

According to the general method for Minisci C-H cross-coupling, phenanthridine (100 mg, 0.558 mmol), 2-methylbut-2-ene (178 µL, 1.67 mmol), $Fe(acac)_2$ (29 mg, 0.112 mmol), TBHP (5.5 M in decanes, 152 µL, 0.837 mmol), TFA (85 µL, 1.12 mmol), in MeOH (0.2 M, 2.86 mL) at room temperature gave after purification by chromatography (hexane → hexane/AcOEt 75:25) **3a** (120 mg, 77%) as a white powder. ^{1}H NMR (400 MHz, $CDCl_3$): δ 10.41 (s, 1H, H-1'), 9.40 (d, *J* = 8.3, 1H, H-7), 8.65 (d, *J* = 8.4 Hz, 1H, H-1), 8.62–8.58 (m, 1H, H-10), 8.34–8.30 (m, 1H, H-4), 7.89 (ddd, *J* = 8.4, 7.0, 1.4 Hz, 1H, H-9), 7.84–7.79 (m, 2H, H-8 and H-3), 7.78 (ddd, *J* = 8.3, 7.0, 1.2 Hz, 1H, H-2). ^{13}C NMR (101 MHz, $CDCl_3$): δ 195.8 (C-1'), 150.4 (C-6), 143.5 (C-4a), 133.6 (C-10a), 131.4 (C-9), 131.3 (C-4), 130.0 (C-3), 129.3 (C-8), 128.9 (C-2), 127.1 (C-7), 125.7 (C-6a), 123.7 (C-10b), 122.4 (C-10), 122.1 (C-1). LRMS (ESI) m/z calcd. for $[C_{14}H_{10}NO]^+$ 208.07, found 208.08.

4-Methylquinoline-2-carbaldehyde (3b)

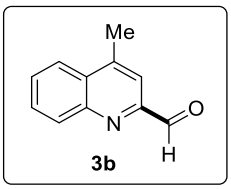

According to the general method for Minisci C-H cross-coupling, phenanthridine (100 mg, 0.698 mmol), 2-methylbut-2-ene (370 µL, 3.49 mmol), $Fe(acac)_2$ (35 mg, 0.139 mmol), TBHP (5.5 M in decanes, 381 µL, 2.094 mmol), TFA (107 µL, 1.39 mmol), in MeOH (0.2 M, 3.50 mL) at room temperature for 96 h gave after purification by chromatography (hexane → hexane/AcOEt 97.5:2.5) **3b** (53 mg, 44%) as a white powder. ^{1}H NMR (400 MHz, $CDCl_3$) δ 10.16 (s, 1H, CHO), 8.21 (ddd, *J* = 8.4, 1.6, 0.8 Hz, 1H, H-8), 8.01 (ddd, *J* = 8.4, 1.6, 0.8 Hz, 1H, H-5), 7.82 (s, 1H, H-3), 7.78 (ddd, *J* = 8, 6.8, 1.2 Hz, 1H, H-7), 7.67 (ddd, *J* = 8.4, 6.8, 1.2 Hz, 1H, H-6), 2.74 (s, 3H, Me); ^{13}C NMR (101 MHz, $CDCl_3$) δ 194.2 (CHO), 152.2 (C-2), 147.8 (C-8a), 146.1 (C-4), 131.1 (C-8), 130.2 (C-7), 130.1 (C-4a), 129.0 (C-6), 124.1 (C-5), 117.9 (C-3), 19.0 (Me). LRMS (ESI) m/z calcd. For $[C_{11}H_{10}NO]^+$ 172.07, found 172.07.

4-Methyl-2-(tetrahydrofuran-2-yl)quinoline (4b)

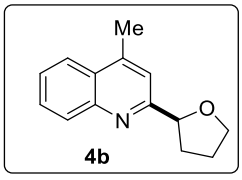

According to the general method for Minisci C-H cross-coupling, lepidine (92 µL, 0.698 mmol), 2-methylbut-2-ene (222 µL, 2.10

mmol), $Fe(acac)_2$ (36 mg, 0.140 mmol), TBHP (5.5 M in decanes, 191 µL, 1.05 mmol), TFA (107 µL, 1.40 mmol), in 4:1 THF/MeOH (0.2 M, 3.49 mL) at room temperature gave after purification by chromatography (hexane → hexane/AcOEt 75:25) **4b** (117 mg, 79%) as pale yellow powder. ^{1}H NMR (400 MHz, $CDCl_3$) δ 8.05 (d, *J* = 8.3 Hz, 1H, H-8), 7.96 (d, *J* = 8.5 Hz, 1H, H-5), 7.67 (ddd, *J* = 8.4, 6.9, 1.4 Hz, 1H, H-7), 7.52 (ddd, *J* = 8.2, 6.8, 1.3 Hz, 1H, H-6), 7.44 (s, 1H, H-3), 5.13 (t, *J* = 7.0 Hz, 1H, H-2'), 4.20–4.15 (m, 1H, H-5'), 4.06–4.01 (m, 1H, H-5'), 2.70 (d, *J* = 1.0 Hz, 3H, H-9), 2.54–2.48 (m, 1H, H-3'), 2.11–1.99 (m, 3H, H-3' and H-4'). ^{13}C NMR (101 MHz, $CDCl_3$) δ 163.2 (C-2), 147.4 (C-8a), 145.1 (C-4), 129.7 (C-8), 129.3 (C-7), 127.6 (C-4a), 125.9 (C-6), 123.8 (C-5), 118.7 (C-3), 82.2 (C-2'), 69.4 (C-5'), 33.5 (C-3'), 26.1 (C-4'), 19.0 (C-9).

1-(Tetrahydrofuran-2-yl)isoquinoline (4c)

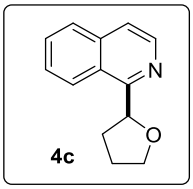

According to the general method for Minisci C-H cross-coupling, isoquinoline (100 mg, 0.774 mmol), 2-methylbut-2-ene (246 µL, 2.32 mmol), $Fe(acac)_2$ (39 mg, 0.155 mmol), TBHP (5.5 M in decanes, 211 µL, 1.16 mmol), TFA (119 µL, 1.55 mmol), in 4:1 THF/MeOH (0.2 M, 3.88 mL) at room temperature gave after purification by chromatography (hexane → hexane/AcOEt 50:50) **4c** (102 mg, 66%) as a brown oil. ^{1}H NMR (400 MHz, $CDCl_3$) d 8.48 (d, *J* = 5.7 Hz, 1H, H-3), 8.32 (d, *J* = 8.32 Hz, 1H, H-8), 7.80 (d, *J* = 8.2 Hz, 1H, H-5), 7.65 (td, *J* = 6.7, 1.2 Hz, 1H, H-6), 7.61–7.58 (m, 1H, H-7), 7.55 (d, *J* = 5.9 Hz, 1H, H-4), 5.71 (t, *J* = 7.1, 1H, H-2'), 4.17 (q, *J* = 6.7 Hz, 1H, H-5'), 4.03 (q, *J* = 6.5 Hz, 1H, H-5'), 2.56–2.47 (m, 1H, H-3'), 2.43–2.35 (m, 1H, H-3'), 2.22–2.04 (m, 2H, H-4'). ^{13}C NMR (101 MHz, $CDCl_3$) d 159.7 (C-1), 141.7 (C-3), 136.6 (C-4a), 129.9 (C-6), 127.4 (C-5), 127.2 (C-7), 126.6 (C-8a), 125.4 (C-8), 120.6 (C-4), 79.2 (C-2'), 69.1 (C-5'), 30.9 (C-3'), 26.2 (C-4').

2-(Tetrahydrofuran-2-yl)quinoline (4d) and 4-(Tetrahydrofuran-2-yl)quinoline (4d')

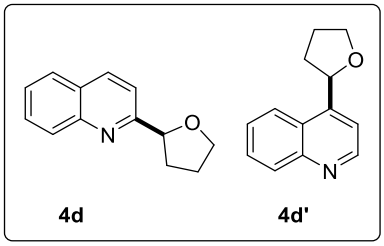

According to the general method for Minisci C-H cross-coupling, quinoline (92 µL, 0.774 mmol), 2-methylbut-2-ene (246 µL, 2.32 mmol), $Fe(acac)_2$ (39 mg, 0.155 mmol), TBHP (5.5 M in decanes, 211 µL, 1.16 mmol), TFA (119 µL, 1.55 mmol), in 4:1 THF/MeOH (0.2 M, 3.88 mL) at room temperature gave after purification by chromatography (hexane → hexane/AcOEt

75:25) **4d** (62 mg, 41%) and **4d'** (40 mg, 26%) as a yellow oil respectively. ^{1}H NMR (400 MHz, $CDCl_3$) of 3u δ 8.13 (d, *J* = 7.8 Hz, 1H, H-4), 8.05 (d, *J* = 8.6 Hz, 1H, H-8), 7.77 (dd, *J* = 8.1, 1.5 Hz, 1H, H-5), 7.67 (ddd, *J* = 8.5, 6.8, 1.5 Hz, 1H, H-7), 7.59 (d, *J* = 8.5 Hz, 1H, H-3), 7.48 (ddd, *J* = 8.0, 6.9, 1.1 Hz, 1H, H-6), 5.18 (t, *J* = 7.0 Hz, 1H, H-2'), 4.19–4.12 (m, 1H, H-5'), 4.06–3.99 (m, 1H, H-5'), 2.57–2.42 (m, 1H, H-3'), 2.12–1.96 (m, 3H, H-3' and H-4'). ^{1}H NMR (400 MHz, $CDCl_3$) of 3u' δ 8.85 (d, *J* = 4.5 Hz, 1H, H-2), 8.11 (d, *J* = 8.5 Hz, 1H, H-8), 7.87 (d, *J* = 8.5 Hz, 1H, H-5), 7.69–7.60 (m, 2H, H-6 and H-7), 7.51 (m, 1H, H-3), 5.57 (t, *J* = 7.1 Hz, 1H, H-2'), 4.21–4.15 (m, 1H, H-5'), 4.03–3.97 (m, 1H, H-5'), 2.60–2.53 (m, 1H, H-3'), 2.04–1.96 (m, 3H, H-3' and H-4'). Spectral data were identical to those previously reported.[320]

2-Methyl-4-(tetrahydrofuran-2-yl)quinoline (4e)

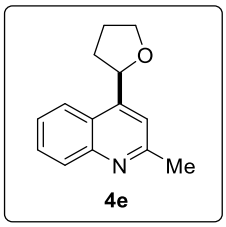

4e

According to the general method for Minisci C-H cross-coupling, 2-methyl quinoline (100 mg, 0.698 mmol), 2-methylbut-2-ene (222 µL, 2.09 mmol), $Fe(acac)_2$ (35 mg, 0.139 mmol), TBHP (5.5 M in decanes, 190 µL, 1.05 mmol), TFA (107 µL, 1.39 mmol), in 4:1 THF/MeOH (0.2 M, 3.50 mL) at room temperature gave after purification by chromatography (hexane → hexane/AcOEt 75:25) to give **4e** (110 mg, 74%) as a yellow oil. ^{1}H NMR (400 MHz, $CDCl_3$) δ 8.05 (dd, *J* = 8.8, 0.8 Hz, 1H, H-5), 7.84 (dd, *J* = 8.4, 2 Hz, 1H, H-8), 7.66 (ddd, *J* = 8.4, 6.8, 1.2 Hz, 1H, H-6), 7.48 (ddd, *J* = 8.4, 6.8, 1.2 Hz, 1H, H-7), 7.44 (s, 1H, H-3), 5.57 (t, *J* = 8 Hz, 1H, H-2'), 4.25–4.20 (m, 1H, H-5') and 4.07–4.01 (m, 1H, H-5'), 2.74 (s, 3H, Me), 2.65–2.57 (m, 1H, H-3'), 2.13–1.95 (m, 2H, H-4'), 1.88–1.79 (m, 1H, H-3'); ^{13}C NMR (101 MHz, $CDCl_3$) δ 159.2 (C-2), 149.5 (C-4), 147.9 (C-8a), 129.5 (C-5), 129.1 (C-6), 125.6 (C-7), 123.9 (C-4a), 123.1 (C-8), 117.3 (C-3), 76.9 (C-2'), 69.1 (C-5'), 25.6 (Me), 34.0 (C-3'), 26.1 (C-4').

Methyl 6-(tetrahydrofuran-2-yl)nicotinate (4j)

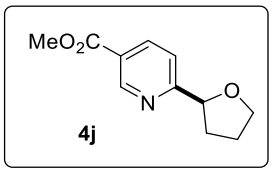

4j

According to the general method for Minisci C-H cross-coupling, methyl nicotinate (100 mg, 0.729 mmol), 2-methylbut-2-ene (232 µL, 2.19 mmol), $Fe(acac)_2$ (37 mg, 0.146 mmol), TBHP (5.5 M in decanes, 199 µL, 1.09 mmol), TFA (112 µL, 1.46 mmol), in 4:1 THF/MeOH (0.2 M, 3.65 mL) at room temperature gave after purification by chromatography (hexane → hexane/AcOEt 75:25) to give **4j** (69 mg, 44%) as a yellow oil. ^{1}H NMR (400 MHz, $CDCl_3$)

δ 9.13 (d, *J* = 2.2 Hz, 1H, H-2), 8.27 (dd, *J* = 8.2, 2.2 Hz, 1H, H-4), 7.54 (d, *J* = 8.1 Hz, 1H, H-5), 5.07 (t, *J* = 5.9 Hz, 1H, H-2'), 4.13–4.08 (m, 1H, H-5'), 4.02–3.97 (m, 1H, H-5'), 3.94 (s, 3H, OMe), 2.49–2.43 (m, 1H, H-3'), 2.01–1.93 (m, 3H, H-3' and H-4'). ^{13}C NMR (101 MHz, $CDCl_3$) δ 167.9 (C-7), 166.0 (C-6), 150.5 (C-2), 137.9 (C-4), 124.6 (C-3), 119.4 (C-5), 81.3 (C-2'), 69.4 (5'), 52.4 (OMe), 33.3 (C-3'), 25.9 (C-4').

4-Phenyl-2-(tetrahydrofuran-2-yl)pyridine (4k)

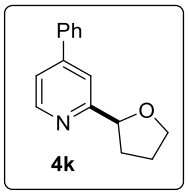

4k

According to the general method for Minisci C-H cross-coupling, 4-phenylpyridine (100 mg, 0.644 mmol), 2-methylbut-2-ene (205 µL, 1.93 mmol), $Fe(acac)_2$ (33 mg, 0.129 mmol), TBHP (5.5 M in decanes, 176 µL, 0.966 mmol), TFA (99 µL, 1.29 mmol), in 4:1 THF/MeOH (0.2 M, 3.22 mL) at room temperature gave after purification by chromatography (hexane → hexane/AcOEt 75:25) **4k** (7 mg, 5%) as a white powder. ^{1}H NMR (400 MHz, $CDCl_3$): δ 8.60 (d, *J* = 5.1 Hz, 1H, H-6), 7.68 (d, *J* = 1.6 Hz, 1H, H-5), 7.66 (s, 1H, H-3), 7.52–7.44 (m, 4H, Ph), 7.39 (dd, *J* = 5.2, 1.8 Hz, 1H, Ph), 5.10 (t, *J* = 6.7 Hz, 1H, H-2'), 4.17–4.12 (m, 1H, H-5'), 4.04–3.99 (m, 1H, H-5'), 2.50–2.44 (m, 1H, H-3'), 2.08–1.98 (m, 3H, H-3' and H-4'). Spectral data were identical to those previously reported.[321]

2-(Tetrahydrofuran-2-yl)quinoxaline (4m)

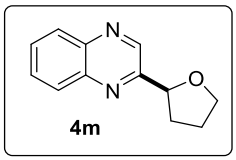

4m

According to the general method for Minisci C-H cross-coupling, quinoxaline (100 mg, 0.768 mmol), 2-methylbut-2-ene (244 µL, 2.31 mmol), $Fe(acac)_2$ (39 mg, 0.154 mmol), TBHP (5.5 M in decanes, 209 µL, 1.15 mmol), TFA (235 µL, 3.07 mmol), in 4:1 THF/MeOH (0.2 M, 3.77 mL) at room temperature gave after purification by chromatography (hexane → hexane/AcOEt 75:25) to give **4m** (109 mg, 71%) as a yellow oil. ^{1}H NMR (400 MHz, $CDCl_3$) δ 9.03 (s, 1H, H-3), 8.12–8.09 (m, 1H, H-5), 8.07–8.04 (m, 1H, H-8), 7.78–7.71 (m, 2H, H-6 and H-7), 5.23 (t, *J* = 6.4 Hz, 1H, H-2'), 4.22–4.16 (m, 1H, H-5') and 4.09–4.03 (m, 1H, H-5'), 2.57–2.49 (m, 1H, H-3') and 2.21–2.14 (m, 1H, H-3'), 2.11–2.04 (m, 2H, H-4'); ^{13}C NMR (101 MHz, $CDCl_3$) δ 157.8 (C-2), 143,7 (C-3), 142.0 (C-4a), 141.7 (C-8a), 130.2 (C-7), 129.6 (C-6), 129.4 (C-5), 129.2 (C-8), 80.7 (C-2'), 69.6 (C-5'), 33.1 (C-3'), 26.1 (C-4').

1-(Tetrahydrofuran-2-yl)phthalazine (4o) and 1-(Tetrahydrofuran-2-yl)-4-(tetrahydrofuran-2-yl)phthalazine (4o')

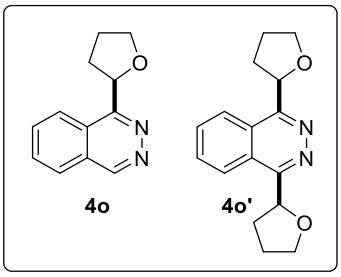

According to the general method for Minisci C-H cross-coupling, phtalazine (100 mg, 0.768 mmol), 2-methylbut-2-ene (244 µL, 2.31 mmol), $Fe(acac)_2$ (39 mg, 0.154 mmol), TBHP (5.5 M in decanes, 209 µL, 1.15 mmol), TFA (235 µL, 3.07 mmol), in 4:1 THF/MeOH (0.2 M, 3.77 mL) at room temperature gave after purification by chromatography (hexane → hexane/AcOEt 75:25) to give **4o** (94 mg, 46%) and **4o'** (45 mg, 30%) as a yellow oil. ^{1}H NMR **4o** (400 MHz, $CDCl_3$) δ 9.43 (s, 1H, H-4), 8.43–8.40 (m, 1H, H-8), 7.95–7.85 (m, 3H, H-5, H-6 and H-7), 5.68 (t, *J* = 7.2 Hz, 1H, H-2'), 4.11–3.99 (m, 2H, H-5'), 2.89–2.81 (m, 1H) and 2.43–2.35 (m, 1H, H-3'), 2.26–2.19 (m, 1H) and 2.16–2.09 (m, 1H, H-4'); ^{1}H NMR **4o'** (400 MHz, $CDCl_3$) δ 8.42–8.39 (m, 2H, H-5 and H-8), 7.86–7.83 (m, 2H, H-6 and H-7), 5.70–5.66 (m, 2H, H-2'), 4.04–3.95 (m, 4H, H-5'), 2.99–2.88 (m, 2H) and 2.37–2.28 (m, 2H, H-3'), 2.26–2.15 (m, 2H) and 2.14–2.03 (m, 2H, H-4'); ^{13}C NMR **4o**(101 MHz, $CDCl_3$) δ 158.1 (C-1), 151.6 (C-4), 132.5 (C-6), 132.1 (C-7), 127.1 (C-4a), 126.9 (C-5), 125.6 (C-8a), 125.0 (C-8), 79.2 (C-2'), 69.1 (C-5'), 29.6 (C-3'), 26.2 (C-4'); ^{13}C NMR **4o'** (101 MHz, $CDCl_3$) δ 158.0 and 157.9 (C-1 and C-4), 131.8 and 131.7 (C-6 and C-7), 126.1 (C-4a and C-8a), 125.4 and 125.3 (C-5 and C-8), 78.6 and 78.4 (C-2'), 69.1 and 69.0 (C-5'), 29.0 and 28.9 (C-3'), 26.1 and 26.0 (C-4').

5-(Benzo[*d*][1,3]dioxol-2-yl)pyrimidine (4r)

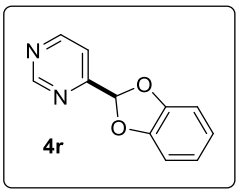

According to the general method for Minisci C-H cross-coupling, pyrimidine (99 µL, 1.25 mmol), 2-methylbut-2-ene (397 µL, 3.75 mmol), $Fe(acac)_2$ (64 mg, 0.250 mmol), TBHP (5.5 M in decanes, 227 µL, 1.87 mmol), TFA (382 µL, 5 mmol), in 4:1 1,3-benzodioxole/MeOH (0.2 M, 6.25 mL) at room temperature gave after purification by chromatography (hexane → hexane/AcOEt 75:25) to give **4r** (77 mg, 31%) as a brownish powder. ^{1}H NMR (400 MHz, $CDCl_3$) δ 9.33 (d, *J* = 1.4 Hz, 1H, H-2), 8.87 (d, *J* = 5.2 Hz, 1H, H-6), 7.67 (dd, *J* = 5.2, 1.4 Hz, 1H, H-5), 6.95 (s, 1H, H-2'), 6.88–6.78 (m, 4H, H-4', H-5', H-6' and H-7').

2-(Benzo[*d*][1,3]dioxol-2-yl)pyrazine (4s)

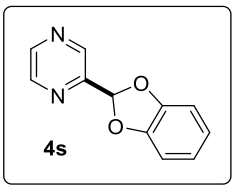

According to the general method for Minisci C-H cross-coupling, pyrazine (100 mg, 1.25 mmol), 2-methylbut-2-ene (397 µL, 3.75 mmol), $Fe(acac)_2$ (64 mg, 0.250 mmol), TBHP (5.5 M in decanes, 227 µL, 1.87 mmol), TFA (382 µL, 5 mmol), in 4:1 1,3-benzodioxole/MeOH (0.2 M, 6.25 mL) at room temperature gave after purification by chromatography (hexane → hexane/AcOEt 90:10) to give **4s** (103 mg, 41%) as a brownish powder. ^{1}H NMR (400 MHz, $CDCl_3$) δ 8.91 (s, 1H, H-3), 8.68–8.65 (m, 2H, H-5 and H-6), 7.05 (s, 1H, H-2'), 6.93-6.90 (m, 4H, H-4', H-5', H-6' and H-7'). ^{13}C NMR (101 MHz, $CDCl_3$) δ 150.7 (C-2), 147.1 (C-3a' and C-7a'), 146.1 (C-6), 144.4 (C-5), 142.9 (C-3), 122.4 (C-5' and C-6'), 109.1 (C-4' and C-7'), 108.0 (C-2').

Copies of ^{1}H and ^{13}C NMR spectra

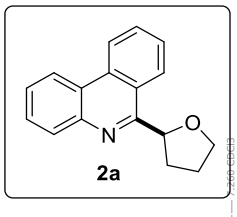

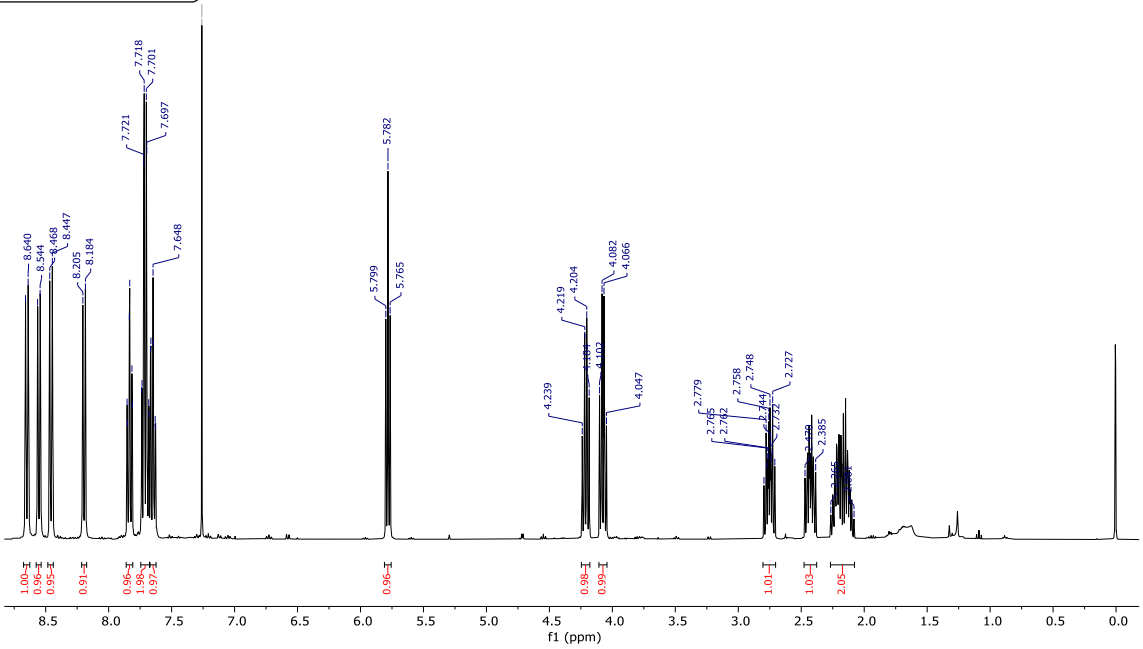

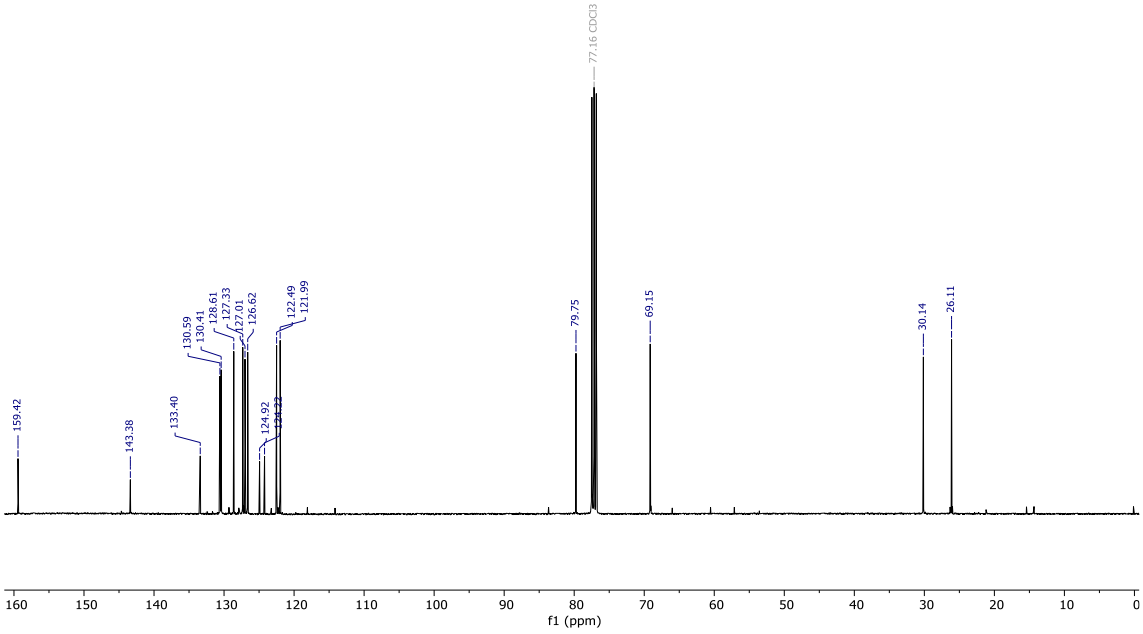

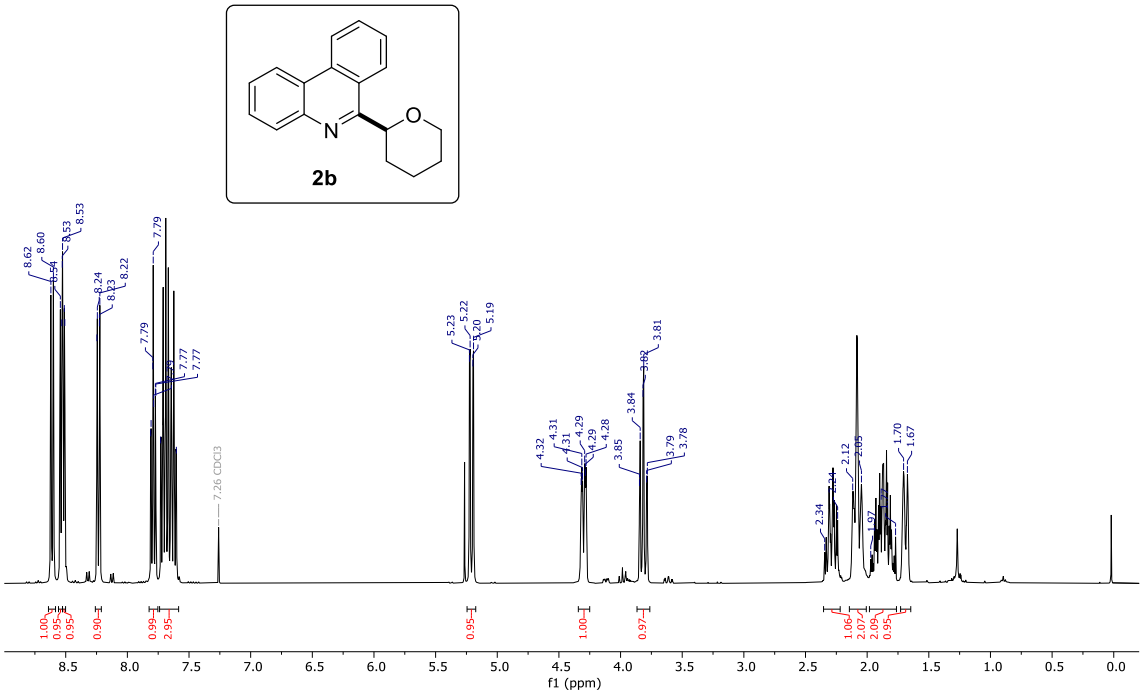
2b
8.62
8.60
8.54
8.53
8.24
8.23
8.22
7.79
7.77
7.77
7.26 CDCl3
5.23
5.22
5.20
5.19
4.32
4.31
4.31
4.29
4.29
4.28
3.85
3.84
3.82
3.81
3.79
3.78
2.34
2.24
2.12
2.09
1.97
1.70
1.67
1.00
0.95
0.95
0.90
0.99
2.95
0.95
1.00
0.97
1.06
2.07
2.09
0.95
f1 (ppm)

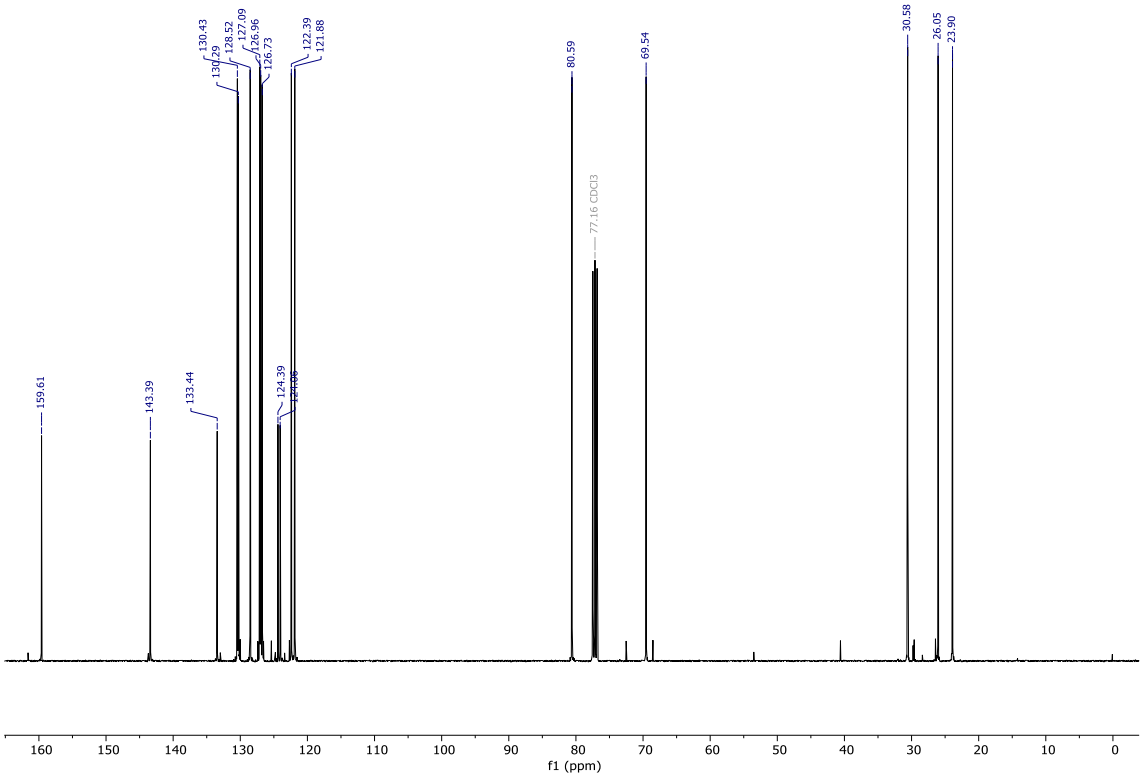
159.61
143.39
133.44
130.43
130.29
128.52
127.09
126.96
126.73
124.39
124.08
122.39
121.88
80.59
77.16 CDCl3
69.54
30.58
26.05
23.90
f1 (ppm)

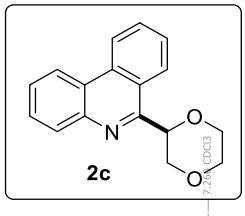
N
O
O
2c

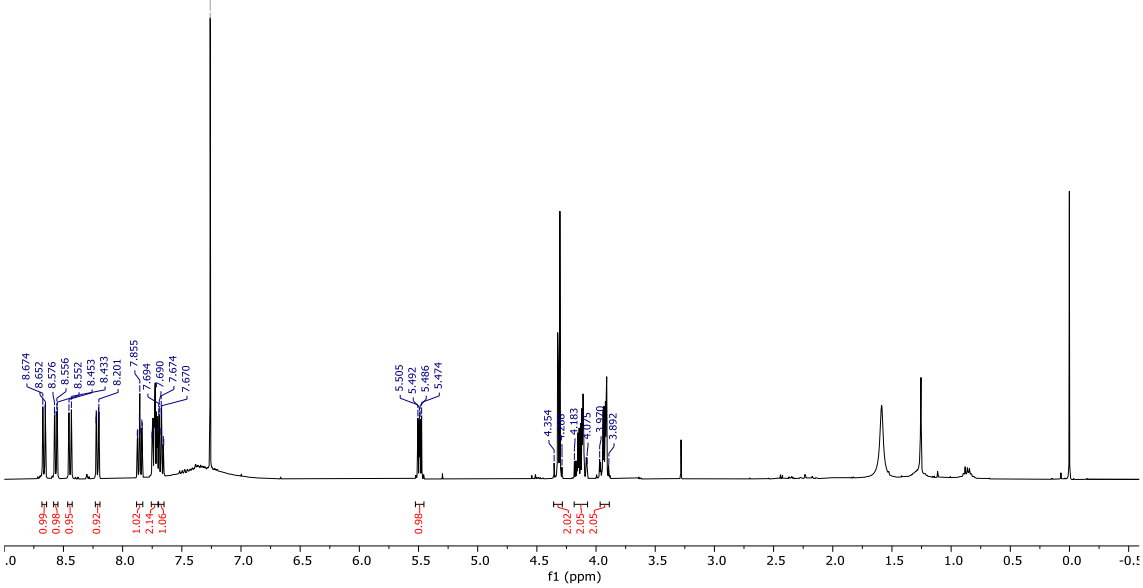
7.26 CDCl3
8.674
8.652
8.576
8.556
8.552
8.453
8.433
8.201
7.855
7.694
7.690
7.674
7.670
5.505
5.492
5.486
5.474
4.354
4.183
4.075
3.970
3.892
0.99
0.98
0.95
0.92
1.02
2.14
1.06
0.98
2.02
2.05
2.05
f1 (ppm)

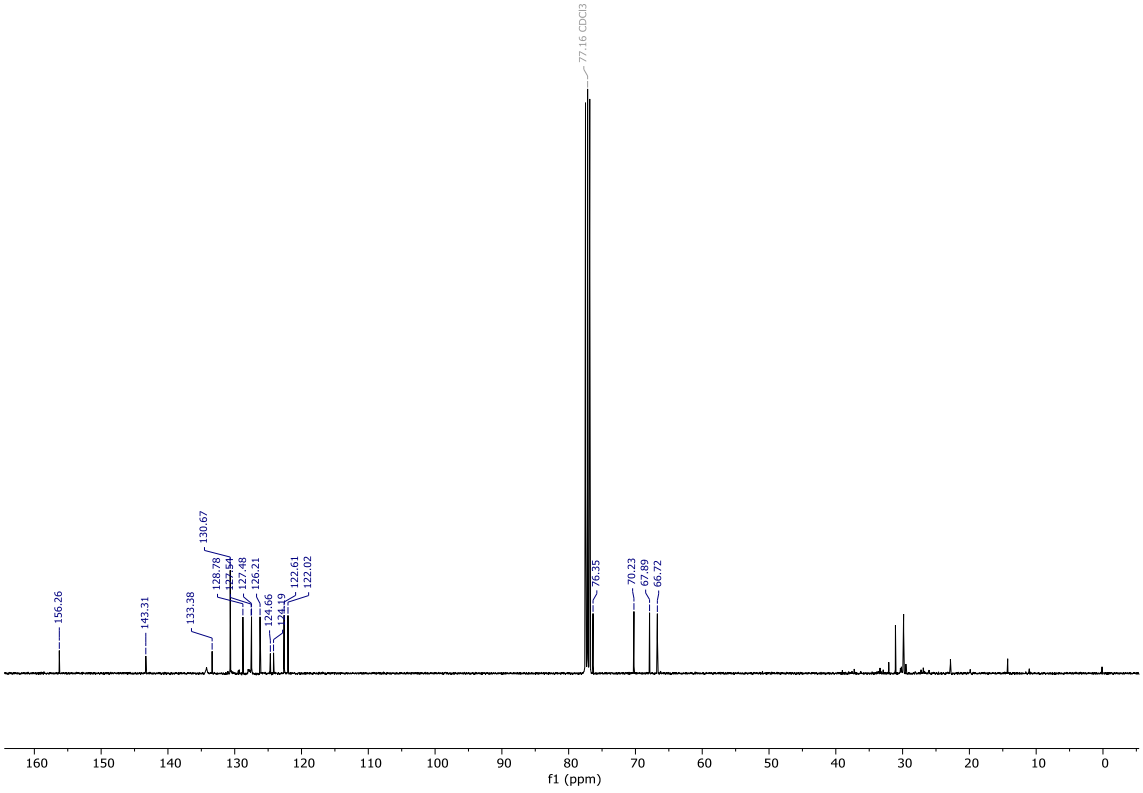
77.16 CDCl3
156.26
143.31
133.38
130.67
128.78
127.54
127.48
126.21
124.66
122.61
122.02
76.35
70.23
67.89
66.72
f1 (ppm)

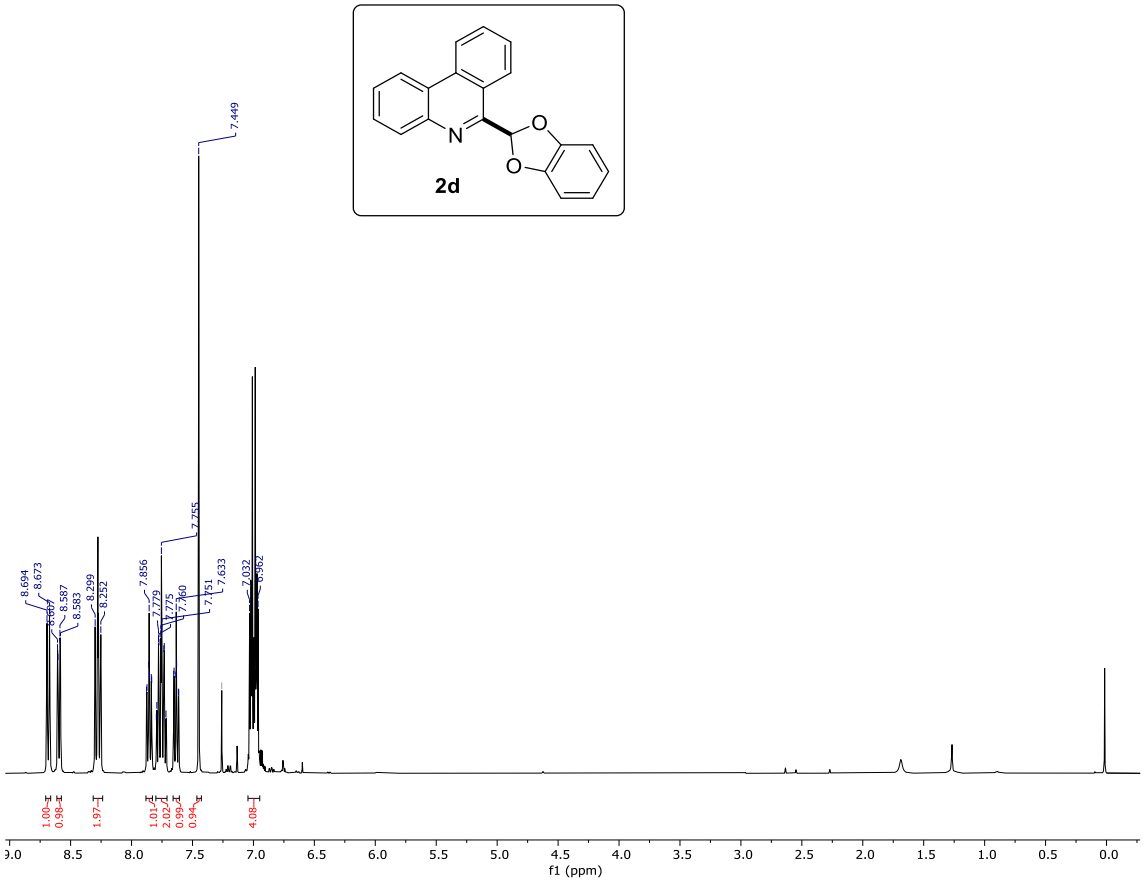
2d
7.449
8.694
8.673
8.587
8.583
8.299
8.252
7.856
7.779
7.775
7.760
7.755
7.751
7.633
7.032
6.962
1.00
0.98
1.97
1.01
2.02
0.99
0.94
4.08
f1 (ppm)

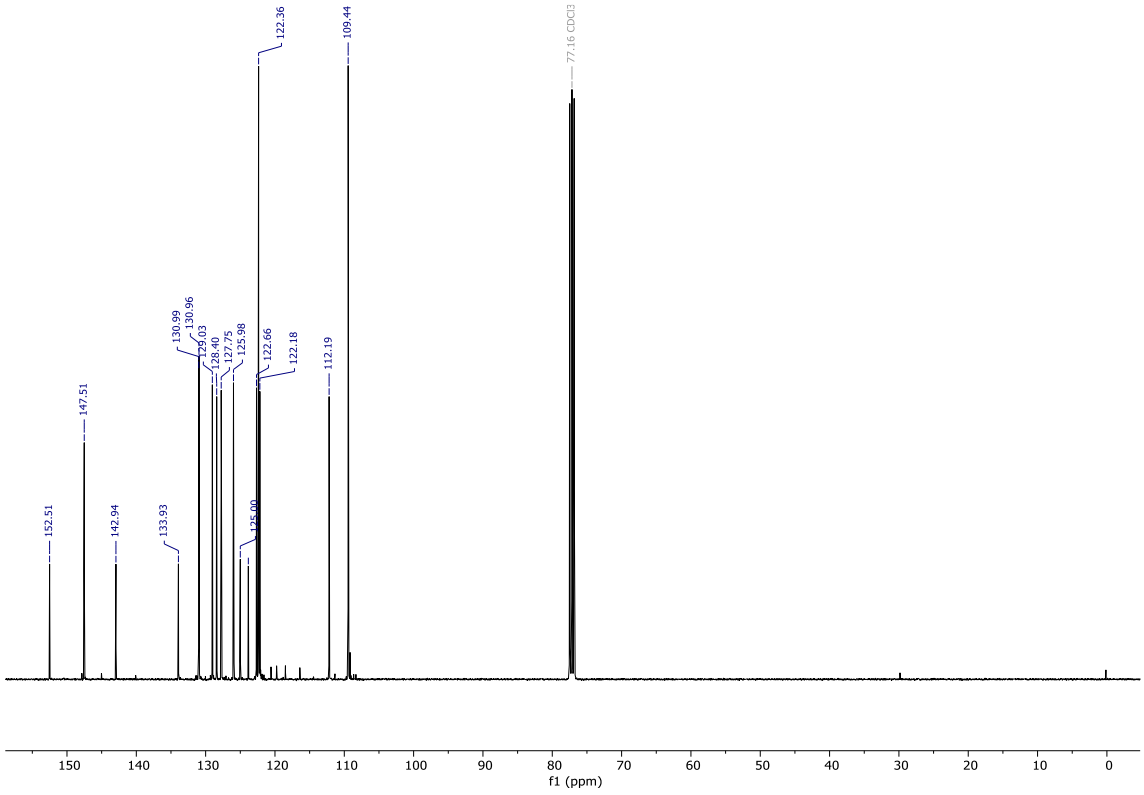
122.36
109.44
77.16 CDCl3
130.99
130.96
129.03
128.40
127.75
125.98
122.66
122.18
112.19
147.51
152.51
142.94
133.93
125.00
f1 (ppm)

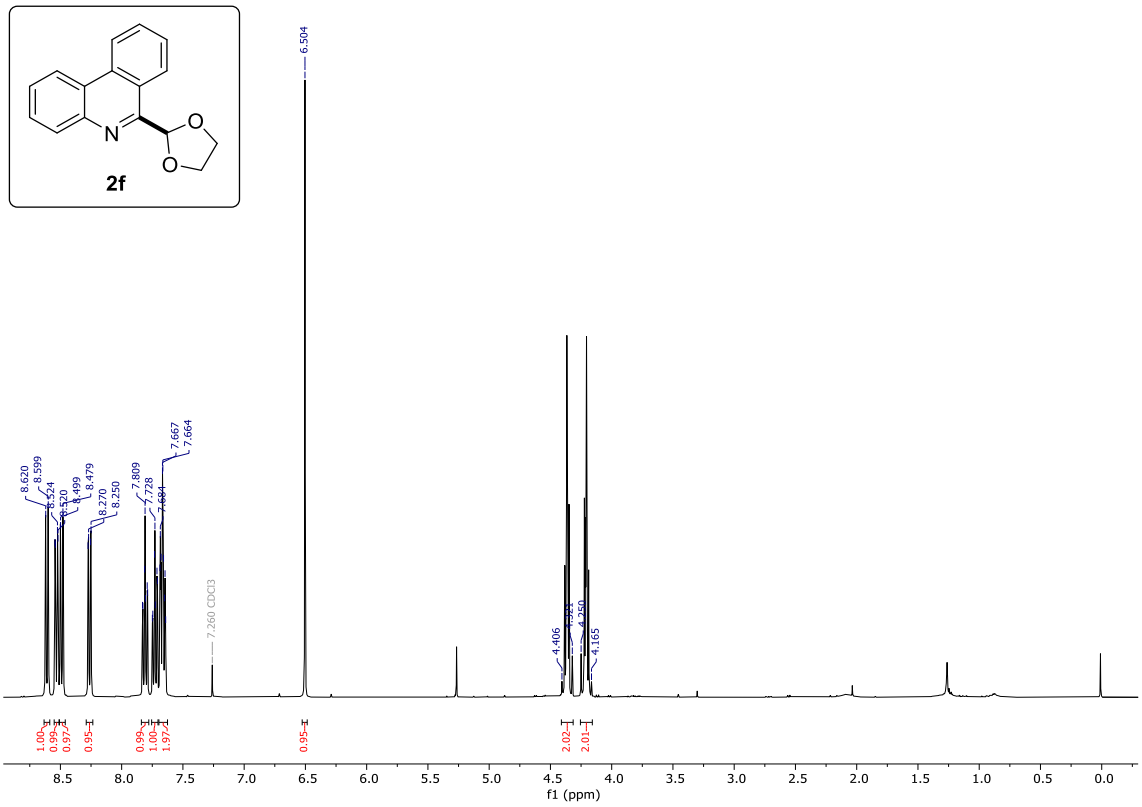
2f
6.504
8.620
8.599
8.524
8.520
8.499
8.479
8.270
8.250
7.809
7.728
7.684
7.667
7.664
7.260 CDCl3
4.406
4.250
4.165
1.05
0.99
0.97
0.95
0.99
1.00
1.97
0.95
2.02
2.01
f1 (ppm)

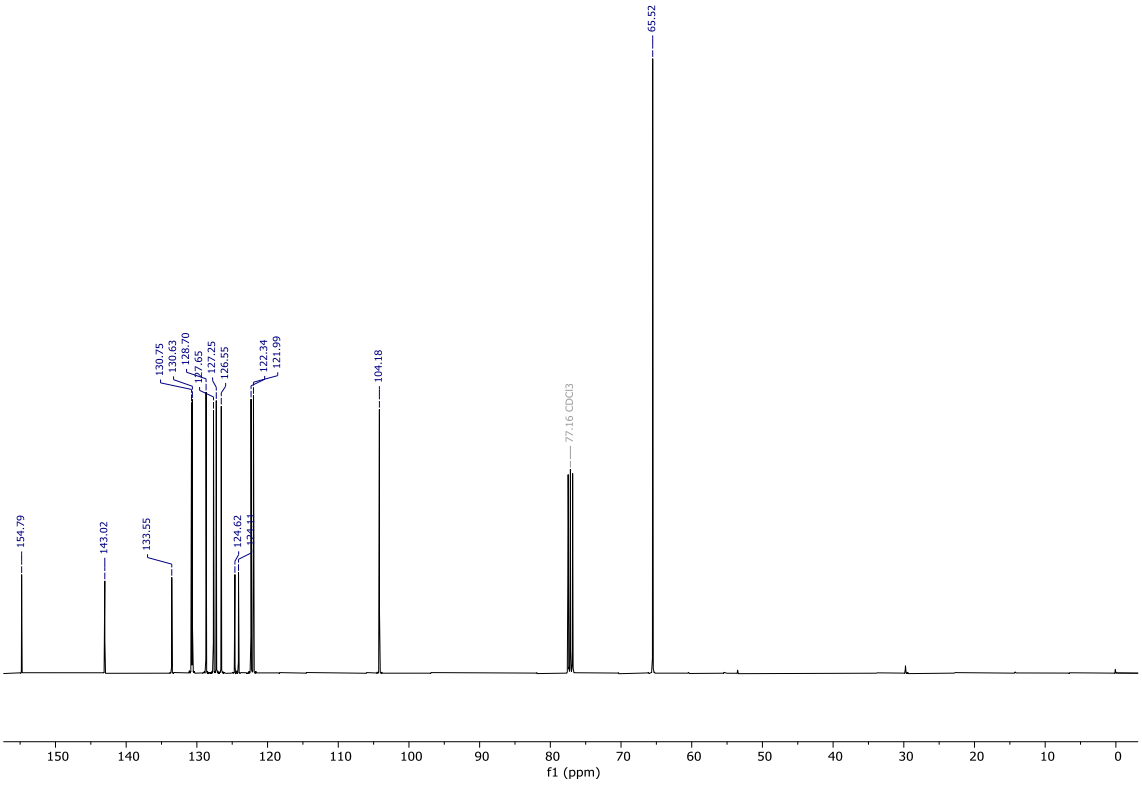
65.52
154.79
143.02
133.55
130.75
130.63
128.70
127.65
127.25
126.55
124.62
124.11
122.34
121.99
104.18
77.16 CDCl3
f1 (ppm)

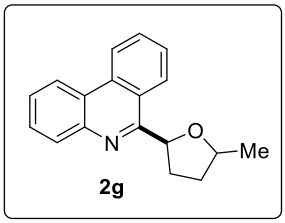
N
O
Me

2g

8.653
8.632
8.561
8.540
8.463
8.199
8.195
8.175
7.846
7.833
7.829
7.825
7.808
7.260 CDCl3
5.936
5.919
5.901
5.718
5.700
5.682
4.524
4.371
4.289
2.911
2.756
2.513
2.366
2.356
2.188
1.851
1.716
1.408
1.401
1.392
1.385
1.00
1.31
0.63
0.92
0.98
3.04
0.64
0.32
0.65
0.32
1.01
1.07
0.99
1.11
2.96
f1 (ppm)

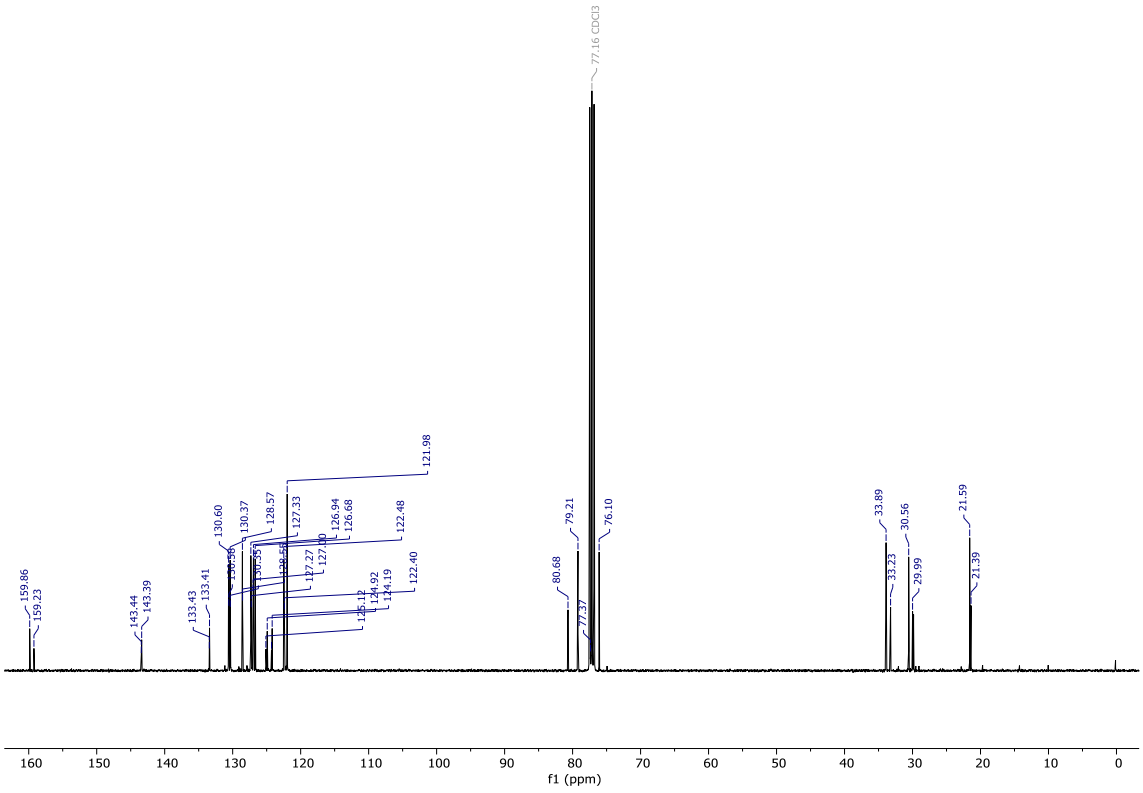
77.16 CDCl3
159.86
159.23
143.44
143.39
133.43
133.41
130.60
130.37
128.57
127.33
126.94
126.68
122.48
122.40
121.98
80.68
79.21
77.37
76.10
33.89
33.23
30.56
29.99
21.59
21.39
f1 (ppm)

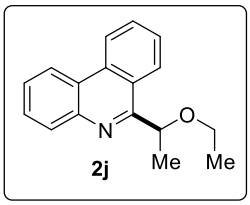
N
O
Me
Me

2j

8.894
8.874
8.618
8.597
8.501
8.197
8.176
8.173
7.790
7.708
7.687
7.674
7.260 CDCl3
5.241
5.224
5.258
5.207
3.621
3.427
1.800
1.783
1.229
1.211
1.194
f1 (ppm)

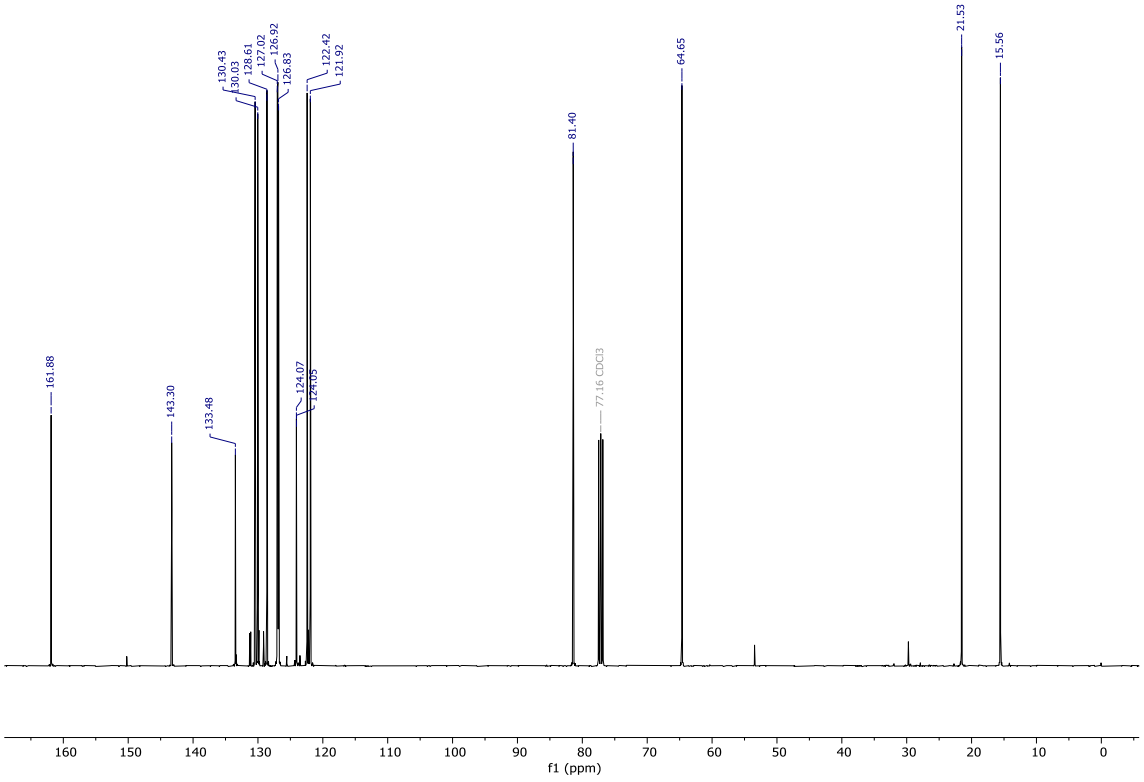
161.88
143.30
133.48
130.43
130.03
128.61
127.02
126.92
126.83
124.07
124.05
122.42
121.92
81.40
77.16 CDCl3
64.65
21.53
15.56
f1 (ppm)

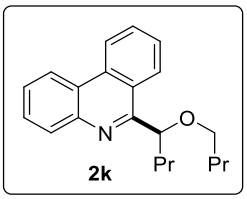
N
O
Pr
Pr

2k

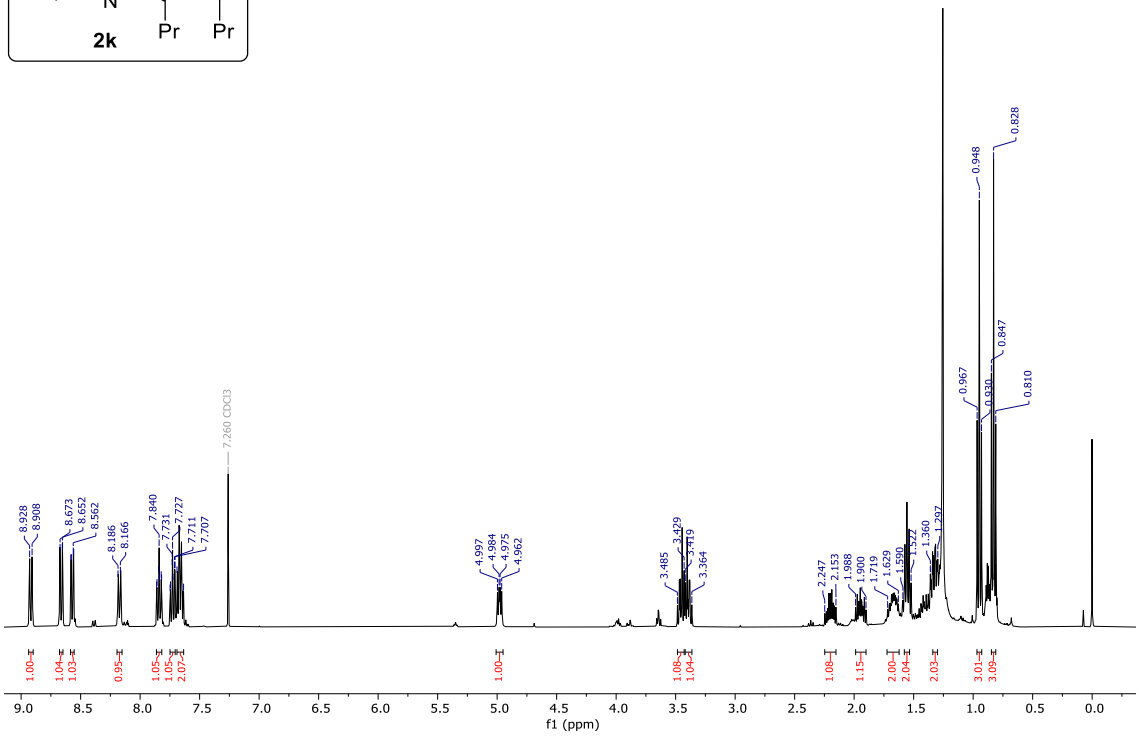
8.928
8.908
8.673
8.652
8.562
8.186
8.166
7.840
7.731
7.727
7.711
7.707
7.260 CDCl3
4.997
4.984
4.975
4.962
3.485
3.429
3.419
3.364
2.247
2.153
1.988
1.900
1.719
1.629
1.590
1.522
1.360
1.297
0.967
0.948
0.930
0.847
0.828
0.810
f1 (ppm)

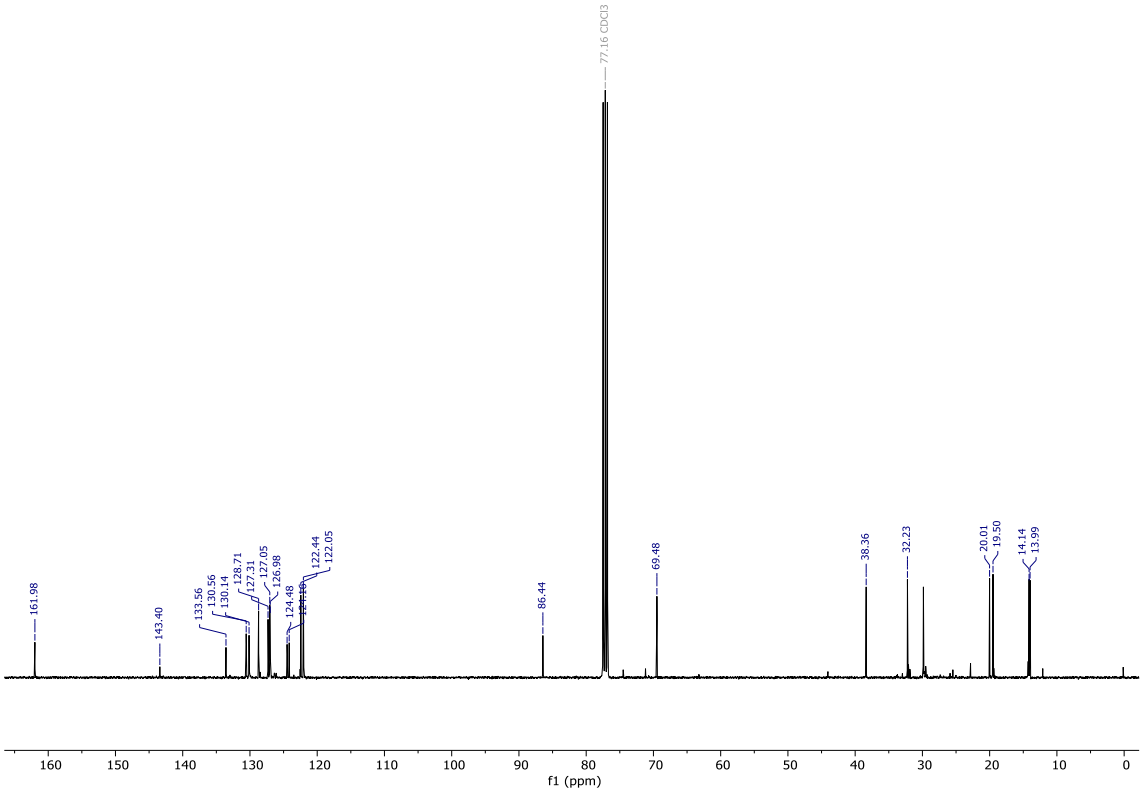
161.98
143.40
133.56
130.56
130.14
128.71
127.31
127.05
126.98
124.48
122.44
122.05
86.44
77.16 CDCl3
69.48
38.36
32.23
20.01
19.50
14.14
13.99
f1 (ppm)

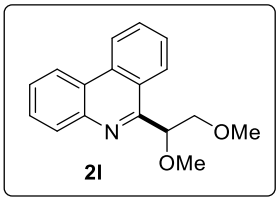
N
OMe
OMe

2l

3.447
3.445
8.748
8.727
8.679
8.657
8.557
8.227
8.211
8.207
7.873
7.869
7.852
7.831
7.761
7.260 CDCl3
5.340
5.331
5.320
5.311
4.165
4.144
4.138
4.118
3.848
3.839
3.822
1.00
1.01
1.00
0.96
1.00
3.08
0.94
1.01
1.00
6.04
f1 (ppm)

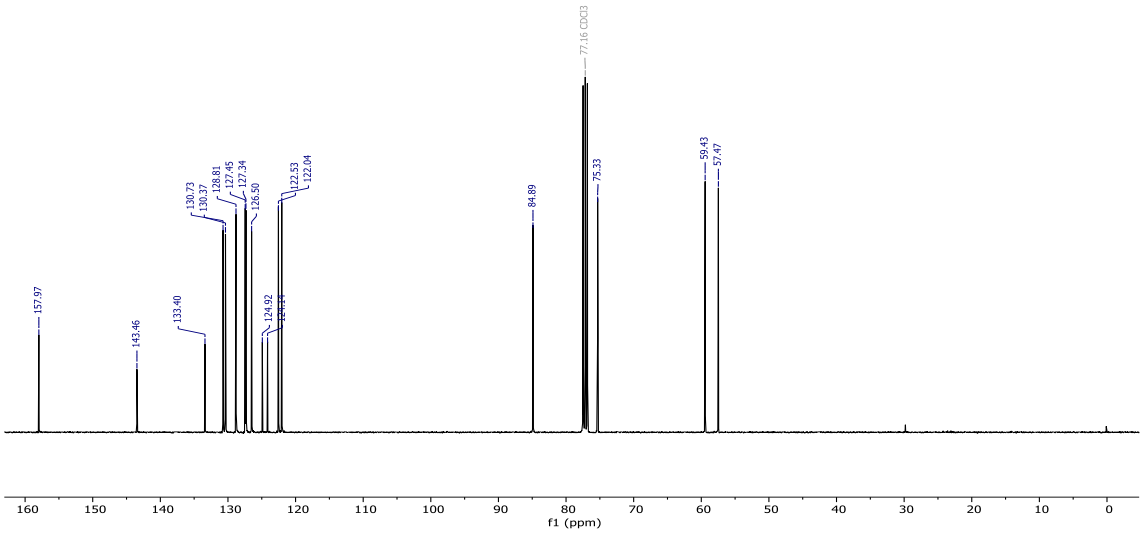
77.16 CDCl3
157.97
143.46
133.40
130.73
130.37
128.81
127.45
127.34
126.50
124.92
122.53
122.04
84.89
75.33
59.43
57.47
f1 (ppm)

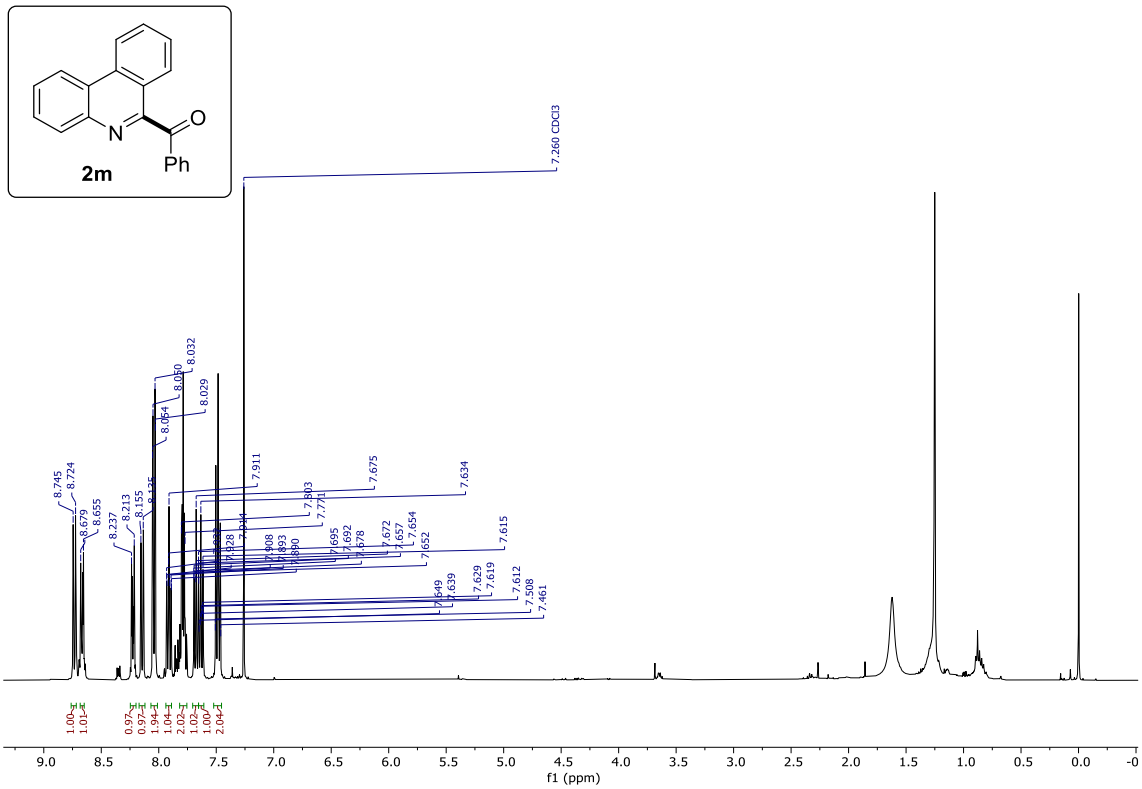
2m
N
O
Ph
7.260 CDCl3
8.745
8.724
8.679
8.655
8.237
8.213
8.155
8.135
8.064
8.050
8.032
8.029
7.911
7.803
7.791
7.675
7.634
7.672
7.657
7.654
7.652
7.615
7.695
7.692
7.678
7.629
7.619
7.612
7.508
7.461
1.00
1.01
0.97
0.97
1.94
1.04
2.03
1.02
1.00
2.04
f1 (ppm)

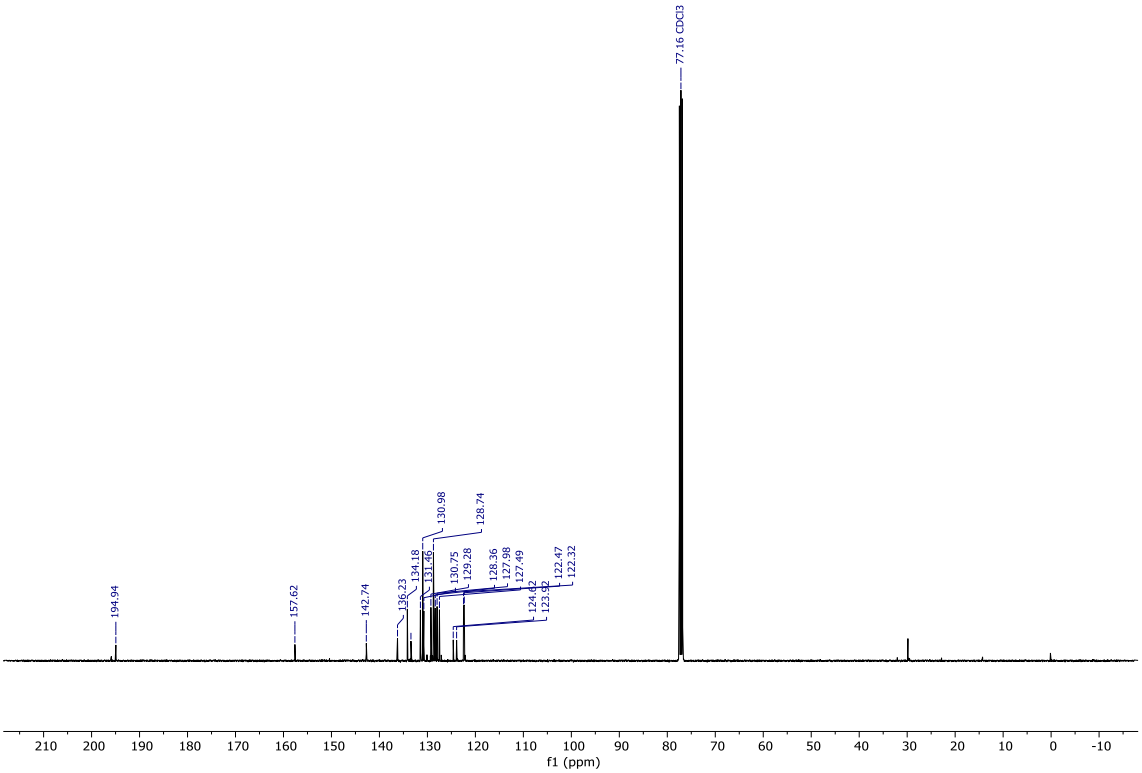
77.16 CDCl3
194.94
157.62
142.74
136.23
134.18
131.46
130.98
130.75
129.28
128.74
128.36
127.98
127.49
124.32
123.32
122.47
122.32
f1 (ppm)

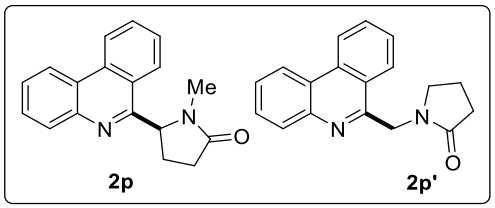
Me
N
O
N
N
O
2p
2p'

8.703
8.583
8.563
8.171
8.164
7.909
7.847
7.760
7.657
7.260 CDCl3
5.573
5.564
5.552
5.542
5.165
3.376
3.359
3.341
2.921
2.610
2.551
2.510
2.493
2.473
2.453
2.217
2.128
1.970
1.951
1.931
1.912
1.07
0.57
1.57
0.50
1.11
1.36
1.62
4.93
1.00
0.99
1.07
3.01
2.31
0.94
1.36
1.41
1.38
f1 (ppm)

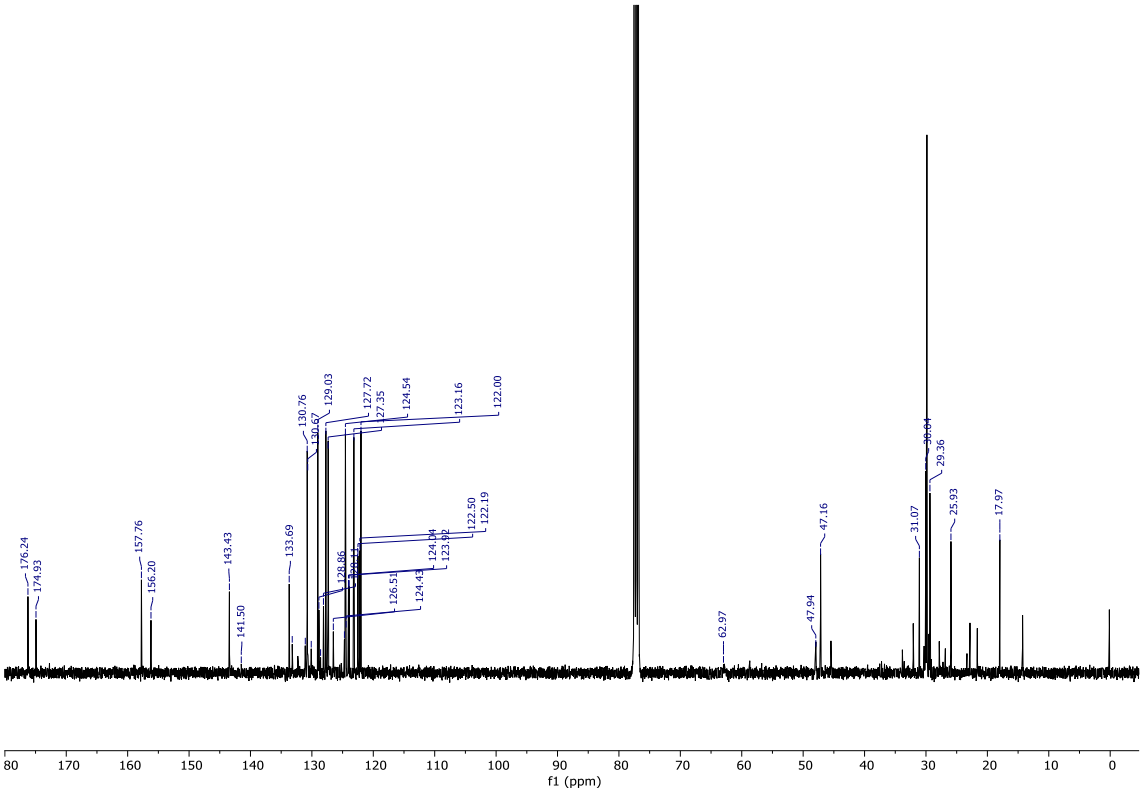
176.24
174.93
157.76
156.20
143.43
141.50
133.69
130.76
130.67
129.03
128.86
127.72
127.35
126.51
124.54
124.43
123.16
122.50
122.19
122.00
62.97
47.16
47.94
31.07
29.36
25.93
17.97
f1 (ppm)

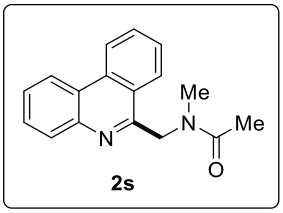
Me
N
N
Me
O

2s

3.005
2.194
5.319
7.260 CDCl3
8.648
8.627
8.576
8.572
8.555
8.552
8.443
8.423
8.150
8.147
7.853
7.850
7.832
7.829
0.22
1.00
1.11
0.97
1.08
1.05
3.21
1.95
0.44
0.71
3.00
3.01
0.73
f1 (ppm)

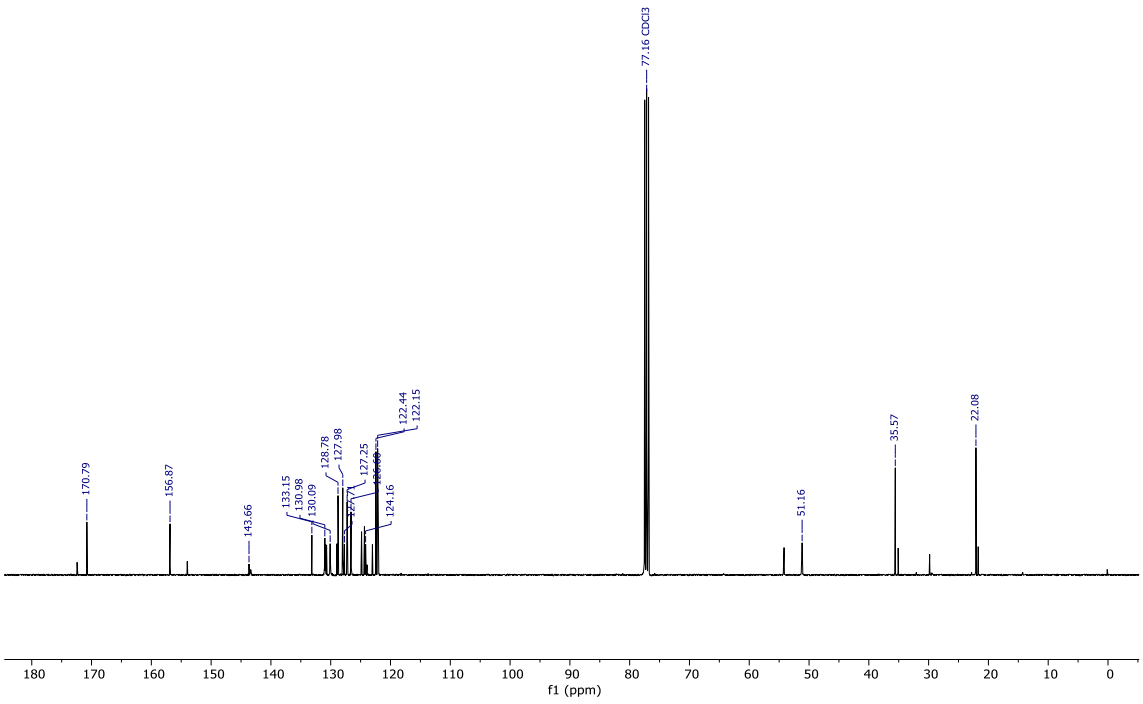
77.16 CDCl3
170.79
156.87
143.66
133.15
130.98
130.09
128.78
127.98
127.25
124.16
122.44
122.15
51.16
35.57
22.08
f1 (ppm)

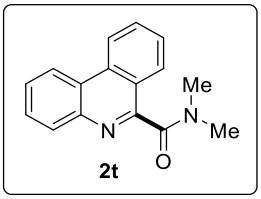
Me
N
Me
N
O

2t

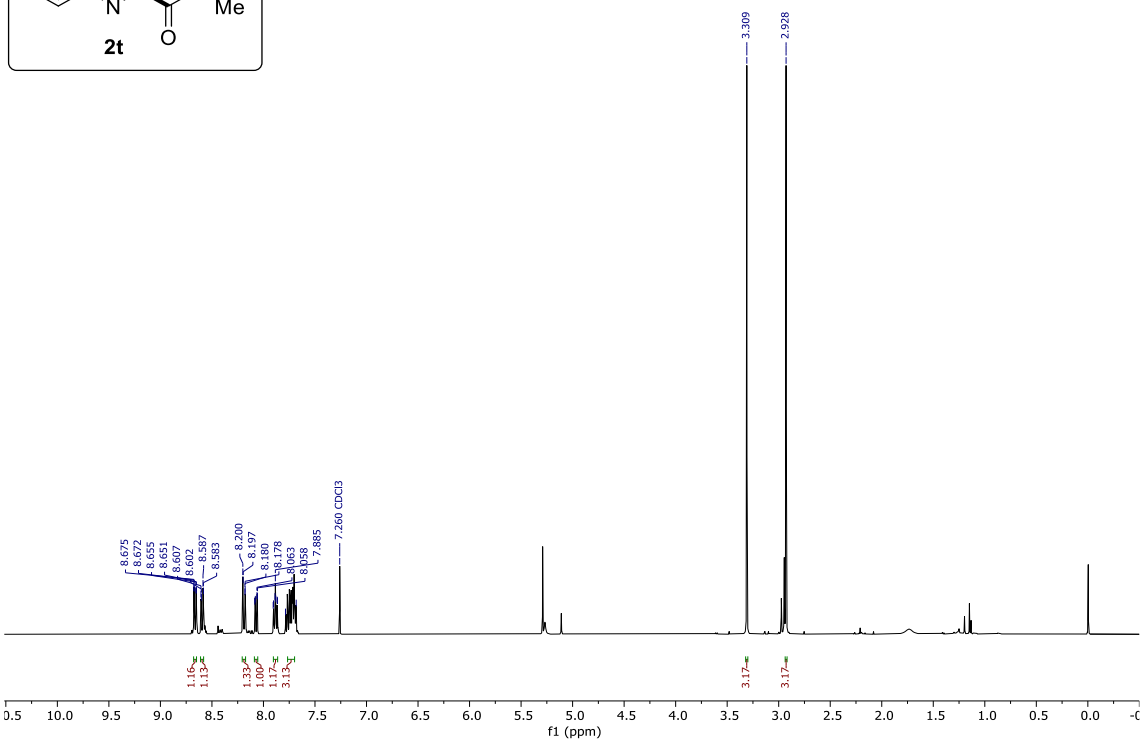
8.675
8.672
8.655
8.651
8.607
8.602
8.587
8.583
8.200
8.197
8.180
8.178
8.063
8.058
7.885
7.260 CDCl3
3.309
2.928
1.16
1.13
1.33
1.00
1.17
3.13
3.17
3.17
f1 (ppm)

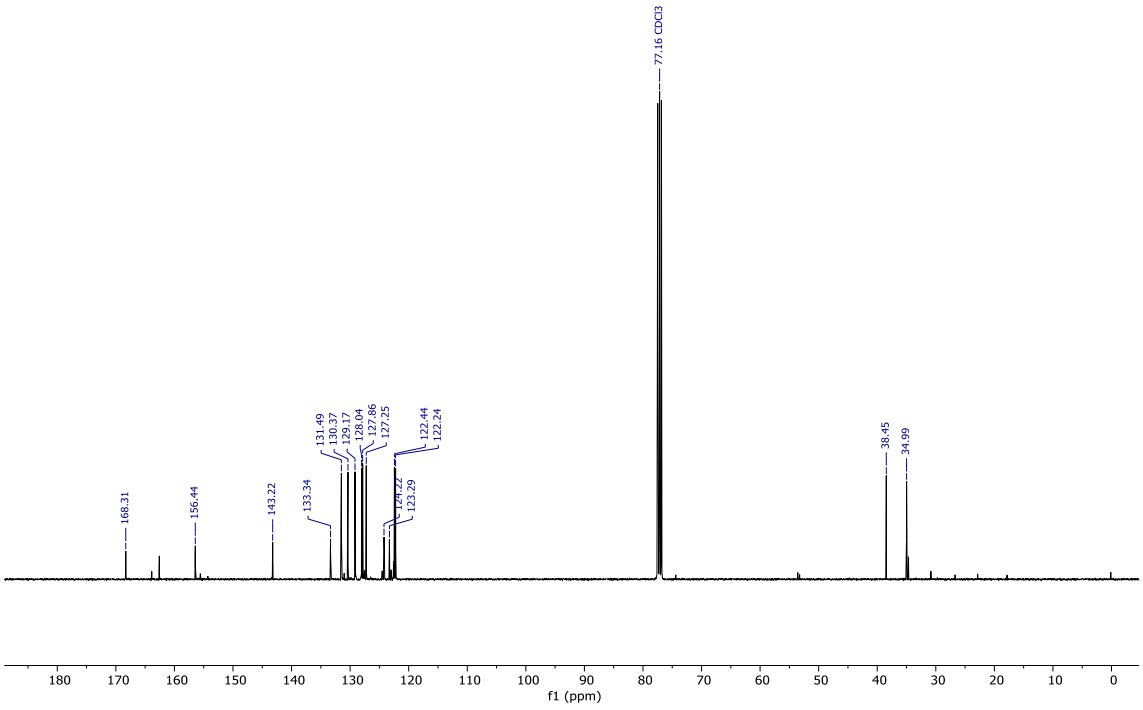
77.16 CDCl3
168.31
156.44
143.22
133.34
131.49
130.37
129.17
128.04
127.86
127.25
124.22
123.29
122.44
122.24
38.45
34.99
f1 (ppm)

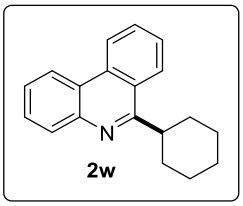
N
2w

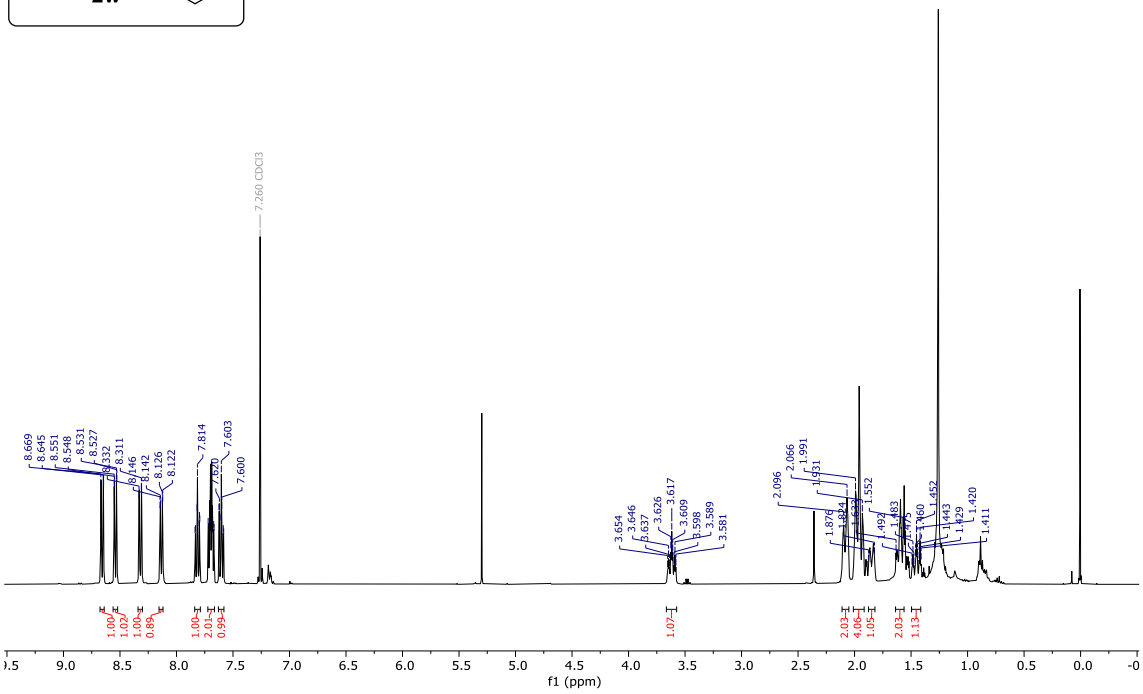
7.260 CDCl3
8.669
8.645
8.551
8.548
8.531
8.527
8.332
8.311
8.146
8.142
8.126
8.122
7.814
7.620
7.603
7.600
3.654
3.646
3.637
3.626
3.617
3.609
3.598
3.589
3.581
2.096
2.066
1.991
1.931
1.876
1.552
1.483
1.460
1.452
1.443
1.429
1.420
1.411
1.00
1.02
1.00
0.89
1.00
2.01
0.99
1.07
2.03
4.06
1.05
2.03
1.13
f1 (ppm)

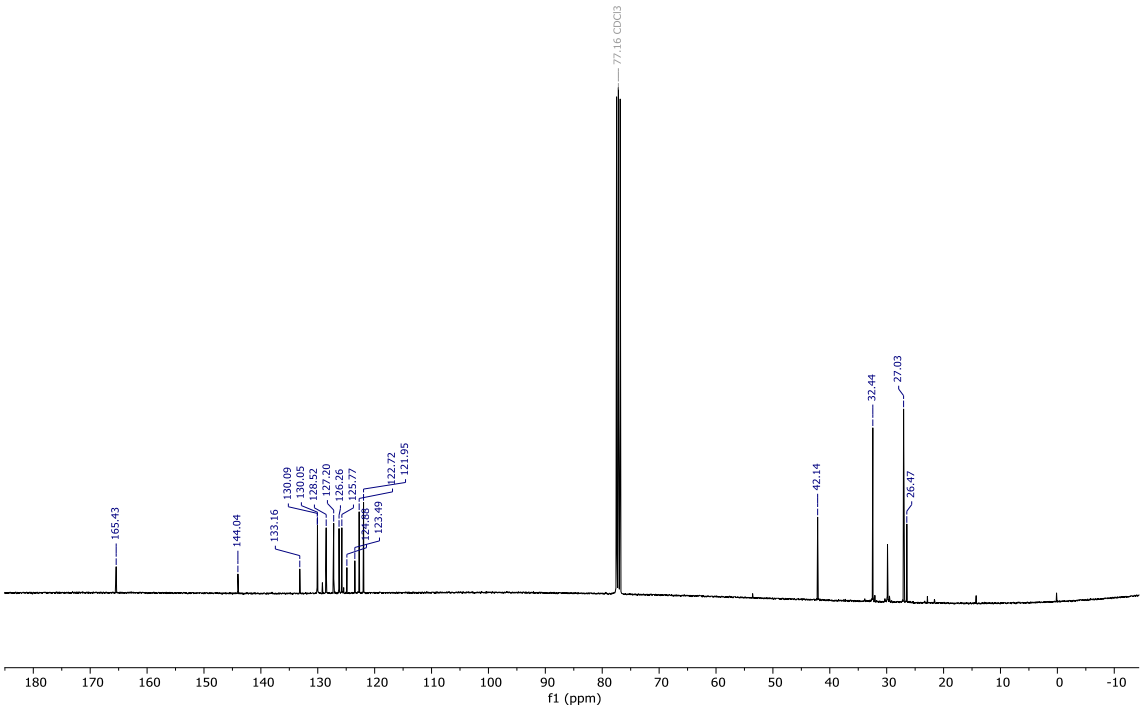
77.16 CDCl3
165.43
144.04
133.16
130.09
130.05
128.52
127.20
126.26
125.77
123.49
122.72
121.95
42.14
32.44
27.03
26.47
f1 (ppm)

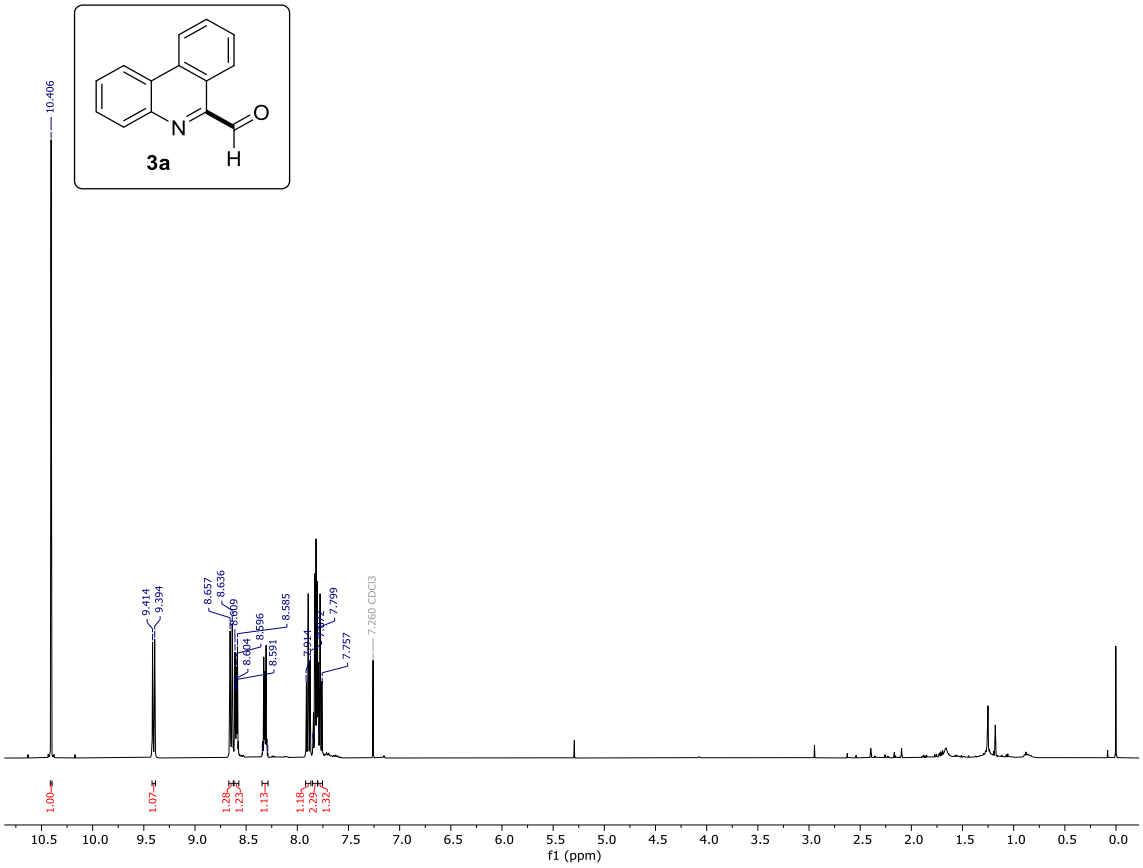
3a
10.406
9.414
9.394
8.657
8.636
8.596
8.585
8.591
7.914
7.799
7.757
7.260 CDCl3
1.00
1.07
1.28
1.23
1.13
1.18
2.29
1.32
f1 (ppm)

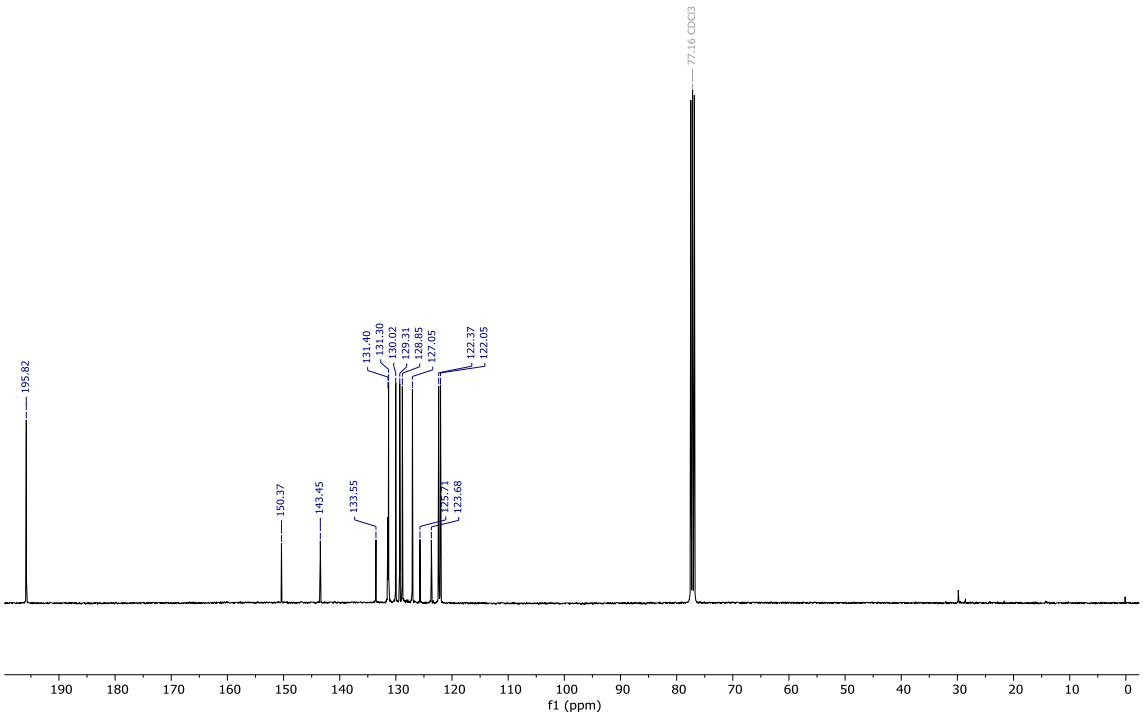
195.82
150.37
143.45
133.55
131.40
131.30
130.03
129.31
128.85
127.05
125.71
123.68
122.37
122.05
77.16 CDCl3
f1 (ppm)

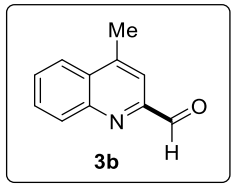
Me
N
O
H

3b

10.162
8.222
8.220
8.203
8.201
8.199
8.005
8.003
7.817
7.776
7.690
7.687
7.669
7.260 CDCl3
2.736
0.92
1.00
1.06
0.97
1.04
1.02
3.09
f1 (ppm)

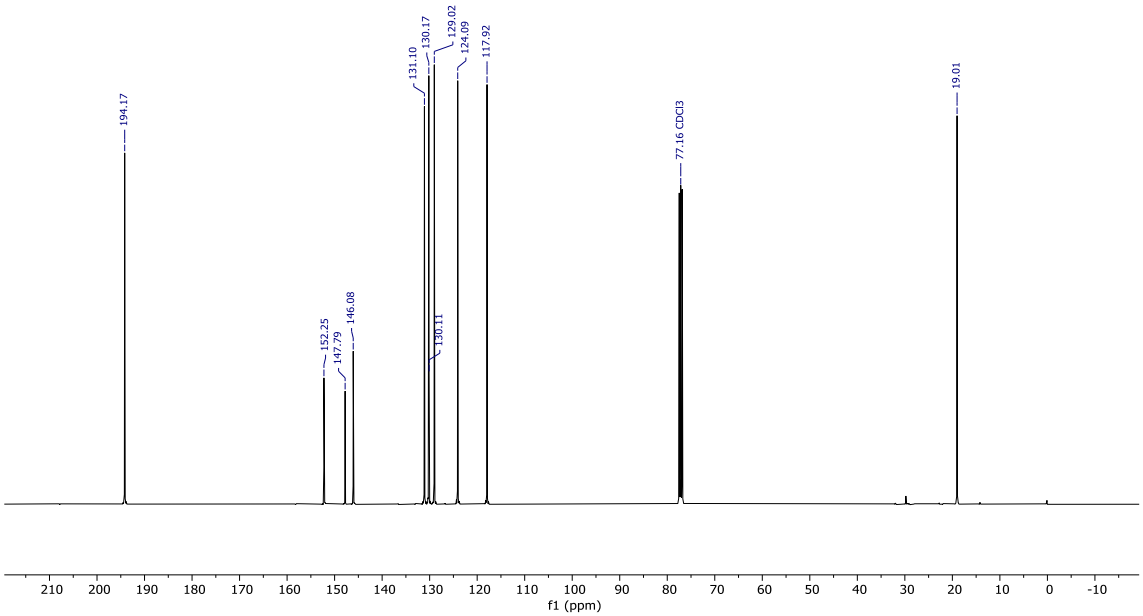
194.17
152.25
147.79
146.08
131.10
130.17
130.11
129.02
124.09
117.92
77.16 CDCl3
19.01
f1 (ppm)

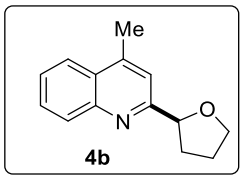
Me
N
O

4b

8.06
8.04
7.98
7.96
7.70
7.68
7.67
7.66
7.65
7.54
7.53
7.52
7.51
7.50
7.49
7.44
7.26 CDCl3
5.15
5.13
5.12
4.20
4.18
4.16
4.06
4.04
4.02
4.01
2.71
2.70
2.54
2.48
2.11
1.99
0.94
1.02
1.04
1.09
0.92
0.93
0.99
0.98
3.00
1.05
3.20
f1 (ppm)

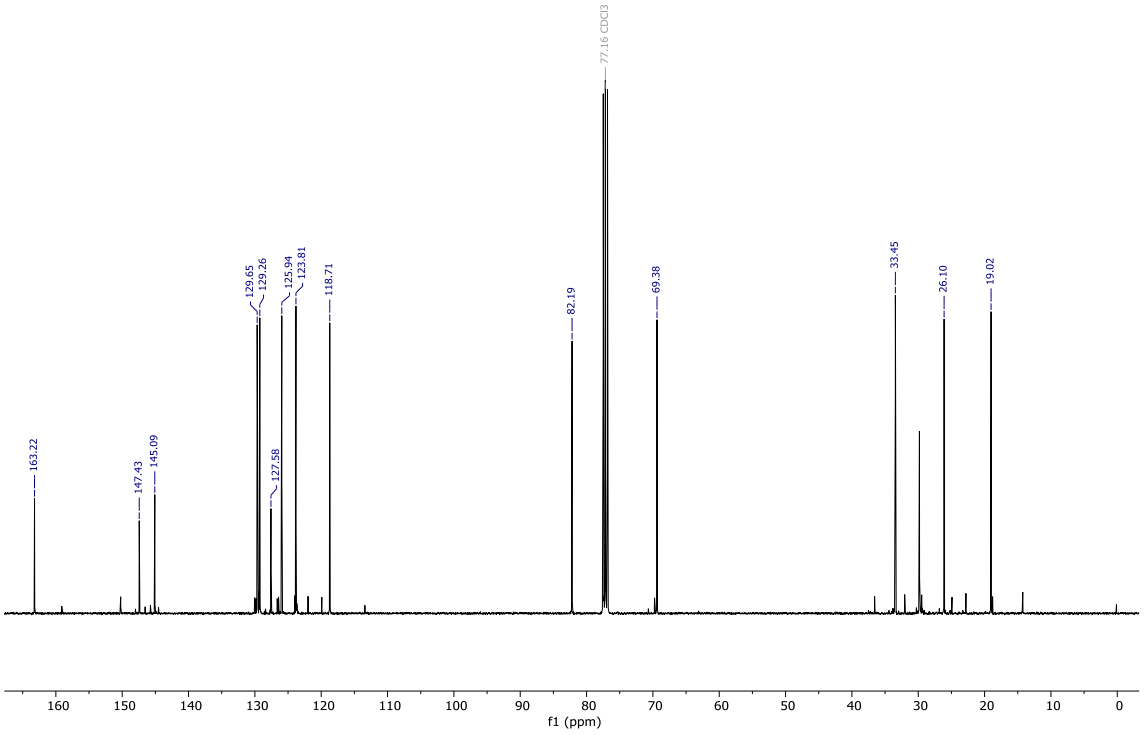
163.22
147.43
145.09
129.65
129.26
127.58
125.94
123.81
118.71
82.19
77.16 CDCl3
69.38
33.45
26.10
19.02
f1 (ppm)

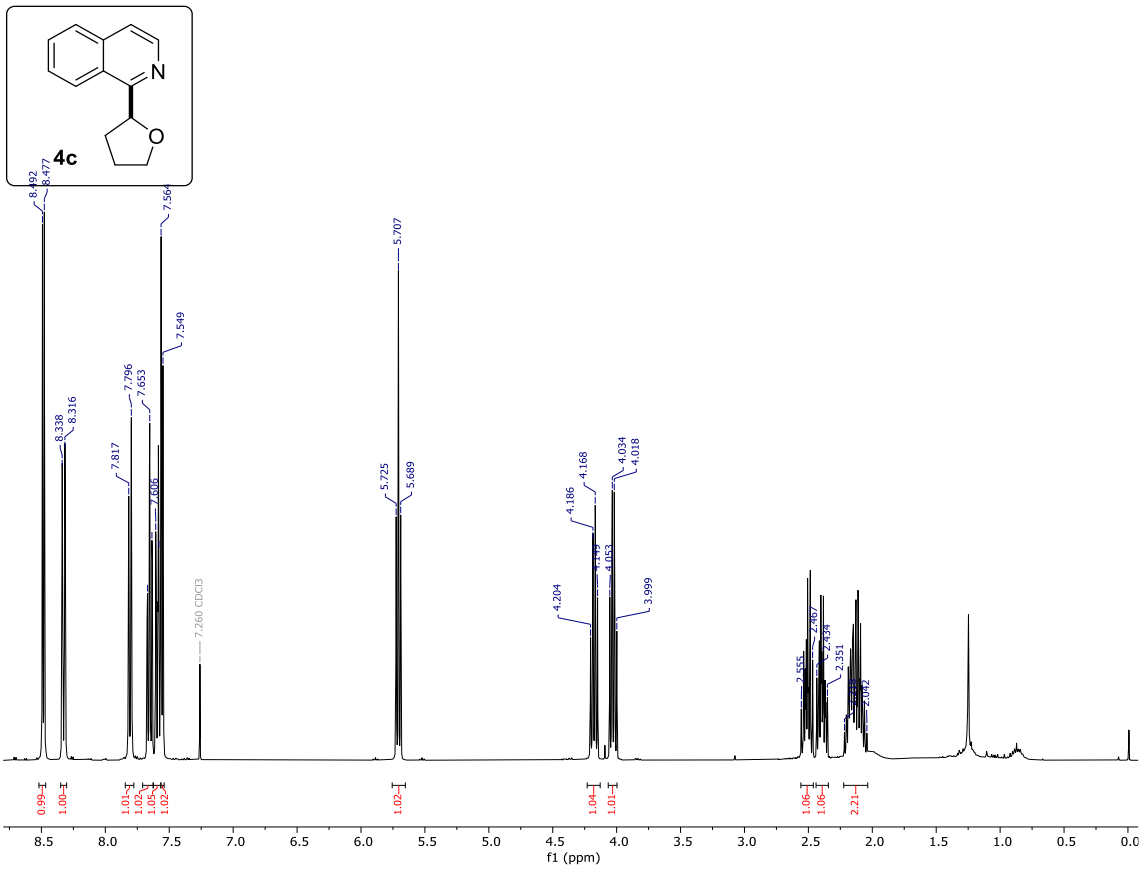
4c
8.492
8.477
7.564
5.707
7.549
7.796
7.653
8.338
8.316
7.817
7.606
5.725
5.689
4.186
4.168
4.034
4.018
4.204
4.053
3.999
7.260 CDCl3
2.555
2.487
2.434
2.351
2.092
0.99
1.00
1.01
1.02
1.05
1.02
1.02
1.04
1.01
1.06
1.06
2.21
f1 (ppm)

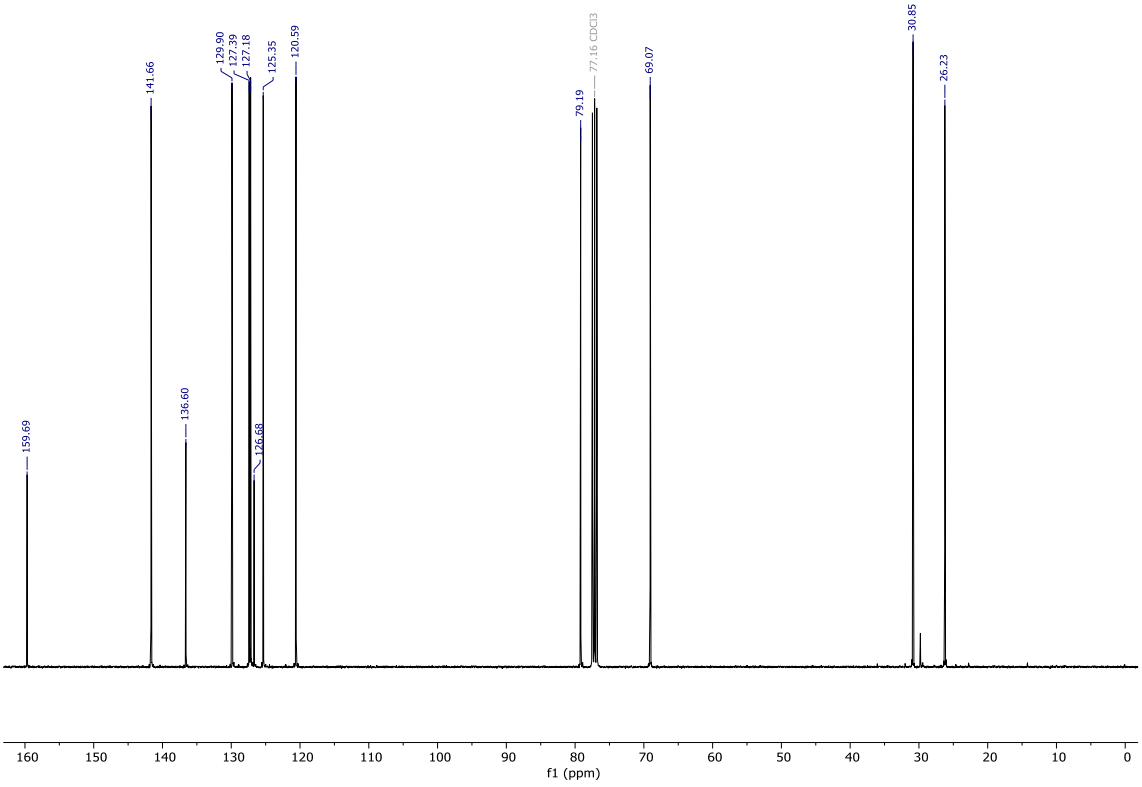
159.69
141.66
136.60
129.90
127.39
127.18
126.68
125.35
120.59
79.19
77.16 CDCl3
69.07
30.85
26.23
f1 (ppm)

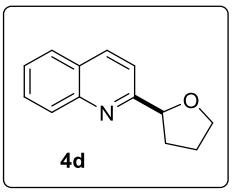
N
O

4d

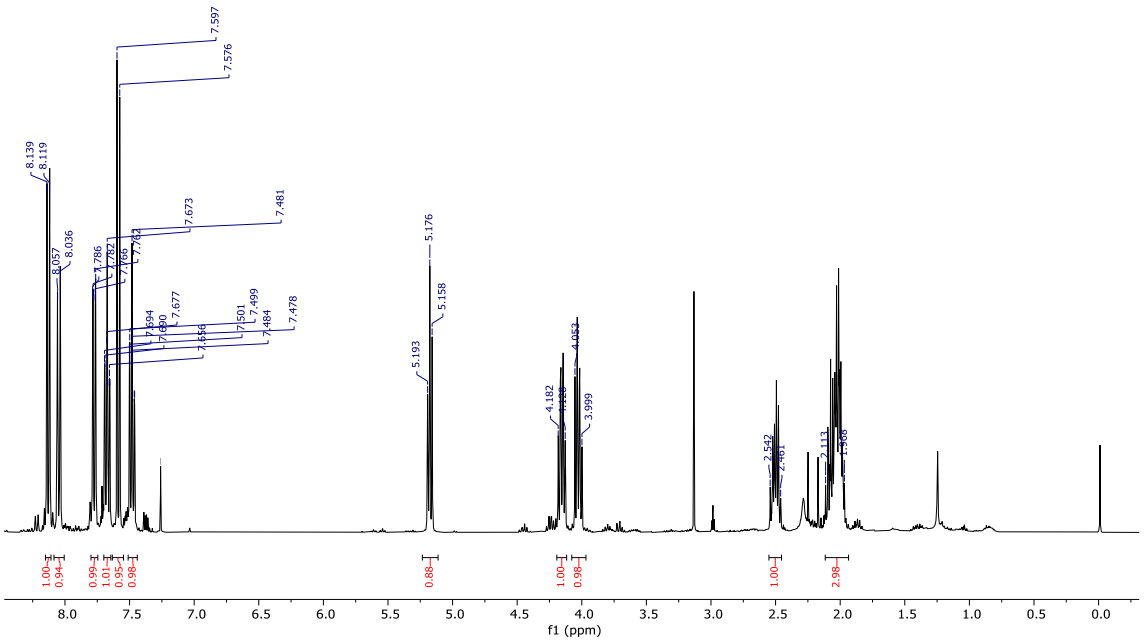
7.597
7.576
8.139
8.119
8.057
8.036
7.786
7.782
7.765
7.743
7.673
7.481
7.677
7.694
7.680
7.656
7.501
7.499
7.484
7.478
5.176
5.158
5.193
4.182
4.053
3.999
2.542
2.113
1.988
1.00
0.94
0.99
1.01
0.95
0.98
0.88
1.00
0.98
1.00
2.98
f1 (ppm)

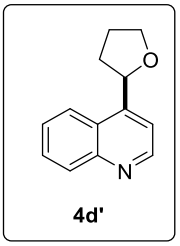
O
N

4d'

8.859
8.848
8.119
8.098
7.878
7.857
7.683
7.525
7.501
7.260 CDCl3
5.568
5.552
5.587
4.205
4.152
4.027
3.971
2.592
2.542
2.027
1.963
1.00
0.99
1.02
1.99
1.03
1.07
1.07
1.06
1.02
3.06
f1 (ppm)

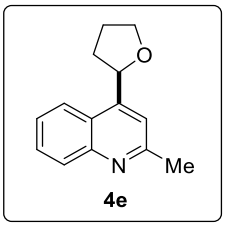
O
N
Me

4e

2.739
8.063
8.061
8.041
8.039
7.856
7.851
7.835
7.830
7.683
7.680
7.666
7.662
7.645
7.641
7.500
7.497
7.483
7.479
7.476
7.462
7.439
7.442
7.260 CDCl3
5.592
5.572
5.556
4.253
4.200
4.068
4.012
2.652
2.566
2.131
1.954
1.880
1.796
1.00
1.01
1.07
1.03
0.95
1.03
1.09
1.12
3.13
1.12
2.34
1.08
f1 (ppm)

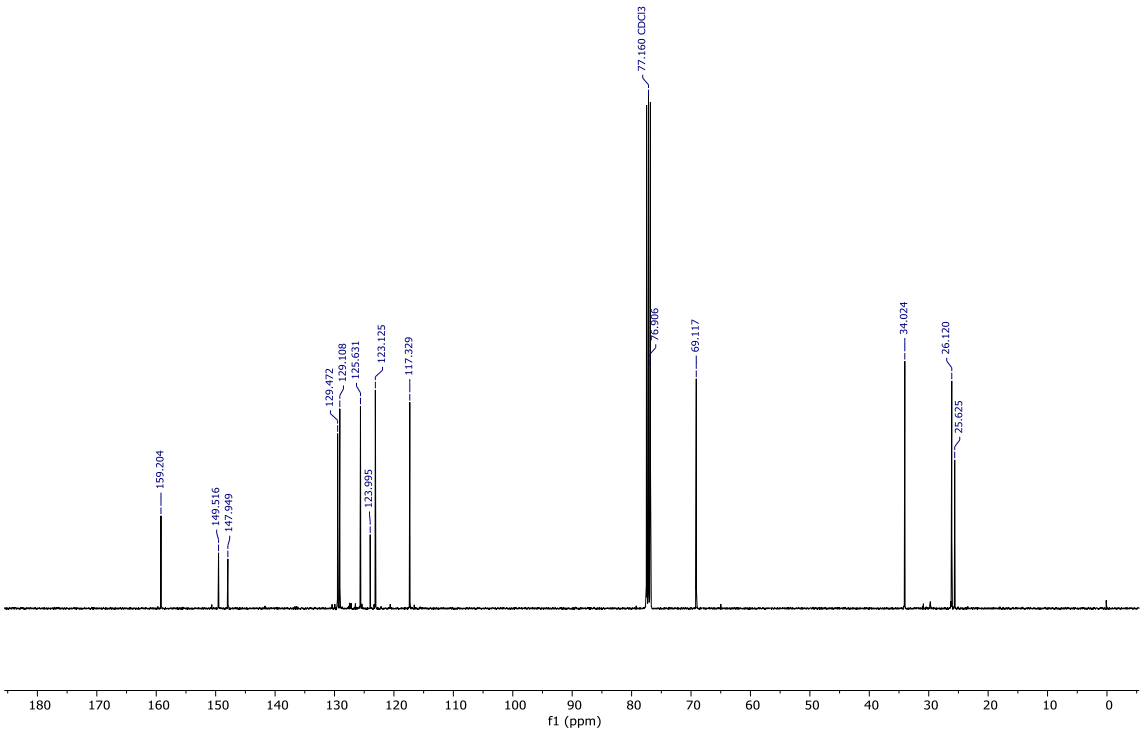
77.160 CDCl3
159.204
149.516
147.949
129.472
129.108
125.631
123.995
123.125
117.329
76.906
69.117
34.024
26.120
25.625
f1 (ppm)

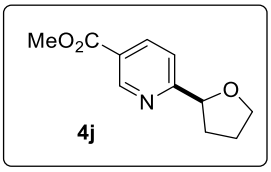
MeO2C
N
O

4j

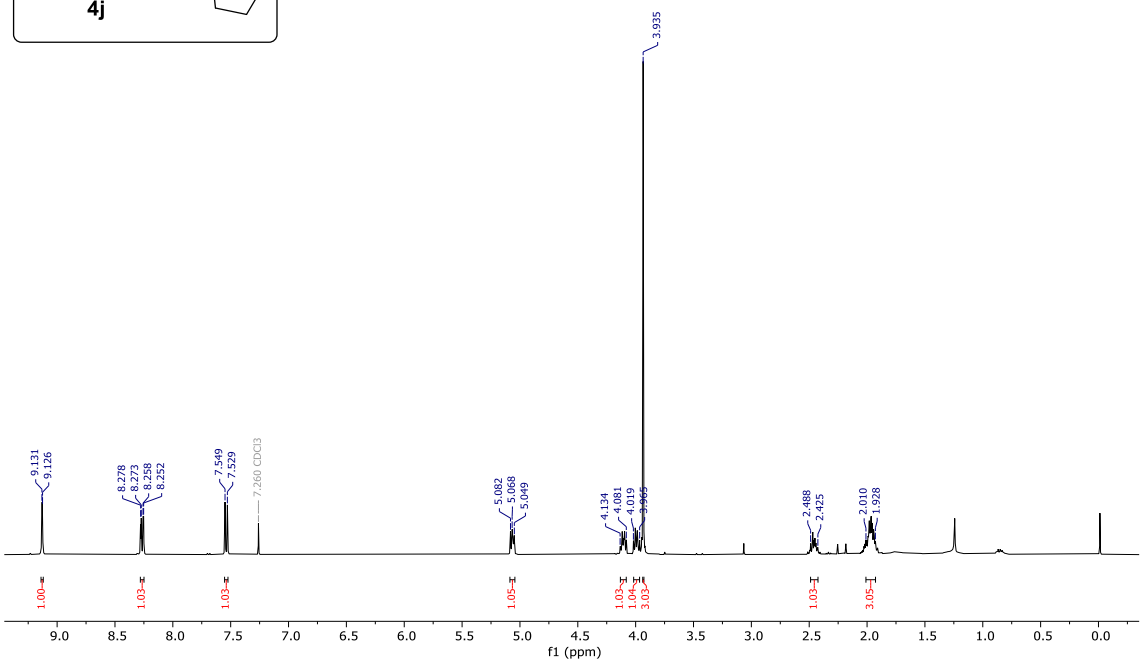
9.131
9.126
8.278
8.273
8.258
8.252
7.549
7.529
7.260 CDCl3
5.082
5.068
5.049
4.134
4.081
4.019
3.935
2.488
2.425
2.010
1.928
1.00
1.03
1.03
1.05
1.03
1.04
3.03
1.03
3.05
f1 (ppm)

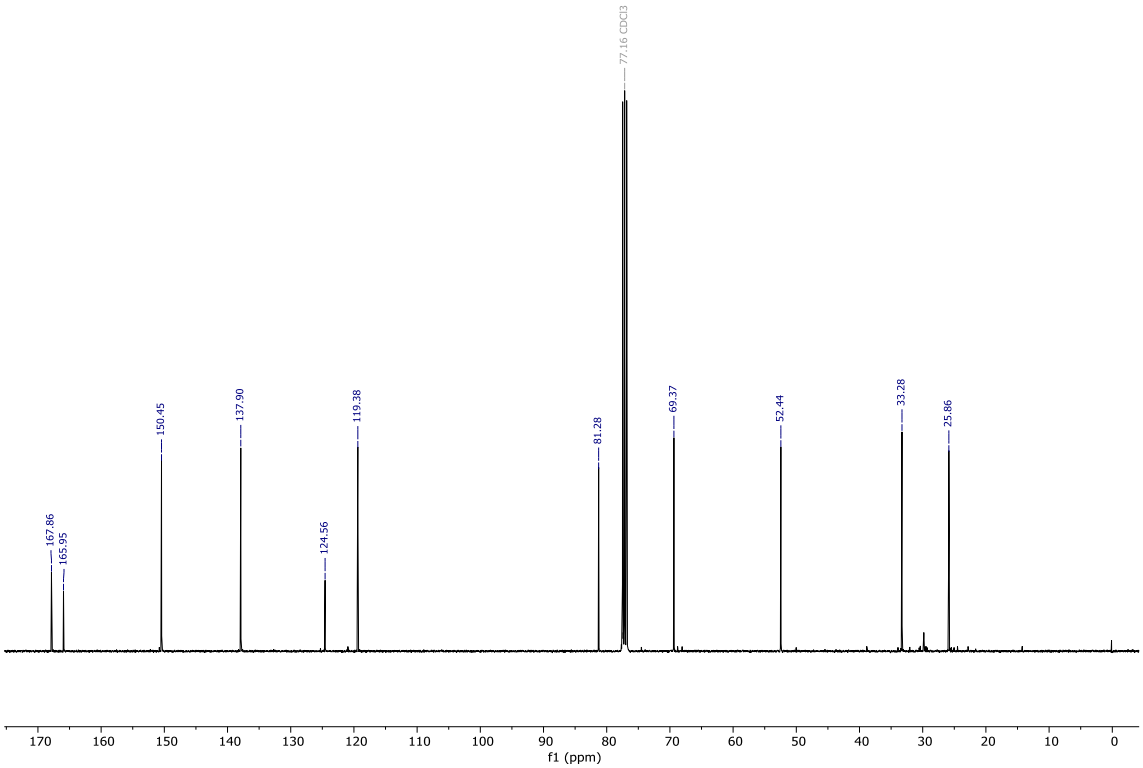
77.16 CDCl3
167.86
165.95
150.45
137.90
124.56
119.38
81.28
69.37
52.44
33.28
25.86
f1 (ppm)

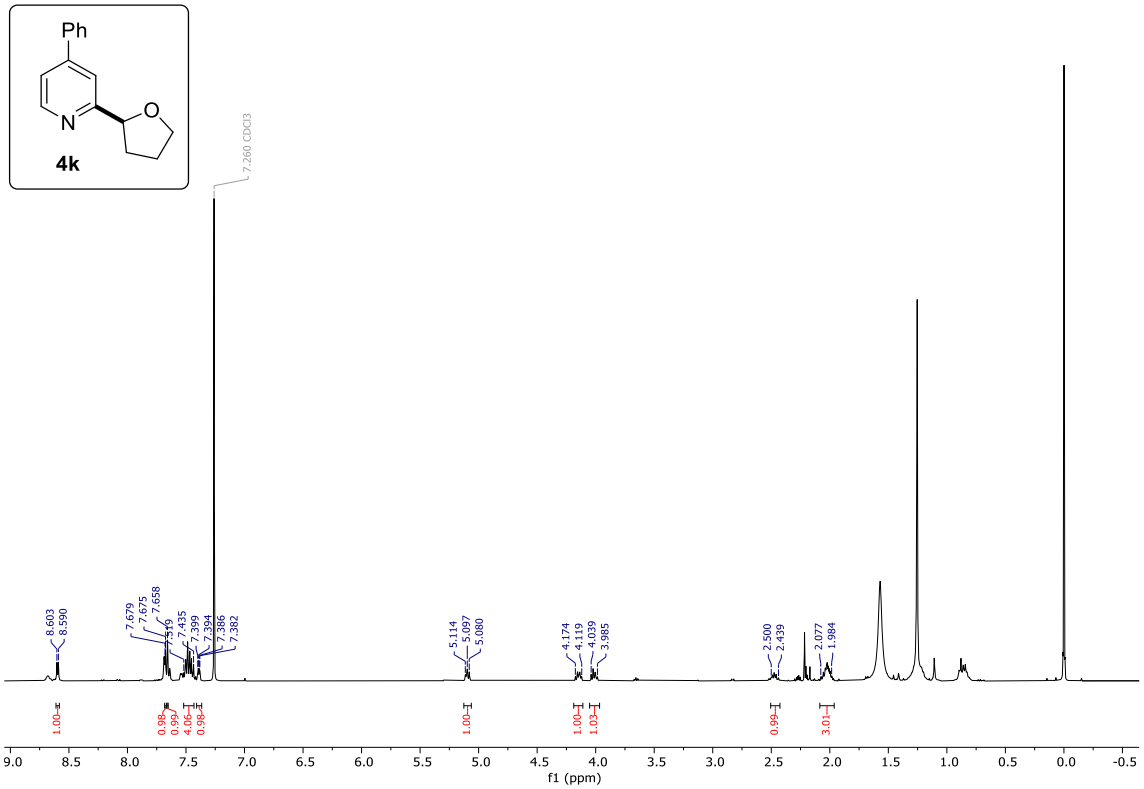
Ph
N
O
4k
7.260 CDCl3
8.603
8.590
7.679
7.675
7.658
7.649
7.435
7.399
7.394
7.386
7.382
5.114
5.097
5.080
4.174
4.119
4.039
3.985
2.500
2.439
2.077
1.984
1.00
0.98
0.99
4.06
0.98
1.00
1.00
1.03
0.99
3.01
9.0 8.5 8.0 7.5 7.0 6.5 6.0 5.5 5.0 4.5 4.0 3.5 3.0 2.5 2.0 1.5 1.0 0.5 0.0 -0.5
f1 (ppm)

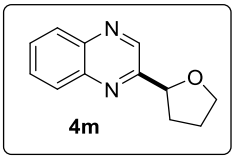
N
N
O

4m

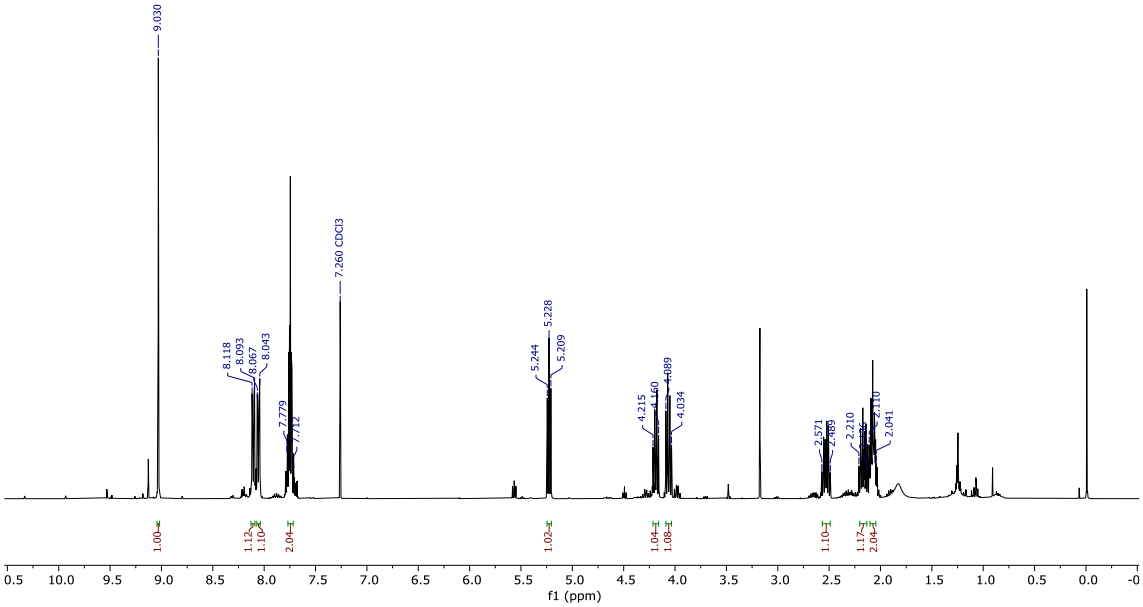
9.030
8.118
8.093
8.067
8.043
7.779
7.712
7.260 CDCl3
5.244
5.228
5.209
4.215
4.160
4.089
4.034
2.571
2.489
2.210
2.110
2.041
1.00
1.12
1.10
2.04
1.02
1.04
1.08
1.10
1.17
2.04
f1 (ppm)

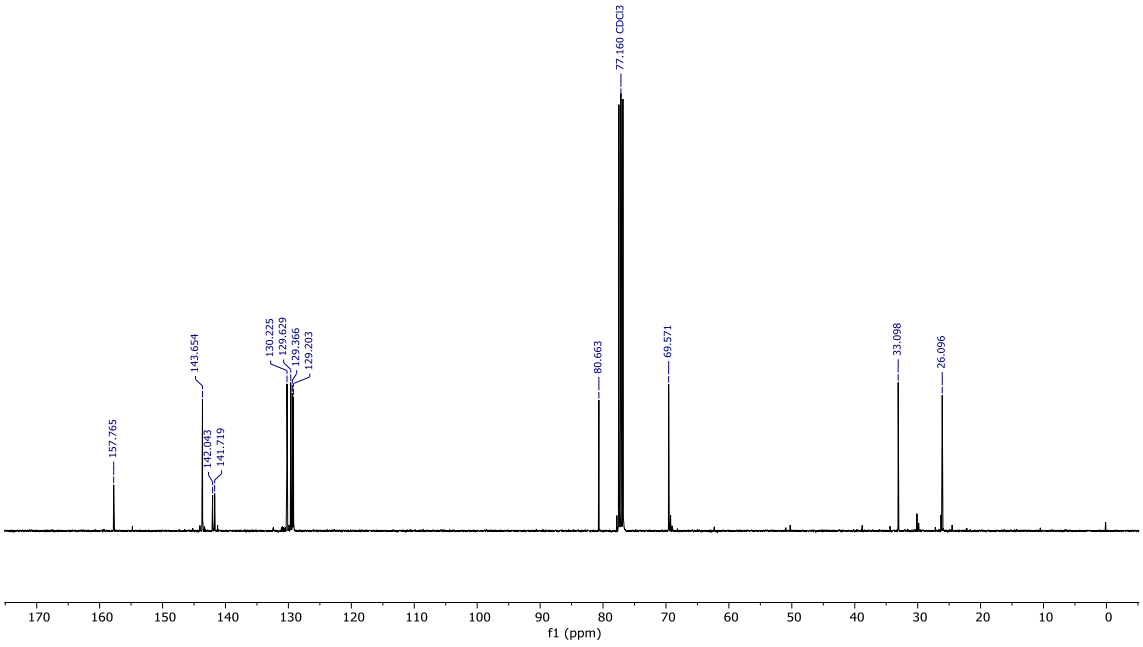
157.765
143.654
142.043
141.719
130.225
129.629
129.366
129.203
80.663
77.160 CDCl3
69.571
33.098
26.096
f1 (ppm)

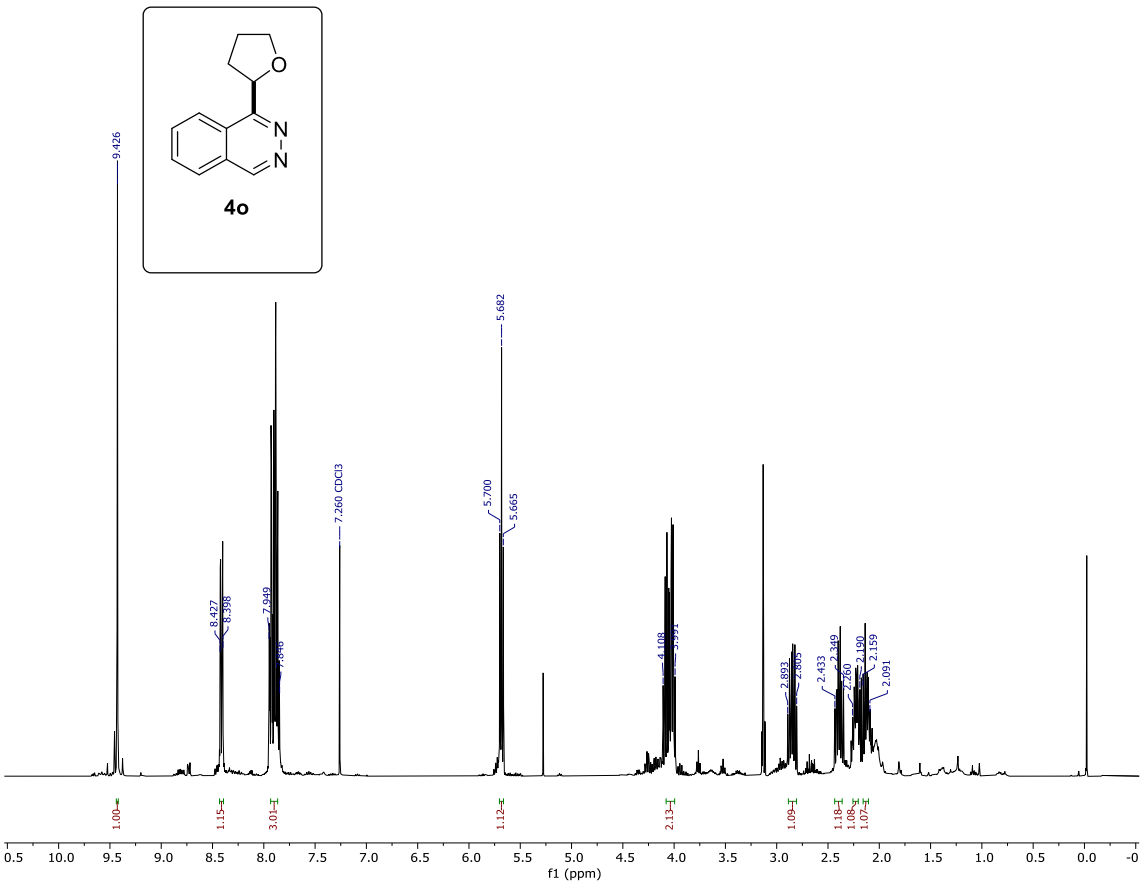
4o
9.426
8.427
8.398
7.949
7.260 CDCl3
5.700
5.682
5.665
4.108
3.991
2.893
2.869
2.433
2.349
2.260
2.190
2.159
2.091
1.00
1.15
3.01
1.12
2.13
1.09
1.18
1.08
1.07
f1 (ppm)

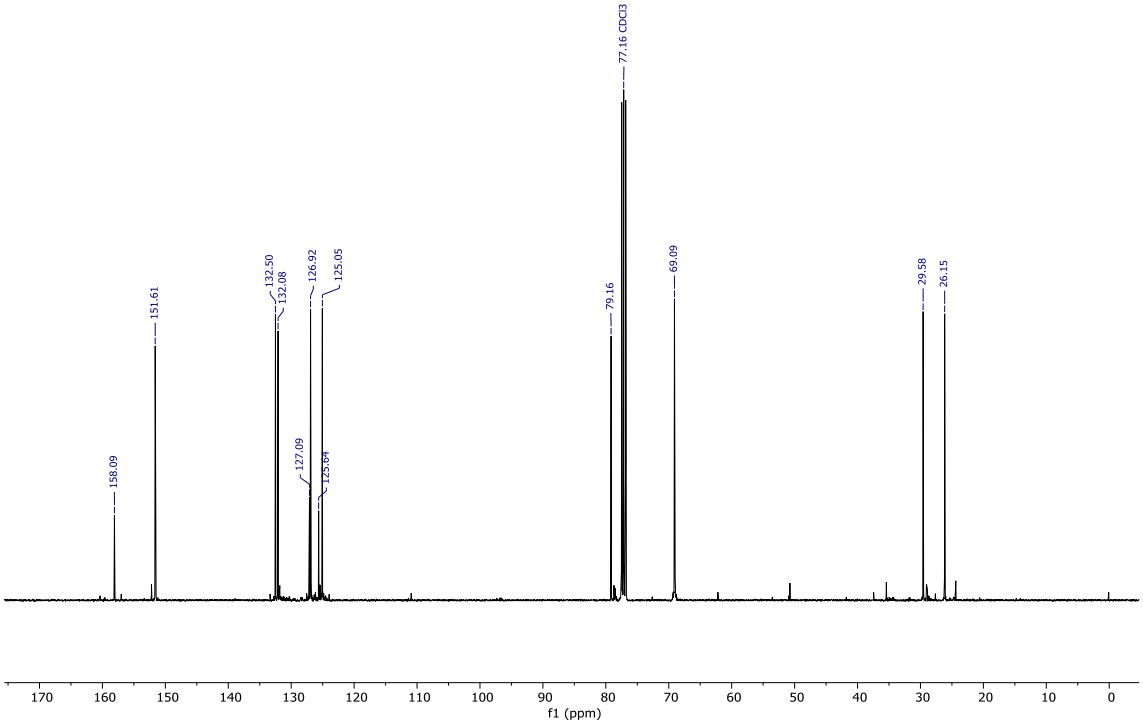
158.09
151.61
132.50
132.08
127.09
126.92
125.64
125.05
79.16
77.16 CDCl3
69.09
29.58
26.15
f1 (ppm)

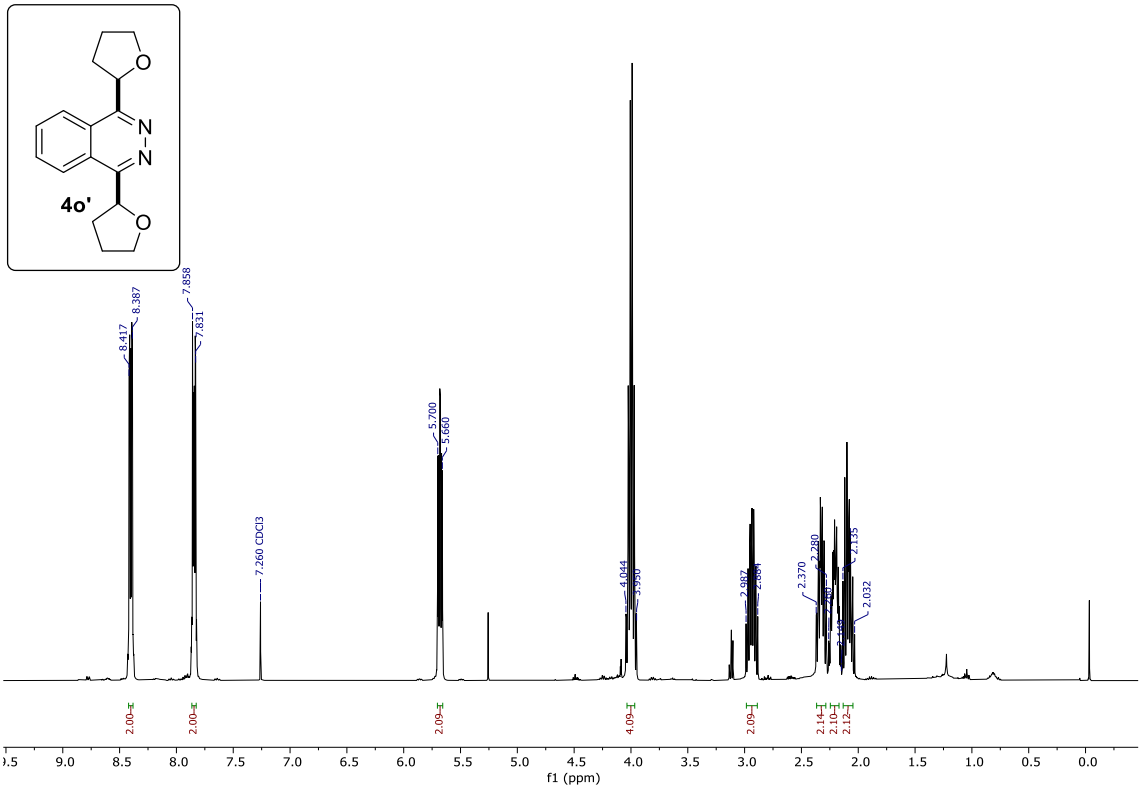
4o'
8.417
8.387
7.858
7.831
7.260 CDCl3
5.700
5.660
4.044
3.350
2.887
2.884
2.370
2.280
2.135
2.032
2.00
2.00
2.09
4.09
2.09
2.14
2.10
2.12
f1 (ppm)

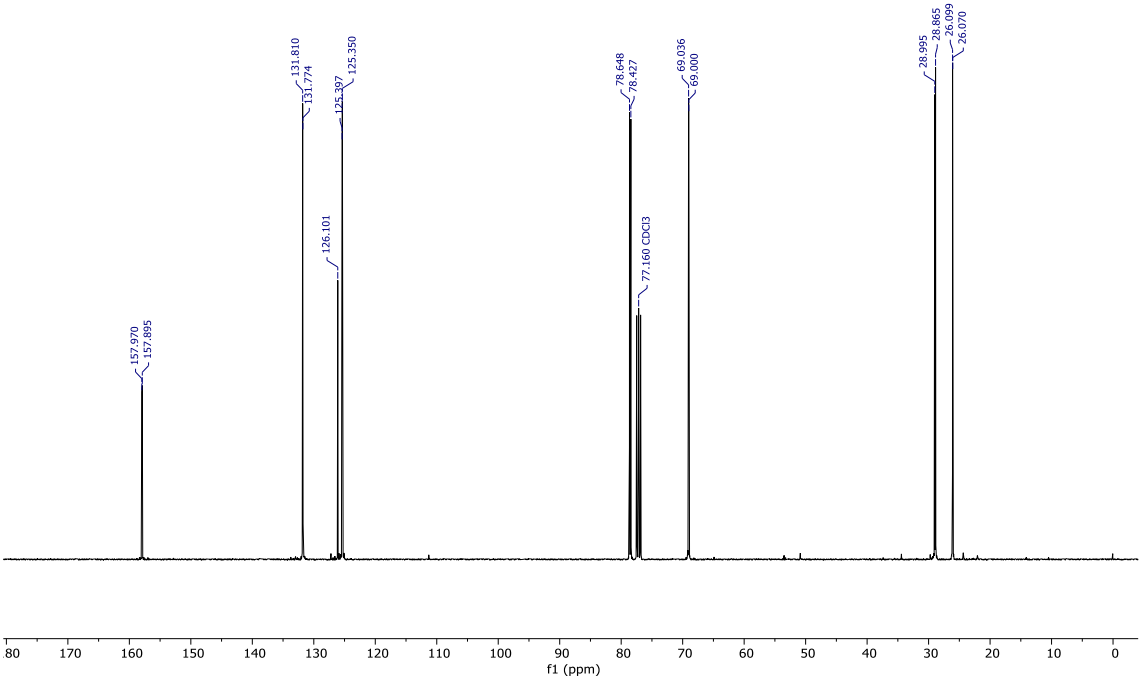
157.970
157.895
131.810
131.774
126.101
125.397
125.350
78.648
78.427
77.160 CDCl3
69.036
69.000
28.995
28.865
26.099
26.070
f1 (ppm)

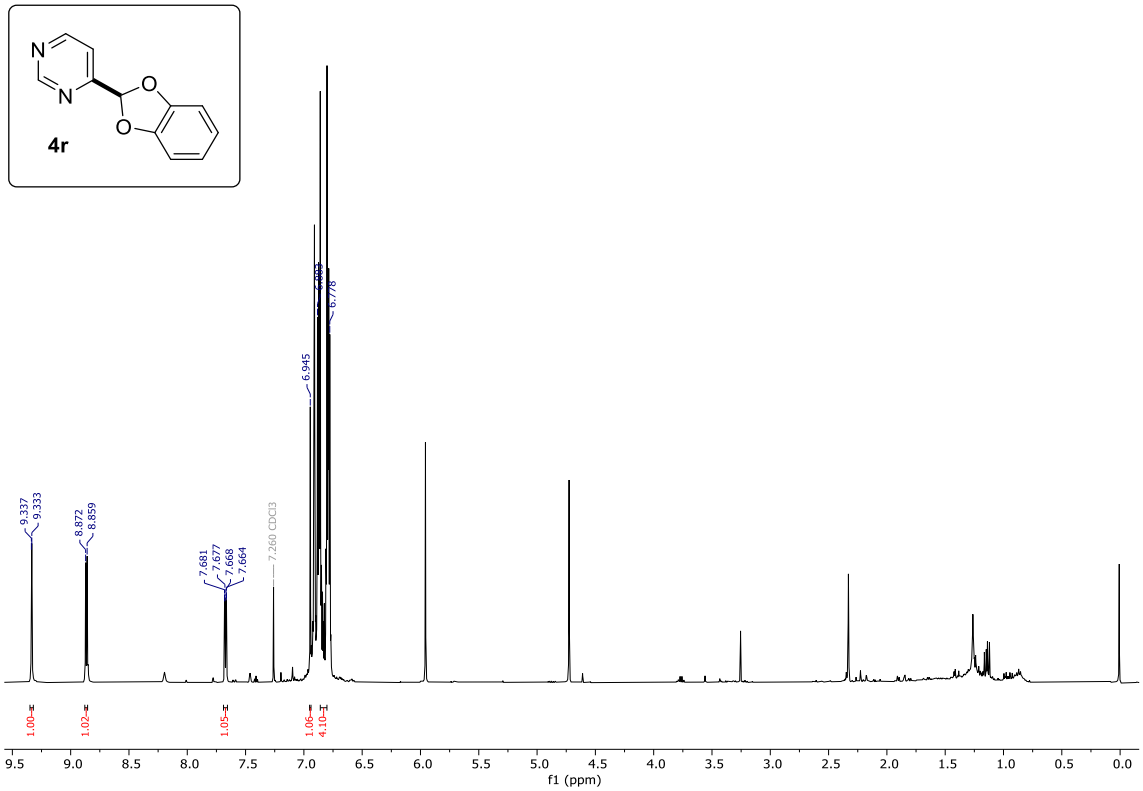
4r
9.337
9.333
8.872
8.859
7.681
7.677
7.668
7.664
7.260 CDCl3
6.945
6.778
1.00
1.02
1.05
1.06
4.10
f1 (ppm)

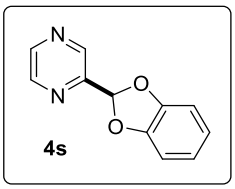
N
N
O
O

4s

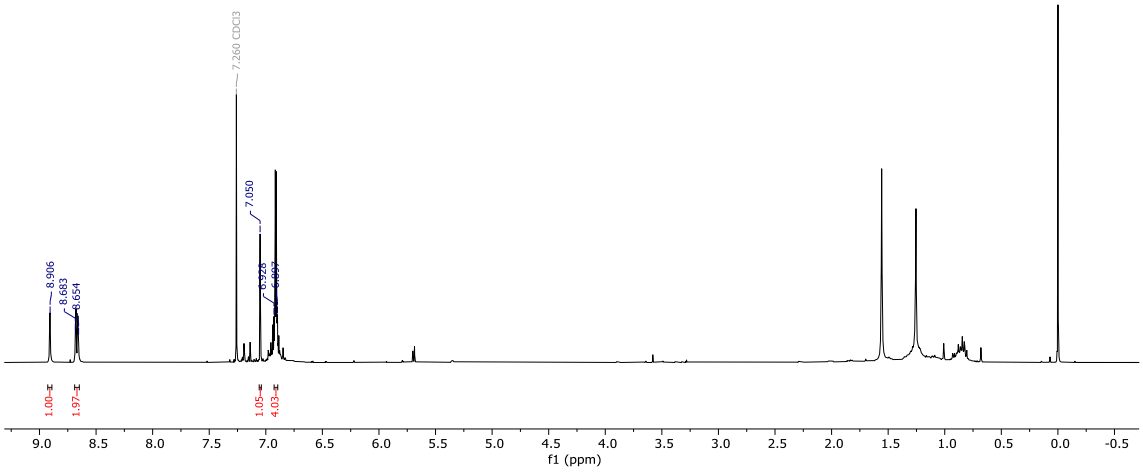
7.260 CDCl3
8.906
8.683
8.654
7.050
6.926
1.00
1.97
1.05
4.03
9.0 8.5 8.0 7.5 7.0 6.5 6.0 5.5 5.0 4.5 4.0 3.5 3.0 2.5 2.0 1.5 1.0 0.5 0.0 -0.5
f1 (ppm)

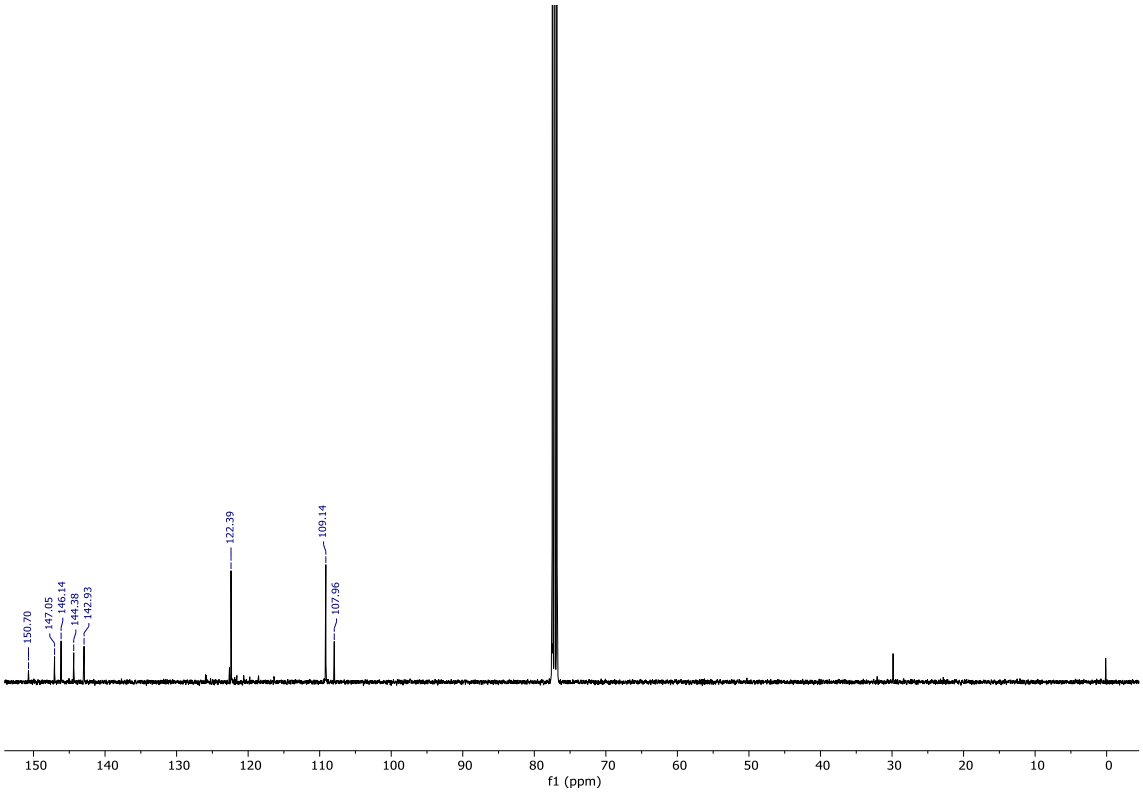
150.70
147.05
146.14
144.38
142.93
122.39
109.14
107.96
150 140 130 120 110 100 90 80 70 60 50 40 30 20 10 0
f1 (ppm)

4. ADAMANTANE BUILDING-BLOCK SYNTHESIS USING MHAT

Preparation of starting materials

Compounds **5a**,[322] **5b**,[54] **8**,[323] **9**,[324] **10**[55] were prepared according to the reported procedure.

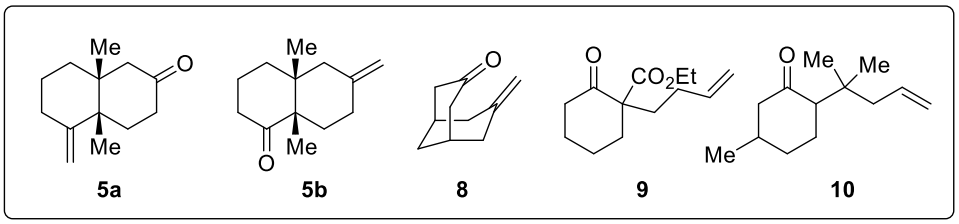

General method 1 for the formation of Wieland-Miescher ketones 3a-c

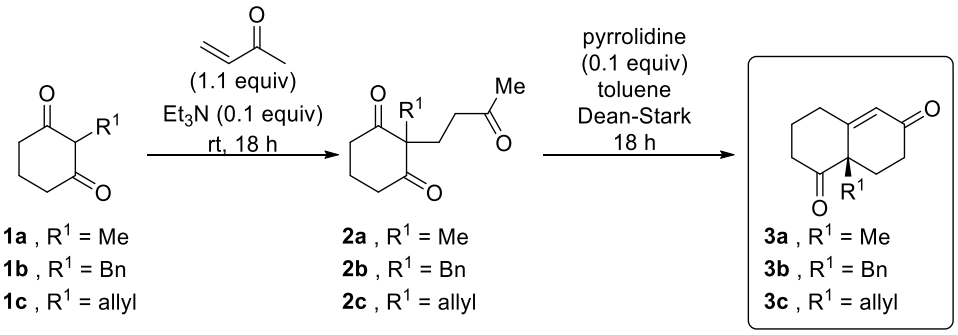

To 1,3-cyclohexadione **1a-c** (1 equiv) in a standard glass vial (10 cm x 3 cm) with stirrer bar was added methyl vinyl ketone (1.1 equiv) and Et_3N (0.1 equiv). The resulting mixture was stirred at room temperature for 18 hours. The product was diluted with CH_2Cl_2, washed with 5% aqueous HCl (15 mL), water (15 mL), and the aqueous phases further extracted with DCM (3 x 15 mL). The combined organic layers were dried, concentrated to afford the product which was used in the next step without further purification.

To a solution of the crude triketone (1 equiv) in toluene (20 mL) was added pyrrolidine (0.1 equiv) before fitting the flask with a Dean-Stark trap. The reaction was heated at reflux for 5 hours, cooled to room temperature, and the solvent removed under reduced pressure. The crude oil was dissolved in CH_2Cl_2, washed with 5% aqueous HCl (15 mL), water (15 mL), and the combined aqueous phases extracted with CH_2Cl_2. The

combined organic layers were washed with brine (10 mL), dried and concentrated. Purification by column chromatography gave the corresponding Wieland-Miescher ketone **3a-c** as a brown/amber oil which solidified to a solid upon storage at – 20 °C. The NMR data obtained for the triketone intermediates **2a-c** and the Wieland-Miescher ketone analogues **3a-c** were identical to those previously reported.[291]

General method 2 for the preparation of acetals 6a-c

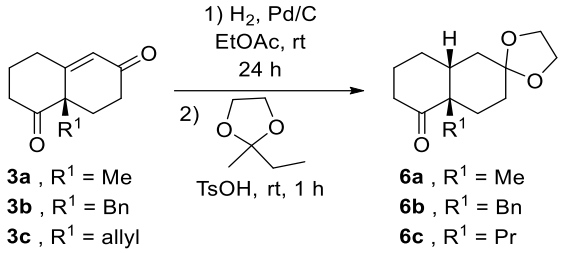

To a solution of the diketone **3a-c** (1 equiv) in EtOAc (0.5 M) was added Pd/C (10 wt%) and the resulting suspension was stirred under H_2 (1 atm) at room temperature for 24 h. The resulting mixture was filtered through Celite® and the filtrate was concentrated to give the corresponding reduced diketone which was used in the next step without further purification. To a solution of the diketone (1 equiv) in 2-ethyl-2-methyl-1,3-dioxolane (5 equiv) was added *p*-toluenesulfonic acid monohydrate (0.05 equiv) and the resulting mixture was stirred for 1 h at room temperature. The reaction was quenched by the addition of saturated aqueous $NaHCO_3$ and extracted with Et_2O three times, the combined organic layers were washed with brine, dried and concentrated. Purification by column chromatography gave the corresponding acetal **6a-c**.

General method 3 for the preparation of ketoalkenes 7a-c

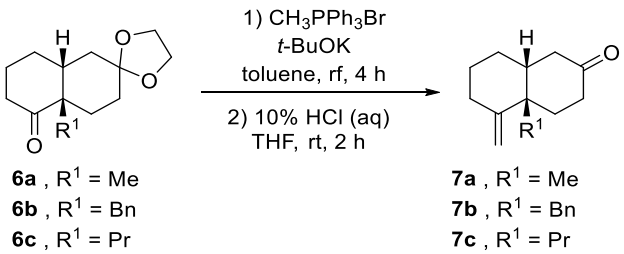

A solution of methyltriphenylphosphonium bromide (5 equiv) and potassium tert-butoxide (5 equiv) in toluene (0.5 M) was stirred at reflux for 1 h. A solution of the corresponding acetal **6a-c** (1 equiv) in toluene (0.3 M) was then added dropwise to the

above solution and the resulting mixture was stirred at reflux for 4 h. The reaction was quenched by the careful addition of acetone, stirring at 100 °C for 30 min and then by the addition of water. The reaction mixture was extracted with Et_2O three times, the combined organic layers were washed with brine, dried and concentrated. The crude was used for the next step without further purification. To the crude acetal in THF (0.3 M) was added 10% aq. HCl solution (0.2 M) and the resulting mixture stirred for 2 h at room temperature. The crude was extracted with Et_2O three times, dried and concentrated. Purification of the residue by chromatography gave the corresponding ketone **7a-c**.

Preparation of ketoalkenes 7a-c

(4aS,8aR)-4a-methyl-5-methyleneoctahydronaphthalen-2(1H)-one (7a)

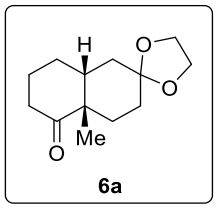

6a

According to the general method **2**, a solution of **3a** (2.00 g, 11.22 mmol, 1 equiv) and Pd/C (10 wt%, 0.20 g) in EtOAc (0.5 M, 22 mL) afforded the diketone as a yellow oil, which was then mixed with *p*-toluenesulfonic acid monohydrate (107 mg, 0.561 mmol, 0.05 equiv) in 2-ethyl-2-methyl-1,3- dioxolane (7 mL, 56.1 mmol, 5 equiv). Purification by column chromatography (hexane → hexane/EtOAc 75:25) gave **6a** (1.862 g, 74%) as a clear oil. ^{1}H NMR δ 3.97 (m, 4H, CH_2O), 2.59–2.50 (m, 1H, CH_2), 2.26–2.10 (m, 4H, CH_2 and H-8a), 1.92–1.85 (m, 2H, CH_2), 1.70–1.58 (m, 2H, CH_2), 1.55–1.46 (m, 3H, CH_2), 1.26–1.18 (m, 1H CH_2), 1.23 (s, 3H, Me); ^{13}C NMR δ 215.1 (C=O), 109.5 (C-2), 64.3 and 64.2 (CH_2O), 46.4 (C-4a), 42.6 (C-8a), 37.8 (CH_2), 37.3 (CH_2), 31.8 (CH_2), 31.7 (CH_2), 26.0 (Me), 25.9 (CH_2), 22.4 (CH_2).

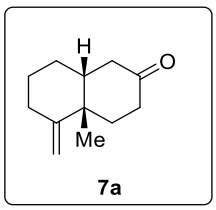

7a

According to the general method **3**, to a solution of methyltriphenylphosphonium bromide (14 g, 40.1 mmol, 5 equiv) and potassium tert-butoxide (4.5 g, 40.1 mmol, 5 equiv) in toluene (0.5 M, 80 mL), was added ketone **6a** (1.80 g, 8.02 mmol, 1 equiv) in toluene (0.3 M, 27 mL). Then, was added THF (0.3 M, 27 mL) and 10% aq. HCl solution (0.2 M, 40 mL) and purification by chromatography (hexane → hexane/EtOAc 95:5) gave **7a** (1.186 g, 83%) as a colorless oil. ^{1}H NMR δ 4.86 (d, *J* = 18 Hz, 2H, $=CH_2$), 2.54–1.45 (m, 1H, CH_2), 2.38–2.21 (m, 6H, CH_2), 1.90–1.85 (m, 1H, H-8a), 1.84–1.78 (m, 1H, CH_2), 1.70–1.60 (m, 1H, CH_2), 1.55–1.46 (m, 2H, CH_2), 1.38–1.31 (m, 1H, CH_2), 1.28 (s,

3H, Me); ^{13}C NMR δ 212.8 (C=O), 151.6 (C-5), 108.5 (=CH_2), 45.2 (C-8a), 44.2 (CH_2), 39.3 (C-4a), 38.3 (CH_2), 35.5 (CH_2), 32.5 (CH_2), 28.5 (CH_2), 26.2 (Me), 24.0 (CH_2).

(4aR,8aR)-4a-benzyl-5-methyleneoctahydronaphthalen-2(1H)-one (7b)

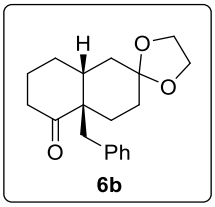

6b

According to the general method **2**, a solution of **3b** (2.11 g, 8.29 mmol, 1 equiv) and Pd/C (10 wt%, 0.21 g) in EtOAc (0.5 M, 17 mL) afforded the diketone as a yellow oil, which was then mixed with *p*-toluenesulfonic acid monohydrate (79 mg, 0.415 mmol, 0.05 equiv) in 2-ethyl-2-methyl-1,3- dioxolane (5.2 mL, 41 mmol, 5 equiv). Purification by column chromatography (hexane → hexane/EtOAc 90:10) gave **6b** (2.29 g, 92%) as a white solid. ^{1}H NMR δ 7.25–7.17 (m, 3H, Ph), 7.01–6.99 (m, 2H, Ph), 3.92–3.88 (m, 4H, OCH_2), 3.40 (d, *J* = 13.6 Hz, 1H, CH_2Ph), 2.89–2.80 (m, 1H, CH_2), 2.73 (d, *J*= 13.6 Hz, CH_2Ph), 2.47–2.29 (m, 3H, CH_2 and H-8a), 2.04–1.96 (m, 2H, CH_2), 1.92 (dt, *J* = 13.6, 3.6 Hz, 1H, CH_2), 1.62 (t, *J* = 13.2 Hz, 2H, CH_2), 1.54–1.48 (m, 3H, CH_2), 1.20 (ddd, *J* = 13.6, 5.2 Hz, 1H, CH_2); ^{13}C NMR δ 213.7 (C=O), 136.9 (C_{ipso}), 129.9 (Ph), 128.3 (Ph), 126.8 (Ph), 109.3 (OCH_2), 64.5 (OCH_2), 64.3 (OCH_2), 53.1 (C-4a), 44.8 (CH_2Ph), 42.2 (C-8a), 38.8 (CH_2), 37.7 (CH_2), 31.4 (CH_2), 29.2 (CH_2), 25.9 (CH_2), 22.7 (CH_2).

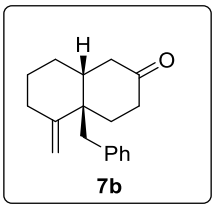

7b

According to the general method **3**, to a solution of methyltriphenylphosphonium bromide (13.6 g, 38.2 mmol, 5 equiv) and potassium tert-butoxide (4.3 g, 38.2 mmol, 5 equiv) in toluene (0.5 M, 76 mL), was added ketone **6b** (2.29 g, 7.63 mmol, 1 equiv) in toluene (0.3 M, 25 mL). Then, was added THF (0.3 M, 25 mL) and 10% aq. HCl solution (0.2 M, 38 mL) purification by chromatography (hexane → hexane/EtOAc 90:10) gave **7b** (1.36 g, 70%) as a colorless solid. ^{1}H NMR δ 7.25–7.19 (m, 3H, Ph), 7.06–7.04 (m, 2H, Ph), 5.08 (s, 1H) and 4.58 (s, 1H, =CH_2), 3.28 (d, *J* = 13.2 Hz, 1H, CH_2), 2.69–2.59 (m, 2H, CH_2), 2.56–2.47 (m, 2H, CH_2), 2.41–2.35 (m, 1H, CH_2), 2.29–2.19 (m, 1H, CH_2), 2.15–2.09 (m, 2H, CH_2), 2.02–1.96 (m, 2H, CH_2), 1.79–1.67 (m, 2H, CH_2), 1.62–1.54 (m, 2H, CH_2), 1.43–1.38 (m, 1H, CH_2); ^{13}C NMR δ 213.3 (C=O), 146.3 (C-5), 137.8 (C_{ipso}), 130.5 (Ph), 127.8 (Ph), 126.4 (Ph), 112.4 (=CH_2), 45.1 (CH_2), 44.4 (CH_2), 43.9 (CH_2), 37.8 (CH_2), 34.3 (CH_2), 32.7 (CH_2), 27.2 (CH_2), 21.7 (CH_2), 43.8 (C-4a).

(4aS,8aR)-5-methylene-4a-propyloctahydronaphthalen-2(1H)-one (7c)

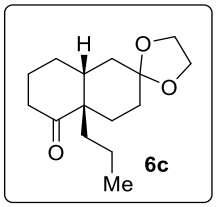

6c

According to the general method **2**, a solution of **3c** (1.01 g, 4.94 mmol, 1 equiv) and Pd/C (10 wt%, 0.10 g) in EtOAc (0.5 M, 10 mL) afforded the diketone as a yellow oil, which was then mixed with *p*-toluenesulfonic acid monohydrate (47 mg, 0.247 mmol, 0.05 equiv) in 2-ethyl-2-methyl-1,3- dioxolane (3.1 mL, 24.7 mmol, 5 equiv). Purification by column chromatography (hexane → hexane/EtOAc 90:10) gave **6c**(1.06 g, 85%) as a clear oil. ^{1}H NMR δ 3.95–3.89 (m, 4H, OCH_2), 2.52–2.43 (m, 1H, CH_2), 2.34–2.19 (m, 4H, CH_2), 1.99–1.86 (m, 2H, CH_2), 1.69–1.54 (m, 4H, CH_2), 1.48–1.29 (m, 4H, CH2), 1.18–1.09 (m, 1H, CH_2), 0.98–0.85 (m, 4H, CH_2 and Me); ^{13}C NMR δ 214.9 (C=O), 109.4 (C-2), 64.4 and 64.3 (OCH_2), 52.3 (C-4a), 41.8 (CH_2), 41.5 (CH_2), 38.4 (CH_2), 37.6 (CH_2), 31.7 (CH_2), 28.8 (CH_2), 25.7 (CH_2), 22.5 (CH_2), 16.9 (CH_2), 14.9 (Me).

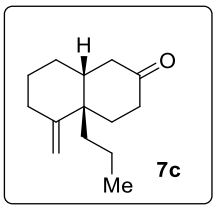

7c

According to the general method **3**, to a solution of methyltriphenylphosphonium bromide (7.50 g, 20.9 mmol, 5 equiv) and potassium tert-butoxide (2.36 g, 20.9 mmol, 5 equiv) in toluene (0.5 M, 42 mL), was added ketone **6c** (1.06 g, 4.19 mmol, 1 equiv) in toluene (0.3 M, 14 mL). Then, was added THF (0.3 M, 14 mL) and 10% aq. HCl solution (0.2 M, 21 mL) and purification by chromatography (hexane → hexane/EtOAc 75:25) gave **7c** (788 mg, 91%) as a pale yellow solid. ^{1}H NMR δ 5.03 (s, 1H) and 4.78 (s, 1H, $=CH_2$), 2.61–2.49 (m, 2H, CH_2), 2.45–2.39 (m, 1H, CH_2), 2.27–2.17 (m, 3H, CH_2), 2.05–1.91 (m, 3H, CH_2), 1.64–1.56 (m, 2H, CH_2), 1.52–1.44 (m, 1H, CH_2), 1.30–1.20 (m, 2H, CH_2), 1.18–1.07 (m, 2H, CH_2), 0.95–0.87 (m, 4H, CH_2 and Me); ^{13}C NMR δ 213.6 (C=O), 147.9 (C-5), 110.6 ($=CH_2$), 44.3 (CH_2), 43.9 (CH_2), 42.8 (C-4a), 41.2 (CH_2), 38.1 (CH_2), 34.2 (CH_2), 32.6 (CH_2), 27.2 (CH_2), 22.1 (CH_2), 16.7 (CH_2), 14.9 (Me).

(4aS,8aR)-4a-butyl-5-methyleneoctahydronaphthalen-2(1H)-one (7d)

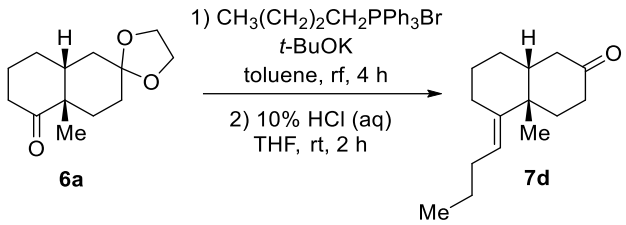

According to the general method **3**, to a solution of butyltriphenylphosphonium bromide (4.45 g, 11.15 mmol, 5 equiv) and potassium tert-butoxide (1.25 g, 11.15 mmol, 5 equiv) in toluene (0.5 M, 22 mL), was added ketone **6a** (500 mg, 2.23 mmol, 1 equiv) in toluene (0.3 M, 7.5 mL). Then, was added THF (0.3 M, 7.5 mL) and 10% aq. HCl solution (0.2 M, 11 mL) and purification by chromatography (hexane → hexane/EtOAc 90:10) gave **7d** (260 mg, 52%) as a clear yellow solid, as a mixture of E/Z (1.5:1) diastereomers. ^{1}H NMR δ 5.35 (t, *J* = 6.8 Hz, 1H, CH), 2.54–2.46 (m, 1H, CH_2), 2.39–2.29 (m, 4H, CH_2), 2.24–2.17 (m, 2H, CH_2), 2.10–1.99 (m, 2H, CH_2), 1.91–1.83 (m, 2H, CH_2), 1.58–1.46 (m, 3H, CH_2), 1.42–1.32 (m, 3H, CH_2), 1.24 (s, 3H, Me), 0.90 (t, *J* = 7.2 Hz, 3H, Me); ^{13}C NMR δ 213.3 (C=O), 140.3 (C-5), 122.6 (CH), 45.3 (CH_2), 44.4 (CH_2), 39.5 (C-4a), 38.5 (CH_2), 36.1 (CH_2), 29.8 (CH_2), 28.3 (CH_2), 26.9 (Me), 24.3 (CH_2), 23.4 (CH_2), 23.1 (CH_2), 13.9 (Me).

General method for the preparation of hydrazones

A solution of the corresponding ketone (1 equiv) and *p*-toluenesulfonyl hydrazide (1 equiv) in EtOH (0.2 M) was stirred at room temperature for 3 h. The mixture was concentrated and purified by chromatography (hexane → hexane/EtOAc 90:10) to afford the corresponding hydrazone.

***N'*-[(4a*RS*,8a*RS*)-4a,8a-Dimethyl-5-methyleneoctahydronaphthalen-2(1*H*)-ylidene]-4-methylbenzenesulfonohydrazide (9a)**

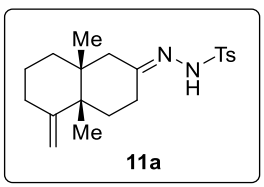

A solution of ketone **5a** (180 mg, 0.94 mmol) and *p*-toluenesulfonyl hydrazide (174 mg, 0.94 mmol) in EtOH (4.7 mL) was stirred at room temperature for 3 h. The mixture was concentrated and purified by chromatography (hexane →

hexane/EtOAc 90:10) to afford the corresponding hydrazone **11a** (333 mg, 98%) as a white solid; ^{1}H NMR (400 MHz, $CDCl_3$) δ 7.87–7.79 (m, 2H, Ts), 7.34–7.26 (m, 2H, Ts), 4.81 (dd, *J* = 2.4, 1.3 Hz, 1H), 4.76–4.70 (m, 1H), 2.42 (two s, 3H, Me), 2.41–2.33 (m, 1H), 2.32–2.13 (m, 4H), 2.08–2.00 (m, 1H), 1.57–1.45 (m, 2H), 1.42–1.33 (m, 1H), 1.35–1.24 (m, 3H), 1.09 (s, 3H, Me), 0.79 and 0.75 (s, 3H, Me); ^{13}C NMR (101 MHz, $CDCl_3$) δ 152.4, 144.0, 135.6, 129.6, 128.2, 108.8, 44.3, 42.8, 42.5, 41.3, 35.1, 32.6, 32.5, 32.4, 31.8, 23.0, 22.9, 22.8, 21.8. HRMS (ESI) *m/z*: $[M+H]^+$ calcd for $[C_{20}H_{29}N_2O_2S]^+$ 361.1944, found 361.1948.

Synthesis of coupled products via MHAT

General Method

To a solution of the corresponding hydrazone (1 equiv) and $Fe(acac)_3$ (2 equiv) in THF (0.08 M) with *t*-BuOH (10 equiv) was added alkene (2.5-10 equiv) and the mixture was degassed and bubbled with argon for 5 minutes. The mixture was heated to 60 °C and $PhSiH_3$ (2.5 equiv) was then added via syringe. After 24 h at this temperature, the reaction mixture was concentrated and purified by column chromatography.

Methyl 3-[(3a*RS*,4*RS*,7a*RS*)-3a,4,7a-Trimethyloctahydro-1*H*-1,4-methanoinden-1-yl)propanoate (12a)

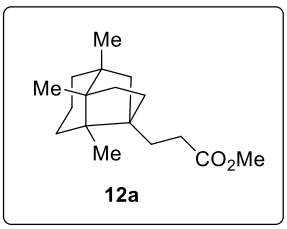

12a

To a solution of hydrazone **11a** (75 mg, 0.208 mmol) and $Fe(acac)_3$ (147 mg, 0.416 mmol) in THF (2.6 mL) with *t*-BuOH (197 μL, 2.08 mmol), methyl acrylate (179 mg, 2.08 mmol) and $PhSiH_3$ (56 mg, 0.52 mmol) were added and stirred at 60 °C in an oil bath for 24 h. Purification by chromatography (hexane → hexane/EtOAc 97.5:2.5) gave the desired compound **12a** (52 mg, 94%) as a yellowish oil; ^{1}H NMR (400 MHz, $CDCl_3$) δ 3.67 (s, 3H, OCH_3), 2.29 (t, *J* = 8.4 Hz, 2H, CH_2CO), 1.76–1.57 (m, 4H, CH_2), 1.51–1.42 (m, 2H, CH_2), 1.41–1.31 (m, 4H, CH_2), 1.28–1.16 (m, 1H, CH_2), 1.18–1.07 (m, 1H, CH_2), 0.96–0.85 (m, 2H, CH_2), 0.86 (s, 3H, CH_3), 0.78 (s, 3H, CH_3), 0.61 (s, 3H, CH_3); ^{13}C NMR (101 MHz, $CDCl_3$) δ 51.7 (OCH_3), 45.2 (CH_2), 35.8 (CH_2), 33.7 (CH_2), 30.9 (CH_2),

29.8 (CH_2), 29.6 (CH_2), 27.0 (CH_2), 22.3 (CH_3), 20.1 (CH_2), 18.2 (CH_3), 11.7 (CH_3). HRMS (ESI) *m/z*: $[M+H]^+$ calcd for $[C_{17}H_{29}O_2]^+$ 265.2162, found 265.2159.

- Subproducts obtained in the coupling-fragmentation reaction (**A**, **B**, **C** and **D**):

4-Methyl-*N'*-[(3a*RS*,4*SR*,7a*SR*)-3a,4,7a-trimethyloctahydro-1*H*-1,4-methanoinden-1-yl)benzenesulfonohydrazide (A)

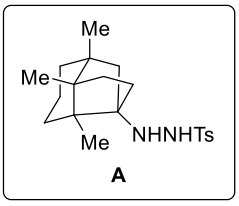

A

^{1}H NMR (400 MHz, $CDCl_3$) δ 7.82 (d, *J* = 8.3 Hz, 2H, Ts), 7.30 (d, *J* = 8.0 Hz, 2H, Ts), 5.68 (br s, 1H, NH), 2.44 (s, 3H, Ts), 1.70–1.63 (m, 2H, CH_2), 1.44–1.31 (m, 4H, CH_2), 1.23–1.09 (m, 3H, CH_2), 0.98–0.90 (m, 3H, CH_2), 0.82 (s, 3H, CH_3), 0.72 (s, 3H, CH_3), 0.62 (s, 3H, CH_3).

(3a*RS*,4*RS*,7a*RS*)-3a,4,7a-Trimethyloctahydro-1*H*-1,4-methanoindene (B)

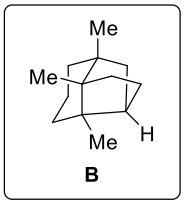

B

^{1}H NMR (400 MHz, $CDCl_3$) δ 1.91 (ddd, *J* = 12.8, 5.2, 3.6 Hz, 1H, CH_2), 1.75–1.65 (m, 3H, CH, CH_2), 1.63–1.57 (m, 1H, CH_2), 1.51–1.36 (m, 4H, CH_2), 1.28–1.20 (m, 2H, CH_2), 1.07–1.01 (m, 1H, CH_2), 0.95 (dd, *J* = 14, 7.6 Hz, 1H, CH_2), 0.87 (s, 3H, Me), 0.77 (s, 3H, Me), 0.74 (s, 3H, Me); ^{13}C NMR (101 MHz, $CDCl_3$) δ 48.6 (C), 47.8 (C), 45.0 (CH), 41.6 (C), 40.9 (CH_2), 34.2 (CH_2), 32.3 (CH_2), 31.6 (CH_2), 30.5 (CH_2), 22.3 (Me), 20.5 (CH_2), 20.4 (Me), 11.2 (Me). HRMS (ESI) *m/z*: $[M+H]^+$ calcd for $[C_{13}H_{23}]^+$ 179.1795, found 179.1799.

(3a*RS*,4*RS*,7a*RS*)-1-Ethoxy-3a,4,7a-trimethyloctahydro-1*H*-1,4-methanoindene (C)

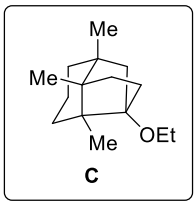

C

Selected peaks in ^{1}H NMR (400 MHz, $CDCl_3$) δ 3.48 (q, *J* = 7.0 Hz, 2H, OCH_2), 1.17 (t, *J* = 7.0 Hz, 3H, OCH_2CH_3), 0.88 (s, 3H, CH_3), 0.76 (s, 3H, CH_3), 0.73 (s, 1H, CH_3).

3-[(3a*RS*,4*RS*,7a*RS*)-3a,4,7a-Trimethyloctahydro-1*H*-1,4-methanoinden-1-yl]pentane-2,4-dione (D)

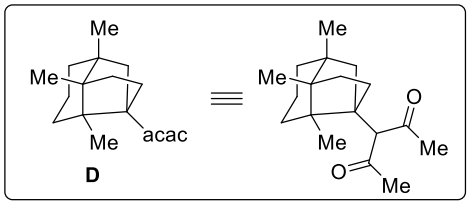

D

^{1}H NMR (400 MHz, $CDCl_3$) δ 2.36 (dd, *J* = 12.3, 4.0 Hz, 1H), 2.32 (s, 3H, $COCH_3$), 2.27–2.20 (m, 1H, CH_2), 2.18 (s, 3H, $COCH_3$), 2.17–2.08 (m, 1H,

CH_2), 1.92–1.72 (m, 3H, CH_2), 1.61–1.52 (m, 2H, CH_2), 1.49–1.36 (m, 3H, CH_2), 1.07 (dd, *J* = 13.0, 7.1 Hz, 1H, CH_2), 1.01 (s, 3H, CH_3), 0.95 (s, 3H, CH_3), 0.85 (s, 3H, CH_3).

Hexyl 3-((3aS,4R,7aS)-3a,4,7a-trimethyloctahydro-1H-1,4-methanoinden-1-yl)propanoate (12b)

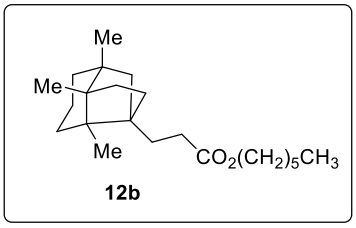

12b

To a solution of hydrazone **11a** (187 mg, 0.520 mmol) and $Fe(acac)_3$ (367 mg, 1.04 mmol) in THF (6.5 mL) with *t*-BuOH (494 μL, 2.77 mmol), hexyl acrylate (812 mg, 5.20 mmol) and $PhSiH_3$ (140 mg, 1.30 mmol) were added and stirred at 60 °C in an oil bath for 24 h. Purification by chromatography (hexane → hexane/EtOAc 95:5) gave the desired compound **12b** (120 mg, 69%) as a yellowish oil; ^{1}H NMR (400 MHz, $CDCl_3$) δ 4.08 (t, *J* = 6.8 Hz, 1H, CH_2), 3.92–3.72 (m, 1H, CH_2), 2.39–2.28 (m, 1H, CH_2), 2.23–2.16 (m, 1H, CH_2), 1.86 (dd, *J* = 12.4, 4 Hz, 2H, CH_2), 1.82–1.74 (m, 2H, CH_2), 1.69–1.61 (m, 4H, CH_2), 1.57 (br s, 6H, CH_2), 1.53–1.46 (m, 3H, CH_2), 1.38–1.25 (m, 6H, CH_2), 1.03 (dd, *J* = 12.4, 7.2 Hz, 2H, CH_2), 0.89 (s, 3H, Me), 0.78 (s, 3H, Me), 0.71 (s, 3H, Me); ^{13}C NMR (101 MHz, $CDCl_3$) δ 173.6 (C=O), 73.2 (CH_2), 68.0 (CH_2), 64.8 (CH_2), 48.8 (C), 47.1 (CH_2), 46.6 (C), 40.5 (C), 38.9 (C), 37.5 (CH_2), 33.5 (CH_2), 32.3 (CH_2), 31.6 (CH_2), 29.1 (CH_2), 28.6 (CH_2), 25.7 (CH_2), 22.7 (CH_2), 22.4 (Me), 19.8 (CH2), 17.4 (Me), 14.1 (CH_2), 12.1 (Me). HRMS (ESI) *m/z*: $[M+H]^+$ calcd for $[C_{22}H_{39}O_2]^+$ 335.2945, found 335.2951.

3-((3aS,4R,7aS)-3a,4,7a-trimethyloctahydro-1H-1,4-methanoinden-1-yl)propanenitrile (12c)

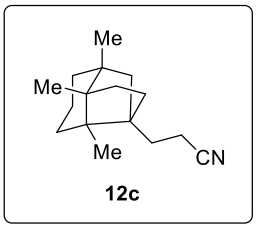

12c

To a solution of hydrazone **11a** (75 mg, 0.208 mmol) and $Fe(acac)_3$ (147 mg, 0.416 mmol) in THF (2.6 mL) with *t*-BuOH (197 mg, 2.08 mmol), acrylonitrile (110 mg, 2.08 mmol) and $PhSiH_3$ (56 mg, 0.52 mmol) were added and stirred at 60 °C in an oil bath for 24 h. Purification by chromatography (hexane → hexane/EtOAc 99:1) gave the desired compound **12c** (44 mg, 92%) as a colorless oil; ^{1}H NMR (400 MHz, $CDCl_3$) δ 2.30 (t, *J* = 8 Hz, 2H, CH_2CN), 1.77–1.60 (m, 4H, CH_2), 1.50–1.37 (m, 5H, CH_2), 1.33–1.26 (m, 2H, CH_2), 1.24–1.16 (m, 1H, CH_2), 0.96–0.93 (m, 2H, CH_2), 0.88 (s, 3H, Me), 0.79 (s, 3H, Me), 0.62 (s, 3H, Me); ^{13}C NMR (101 MHz, $CDCl_3$) δ 120.9 (CN), 50.4 (C), 50.1 (C), 49.5

(C), 44.9 (CH_2), 40.9 (C), 35.5 (CH_2), 33.5 (CH_2), 29.7 (CH_2), 29.5 (CH_2), 28.1 (CH_2), 22.2 (Me), 20.0 (CH_2), 18.1 (Me), 13.9 (CH_2CN), 11.6 (Me). HRMS (ESI) *m/z*: $[M+H]^+$ calcd for $[C_{16}H_{26N}]^+$ 232.2024, found 232.2055.

N,N-dimethyl-3-((3aS,4R,7aS)-3a,4,7a-trimethyloctahydro-1H-1,4-methanoinden-1-yl)propanamide (12d)

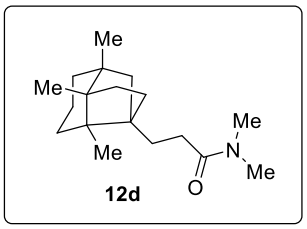

12d

To a solution of hydrazone **11a** (187 mg, 0.520 mmol) and $Fe(acac)_3$ (367 mg, 1.04 mmol) in THF (6.5 mL) with *t*-BuOH (385 mg, 5.20 mmol), *N,N*-dimethylacrylamide (134 μL, 1.30 mmol) and $PhSiH_3$ (140 mg, 1.30 mmol) were added and stirred at 60 °C in an oil bath for 24 h. Purification by chromatography (hexane → hexane/EtOAc 72:25) gave the desired compound **12d** (96 mg, 66%) as a colorless oil; ^{1}H NMR (400 MHz, $CDCl_3$) δ 3.00(s, 3H, Me), 2.93 (s, 3H, Me), 2.27 (d, *J* = 7.2 Hz, 2H, CH_2), 1.72–1.63 (m, 2H, CH_2), 1.62–1.57 (m, 2H, CH_2), 1.50–1.45 (m, 2H, CH_2), 1.42–1.33 (m, 4H, CH_2), 1.25–1.12 (m, 2H, CH_2), 0.91–0.89 (m, 2H, CH_2), 0.86 (s, 3H, Me), 0.77 (s, 3H, Me), 0.61 (s, 3H, Me); ^{13}C NMR (101 MHz, $CDCl_3$) δ 173.9 (C=O), 50.2 (C), 50.1 (C), 49.4 (C), 45.4 (CH_2), 40.7 (C), 37.5 (Me), 35.9 (CH_2), 35.5 (Me), 33.7 (CH_2), 29.9 (CH_2), 29.8 (CH_2), 29.6 (CH_2), 27.1 (CH_2), 22.3 (Me), 20.1 (CH_2), 18.2 (Me), 11.5 (Me). HRMS (ESI) *m/z*: $[M+H]^+$ calcd for $[C_{18}H_{32}NO]^+$ 278.2479, found 278.2487.

Methyl 2-methyl-3-((3aS,4R,7aS)-3a,4,7a-trimethyloctahydro-1H-1,4-methanoinden-1-yl)propanoate (12e)

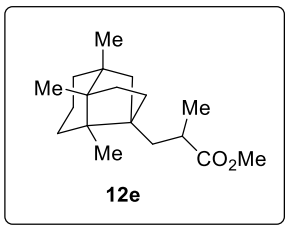

12e

To a solution of hydrazone **11a** (187 mg, 0.520 mmol) and $Fe(acac)_3$ (367 mg, 1.04 mmol) in THF (6.5 mL) with *t*-BuOH (494 μL, 5.20 mmol), methyl methacrylate (520 mg, 5.20 mmol) and $PhSiH_3$ (140 mg, 1.30 mmol) were added and stirred at 60 °C in an oil bath for 24 h. Purification by chromatography (hexane → hexane/EtOAc 97.2:2.5) gave the desired compound **12e** (109 mg, 75%) as a colorless oil, as a mixture of epimers (1:1) at C-2', selected peaks for one epimer: ^{1}H NMR (400 MHz, $CDCl_3$) δ 3.66 (s, 3H, OMe), 2.54–2.45 (m, 1H, CH), 1.86–1.76 (m, 1H, CH_2), 1.73–1.64 (m, 1H, CH_2), 1.61–1.53 (m, 1H, CH_2), 1.48–1.41 (m, 2H, CH_2), 1.38–1.29 (m, 6H, CH_2), 1.22–1.15 (m, 4H, CH_2 and CH-Me), 1.05–0.98 (m, 1H, CH_2), 0.94–0.89 (m, 1H,

CH_2), 0.86 (s, 3H, Me), 0.77 (s, 3H, Me), 0.59 (s, 3H, Me); ^{13}C NMR (101 MHz, $CDCl_3$) δ 178.6 (C=O), 51.7 (OMe), 50.6 (C), 50.2 (C), 48.9 (C), 45.9 (CH_2), 44.8 (CH_2), 40.9 (C), 37.4 (CH), 36.0 (CH_2), 33.6 (CH_2), 30.0 (CH_2), 29.6 (CH_2), 22.3 (Me), 20.1 (CH_2), 19.9 (CH-Me), 18.2 (Me), 11.7 (Me). HRMS (ESI) *m/z*: $[M+H]^+$ calcd for $[C_{18}H_{31}O_2]^+$ 279.2319, found 279.2321.

Methyl 3-((3aS,4R,7aS)-3a,4,7a-trimethyloctahydro-1H-1,4-methanoinden-1-yl)butanoate (12f)

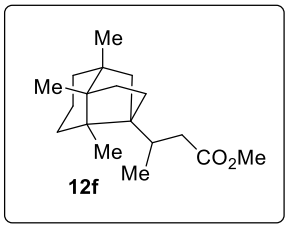

To a solution of hydrazone **11a** (187 mg, 0.520 mmol) and $Fe(acac)_3$ (367 mg, 1.04 mmol) in THF (6.5 mL) with *t*-BuOH (494 μL, 5.20 mmol), methyl but-2-enoate (520 mg, 5.20 mmol) and $PhSiH_3$ (140 mg, 1.30 mmol) were added and stirred at 60 °C in an oil bath for 24 h. Purification by chromatography (hexane → hexane/EtOAc 97.5:2.5) gave the desired compound **12f** (124 mg, 85%) as a colorless oil, as a mixture of epimers (1:1) at C-2', selected peaks for one epimer: ^1H NMR (400 MHz, $CDCl_3$) δ 3.67 (s, 3H, OMe), 2.53 (ddd, *J* = 23.6, 13.6, 2.8 Hz, 1H, CH_2CO), 2.24–2.17 (m, 1H, CH), 2.05 (ddd, *J* = 25.2, 14.4, 11.6 Hz, 1H, CH_2CO), 1.72–1.56 (m, 5H, CH_2), 1.52–1.39 (m, 5H, CH_2), 1.25–1.13 (m, 2H, CH_2), 0.97 (d, *J* = 6.8 Hz, 3H, Me-CH), 0.86 (s, 3H, Me), 0.75 (s, 3H, Me), 0.74 (s, 3H, Me); ^{13}C NMR (101 MHz, $CDCl_3$) δ 174.6 (C=O), 53.6 (C), 51.6 (OMe), 50.5 (C), 50.3 (C), 45.0 (CH_2), 39.9 (C), 39.0 (CH_2), 38.7 (CH_2CO), 34.9 (CH_2), 33.8 (CH_2), 31.1 (CH_2), 29.3 (CH_2), 22.5 (Me), 19.3 (Me), 16.2 (Me-CH), 11.8 (Me). HRMS (ESI) *m/z*: $[M+H]^+$ calcd for $[C_{18}H_{31}O_2]^+$ 279.2319, found 279.2325.

2-((3aS,4R,7aS)-3a,4,7a-trimethyloctahydro-1H-1,4-methanoinden-1-yl)-2,3-dihydronaphthalene-1,4-dione (12g)

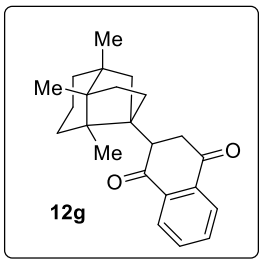

To a solution of hydrazone **11a** (187 mg, 0.520 mmol) and $Fe(acac)_3$ (367 mg, 1.04 mmol) in THF (6.5 mL) with *t*-BuOH (385 mg, 5.20 mmol), naphthalene-1,4-dione (411 mg, 2.60 mmol) and $PhSiH_3$ (140 mg, 1.30 mmol) were added and stirred at 60 °C in an oil bath for 24 h. Purification by chromatography (hexane → hexane/EtOAc 95:5) gave the desired compound **12g** (132 mg, 76%) as a brownish oil; ^1H NMR (400 MHz, $CDCl_3$) δ 7.58 (d, *J* = 8 Hz, 2H, Ph), 7.31 (d, *J* = 8 Hz, 2H, Ph), 2.42

(s, 1H, CH), 2.40–2.32 (m, 2H, CH_2CO), 2.06–1.98 (m, 1H, CH_2), 1.95–1.80 (m, 2H, CH_2), 1.76–1.66 (m, 1H, CH_2), 1.63–1.39 (m, 7H, CH_2), 1.14–1.07 (m, 1H, CH_2), 0.93 (s, 3H, Me), 0.81 (s, 3H, Me), 0.79 (s, 3H, Me); ^{13}C NMR (101 MHz, $CDCl_3$) δ 144.0 (C=O), 142.2 (C=O), 130.2 (C_{ipso}), 129.7 (C_{ipso}), 129.6 (Ph), 125.1 (Ph), 50.4 (C), 45.9 (C), 45.6 (CH_2CO), 45.5 (C), 41.9 (C), 35.9 (CH_2), 33.5 (CH_2), 29.8 (CH_2), 29.5 (CH_2), 28.7 (CH_2), 22.4 (Me), 21.6 (CH), 19.6 (CH_2), 17.7 (Me), 11.7 (Me). HRMS (ESI) *m/z*: $[M+H]^+$ calcd for $[C_{23}H_{29}O_2]^+$ 337.2162, found 337.2155.

3-((3aS,4R,7aS)-3a,4,7a-trimethyloctahydro-1H-1,4-methanoinden-1-yl)cyclohexan-1-one (12h)

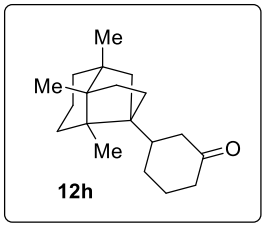

12h

To a solution of hydrazone **11a** (187 mg, 0.520 mmol) and $Fe(acac)_3$ (367 mg, 1.04 mmol) in THF (6.5 mL) with *t*-BuOH (385 mg, 5.20 mmol), cyclohex-2-en-1-one (500 mg, 5.20 mmol) and $PhSiH_3$ (140 mg, 1.30 mmol) were added and stirred at 60 °C in an oil bath for 24 h. Purification by chromatography (hexane → hexane/EtOAc 95:5) gave the desired compound **12h** (128 mg, 90%) as a mixture of diastereomers, as a yellowish oil; ^{1}H NMR (400 MHz, $CDCl_3$) δ 2.54–2.41 (m, 2H, CH_2), 2.36–2.34 (m, 1H, CH_2), 2.28–2.22 (m, 1H, CH_2), 2.17 (br s, 1H, CH), 2.13–2.06 (m, 1H, CH_2), 1.98–1.90 (m, 1H, CH_2), 1.79–1.67 (m, 2H, CH_2), 1.58–1.39 (m, 8H, CH_2), 1.28–1.10 (m, 2H, CH_2), 1.00–0.94 (m, 2H, CH_2), 0.87 (s, 3H, Me), 0.75 (s, 3H, Me), 0.69 (s, 3H, Me); ^{13}C NMR (101 MHz, $CDCl_3$) δ 213.3 (C=O), 53.6 (C), 50.4 (C), 50.3 (C), 45.6 (CH_2), 44.3 (CH_2), 42.8 (CH_2), 41.7 (CH_2), 40.1 (C), 34.3 (CH_2), 34.0 (CH_2), 31.0 (CH), 29.3 (CH_2), 27.7 (CH_2), 26.0 (CH_2), 22.5 (Me), 20.2 (CH_2), 19.5 (Me), 11.7 (Me). HRMS (ESI) *m/z*: $[M+NH_4]^+$ calcd for $[C_{19}H_{34}NO]^+$ 292.2635, found 292.2631.

1,4-diphenyl-2-((3aS,4R,7aS)-3a,4,7a-trimethyloctahydro-1H-1,4-methanoinden-1-yl)butane-1,4-dione (12i)

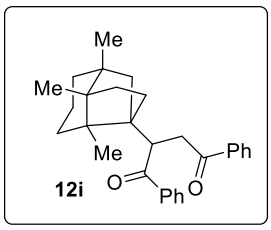

12i

To a solution of hydrazone **11a** (187 mg, 0.520 mmol) and $Fe(acac)_3$ (367 mg, 1.04 mmol) in THF (6.5 mL) with *t*-BuOH (385 mg, 5.20 mmol), 1,4-diphenylbut-2-ene-1,4-dione (307 mg, 1.30 mmol) and $PhSiH_3$ (140 mg, 1.30 mmol) were added and stirred at 60 °C in an oil bath for 5 h. Purification by chromatography (hexane →

hexane/EtOAc 95:5) gave the desired compound **12i** (167 mg, 92%) as a mixture of diastereomers, as a yellow oil; ^{1}H NMR (400 MHz, $CDCl_3$) δ 8.22–8.17 (m, 4H, Ph), 7.96–7.93 (m, 4H, Ph), 7.56–7.47 (m, 8H, Ph), 7.45–7.40 (m, 4H, Ph), 4.38 (ddd, *J* = 10.8, 6.4, 2.4 Hz, 2H, H-2'), 4.06 (dd, *J* = 18, 11.2 Hz, 1H, H-3'), 3.93 (dd, *J* = 18, 10.8 Hz, 1H, H-3'), 3.41 (dd, *J* = 18, 2.8 Hz, 1H, H-3'), 3.31 (dd, *J* = 18, 2.8 Hz, 1H, H-3'), 2.04 (ddd, *J* = 12.4, 9.2, 4 Hz, 2H, CH_2), 1.83–1.62 (m, 5H, CH_2), 1.58–1.22 (m, 12H, CH_2), 1.18–0.95 (m, 5H, CH_2), 0.89 (s, 3H, Me), 0.84 (s, 3H, Me), 0.78 (s, 3H, Me), 0.75 (s, 3H, Me), 0.74 (s, 3H, Me), 0.63 (s, 3H, Me); ^{13}C NMR (101 MHz, $CDCl_3$) δ 204.1, (C=O), 203.8 (C=O), 199.3 (C=O), 139.5 (C_{ipso}), 139.4 (C_{ipso}), 136.7(C_{ipso}), 136.6 (C_{ipso}), 133.2 (Ph), 133.1 (Ph), 132.6 (Ph), 132.5 (Ph), 128.9 (Ph), 128.8 (Ph), 128.7 (Ph), 128.6 (Ph), 128.5 (Ph), 128.4 (Ph), 128.2 (Ph), 128.1 (Ph), 52.7(C), 52.3 (C), 51.0 (C), 50.8 (C), 49.8 (C), 44.2 (CH_2), 43.7 (CH_2), 42.2 (C-2'), 41.8 (C-2'), 40.5 (C-3'), 40.2 (C), 40.1 (C), 39.7 (C-3'), 36.8 (CH_2), 36.0 (CH_2), 33.9 (CH_2), 33.7 (CH_2), 30.8 (CH_2), 29.9 (CH_2), 29.1 (CH_2), 22.4 (Me), 22.3 (Me), 19.7 (Me), 19.4 (Me), 11.7 (Me), 11.6 (Me). HRMS (ESI) *m/z*: $[M+H]^+$ calcd for $[C_{29}H_{35}O_2]^+$ 415.2632, found 415.2638.

Methyl 3-((3aS,4R,7aS)-3a,7a-dimethyloctahydro-1H-1,4-methanoinden-1-yl) propanoate (13a)

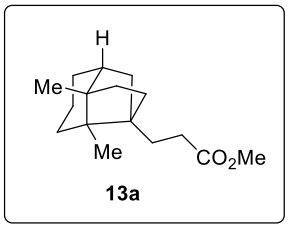

13a

To a solution of hydrazone **7a** (194 mg, 0.561 mmol) and $Fe(acac)_3$ (396 mg, 1.12 mmol) in THF (7 mL) with *t*-BuOH (532 μL, 5.61 mmol), methyl acrylate (483 mg, 5.61 mmol) and $PhSiH_3$ (152 mg, 1.40 mmol) were added and stirred at 60 °C in an oil bath for 24 h. Purification by chromatography (hexane → hexane/EtOAc 97.2:2.5) gave the desired compound **13a** (129 mg, 95%) as a yellowish oil; ^{1}H NMR (400 MHz, $CDCl_3$) δ 3.68 (s, 3H, OMe), 2.31 (t, *J* = 8 Hz, 2H, CH_2CO), 1.80–1.77 (m, 1H, CH), 1.70–1.61 (m, 2H, CH_2), 1.53–1.46 (m, 1H, CH_2), 1.41–1.30 (m, 6H, CH_2), 1.27–1.22 (m, 2H, CH_2), 1.15–1.11 (m, 2H, CH_2), 1.06–0.98 (m, 1H, CH_2), 0.92 (s, 3H, Me), 0.57 (s, 3H, Me); ^{13}C NMR (101 MHz, $CDCl_3$) δ 175.2 (C=O), 51.7 (OMe), 50.3 (C), 49.6 (C), 48.7 (C), 38.9 (CH), 36.5 (CH_2), 34.9 (CH_2), 32.7 (CH_2), 30.9 (CH_2CO), 29.2 (CH_2), 26.7 (CH_2), 24.9 (CH_2), 18.4 (CH_2), 17.7 (Me), 15.5 (Me). HRMS (ESI) *m/z*: $[M+H]^+$ calcd for $[C_{16}H_{27}O_2]^+$ 251.2006, found 251.2012.

Methyl 3-((3aR,4R,7aS)-3a-benzyl-7a-methyloctahydro-1H-1,4-methanoinden-1-yl)propanoate (13b)

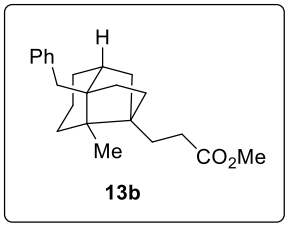

13b

To a solution of hydrazone **7b** (166 mg, 0.393 mmol) and $Fe(acac)_3$ (278 mg, 0.786 mmol) in THF (4.9 mL) with *t*-BuOH (373 μL, 3.93 mmol), methyl acrylate (80 mg, 3.93 mmol) and $PhSiH_3$ (106 mg, 0.983 mmol) were added and stirred at 60 °C in an oil bath for 24 h. Purification by chromatography (hexane → hexane/EtOAc 97.5:2.5) gave the desired compound **13b** (112 mg, 88%) as a colorless oil; ^{1}H NMR (400 MHz, $CDCl_3$) δ 7.25–7.14 (m, 5H, Ph), 3.66 (s, 3H, OMe), 3.06 (d, *J* = 13.6 Hz, 1H) and 2.37 (d, *J* = 13.2 Hz, 1H, CH_2Ph), 2.29 (t, *J* = 8.4 Hz, 2H, CH_2CO), 2.01–1.93 m, 1H, CH_2), 1.74–1.62 (m, 3H, CH_2 and 1H, CH), 1.58–1.54 (m, 1H, CH_2), 1.49–1.44 (m, 2H, CH_2), 1.40–1.34 (m, 2H, CH_2), 1.26–1.15 (m, 3H, CH_2), 1.11–1.06 (m, 1H, CH_2), 1.03–0.96 (m, 1H, CH_2), 0.70 (s, 3H, Me); ^{13}C NMR (101 MHz, $CDCl_3$) δ 174.9 (C=O), 140.4 (C_{ipso}), 129.9 (Ph), 127.9 (Ph), 125.6 (Ph), 51.6 (OMe), 50.5 (C), 50.4 (C), 49.1 (C), 38.7 (CH), 36.5 (CH_2), 34.8 (CH_2), 34.6 (CH_2Ph), 32.6 (CH_2), 30.8 (CH_2CO), 29.5 (CH_2), 26.5 (CH_2), 25.6 (CH_2), 18.5 (CH_2), 17.8 (Me). HRMS (ESI) *m/z*: $[M+H]^+$ calcd for $[C_{22}H_{31}O_2]^+$ 327.2319, found 327.2321.

Methyl 3-((3aS,4R,7aS)-7a-methyl-3a-propyloctahydro-1H-1,4-methanoinden-1-yl)propanoate (13c)

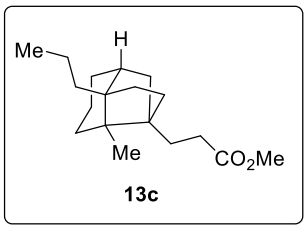

13c

To a solution of hydrazone **7c** (181 mg, 0.485 mmol) and $Fe(acac)_3$ (343 mg, 0.970 mmol) in THF (6 mL) with *t*-BuOH (460 μL, 4.85 mmol), methyl acrylate (417 mg, 4.85 mmol) and $PhSiH_3$ (131 mg, 1.213 mmol) were added and stirred at 60 °C in an oil bath for 24 h. Purification by chromatography (hexane → hexane/EtOAc 99:1) gave the desired compound **13c** (108 mg, 80%) as a colorless oil; ^{1}H NMR (400 MHz, $CDCl_3$) δ 3.67 (s, 3H, OMe), 2.31 (t, *J* = 8 Hz, 2H, CH_2CO), 1.80–1.76 (m, 1H, CH), 1.69–1.57 (m, 3H, CH_2), 1.52–1.44 (m, 2H, CH_2), 1.40–1.28 (m, 8H, CH_2), 1.26–1.20 (m, 2H, CH_2), 1.15–1.10 (m, 2H, CH_2), 1.05–0.98 (m, 1H, CH_2), 0.92 (t, *J* = 7.2 Hz, 3H, Me), 0.56 (s, 3H, Me); ^{13}C NMR (101 MHz, $CDCl_3$) δ 175.1 (C=O), 51.6 (OMe), 50.2 (C), 49.5 (C), 48.7 (C), 38.8 (CH), 36.5 (CH_2), 35.0 (CH_2), 32.7 (CH_2), 31.4 (CH_2), 31.0 (CH_2CO), 29.2

(CH_2), 26.6 (CH_2), 24.9 (CH_2), 18.4 (CH_2), 17.9 (CH_2), 17.6 (Me), 15.5 (Me). HRMS (ESI) *m/z*: $[M+H]^+$ calcd for $[C_{18}H_{31}O_2]^+$ 279.2319, found 279.2321.

Synthesis of adamantyl-substituted heterocycles 14 and 15

2,5-diphenyl-3-((3aS,4R,7aR)-3a,4,7a-trimethyloctahydro-1H-1,4-methanoinden-1-yl)-1H-pyrrole (14)[325]

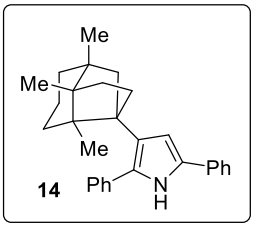

A solution of **12i** (140 mg, 0.34 mmol, 1 equiv) and ammonium acetate (520 mg, 6.75 mmol, 20 equiv) in a mixture of EtOH (8.1 mL) and $CHCl_3$ (5.4 mL) was stirred at 50 °C for 24 h. Concentration and purification by column (hexane → hexane/EtOAc 97.5:2.5) gave the desired compound **14** (112 mg, 84%) as a brownish oil; ^{1}H NMR (500 MHz, $CDCl_3$) δ 8.05 (br s, 1H, NH), 7.46 (br s, 4H, Ph), 7.38–7.33 (m, 5H, Ph), 7.17 (t, *J* = 7 Hz, 1H, Ph), 6.69 (s, 1H, CH), 2.11 (dd, *J* = 12.5, 3.5 Hz, 1H, CH_2), 1.77–1.59 (m, 4H, CH_2), 1.55–1.38 (m, 3H, CH_2), 1.27–1.12 (m, 3H, CH_2), 1.02–0.96 (m, 1H, CH_2), 0.86 (s, 3H, Me), 0.80 (s, 3H, Me), 0.69 (s, 3H, Me); ^{13}C NMR (126 MHz, $CDCl_3$) δ 136.4 (C_{ipso}), 134.7 (C_{ipso}), 132.8 (C_{ipso}), 131.6 (Ph), 131.4 (Ph), 130.2 (C_{ipso}), 128.9 (Ph), 127.8 (Ph), 125.9 (Ph), 124.9 (C-CH), 123.6 (Ph), 106.4 (CH), 58.9 (C), 52.6 (C), 51.4 (C), 49.8 (CH_2), 49.5 (CH_2), 40.8 (C), 38.7 (CH_2), 34.1 (CH_2), 30.3 (CH_2), 29.9 (CH_2), 22.5 (Me), 20.4 (CH_2), 19.1 (Me), 12.3 (Me). HRMS (ESI) *m/z*: $[M+H]^+$ calcd for $[C_{29}H_{34}N]^+$ 396.2686, found 396.2688.

2,5-Diphenyl-3-((3aS,4R,7aR)-3a,4,7a-trimethyloctahydro-1H-1,4-methanoinden-1-yl)furan (15)[326]

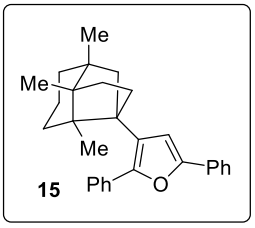

To a stirred solution of **12i** (60 mg, 0.144 mmol) in toluene (3 mL, 0.1 M) was added TsOH (13 mg, 0.072 mmol) at room temperature. The mixture was heated to 110 °C and stirred for 8 h. Purification by column chromatography (hexane → hexane/EtOAc 97.5:2.5) gave the desired compound **15** (50 mg, 88%) as a pale yellow oil; ^{1}H NMR (400 MHz, $CDCl_3$) δ 7.71–7.68 (m, 2H, Ph), 7.52–7.50 (m, 2H, Ph), 7.42–7.35 (m, 5H, Ph), 7.24 (tt, *J* = 6.8, 1.2 Hz, 1H, Ph), 6.87 (s, 1H, C-3'), 2.09 (dd, *J* = 12.8, 3.6 Hz, 1H, CH_2), 1.79–1.71 (m, 2H, CH_2), 1.64–1.54 (m, 2H, CH_2), 1.52–1.45 (m, 2H, CH_2), 1.30–1.20 (m, 3H, CH_2), 1.04–0.97 (m, 2H, CH_2), 0.90 (s, 3H, Me), 0.82 (s, 3H, Me), 0.72 (s,

3H, Me); ^{13}C NMR (101 MHz, $CDCl_3$) δ 151.8 (C-Ph), 150.9 (C-Ph), 134.1 (C_{ipso}),131.2 (Ph), 131.1 (C_{ipso}), 128.7 (Ph), 128.5 (Ph), 127.7 (Ph), 127.1 (Ph), 125.5 (C-2'), 123.8 (Ph), 106.8 (C-3'), 52.8 (C), 49.9 (C), 48.6 (CH_2), 40.9 (C), 38.2 (CH_2), 33.9 (CH_2), 30.3 (CH_2), 29.9 (CH_2), 22.4 (Me), 20.3 (CH_2), 19.0 (Me), 12.2 (Me). HRMS (ESI) *m/z*: $[M+H]^+$ calcd for $[C_{29}H_{33}O]^+$ 397.2526, found 397.2533.

Copies of ^{1}H and ^{13}C NMR spectra

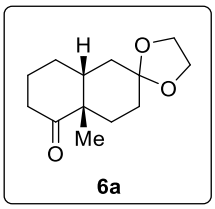

6a

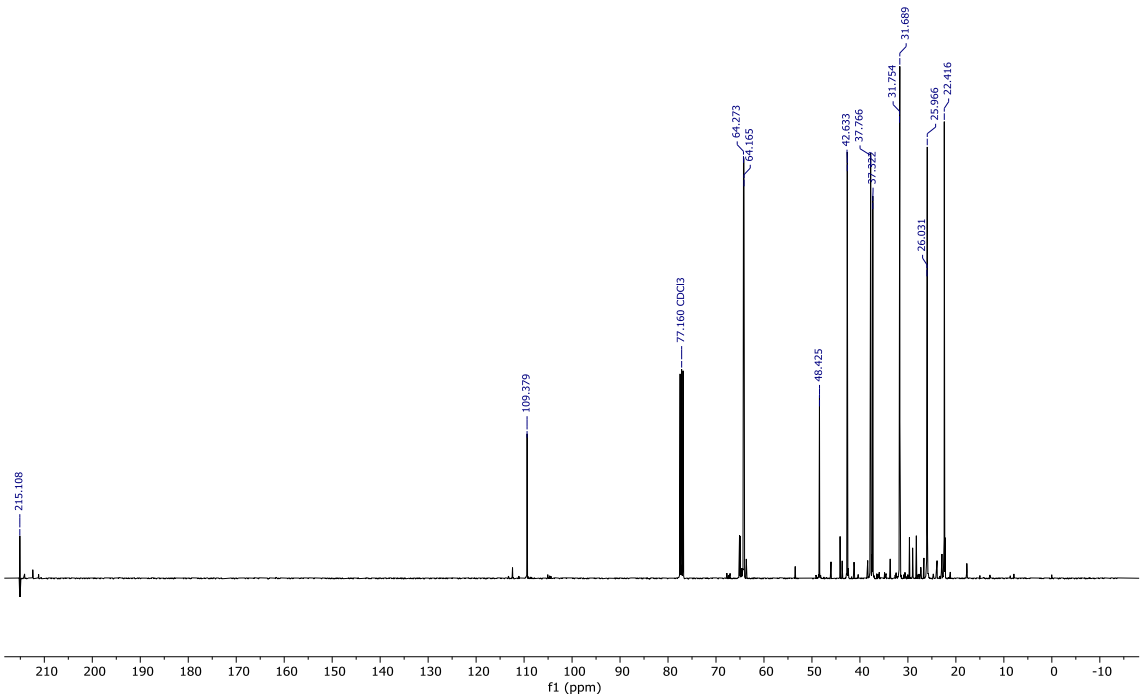

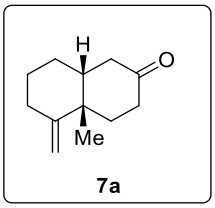
H
O
Me

7a

1.279
4.880
4.835
7.260 CDCl3
2.537
2.449
2.206
1.900
1.850
1.842
1.778
1.703
1.602
1.546
1.464
1.380
1.306
1.98
1.07
6.06
1.04
1.01
1.06
2.09
1.07
3.00
f1 (ppm)

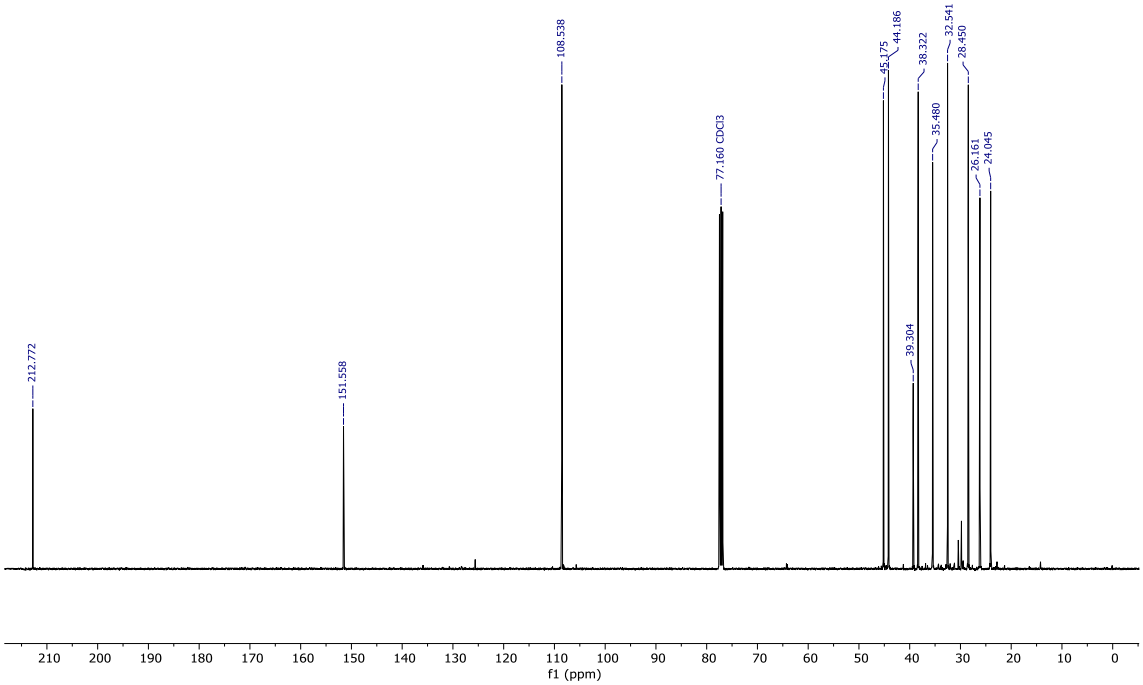
212.772
151.558
108.538
77.160 CDCl3
45.175
44.186
39.304
38.322
35.480
32.541
28.450
26.161
24.045
f1 (ppm)

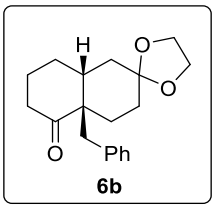
H
O
O
O
Ph

6b

7.260 CDCl3
7.014
6.990
7.171
3.915
3.882
3.417
3.383
2.754
2.720
2.889
2.800
2.469
2.287
1.945
1.936
1.902
1.621
1.588
1.537
1.245
1.232
1.211
1.198
1.180
1.167
2.96
1.99
4.01
0.98
0.99
0.96
3.03
2.00
1.05
2.02
3.04
1.04
f1 (ppm)

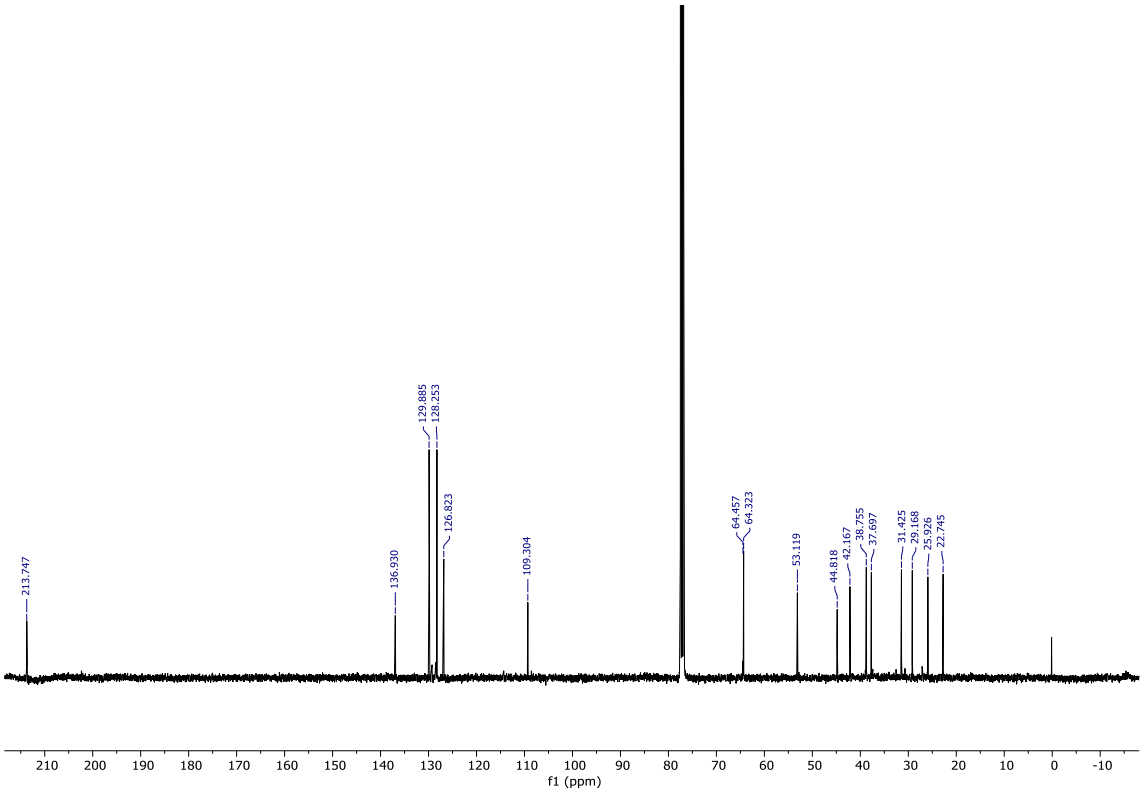
213.747
136.930
129.885
128.253
126.823
109.304
64.457
64.323
53.119
44.818
42.167
38.755
37.697
31.425
29.168
25.926
22.745
f1 (ppm)

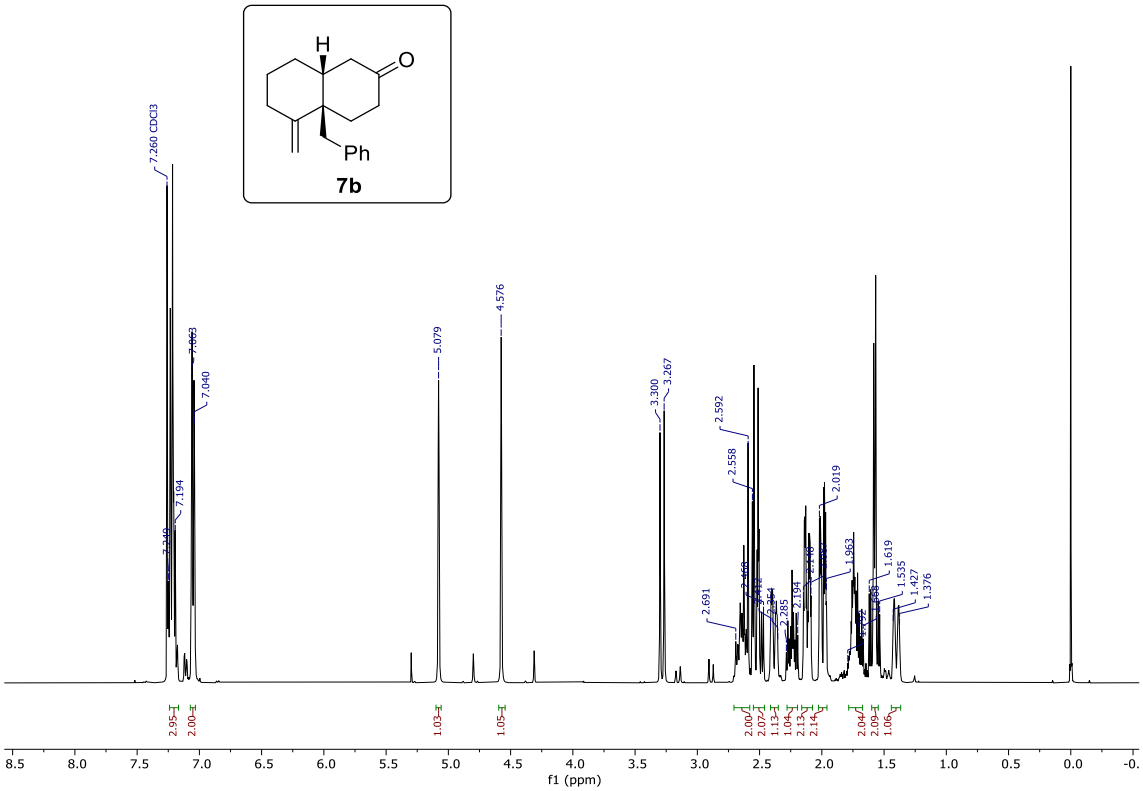
H
O
Ph
7b
7.260 CDCl3
7.349
7.194
7.040
5.079
4.576
3.300
3.267
2.691
2.592
2.558
2.019
1.863
1.619
1.535
1.427
1.376
f1 (ppm)

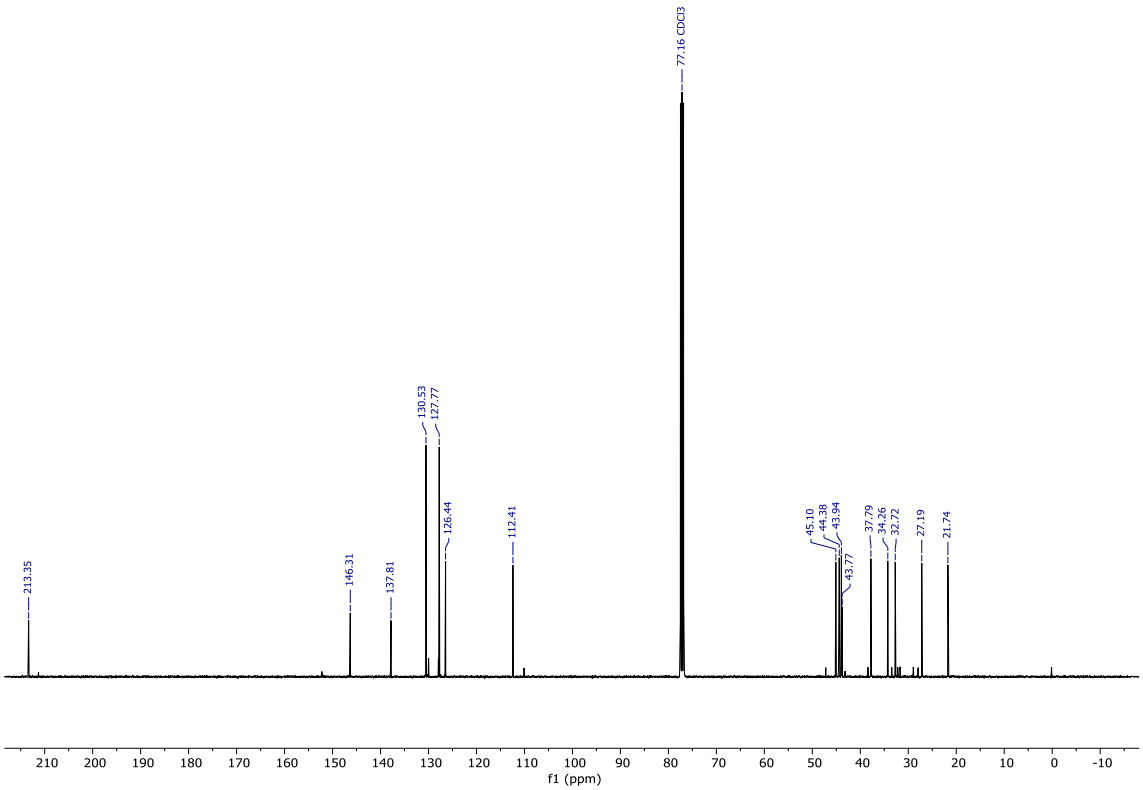
77.16 CDCl3
213.35
146.31
137.81
130.53
127.77
126.44
112.41
45.10
44.38
43.94
43.77
37.79
34.26
32.72
27.19
21.74
f1 (ppm)

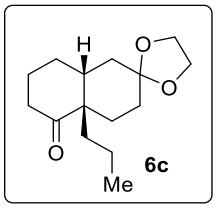
H
O
O
O
Me
6c

7.260 CDCl3
3.948
3.892
2.517
2.428
2.306
2.188
2.097
1.980
1.687
1.535
1.279
1.177
1.098
0.850
4.00
1.04
3.93
2.14
4.05
4.01
0.98
4.19
f1 (ppm)

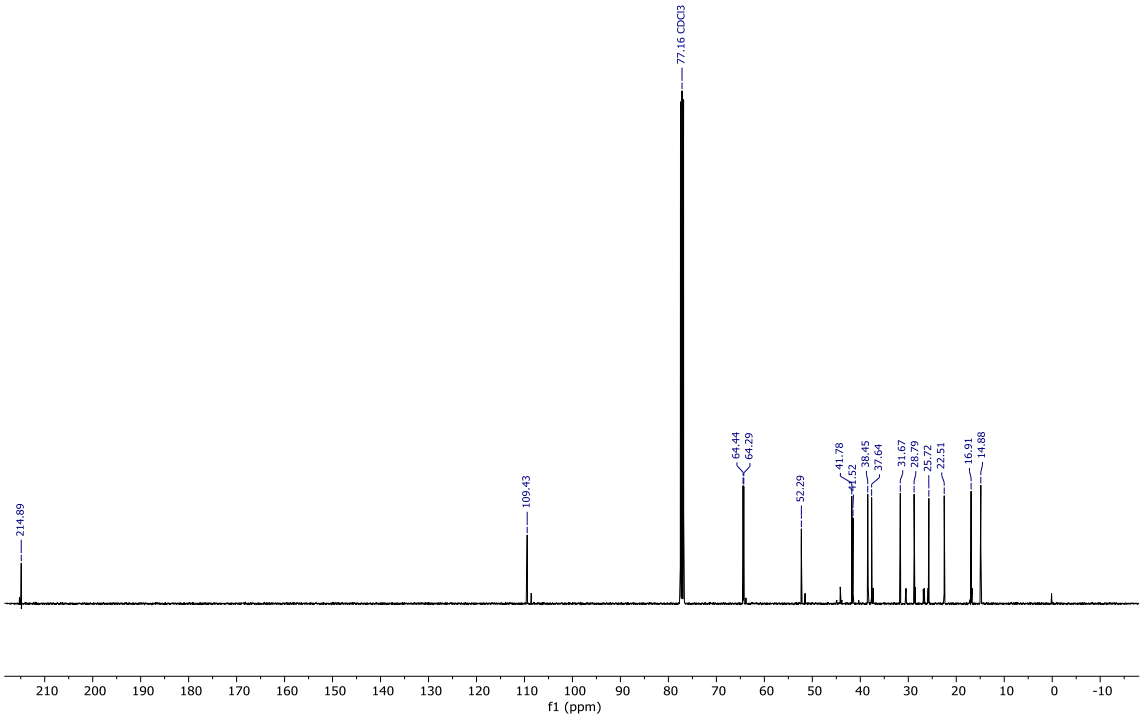
214.89
109.43
77.16 CDCl3
64.44
64.29
52.29
41.78
41.52
38.45
37.64
31.67
28.79
25.72
22.51
16.91
14.88
f1 (ppm)

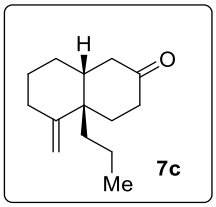
H
O
Me

7c

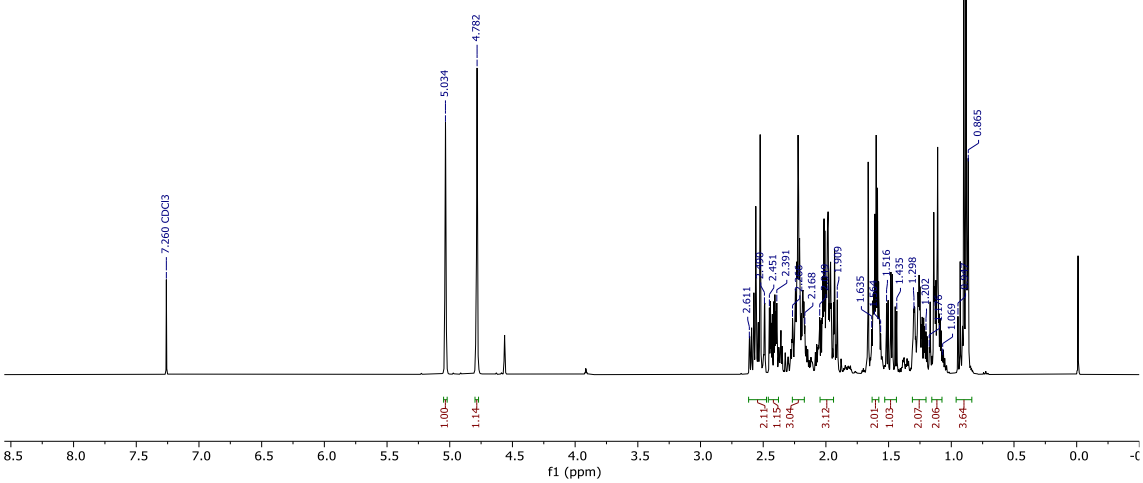
7.260 CDCl3
5.034
4.782
0.865
2.611
2.451
2.391
2.168
1.635
1.516
1.435
1.298
1.069
1.00
1.14
2.11
1.15
3.04
3.12
2.01
1.03
2.07
2.06
3.64
f1 (ppm)

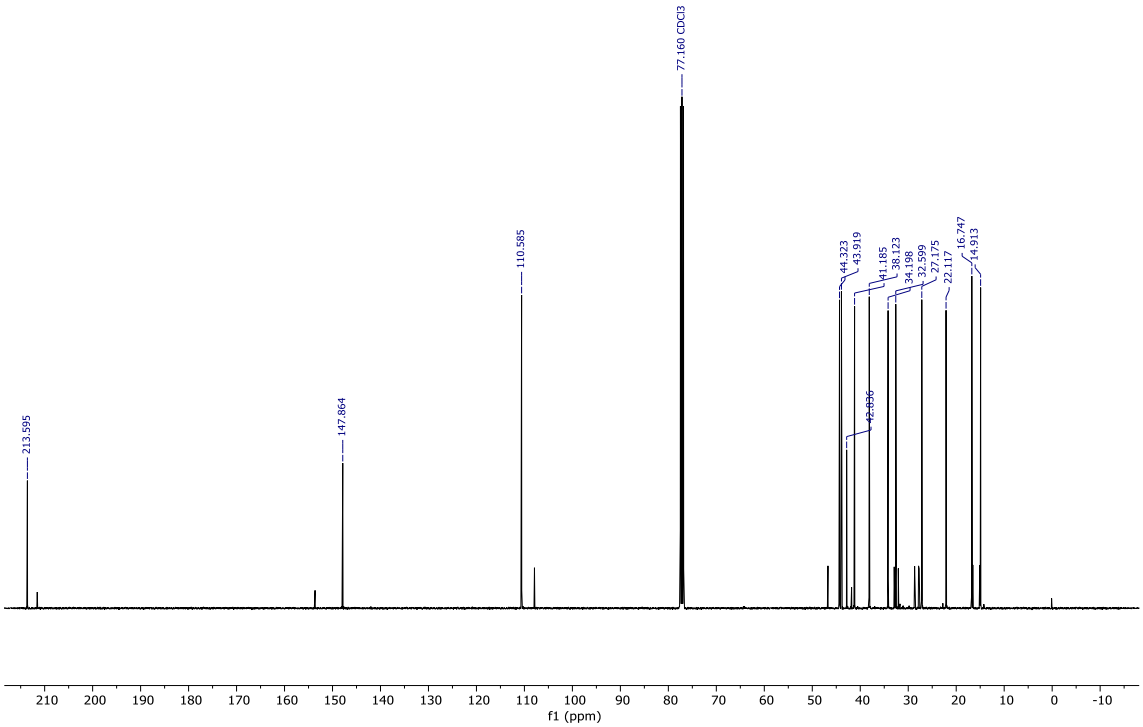
77.160 CDCl3
213.595
147.864
110.585
44.323
43.919
41.185
38.123
34.198
32.599
27.175
22.117
16.747
14.913
f1 (ppm)

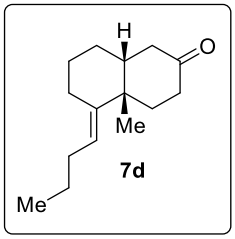
H
O
Me
Me

7d

7.260 CDCl3
5.365
5.348
5.330
2.538
2.460
2.385
2.293
2.241
2.169
2.102
1.991
1.907
1.828
1.575
1.457
1.415
1.322
1.244
0.899
0.917
0.880
1.00
0.66
1.11
4.15
2.10
2.23
1.99
3.06
3.04
3.10
3.34
f1 (ppm)

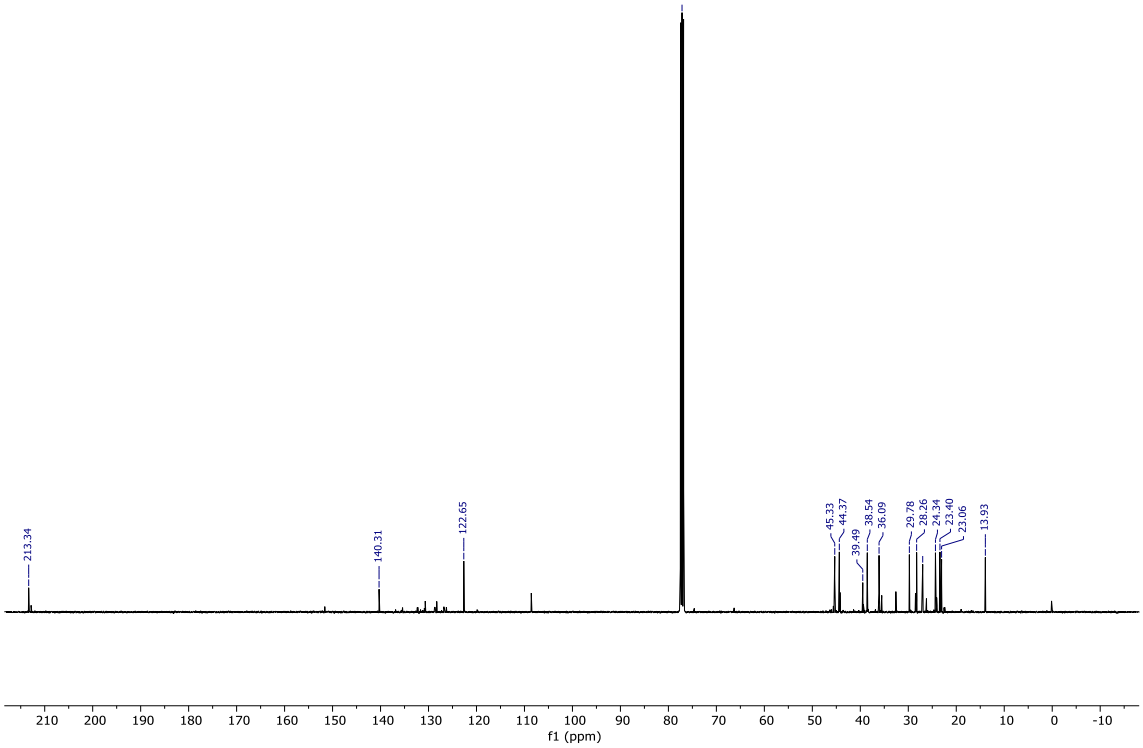
213.34
140.31
122.65
45.33
44.37
39.49
38.54
36.09
29.78
28.26
24.34
23.40
23.06
13.93
f1 (ppm)

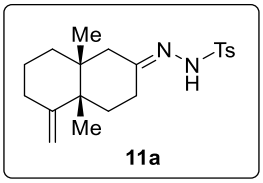
Me
N
N
H
Ts
Me

11a

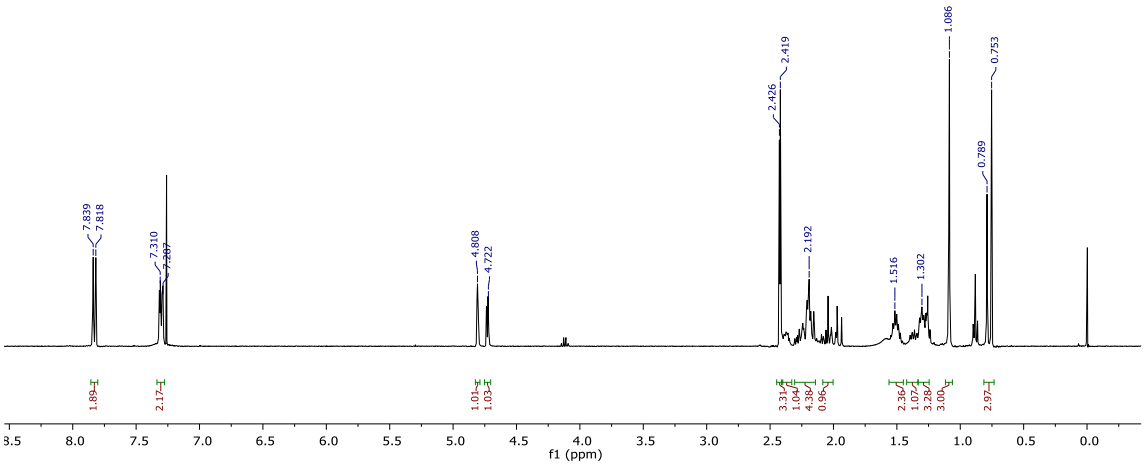
7.839
7.818
7.310
7.287
4.808
4.722
2.426
2.419
2.192
1.516
1.302
1.086
0.789
0.753
1.89
2.17
1.01
1.03
3.31
1.04
4.38
0.96
2.36
1.07
3.28
3.00
2.97
f1 (ppm)

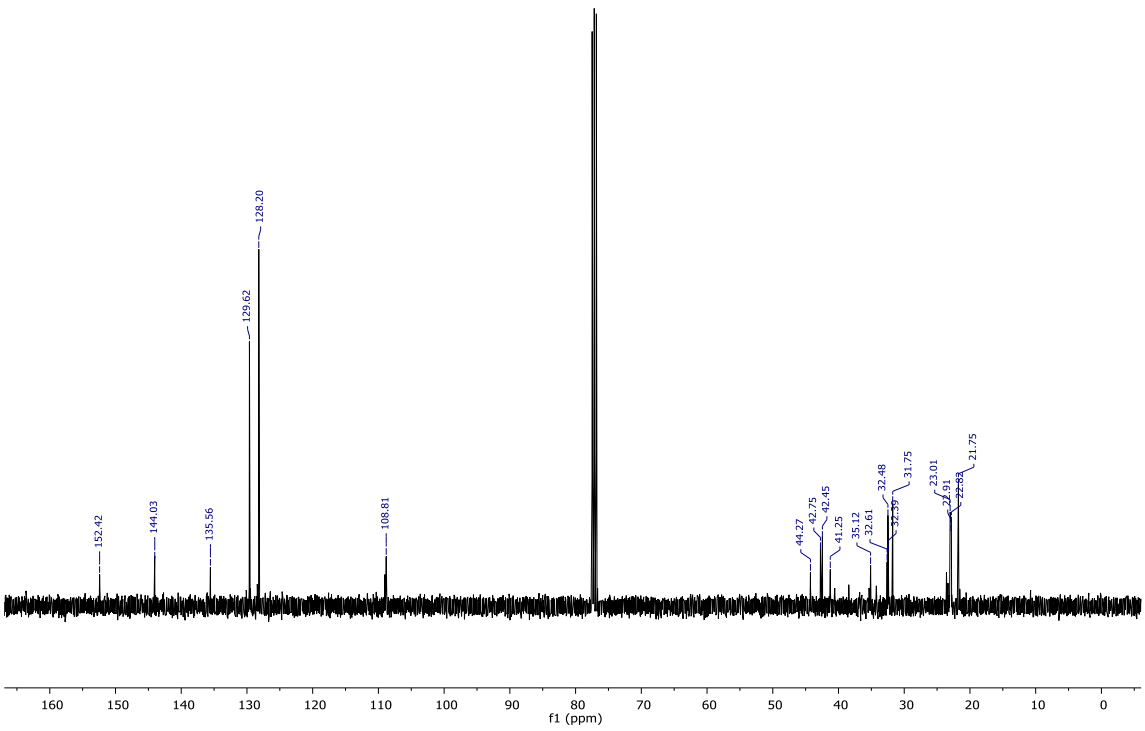
152.42
144.03
135.56
129.62
128.20
108.81
44.27
42.75
42.45
41.25
35.12
32.61
32.48
31.75
23.01
22.91
22.83
21.75
f1 (ppm)

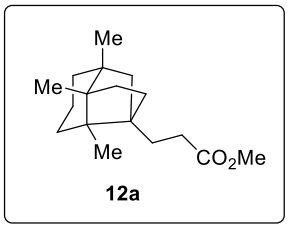
Me
Me
Me
CO_2Me

12a

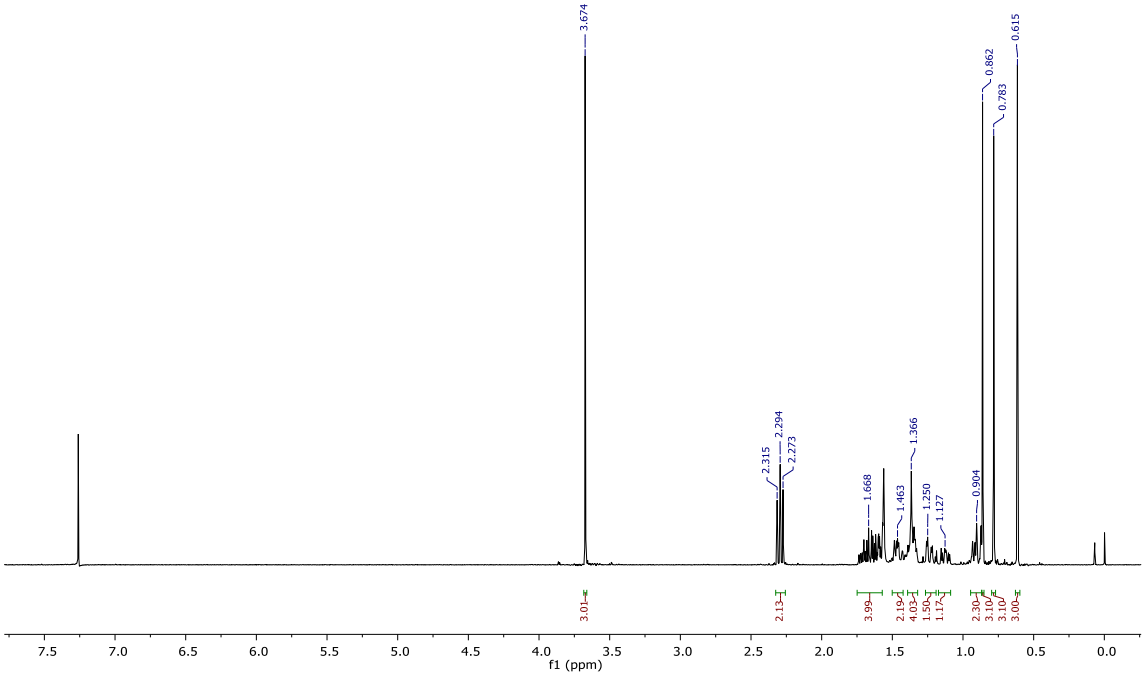
3.674
2.315
2.294
2.273
1.668
1.463
1.366
1.250
1.127
0.904
0.862
0.783
0.615
3.01
2.13
3.99
2.19
4.03
1.50
1.17
2.30
3.10
3.10
3.00
7.5 7.0 6.5 6.0 5.5 5.0 4.5 4.0 3.5 3.0 2.5 2.0 1.5 1.0 0.5 0.0
f1 (ppm)

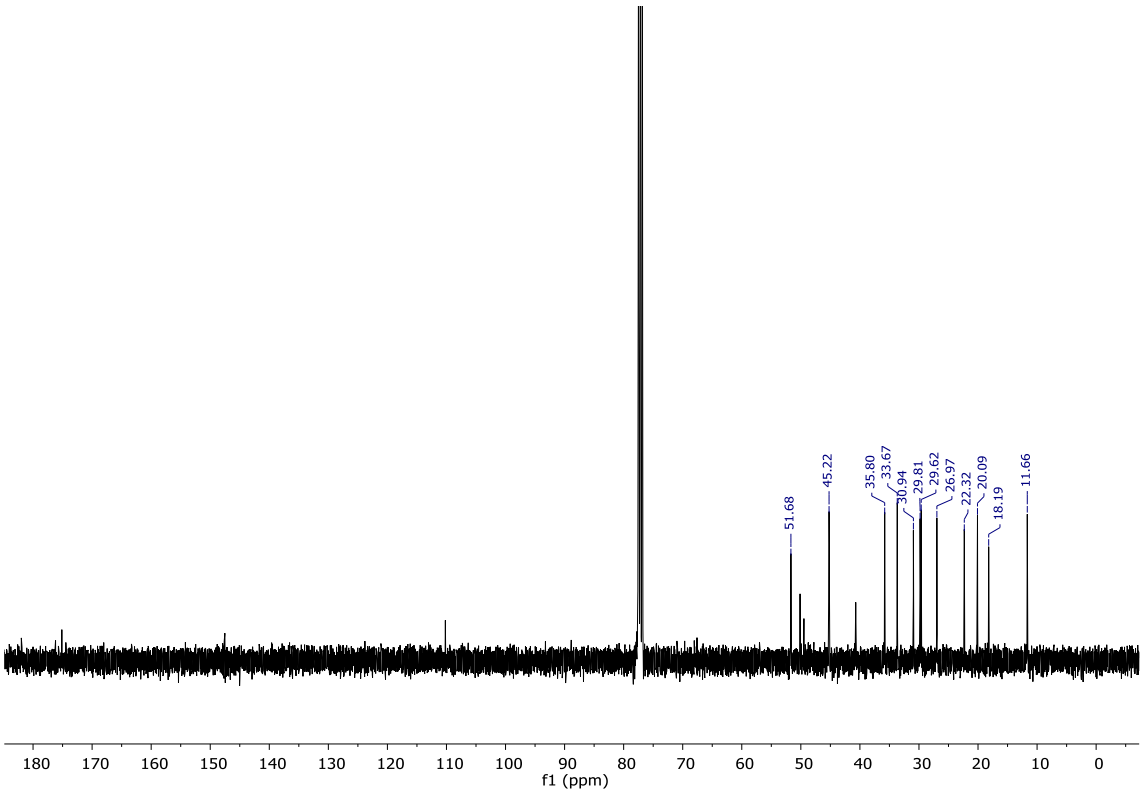
51.68
45.22
35.80
33.67
30.94
29.81
29.62
26.97
22.32
20.09
18.19
11.66
180 170 160 150 140 130 120 110 100 90 80 70 60 50 40 30 20 10 0
f1 (ppm)

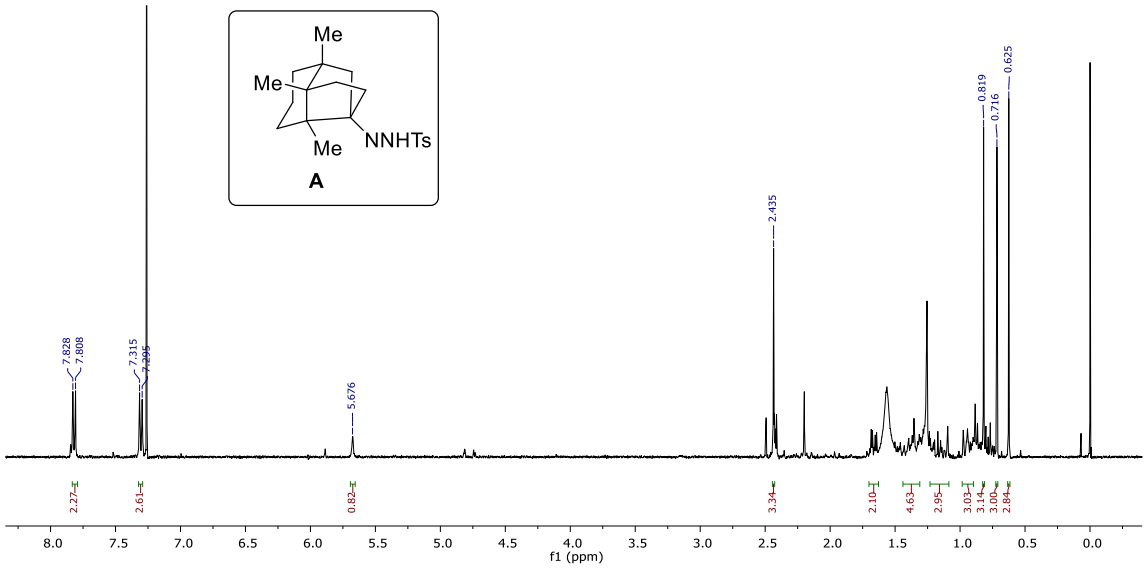
Me
Me
Me
NNHTs
A
7.828
7.808
7.315
7.296
5.676
2.435
0.819
0.716
0.625
2.27
2.61
0.82
3.34
2.10
4.63
2.95
3.03
3.14
3.00
2.84
f1 (ppm)

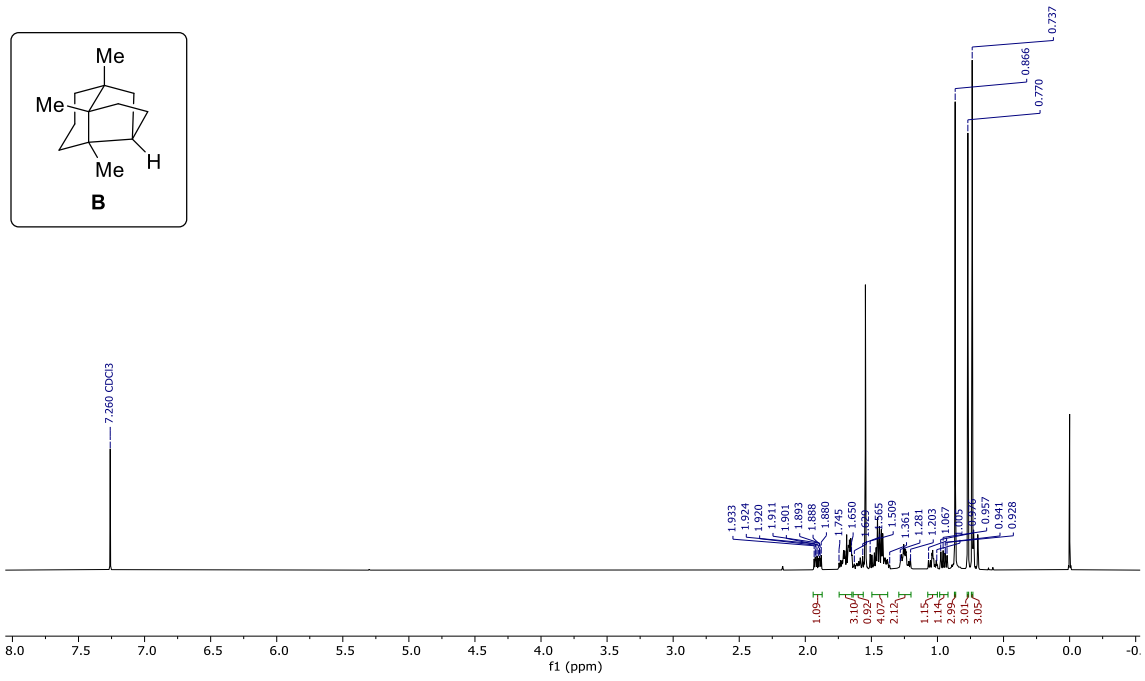
Me
Me
Me
H
B
7.260 CDCl3
0.737
0.866
0.770
1.933
1.924
1.920
1.911
1.901
1.893
1.888
1.880
1.745
1.650
1.629
1.565
1.509
1.361
1.281
1.203
1.067
1.005
0.976
0.957
0.941
0.928
1.09
3.10
0.92
4.07
2.12
1.15
1.14
2.99
3.01
3.05
f1 (ppm)

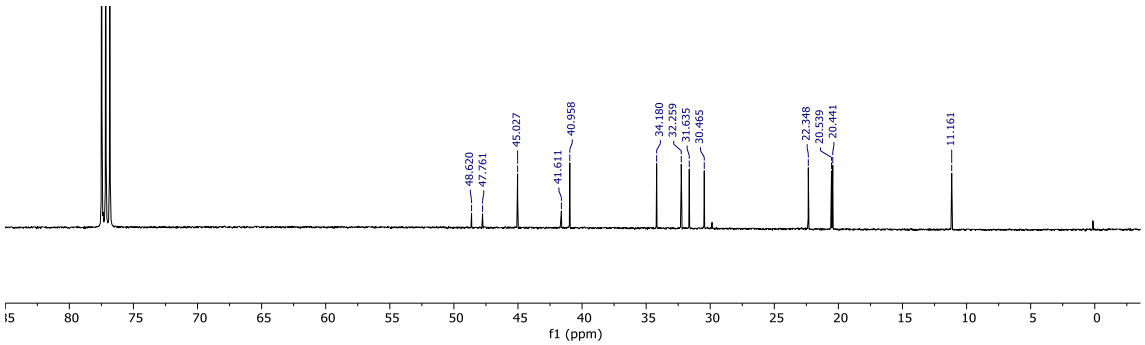
48.620
47.761
45.027
41.611
40.958
34.180
32.259
31.635
30.465
22.348
20.539
20.441
11.161
f1 (ppm)

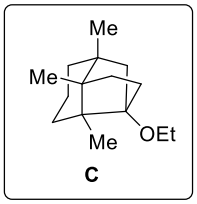
Me
Me
Me
OEt

C

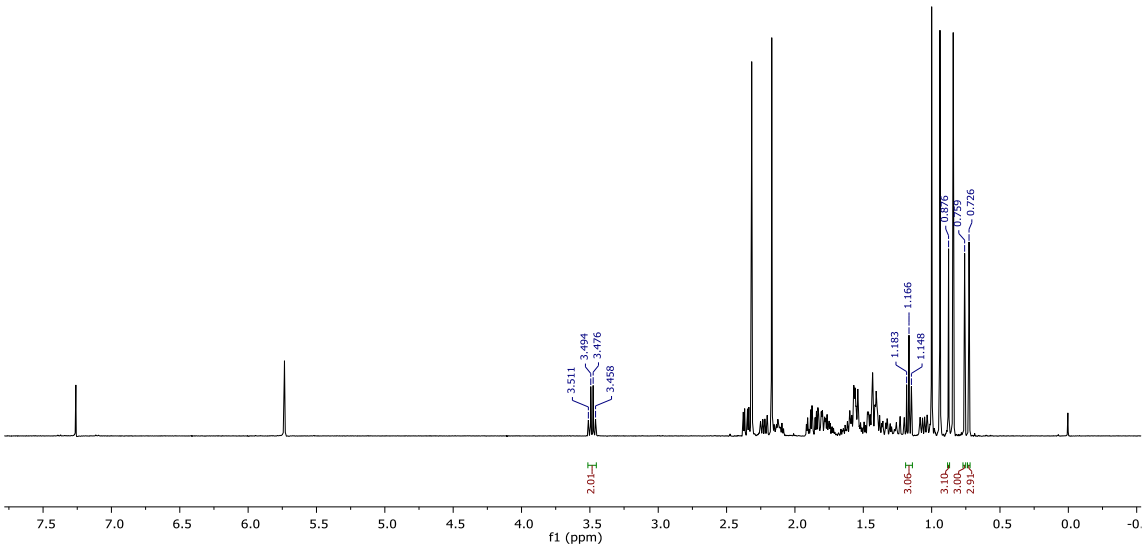
3.511
3.494
3.476
3.458
1.183
1.166
1.148
0.876
0.759
0.726
2.01
3.06
3.10
3.00
2.91
7.5 7.0 6.5 6.0 5.5 5.0 4.5 4.0 3.5 3.0 2.5 2.0 1.5 1.0 0.5 0.0
f1 (ppm)

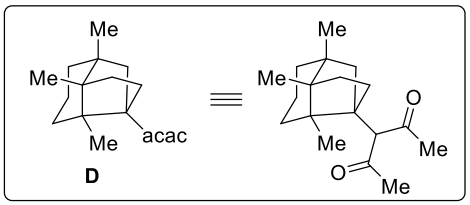
Me
Me
Me
acac

D

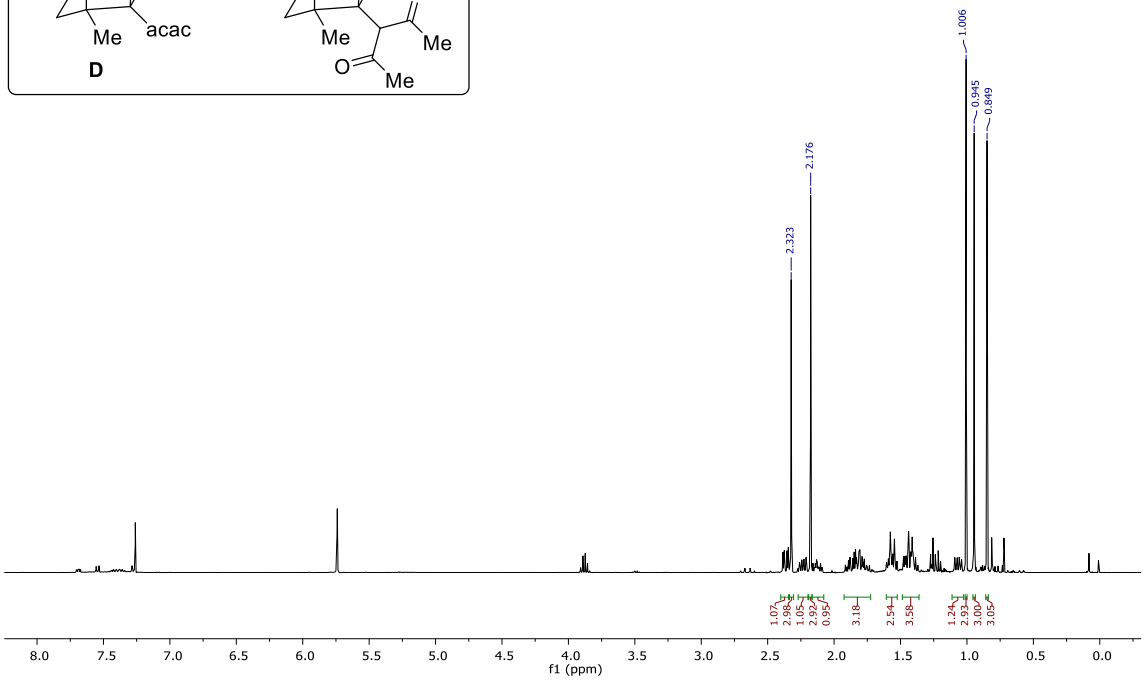
2.323
2.176
1.006
0.945
0.849
1.07
2.98
1.05
2.92
0.95
3.18
2.54
3.58
1.24
2.93
3.00
3.05
8.0 7.5 7.0 6.5 6.0 5.5 5.0 4.5 4.0 3.5 3.0 2.5 2.0 1.5 1.0 0.5 0.0
f1 (ppm)

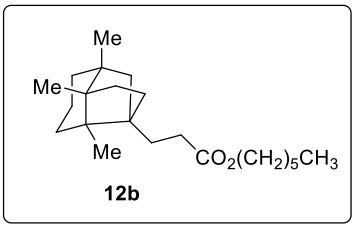
Me
Me
Me
$CO_2(CH_2)_5CH_3$

12b

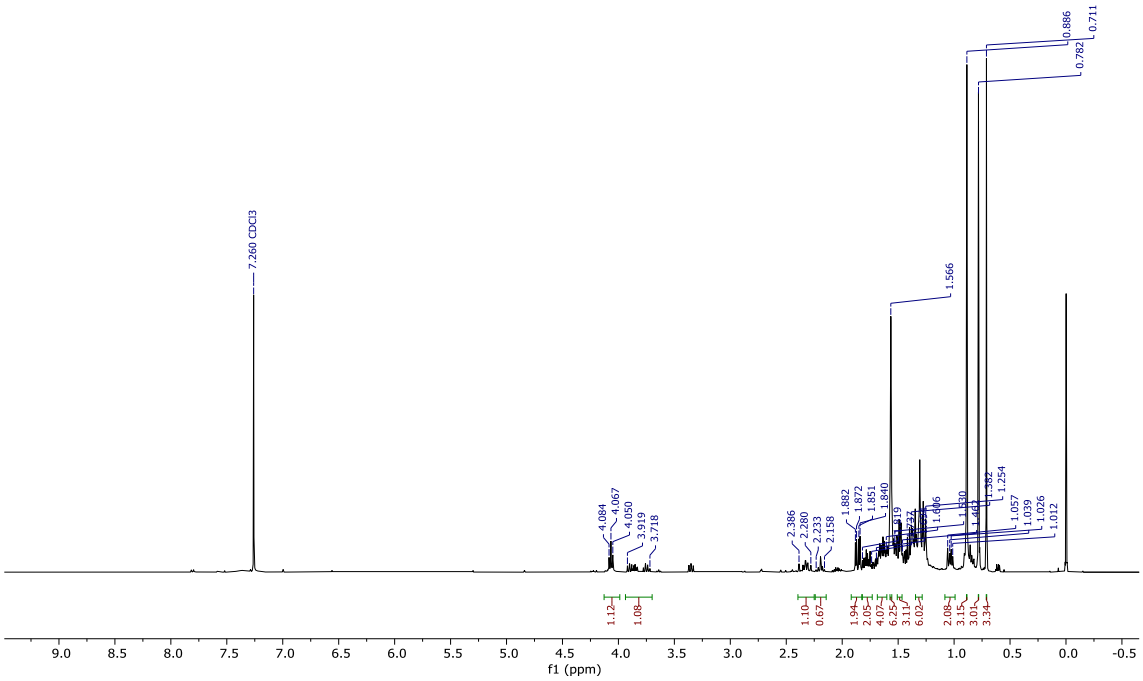
7.260 CDCl3
0.886
0.782
0.711
1.566
4.094
4.067
4.050
3.919
3.718
2.386
2.280
2.233
2.158
1.882
1.872
1.851
1.840
1.254
1.057
1.039
1.026
1.012
f1 (ppm)

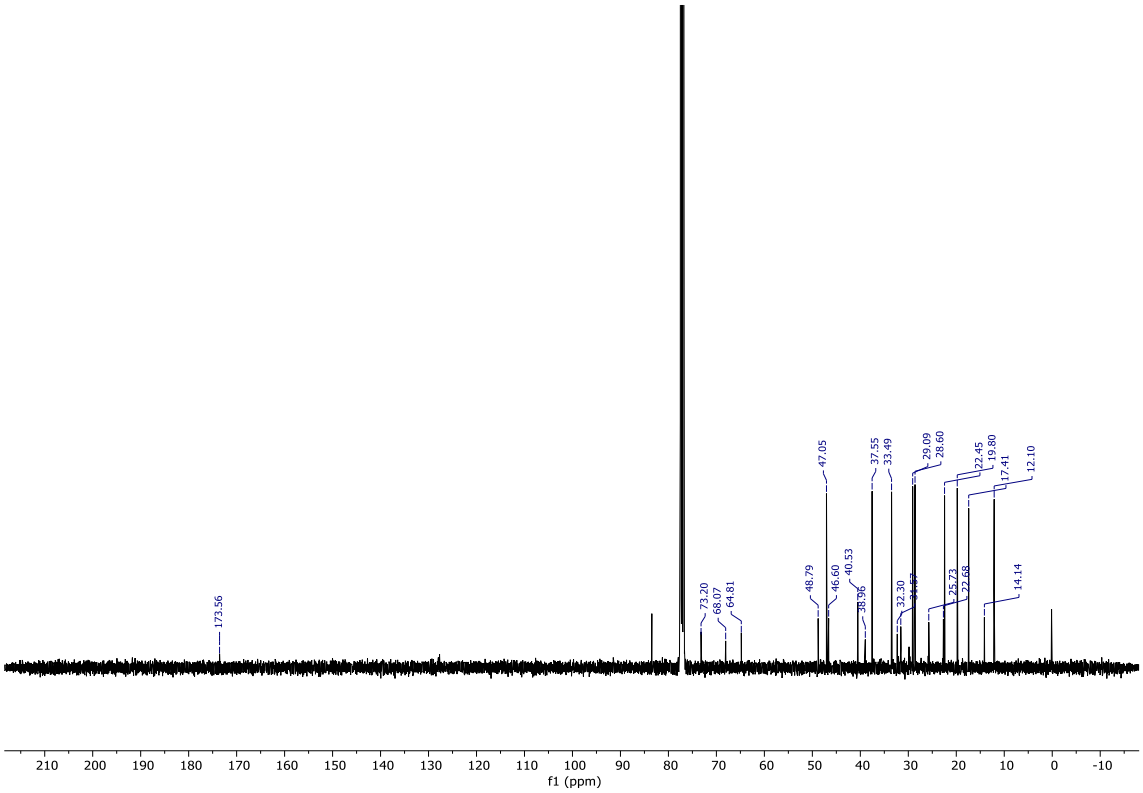
173.56
73.20
68.07
64.81
48.79
47.05
46.60
40.53
38.96
37.55
33.49
32.30
29.09
28.60
25.72
22.68
22.45
19.80
17.41
14.14
12.10
f1 (ppm)

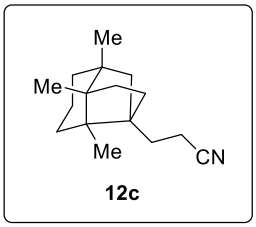
Me
Me
Me
CN

12c

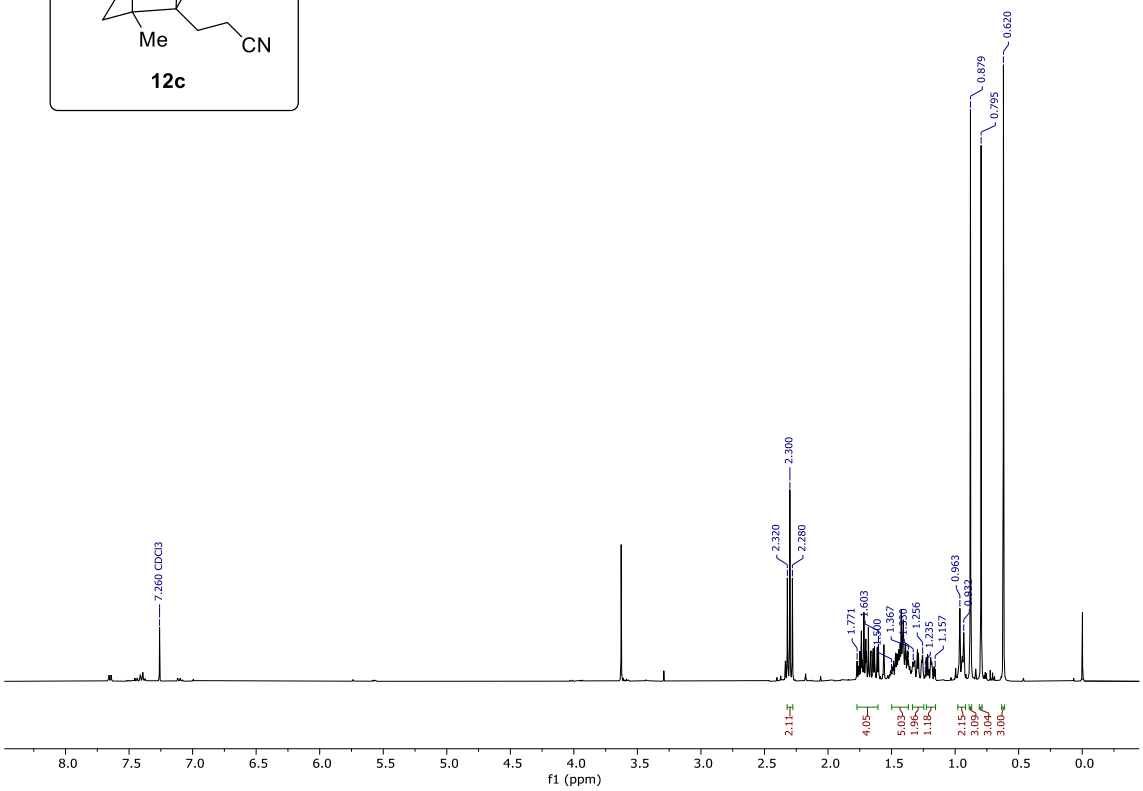
7.260 CDCl3
2.320
2.300
2.280
1.771
1.603
1.500
1.367
1.330
1.256
1.235
1.157
0.963
0.879
0.795
0.620
2.11
4.05
5.03
1.96
1.18
2.15
3.09
3.04
3.00
f1 (ppm)

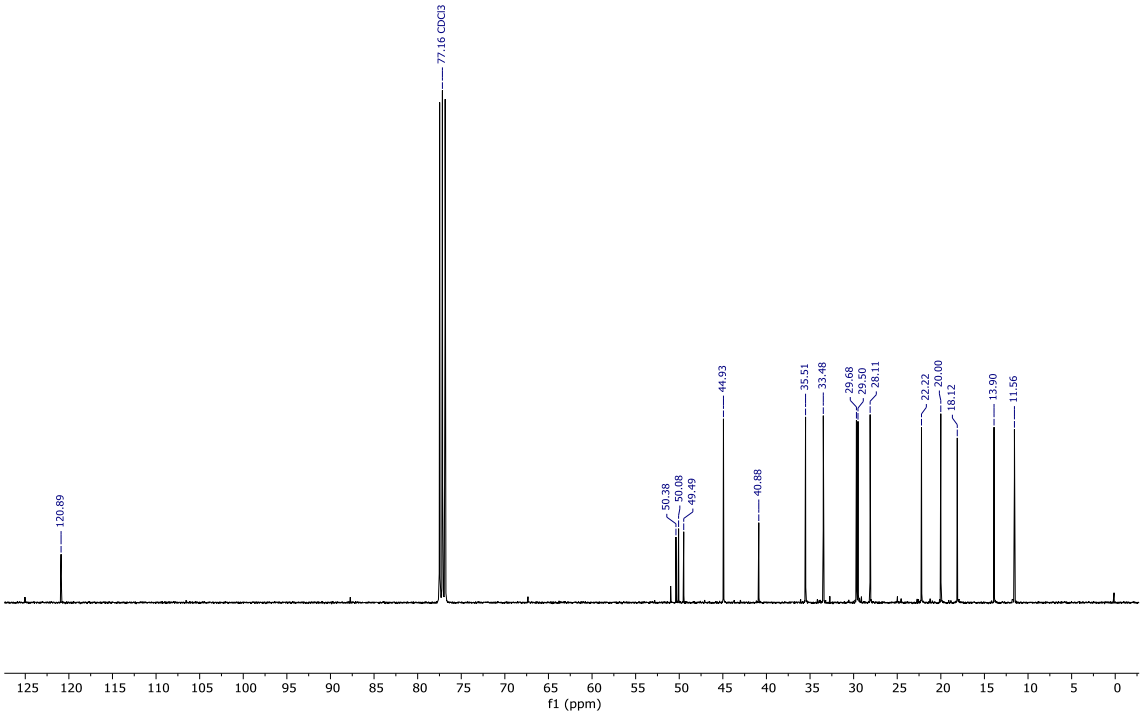
77.16 CDCl3
120.89
50.38
50.08
49.49
44.93
40.88
35.51
33.48
29.68
29.50
28.11
22.22
20.00
18.12
13.90
11.56
f1 (ppm)

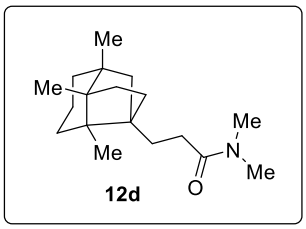
Me
Me
Me
Me
N
Me
O

12d

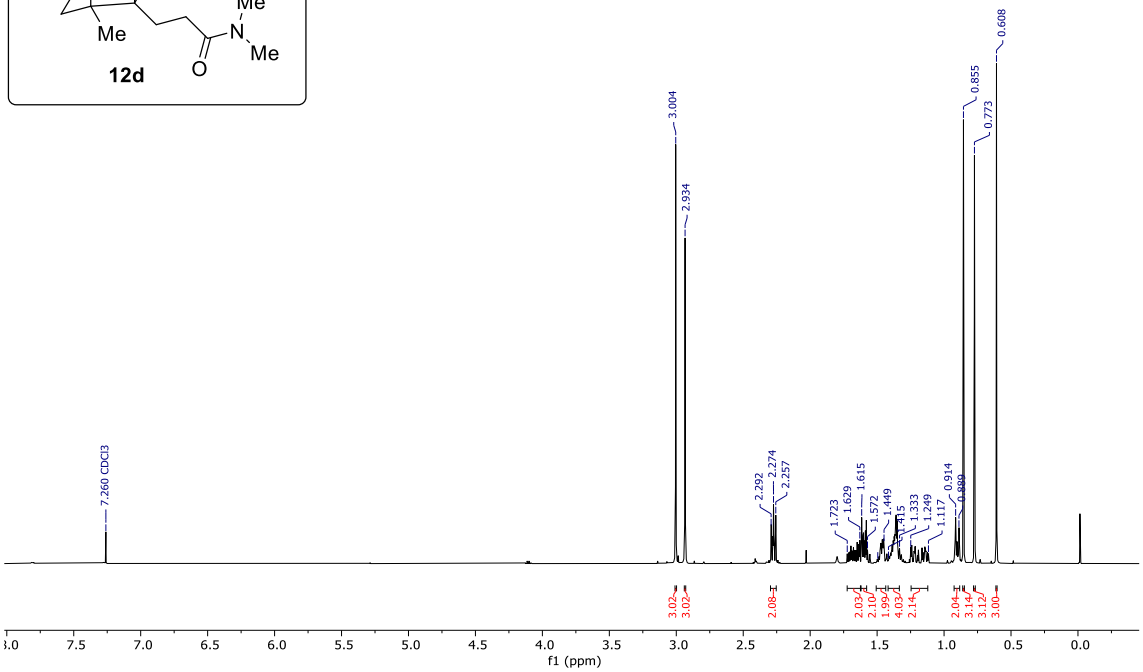
7.260 CDCl3
3.004
2.934
2.292
2.274
2.257
1.723
1.629
1.615
1.572
1.449
1.333
1.249
1.117
0.914
0.889
0.855
0.773
0.608
3.02
3.02
2.08
2.03
2.10
1.99
4.03
2.14
2.04
3.14
3.12
3.00
f1 (ppm)

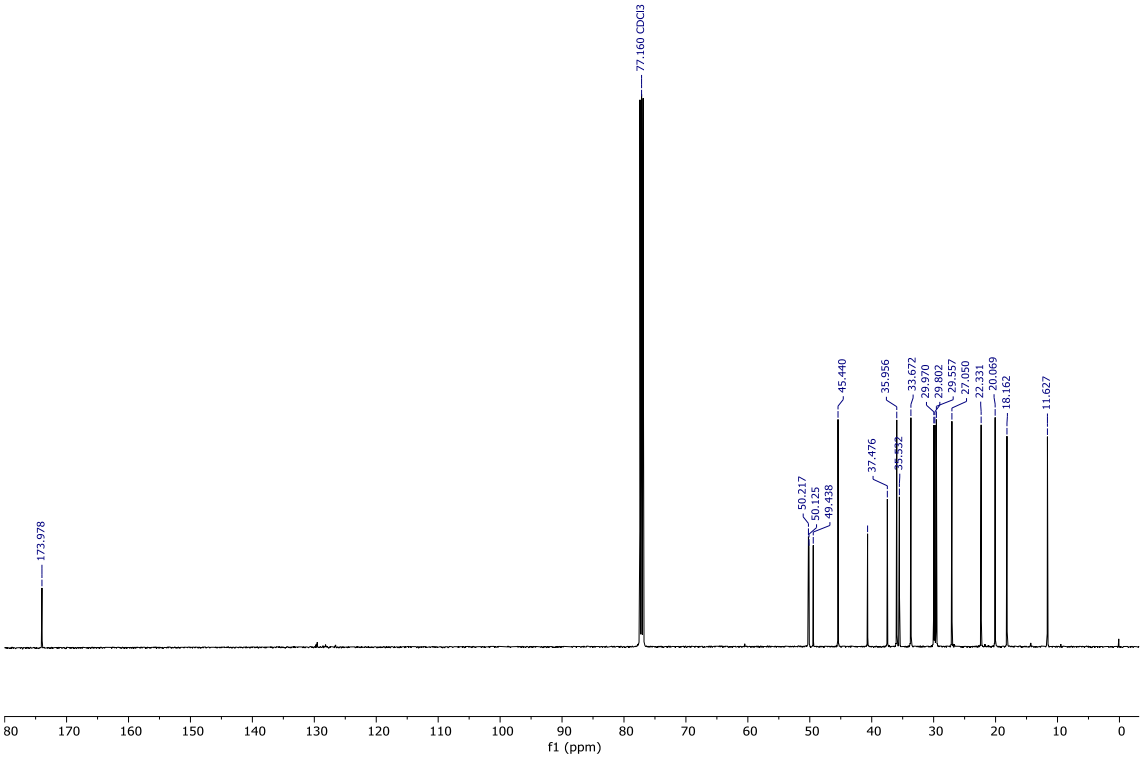
77.160 CDCl3
173.978
50.217
50.125
49.438
45.440
37.476
35.956
33.672
29.970
29.802
29.557
27.050
22.331
20.069
18.162
11.627
f1 (ppm)

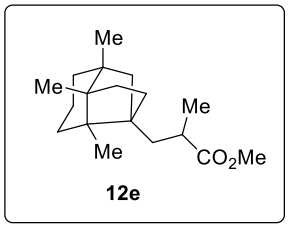
Me
Me
Me
Me
CO2Me

12e

0.767
3.664
3.654
0.592
0.583
0.855
0.833
7.260 CDCl3
2.542
2.453
1.856
1.756
1.726
1.636
1.609
1.525
1.481
1.410
1.376
1.289
1.219
1.146
1.050
0.885
3.00
0.98
1.16
1.12
1.07
1.94
6.12
4.08
1.32
0.88
3.09
2.98
3.04
f1 (ppm)

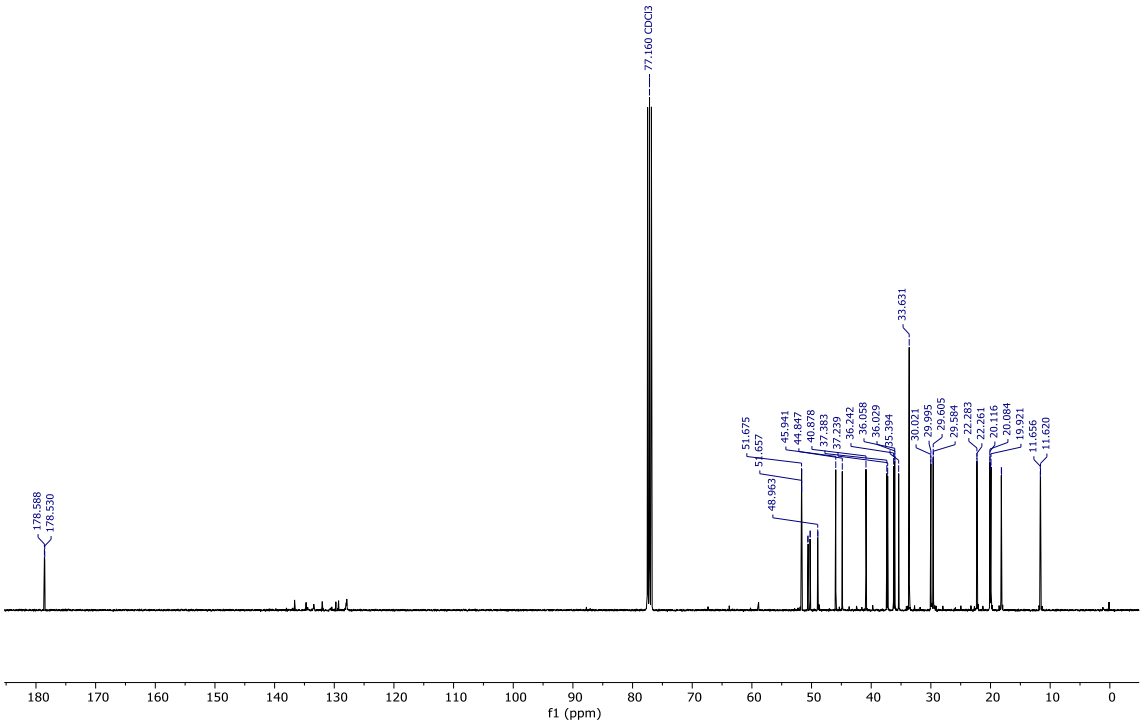
77.160 CDCl3
33.631
178.588
178.530
51.675
51.657
48.963
45.941
44.847
40.878
37.383
37.239
36.242
36.058
36.029
35.394
30.021
29.995
29.605
29.584
22.283
22.261
20.116
20.084
19.921
11.656
11.620
f1 (ppm)

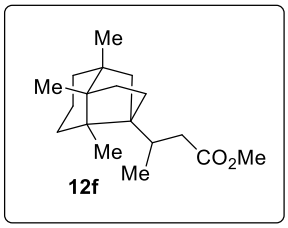
Me
Me
Me
Me
CO2Me

12f

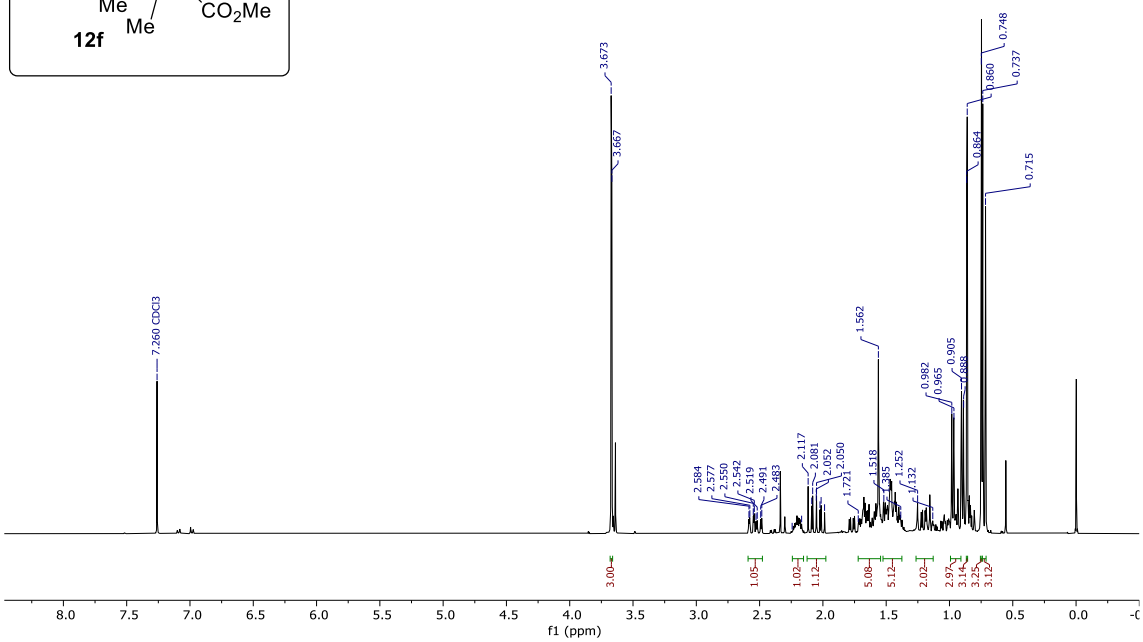
7.260 CDCl3
3.673
3.667
2.584
2.577
2.550
2.542
2.519
2.491
2.483
2.117
2.091
2.052
2.050
1.721
1.562
1.518
1.485
1.252
1.132
0.982
0.965
0.905
0.748
0.737
0.860
0.864
0.715
3.00
1.05
1.02
1.12
5.08
5.12
2.02
2.97
3.14
3.25
3.12
f1 (ppm)

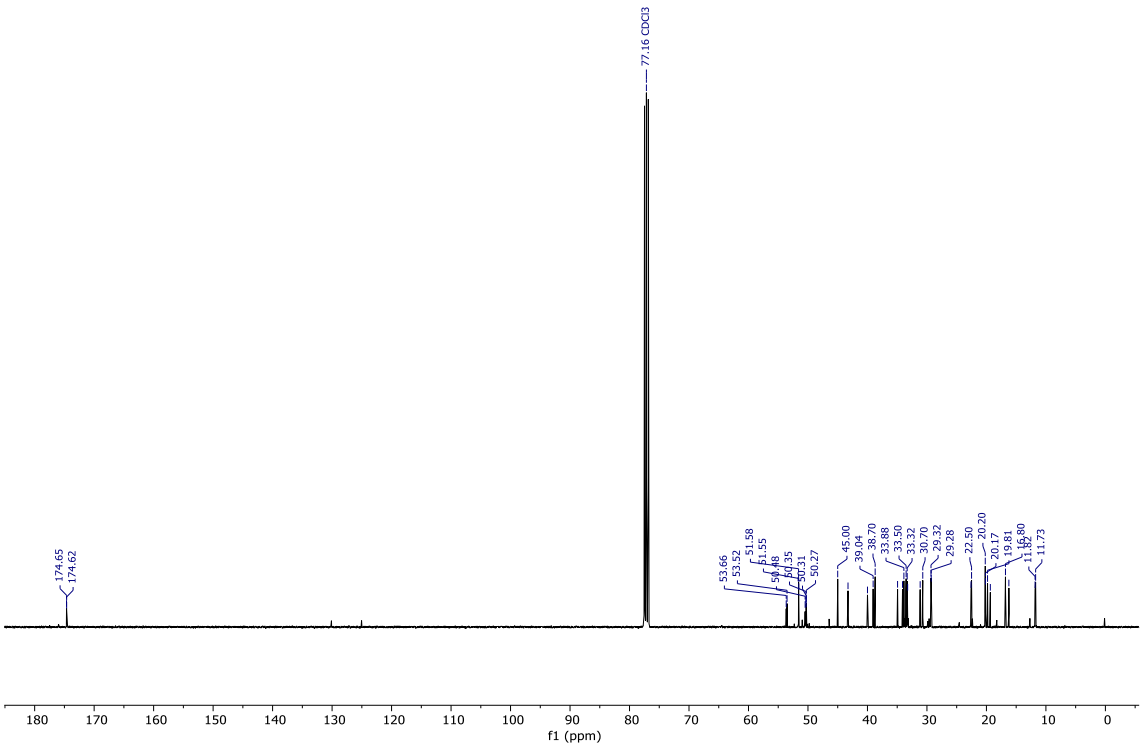
77.16 CDCl3
174.65
174.62
53.66
53.52
51.58
51.55
50.48
50.35
50.31
50.27
45.00
39.04
38.70
33.88
33.50
33.22
30.70
29.32
29.28
22.50
20.20
20.17
19.81
16.80
11.82
11.73
f1 (ppm)

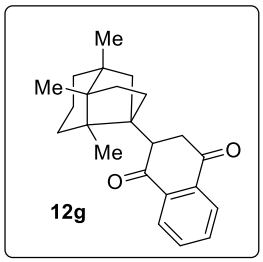
Me
Me
Me
O
O

12g

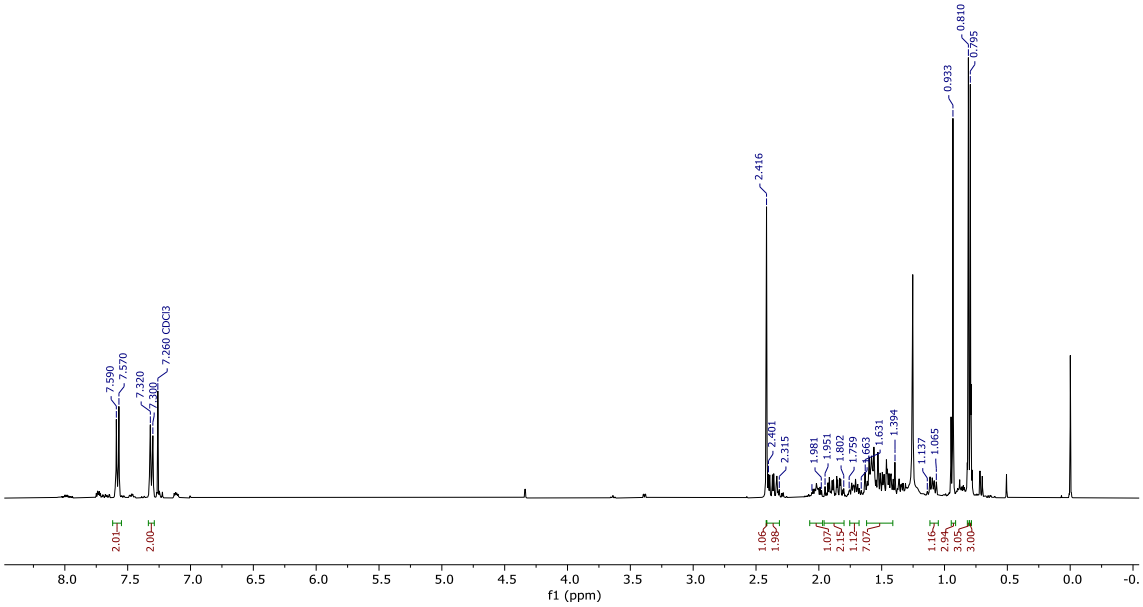
7.590
7.570
7.330
7.300
7.260 CDCl3
2.416
2.401
2.315
1.981
1.951
1.802
1.759
1.663
1.631
1.394
1.137
1.065
0.933
0.810
0.795
2.01
2.00
1.06
1.98
1.07
2.15
1.12
7.07
1.16
2.94
3.05
3.00
f1 (ppm)

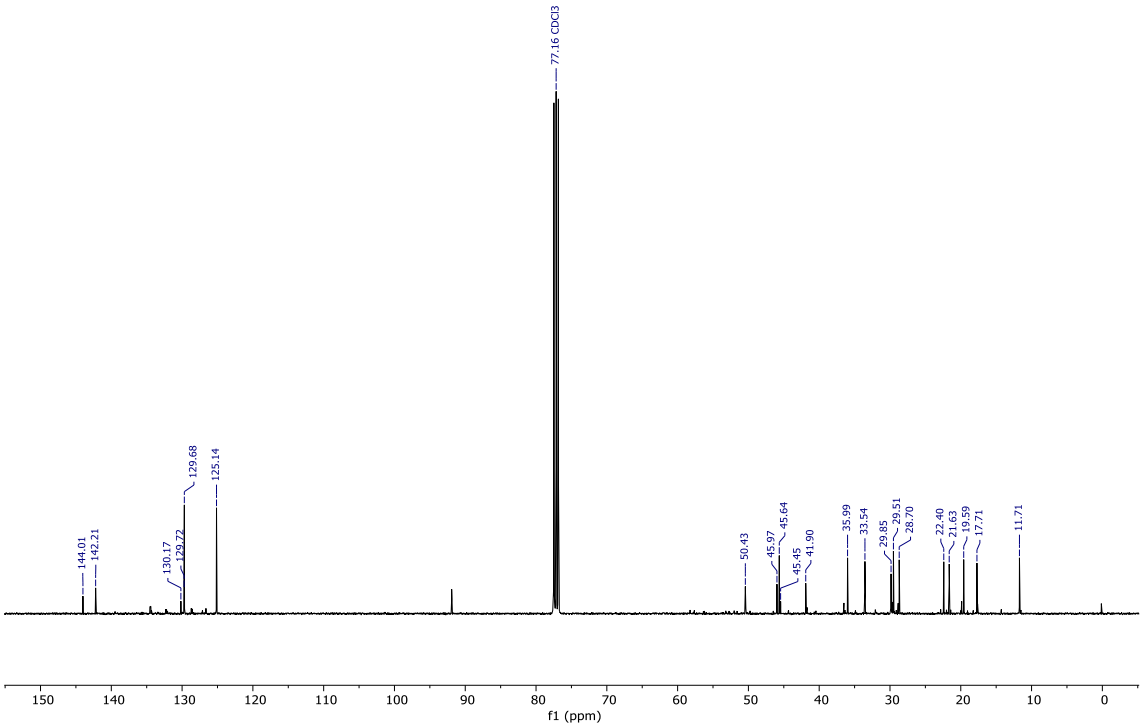
77.16 CDCl3
144.01
142.21
130.17
129.72
129.68
125.14
50.43
45.97
45.64
45.45
41.90
35.99
33.54
29.85
29.51
28.70
22.40
21.63
19.59
17.71
11.71
f1 (ppm)

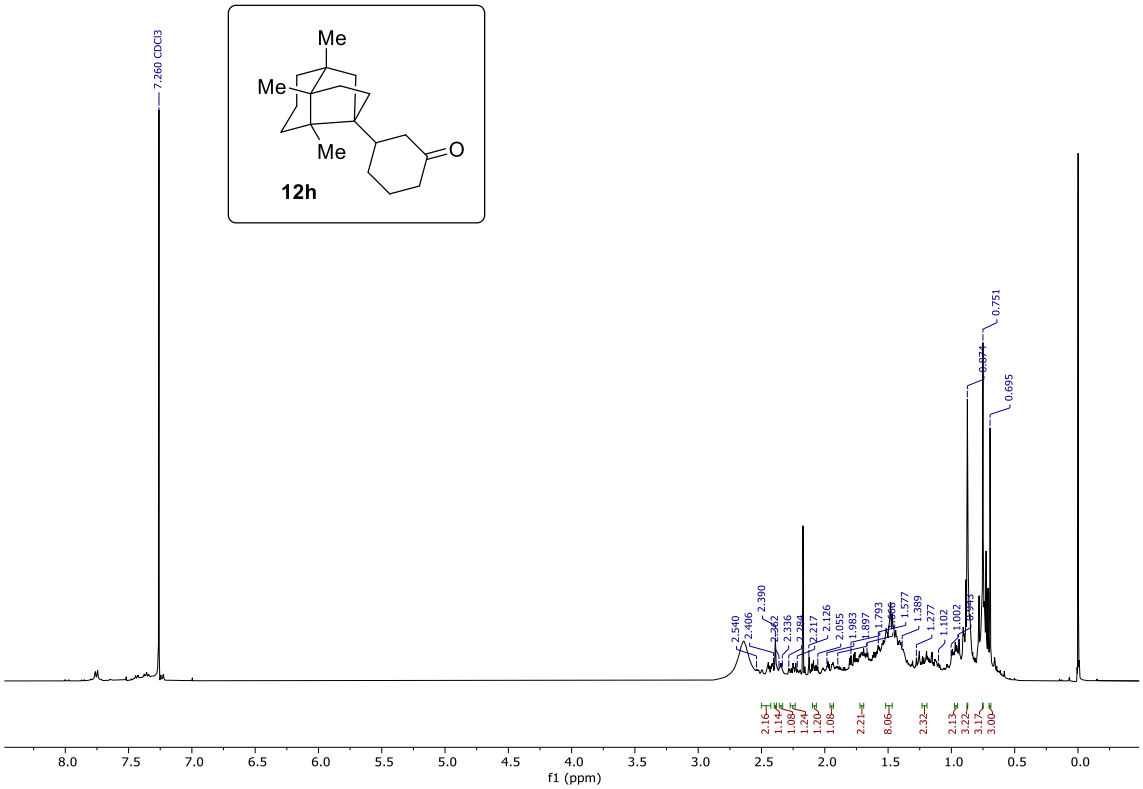
Me
Me
Me
O
12h
7.260 CDCl3
0.751
0.695
f1 (ppm)

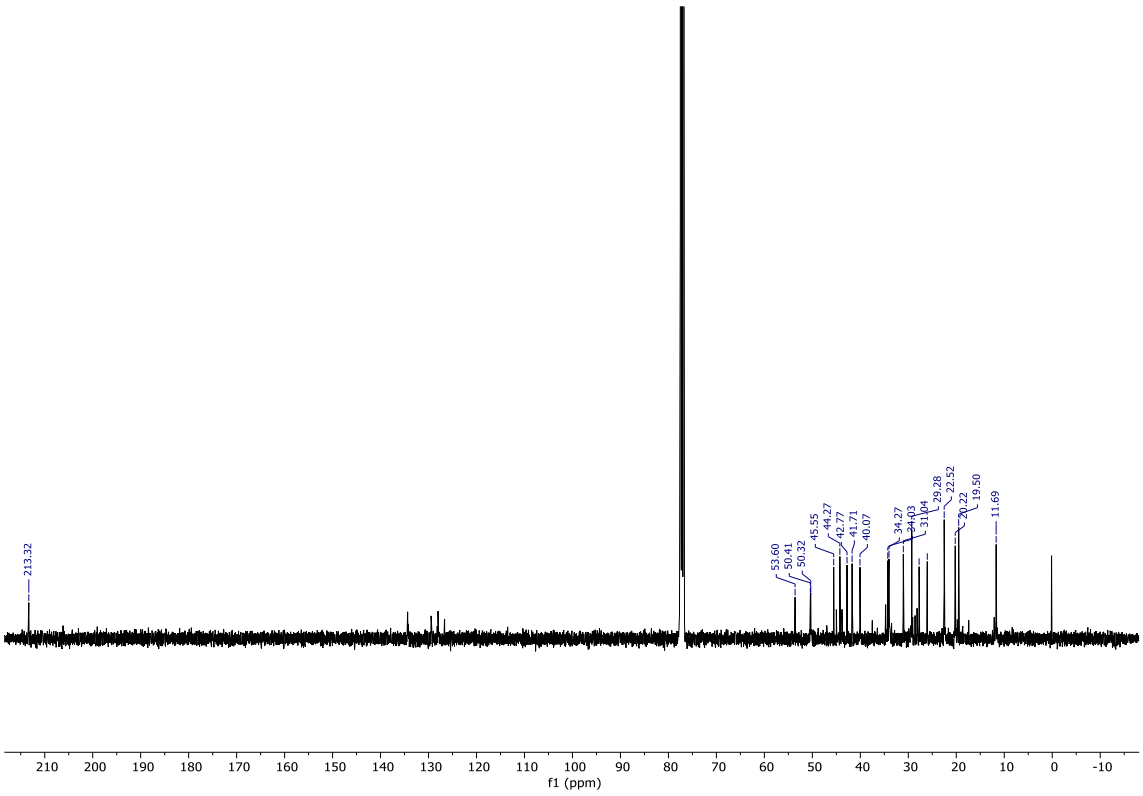
213.32
53.60
50.41
50.32
45.55
44.27
42.77
41.71
40.07
34.27
34.03
31.04
29.28
22.52
20.22
19.50
11.69
f1 (ppm)

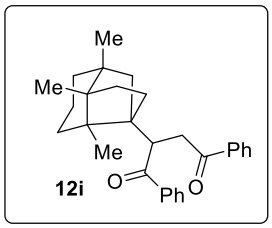
Me
Me
Me
Ph
O
Ph
O
12i

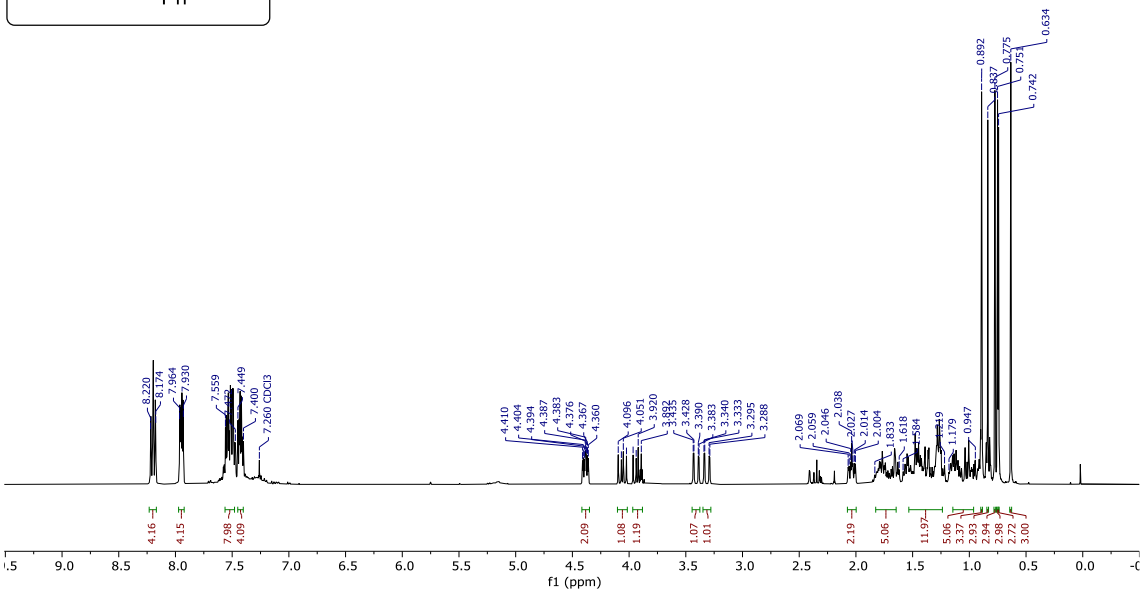
8.220
8.174
7.964
7.930
7.559
7.449
7.400
7.260 CDCl3
4.410
4.404
4.394
4.387
4.383
4.376
4.367
4.360
4.096
4.051
3.920
3.428
3.390
3.383
3.340
3.333
3.295
3.288
2.069
2.059
2.046
2.038
2.027
2.014
2.004
1.833
1.618
1.584
1.179
0.947
0.892
0.837
0.775
0.751
0.742
0.634
4.16
4.15
7.98
4.09
2.09
1.08
1.19
1.07
1.01
2.19
5.06
11.97
5.06
3.37
2.93
2.94
2.98
2.72
3.00
f1 (ppm)

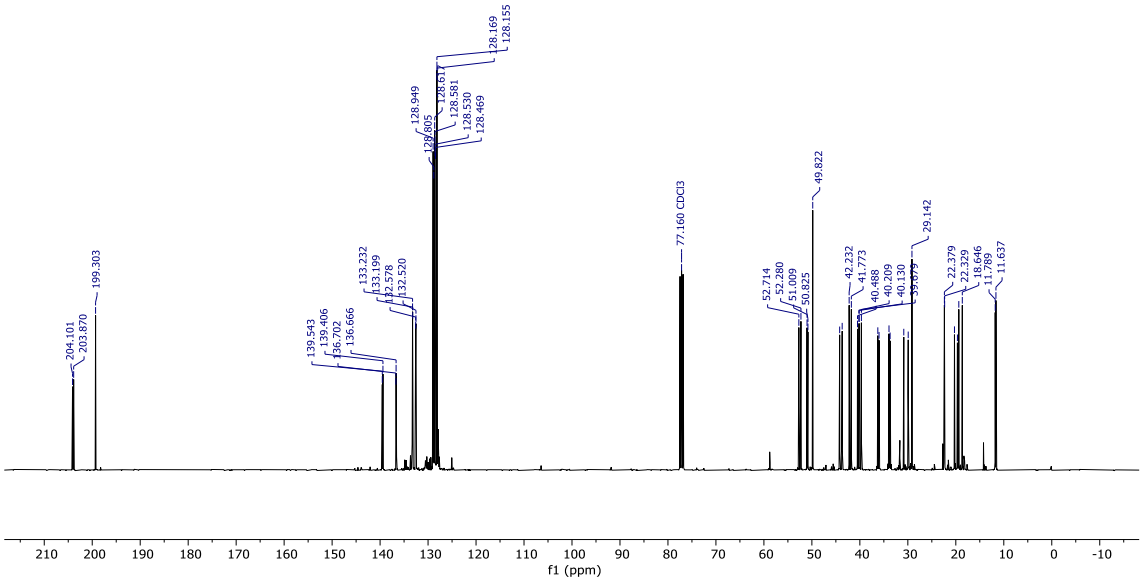
204.101
203.870
199.303
139.543
139.406
136.670
136.666
133.232
133.199
132.578
132.520
128.949
128.805
128.617
128.581
128.530
128.469
128.169
128.155
77.160 CDCl3
52.714
52.280
51.009
50.825
49.822
42.232
41.773
40.488
40.209
40.130
29.142
22.379
22.329
18.646
11.789
11.637
f1 (ppm)

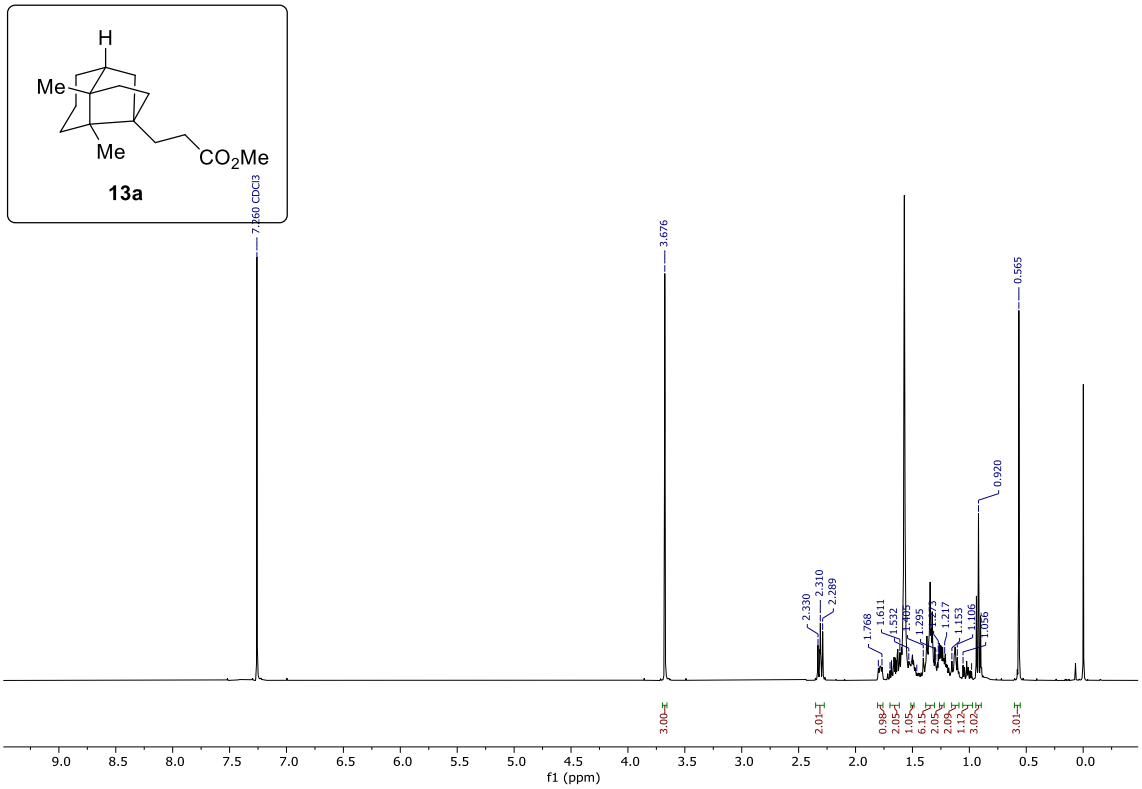
H
Me
Me
CO2Me
13a
7.260 CDCl3
3.676
2.330
2.310
2.289
1.768
1.611
1.532
1.465
1.295
1.273
1.217
1.153
1.106
1.056
0.920
0.565
3.00
2.01
0.98
2.08
1.05
6.15
2.05
2.09
1.12
3.02
3.01
f1 (ppm)

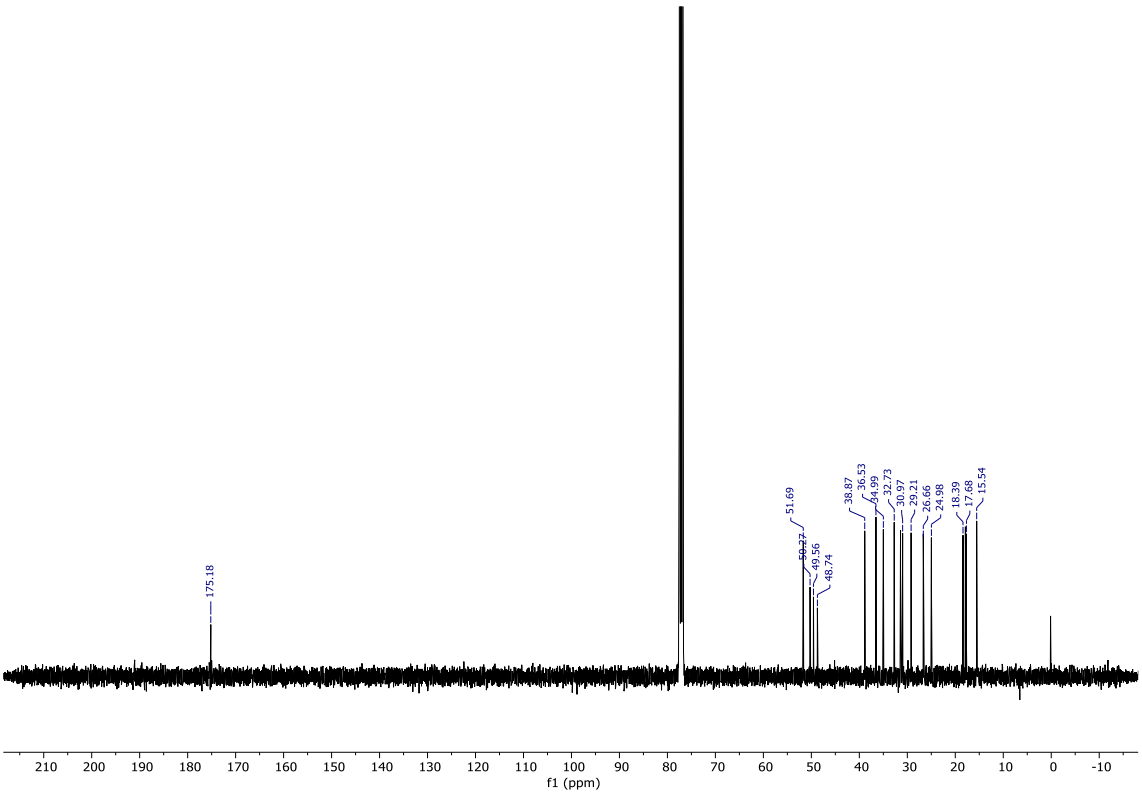
175.18
51.69
50.22
49.56
48.74
38.87
36.53
34.99
32.73
30.97
29.21
26.66
24.98
18.39
17.68
15.54
f1 (ppm)

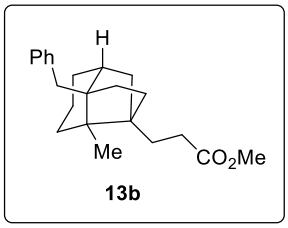
H
Ph
Me
CO_2Me

13b

3.662
0.700
7.250
7.139
3.083
3.049
2.388
2.355
2.315
2.294
2.274
1.744
1.634
1.536
1.490
1.438
1.339
1.262
1.153
1.112
1.055
1.029
0.000 TMS
5.12
3.00
1.14
1.20
2.07
1.14
4.18
0.93
2.15
2.04
3.07
1.09
1.18
3.06
8.0
7.5
7.0
6.5
6.0
5.5
5.0
4.5
4.0
3.5
3.0
2.5
2.0
1.5
1.0
0.5
0.0
f1 (ppm)

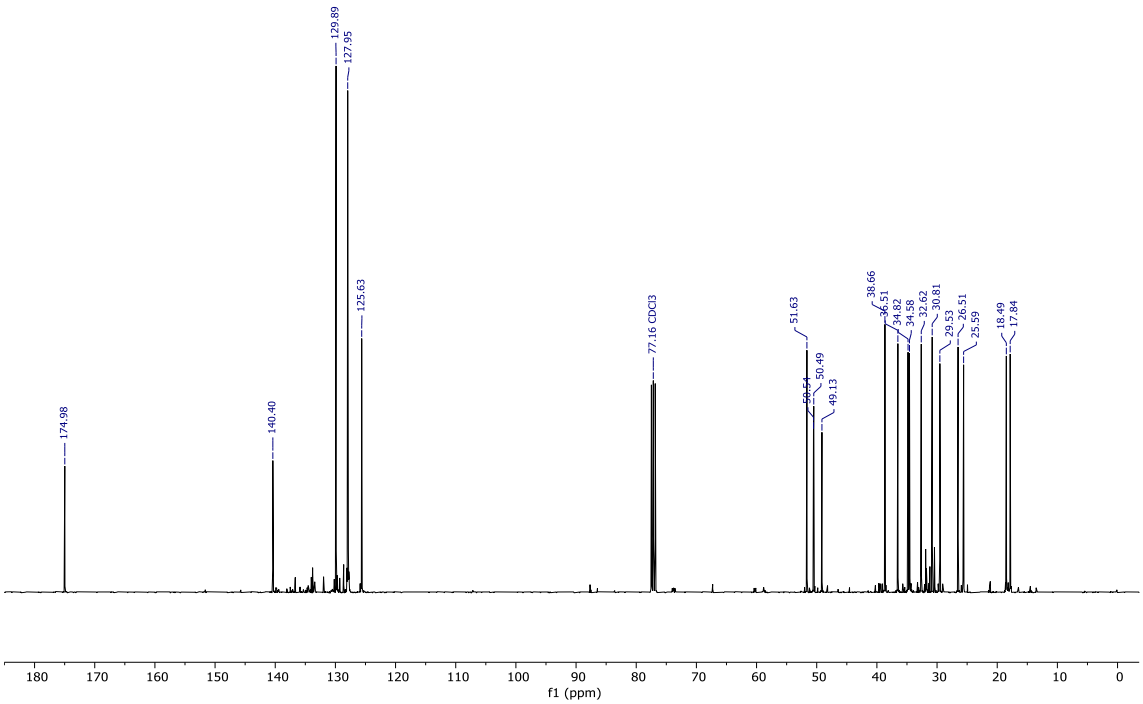
129.89
127.95
125.63
174.98
140.40
77.16 CDCl3
51.63
50.49
49.13
38.66
36.51
34.82
34.58
32.62
30.81
29.53
26.51
25.59
18.49
17.84
180
170
160
150
140
130
120
110
100
90
80
70
60
50
40
30
20
10
0
f1 (ppm)

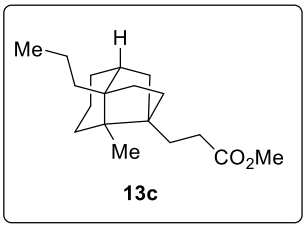
Me
H
Me
CO2Me

13c

7.260 CDCl3
3.671
2.325
2.305
2.284
1.796
1.763
1.693
1.524
1.401
1.276
1.255
1.149
1.102
1.052
0.977
0.916
0.897
0.561
3.00
2.03
1.03
3.06
2.06
8.06
2.14
2.01
1.08
3.09
3.01
f1 (ppm)

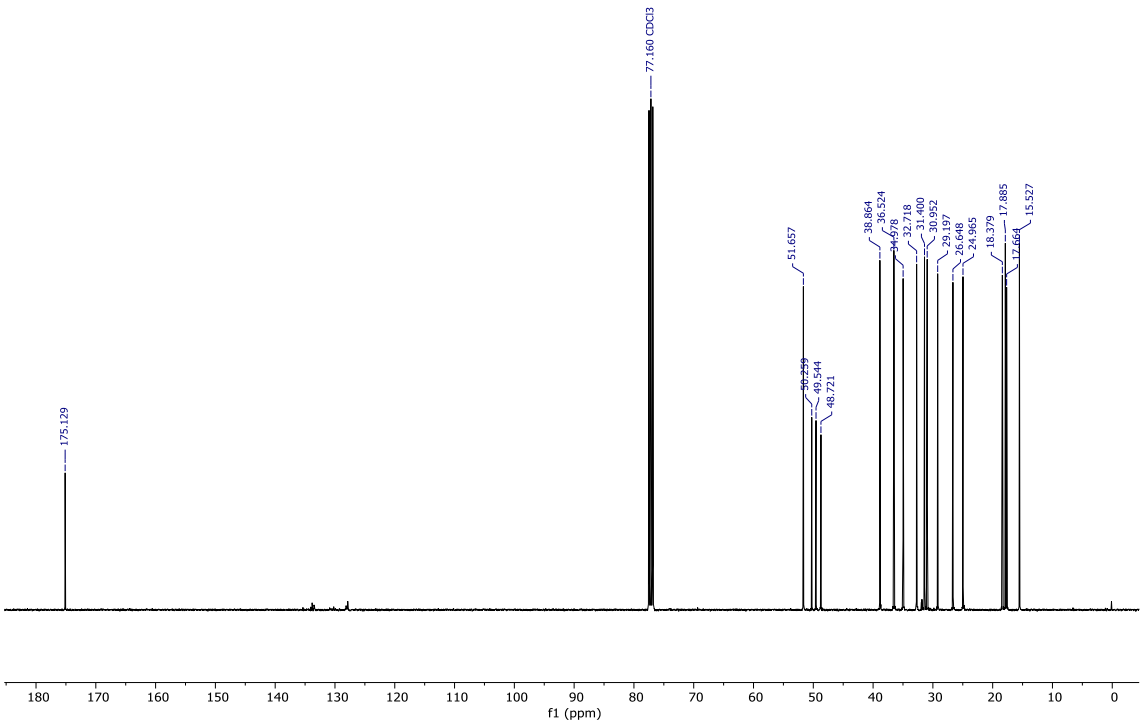
77.160 CDCl3
175.129
51.657
50.239
49.544
48.721
38.864
36.524
34.678
32.718
31.400
30.952
29.197
26.648
24.965
18.379
17.885
17.664
15.527
f1 (ppm)

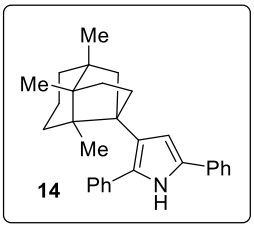
Me
Me
Me
Ph
Ph
N
H

14

0.685
0.861
0.797
7.459
7.377
7.260 CDCl3
8.054
6.688
2.135
2.128
2.110
2.102
1.769
1.589
1.554
1.378
1.270
1.015
0.963
f1 (ppm)

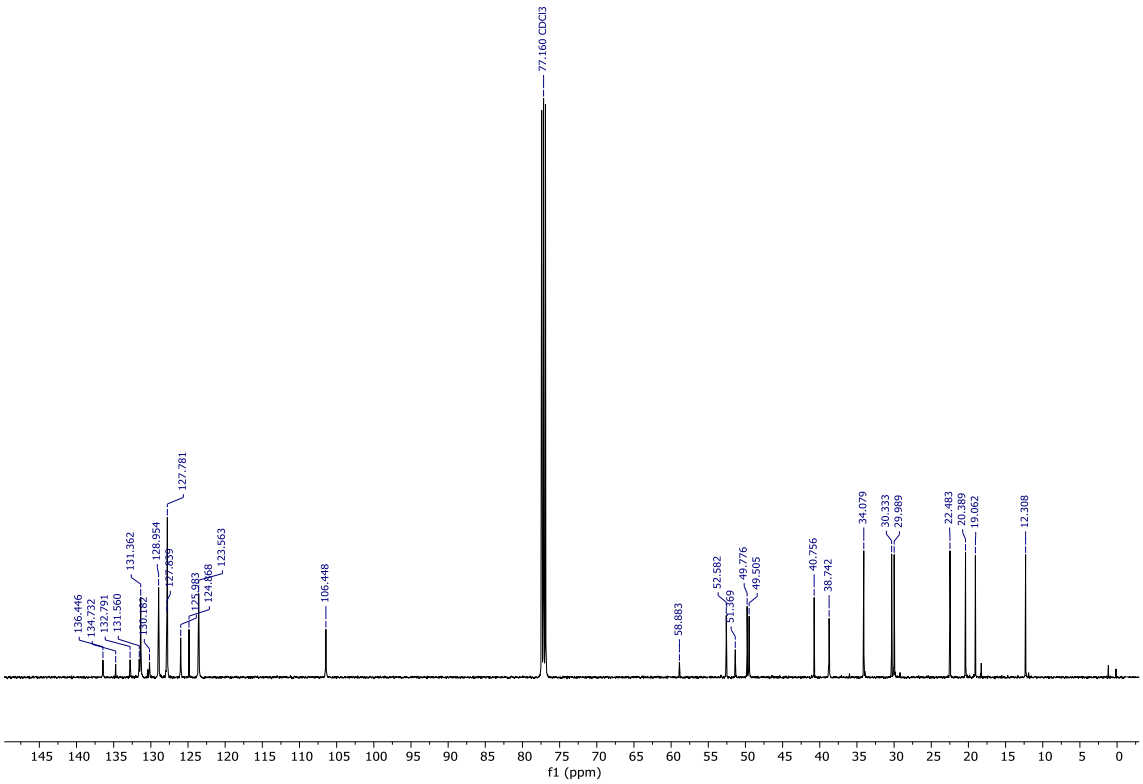
77.160 CDCl3
127.781
128.954
131.362
123.563
106.448
58.883
52.582
51.369
49.776
49.505
40.756
38.742
34.079
30.333
29.989
22.483
20.389
19.062
12.308
f1 (ppm)

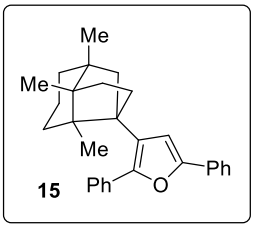
Me
Me
Me
Ph
Ph
O

15

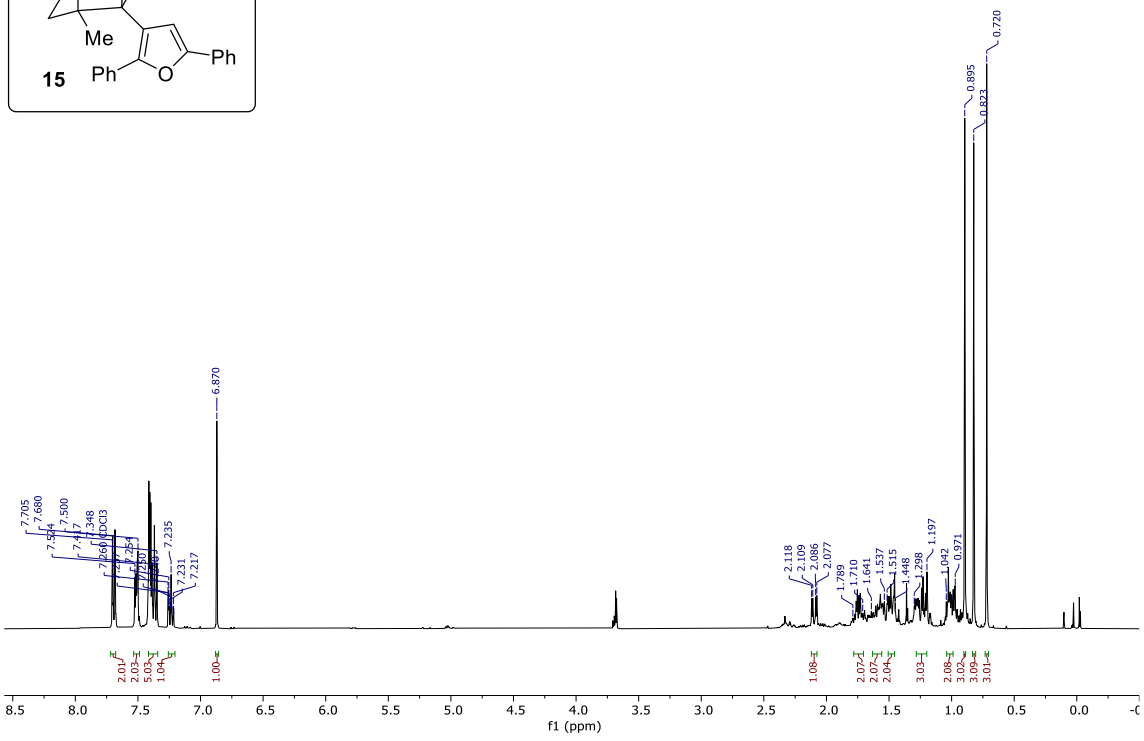
7.705
7.680
7.504
7.500
7.417
7.348
CDCl3
7.260
7.235
7.231
7.217
6.870
2.118
2.109
2.086
2.077
1.760
1.710
1.641
1.537
1.515
1.448
1.298
1.197
1.042
0.971
0.895
0.823
0.720
2.01
2.03
5.03
1.04
1.00
1.08
2.07
2.07
2.04
3.03
2.08
3.02
3.09
3.01
f1 (ppm)

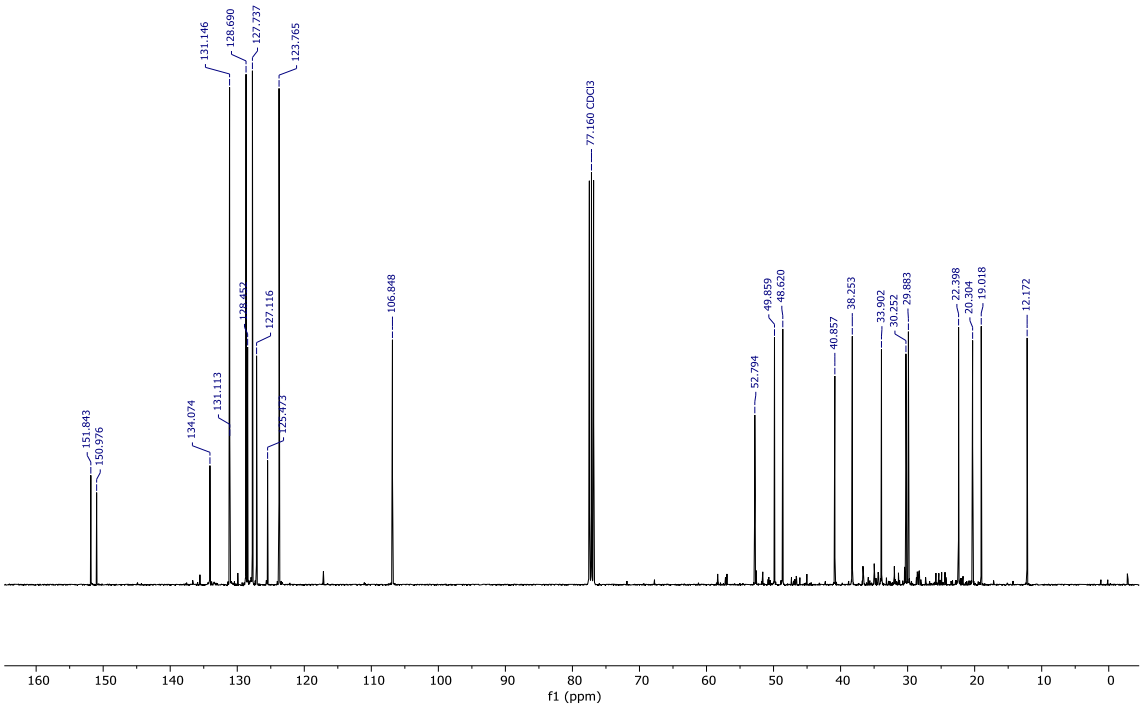
151.843
150.976
134.074
131.146
131.113
128.690
128.452
127.737
127.116
125.473
123.765
106.848
77.160 CDCl3
52.794
49.859
48.620
40.857
38.253
33.902
30.252
29.883
22.398
20.304
19.018
12.172
f1 (ppm)

REFERENCES

(1) Gomberg, M. An Instance of Trivalent Carbon: Triphenylmethyl. *J. Am. Chem. Soc.*, **1900**, *22*, 757–771. https://doi.org/10.1021/ja02049a006

(2) (a) Lewis, G. N. The Atom and the Molecule. *J. Am. Chem. Soc.*, **1916**, *38*, 762-785. https://doi.org/10.1021/ja02261a002 (b) Langmuir, I. The Arrangement of Electrons in Atoms and Molecules. *J. Am. Chem. Soc.*, **1919**, *41*, 868–934. https://doi.org/10.1021/ja02227a002

(3) Studer, A.; Curran, D. P. Catalysis of Radical Reactions: A Radical Chemistry Perspective. *Angew. Chem. Int. Ed.*, **2016**, *55*, 58–102. https://doi.org/10.1002/anie.201505090

(4) (a) Yan, M.; Lo, J. C.; Edwards, J. T.; Baran, P. S. Radicals: Reactive Intermediates with Translational Potential. *J. Am. Chem. Soc.* **2016**, *138*, 12692–12714. https://doi.org/10.1021/jacs.6b08856 (b) Smith, J. M.; Harwood, S. J.; Baran, P. S. Radical Retrosynthesis. *Acc. Chem. Res.* **2018**, *51*, 1807–1817. https://doi.org/10.1021/acs.accounts.8b00209

(5) Zard, S. Z. Radicals in Action: A Festival of Radical Transformations. *Org. Lett.* **2017**, *19*, 1257–1269. https://doi.org/10.1021/acs.orglett.7b00531

(6) (a) Cao, H.; Tang, X.; Tang, H.; Yuan, Y.; Wu, J. Photoinduced intermolecular hydrogen atom transfer reactions in organic synthesis. *Chem. Catalysis.*, **2021**, *1*, 1–76. https://doi.org/10.1016/j.checat.2021.04.008 (b) Marzo, L.; Pagire, S. K.; Reiser, O.; König, B. Visible-Light Photocatalysis: Does It Make a Difference in Organic Synthesis? *Angew. Chem. Int. Ed.* **2018**, *57*, 10034. https://doi.org/10.1002/anie.201709766 (c) Garrido-Castro, A. F.; Maestro, M. C.; Alemán, J. α-Functionalization of Imines via Visible Light Photoredox Catalysis. *Catalysts,* **2020**, *10*, 562; https://doi.org/10.3390/catal10050562

(7) (a) Ghosh, M.; Shinde, V. S.; Rueping, M. A review of asymmetric synthetic organic electrochemistry and electrocatalysis: concepts, applications, recent developments and future directions. *Beilstein J. Org. Chem.*, **2019**, *15*, 2710–2746. https://doi.org/10.3762/bjoc.15.264 (b) Zhu, C.; Ang, N. W. J.; Meyer, T. H.; Qiu, Y. Ackermann, L. Organic Electrochemistry: Molecular Syntheses with Potential. *ACS Cent. Sci.*, **2021**, *7*, 415–431. https://doi.org/10.1021/acscentsci.0c01532

(8) (a) Zuo, Z.; Ahneman, D. T.; Chu, L.; Terret, J. A.; Doyle, A. G.; MacMillan, D. W. C. Merging photoredox with nickel catalysis: Coupling of α-carboxyl sp^3-carbons with aryl halides. *Science*, **2014**, *345*, 437–440. https://doi.org/10.1126/science.1255525 (b) Twilton, J.; Le, C.; Zhang, P.; Shaw, M. H.; Evans, R. W.; MacMillan, D. W. C. The merger of transition metal and photocatalysis. *Nature Rev. Chem.*, **2017**, *1*, 0052, 1–17. https://doi.org/10.1038/s41570-017-

0052 (c) Zhu, C.; Yue, H.; Chu, L.; Rueping, M. Recent advances in photoredox and nickel dual-catalyzed cascade reactions: pushing the boundaries of complexity. *Chem. Sci.*, **2020**, *11*, 4051–4064. https://doi.org/10.1039/D0SC00712A

(9) Mondal, S.; Dumur, F.; Gigmes, D.; Sibi, M. P.; Bertrand, M. P.; Nechab, M. Enantioselective Radical Reactions Using Chiral Catalysts. *Chem. Rev.*, **2022**, *122*, 5842–5976. https://doi.org/10.1021/acs.chemrev.1c00582

(10) Green, S. A.; Crossley, S. W. M.; Matos, J. L. M.; Vásquez-Céspedes, S.; Shevick, S. L.; Shenvi, R. A. The High Chemofidelity of Metal-Catalyzed Hydrogen Atom Transfer. *Acc. Chem. Res*., **2018**, *51*, 2628–2640. https://doi.org/10.1021/acs.accounts.8b00337

(11) (a) Ai, W.; Zhong, R.; Liu, X.; Liu, Q. Hydride Transfer Reactions Catalyzed by Cobalt Complexes. *Chem. Rev.* **2019**, *119*, 2876–2953. https://doi.org/10.1021/acs.chemrev.8b00404. (b) Lübken, D.; Saxarra, M.; Kalesse, M. Tris(Acetylacetonato) Iron(III): Recent Developments and Synthetic Applications. *Synthesis* **2019**, *51*, 161–177. https://doi.org/10.1055/s-0037-1610393 (c) Gualandi, A.; Mengozzi, L.; Cozzi, P. G. Iron-Promoted Radical Reactions: Current Status and Perspectives. *Asian J. Org. Chem*. **2017**, *6*, 1160–1179. https://doi.org/10.1002/ajoc.201700151

(12) Hoffmann, R. W. Markovnikov Free Radical Addition Reactions, a Sleeping Beauty Kissed to Life. *Chem. Soc. Rev.* **2016**, *45*, 577–583. https://doi.org/10.1039/c5cs00423c

(13) Wua, J.; Ma, Z. Metal-hydride hydrogen atom transfer (MHAT) reactions in natural product synthesis. *Org. Chem. Front.*, **2021**, 8, 7050–7076. https://doi.org/10.1039/D1QO01139A

(14) (a) Huang, Z.; Dong, G. Site-Selectivity Control in Organic Reactions: A Quest To Differentiate Reactivity among the Same Kind of Functional Groups. *Acc. Chem. Res.* **2017**, *50*, 465–471. https://doi.org/10.1021/acs.accounts.6b00476 (b) Ma, X.; Herzon, S. B. Non-Classical Selectivities in the Reduction of Alkenes by Cobalt-Mediated Hydrogen Atom Transfer. *Chem. Sci.* **2015**, *6*, 6250–6255. https://doi.org/10.1039/c5sc02476e

(15) (a) Kwiatek, J.; Mador, I.L.; Seyler, J. K. Catalytic Hydrogenation of Organic Compounds by Pentacyanocobaltate(II). *J. Am. Chem. Soc.*, **1962**, *84*, 305–305. https://doi.org/10.1021/ja00861a034 (b)Kwiatek, J.; Seyler, J. K. Preparation of organocyanocobaltate(III) complexes. *J. Organomet. Chem.*, **1965**, *3*, 421–432. https://doi.org/10.1016/S0022-328X(00)83570-6

(16) Zombeck, A.; Hamilton, D. E.; Drago, R. S.; Zombeck, A.; Hamilton, D. E.; Drago, R. S. Novel Catalytic Oxidations of Terminal Olefins by Cobalt(II)-Schiff Base Complexes. *J. Am. Chem. Soc.* **1982**, *104*, 6782–6784. https://doi.org/10.1021/ja00388a051

(17) (a) Mukayama, T.; Isayama, S. Inoki, S.; Kato, K.; Yamada, T.; Takai, T. Oxidation-Reduction Hydration of Olefins with Molecular Oxygen and 2-Propanol Catalyzed by Bis(acetylacetonato)cobalt (II). *Chem. Lett.*, **1989**, 18, 449–452. https://doi.org/10.1246/cl.1989.449 (b) Inoki, S.; Kato, K.; Takai, T.; Isayama, S.; Yamada, T.; Mukayama, T. Bis(trifluoroacetylacetonato)cobalt (II) Catalyzed Oxidation-Reduction Hydration of Olefins Selective Formation of Alcohols from Olefins. *Chem. Lett.*, **1989**, *18*, 515–518. https://doi.org/10.1246/cl.1989.515

(18) (a) Ishikawa, H.; Colby, D. A.; Seto, S.; Va, P.; Tam, A.; Kakei, H.; Rayl, T. J.; Hwang, I.; Boger, D. L. Total Synthesis of Vinblastine, Vincristine, Related Natural Products, and Key Structural Analogues. *J. Am. Chem. Soc.*, **2009**, *131*, 4904–4916. https://doi.org/10.1021/ja809842b (b) Schindler, C. S.; Stephenson, C. R. J.; Carreira, E. M. Enantioselective Synthesis of the Core of Banyaside, Suomilide, and Spumigin HKVV. *Angew. Chem. Int. Ed.*, **2008**, *47*, 8852–8855. https://doi.org/10.1002/anie.200803655 (c)Shenvi, R. A.; Guerrero, C. A.; Shi, J.; Li, C.; Baran, P. S. Synthesis of (+)-Cortistatin A. *J. Am. Chem. Soc.*, **2008**, *130*, 7241–7243. https://doi.org/10.1021/ja8023466

(19) Isayama, S. An Efficient Method for the Direct Peroxygenation of Various Olefinic Compounds with Molecular Oxygen and Triethylsilane Catalyzed by a Cobalt(II) Complex. *Bull. Chem. Soc. Jpn.*, **1990**, *63*, 1305–1310. https://doi.org/10.1246/bcsj.63.1305

(20) (a) Shigehisa, H.; Aoki, T.; Yamaguchi, S.; Shimizu, N.; Hiroya, K. Hydroalkoxylation of Unactivated Olefins with Carbon Radicals and Carbocation Species as Key Intermediates. *J. Am. Chem. Soc.*, **2013**, *135*, 10306–10309. https://doi.org/10.1021/ja405219f (b) Shi, S.; Kuo, J. L.; Chen, T.; Norton, J. R. Catalytic Cycloisomerization onto a Carbonyl Oxygen. *Org. Lett*. **2020**, *22*, 6171–6176. https://doi.org/10.1021/acs.orglett.0c02272

(21) Shigehisa, H.; Koseki, N.; Shimizu, N.; Fujisawa, M.; Niitsu, M.; Hiroya, K. Catalytic Hydroamination of Unactivated Olefins Using a Co Catalyst for Complex Molecule Synthesis *J. Am. Chem. Soc.*, **2014**, *136*, 13534–13537. https://doi.org/10.1021/ja507295u

(22) Waser, J.; Gaspar, B.; Nambu, H.; Carreira, E. M. Hydrazines and Azides via the Metal-Catalyzed Hydrohydrazination and Hydroazidation of Olefins. *J. Am. Chem. Soc.*, **2006**, *128*, 11693–11712. https://doi.org/10.1021/ja062355+

(23) Okamoto, T.; Kobayashi, K.; Oka, S.; Tanimoto, S. Cobalt-catalyzed reaction of nitric oxide with aryl-substituted olefins in the presence of tetrahydroborate ion. *J. Org. Chem.*, **1987**, *52*, 5089–5092. https://doi.org/10.1021/jo00232a005

(24) Girijavallabhan, V.; Alvarez, C.; Njogoroge, F. G. Regioselective Cobalt-Catalyzed Addition of Sulfides to Unactivated Alkenes. *J. Org. Chem.*, **2011**, *76*, 6442–6446. https://doi.org/10.1021/jo201016z

(25) Barker, T. J.; Boger, D. L. Fe(III)/$NaBH_4$-Mediated Free Radical Hydrofluorination of Unactivated Alkenes. *J. Am. Chem. Soc.*, **2012**, *134*, 13588–13591. https://doi.org/10.1021/ja3063716

(26) Gaspar, B.; Carreira, E. M. Catalytic Hydrochlorination of Unactivated Olefins with para-Toluenesulfonyl Chloride. *Angew. Chem. Int. Ed.*, **2008**, *47*, 5758–5760. https://doi.org/10.1002/anie.200801760

(27) Ma, X.; Herzon, S. B. Non-classical selectivities in the reduction of alkenes by cobalt-mediated hydrogen atom transfer. *Chem. Sci.*, **2015**, *6*, 6250–6255. https://doi.org/10.1039/C5SC02476E

(28) Iwasaki, K.; Wan, K. K.; Oppedisano, A.; Crossley, S. W. M.; Shenvi, R. A. Simple, Chemoselective Hydrogenation with Thermodynamic Stereocontrol. *J. Am. Chem. Soc.*, **2014**, *136*, 1300–1303. https://doi.org/10.1021/ja412342g

(29) Ma, X.; Herzon, S. B. Cobalt Bis(acetylacetonate)–tert-butyl Hydroperoxide–Triethylsilane: A General Reagent Combination for the Markovnikov Selective Hydrofunctionalization of Alkenes by Hydrogen Atom Transfer. *Beilstein J. Org. Chem.*, **2018**, *14*, 2259–2265. https://doi.org/10.3762/bjoc.14.201

(30) Crossley, S. W. M.; Obradors, C.; Martinez, R. M.; Shenvi, R. A. Mn-, Fe-, and Co-Catalyzed Radical Hydrofunctionalizations of Olefins. *Chem. Rev.* **2016**, *116*, 8912–9000. https://doi.org/10.1021/acs.chemrev.6b00334

(31) Lo, J. C.; Yabe, Y.; Baran, P. S. A Practical and Catalytic Reductive Olefin Coupling. *J. Am. Chem. Soc.* **2014**, *136*, 1304–1307. https://doi.org/10.1021/ja4117632

(32) Lo, J. C.; Gui, J.; Yabe, Y.; Pan, C. M.; Baran, P. S. Functionalized Olefin Cross-Coupling to Construct Carbon-Carbon Bonds. *Nature* **2014**, *516*, 343–348. https://doi.org/10.1038/nature14006

(33) Lo, J. C.; Kim, D.; Pan, C. M.; Edwards, J. T.; Yabe, Y.; Gui, J.; Qin, T.; Gutiérrez, S.; Giacoboni, J.; Smith, M. W.; Holland, P. L.; Baran, P. S. Fe-Catalyzed C-C Bond Construction from Olefins via Radicals. *J. Am. Chem. Soc.* **2017**, *139*, 2484–2503. https://doi.org/10.1021/jacs.6b13155

(34) Kim, D.; Rahaman, S. M. W.; Mercado, B. Q.; Poli, R.; Holland, P. L. Roles of Iron Complexes in Catalytic Radical Alkene Cross-Coupling: A Computational and Mechanistic Study. *J. Am. Chem. Soc.* **2019**, *141*, 7473–7485. https://doi.org/10.1021/jacs.9b02117

(35) Leifert, D.; Studer, A. The Persistent Radical Effect in Organic Synthesis. *Angew. Chem., Int. Ed.* **2020**, *59*, 74–108. https://doi.org/10.1002/anie.201903726

(36) Zheng, J.; Wang, D.; Cui, S. Fe-Catalyzed Reductive Coupling of Unactivated Alkenes with β-Nitroalkenes. *Org. Lett.* **2015**, *17*, 4572–4575. https://doi.org/10.1021/acs.orglett.5b02294

(37) Shen, Y.; Qi, J.; Mao, Z.; Cui, S. Fe-Catalyzed Hydroalkylation of Olefins with *para*-Quinone Methides. *Org. Lett.* **2016**, *18*, 2722–2725. https://doi.org/10.1021/acs.orglett.6b01173

(38) Qi, J.; Zheng, J.; Cui, S. Fe(III)-Catalyzed Hydroallylation of Unactivated Alkenes with Morita-Baylis-Hillman Adducts. *Org. Lett.* **2018**, *20*, 1355–1358. https://doi.org/10.1021/acs.orglett.8b00108

(39) Yang, L.; Ji, W. W.; Lin, E.; Li, J. L.; Fan, W. X.; Li, Q.; Wang, H. Synthesis of Alkylated Monofluoroalkenes via Fe-Catalyzed Defluorinative Cross-Coupling of Donor Alkenes with Gem -Difluoroalkenes. *Org. Lett.* **2018**, *20*, 1924–1927. https://doi.org/10.1021/acs.orglett.8b00471

(40) Tardieu, D.; Desnoyers, M.; Laye, C.; Hazelard, D.; Kern, N.; Compain, P. Stereoselective Synthesis of C,C-Glycosides from *exo*-Glycals Enabled by Iron-Mediated Hydrogen Atom Transfer. *Org. Lett.* **2019**, *21*, 7262–7267. https://doi.org/10.1021/acs.orglett.9b02496

(41) Zhang, M.; Yang, L.; Tian, C.; Zhou, M.; An, G.; Li, G. A Hydrate Salt-Promoted Reductive Coupling Reaction of Nitrodienes with Unactivated Alkenes. *Org. Biomol. Chem.,* **2019**, *17*, 2258–2264. https://doi.org/10.1039/C9OB00136K

(42) Qi, J.; Tang, H.; Chen, C.; Cui, S.; Xu, G. Reductive coupling of Alkenes with unsaturated imines *via* a radical pathway. *Org. Chem. Front.*, **2019**, *6*, 2760–2764. https://doi.org/10.1039/C9QO00653B

(43) Zhu, T.; Zhang, X. J.; Zhou, Z.; Xu, Z.; Ma, M.; Zhao, B. Synthesis of functionalized malononitriles *via* Fe-catalysed hydrogen atom transfers of alkenes. *Org. Biomol. Chem.* **2022**, *20*, 1480–1487. https://doi.org/10.1039/D1OB02332B

(44) Fang, X. Zhang, N.; Chen, S. C.; Luo, T. Scalable Total Synthesis of (-)-Triptonide: Serendipitous Discovery of a Visible-Light Promoted Olefin Coupling Initiated by Metal-Catalyzed Hydrogen Atom Transfer (MHAT). *J. Am. Chem. Soc.*, **2022**, *144*, 2292–2300. https://doi.org/10.1021/jacs.1c12525

(45) Jana, K.; Studer, A. Allylboronic Esters as Acceptors in Radical Addition, Boron 1,2-Migration, and Trapping Cascades. *Org. Lett.*, **2022**, *24*, 1100–1104. https://doi.org/10.1021/acs.orglett.2c00039

(46) Iwasaki, K.; Wan, K. K.; Oppedisano, A.; Crossley, S. W. M.; Shenvi, R. A. Simple, Chemoselective Hydrogenation with Thermodynamic Stereocontrol. *J. Am. Chem. Soc.* **2014**, *136*, 1300–1303. https://doi.org/10.1021/ja412342g

(47) Crossley, S. W. M.; Barabé, F.; Shenvi, R. A. Simple, Chemoselective, Catalytic Olefin Isomerization. *J. Am. Chem. Soc.*, **2014**, *136*, 16788–16791. https://doi.org/10.1021/ja5105602

(48) Kuo, J. L.; Hartung, J.; Han, A.; Norton, J. R. Direct Generation of Oxygen-Stabilized Radicals by H· Transfer from Transition Metal Hydrides. *J. Am. Chem. Soc.*, **2015**, *137*, 1036–1039. https://doi.org/10.1021/ja511883b

(49) Gnaim, S.; Bauer, A.; Zhang, H. J.; Chen, L.; Gannett, C.; Malapit, C. A.; Hill, D. E.; Vogt, D.; Tang, T.; Daley, R. A.; Hao, W.; Zeng, R.; Quertenmont, M.; Beck, W. D.; Kandahari, E.; Vantourout, J. C.; Echeverria, P. G.; Abruna, H. D.; Blackmond, D. G.; Minteer, S. D.; Reisman, S. E.; Sigman, M. S.; Baran, P. S. Cobalt-electrocatalytic HAT for functionalization of unsaturated C–C bonds. *Nature*, **2022**, *605*, 687–695. https://doi.org/10.1038/s41586-022-04595-3

(50) Shen, Y.; Huang, B.; Zheng, J.; Lin, C.; Cui, S. Csp–Csp3 Bond Formation via Iron(III)-Promoted Hydroalkynylation of Unactivated Alkenes. *Org. Lett.*, **2017**, *19*, 1744–1747. https://doi.org/10.1021/acs.orglett.7b00499

(51) Xia, X. F.; He, W.; Zhang, G. W.; Wang, D. Iron-catalyzed reductive cyclization reaction of 1,6-enynes for the synthesis of 3-acylbenzofurans and thiophenes. *Org. Chem. Front.*, **2019**, *6*, 342–346. https://doi.org/10.1039/C8QO01190G

(52) Zhao, M.; He, W.; Zou, L. H.; Wang, D.; Sun, T. Y.; Xia, X. F. Iron-catalyzed hydrogen atom transfer induced cyclization of 1,6-enynes for the synthesis of ketoximes: a combined experimental and computational study. *Org. Chem. Front.,* **2021**, *8*, 643–652. https://doi.org/10.1039/D0QO01341B

(53) Zhao, B.; Zhu, T.; Ma, M.; Shi, Z. SOMOphilic Alkynylation of Unreactive Alkenes Enabled by Iron-Catalyzed Hydrogen Atom Transfer. *Molecules*, **2022**, *27*, 33. https://doi.org/10.3390/molecules27010033

(54) Saladrigas, M.; Bosch, C.; Saborit, G. V.; Bonjoch, J.; Bradshaw, B. Radical Cyclization of Alkene-Tethered Ketones Initiated by Hydrogen-Atom Transfer. *Angew. Chem., Int. Ed.* **2018**, *57*, 182–186. https://doi.org/10.1002/anie.201709659

(55) Saladrigas, M.; Gómez-Bengoa, E.; Bonjoch, J.; Bradshaw, B. Four-Step Synthesis of (-)-4-epi-Presilphiperfolan-8α-ol by Intramolecular Iron Hydride Atom Transfer-Mediated Ketone-

Alkene Coupling and Studies to Access trans-Hydrindanols with a Botryane Scaffold. *Chem. Eur. J.* **2023**, *29*, e202203286. https://doi.org/10.1002/chem.202203286

(56) Matos, J. L. M.; Vásquez-Céspedes, S.; Gu, J.; Oguma, T.; Shenvi, R. A. Branch-Selective Addition of Unactivated Olefins into Imines and Aldehydes. *J. Am. Chem. Soc*. **2018**, *140*, 16976−16981. https://doi.org/10.1021/jacs.8b11699

(57) Saladrigas, M.; Puig, J.; Bonjoch, J.; Bradshaw, B. Iron-Catalyzed Radical Intermolecular Addition of Unbiased Alkenes to Aldehydes. *Org. Lett.* **2020**, *22*, 8111–8115. https://doi.org/10.1021/acs.orglett.0c03081

(58) Wu, B.; Zhu, R. Radical Philicity Inversion in Co- and Fe-Catalyzed Hydrogen-Atom-Transfer-Initiated Cyclizations of Unsaturated Acylsilanes. *ACS Catal.* **2020**, *10*, 510–515. https://doi.org/10.1021/acscatal.9b04774

(59) Zhang, B.; He, J.; Li, Y.; Song, T.; Fang, Y.; Li, C. Cobalt-Catalyzed Markovnikov-Selective Radical Hydroacylation of Unactivated Alkenes with Acylphosphonates. *J. Am. Chem. Soc.* **2021**, *143*, 4955–4961. https://doi.org/10.1021/jacs.1c02629

(60) Mayerhofer, V. J.; Lippolis, M.; Teskey, C. J. Dual-Catalysed Intermolecular Reductive Coupling of Dienes and Ketones. *Angew. Chem. Int. Ed.* **2024**, *63*, e202314870. https://doi.org/10.1002/anie.202314870

(61) Yan, H.; Shan, J. R.; Shi, L. Photochemical Metal-Hydride Hydrogen Atom Transfer Mediated Radical Hydrofunctionalization of Dienes and Allenes. *Chem. Cat. Chem.*, **2024**, *16*, e202301344. https://doi.org/10.1002/cctc.202301344

(62) Ma, X.; Herzon, S. B. Intermolecular Hydropyridylation of Unactivated Alkenes. *J. Am. Chem. Soc.*, **2016**, *138,* 8718–8721. https://doi.org/10.1021/jacs.6b05271

(63) Bordi, S.; Starr, J. T. Hydropyridylation of Olefins by Intermolecular Minisci Reaction. *Org. Lett.,* **2019**, *19*, 2290–2293. https://doi.org/10.1021/acs.orglett.7b00833

(64) Lo, J. C.; Kim, D.; Pan, C. M.; Edwards, J. T.; Yabe, Y.; Gui, J.; Qin, T.; Gutiérrez, S.; Giacoboni, J.; Smith, M. W.; Holland, P. L.; Baran, P. S. Fe-Catalyzed C-C Bond Construction from Olefins via Radicals. *J. Am. Chem. Soc.* **2017**, *139*, 2484–2503. https://doi.org/10.1021/jacs.6b13155

(65) Qin, J.; Barday, M.; Jana, S.; Sanosa, N.; Funes-Ardoiz, I.; Teskey, C. J. Photoinduced Cobalt Catalysis for the Reductive Coupling of Pyridines and Dienes Enabled by Paired Single-Electron Transfer. *Angew. Chem. Int. Ed.*, **2023**, *62*, e202310639. https://doi.org/10.1002/anie.202310639

(66) Gharpure, S. J.; Chavan, R. S.; Narang, S. R. Iron-Mediated Hydrogen Atom Transfer Radical Cyclization of Alkenyl Indoles and Pyrroles Gives Their Fused Derivatives: Total

Synthesis of Bruceolline E and H. *Org. Lett.*, **2024**, article ASAP. https://doi.org/10.1021/acs.orglett.4c00032

(67) Green, S. A.; Matos, J. L. M.; Yagi, A.; Shenvi, R. A. Branch-Selective Hydroarylation: Iodoarene-Olefin Cross-Coupling. *J. Am. Chem. Soc.* **2016**, *138*, 12779–12782. https://doi.org/10.1021/jacs.6b08507

(68) Crossley, S. W. M.; Martinez, R. M.; Guevara-Zuluaga, S.; Shenvi, R. A. Synthesis of the Privileged 8-Arylmenthol Class by Radical Arylation of Isopulegol. *Org. Lett.,* **2016**, *18*, 2620–2623. https://doi.org/10.1021/acs.orglett.6b01047

(69) Shigehisa, H.; Ano, T.; Honma, H.; Ebisawa, K.; Hiroya, K. Co-Catalyzed Hydroarylation of Unactivated Olefins. *Org. Lett.*, **2016**, *18*, 3622–3625. https://doi.org/10.1021/acs.orglett.6b01662

(70) Ji, Y.; Xin, Z.; He, H.; Gao, S. Total Synthesis of Viridin and Viridiol. *J. Am. Chem. Soc.* **2019**, *141*, 16208–16212. https://doi.org/10.1021/jacs.9b08577

(71) Gaspar, B.; Carreira, E. M. Mild Cobalt-Catalyzed Hydrocyanation of Olefins with Tosyl Cyanide. *Angew. Chem., Int. Ed.* **2007**, *46*, 4519–4522. https://doi.org/10.1002/anie.200700575

(72) Liu, J.; Ma, D. A Unified Approach for the Assembly of Atisine- and Hetidine-Type Diterpenoid Alkaloids: Total Syntheses of Azitine and the Proposed Structure of Navirine C. *Angew. Chem., Int. Ed.* **2018**, *57*, 6676–6680. https://doi.org/10.1002/anie.201803018

(73) Turner, O. J.; Murphy, J. A.; Hirst, D. J.; Talbot, E. P. A. Hydrogen Atom Transfer-Mediated Cyclisations of Nitriles. *Chem. Eur. J.* **2018**, *24*, 18658–18662. https://doi.org/10.1002/chem.201805236

(74) Turner, O. J.; Hirst, D. J.; Murphy, J. A. Hydrogen Atom Transfer-Mediated Domino Cyclisation Reaction to Access (Spiro)-Quinazolinones. *Chem. Eur. J.*, **2020**, *26*, 3026−3029. https://doi.org/10.1002/chem.201905712

(75) Song, L.; Fu, N.; Ernst, B. G. Lee, W. H.; Frederick, M. O.; DiStasio, R. A.; Lin, S. Dual Electrocatalysis, Enables Enantioselective Hydrocyanation of Conjugated Alkenes. *Nat. Chem.* **2020**, *12*, 747–754. https://doi.org/10.1038/s41557-020-0469-5

(76) Gaspar, B.; Carreira, E. M. Cobalt Catalyzed Functionalization of Unactivated Alkenes: Regioselective Reductive C-C Bond Forming Reactions. *J. Am. Chem. Soc.* **2009**, *131*, 13214–13215. https://doi.org/10.1021/ja904856k

(77) Dao, H. T.; Li, C.; Michaudel, Q.; Maxwell, B. D.; Baran, P. S. Hydromethylation of Unactivated Olefins. *J. Am. Chem. Soc.* **2015**, *137*, 8046–8049. https://doi.org/10.1021/jacs.5b05144

(78) Saladrigas, M.; Loren, G.; Bonjoch, J.; Bradshaw, B. Hydrogen Atom Transfer (HAT)-Triggered Iron-Catalyzed Intra- and Intermolecular Coupling of Alkenes with Hydrazones: Access to Complex Amines. *ACS Catal.* **2018**, *8*, 11699–11703. https://doi.org/10.1021/acscatal.8b03794

(79) Matos, J. L. M.; Vásquez-Céspedes, S.; Gu, J.; Oguma, T.; Shenvi, R. A. Branch-Selective Addition of Unactivated Olefins into Imines and Aldehydes. *J. Am. Chem. Soc.* **2018**, *140* (49), 16976–16981.https://doi.org/10.1021/jacs.8b11699

(80) Wang, Y. Y.; Bode, J. W. Olefin Amine (OLA) Reagents for the Synthesis of Bridged Bicyclic and Spirocyclic Saturated *N*-Heterocycles by Catalytic Hydrogen Atom Transfer (HAT) Reactions. *J. Am. Chem. Soc.* **2019**, *141*, 9739–9745. https://doi.org/10.1021/jacs.9b05074

(81) Saladrigas, M.; Bonjoch, J.; Bradshaw, B. Iron Hydride Radical Reductive Alkylation of Unactivated Alkenes. *Org. Lett.* **2020**, *22*, 684–688. https://doi.org/10.1021/acs.orglett.9b04459

(82) Green, S. A.; Huffman, T. R.; McCourt, R. O.; van der Puyl, V.; Shenvi, R. A. Hydroalkylation of Olefins To Form Quaternary Carbons. *J. Am. Chem. Soc.*, **2019**, *141*, 7709–7714. https://doi.org/10.1021/jacs.9b02844

(83) Zeng, M.; Yu, C.; Wang, Y.; Wang, J.; Wang, J.; Liu, H. Cobalt(II)-Catalyzed C(sp^3)-C(sp^3) Coupling for the Direct Stereoselective Synthesis of 2-Deoxy-*C*-Glycosides from Glycals. *Angew. Chem. Int. Ed.*, **2023**, *62*, e202300424. https://doi.org/10.1002/anie.202300424

(84) Liu, B.; Liu, D.; Rong, X.; Lu, X.; Fu, Y.; Liu, Q. Ligand-Controlled Stereoselective Synthesis of 2-Deoxy-b-C-glycosides by Cobalt Catalysis. *Angew. Chem. Int. Ed.*, **2023**, *62*, e202218544. https://doi.org/10.1002/anie.202218544

(85) Puig, J.; Bonjoch, J.; Bradshaw, B. Isocyanides as Acceptor Groups in MHAT Reactions with Unactivated Alkenes. *Org. Lett.* **2023**, *25*, 6539–6543. https://doi.org/10.1021/acs.orglett.3c02358

(86) Zhang, B.; Studer, A. Recent Advances in the Synthesis of Nitrogen Heterocycles via Radical Cascade Reactions Us-ing Isonitriles as Radical Acceptors. *Chem. Soc. Rev.* **2015**, *44*, 3505–3521. https://doi.org/10.1039/C5CS00083A

(87) Vitaku, E.; Smith, D. T.; Njardarson, J. T. Analysis of the structural diversity, substitution patterns, and frequency of nitrogen heterocycles among U.S. FDA approved pharmaceuticals. *J. Med. Chem.*, **2014**, 57, 10257–10274. https://doi.org/10.1021/jm501100b

(88) Cahlíková, L.; Vrabec, R.; Pidaný, F.; Peřinová, R.; Maafi, N.; Mamun, A.; Ritomská, A.; Wijaya, V.; Blunden, G. Recent progress on biological activity of amaryllidaceae and further

isoquinoline alkaloids in connection with alzheimer's disease. *Molecules*, **2021**, *26*, 5240. https://doi.org/10.3390/molecules26175240

(89) Ashrafi, S.; Alam, S.; Sultana, A.; Raj, A.; Emon, N. U.; Richi, F. T.; Sharmin, T.; Moon, M.; Park, M. N.; Kim, B. Papaverine: A Miraculous Alkaloid from Opium and Its Multimedicinal Application. *Molecules*, **2023**, *28*, 3149. https://doi.org/10.3390/molecules28073149

(90) Kolobaric, A.; Hewlings, S. J.; Bryant, C.; Colwell, C. S.; R D'Adamo, C.; Rosner, B.; Chen, J.; Pauli, E. K. A Randomized, Double-Blind, Placebo-Controlled Decentralized Trial to Assess Sleep, Health Outcomes, and Overall Well-Being in Healthy Adults Reporting Disturbed Sleep, Taking a Melatonin-Free Supplement. *Nutrients*, **2023**, *15*, 3788. https://doi.org/10.3390/nu15173788

(91) Lygin, A. V.; de Meijere, A. Isocyanides in the synthesis of nitrogen heterocycles. *Angew. Chem. Int. Ed.*, **2010**, *49*, 9094–9124. https://doi.org/10.1002/anie.201000723

(92) Ryu, I.; Sonoda, N.; Curran, D. P. Tandem Radical Reactions of Carbon Monoxide, Isonitriles, and Other Reagent Equivalents of the Geminal Radical Acceptor/Radical Precursor Synthon. *Chem. Rev.* **1996**, *96*, 177−194. https://doi-org/10.1021/cr9400626

(93) Renaud, P.; Sibi, M.P. Isonitriles: a Useful Trap in Radical Chemistry In *Radicals in Organic Synthesis vol.2*, 1st ed.; Wiley-VCH, **2001**; 44–61.

(94) Hoffman, P.; Marquarding, D.; Kliimann, H.; Ugi, I. Isonitriles In *The Chemistry of the Cyano Group*, Wiley, **1970**.

(95) (a) Kühle, E. Kohlensäurederivate aus Formamiden. *Angew. Chem.* **1952**, *74,* 861. https://doi.org/10.1002/ange.19620742113 (b) Lentz, D. Trifluormethylisocyanid. Eine neue synthese. *J. Fluorine Chem.* **1984**, *24*, 523–530. https://doi.org/10.1016/S0022-1139(00)83172-3

(96) Gautier, A. Ueber die Einwirkung des Chlorwasserstoffs u. a. auf das Aethyl- und Methylcyanur. *Justus Liebigs Ann. Chem.* **1957**, *142*, 289–294. https://doi.org/10.1002/jlac.18671420304

(97) (a) Hagedorn, I., Tönjes, H., Structure of Xanthocillin, a New Antibiotic. *Pharmazie*, **1956**, *11*, 409. (b) Ugi, I.; Meyr, R. Darstellung von Isonitrilen aus monosubstituierten Formamiden durch Wasserabspaltung. *Chem. Ber.* **1960**, 93, 239–248. https://doi.org/10.1002/cber.19600930136

(98) (a) Mukaiyama, T.; Nambu, H.; Okamoto, M. Deoxygenations of Isocyanates and Diphenylketene by Tertiary Phosphites. *J. Org. Chem.* **1962**, 27, 3651–3654. https://doi-org /10.1021/jo01057a060 (b) Lorenz, D.H.; Becker, E.I. *J. Org. Chem.* **1963**, *28*, 1707–1708. https://doi.org/10.1021/jo01041a508

(99) Witczak, Z.J. Desulfuration of Glycosyl Isothiocyanates with Tributyltin Hydride. *Tetrahedron,* **1986**, *27*, 155–158. https://doi-org /10.1016/S0040-4039(00)83965-9

(100) Gassman, P.G.; Guggenheim, T.L. Opening of epoxides with trimethylsilyl cyanide to produce beta-hydroxy isonitriles. A general synthesis of oxazolines and beta-amino alcohols. *J. Am. Chem. Soc.* **1982**, *104*, 5849–5850. https://doi-org/10.1021/ja00385a078

(101) Baldwin, J. E.; Bottaro, J. C.; Riordan, P. D.; Derome, A. E. A New Method for the Reduction of Isocyanates to Isocyanides. ***J. Chem. Soc., Chem. Commun.***, **1982**, 942–943. https://doi.org/10.1039/C39820000942

(102) Sasaki, T.; Nakanishi, A.; Ohno, M. Synthesis of adamantane derivatives. 56. Reaction of 1-adamantyl chloride with trimethylsilyl pseudohalide. *J. Org. Chem.* **1981**, *46*, 5445–5447 https://doi.org/10.1021/jo00339a050

(103) Ritter, J.J.; Minieri, P.P. A New Reaction of Nitriles. I. Amides from Alkenes and Mononitriles. *J. Am. Chem. Soc.* **1948**, *70*, 4045–4048. https://doi.org/10.1021/ja01192a022

(104) (a) Passerini, M. *Gazz. Chim. Ital.* **1921**, *51*, 126. (b) Ugi, I. Neuere Methoden der präparativen organischen Chemie. Mit Sekundär-Reaktionen gekoppelte α-Additionen von Immonium-Ionen und Anionen an Isonitrile. *Angew. Chem.* **1962,** *74*, 9–22. https://doi.org/10.1002/ange.19620740103

(105) Gomes, G.; Loginova, Y.; Vatsadze, S.Z.; Alabugin, I.V. Isonitriles as Stereoelectronic Chameleons: The Donor−Acceptor Dichotomy in Radical Additions. *J. Am. Chem. Soc.* 2018, **140**, 14272–14288. https://doi.org/10.1021/jacs.8b08513

(106) Shaw, D.H.; Pritchard, H.O. Free-radical-catalyzed isomerization of isocyanides. *Can. J. Chem.* **1967**, *45*, 2749–2754. https://doi.org/10.1139/v67-445

(107) Saegusa, T.; Kobayashi, S.; Yoshihiko, I.; Yasuda, N. Radical reaction of isocyanide with organotin hydride. *J. Am. Chem. Soc.* **1968**, *90*, 4182. https://doi.org/10.1021/ja01017a061

(108) (a) Saegusa, T.; Kobayashi, S.; Ito, Y. Radical reaction of isocyanide with thiol. *J. Org. Chem.* **1970**, *35*, 2118–2121. https://doi.org/10.1021/jo00832a003 (b) Banks, R.E.; Haszeldine, R.N.; Stephens C.W. Free-radical attack on isocyanides: reactions between bistrifluoromethylamino-oxyl and t-butyl or trifluoromethyl isocyanide. *Tetrahedron*. **1972**, *13*, 3699–3701. https://doi.org/10.1016/S0040-4039(01)94139-5 (c) Singer, L.A.; Kim, S.S. Addition of t-butyl and t-butyoxy radicals to t-butylisocyanide. Fragmentation patterns in resulting imidoyl radicals. *Tetrahedron*. **1974**, *15*, 861–863. https://doi.org/10.1016/S0040-4039(01)82353-4 (d) Blum, P.M.; Roberts, B.P. Electron spin resonance study of radical addition to alkyl isocyanides. *J. Chem. Soc., Chem. Commun*., **1976**, 535–536. https://doi.org/10.1039/C39760000535 (e) Kim. S.S. Addition of phenyl radical to t-butyl

isocyanide an example of a cyanide transfer reaction. *Tetrahedron*, **1977**, *18*, 2741–2744. https://doi.org/10.1016/S0040-4039(01)83060-4 (f) Blum, P.M.; Roberts, B.P. An electron spin resonance study of radical addition to alkyl isocyanides. *J. Chem. Soc., Perkin Trans. 2,* **1978**, 1313–1319. https://doi.org/10.1039/P29780001313 (g) Barton, D.H.R.; Bringmann, G.; Motherwell, W.B. Reactions of relevance to the chemistry of aminoglycoside antibiotics. Part 15. The selective modification of neamine by radical-induced deamination. *J. Chem. Soc., Perkin Trans. 1*, **1980**, 2665–2669. https://doi.org/10.1039/P19800002665 (h) Stork, G.; Sher, P.M. Regiospecific trapping of radicals from cyclization reactions. Cyclic nitriles via isocyanide trapping. *J. Am. Chem. Soc.* **1983**, *105*, 6765–6766. https://doi.org/10.1021/ja00360a062

(109) Leardini, R.; Pedulli, G. F.; Tundo, A.; Zanardi, G. Aromatic Annelation by Reaction of Arylimidoyl Radicals with Alkynes: A New Synthesis of Quinolines. ***J. Chem. Soc., Chem. Commun.***, **1984**, 1320–1321. https://doi.org/10.1039/C39840001320

([110]) Curran, D. P.; Liu, H. 4 + 1 Radical Annulations with Isonitriles: A Simple Route to Cyclopenta-Fused Quinolines. *J. Am. Chem. Soc.*, **1991**, *113*, 2127–2132. https://doi.org/10.1021/ja00006a033

(111) Leardini, R.; Nanni, D.; Pedulli, G. F.; Tundo, A.; Zanardi, G. Aromatic Annelation by Reaction of Arylimidoyl Radicals with Alkynes: Evidence for the Intervention of a Spirocyclohexadienyl Radical in the Synthesis of Substituted Quinolines. *J. Chem. Soc., Perkin Trans. 1*, **1986**, 1591-1594. https://doi.org/10.1039/P19860001591

(112) Curran, D. P.; Liu, H. New 4 + 1 radical annulations. A formal total synthesis of (+-)-camptothecin. *J. Am. Chem. Soc*. **1992**, *114*, 5863–5864. https://doi.org/10.1021/ja00040a060

(113) Nanni, D.; Pareschi, P.; Rizzoli, C.; Sgarabotto, P.; Tundof, A. Radical Annulations and Cyclisations with Isonitriles: the Fate of the Intermediate Imidoyl and Cycfohexadienyl Radicals. *Tetrahedron*, **1995**, *51*, 9045–9062. https://doi.org/10.1016/0040-4020(95)00348-C

(114) Camaggi, C. M.; Leardini, R.; Nanni, D.; Zanardi, G. Radical Annulations with Nitriles: Novel Cascade Reactions of Cyano-Substituted Alkyl and Sulfanyi Radicals with Isonitriles. *Tetrahedron*, **1998**, *54*, 5587–5598. https://doi.org/10.1016/S0040-4020(98)00230-0

(115) Lenoir, I.; Smith, M. L. Vinyl isonitriles in radical cascade reactions: Formation of cyclopenta-fused pyridines and pyrazines. *J. Chem. Soc., Perkin Trans. 1,* **2000**, *5*, 641–643. https://doi.org/10.1039/a908630g

(116) Fukuyama, T.; Chen, X.; Peng, G. A Novel Tin-Mediated Indole Synthesis. *J. Am. Chem. Soc.* **1994**, *116*, 3127–3128. https://doi.org/10.1021/ja00086a054

(117) Tokuyama, H.; Yamashita, T.; Reding, M. T.; Kaburagi, Y.; Fukuyama, T. Radical cyclization of 2-alkenylthioanilides: A Novel synthesis of 2,3- disubstituted indoles. *J. Am. Chem. Soc.*, **1999**, *121*, 3791–3792. https://doi.org/10.1021/ja983681v

(118) Kobayashi, Y.; Fukuyama, T. Development of a novel indole synthesis and its application to natural products synthesis. *J. Heterocyclic Chem.*, **1998**, *35*, 1043–1056. https://doi.org/10.1002/jhet.5570350504

(119) Rainier, J. D.; Kennedy, A. R.; Chase, E. An isonitrile-alkyne cascade to di-substituted indoles. *Tetrahedron,* **1999**, *40*, 6325–6327. https://doi.org/10.1016/S0040-4039(99)01169-7

(120) (a) Bachi, M. D.; Balanov, A.; Bar-Ner, N. Thiol-Mediated Free Radical Cyclization of Alkenyl and Alkynyl Isocyanides. *J. Org. Chem.*, **1994**, *59*, 7752–7758. https://doi-org /10.1021/jo00104a035 (b) Bachi, M.D.; Melman, A. Stereocontrolled 5-Exo-Trig Cyclization of Imidoyl Radicals in the Synthesis of Substituted (Alkylthio)pyrrolines, Pyroglutamates, and Thiopyroglutamates. *J. Org. Chem.* **1996**, *60*, 6242–6244. https://doi-org/10.1021/jo00124a056.

(121) Bachi, M. D.; Melman, A. Enantioselective total synthesis of (−)-α-kainic acid. Pure Appl. Chem. 1998, 79, 259–262. http://doi.org/10.1351/pac199870020259

(122) Tumir, L.M.; Stojkovic, M.R.; Piantanida I. Come-back of phenanthridine and phenanthridinium derivatives in the 21st century. *Beilstein. J. Org. Chem.* **2014**, *10*, 2930–2954. http://doi.org/10.3762/bjoc.10.312

(123) (a) Zhu, Z. Q.; Wang, T. T.; Baia, P.; Huang, Z. Z. A cascade alkylarylation reaction of 2-isocyanobiphenyls with simple alkanes for 6-alkyl phenanthridines via dual C(sp^3)–H/C(sp^2)–H functionalization. *Org. Biomol. Chem.*, **2014**, *12*, 5839–5842. http://doi.org/10.1039/c4ob01256a (b) Li, Z.; Fan, F.; Yang, J.; Liu, Z. Q. A Free Radical Cascade Cyclization of Isocyanides with Simple Alkanes and Alcohols. *Org. Lett*. **2014**, *16*, 3396-3399. http://doi.org/10.1021/ol501461u (c) Sha, W.; Yu, J. T.; Jiang, Y.; Yang, H.; Cheng, J. The benzoyl peroxide-promoted functionalization of simple alkanes with 2-aryl phenyl isonitrile. *Chem. Commun.*, **2014**, *50*, 9179–9181. http://doi.org/10.1039/c4cc03304c (d) [123] Li, Z.; Fan, F.; Yang, J.; Liu, Z. Q. A Free Radical Cascade Cyclization of Isocyanides with Simple Alkanes and Alcohols. *Org. Lett*. **2014**, *16*, 3396-3399. http://doi.org/10.1021/ol501461u

(124) (a) Wang, L.; Sha, W.; Dai, Q.; Feng, X.; Wu, W.; Peng, H.; Chen, B.; Cheng, J. The Benzoyl Peroxide Dual C-C Bond Formation *via* Dual C-H Bond Cleavage: -Phenanthridinylation of Ether by Isocyanide. *Org. Lett*. **2014**, *16*, 2088-2091. http://doi.org/10.1021/ol500277u (b) Cao, J. J.; Zhu, T. H.; Wang, S. Y.; Gu, Z. Y.; Wang, X.; Ji, S. J. *tert*-Butyl peroxybenzoate (TBPB)-mediated 2-isocyanobiaryl insertion with 1,4-dioxane:

efficient synthesis of 6-alkyl phenanthridines *via* C(sp^3)-H/ C(sp^2)-H bond functionalization. *Chem. Commun*. **2014**, *50*, 6439-6442. http://doi.org/10.1039/c4cc00743c (c) Xu, Y.; Chen, Y.; Li W.; Xie, Q.; Shao, L. Microwave-Assisted Synthesis of Phenanthridines by Radical Insertion/Cyclization of Biphenyl Isocyanides. *J. Org. Chem.* **2016**, *81*, 8426−8435. http://doi.org/10.1021/acs.joc.6b01589 (d) Feng, S.; Li, T.; Du, C.; Chen, P.; Song, D.; Li, J.; Xie, X.; She, X. Visible-light-mediated radical insertion/cyclization cascade reaction: synthesis of phenanthridines and isoquinolines from isocyanides. *Chem. Commun*., **2017**, *53*, 4585–4588. http://doi.org/10.1039/c7cc01813d (e) Guo, A.; Han, J. B.; Tang, X. Y. Boryl Radicals-Triggered Selective C−H Functionalization for the Synthesis of Diverse Phenanthridine Derivatives. *Org. Lett*. **2018**, *20*, 2351−2355. http://doi.org/10.1021/acs.orglett.8b00642

(125) (a) Feng, X.; Zhu, H.; Wang, L.; Jiang, Y.; Cheng, J.; Yu, J. T. TBHP-promoted Sequential Carboxamidation and Aromatisation of Aryl Isonitriles with Formamides. *Org. Biomol. Chem*. **2014**, *12*, 9257–9263. http://doi.org/10.1039/c4ob01850h (b) Tu, H. Y.; Liu, Y. R.; Chu, J. J.; Hu, B. L.; Zhang, X. G. $FeCl_3$-Promoted Carboxamidation and Cyclization of Aryl Isonitriles with Formamides toward Phenanthridine-6-carboxamides. *J. Org. Chem.* **2014**, *79*, 9907−9912. http://doi.org/10.1021/jo502022c

(126) Leifert, D.; Daniliuc, C. G.; Studer, A. 6-Aroylated Phenantridines via Base Promoted Homolytic Aromatic Substitution (BHAS). *Org. Lett.* **2013**, *15*, 6286-6289. http://doi.org/10.1021/ol403147v

(127) (a) Liu, J.; Fan, C.; Yin, H.; Qin, C.; Zhang, G.; Zhang, X.; Yia, H.; Lei, A. Synthesis of 6-Acyl Phenanthridines by Oxidative Radical Decarboxylation–Cyclization of a-Oxocarboxylates and Isocyanides. *Chem. Commun.*, **2014**, *50*, 2145—2147. http://doi.org/10.1039/c3cc49026b (b) Cao, J. J.; Wang, X.; Wang, S. Y.; Ji, S. J. Mn(III)-Mediated Reactions of 2-Isocyanobiaryl with 1,3-Dicarbonyl Compounds: Efficient Synthesis of 6-Alkylated and 6-Monofluoro-Alkylated Phenanthridines. *Chem. Commun.* **2014**, *50*, 12892–12895. http://doi.org/10.1039/c4cc05324a (c) Lu, S. C.; Li, H. S.; Gong, Y. L.; Zhang, S. P.; Zhang, J. G.; Xu, S. Combination of $PhI(OAc)_2$ and 2-Nitropropane as the Source of Methyl Radical in Room-Temperature Metal-Free Oxidative Decarboxylation/Cyclization: Construction of 6-Methyl Phenanthridines and 1-Methyl Isoquinolines. *J. Org. Chem.* **2018**, *83*, 15415−15425. http://doi.org/10.1021/acs.joc.8b02701 (d) Yao, Q.; Zhou, X.; Zhang, X.; Wang, C.; Wang, P.; Li, M. Convenient Synthesis of 6-Alkyl Phenanthridines and 1-Alkyl Isoquinolines via Silver-Catalyzed Oxidative Radical Decarboxylation. *Org. Biomol. Chem*., **2017**, *15*, 957–971. http://doi.org/10.1039/c6ob02331b (e) Xiang, H.; Yu, Z.; Xie, T.; Ye, X. Y.; Ye, T. Zn-Mediated Reductive Addition of Isocyanides with

Unactivated Tertiary Alkyl Oxalates. *Eur. J. Org. Chem*. **2022**, e202200937. http://doi.org/10.1002/ejoc.202200937

(128) (a)Lu, S.; Gong, Y.; Zhou, D. Transition Metal-Free Oxidative Radical Decarboxylation/Cyclization for the Construction of 6-Alkyl/Aryl Phenanthridines. *J. Org. Chem.* **2015**, *80*, 9336−9341. http://doi.org/10.1021/acs.joc.5b01518 (b) Lu, S. C.; Li, H. S.; Gong, Y. L.; Wang, X. L.; Li, F. R.; Li, F.; Duan, G. Y.; Xu, S. Use of Unprotected Amino Acids in Metal-free Tandem Radical Cyclization Reactions: Divergent Synthesis of 6-Alkyl/Acyl Phenanthridines. *RSC Adv*., **2017**, *7*, 55891–55896. http://doi.org/10.1039/c7ra12318c (c) Shi, W. Q.; Liu, S.; Wang, C. Z.; Huang, Y.; Qing, F. L.; Xu, X. H. Synthesis of CMe_2CF_3-Containing Heteroarenes via Tandem 1,1-Dimethyltrifluoroethylation and Cyclization of Isonitriles. *J. Org. Chem*. **2018**, *83*, 15236−15244. http://doi.org/10.1021/acs.joc.8b02506 (d) Luo, Z.; Li, R.; Zhu, T.; Liu, C. F.; Feng, H.; Nartey, K. A.; Liu, Q.; Xu, X. Iron-Catalyzed Oxidative Decabonylation/Radical Cyclization of Aliphatic Aldehydes with Biphenyl Isocyanides: A New Pathway For the Synthesis of 6-Alkylphenanthridines. *Asian J. Org. Chem.,* **2021**, *10*, 926–930. http://doi.org/10.1002/ajoc.202100112

(129) (a) Zhuang, Y. J.; Qu, J. P.; Kang, Y. B. Deprotonated Salicylaldehyde as Visible Light Photocatalyst. *J. Org. Chem.* **2020**, *85*, 4386−4397. http://doi.org/10.1021/acs.joc.0c00102 (b) Wadekar, K.; Aswale, S.; Yatham, V. R. PPh_3/NaI Driven Photocatalytic Decarboxylative Radical Cascade Alkylarylation Reaction of 2-Isocyanobiaryls. *RSC Adv.*, **2020**, *10*, 16510–16514. http://doi.org/10.1039/d0ra03211e (c) Zhou, Q.; Sun, C. G.; Liu, X.; Li, X.; Shao, Z.; Tan, K.; Shen, Y. Electron donor–acceptor complex-catalyzed photoredox reactions mediated by DIPEA and inorganic carbonates. *Org. Chem. Front*., **2022**, *9*, 5264–5271. http://doi.org/10.1039/d2qo00868h (d) Liu, M. T.; Liu, D. G.; Qin, Z. W.; Wang, G. Z. Visible Light-induced Decarboxylative Alkylations Enabled by Electron Donor-Acceptor Complex. *Asian J. Org. Chem*. **2022**, *11*, e202200335. http://doi.org/10.1002/ajoc.202200335

(130) Rohe, S.; McCallum, T.; Morris, A. O.; Barriault, L. Transformations of Isonitriles with Bromoalkanes Using Photoredox Gold Catalysis. *J. Org. Chem.* **2018**, *83*, 10015−10024. https://doi.org/10.1021/acs.joc.8b01380

(131) (a) Jiang, H.; Cheng, Y.; Wang, R.; Zheng, M.; Zhang, Y. and Yu, S. Synthesis of 6-Alkylated Phenanthridine Derivatives Using Photoredox Neutral Somophilic Isocyanide Insertion. *Angew. Chem. Int. Ed.* **2013**, *52*, 13289-13292. http://doi.org/10.1002/anie.201308376 (b) Liu, X.; Wu, C.; Zhang, J.; Shi, Y.; Zhang, S.; Geng, Y.; Tunga, C. H.; Wang, W. Cobalt-catalyzed radical cyclization of isocyanides forming phenanthridine derivatives. *Org. Chem. Front.*, **2018**, *5*, 2997–3002.

http://doi.org/10.1039/c8qo00887f (c) Li, Q.; Zhou, C. Y.; Wang, C. Divergent Construction of Heterocycles by SOMOphilic Isocyanide Insertion under N-Heterocyclic Carbene Catalysis. *Org. Lett*. **2022**, *24*, 7654−7658. https://doi.org/10.1021/acs.orglett.2c03148

(132) Zhang, B.; Studer, A. 6-Perfluoroalkylated Phenanthridines via Radical Perfluoroalkylation of Isonitriles. *Org. Lett*. **2014**, *16*, 3990-3993. https://doi.org/10.1021/ol5018195

(133) (a) Pei, C.; Yang, Z.; Koenigs, R. M. Photochemical palladium-catalyzed methylation and alkylation reactions in cascade reactions of isonitriles. *Tetrahedron*, **2022**, *123*, 132939. https://doi.org/10.1016/j.tet.2022.132939 (b) Tripathy, A. R.; Rahmathulla, R.; Kumar, A.; Yatham, V. R. Photocatalyzed alkylative cyclization of 2-isocyanobiphenyls with unactivated alkyl iodides. *Org. Biomol. Chem.*, **2022**, *20*, 3136–3144. http://doi.org/10.1039/d2ob00314g

(134) Chen, J. Y.; Wu, H. Y.; Song, H. Y.; Li, H. X.; Jiang, J.; Yang, T. B.; He, W. M. Visible-Light-Induced Annulation of Iodonium Ylides and 2-Isocyanobiaryls to Access 6-Arylated Phenanthridines. *J. Org. Chem.* **2023**, *88*, 8360−8368. http://doi.org/10.1021/acs.joc.3c00380

(135) Xia, Z.; Huang, J.; He, Y.; Zhao, J.; Lei, J.; Zhu, Q. Arylative Cyclization of 2-Isocyanobiphenyls with Anilines: One-Pot Synthesis of 6-Arylphenantridines via Competitive Reaction Pathways. *Org. Lett*., **2014**, *16*, 2546-2549. http://doi.org/10.1021/ol500923t

(136) (a) Xiao, T.; Li, L.; Lin, G.; Wang, Q.; Zhang, P.; Mao, Z.; Zhou, L. Synthesis of 6-Substituted Phenanthridines by Metal-Free, Visible-Light Induced Aerobic Oxidative Cyclization of 2-Isocyanobiphenyls with Hydrazines. *Green Chem*. **2014**, *16*, 2418-2421. http://doi.org/10.1039/c3gc42517g (b) Pan, C.; Han, J.; Zhang, H.; Zhu, C. Radical Arylalkoxycarbonylation of 2-Isocyanobiphenyl with Carbazates: Dual C-C Bond Formation toward Phenantridine-6-carboxylates. *J. Org. Chem*. **2014**, *79*, 5374–5378. http://doi.org/10.1021/jo500842e (c) Liu, S.; Pan, W.; Wu, S.; Bu, X.; Xin, S.; Yu, J.; Xu, H.; Yang, X. Visible-Light-Induced Tandem Radical Addition–Cyclization of 2-Aryl Phenyl Isocyanides Catalysed by Recyclable Covalent Organic Frameworks. *Green Chem*., **2019**, *21*, 2905–2910. http://doi.org/10.1039/c9gc00022d

(137) Ye, H. B.; Zhou, X. Y.; Li, L.; He, X. K.; Xuan, J. Photochemical Synthesis of Succinic Ester-Containing Phenanthridines from Diazo Compounds as 1,4-Dicarbonyl Precursors. *Org. Lett.* **2022**, *24*, 6018−6023. https://doi.org/10.1021/acs.orglett.2c02313

(138) Xu, Z.; Yan, C.; Liu, Z. Q. A Free-Radical Cascade Methylation/Cyclization of N-Arylacrylamides and Isocyanides with Dicumyl Peroxide. *Org. Lett.* **2014**, *16*, 5670–5673. http://doi.org/10.1021/ol502738a

(139) (a) Zhang, B.; Daniliuc, C. G.; Studer, A. 6-Phosphorylated Phenanthridines from 2-Isocyanobiphenyls via Radical C–P and C–C Bond Formation. *Org. Lett*. **2014**, *16*, 250-253. http://doi.org/10.1021/ol403256e (b) Li, Y.; Qiu, G.; Ding, Q.; Wu, J. Synthesis of phenanthridin-6-yldiphenylphosphine oxides by oxidative cyclization of 2-isocyanobiphenyls with diarylphosphine oxides. *Tetrahedron*, **2014**, *70*, 4652–4656. https://doi.org/10.1016/j.tet.2014.05.039

(140) (a) Xue, D.; Liu, R.; Zhang, D.; Li, N.; Xue, Y.; Gea, Q.; Shao, L. Iron-Catalyzed Radical Cascade Cyclization of Oxime Esters with Isocyanides: Synthesis of 1-Cyanoalkyl Isoquinolines and 6-Cyanoalkyl Phenanthridines. *Org. Biomol. Chem*., **2021**, *19*, 8597–8606. http://doi.org/10.1039/d1ob01556g (b) Li, Q.; Zhou, C. Y.; Wang, C. Metal-Free Generation of γ-Cyanoalkyl Radicals by N-Heterocyclic Carbene Catalysis: Assembly of 6-Cyanoalkyl Phenanthridines. *Org. Lett*. **2022**, *24*, 9243–9247. https://doi.org/10.1021/acs.orglett.2c03808

(141) (a) Cheng, Y.; Jian, H.; Zhang, Y.; Yu, S. Isocyanide Insertion: De Novo Synthesis of Trifluoromethylated Phenanthridine Derivatives. *Org. Lett.* **2013**, *15*, 5520-5523. http://doi.org/10.1021/ol4026827 (b) Gu, L.; Jin, C.; Liu, J.; Ding, H. and Fan, B. Transition-metal-free, visible-light induced cyclization of arylsulfonyl chlorides with 2-isocyanobiphenyl to produce phenanthridines. *Chem. Commun*. **2014**, *50*, 4643-4645. http://doi.org/10.1039/c4cc01487a (c) Natarajan, P.; Pooja, P. A Photocatalyst-Free Method for the Synthesis of 6-Alkyl(aryl)phenanthridines under Visible Light Irradiation. *New J. Chem*., **2022**, *46*, 22862–22868. http://doi.org/10.1039/d2nj04414e

(142) Qile Wang, Q.; Dong, X.; Xiao, T.; Zhou, L. $PhI(OAc)_2$-Mediated Synthesis of 6-(Trifluoromethyl)phenanthridines by Oxidative Cyclization of 2-Isocyanobiphenyls with CF_3SiMe_3 under Metal-Free Conditions. *Org. Lett.*, **2013**, *15*, 4846–4849. http://doi.org/10.1021/ol4022589

(143) Wang, L.; Zhu, H.; Guo, S.; Cheng, J.; Yu, J-T. TBHP-promoted sequential radical silylation and aromatisation of aryl isonitriles with silanes. *Chem. Commun*. **2014**, *50*, 10864-10867. http://doi.org/10.1039/c4cc04773g

(144) (a) Tobisu, M.; Koh, K.; Furukawa, T.; Chatani, N. Modular Synthesis of Phenanthridine Derivatives by Oxidative Cyclization of 2-Isocyanobiphenyls with Organoboron Reagents. *Angew. Chem. Int. Ed.*, **2012**, *51*, 11363 –11366. http://doi.org/10.1002/anie.201206115 (b) Ding, S.; Zhao, Y.; Ma, Q.; Tian, S.; Ren, H.; Zhu, M.; Li, K.; Miao, Z. Silver(I)-mediated Reaction of 2-Isocyanobiaryl with Alkyl Trifluoroborates: Efficient Synthesis of 6-Alkylated Phenanthridines. *Chem. Lett*. **2018**, *47*, 562–565. http://doi.org/10.1246/cl.180009

(145) Liu, Y.; Li, J. L.; Liu, X. G.; Wu, J. Q.; Huang, Z. S.; Li, Q.; Wang, H. Radical Borylative Cyclization of Isocyanoarenes with N-Heterocyclic Carbene Borane: Synthesis of Borylated Aza-arenes. *Org. Lett*. **2021**, *23*, 1891−1897. https://doi.org/10.1021/acs.orglett.1c00309

(146) Hua, S.; Chena, J.; Cao, J. X.; Zhang, S. S.; Gu, S. X.; Chen, F. E. Quinolines and isoquinolines as HIV-1 inhibitors: Chemical structures, action targets, and biological activities. *Bioorg. Chem*. **2023**, *136*, 106549. https://doi.org/10.1016/j.bioorg.2023.106549

(147) Xue, D.; Xue, Y.; Yu, H.; Shao, L. Metal-Free Radical Cyclization of Vinyl Isocyanides with Alkanes: Synthesis of 1-Alkylisoquinolines. *Synthesis*, **2019**, *51*, 874–884. https://doi.org/10.1055/s-0037-1610661

(148) (a) Ping Qian, P.; Du, B.; Zhou, J.; Mei, H.; Han, J.; Pan, Y. DBU-promoted cyclization of vinyl isocyanides with ethers via the functionalization of a C(sp^3)–H bond for the synthesis of isoquinolines. *RSC Adv.*, **2015**, *5*, 64961–64965. https://doi.org/10.1039/c5ra11530b (b) Xu, Y.; Chen, H.; Li, W.; Xie, Q.; Yu, L.; Shao, L. Microwave-Assisted Radical Insertion/Cyclization of Vinyl Isocyanides for the Synthesis of Multi-Substituted Isoquinolines. *ChemistrySelect.* **2017**, *2*, 8033–8038. http://doi.org/10.1002/slct.201701896

(149) Xue, D.; Chen, H.; Xu Y.; Yu, H.; Yu, L.; Li, W.; Xie, Q.; Shao, L. Microwave-assisted synthesis of hydroxyl-containing isoquinolines by metal-free radical cyclization of vinyl isocyanides with alcohols. *Org. Biomol. Chem.*, **2017**, *15*, 10044–10052. http://doi.org/10.1039/c7ob02221b

(150) (a) Qian Yao, Q.; Zhou, X.; Zhang, X.; Wang, C.; Wang, P.; Li, M. Convenient synthesis of 6-alkyl phenanthridines and 1-alkyl isoquinolines via silver-catalyzed oxidative radical decarboxylation. *Org. Biomol. Chem.*, **2017**, *15*, 957–971. http://doi.org/10.1039/c6ob02331b (b) He, Y.; Wang, X.; Xiao, J.; Pang, J.; Gan, C.; Huang, Y.; Huang, C. Metal-free oxidative isocyanides insertion with aromatic aldehydes to aroylated N-heterocycles. *RSC Adv*., **2018**, *8*, 3036–3040. https://doi.org/10.1039/c7ra12755c (c) Shi, W. Q.; Liu, S.; Wang, C. Z.; Huang, Y.; Qing, F. L.; Xu, X. H. Synthesis of CMe_2CF_3-Containing Heteroarenes via Tandem 1,1-Dimethyltrifluoroethylation and Cyclization of Isonitriles. *J. Org. Chem.* **2018**, *83*, 15236−15244. http://doi.org/10.1021/acs.joc.8b02506

(151) (a) Zhang, B.; Studer, A. 1-Trifluoromethylated isoquinolines via radical trifluoromethylation of isonitriles. *Org. Biomol. Chem*., **2014**, *12*, 9895–9898. http://doi.org/10.1039/c4ob02145b (b) Jiang, H.; Cheng, Y.; Wang, R.; Zhang, Y.; Yu, S. Synthesis of isoquinolines via visible light-promoted insertion of vinyl isocyanides with diaryliodonium salts. *Chem. Commun.,* **2014**, *50*, 6164–6167. http://doi.org/10.1039/c4cc01122h (c) Ding, F.; Jiang, Y.; Lin, K.; Shi, L. Tandem radical

cyclization for the construction of 1-difluoroalkylated isoquinolines via Cu catalyzed and visible light-promoted pathways. *Org. Biomol. Chem*., **2018**, *16*, 1812–1815. http://doi.org/10.1039/c8ob00232k

(152) Mao, H.; Gao, M.; Liu, B.; Xu, B. Manganese(II)-catalyzed modular synthesis of isoquinolines from vinyl isocyanides and hydrazines. *Org. Chem. Front*., **2016**, *3*, 516–521. https://doi.org/10.1039/c6qo00048g

(153) Yulong Xu, Y.; Chen, H.; Li, W.; Xie, Q.; Yu, L.; Shao, L. Synthetic access to isoxazoline-functionalized isoquinolines via microwave-assisted iminoxyl radical-participated cascade cyclization of vinyl isocyanides. *Org. Biomol. Chem.*, **2018**, *16*, 4996–5005. https://doi.org/10.1039/c8ob01229f

(154) Wang, H.; Yu, Y.; Hong, X.; Xu, B. Mn(II)/O_2-promoted oxidative annulation of vinyl isocyanides with boronic acids: synthesis of multi-substituted isoquinolines. *Chem. Commun.*, **2014**, *50*, 13485—13488. http://doi.org/10.1039/c4cc06427e

(155) Cheng, Y.; Yuan, X.; Jiang, H.; Wang, R.; Ma, J.; Zhang, Y.; Yu, S. Regiospecific Synthesis of 1-Trifluoromethylisoquinolines Enabled by Photoredox Somophilic Vinyl Isocyanide Insertion. *Adv. Synth. Catal*. **2014**, *356*, 2859–2866. http://doi.org/10.1002/adsc.201400504

(156) Niu, J.; Qi, J.; Wang, P.; Liu, C.; Gao, J. M. The chemical structures and biological activities of indole diterpenoids. *Nat. Prod. Bioprospect*. **2023**, *13*, 3. https://doi.org/10.1007/s13659-022-00368-7

(157) Tobisu, M.; Fujihara, H.; Koh, K.; Chatani, N. Synthesis of 2-Boryl- and Silylindoles by Copper-Catalyzed Borylative and Silylative Cyclization of 2-Alkenylaryl Isocyanides. *J. Org. Chem*. **2010**, *75*, 4841–4847. https://doi.org/10.1021/jo101024f

(158) (a) Evoniuk, C. J.; Ly, M.; Alabugin, I.V. Coupling cyclizations with fragmentations for the preparation of heteroaromatics: quinolines from *o*-alkenyl arylisocyanides and boronic acids. *Chem. Commun.* **2015**, 51, 12831-12834. https://doi.org/10.1039/C5CC04391C (b) Evoniuk, C. J.; dos Passos Gomes, G.; Ly, M.; Frankie D. White, F. D.; Alabugin I. V. Coupling Radical Homoallylic Expansions with C−C Fragmentations for the Synthesis of Heteroaromatics: Quinolines from Reactions of *o*-Alkenylarylisonitriles with Aryl, Alkyl, and Perfluoroalkyl Radicals. *J. Org. Chem*. **2017**, *82*, 4265−4278. https://doi.org/10.1021/acs.joc.7b00262 (c) Heckman, L. M.; He, Z.; Jamison, T. F. Synthesis of Highly Substituted 2-Arylindoles via Copper-Catalyzed Coupling of Isocyanides and Arylboronic Acids. *Org. Lett.* **2018**, *20*, 3263−3267. https://doi.org/10.1021/acs.orglett.8b01132

(159) (a) Zhang, B.; Studer, A. 2-Trifluoromethylated Indoles via Radical Trifluoromethylation of Isonitriles. *Org. Lett.* **2014**, *16*, 1216−1219. https://doi.org/10.1021/ol5001395 (b)

Drennhaus, T.; Leifert, D.; Lammert, J.; Drennhaus, J. P.; Bergander, K.; Daniliuc, C. G.; Studer, A. Enantioselective Copper-Catalyzed Fukuyama Indole Synthesis from 2-Vinylphenyl Isocyanides. *J. Am. Chem. Soc.* **2023**, *145*, 8665-8676. https://doi.org/10.1021/jacs.3c01667

(160) (a) Zhang, X.; Zhu, P.; Zhang, R.; Li, X.; Yao, T. Visible-Light-Induced Decarboxylative Cyclization of 2-Alkenylarylisocyanides with α-Oxocarboxylic Acids: Access to 2-Acylindoles. *J. Org. Chem*. **2020**, *85*, 9503−9513. https://doi.org/10.1021/acs.joc.0c00039 (b) Tang, M.; Cameron, L.; Poland, E. M.; Yu, L. J.; Moggach, S. A.; Fuller, R. O.; Huang, H.; Sun, J.; Thickett, S. C.; Massi, M.; Coote, M. L.; Ho, C. C.; Bissember, A. C. Photoactive Metal Carbonyl Complexes Bearing N-Heterocyclic Carbene Ligands: Synthesis, Characterization, and Viability as Photoredox Catalysts. *Inorg. Chem.* **2022**, *61*, 1888-1898. https://doi.org/10.1021/acs.inorgchem.1c02964

(161) Zhang, T.; Yu, M.; Huang, H. Fe-catalyzed Fukuyama-type indole synthesis triggered by hydrogen atom transfer. *Chem. Sci.*, **2021**, *12*, 10501-10505. https://doi.org/10.1039/D1SC03058B

(162) (a) Vidyasagar, A.; Shi, J.; Kreitmeier, P.; Reiser, O. Bromo- or Methoxy-Group-Promoted Umpolung Electron Transfer Enabled, Visible-Light-Mediated Synthesis of 2-Substituted Indole-

3-glyoxylates. *Org. Lett.* **2018**, *20*, 6984−6989. https://doi.org/10.1021/acs.orglett.8b02725 (b) Ye, H. B.; Zhou, X. Y.; Li, L.; He, X. K.; Xuan, J. Photochemical Synthesis of Succinic Ester-Containing Phenanthridines from Diazo Compounds as 1,4-Dicarbonyl Precursors. *Org. Lett*. **2022**, *24*, 6018−6023. https://doi.org/10.1021/acs.orglett.2c02313

(163) Tokuyama, H.; Watanabe, M.; Hayashi, Y.; Kurokawa, T.; Peng, G.; Fukuyama, T. A Novel Protocol for Construction of Indolylmethyl Group at Aldehydes or Ketones. *Synlett.* **2001**, *9*, 1403–1406. https://doi.org/10.1055/s-2001-16808

(164) (a) Mitamura, T.; Iwata, K.; Ogawa, A. Photoinduced Intramolecular Cyclization of *o*-Ethenylaryl Isocyanides with Organic Disulfides Mediated by Diphenyl Ditelluride. *J. Org. Chem*. **2011**, *76*, 3880–3887. https://doi.org/10.1021/jo200299d (b) Mitamura, T.; Tsuboi, Y.; Iwata, K.; Tsuchii, K.; Nomoto, A.; Sonoda, M.; Ogawa, A. Photoinduced thiotelluration of isocyanides by using a $(PhS)_2$–$(PhTe)_2$ mixed system, and its application to bisthiolation via radical cyclization. *Tetrahedron*, **2007**, *48*, 5953–5957. https://doi.org/10.1016/j.tetlet.2007.06.126

(165) Yamakawa, T.; Ideue, E.; Iwaki, Y.; Sato, A.; Tokuyama, H.; Shimokawa, J.; Fukuyama, T. Total synthesis of tryprostatins A and B. *Tetrahedron*, **2011**, *67*, 6547-6560. https://doi.org/10.1016/j.tet.2011.05.112

(166) Tokuyama, H.; Kaburagi, Y.; Chen, X.; Fukuyama, T. Synthesis of 2,3-Disubstituted Indoles by Palladium-Mediated Coupling of 2-Iodoindoles. *Synthesis*, **2000**, *3*, 429–434. https://doi.org/10.1055/s-1971-21756

(167) Xiang, H.; Yu, Z.; Xie, T.; Ye, X. Y.; Ye, Y. Zn-Mediated Reductive Addition of Isocyanides with Unactivated Tertiary Alkyl Oxalates. *Eur. J. Org. Chem.,* **2022**, *38*, e202200937. https://doi.org/10.1002/ejoc.202200937

(168) Rong, J.; Deng, L.; Tan, P.; Ni, C.; Gu, Y.; Hu, J. Radical Fluoroalkylation of Isocyanides with Fluorinated Sulfones by Visible-Light Photoredox Catalysis. *Angew. Chem. Int. Ed.* **2016**, *55*, 2743−2747. https://doi.org/10.1002/anie.201510533

(169) Hu, W.; Teng, F.; Hu, H.; Luo, S.; Zhu, Q. Pd-Catalyzed C(sp^2)−H Imidoylative Annulation: A General Approach To Construct Dibenzoox(di)azepines. *J. Org. Chem.* **2019**, *84*, 6524−6535. http://doi.org/10.1021/acs.joc.9b00683

(170) Proctor, R.S.J.; Phipps, R.J. Recent Advances in Minisci-Type Reactions. *Angew. Chem. Int. Ed.* **2019**, *58*, 13666–13699. https://doi.org/10.1002/anie.201900977

(171) Lo, J. C.; Kim, D.; Pan, C. M.; Edwards, J. T.; Yabe, Y.; Gui, J.; Qin, T.; Gutiérrez, S.; Giacoboni, J.; Smith, M. W.; Holland, P. L.; Baran, P. S. Fe-Catalyzed C-C Bond Construction from Olefins via Radicals. *J. Am. Chem. Soc*. **2017**, *139*, 2484–2503. https://doi.org/10.1021/jacs.6b13155

(172) Bertho, S.; Rey-Rodriguez, R.; Colas, C.; Retailleau, P.; Gillaizeau, I. Regio- and Stereoselective Iron-Catalyzed Oxyazidation of Enamides Using a Hypervalent Iodine Reagent. *Chem. Eur. J.* **2017**, *23*, 17674–17677. http://doi.org/10.1002/chem.201704499

(173) Xu, Y.; Chen, H.; Li, W.; Xie, Q.; Yu, L.; Shao, L. Microwave-Assisted Radical Insertion/Cyclization of Vinyl Isocyanides for the Synthesis of Multi-Substituted Isoquinolines. *Chemistry Select.*, **2017**, *2*, 8033–8038. https://doi.org/10.1002/slct.201701896

(174) Nguyen, T. B.; Retailleau, P. Redox-Neutral Access to Sultams from 2-Nitrochalcones and Sulfur with Complete Atom Economy. *Org. Lett*. **2017**, *19*, 3879–3882. https://doi.org/10.1021/acs.orglett.7b01766

(175) Shrestha-Dawadi, P. B.; Lugtenburg, J. Preparation of [1,2,3,4,5-$^{13}C_5$]-5-Amino-4-oxopentanoic Acid (ALA)-Design of a Synthetic Scheme to Prepare Any ^{13}C- and ^{15}N-Isotopomer with High Isotopic Enrichment. *Eur. J. Org. Chem.* **2003**, 4654–4663. http://doi.org/10.1002/ejoc.200300408

(176) Aeluri, M.; Gaddam, J.; Trinath, D. V. K. S.; Chandrasekar, G.; Kitambi, S. S.; Arya, P. An Intramolecular Heck Approach To Obtain 17-Membered Macrocyclic Diversity and the

Identification of an Antiangiogenesis Agent from a Zebrafish Assay. *Eur. J. Org. Chem.* **2013**, *19*, 3955–3958. https://doi.org/10.1002/ejoc.201300408

(177) Evoniuk, C. J.; Gomes, G. P.; Ly, F.; White, F. D.; Alabugin, I. V. Coupling Radical Homoallylic Expansions with C–C Fragmentations for the Synthesis of Heteroaromatics: Quinolines from Reactions of o-Alkenylarylisonitriles with Aryl, Alkyl, and Perfluoroalkyl Radicals. *J. Org. Chem.* **2017**, *82*, 4265–4278. https://doi.org/10.1021/acs.joc.7b00262

(178) Lyrgin, A. V.; de Mejiere, A. *Ortho*-Lithiophenyl Isocyanide: A Versatile Precursor for 3H-Quinazolin-4-ones and 3H-Quinazolin-4-thiones. *Org. Lett.*, **2009**, *11*, 389–392. https://doi.org/10.1021/ol802659m

(179) Saavedra, B.; Ramón, D. J. Deep Eutectic Solvent as a Sustainable Medium for C−C Bond Formation Via Multicomponent Radical Conjugate Additions. *ACS Sustainable Chem.*, **2021**, *9*, 7941−7947. https://doi.org/10.1021/acssuschemeng.1c02193?rel=cite-as&ref=PDF&jav=VoR

(180) Zhang, T.; Yu, M.; Huang, H. Fe-catalyzed Fukuyama-type indole synthesis triggered by hydrogen atom transfer. *Chem. Sci.*, **2021**, *12*, 10501−10505. https://doi.org/10.1039/D1SC03058B

(181) Wu, X.; Chen, P.; Gan, M.; Ji, X.; Deng, G. J.; Huang, H. Redox-Neutral Cyclization of 2-Isocyanobiaryls through Photoredox/PPh_3 Dual Catalysis. *Org. Lett.*, **2023**, *25*, 9186–9190. https://doi.org/10.1021/acs.orglett.3c03744

(182) Proctor, R.S.J.; Phipps, R.J. Recent Advances in Minisci-Type Reactions. *Angew. Chem. Int. Ed.* **2019**, *58*, 13666–13699. https://doi.org/10.1002/anie.201900977

(183) Lynch, B. M.; Chang, H. S. Concentration-dependent orientations in free-radical phenylations of heteroaromatic compounds. *Tetrahedron*, **1964**, *40*, 2965–2968. https://doi.org/10.1016/0040-4039(64)83071-9

(184) Minisci, F.; Galli, R.; Cecere, M.; Malatesta, V.; Caronna, T. Nucleofilic Character of Alkyl Radicals: New Synthesis by Alkyl Radicals Generated in Redox Processes. *Tetrahedron*, 1968, *54*, 5609–5612. https://doi.org/10.1016/S0040-4039(00)70732-5

(185) Minisci, F.; Galli, R.; Malatesta, V.; Caronna, T. Nucleophilic Character of Alkyl Radicals-II: Selective Alkylation of Pyridine, Quinoline and Acridine by Hydroperoxides and Oxaziranes. *Tetrahedron,* **1970**, *26*, 4083–4091. https://doi.org/10.1016/S0040-4020(01)93049-2

(186) Minisci, F.; Bernardi, R.; Bertini, F.; Galli, R.; Perchinummo, M. Nucleophilic Character of Alkyl Radicals-VI: A New Convenient Selective Alkylation of Heteroaromatic Bases. *Tetrahedron*, **1971**, *27*, 3575–3579. https://doi.org/10.1016/S0040-4020(01)97768-3

(187) Ritchie, T. J.; MacDonald, S. J. F.; Young, R. J.; Pickett, S. D. The impact of aromatic ring count on compound developability: Further insights by examining carbo- and hetero-aromatic and -aliphatic ring types. *Drug Discovery Today*, **2011**, *16*, 164–171. https://doi.org/10.1016/j.drudis.2010.11.014

(188) Duncton, M. A. J. Minisci reactions: Versatile CH-functionalizations for medicinal chemists. In *Med. Chem. Commun.,* **2011**, *2*, 1135–1161. https://doi.org/10.1039/c1md00134e

(189) O'Hara, F.; Blackmond, D. G.; Baran, P. S. Radical-based regioselective C-H functionalization of electron-deficient heteroarenes: Scope, tunability, and predictability. *J. Am. Chem. Soc.*, **2013**, *135*, 12122–12134. https://doi.org/10.1021/ja406223k

(190) Tauber, J.; Imbri, D.; Opatz, T. Radical Addition to Iminium Ions and Cationic Heterocycles. *Molecules*, **2014**, *19*, 16190–16222. https://doi.org/10.3390/molecules191016190

(191) Minisci, F.; Vismara, E.; Fontana, F.; Morini,G.; Serravalle, M. Polar Effects in Free-Radical Reactions. Solvent and Isotope Effects and Effects of Base Catalysis on the Regio- and Chemoselectivity of the Substitution of Protonated Heteroaromatic Bases by Nucleophilic Carbon-Centered Radicals. *J. Org. Chem.*, **1987**, *52*, 730–736. https://doi-org/10.1021/jo00381a004

(192) Demir, A. S.; Reis, O.; Emrullahogu, M. Generation of Aryl Radicals from Arylboronic Acids by Manganese(III) Acetate: Synthesis of Biaryls and Heterobiaryls. *J. Org. Chem.*, **2003**, *68*, 578–580. https://doi.org/10.1021/jo026466c

(193) (a)Baciocchi, E.; Muraglia, E. Synthesis of perfluoroalkylpyrroles by homolytic substitution with perfluoroalkyl radicals. *Tetrahedron Lett.*, **1993**, *34*, 3799–3800. https://doi-org.sire.ub.edu/10.1016/S0040-4039(00)79233-1 (b)Antonietti, F.; Mele, A.; Minisci, F.; Punta, C.; Recupero, F.; Fontana, F. Enthalpic and polar effects in the reactions of perfluoroalkyl radicals: New selective synthetic developments with alkenes and heteroaromatic bases. *J. Fluorine Chem.*, **2004**, *125*, 205–211. https://doi.org/10.1016/j.jfluchem.2003.07.012

(194) Roughley, S. D.; Jordan, A. M. The Medicinal Chemist's Toolbox: An Analysis of Reactions Used in the Pursuit of Drug Candidates. *J. Med. Chem.* **2011**, *54*, 3451–3479. https://doi.org/10.1021/jm200187y

(195) Liu, S.; Liu, A.; Zhang, Y.; Wang, W. Direct Cα-heteroarylation of structurally diverse ethers via a mild N-hydroxysuccinimide mediated cross-dehydrogenative coupling reaction. *Chem*. *Sci*. **2017**, *8*, 4044–4050. https://doi.org/10.1039/C6SC05697K

(196) Roughley, S. D.; Jordan, A. M. The Medicinal Chemist's Toolbox: An Analysis of Reactions Used in the Pursuit of Drug Candidates. *J. Med. Chem*. **2011**, 54, 3451–3479. https://doi.org/10.1021/jm200187y

(197) Okugawa, N.; Moriyama, K.; Togo, H. Introduction of Ether Groups onto Electron-Deficient Nitrogen-Containing Heteroaromatics Using Radical Chemistry under Transition-Metal-Free Conditions. *Eur. J. Org. Chem.*, **2015***, 22*, 4973–4981. https://doi.org/10.1002/ejoc.201500584

(198) McCallum, T.; Jouanno, L. A.; Cannillo, A.; Barriault, L. Persulfate-Enabled Direct C-H Alkylation of Heteroarenes with Unactivated Ethers. *Synlett.*, **2016**, *27*, 1282–1286. https://doi.org/10.1055/s-0035-1561338

(199) Salman, M.; Huang, X. F.; Huang, Z. Z. Highly chemoselective and regioselective dehydrogenative cross-coupling reaction between pyridines and ethers. *Synlett.*, **2015**, *26*, 1391–1394. https://doi.org/10.1055/s-0034-1380694

(200) Ambala, S.; Thatikonda, T.; Sharma, S.; Munagala, G.; Yempalla, K. R.; Vishwakarma, R. A.; Singh, P. P. Cross-dehydrogenative coupling of α-C(sp3)-H of ethers/alkanes with C(sp2)-H of heteroarenes under metal-free conditions. *Org. Biomol. Chem.*, **2015**, *13*, 11341–11350. https://doi.org/10.1039/c5ob01268f

(201) Antonchick, A.P.; Burgmann, L. Direct Selective Oxidative Cross-Coupling of Simple Alkanes with Heteroarenes. *Angew. Chem. Int. Ed.* **2013**, *52*, 3267–3271. https://doi-org/10.1002/anie.201209584

(202) Wu, Z.; Pi, C.; Cui, X.; Bai, J.; Wu, Y. Direct C-2 alkylation of quinoline N-oxides with ethers via palladium-catalyzed dehydrogenative cross-coupling reaction. *Adv. Synth. Catal.*, **2013**, *355*, 1971–1976. https://doi.org/10.1002/adsc.201300111

(203) Fang, L.; Chen, L.; Yu, J.; Wang, L. Benzoyl peroxide promoted radical ortho-alkylation of nitrogen heteroaromatics with simple alkanes and alcohols. *Eur. J. Org. Chem.*, **2015***, 9*, 1910–1914. https://doi.org/10.1002/ejoc.201403479

(204) Wang, L.; Sha, W.; Dai, Q.; Feng, X.; Wu, W.; Peng, H.; Chen, B.; Cheng, J. The benzoyl peroxide promoted dual C-C bond formation via dual C-H bond cleavage: α-phenanthridinylation of ether by isocyanide. *Org. Lett.*, **2014**, *16*, 2088–2091. https://doi.org/10.1021/ol500277u

(205) Jin, J.; MacMillan, D.W.C. Direct α-Arylation of Ethers through the Combination of Photoredox-Mediated C-H Functionalization and the Minisci Reaction. *Angew. Chem. Int. Ed.*, **2015**, *127*, 1585–1589. https://doi.org/10.1002/ange.201410432

(206) Cai, Z.; An, G.; Li, G. Quinoline-polyoxometalate conglomerate as efficient heterogeneous catalysts for visible-light-mediated Minisci reactions. *J. Organomet. Chem.*, **2023**, *996*. https://doi.org/10.1016/j.jorganchem.2023.122757

(207) Laze, L.; Quevedo-Flores, B.; Bosque, I.; Gonzalez-Gomez, J.C. Alkanes in Minisci-Type Reaction under Photocatalytic Conditions with Hydrogen Evolution. *Org. Lett*. **2023**, *48*, 8541−8546. https://doi.org/10.1021/acs.orglett.3c02619

(208) Pan, Z. T.; Shen, L. M.; Dagnaw, F. W.; Zhong, J. J.; Jian, J. X.; Tong, Q. X. Minisci reaction of heteroarenes and unactivated C(sp3)-H alkanes via a photogenerated chlorine radical. *Chem. Commun.*, **2023**, *59*, 1637–1640. https://doi.org/10.1039/d2cc06486c

(209) Devari, S.; Shah, B. A. Visible light-promoted C-H functionalization of ethers and electron-deficient arenes. *Chem. Commun.*, **2016**, *52*, 1490–1493. https://doi.org/10.1039/c5cc08817h

(210) Huang, C. Y., Li, J., Liu, W., Li, C. J. Diacetyl as a “traceless” visible light photosensitizer in metal-free cross-dehydrogenative coupling reactions. *Chem. Sci.*, **2019**, *10*, 5018–5024. https://doi.org/10.1039/c8sc05631e

(211) Li, X.; Liu, C.; Guo, S.; Wang, W.; Zhang, Y. PIFA-Mediated Cross-Dehydrogenative Coupling of N-Heteroarenes with Cyclic Ethers: Ethanol as an Efficient Promoter. *Eur. J. Org. Chem.*, **2021***,* 3, 411–421. https://doi.org/10.1002/ejoc.202001354

(212) Zhao, H.; Jin, J. Visible Light-Promoted Aliphatic C-H Arylation Using Selectfluor as a Hydrogen Atom Transfer Reagent. *Org. Lett.*, **2019**, *21*, 6179–6184. https://doi.org/10.1021/acs.orglett.9b01635

(213) Tian, H.; Yang, H.; Tian, C.; An, G.; Li, G. Cross-Dehydrogenative Coupling of Strong C(sp3)-H with N-Heteroarenes through Visible-Light-Induced Energy Transfer. *Org. Lett.*, **2020**, *22*, 7709–7715. https://doi.org/10.1021/acs.orglett.0c02912

(214) Bhakat, M.; Biswas, P.; Dey, J.; Guin, J. Heteroarylation of Ethers, Amides, and Alcohols with Light and O2. *Org. Lett.*, **2021**, *23*, 6886–6890. https://doi.org/10.1021/acs.orglett.1c02440

(215) Lopat’eva, E. R.; Krylov, I. B.; Segida, O. O.; Merkulova, V. M.; Ilovaisky, A. I.; Terent’ev, A. O. Heterogeneous Photocatalysis as a Potent Tool for Organic Synthesis: Cross-Dehydrogenative C–C Coupling of N-Heterocycles with Ethers Employing TiO2/N-Hydroxyphthalimide System under Visible Light. *Molecules*, **2023**, *28*. https://doi.org/10.3390/molecules28030934

(216) Dong, J.; Xia, Q.; Lv, X.; Yan, C.; Song, H.; Liu, Y.; Wang, Q. Photoredox-Mediated Direct Cross-Dehydrogenative Coupling of Heteroarenes and Amines. *Org. Lett.*, **2018**, *20*, 5661–5665. https://doi.org/10.1021/acs.orglett.8b02389

(217) Zhou, J.; Ren, Q.; Xu, N.; Wang, C.; Song, S.; Chen, Z.; Li, J. $K_2S_2O_8$-catalyzed highly regioselective amidoalkylation of diverse N-heteroaromatics in water under visible light irradiation. *Green Chem.*, **2021**, *23*, 5753–5758. https://doi.org/10.1039/d1gc02107a

(218) Potopnyk, M. A.; Jarosz, S. Nitrogen-Containing Macrocycles Having a Carbohydrate Scaffold. *Advances in Carbohydrate Chemistry and Biochemistry*, **2014**, *71*, 227–295. https://doi-org.sire.ub.edu/10.1016/B978-0-12-800128-8.00003-0

(219) Burns, C. J.; Neu, M.P.; Boukhalfa, H.; Gutowski, K. E.; Bridges, N. J.; Rogers, R. D. The Actinides. *Comprehensive Coordination Chemistry II*. **2003**, *3*, 189–345. https://doi.org/10.1016/B0-08-043748-6/02001-6

(220) Anton-Torrecillas, C.; Felipe-Blanco, D.; Gonzalez-Gomez, J. C. A Radical Addition/Cyclization of Diverse Ethers to 2-Isocyanobiaryls Under Mildly Basic Aqueous Conditions. *Org. Biomol. Chem.* **2016**, *14*, 10620–10629. https://doi.org/10.1039/c6ob02103d

(221) Nie, Z.; Ding, Q.; Peng, Y. Synthesis of 6-Aroylphenanthridines by Fe-Catalyzed Oxidative Radical Cyclization of 2-Isocyanobiphenyls with Benzylic Alcohols. *Tetrahedron*, **2016**, *72*, 8350–8357. https://doi.org/10.1016/j.tet.2016.11.010

(222) Xu, Z.; Zhang, L. Methanol as a formylating agent in nitrogen heterocycles. *Org. Biomol. Chem.* **2021**, *19*, 9476–9482. https://doi.org/10.1039/D1OB01807H

(223) (a)Giordano, C.; Minisci, F.; Vismara, E.; Levi, S. A general, selective, and convenient procedure of homolytic formylation of heteroaromatic bases. *J. Org. Chem.* **1986**, *51*, 536–537. https://doi.org/10.1021/jo00354a026 (b)Dong, J.; Wang, X.; Song, H.; Liu, Y.; Wang, Q. Photoredox-Catalyzed Redox-Neutral Minisci C-H Formylation of N-Heteroarenes. *Adv. Synth. Catal.* **2020**, *362*, 2155–2159. https://doi.org/10.1002/adsc.201901481 (c) Xu, Z.; Zhang, L. Methanol as a formylating agent in nitrogen heterocycles. *Org. Biomol. Chem*., **2021**, *19*, 9476–9482. https://doi.org/10.1039/D1OB01807H (d) Zhang, Y.; Yue, X.; Zhu, J.; Peng, J.; Zhou, C.; Wu, J.; Zhang, P. Visible light-induced hydroxymethylation and formylation of (iso)quinolines with alcohols. *Molecular Catalysis*, **2022**, *530*, 112594. https://doi.org/10.1016/j.mcat.2022.112594 (e) Liao, Y.; Jiang, C.; Qiang, C.; Liu, P.; Sun, P. HAT-mediated Electrochemical C(sp2)–H Acylation of Quinolines with Alcohols. *Org. Lett.* **2023**, *25*, 7327-7331. https://doi.org/10.1021/acs.orglett.3c02668

(224) Salamone, M.; Milan, M.; DiLabio, G. A.; Bietti, M. Absolute Rate Constants for Hydrogen Atom Transfer from Tertiary Amides to the Cumyloxyl Radical: Evaluating the Role of

Stereoelectronic Effects. *J. Org. Chem.* **2014**, *79*, 7179−7184. https://doi.org/10.1021/jo5013459

(225) Shi, G.; Kim, H.; Koo, S. Oxo-Carotenoids as Efficient Superoxide Radical Scavengers. *Antioxidants,* **2022**, *11*, 1525. https://doi.org/10.3390/antiox11081525

(226) (a) Fan, X. Z.; Rong, J. W.; Wu, H. L.; Zhou, Q.; Deng, H. P.; Tan, J. D.; Xue, C. W.; Wu, L. Z.; Tao, H. R.; Wu, J. Eosin Y as a Direct Hydrogen-Atom Transfer Photocatalyst for the Functionalization of C-H Bonds. *Angew. Chem. Int. Ed.* **2018**, *57*, 8514–8518. https://doi.org/10.1002/anie.201803220 (b) Lee, G. S.; Hong, S. H. Formal Giese addition of C(sp3)–H nucleophiles enabled by visible light mediated Ni catalysis of triplet enone diradicals. Chem.Sci., 2018, 9, 5810−5815. https://doi.org/10.1039/C8SC01827H

(227) Devari, S.; Shah, B. A. Visible light-promoted C–H functionalization of ethers and electron-deficient arenes. *Chem. Commun.*, **2016**, *52*, 1490–1493. https://doi.org/10.1039/C5CC08817H

(228) Leifert, D.; Daniliuc, C. G.; Studer, A. 6-Aroylated phenanthridines via base promoted homolytic aromatic substitution (BHAS). *Org. Lett.*, **2013**, *15*, 6286–6289. https://doi.org/10.1021/ol403147v

(229) Landa, S.; Macháček, V. Sur l'Adamantane, Nouvel Hydrocarbure Extrait du Naphte. *Collect. Czech. Chem. Commun.* **1933**, *5*, 1−5. https://doi.org/10.1135/cccc19330001

(230) Prelog, V.; Seiwerth, R. Über die Synthese des Adamantans. *Ber. Dtsch. Chem. Ges.* **1941**, *74*, 1644–1648. https://doi.org/10.1002/cber.19410741004

(231) Stetter, H.; Bänder, O. E.; Neumann, W. Über Verbindungen mit Urotropin-Struktur, VIII. Mitteil.: Neue Wege der Adamantan-Synthese. *Chem. Ber.* **1956**, *89*, 1922−1926. https://doi.org/10.1002/cber.19560890820

(232) Schleyer, P. R. A. A Simple Preparation of Adamantane. *J. Am. Chem. Soc.* **1957**, 3292. https://doi.org/10.1021/ja01569a086

(233) Farooq, O.; Farnia, S. M. F.; Stephenson, M.; Olah, G. A. Superacid-catalyzed near-quantitative isomerization of C4n+6H4n+12 (n = 1-3) polycyclic precursors to diamondoid cage hydrocarbons promoted by 1-haloadamantanes and sonication. *J.Org.Chem.*, **1988**, *53*, 2840. https://doi.org/10.1021/jo00247a035

(234) Mckervey,M. A. Synthetic approaches to large diamondoid hydrocarbons. *Tetrahedron*, **1980**, *36*, 971. https://doi.org/10.1016/0040-4020(80)80050-0

(235) Stetter, H.; Schwarz, M.; Hirschhorn, A. Über Verbindungen mit Urotropin-Struktur, XII. Monofunktionelle Adamantan-Derivate. *Chem. Ber.*, **1959**, *92*, 1629-1635. https://doi.org/10.1002/cber.19590920722

(236) Webber, W. C.; Harthoorn, P. A. Chlorinated and brominated polycyclic hydrocarbons. *Br. Patent Appl.* 819240, Sep 02, **1959**.

(237) Stetter, H.; Mayer, J.; Schwarz, M.; Wulff, K. Über Verbindungen mit Urotropin-Struktur, XVI. Beiträge zur Chemie der Adamantyl-(1)-Derivate. *Chem. Ber.* **1960**, *93*, 226−230. https://doi.org/10.1002/cber.19600930133

(238) Davies,W. L.; Grunert, R. R.; Haff, R. F.; McGahen, J. W.; Neumayer, E. M.; Paulshock, M.; Watts, J. C.; Wood, T. R.; Hermann, E. C.; Hoffmann, C.E. Antiviral Activity of 1-Adamantanamine (Amantadine). *Science*, **1964**, *144*, 862–863. https://doi.org/10.1126/science.144.3620.862

(239) Hubsher, G.; Haider, M.; Okun, M. S. *Neurology,* **2012**, *78*, 1096−1099. https://doi.org/10.1212/wnl.0b013e31824e8f0d

(240) Tsunoda, A.; Maassab, H. F.; Cochran, K. W.; Eveland, W. C. Antiviral activity of alpha-methyl-1-adamantanemethylamine hydrochloride. *Antimicrob. Agents Chemother.* **1965**, *5*, 553−560. https://doi.org/10.1128/aac.5.6.553

(241) Rosenthal, K. S.; Sokol, M. S.; Ingram, R. L.; Subramanian, R.; Fort, R. C. Tromantadine: inhibitor of early and late events in herpes simplex virus replication. *Antimicrob. Agents Chemother*. **1982**, *22*, 1031–1036. https://doi.org/10.1128/aac.22.6.1031

(242) (a) Kornhuber, J.; Schoppmeyer, K.; Riederer, P. Affinity of 1-aminoadamantanes for the sigma binding site in post-mortem human frontal cortex *Neurosci. Lett.* **1993**, *163*, 129–131. https://doi.org/10.1016/0304-3940(93)90362-o (b) Barnett, A. DPP-4 inhibitors and their potential role in the management of type 2 diabetes. *Int. J. Clin. Pract.* **2006**, *60*, 1454. https://doi.org/10.1111/j.1742-1241.2006.01178.x

(243) Wanka, L.; Iqbal, K.; Schreiner, P. R. The lipophilic bullet hits the targets: Medicinal chemistry of adamantane derivatives. *Chem. Rev*., **2013**, *113*, 3516–3604. https://doi.org/10.1021/cr100264t

(244) Gerzon, K.; Krumalns, E. V.; Brindle, R. L.; Marshall, F. J.; Root, M. A. *J. Med. Chem.* **1963**, *6*, 760. https://doi.org/10.1021/jm00342a029

(245) Gerzon, K.; Kau, D. *J. Med. Chem.* **1967**, *10*, 189. https://doi.org/10.1021/jm00314a014

(246) Rapala, R. T.; Kraay, R. J.; Gerzon, K. *J. Med. Chem.* **1965**, *8*, 580. https://doi.org/10.1021/jm00329a007

(247) Agnew-Francis, K. A.; Williams, C. M. Catalysts Containing the Adamantane Scaffold. *Adv. Synth. Catal.* **2016**, *358*, 675 –700. https://doi.org/10.1002/adsc.201500949

(248) Schweighauser, L.; Strauss, M. A.; Bellotto, S.; Wegner, H. A. Anziehung oder Abstoßung? London-Dispersionswechselwirkungen kontrollieren Azobenzol-basierte

molekulare Schalter. *Angew. Chem.* **2015**, *127*, 13636–13639. https://doi.org/10.1002/ange.201506126

(249) Tolman, C. A. Steric effects of phosphorus ligands in organometallic chemistry and homogeneous catalysis. *Chem. Rev.* **1977**, *77*, 313–348. https://doi.org/10.1021/cr60307a002

(250) Zapf, A.; Ehrentraut, A.; Beller, M. A New Highly Efficient Catalyst System for the Coupling of Nonactivated and Deactivated Aryl Chlorides with Arylboronic Acids. *Angew. Chem*. **2000**, *112*, 4315–4317. https://doi.org/10.1002/1521-3773(20001117)39:22%3C4153::AID-ANIE4153%3E3.0.CO;2-T

(251) (a) Arduengo, A. J.; Harlow, R. L.; Kline, M. A Stable Crystalline Carbene. *J. Am. Chem. Soc.* **1991**, *113*, 361–363. https://doi.org/10.1021/ja00001a054 (b) Flores-Gaspar, A.; Gutiérrez-Bonet, A.; Martin, R. N-Heterocyclic Carbene Dichotomy in Pd-Catalyzed Acylation of Aryl Chlorides via C–H Bond Functionalization. *Org. Lett*. **2012**, *14*, 5234–5237. https://doi.org/10.1021/ol3023819

(252) Endo, K.; Grubbs, R. H. Chelated Ruthenium Catalysts for Z-Selective Olefin Metathesis. *J. Am. Chem. Soc.* **2011**, *133*, 8525–8527. https://doi.org/10.1021/ja202818v

(253) D. E. Chavez, E. N. Jacobsen, An Efficient, Highly Diastereo- and Enantioselective Hetero-Diels-Alder Catalyst. *Org. Synth.* **2005**, *82*, 34. https://doi.org/10.15227/orgsyn.082.0034

(254) Imamoto, T.; Watanabe, J.; Wada, Y.; Masuda, H.; Yamada, H.; Tsuruta, H.; Matsukawa, S.; Yamaguchi, K. *J. Am. Chem. Soc.* **1998**, *120*, 1635–1636. https://doi.org/10.1021/ja973423i

(255) Manna, M. S.; Mukherjee, S. Catalytic Asymmetric Direct Vinylogous Michael Addition of Deconjugated Butenolides to Maleimides for the Construction of Quaternary Stereogenic Centers. *Chem. Eur. J.* **2012**, *18*, 15277–15282. https://doi.org/10.1002/chem.201203180

(256) Hu, L.-H.; Sim, K.-Y. Complex caged polyisoprenylated benzophenone derivatives, sampsoniones A and B, from Hypericum sampsonii. *Tetrahedron Lett.* **1998**, *39*, 7999–8002. https://doi.org/10.1016/S0040-4039(98)01741-9

(257) Christian, O. E.; Henry, G. E.; Jacobs, H.; McLean, S.; Reynolds, W. F. Prenylated Benzophenone Derivatives from *Clusia havetiodes* var*. stenocarpa*. *J. Nat. Prod*. **2001**, *64*, 23–25. https://doi.org/10.1021/np000321o

(258) Tanaka, N.; Takaishi, Y.; Shikishima, Y.; Nakanishi, Y.; Bastow, K.; Lee, K.-H.; Honda, G.; Ito, M.; Takeda, Y.; Kodzhimatov, O. K.; Ashurmetov, O. Prenylated Benzophenones and Xanthones from *Hypericum scabrum*. *J. Nat. Prod.* **2004**, *67*, 1870–1875. https://doi.org/10.1021/np040024

(259) Hinman, A.; Du Bois, J. A Stereoselective Synthesis of (−)-Tetrodotoxin *J. Am. Chem. Soc.* **2003**, *125*, 11510–11511. https://doi.org/10.1021/ja0368305

(260) Roll, D. M.; Biskupiak, J. E.; Mayne, C. L.; Ireland, C. M. Muamvatin, a novel tricyclic spiro ketal from the Fijian mollusk Siphonaria normalis. *J. Am. Chem. Soc.* **1986**, *108*, 6680–6682. https://doi.org/10.1021/ja00281a039

(261) Blanchfield, J. T.; Brecknell, D. J.; Brereton, I. M.; Garson, M. J.; Jones, D. D. Caloundrin B and Funiculatin A: New Polypropionates From Siphonariid Limpets Aust. J. Chem. 1994, 47, 2255–

2269. https://doi.org/10.1071/CH9942255

(262) Tanner, J. A.; Zheng, B.-J.; Zhou, J.; Watt, R. M.; Jiang, J.-Q.; Wong, K.-L.; Lin, Y.-P.; Lu, L.-Y.; He, M.-L.; Kung, H.-F.; Kesel, A. J.; Huang, J.-D. The Adamantane-Derived Bananins Are Potent Inhibitors of the Helicase Activities and Replication of SARS Coronavirus. *Chem. Biol.* **2005**, *12*, 303–311. https://doi.org/10.1016/j.chembiol.2005.01.006

(263) Yeung, K. W.; Dong, Y.; Chen, L.; Tang, C. Y.; Law, W. C.; Tsui, G. C. P. Nanotechnology of diamondoids for the fabrication of nanostructured systems. *Nanotechnology Reviews*. **2020,** *9,* 650–669. https://doi.org/10.1515/ntrev-2020-0051

(264) Mathias, L. J.; Jensen, J. J.; Reichert, V. T.; Lewis, C. M.; Tullos, G.L. Adamantane-containing polymers. *ACS Sym Ser.* **1996**, *624*, 197–207. https://doi.org/10.1021/bk-1996-0624.ch011

(265) Yang, W.; Fabbri, J. D.; Willey, T. M.; Lee, J. R. I.; Dahl, J. E. P.; Carlson, R. M. Monochromatic electron photoemission from diamondoid monolayers. *Science*, **2007**, *316*, 1460–1462. https://doi.org/10.1126/science.1141811

(266) (a)Zheng, H.; Zhang, Q.; Hong, Z.; Lin, Y.; Dai, H. A bifunctional catalyst based ECL immunosensor for a cardiac biomarker regulated by oxygen evolution reaction. *Electrochim. Acta.* **2016**, *215*, 326–333. https://doi.org/10.1016/j.electacta.2016.08.120 (b) Gunawan, M. A.; Moncea, O.; Poinsot, D.; Keskes, M.; Domenichini, B.; Heintz, O. Nanodiamond-palladium core–shell organohybrid synthesis: a mild vapor-phase procedure enabling nanolayering metal onto functionalized sp^3-carbon. *Adv. Funct. Mater.* **2018**, *28*, 1705786. https://doi.org/10.1002/adfm.201705786

(267) Zheng, S.; Shi, J.; Mateu, R. Novel blue light emitting polymer containing an adamantane moiety. *Chem. Mater.* **2000**, *12*, 1814–1817. https://doi.org/10.1021/cm000228l

(268) Chu, P. L. E.; Wang, L. Y.; Khatua, S.; Kolomeisky, A. B.; Link, S.; Tour, J. M. Synthesis and Single-Molecule Imaging of Highly Mobile Adamantane-Wheeled Nanocars. *ACS Nano*. **2013**, *7*, 35–41. https://doi-org.sire.ub.edu/10.1021/nn304584a

(269) Weigel, W. K.; Dang, H. T.; Feceu, A.; Martin, D. B. C. Direct radical functionalization methods to access substituted adamantanes and diamondoids. *Org. Biomol. Chem.* **2022**, *20*, 10–36. https://doi.org/10.1039/D1OB01916C

(270) Tabushi, I.; Hamuro, J.; Oda, R. Chlorocarbonylation of adamantane. *J. Org. Chem*., **1968**, *33*, 2108–2109. https://doi.org/10.1021/jo01269a090

(271) Tabushi, I.; Kojo, S.; Yoshida, Z. Photoacetylation of substituted adamtanes. Exclusive bridgehead substitution and a large ϱ value. *Tetrahedron Lett.*, **1973**, *14*, 2329–2332. https://doi.org/10.1016/S0040-4039(01)96210-0

(272) Kamijo, S.; Takao, G.; Kamijo, K.; Hirota, M.; Tao, K.; Murafuji, T. Photo-induced Substitutive Introduction of the Aldoxime Functional Group to Carbon Chains: A Formal Formylation of Non-Acidic C(sp^3)−H Bonds. *Angew. Chem. Int. Ed.*, **2016**, *55*, 9695–9699. https://doi.org/10.1002/anie.201603810

(273) Ackerman, L. K. G.; Alvarado, J. I. M.; Doyle, A. G. Direct C–C Bond Formation from Alkanes Using Ni-Photoredox Catalysis. *J. Am. Chem. Soc.*, **2018**, *140*, 14059–14063. https://doi.org/10.1021/jacs.8b09191

(274) Yuan, H.; Liu, Z.; Shen, Y.; Zhao, H.; Li, C.; Jia X.; Li, J. Iron-Catalyzed Oxidative Coupling Reaction of Isocyanides and Simple Alkanes towards Amide Synthesis. *Adv. Synth. Catal.*, **2019**, *361*, 2009–2013. https://doi.org/10.1002/adsc.201801619

(275) Kato, S.; Iwahama, T.; Sakaguchi, S.; Ishii, Y. *N*-Hydroxyphthalimide-Catalyzed Carboxylation of Polycyclic Alkanes with Carbon Monoxide in the Presence of Dioxygen. *J. Org. Chem.*, **1998**, *63*, 222–223. https://doi.org/10.1021/jo9718556

(276) Tabushi, I.; Fukunishi, K. Free radical alkylation of adamantanes. *J. Org. Chem.*, **1974**, *39*, 3748–3750. https://doi.org/10.1021/jo00939a031

(277) González-Cameno, A. M.; Mella, M.; Fagnoni, M.; Albini, A. Photochemical Alkylation of Ketene Dithioacetal *S,S*-Dioxides. An Example of Captodative Olefin Functionalization. *J. Org. Chem.*, **2000**, *65*, 297–303. https://doi.org/10.1021/jo990817e

(278) Ji, J.; Liu, P.; Sun, P. Peroxide promoted tunable decarboxylative alkylation of cinnamic acids to form alkenes or ketones under metal-free conditions. *Chem. Commun.*, **2015**, *51*, 7546–7549. https://doi.org/10.1039/C5CC01762A

(279) Kamijo, S.; Kamijo, K.; Maruoka, K.; Murafuji, T. Aryl Ketone Catalyzed Radical Allylation of C(sp^3)–H Bonds under Photoirradiation. *Org. Lett.*, **2016**, *18*, 6516–6519. https://doi.org/10.1021/acs.orglett.6b03586

(280) Amaoka, Y.; Nagatomo, M.; Watanabe, M.; Tao, K.; Kamijo, S.; Inoue, M. Photochemically induced radical alkenylation of C(sp^3)–H bonds. *Chem. Sci.*, **2014**, *5*, 4339–4345. https://doi.org/10.1039/C4SC01631A

(281) Ma, D.; Pan, J.; Yin, L.; Xu, P.; Gao, Y.; Yin, Y.; Zhao, Y. Copper-Catalyzed Direct Oxidative C–H Functionalization of Unactivated Cycloalkanes into Cycloalkyl Benzo[*b*]phosphole Oxides. *Org. Lett.*, **2018**, *20*, 3455–3459. https://doi.org/10.1021/acs.orglett.8b01108

(282) Gong, J.; Fuchs, P. L. Alkynylation of C−H Bonds via Reaction with Acetylenic Triflones. *J. Am. Chem. Soc.*, **1996**, *118*, 4486–4487. https://doi.org/10.1021/ja953518p

(283) Mella, M.; Freccero, M.; Soldi, T.; Fasani, E.; Albini, A.; Oxidative Functionalization of Adamantane and Some of Its Derivatives in Solution. *J. Org. Chem.*, **1996**, *61*, 1413–1422. https://doi.org/10.1021/jo951645y

(284) Nayyar, A.; Monga, V.; Malde, A.; Coutinho, E.; Jain, R. Synthesis, anti-tuberculosis activity, and 3D-QSAR study of 4-(adamantan-1-yl)-2-substituted quinolines. *Bioorg. Med. Chem.*, **2007**, *15*, 626–640. https://doi.org/10.1016/j.bmc.2006.10.064

(285) Perry, I. B.; Brewer, T. F.; Sarver, P. J.; Schultz, D. M.; DiRocco D. A.; MacMillan, D. W. C. Direct arylation of strong aliphatic C–H bonds. *Nature*, **2018**, *560*, 70–75. https://doi.org/10.1038/s41586-018-0366-x

(286) Yadav, A. K.; Yadav, L. D. S. Direct construction of 2-alkylbenzo-1,3-azoles via C–H activation of alkanes for C–C and C–X (X = O, S) bond formation. *Org. Biomol. Chem.*, **2015**, *13*, 2606–2611. https://doi.org/10.1039/C4OB02488E

(287) Kamijo, S.; Hoshikawa, T.; Inoue, M. Photochemically Induced Radical Transformation of C(sp^3)–H Bonds to C(sp^3)–CN Bonds. *Org. Lett.*, **2011**, *13*, 5928–5931. https://doi.org/10.1021/ol202659e

(288) Peng, H.; Yu, J. T.; Jiang, Y.;Yang, H.; Cheng, J. Di-*tert*-butyl Peroxide-Promoted α-Alkylation of α-Amino Carbonyl Compounds by Simple Alkanes *J. Org. Chem.*, **2014**, *79*, 9847–9853. https://doi.org/10.1021/jo5017426

(289) Kim, S.; Kee, I. S.; Lee, S. Novel Radical Cyclization of *N*-Aziridinyl Imines. *J. Am. Chem. Soc.* **1991**, *113*, 9882–9883. https://doi.org/10.1021/ja00026a041

(290) Muller, R. K.; Joos, R.; Felix, D.; Schreiber, J.; Wintner, C.; Eschenmoser, A. Preparation of N-Aminoaziridines: trans-1-Amino-2,3-diphenylaziridine, 1-Amino-2-phenylaziridine, and 1-Amino-2-phenylaziridinium Acetate. *Org. Synth.* **1976**, *55*, 114. https://doi.org/10.15227/orgsyn.055.0114

(291) Bradshaw,B.; Etxebarría-Jardi, G.; Bonjoch, J.; Viózquez, S. F.; Guillena, G.; Nájera, C. Efficient Solvent-Free Robinson Annulation Protocols for the Highly Enantioselective Synthesis of the Wieland–Miescher Ketone and Analogues. *Adv. Synth. Catal.* **2009**, *351*, 2482–2490. https://doi.org/10.1002/adsc.200900321

(292) Henze, W.; Gärtner, T.; Gschwind, R. M. Organocuprate Conjugate Addition: Structural Features of Diastereomeric and Supramolecular π-Intermediates. *J. Am. Chem. Soc.*, **2008**, *130*, 13718–13726. https://doi.org/10.1021/ja8041433

(293) Sakata, K.; Wang, Y.; Urabe, D.; Inoue, M. Synthesis of the Tetracyclic Structure of Batrachotoxin Enabled by Bridgehead Radical Coupling and Pd/Ni-Promoted Ullmann Reaction. Organic Letters 2018, 20, 130–133. https://doi.org/10.1021/acs.orglett.7b03482

(294) Shibuya, M.; Tomizawa, M.; Suzuki, I.; Iwabuchi, Y. 2-Azaadamantane *N*-Oxyl (AZADO) and 1-Me-AZADO: Highly Efficient Organocatalysts for Oxidation of Alcohols. *J. Am. Chem. Soc.* **2006**, *128*, 8412–8413. https://doi.org/10.1021/ja0620336

(295) Liu, R.; Wei, Z.; Wang, J.; Liu, Y.; Xue, H. Highly selective hydrosilylation of equilibrating allylic azides. *Chem. Commun*., **2020**, *56*, 5038–5041. https://doi.org/10.1039/D0CC01316A

(296) Kobayashi, T.; Shiroi, H.; Abe, H.; Ito, H. Synthetic Study of Presilphiperfolan-8-ol: Construction of the Tricyclo[5.3.1.$0^{4,11}$]undecane Framework Utilizing Intramolecular Aldol Condensation and McMurry Coupling. *Chem. Lett.* **2013**, *42*, 975–976. https://doi.org/10.1246/cl.130394

(297) Saladrigas, M. *Reductive Radical Coupling of Alkenes with Aldehydes, Ketones and Hydrazones by Iron-Catalyzed Hydrogen-Atom Transfer Reactions.* Directors: Josep Bonjoch, Ben Bradshaw. **2021**, Universitat de Barcelona. Id.GREC: 063745.

(298) Wu, X.; Gannett, C.N.; Liu, J.; Zeng, R.; Novaes, L.F.T.; Wang, H.; Abruna, H.D.; Lin, S. Intercepting Hydrogen Evolution with Hydrogen-Atom Transfer: Electron-Initiated Hydrofunctionalization of Alkenes. *J. Am. Chem. Soc.* **2022**, *144*, 17783−17791. https://doi.org/10.1021/jacs.2c08278

(299) Mao, C.L.; Zhao, S.; Zang, Z.L.; Xiao, L.; Zhou, C.H.; He, Y.; Cai G.C. Pd-Catalyzed Remote Site-Selective and Stereoselective C(Alkenyl)−H Alkenylation of Unactivated Cycloalkenes. *J. Org. Chem.* **2020**, *85*, 774−787. https://doi.org/10.1021/acs.joc.9b02797

(300) Bertho, S.; Rey-Rodriguez, R.; Colas, C.; Retailleau, P.; Gillaizeau, I. Regio- and Stereoselective Iron-Catalyzed Oxyazidation of Enamides Using a Hypervalent Iodine Reagent. *Chem. Eur. J.* **2017**, *23*, 17674–17677. http://doi.org/10.1002/chem.201704499

(301) Si, Y. X.; Zhu, P. F.; Zhang, S. L. Synthesis of Isocyanides by Reacting Primary Amines with Difluorocarbene. *Org. Lett*., **2020**, *22*, 9086–9090. https://doi.org/10.1021/acs.orglett.0c03472

(302) Lyrgin, A. V.; de Mejiere, A. *Ortho*-Lithiophenyl Isocyanide: A Versatile Precursor for 3H-Quinazolin-4-ones and 3H-Quinazolin-4-thiones. *Org. Lett.*, **2009**, *11*, 389–392. https://doi.org/10.1021/ol802659m

(303) Patl, P.; Ahmadian-Moghaddma, M.; Dömling, A. Isocyanides 2.0. *Green Chem.*, **2020**, *22*, 6902–6911. https://doi.org/10.1039/D0GC02722G

(304) Xiang, H.; Yu, Z.; Xie, T.; Ye, X. Y.; Ye, Y. Zn-Mediated Reductive Addition of Isocyanides with Unactivated Tertiary Alkyl Oxalates. *Eur. J. Org. Chem.,* **2022**, *38*, e202200937. https://doi.org/10.1002/ejoc.202200937

(305) a) Leifert, D.; Daniliuc, C.G.; Studer, A. 6-Aroylated Phenanthridines via Base Promoted Homolytic Aromatic Substitution (BHAS). *Org. Lett.*, **2013**, *15*, 6286−6289. https://doi.org/10.1021/ol403147v b) Patil, P.; Ahmadian-Moghaddam, M.; Dömling, A. Isocyanide 2.0. *Green Chem.* **2020**, *22*, 6902−6911. https://doi.org/10.1039/D0GC02722G

(306) Rong, J.; Deng, L.; Tan, P.; Ni, C.; Gu, Y.; Hu, J. Radical Fluoroalkylation of Isocyanides with Fluorinated Sulfones by Visible-Light Photoredox Catalysis. *Angew. Chem. Int. Ed.* **2016**, *55*, 2743−2747. https://doi.org/10.1002/anie.201510533

(307) Wang, H.; Yu, Y.; Hong, X.; Xu, B. Mn(II)/O_2-promoted oxidative annulation of vinyl isocyanides with boronic acids: synthesis of multi-substituted isoquinolines. *Chem. Commun.* **2014**, *50*, 13485-13488. https://doi.org/10.1039/C4CC06427E

(308) Hu. Z.; Yuan, H.; Men, Y.; Liu, Q.; Zhang, J.; Xu, X. Cross-Cycloaddition of Two Different Isocyanides: Chemoselective Heterodimerization and [3+2]-Cyclization of 1,4-Diazabutatriene. *Angew. Chem. Int. Ed.* **2016**, *55*, 7077-7080. https://doi.org/10.1002/anie.201600257

(309) Heckman, L.; He, Z.; Jamison, T.F. Synthesis of Highly Substituted 2-Arylindoles via Copper-Catalyzed Coupling of Isocyanides and Arylboronic Acids. *Org. Lett.* **2018**, *20*, 3263-3267. https://doi.org/10.1021/acs.orglett.8b01132

(310) Evoniuk, C.J.; Gomes, G.D.P.; Ly, M.; White, F.D.; Alabugin, I.V. Coupling Radical Homoallylic Expansions with C–C Fragmentations for the Synthesis of Heteroaromatics: Quinolines from Reactions of o-Alkenylarylisonitriles with Aryl, Alkyl, and Perfluoroalkyl Radicals. *J. Org. Chem.* **2017**, *82*, 4265-4278. https://doi.org/10.1021/acs.joc.7b00262

(311) Linsenmeier, A. M.; Williams, C.M.; Bräse, S. Synthesis of Phenanthridine Derivatives via Photolysis. *J. Org. Chem.* **2011**, *76*, 9127-9132. https://doi.org/10.1021/jo201542x

(312) Qian, P.; Du, B.; Zhou, J.; Mei, H.; Han, J.; Pan, Y. DBU-promoted cyclization of vinyl isocyanides with ethers via the functionalization of a C(sp^3)–H bond for the synthesis of isoquinolines. *RSC Adv.*, **2015**, *5*, 64961-64965. https://doi.org/10.1039/C5RA11530B

(313) Wang, P.; Zhao, J.Z.; Li, H.F.; Liang, X.M.; Zhang, Y.L.; Da, C.S. Acid-catalyzed highly diastereoselective and effective synthesis of 1,3-disubstituted tetrahydropyrano[3,4-b]indoles. *Tetrahedron Lett.* **2017**, *58*, 129-133. https://doi.org/10.1016/j.tetlet.2016.11.110

(314) Vargas, D.A.; Tinoco, A.; Tyagi, V.; Fasan, R. Myoglobin-Catalyzed C−H Functionalization of Unprotected Indoles. *Angew. Chem. Int. Ed.* **2018**, *57*, 9911-9915. https://doi.org/10.1002/anie.201804779

(315) Sha, W.; Yu, J.T.; Jiang, Y.; Yang, H.; Cheng, J. The benzoyl peroxide-promoted functionalization of simple alkanes with 2-aryl phenyl isonitrile. *Chem. Commun.* **2014**, *50*, 9179-9181. https://doi.org/10.1039/C4CC03304C

(316) Mao, H., Gao, M., Liu, B., Xu, B. Manganese(II)-catalyzed modular synthesis of isoquinolines from vinyl isocyanides and hydrazines. *Org. Chem. Front.*, **2016**, *3*, 516-521. https://doi.org/10.1039/C6QO00048G

(317) Lu, Y. C.; Kao, S. C.; West, J. G. Decatungstate-Catalysed C(sp^3)–H Azidation. *Chem. Commun*., **2022**, *58*, 4869−4872. https://doi.org/10.1039/D2CC00425A

(318) Yan, J.; Zhang, W.; He, Q.; Hou, J.; Zeng, H.; Wei, H.; Xie, W. Enantioselective Direct Vinylogous Michael Addition for Constructing Enantioenriched γ,γ-Dialkyl Substituted Butyrolactams and Octahydroindoles. *Org. Biomol. Chem.***,** **2022**, *20*, 2387−2391. https://doi.org/10.1039/D2OB00112H

(319) Fang, H.; Zhao, J.; Ni, S.; Mei, H.; Han, J.; Pan, Y. Metal-Free Oxidative Functionalization of a C(sp^3)–H Bond Adjacent to Nitrogen and Intramolecular Aromatic Cyclization for the Preparation of 6-Amidophenanthridines. *J. Org. Chem.* **2015**, *80*, 3151−3158. https://doi.org/10.1021/acs.joc.5b00058

(320) Ambala, S.; Thatikonda, T.; Sharma, S.; Munagala, G.; Yempalla, K. R.; Vishwakarma, R. A.; Singh, P. P. Cross-dehydrogenative coupling of α-C(sp^3)–H of ethers/alkanes with C(sp^2)–H of heteroarenes under metal-free conditions. *Org. Biomol. Chem.*, **2015**, *13*, 11341–11350. https://doi.org/10.1039/C5OB01268F

(321) Li, Z.; Liu, C.; Guo, S.; Wang, W.; Zhang, Y. PIFA-Mediated Cross-Dehydrogenative Coupling of N-Heteroarenes with Cyclic Ethers: Ethanol as an Efficient Promoter. *Eur. J. Org. Chem.*, **2021**, 3, 411–421. https://doi.org/10.1002/ejoc.202001354

(322) Bradshaw, B.; Etxebarria-Jardí, G.; Bonjoch, J. Polycyclic Framework Synthesis of Anominine and Tubingensin A Indole Diterpenoids. *Org. Biomol. Chem*. **2008**, *6*, 772–778. https://doi.org/10.1039/b718280e.

(323) Shibuya, M.; Tomizawa, M.; Suzuki, I.; Iwabuchi, Y. 2-Azaadamantane *N*-Oxyl (AZADO) and 1-Me-AZADO: Highly Efficient Organocatalysts for Oxidation of Alcohols. *J. Am. Chem. Soc.* **2006**, *128*, 8412–8413. https://doi.org/10.1021/ja0620336

(324) Liu, R.; Wei, Z.; Wang, J.; Liu, Y.; Xue, H. Highly selective hydrosilylation of equilibrating allylic azides. *Chem. Commun*., **2020**, *56*, 5038–5041. https://doi.org/10.1039/D0CC01316A

(325) Rostoll-Berenguer, J.; Blay, G.; Pedro, J.R.; Vila, C. Photocatalytic Giese Addition of 1,4-Dihydroquinocalin-2-ones to Electron-Poor Alkenes Using Visible Light. *Org. Lett*., **2020**, *22*, 8012-8017. https://doi.org/10.1021/acs.orglett.0c02953

(326) Liu, J.; Lu, L. Q.; Luo, Y.; Zhao, W.; Sun, P. C.; Jin, W.; Qi, X.; Cheng, Y.; Xiao, W. J. Photoredox-Enabled Chromium-Catalyzed Alkene Diacylations. *ACS Catal*. **2022**, *12*, 1879–1885. https://doi.org/10.1021/acscatal.1c05672